e-ISSN : 2320-0847
p-ISSN : 2320-0936

American Journal of Engineering Research (AJER)

Volume 3 Issue 3 – March 2014

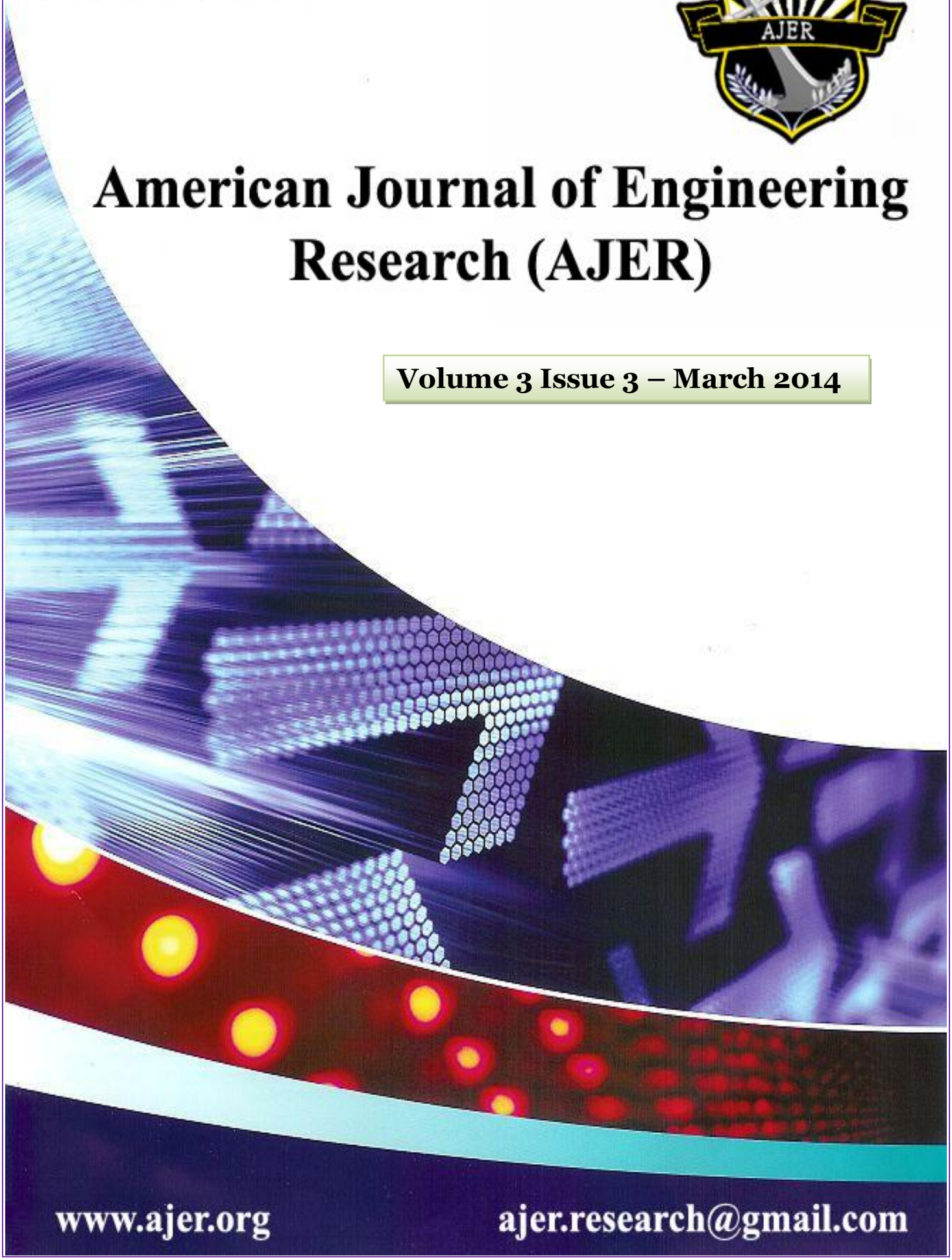

www.ajer.org ajer.research@gmail.com

Editorial Board

American Journal of Engineering Research (AJER)

Volume-3 Issue-3

American Journal of Engineering Research (AJER)
e-ISSN : 2320-0847 p-ISSN : 2320-0936
Volume-03, Issue-03, pp-01-07
www.ajer.org

Research Paper Open Access

Physico Chemical Properties of higher polymers in petroleum Industry

*Sudhaker Dubey ** Kartikeya Dwivedi *** Aarti Chaturvedi
****Prashant Dwivedi
** Maharaj Singh College ; C.C.S University;Meerut (U.P);India*
*** Maharaj Singh College ; C.C.S University;Meerut (U.P);India*
****Maharaja Agrasen University;Baddi;Solen;(H.P) ;India*
***** International College of Engineering;Uttar Pradesh Technical University ;Lucknow; (U.P) ; India*

Abstract: - This paper deals with the phase inversion and the stability of emulsion. This phenomenon of inversion of emulsion is the sudden reversal of phase by which an oil/water emulsions becomes a water/oil emulsion. As the percentage of kerosene and turpentine oil increases from 10% to 90% in the oil/water emulsion, the oil/water type emulsion changes into water/oil types. There is a sudden fall in the conductance when oil phase concentration changes from 70-80% in all cases. The plots of log conductance against oil percentage shows that in all the cases horizontal portions are obtained. Thus for all the surfactants phase inversion from oil/water to water/oil occurs at an oil concentration of 70% in the case of both kerosene oil and turpentine oil. The lowest horizontal portion is indicative of water/oil emulsions. The highest horizontal portion corresponding to oil/water emulsions is case of RL-1, RL-2 & RL-3 up to a concentration of 30% oil, it is mainly oil/water emulsions. The study of stability shows that kerosene oil/water emulsion stabilized by adding 1% surfactant viz RL-1, RL-2,RL-3 remain stable upto 9 days, 9days and 19 days respectively. A demulsifier used in the petroleum industry to demulsify and the emulsion was tested here and found that emulsion stabilized by adding 1% RL-1 and RL-2 surfactant were stable upto 4 hours while emulsion stabilized by RL-3 surfactant remain stable upto 5 hrs respectively. After 10 hrs 100% demulsification is noticed in the case of all the emulsion.

Keywords: *- emulsion, phase inversion, conductance, demulsification, surfactants.*

I. INTRODUCTION

The phenomena of phase inversion in emulsion i.e. the sudden reversal of phase by which an oil/water emulsion becomes water/oil emulsion (and vice-versa) is of considerable interest both from the practical as well as the theoretical point of view the importance resides in the fact that many commercial emulsion are prepared by, initially producing the wrong type of emulsions and inducing inversion to the desired type by addition of the phase which will ultimately be the external phase.

Robertson (1) was one of the first to record experiments of this kind, but his work was really an investigation on phase/volume relationship. Newmen (2) investigated two types of emulsions obtained with water and benzene. He found that when sodium-oleate was used as emulsifier, water was always the external phase. However, when magnesium-oleate was the emulsifying agent, he obtained emulsion of water/benzene type Newman found that emulsions of water/benzene stabilized by magnesium-oleate could be inverted by adding sufficient sodium oleate a phase inversion can some times be brought about on shaking an aged emulsion or both types can be prepared by the use of different types of mechanical methods.

The effect of electrolytes on emulsion is of great importance specially the divalent cations, normally found in hard water which tend to invert oil/water emulsion made with soaps and many other agents. Thus to an oil in water emulsion stabilized by sodium oleate and aluminium salts are added in a slight excess, the phase inversion takes place and water/oil emulsion is obtained.

Physical theories of emulsion inversion has been proposed which describe the formation of one type or the other to excess of positive or negative ions absorbed by the stabilizing film of the emulsifying agents. According to Clows (3) emulsion equilibrium depend on the relative proportion of the positive and negative ions absorbed by the film when negative ions are in excess the oil in water emulsion is favoured. Whereas an excess of positive ions has the reverse effect. The idea was accepted and extended by Bhatnagar(4) to explain the result of his own extensive experiments on the inversion of emulsion by electrolytes. Employing the electrical method suggested by Cayton(5) a sensitive means of detecting the inversion point. He found that(a) There is distinct valency effect of electrolytes. Trivalent electrolytes such as sulphates of Al^{+3} and Cr^{+3} are required in such a small amounts to effect inversion of oil/water emulsions than the bivalent electrolytes (b) The inverting capacity of the electrolytes follows the order Al>Cr>Ni>Pb>Ba>Sr and (c) The nature of the soap present influences the amount of electrolytes required to effect the reversal of phase. But the valency effect of the electrolyte still appears. He formulated two empirical rules from his results. (1) An emulsion of water/oil type can be transformed into one of the oil/water type by electrolytes having reactive ions like OH^- and PO_4^{-3}.
(2) An emulsion of oil/water type can be transformed into the reverse type i.e. water/oil type with electrolyte having reactive cations like Al^{3+} and Fe^{3+} and Th^{3+} Ostwald(6) & (7) apparently the first to point out the possibility of the existence of two emulsion types. Ostwald's theory is based on solid geometry, namely that in the assembly of spheres occupy 74.02% of the available space. Thus Ostwald was led to conclusion that if an emulsion contained more than 74% of the internal phase, inversion must necessarily occur, resulting in an emulsion of the opposite type which would contain only 26% internal phase. In other words in the regions 0-26% and 74-100% only one type of emulsion may exist in the intermediate region, both types are possible.
Bechere(8) shows the dependence of the inversion phase concentration on the emulsifier concentration for the inversion oil/water to water/oil. As the concentration of emulsifier increases the volume of the inversion phase at which the inversion occur decreases. The inversion concentration of an emulsion is a function of the concentration and the chemical nature of the surfactant. A Salager proposed that atleast two types of inversion occurs. A Catastrophic 'C' (9,10) inversion occurs when the inversion takes place because of the change in volume fraction (i.e. increasing the volume fraction of the dispersed phase it was first suggested that this inversion is caused by the complete coalescence of the dispersed phase at the closer packing arrangement of the drop(11).
Recently experiments were performed(12) for the surfactant/ oil-water system $C_6H_{13}(OC_2H_4)OH$/-n tetradecane/aqueous 10 mL of NaCl at temperature from 298K down to 285K near the lower critical end point temperature.
Morphologies and phase volume fraction at which inversion occurred were determined for emulsion by electrical conductivity measurements. The inversion-hysteresis lines were found to confirm the dispersion-morphology diagram proposed by Smith(13).In the literature cited above following techniques have been utilized in the detection of phase inversion.

1) The Indicator Method:- In this method a oil soluble water insoluble or water soluble dye is dusted on the surface of emulsion to be examined. If the oil phase is continuous, the oil soluble dye will gradually spread throughout the system owing to its dissolving in the oil. If however, water is continuous phase, then dye will not spaced.
2) The Drop Dilution Method:- The principle of this method is that emulsion can be diluted by addition of the external or continuous phase by not by adding the disperse phase.
3) The Electrical Conductance Method:- Bhatnagar(14) proposed a way of differentiating between oil/water and water/oil emulsion . A water continuous phase would be expected to show a very much higher conductance than an oil continuous phase sudden rise ir fall in the conductance could be imply phase inversion during investigation.

In the present investigation phase inversion studies of oil/water emulsion stabilized by surfactants (RL-1,RL-2 and RL-3) has been carried out by measuring the electrical-conductance of the emulsion.

II. EXPERIMENTAL

Materials:- Double distilled kerosene and turpentine oil having specific gravity 0.7948 g/mL and 0.9145 g/mL at 70^0C respectively were stored to use in all the experiments. Double distilled water (conductance $1X10^{-6}$ $ohm^{-1}cm^{-1}$) was employed throughout the course of investigations.
RL-1, RL-2 & RL-3 surfactants studied were synthesized as described Daitrolite 400 demulsifier was obtained from Daichi-chemical Bombay.

Preparation of Emulsion:-

(a) Oil/water emulsion of kerosene and turpentine oil were prepared by taking concentration of each of the single surfactant viz, RL-1, RL-2 and RL-3. The percentage of oil phase was then varied as 10%, 20%, 30%, 40%, 50%, 60%, 70%, 80% and 90% respectively

(b) For demulsification studies, oil/water emulsion of kerosene were, prepared by taking concentration each of the single surfactant viz RL-1, RL-2, and RL-3. Oil/water was kept 1:1 constant. Demulsification was studied with the treatment of 50ppm Daitrolite, 400 and without demulsifier. The emulsion were prepared by agent in water method(15) by adding oil with constant stirring to the aqueous solution of surfactant and then finally agitated by redimix mixer to prepare final emulsion.

Measurement of Conductance:-

Conductance of emulsion was measured by German make (WTW) conductance meter with magic eye(16). The conductance of kerosene oil/water and turpentine oil/water emulsion having surfactant concentration 1% and obtaining varying percentage of oil in the range of 10% to 90% at room temperature viz 25 ± 1^0C respectively have been measured and the result are summarized in table 1-II and figure 1-6.

(c) Measurement of Demulsification :- The demulsification was measured by keeping emulsion samples in the carked measuring cylinders in the oven at 25 ± 1^0C . The demulsification phenomena was observed visually with time . After creaming when the breaking of emulsion started, the separated oil also measured regularly at the interval 0-1,10, 20,30,40, 50 and 60 days while by adding demulsifier emulsion sample were checked at the interval of 0-4,5,6,7,8,9, and 10 hours respectively. Results presented in the table III and IV.

III. RESULTS & DISCUSSION

The table I & II and figure 1-6 reveals that when in the experiments kerosene and turpentine oil were added to the 1% (aqueous solution of surfactant) and agitated for final emulsification in mixer, oil/water emulsion were initially formed. When the percentage of oil phase, were increased by adding different amounts such as 10%, 20%, 30%, 40%, 50%, 60%, 70%, 80% and 90% respectively, the oil/water emulsion change to water/oil type.

While studying the effect of phase volume ratio, it is evident from the table that there is sudden fall in conductance when oil phase concentration changes from 70% to 80%. Both in all the cases, the better picture emerges when log conductance is plotted against the oil phase concentration represented in figure 1-6. In all the cases three horizontal portion are obtained. Thus for all the surfactants, phase inversion from oil/water to water/oil occurs at an oil concentration of 70% in the case of both oil. The lowest horizontal portion is indicative of water/oil emulsion. The highest horizontal portion corresponds to oil/water emulsions. While the middle horizontal portion shows the mixed-emulsion profile. The phenomena of phase inversion is of significance both from practical as well as the theoretical point of view, many times a commercial emulsion initially of the wrong type may be obtained and later on change to the desired type by addition of suitable phase. Various theories have been advanced in order to explain the phenomena of phase inversion. According to Clows(17) the droplets of the internal themselves into filaments which weave around the experiments phase. The result is that the external phase breaks down into internal phase while the filaments coalescence in the process changing into continuous or external phase. According to Schulman & Cockbain (8) the process of phase inversion is supposed to consist loose flocculation of droplets of internal phase, whereby the external phase is trapped in the interior of the flocculate. The internal phase where (say the oil) coagulate due to reorganization of the emulsifying agent at the oil/water interface while external phase (say water) is dispersed in the form of irregularly shaped sacks and the oil/water emulsion change into water/oil type. Ostwald (10,11) has, proposed a simple stereometric theory based on the fact of solid geometry viz. in assembly of uniform share, arranged in closest possible packing, the space occupied by them would be 100% of the total. Accordingly, if an emulsion contained 74% of internal phase, inversion should occur producing the opposite type emulsion containing only 26% of internal phase. In the other words in the region 0-26% and 74-10 only one type of emulsion exist while in intermediate range both types are possible. In the present investigations the horizontal portions observed from 0-30% & 70-100% shows one type of emulsion and middle horizontal portion shows the mixed emulsion are in general agreement with Ostwald's theory.

Thus in the range 70-100% of oil, it is purely water-oil emulsion, while in the range of 0-30%, it is purely oil/water system. In the intermediate range both the systems occurs as would be obvious from the figures. Table –III and IV shows that the demulsification data of oil/water emulsions of kerosene oil, stabilized by adding surfactants viz RL-1, RL-2, RL-3 respectively. The results shows that emulsion stabilized by RL-1 and RL-2 were stable upto 9 days, after the preparation of emulsion and then at 10^{th} day clearing start in the case of both the emulsions. In case of emulsion stabilized by RL-3 surfactant, breaking of emulsion starts on 20^{th} day and oil separation on 50^{th} day onward respectively, on 60^{th} day complete breaking of emulsion is noticed. While emulsion stabilized by RL-2 shows creaming on 10^{th} day, after preparation of emulsion on 40^{th} day and complete breaking on 60^{th} day respectively. The emulsion stabilized by surfactant RL-3 shows emulsion remain stable upto 19^{th} day and after that creaming start and emulsion breaking starts an 40^{th} day and breaks completely after 60^{th} day.

A demulsifier used in petroleum industry to demulsify emulsion is checked for efficiency. The results shows, that emulsion stabilized by RL-1 and RL-2 remain stable upto 4 hours while emulsion stabilized by RL-3

surfactant remain stable up to 5 hours respectively. After 9th hour 80%, 75% and 70% oil get separated in cases of emulsion stabilized by RL-1, RL-2 and RL-3 surfactant respectively. After 10 hours 100% demulsification is achieved in all the cases.

Emulsification studies carried out in the earlier papers and in this paper reveal that physio-chemical properties such as surface tension, viscosity, particle size and conductance are the parameters which provides information regarding the formation of emulsions and maintaining their stability. Our result shows that lower the surface tension and higher the values of viscosity, particle size, and conductance favors emulsification and makes the emulsion more stable.

Table-I

Sl. No.	Oil Phase	Conductance RL-1	Ohm RL-2	cm RL-3	Type of Emulsion
1	10	-5.775	-5.762	-5.755	O/W
2	20	-5.807	-5.833	-5.856	O/W
3	30	-5.867	-5.875	-5.890	O/W
4	40	-6.097	-6.036	-6.070	O/W/ O/W
5	50	-6.195	-6.036	-6.100	O/W+ O/W
6	60	-6.208	-6.100	-6.126	O/W+ O/W
7	70	-6.266	-6.180	-6.204	O/W+ O/W
8	80	-7.833	-7.848	-7.863	O/W
9	90	-7.862	-7.877	-7.890	O/W

Table-II

Sl. No.	Oil Phase	Conductance RL-1	Ohm RL-2	cm RL-3	Type of Emulsion
1	10	-5.750	-5.780	-5.828	O/W
2	20	-5.903	-5.920	-5.955	O/W
3	30	-6.012	-6.063	-6.088	O/W
4	40	-6.092	-6.100	-6.173	O/W/ O/W
5	50	-6.106	-6.110	-6.173	O/W+ O/W
6	60	-6.115	-6.160	-6.181	O/W+ O/W
7	70	-6.124	-6.210	-6.241	O/W+ O/W
8	80	-7.121	-7.041	-7.052	O/W
9	90	-7.152	-7.062	-7.074	O/W

Table-III

Sl.	Time	RL-1	RL-2	RL-3
1	01	stable	stable	stable
2	10	creaming	creaming	stable
3	20	creaming	creaming	creaming
4	30	breaking	creaming	creaming
5	40	breaking	breaking	breaking
6	50	60% oil separated	breaking	breaking
7	60	70% oil separated	50% oil separated	40% oil separated

Table-IV

Sl. No.	Time in Days	RL-1	RL-2	RL-3
1	0-4	stable	stable	stable
2	5	creaming	creaming	stable
3	6	breaking	creaming	creaming
4	7	breaking	breaking	breaking
5	8	60% oil separation	breaking	breaking
6	9	80% oil separation	75% oil separation	70% oil separation
7	10	100% oil separation	100% oil separation	100% oil separation

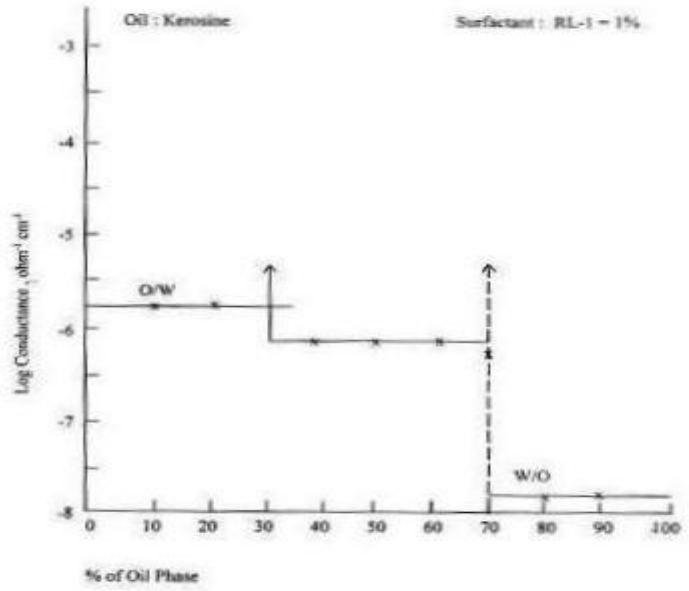

Fig-1: Phase Inversion of Emulsion

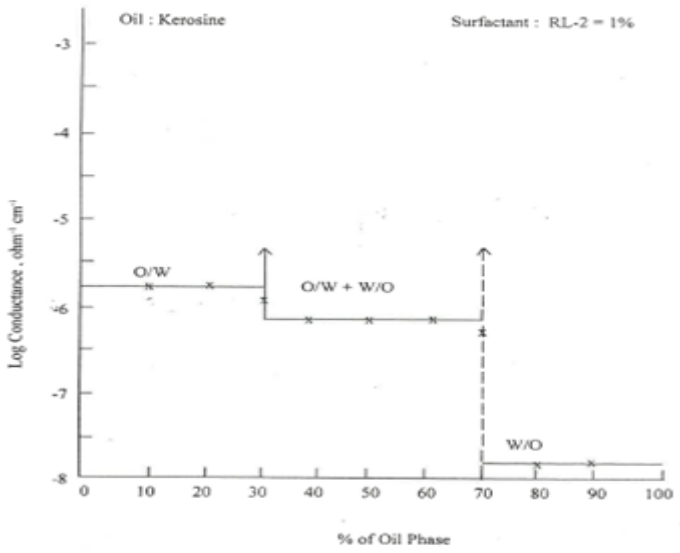

Fig-2: Phase Inversion of Emulsion

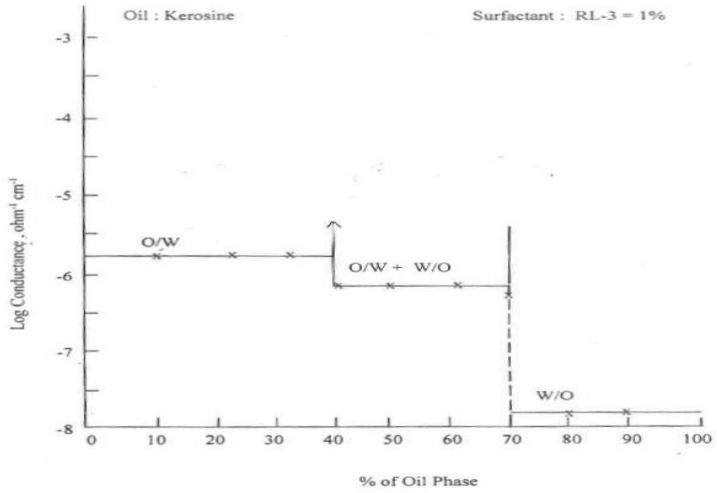

Fig-3: Phase Inversion of Emulsion.

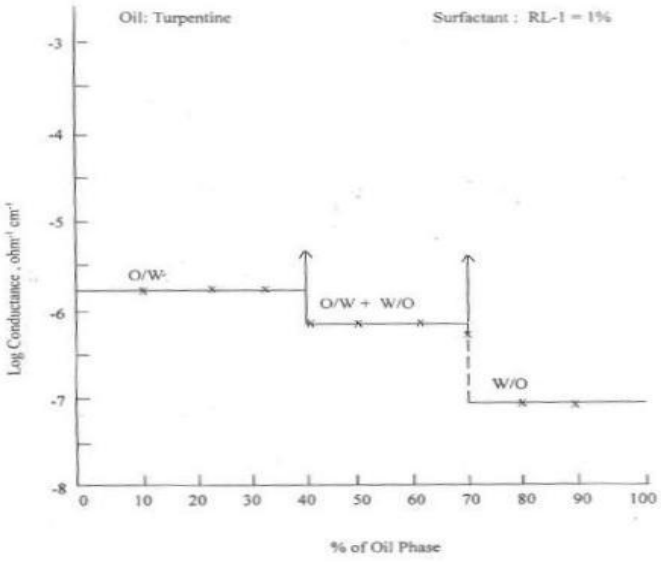

Fig-4: Phase Inversion of Emulsion

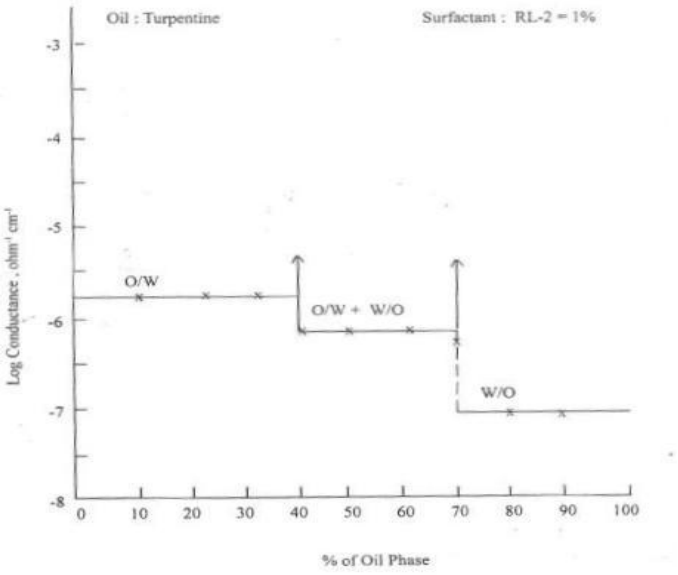

Fig-5: Phase Inversion of Emulsion

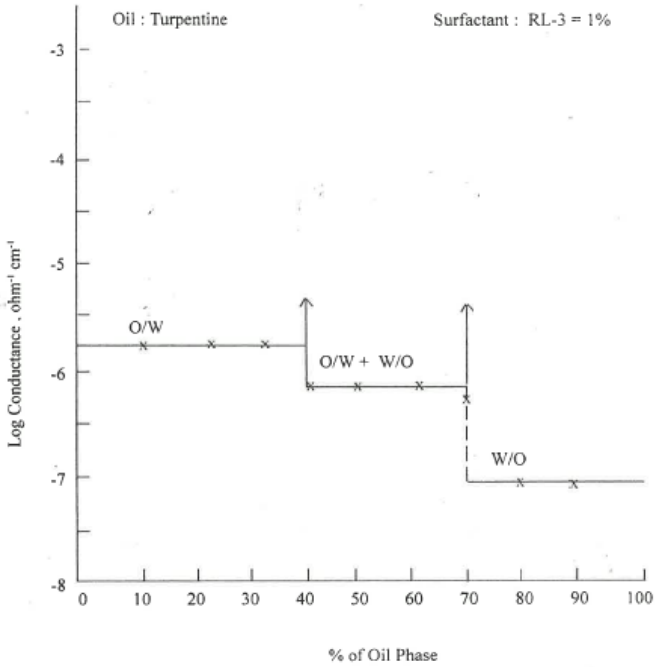

Fig-6:- Phase Inversion of Emulsion

REFERENCES

[1] Robertson K.Kolloid-z,77, 1910.
[2] Newman.J., Phys.chem 18-34,1914.
[3] Clows G.H.A., Proc,Soc.Exp.Biol And-med 11,1,1913.
[4] Bhatnagar,S.S. J.chem soc. 119,61,1921.
[5] Clayton W., Britcoll.reports 2, 114, 1918.
[6] Ostwald W.O., Kolloid-Z, 6, 103, 1910.
[7] Becher,P.,J.Soc.cosmetic chem., IX,3,141, 1958.
[8] Salager J.L., Phase transformation and emulsion inversion on the basis of castastroph theory in P.Becher (Ed) Encyclopedia of emulsion science, vol 3, Marcel-Dekker New York 99, 79-134, 1988.
[9] B.W.Brroks, H.N.Reymond, phase inversion non ionic surfactant-oil-water-system-3. The effect of oil phase viscosity on catastrophic inversion and the relationship between the drop sizes present before and after catastrophic inversion; chem.-eng.sic.49, 1843-1853, 1994.
[10] Ostwald w., Emulsion Kolloids Z., 8, 103-109, 1910,chem. Abs. 1705.

American Journal of Engineering Research (AJER)
e-ISSN : 2320-0847 p-ISSN : 2320-0936
Volume-03, Issue-03, pp-08-15
www.ajer.org

Research Paper Open Access

Suitability of Birnin Gwari and Maraban Rido Clays as Refracory Materials

S.O Yakubu[*1] M.Y. Abdulrahim[2]
[1]*Department of Mechanical Engineering, Faculty of Engineering, Nigerian Defence Academy, PMB 2109, Kaduna, Nigeria GSM: 08028271895 ;email:ysochetengwu@yahoo.com*
[2]*Department of Mechanical Engineering, Faculty of Engineering, Nigerian Defence Academy, PMB 2109, Kaduna, Nigeria GSM: 08052332634*

Abstract: - Most of the industries in Nigeria depend heavily on the use of refractory materials. For instance the iron and steel industries, cement, glass, refineries, bakeries and ceramic industries. However, almost all the refractory materials used by these industries are imported. Consequently, it leads to the draining of Nigeria's foreign reserve and this in turn negatively affects the economy of the Country. Therefore, there is the need to increase the local production of the refractory materials in order to reduce their importation and thereby boost the economy Nigeria. Hence this researched work was carried out to investigate and see if the Birnin Gwari and Maraban Rido clays in Kaduna state, Nigeria can serve as refractory materials. The clay samples were obtained from the mining sites and processed to produce fireclay brick test specimens which were fired between 250^{o}C and 1400 ^{o}C. The fired bricks were then tested for refractory properties such as: the linear shrinkage, bulk density, apparent porosity, cold crushing strength, thermal shock resistance and refractoriness (Pyrometric Cone Equivalent) using ASTM standards. The obtained results were as follows: The Linear shrinkage was 10% and 8.0%; apparent porosity 24.65% and 21.55%; bulk density 1.75 g/cm^3 and 1.96 g/cm^3, cold crushing strength 165.0 Kg/cm^2 and 216.9 Kg/cm^2 , refractoriness 1300 ^{o}C and 1400 ^{o}C and thermal shock resistance 16.67 and 32 cycles for Maraban Rido and Birnin Gwari clays respectively. The results as compared with the standard refractory bricks, showed that both clays are suitable for fire clay refractory materials while bricks produced from Birnin Gwari clay are also suitable for batch furnace applications. Both clays can be used for lining of non-metallic melting furnances.

Keywords: *- Birnin Gwari, Maraban Rido, Clay, Refractory Material, Bricks*

I. INTRODUCTION

According to Aigbodion V.S. (2008), Aigbodion V.S., et al (2007), a refractory material is one which has the ability to withstand high temperature, physical and chemical actions of molten metal slag and gases without deformation failure or change in the chemical composition under their own weight. It is said in Akingbode E.O (1996) and Hassan S.B. (2000) works that refractory materials are used for furnace linings and construction of tubes for electric furnaces, crucibles pots, thermocouple sheaths, refractory cements, among others. These properties are extremely very useful at enhancing both the process control and product quality according to Chesti A.R. (1986) et al.

i) Reinhard S.J. (1982) in his work said Refractories are considered as inorganic materials, which are mainly mixtures of oxides, obtained from naturally occurring minerals, which are capable of withstanding very high temperature condition, without any undue deformation, softening, change in composition. They include silica, magnetite, chrome, carbon, dolomite and alumino-silicates. From Okeugo C.O. and Nwabineli (2012) and Irabor P.S.A., (2002) works, we know that most industries dealing with the treatment of ores and other materials for the manufacture of metallurgical, chemical and ceramic products operates at a very high temperature condition, so the equipment used for the treatment of this materials must sustain the operating temperatures and other working condition such as erosive and local conditions. The industries in Nigeria such as the Iron and Steel, Cement, Glass, Refineries, Bakeries and Ceramic industries etc depend heavily on the use of refractories and their demand are presently met, to a large extent by the importation of theses refractories. Therefore, it has

become imperative to produce these refactories locally. Nigeria is endowed with large quantity of clay deposits all over the country, which has not yet been fully explored. Such areas are Birnin Gwari and maraban rido clay deposits. Thus, the study covers the investigation of refractory properties of Birnin Gwari and Maraban Rido clay deposits. The success of the research will bring about a reduction in importation of the refractory bricks thereby preserving our much needed foreign reserve, creation of more jobs, add economic value to the abundant Birnin Gwari and Maraban Rido clays in Nigeria, the production of Cheaper Refractory. Consequently, with locally sourced raw materials, it is expected that both the cost of materials and production will be low hence the refractory materials will be cheaper.

II. METHODOLOGY

2.1 Materials and Equipment

The materials used were Birnin Gwari and Maraban Rido clays (Kaduna State)

The major equipment used were: X-ray Flouresence (XRF) Machine, Carbolite furnace, Standard Pyrometric cone and roll crusher, Paul Weber hydraulic press, Densometer Electric Water Heater, Electrical Resistance Furnace

2.2 Experimental Procedures

- **Winning:**

The process of collecting clay material is called winning. The available basic winning methods for obtaining clay are mechanical winning and hand digging. Hand digging was employed in this work based on the ease of the process and the low cost involved**.**

- **Crushing and grinding**

The collected clay samples were in wet lump. The samples were dried (dehydrated) in sun for a day for easy crushing to smaller particles before further processing. The crushing and grinding of clay were done by mechanical means using pulverizing machine. The dried clay was crushed and ground into powder form. The ground clays were then sieved with a sieve of 300µm aperture according to ASTM C1054-03 (2008)

- **Chemical Analysis*:***

The elemental composition of the two clays was determined through the X-Ray Fluorescence (XRF) analysis in accordance with American Society of Testing of Materials (ASTM) C25-06. (2010) The results are presented in table 3.1

- **Samples/Brick Production**:

Preparation of the test samples involved mixing of the freshly sieved clay with water. The clay mixture was found to be plastic at 15% water content level. The mixed blend was packed into a metal moulding box and pressed using hydraulic press. A pressure of 10kg/cm^2 was applied to enhance homogeneity and surface smoothness of the samples.

- The moulds used for forming the sample bricks was made from mild steel with internal cross section of 50mm X 50mm and lengths of 40mm, 50mm and 60mm.

Fig 3.1 : Hydraulic Press for Moulding

- The moulded bricks were dried in open air for three days, followed by drying in oven for 12 hours at 110^{O}C to expel any moisture left in them and to avoid crack during firing. Firing was carried out in electric heating furnace pre set at heating rate of 7^{o}C/minute. The firing procedure used involved heating and soaking the samples at various temperatures using ASTM-C16-03 (2009), as shown below:
- a) 250^{O}C for 6 hours
- b) 650 ^{O}C hours for 4 hours
- c) 950 ^{O}C for 3 hours
- d) 1100 ^{O}C hours for 8 hours
- e) 1400 ^{O}C hours for 8hours
- The bricks were then allowed to cool in the furnace at a cooling rate of 1^{o}C /minute immediately after firing to avoid sudden cracks according to ASTM-C16-03 (2009). The cooling rate was achieved with a digital pre-set furnace and this was done to avoid sudden cooling that may result to cracking of the bricks after firing.

1.3.1. TEST PROCEDURE:

The refractory properties of the fired bricks were tested, which includes: linear shrinkage, apparent porosity, bulk density, cold crushing strength, Refractoriness and thermal shock resistance, in accordance to the recommended standard.

a. Measurement of Linear Shrinkage:

The green and fired dimensions of the bricks were measured. The linear shrinkage was then calculated as a percentage of the original wet length as shown below

Percentage of fired shrinkage = $\frac{l_{b-} l_c}{l_b} x100\,(\%)$ ……..(1)

l_b-- dimension of green bricks
l_c--- dimension of fired bricks

b. Apparent Porosity and Bulk Density

The fired brick of 50mm x 50mm x 40mm size was kept in the oven at 110^{O}C for 3 hours to obtained constant weight D, the brick was then suspended in distilled water and boiled on a hot plate for 30 minutes, after boiling, while still in hot water, the water was now displaced with cold water and the weight W was measured on a spring balance hinged on the a tripod stand. The test samples were removed from the water and extra water wiped off from the surface by lightly blotting the sample with wet towel and the weight S in air was measured, the apparent porosity (P_a) of the bricks was determined from the relationship below in accordance with ASTM - C20–80 (2011):

$P_a = \frac{W-D}{W-S} x100(\%)$ ……..(2)

Pa=apparent porosity

The bulk density (B_d) was also calculated from the relationship as:

Bd = $\frac{D}{W-S}$ (g\cm^3) ……..(3)

Bd=bulk density, D = Dried weight, W = Soaked weight, S = Suspended weight

c. Cold Crushing Strength

The fired bricks with 50mm wide and 50mm high were tested for crushing strength, using hydraulic machine. The load was applied axially by turning the hand wheel at a uniform rate until fracture occurs. The crushing strength was then calculated using the relationship below in accordance with ASTM C133-97 (2010):

Cold Crushing strength = $\frac{load(KN)}{Area(m^2)}$ ……..... (4)

d. Thermal Shock Resistance

The fired bricks of 50mmx50mmx60mm were used. The thermal shock was carried out using the test rig according with ASTM-C16-03 (2009) [Standard Test Method for Load Testing Refractory Shapes at High Temperatures]. The test rig consists of a sample holding table which is designed so that the heat transfer due to conduction is reduced to its minimum value. Stainless steel sheathed K-type insulated junction thermocouples of

0.5 mm in diameter; 150 mm long were used to measure the surface and the centre temperatures. These thermocouples can measure temperatures ranging from 0 to 1100^{o}C. The sample was placed in the test rig and maintained at about 1100°C and soaked for 15 minutes, after which, it was air cooled and observed for any cracks. If none were observed, it was returned to the furnace and the same process repeated until the sample cracked. The result of the number of cycles of the samples is presented in Table 3.7.

e. Refractoriness

The clay samples were made into sample cones of 1.27cm base side and a perpendicular vertical length of 3.81cm, this size is the recommended shape for refractoriness test by ASTM-C24-79 (2002). The cones were mounted on refractory base along with several other standard compositions. The cones were heated at a rate of 5^{0}C/min in an oxidizing atmosphere in the furnace until the test cone squatted was compared with the standard cones, the test material is said to have the pyrometric cone equivalence of the standard cone whose behavior most resembled the test cone. The refractoriness or softening point was determined using the method of pyrometric cone equivalence (PCE) in accordance with ASTM C24 – 79 (2002). The refractoriness for each test cone is the number of the standard pyrometric cone that has bent over to a similar extent as the test cone. The temperature corresponding to the cone number was read off from the ASTM Orton Series. The result of the refractoriness of the samples is presented in Table 3.8.

III. RESULTS AND DISCUSSION

3.1 Chemical Composition

The average values of the elemental composition analysis of raw samples of Maraban Rido and Birnin Gwari clays were done using X-ray fluorescence (XRF) machine and are presented in Table 3.1.

Table 3.1: Elemental (XRF) Analysis of Raw Clay samples

Composition	Maraban Rido %	Birnin Gwari %
Al_2O_3	33.42	35.67
SiO_2	45.94	44.59
Fe_2O_3	0.70	0.23
CaO	1.30	0.08
MgO	0.04	0.06
K_2O	0.36	0.52
Na_2O	0.36	0.14
TiO_2	1.28	1.10
Cr_2O_3	2.23	1.85
MnO	0.36	0.43
Moisture	13.93	15.23
LOI	0.08	0.10

The chemical composition of both clay samples tested showed that the alumina (Al_2O_3) content for Maraban Rido was 33.42% while that for Birnin Gwari was 35.67%. Both of them were found to qualify as high melting clays. This is because the values of their alumina content lie within the recommended range for high melting clays (ASTM, 1982). Also the silica (SiO_2) content of Maraban Rido was 45.94% while that for Birnin Gwari was 44.59% and both meet the standard for fireclay refractory. (ASTM, 1982). This means that these clays can be used for lining of heat treatment furnaces and portions of blast furnaces in accordance with the Annual Book of ASTM Standards, 1982.

The iron oxide content of both clay samples is low and these levels of oxide will not impart a reddish colour to the clay when fired. The iron oxide of Maraban Rido was 0.70% and the Birnin Gwari was 0.23% which meets the iron oxide requirement for both refractory clays and high melting clays. According to the Annual Book of ASTM Standards (1982), the maximum amount of iron oxide for fireclay must not exceed 2%.

3.2 Surface Appearance

The physical appearance of the bricks after firing revealed that there was no crack in all the bricks after firing. This means that both clays bond very well during firing (see Table 3.2 and Photograph 3.1).

Table 3.2: The surface appearance the bricks

Samples	After Drying	After Firing	Colour Change
Maraba Rido clay	No crack	No crack	No colour change
Birni Gwari clay	No crack	No crack	No colour change

Photograph 3.1: Sample placed inside the Oven

3.3 Linear Shrinkage

The results of the linear shrinkage are show in Table 3.3.

Table 3.3: Firing Shrinkage of Bricks Samples

S/N	Sample Name	Initial Length (cm)	Final Length (cm)	Firing Shrinkage %
A	Maraban Rido	10.0	9.0	10.0
B	Birnin Gwari	10.0	9.2	8.0

The linear shrinkage of Maraban Rido clay was found to be 10.0%, while that of Birnin Gwari clay was 8.0% as reflected in Table 3.3. Both clays are within the recommended values of fireclay bricks which have values from 7.0-10.0 % (see Table 3.9). These values are satisfactory, because higher shrinkage values may result in warping and cracking of the brick and this may cause loss of heat in the furnace.

3.4 Apparent Porosity and Bulk Density

The results of the apparent porosity and bulk density of the two clays are shown in Table 3.4 - 3.5 respectively.

Table 3.4: Apparent Porosity of Brick Samples

S/N	Name	D (g)	S (g)	W (g)	% Porosity
A	Maraban Rido	11.54	6-19	13.39	25.70
		10.45	5.48	12.05	23.68
Average Porosity					**24.65**
B	Birnin Gwari	16.66	8.41	14.87	22.10
		13.66	6.94	15.45	21.00
Average Porosity					**21.55**

The **apparent porosity** values of the bricks were 24.65% and 21.55% for Maraban Rido and Birnin Gwari clays respectively. Hence the porosity of the clays fall within acceptable level as recommended for fireclay bricks of 15-25% as reflected in Table 3.9. Maraban Rido has a higher value of apparent porosity than Birnin Gwari clay, because Birnin Gwari clay underwent good vitrification during firing.

The **bulk density** values of the bricks were 1.75g/cm^3 and 1.96g/cm^3 for Maraban Rido and Birnin Gwari clays respectively as shown in Table 3.5. Bricks made from Birnin Gwari clay were within the recommended standard for fireclay which has value range of 1.9 – 2.3 g/cm^3 as presented in Table 3.9. The bulk density is a useful property of refractories, which is the amount of refractory material within a volume (g/cm^3). High bulk density

observed for the Birnin Gwari clay bricks indicates an increase in heat capacity and resistance to slag penetration.

Table 3.5: Bulk Density of Brick Samples

S/N	Sample Name	W_1 (g)	W_2 (g)	Bulk D (g/cm^3)
A	Maraban Rido	14.18	109.16	1.75
		13.05	100.61	1.75
		Average		**1.75**
B	Birnin Gwari	16.99	120.48	1.907
		21.22	142.39	2.016
		Average		**1.96**

3.6 Cold Crushing Strength

The average cold crushing strength was 165.0 and 216.9kg/cm^2 for Maraban Rido and Birnin Gwari clays respectively as presented in Table 3.6. The two clays meet the standard of cold crushing strength of 150kg/cm^2 minimum for fireclay as presented in Table 3.9. But bricks made from Birnin Gwari clay have higher cold crushing strength which means it can withstand handling, transportation and abrasion more than bricks made from Maraban Rido clay.

Table 3.6: Cold Crushing Strength of Brick Samples

S/N	Sample Name	L (cm)	B (cm)	Area (cm^2)	Force (KN)	Mass (kg)	C.CS (Kg/cm^2)
A	Maraban Rido	2.5	2.5	6.25	10	1000	160
		2.4	2.4	5.76	9.8	980	170
		Average					**165**
B	Birnin Gwari	2.4	2.4	5.76	13.5	1350	234.4
		2.7	2.6	7.02	14	1400	199.4
		Average					**216.9**

3.7 Thermal Shock Resistance

The thermal shock resistance values were 16.67 and 30 cycles for bricks made with Maraban Rido and Birnin Gwari clays respectively as presented in Table 3.7. Bricks produced from Birnin Gwari clay fall within the acceptable ranges of 20-30 cycles for fire clay as presented in Table 3.9. This might be due to the fact that no degree of fusion might have taken place that may have burn off the brick which would have resulted to low thermal shock resistance.

Table 3.7: Thermal Shock Resistance of Brick Samples

S/N	Sample Name	No of Circles	Average No. of Circles
A	Maraban Rido	16, 15, 19	**16.67**
B	Birnin Gwari	30, 29, 30	**30.0**

3.8 Refractoriness

The refractoriness values were 1300 and 1400^{o}C for bricks made with Maraban Rido and Birnin Gwari clays respectively as shown in Table 3.8. The bricks made with Birnin Gwari clay can withstand higher temperature than bricks made with Maraban Rido clay. These low values of refractoriness were as a result of the alkali content in the clays. Because of the limitation of furnace in temperature (i.e. maximum furnace temperature was 1400^{O}C), the refractoriness of Birnin Gwari clay could not be obtained above this temperature, and hence their refractoriness for ferrous metals cannot be ascertained. However, there were indications that the refractoriness of Birnin Gwari bricks can be higher than 1400^{O}C

Table 3.8: Refractoriness of Brick Samples

S/N	Name	Refractoriness
A	Maraban Rido	1300^o
B	Birnin Gwari	1400^o

Table 3.9: Summary and Comparison of Properties of the Clays with Standard Fireclay Brick

Refractory properties	Maraban Rido	Birnin Gwari	Fireclay (ASTM), 1982
Bulk Density (g/cm^3)	1.75	1.96	1.9 - 2.3
Apparent Porosity (%)	24.65	21.55	15 – 25
Linear Shrinkage (%)	10.0	8.0	7 – 10
Thermal Shock Resistance	16.67	30	20 – 30
Cold Crushing Strength (kg/m^2)	165	216.9	150 minimum
Refractoriness (^{o}C)	1300	1400	1500 - 1700

IV. CONCLUSION AND RECOMMENDATIONS

4.1 Conclusion

The present research was centered on the development and characterization of Maraban Rido and Birnin Gwari clays as refractory materials. From the forgoing results and discussions, the following conclusions were arrived at:

1) The investigated clays are high silicate clays with moderate alumina content, low ferrous oxide content and possess very low contents of other metal oxides.
2) Bricks produced from Birnin Gwari clay have higher refractoriness. This means that Birnin Gwari clays do not easily burn off or fused. This suggests there was an improved vitrification which improved bonding and the cold crushing strength of the bricks.
3) The cold crushing strengths of the two clays meet standard values of 150kg/cm^2 minimum for fireclay. This means that high strength bricks can be made from this clay.
4) Bricks produced from Birnin Gwari clay have a thermal shock resistance of 30 cycles which makes them suitable for heat treatment furnaces application.
5) It can be seen that the physical properties of Birnin Gwari clays compare very favorably with those for international standard fire clay refractory bricks as presented in Table 4.9.

4.2 Recommendations

The research has yielded some important information on the suitability of Maraban Rido and Birnin Gwari clay deposits as refractory materials and thus, the following recommendations are made:

1. Birnin Gwari clay is recommended to be use as fireclay bricks
2. It is recommended that further investigation on the micro structural analysis of these bricks be carried out to be able to known the particles' spacing and interfacial bonding of the clay
3. Both Maraban Rido and Birnin Gwari clays are recommended to be used in casting non-ferrous materials only. However, further studies should carried out to investigate the properties of these clays by firing above 1400 ^{o}C in order to find the suitability of these clays for ferrous materials.
4. The geological survey of the Birnin Gwari and Maraban Rido Clay deposits should be carried out to determine the extent of the deposits so as to form the basis of establishing a refractory company there.

V. REFERENCES

[1] Aigbodion V.S (2008): "An Investigation of the effect of Ile-Oluji Clay on some
[2] Refractory Properties of Alkaleri Clay"; Insights on Science and Technology, Afro-Euro Centre for Development Studies, Printed in the Kingdom of Spain, Pp 21-29.
[3] Aigbodion.V.S, AbdulRahman .A.S and Madugu. I.A (2007): "Characterisation Study of the Effect of Zircon sand on some Refractory Properties of Alkaleri clay"; International Research Journal in Engineering, Science and Engineering Vol 4, Pp 135-142.
[4] Akinbode, E.O.(1996): "An Investigation on the properties of Termite hill as Refractory Material for furnace lining"; Indian Foundry Journal, Pp10-13
[5] Chesti, A.R (1986): "Refractories Manufacture, Properties and Application" Prentice Hall of Private Limited, London. Pp 1-140.
[6] Hassan, S.B (2000): "Refractory Properties of Bauchi and Onibode clay of Nigeria for Furnace Lining"; African Journal of Sciences and Technology, Vol.1 Pp 56-60.
[7] Irabor, P.S.A. (2002): "Physical and Chemical Investigation on some Nigerian Kaoline Clays for use in the ceramic and Allied Industries"; Nigerian J.Eng. Res. Devel.. 1(1): 54-56.
[8] Okeugo.C.O, Nwabineli.E.O (2012): "Production of Insulating Bricks using Unwana Clay, Edda Clay, Kaolin and Wood Soft Dust"; International Journal of Engineering And Science (IJES), Volume 1 Issue 2 Pages 184-187
[9] Reinhard S. J (1982): "Metallurgy Engineering"; Vol.1, Addison Wesley Pub. Co.Inc. Trinks, W.Industrial Furnaces (Vol-2). John Wiley and Sons Inc, New York, 1925.

[10] ASTM (1982): Annual Book of ASTM Standards, Part 17: Refractories, Glass, Ceramic Materials, Carbon and Graphite Products Philadelphia; Pp. 7- 15, 18, 51 - 55, 59 - 61, 190- 93, 498 – 510.
[11] ASTM-C16-03(2009): Standard Test Method for Load Testing Refractory Shapes at High Temperatures.
[12] ASTM-C20–80(2011): Standard Test Methods for Apparent Porosity, Water Absorption, Apparent Specific Gravity, and Bulk Density of Burned Refractory Brick and Shapes by Boiling Water.
[13] ASTM-C24–79(2002): Standard Test Methods for Pyrometric Cone Equivalent of Refractory Materials.
[14] ASTM- C25-06 (2010): Standard Test Methods for Chemical Analysis of Clay, Limestone, Quicklime and Hydrated Lime.
[15] ASTM C133-97(2010): Standard Test Methods for Cold Crushing Strength and Modulus of Rupture of Refractories.
[16] ASTM-C1054-0(2008): Standard practice for washing, Pressing and drying of Refractory plastic and ramming mix.

American Journal of Engineering Research (AJER)
e-ISSN : 2320-0847 p-ISSN : 2320-0936
Volume-03, Issue-03, pp-16-21
www.ajer.org

Research Paper Open Access

Fines Content and Angle of Internal Friction of a Lateritic Soil: An Experimental Study

G.O. Adunoye
Department of Civil Engineering, Obafemi Awolowo University, Ile-Ife, Nigeria

Abstract: **-** Soils in nature are mixture of fine and coarse soils. Fines in soil play a major role in the geotechnical properties of soil. The research focused on experimental study of the relationship between fines content and internal friction angle of lateritic soil. This was with a view to obtaining empirical relationships between the two parameters. Three samples of reddish brown tropical soils were obtained. The samples were subjected to laboratory analysis in their natural states and the index properties were determined. The fines contents were separated from the coarse components of the soils, and the samples were remoulded in varying ratios (fines:coarse). The resulting samples were subjected to triaxial tests to determine the shear strength parameters. Quantitative relationships between fines content and angle of internal friction of the soil samples were developed. The polynomial relationships gave the best relationship between the fines content and angle of internal friction of the soil samples.

Keywords: **-** *Angle of internal friction, correlation, fines content, lateritic soil, triaxial test*

I. INTRODUCTION

The shear strength of a soil mass is the internal resistance per unit area that the soil mass can offer to resist failure along any plane inside it [1]. When this resistance is exceeded failure occurs. Shear strength of a soil refers to the maximum or limiting value of shear stress induced within its matrix before yielding. Shear strength within a soil matrix is due to cohesive and frictional forces between adjacent particles. Therefore, the soil shear strength is to some extent surface dependent. Any action that will hinder or promote the interlocking or welding of soil particles will invariably affect soil shear strength [2]. The shear strength is usually made up of: (a) internal friction or the resistance due to interlocking of the particles, represented by an angle, ϕ; (b) cohesion or the resistance due to the forces tending to hold the particles together in a solid mass. The cohesion of a soil is generally symbolized by the letter 'c'. The law governing the shear failure of soils was first put forward by Coulomb and is given in equation as

$$s = c + \sigma\tan\phi \qquad (1)$$

where s is the shear strength and σ is the normal stress. Therefore, angle of internal friction, ϕ is one of the important parameters considered as a typical characteristic for reconnaissance of granular soils. Angle of internal friction could be described as a measure of the ability of a unit of rock or soil to withstand a shear stress. It is the angle (ϕ), measured between the normal force (N) and resultant force (*R*), that is attained when failure just occurs in response to a shearing stress (S). Its tangent (S/N) is the coefficient of sliding friction. Its value is determined experimentally. Determination of shear strength parameters must take place prior to analytical and design procedures in connection with foundations, retaining walls and earth retaining structures [3].

Fines in soils consist of silts and clays while coarse component consists of sands and gravels. As defined by Unified Soil Classification System (USCS) and the American Association of State Highway Transportation Officials (AASHTO) fines in soil are soil particles passing through sieve No. 200 (75µm opening). The fines contents in coarse soils are carefully considered because they determine the composition and type of soil and affect certain soil properties such as permeability, particle friction and cohesion. The fines content in soil also plays an important role in phase problems including minimum and maximum void ratios and porosity [4]. Fines have also been found to affect the liquefaction potential, compressional characteristics and stress-strain behaviour of soil [5, 6, 7, 8]. According to Wang *et al.*[9], fines content could affect the dynamic response of soils significantly. Tatlisoz *et al.* [10] studied the effect of fines on mechanical properties of soil-

tyre chip mixtures and found out that the fines have significant effect on the mechanical properties of the soil-tyre mixture. During dynamic compact loading, dynamic forces disrupt the soil skeleton and force the particles to compact into a denser arrangement. Obviously, the fines contents play an important role on the mechanical response of soils, especially when the soils are subjected to loading. Ayodele[11] studied the effect of fines content on the performance of soil as sub-base material for road construction and found out that the engineering properties of the studied soil samples generally reduced with increase in fines content [12].

Bello[13] analyzed the shear strength of some compacted lateritic soils. Bareither *et al* [3] studied the geological and physical factors affecting the friction angle of compacted sands and developed a multivariate regression model that can be used to predict friction angle, ϕ of compacted sands from comparable geological origins based on effective particle size, D_{10}, maximum dry unit weight d_{max}, and Krumbein roundness R_s. As reported by Bareither *et al* [3], methods to predict the friction angle of granular materials from physical and engineering properties have also been presented in NAVFAC [14]. NAVFAC [14] presents one of the most widely referenced correlations, where ϕ is estimated with respect to USCS classification and dry unit weight or relative density. The correlation presented in Schmertmann [15] provides an estimate of ϕ based on relative density and generalised material descriptions. The method in Terzaghi *et al* [16] uses a secant definition for the friction angle that is a function of effective normal stress as well as generalized material descriptions and porosity.

The specific relationship between fines content and angle of internal friction of soil is not clear. Also, there is need to advance the effect of fines on angle of internal friction of soil, ϕ. Therefore, in this research it is tried to provide a proper correlation (quantitative relationship) between the angle of internal friction and the fines content of lateritic soils. The primary objectives were to (i) determine the effects of fines content on angle of internal friction ϕ of selected soil samples; and hence (ii) develop regression models (equations) relating fines content to the angle of internal friction ϕ of the soil samples.

II. MATERIALS AND METHODS

2.1 Materials

The soil samples used in this research work are a natural material, that is, reddish brown lateritic soil from three selected locations in Obafemi Awolowo University (OAU) campus, Ile-Ife, Southwestern Nigeria (between latitude 7° and 28°N and longitude 4° and 34°E). The method of disturbed sampling was employed. The soil samples were obtained at depths of 0.60 – 1.00m and the locations are designated as S1, S2 and S3. Fig. 1 is a location map of OAU showing the sampling locations[12].

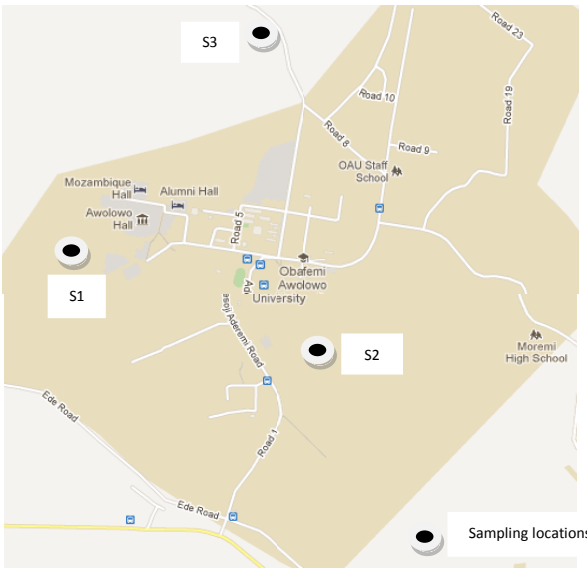

Figure 1: Location map of OAU campus (Google, 2012)

2.2 Methods

Some of the methods for this work were as described by Adunoye and Agbede [17] and Adunoye [12]. Laboratory tests were carried out to determine the index properties of the sample specimen in accordance with BS 1377 [18]. The soil samples were then soaked in water containing 4% sodium hexametaphosphate, a dispersing agent (commercially named Calgon) in the laboratory for 12-24 hours so that all the fines would get soaked and detached from the coarser soil samples. The soil was then washed through sieve size No. 200 with

75µm opening. The soil passing 75µm sieve size was oven dried and referred to as 100% fines. The soil sample retained on sieve 75µm opening was also oven dried (after thorough mixing) and referred to as 100% coarse.

The pulverized fines and the coarse fractions were added together in varying ratios (fines:coarse) from 10:100 to 100:0 in 10% increment. The ratio started with 10:100 and not 0:100 because, laboratory compaction test could not be carried out on the sample containing 0% fines (i.e. 100% coarse) and thus cohesionless. This is because the process of lubrication which aids compaction is limited to soils containing fines and cohesionless soils are compacted or densified by vibration and not by impact which laboratory compaction utilizes [19].

The resulting samples were allowed to homogenise and compacted in the laboratory using standard proctor test to determine the optimum moisture content (OMC) and the maximum dry density (MDD) of each sample. The values of the OMC were used in subsequent unconsolidated undrained triaxial tests (Adunoye and Agbede, 2013). The remoulded soil samples were then subjected to unconsolidated-undrained triaxial test, in accordance with BS 1377 [18], to determine their shear strength parameters (i.e c and ϕ).

Quantitative relationships between fines content and angle of internal friction of soils were then developed using regression analysis . The validity of the developed relationships was verified by the coefficient of determination (R^2), which compares estimated and actual y-values, and ranges in value from 0 to 1. The closer the R^2 to 1, the better the representations.

III. RESULTS AND DISCUSSION

Index properties of the soil samples are summarized in Table 1 Sample S2 has the highest fines content of 55.00%, liquid limit (LL) of 41.00% and plastic limit (PL) of 30.73%. Sample S1 on the other hand, has the lowest fines content of 32.70%, LL of 45.29% and PL of 32.68%. Sample S1 has the highest plasticity index (PI) of 12.61%, which implies that sample S1 has the highest inherent swelling potential shrinkage tendency [12, 17].

Table 1: Index properties of soil samples (Adunoye, 2014)

Property	Sample Identification		
	S1	S2	S3
Natural moisture content (%)	19.74	16.90	17.05
Specific gravity	2.66	2.86	2.69
Percentage passing sieve No. 200 (Fines content)	32.70	55.00	41.07
Liquid Limit, LL (%)	45.29	41.00	39.87
Plastic Limit, PL (%)	32.68	30.73	31.01
Plasticity Index, PI (%)	12.61	10.27	8.86
OMC (%)	17.39	19.42	16.38
MDD (mg/m3)	1.77	1.91	1.71

Table 2 gives a summary of the values of shear strength parameters (c and ϕ) at various fines content of the soil samples. For sample S1, the ϕ values range between 42^o (for 10% fines) and 0^o (for 100% fines). This represents a decrease of 42^o (100%). For sample S2, the ϕ values range between 41^o (for 10% fines) and 0^o (for 100% fines). This represents 41^o (100%) decrease. Similarly, for sample S3, the ϕ values range between 36^o (for 10% fines) and 0^o (for 100% fines). This represents 36^o (100%) decrease. For all the samples, ϕ decreases as fines content increases. At 100% angle of internal friction is 0^o.

On the other hand and as earlier reported by Adunoye [12], for sample S1, the cohesion values range between 8 kN/m^2 (for 10% fines) and 63 kN/m^2 (for 100% fines). This represents 55 kN/m^2 (687.5%) increase. For sample S2, the cohesion values range between 5 kN/m^2 (for 10% fines) and 67 kN/m^2 (for 100% fines). This represents 62 kN/m^2 (1240%) increase. Similarly, for sample S3, the cohesion values range between 10 kN/m^2 (for 10% fines) and 66 kN/m^2 (for 100% fines). This represents 56 kN/m^2 (560%) increase. The cohesion generally increases with increase in fines content of the soils. This is so because cohesion is majorly dependent on clay content in soils [20].

Table 2: Values of shear strength parameters at various fines contents

% Fines	Angle of internal friction, ϕ (degrees)			Cohesion, c (kN/m^2)		
	S1	S2	S3	S1	S2	S3
10	42	41	36	8	5	10
20	39	40	29	10	9	14
30	31	32	27	20	13	19
40	28	30	22	26	19	31
50	27	29	16	41	28	38
60	20	24	13	49	34	46
70	12	19	8	52	51	49
80	5	9	5	57	59	62
90	2	3	2	59	62	64
100	0	0	0	63	67	66

The results of the correlations between fines content and ϕ are as shown in Figs.2 to 4, while Table 3 gives a summary of the equations representing relationships between ϕ and fines content of soil samples. Considering the values of R^2 all the empirical equations are valid for the soil samples as they are all close to 1. However, the linear relationships cannot be said to be valid. This is because there cannot be negative angle of internal friction (Fig. 2). Polynomial relationships give the highest R^2 values for all the samples (0.980 for S1; 0.980 for S2 and 0.994 for S3). This could be as a result of the fact that polynomials have the attractive property of being able to approximate many kinds of functions [12, 21].. The polynomial equations fit the data best and thus give the best representations between fines content and angle of internal friction of the soil samples.

IV. CONCLUSION

From the findings of this research work, the following conclusions are made in relation to the objectives of the research: (i) The angle of internal friction of the studied soil samples generally decreased with increase in fines content; (ii) the best fitting between fines content and cohesion of the soil samples was found by the polynomial expression: $\phi = -0.000f^2 - 0.456f + 47.16$; $\phi = -0.002f^2 - 0.19f + 43.06$; $\phi = 0.001f^2 - 0.571f + 41.4$. Where ϕ is angle of internal friction in degrees and f is fines content in % . The empirical equations are valid for the soil samples and test procedure used in this research. More experiments with various soils and from different locations are required to generalise these expressions.

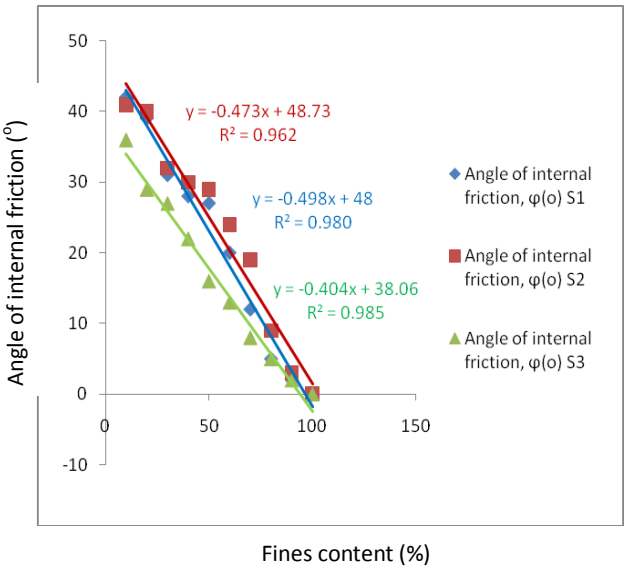

Figure 2: Angle of internal friction vs Fines content (Linear)

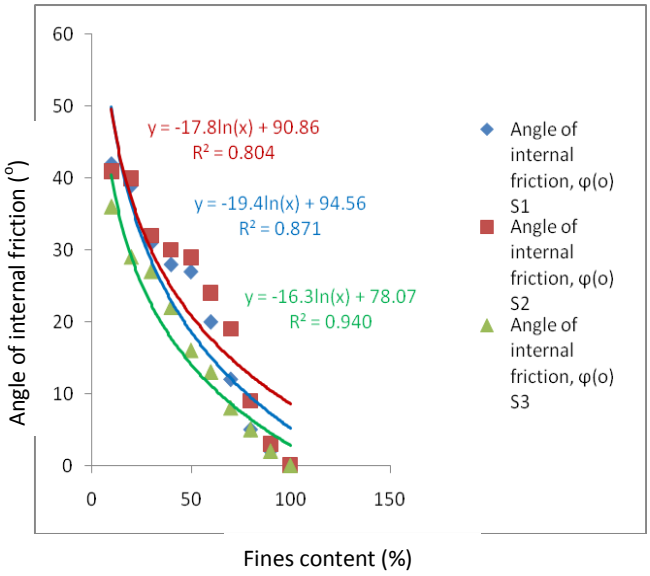

Figure 3: Angle of internal friction vs Fines content (Logarithmic)

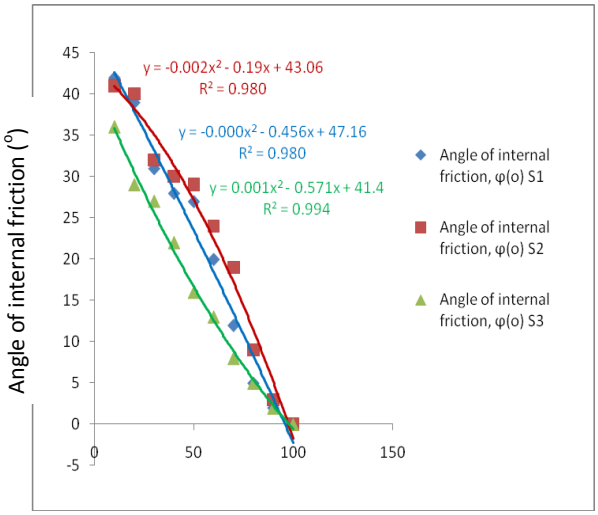

Figure 4: Angle of internal friction vs Fines content (Polynomial)

Table 3: Equations representing relationship between angle of internal friction and fines content of soil samples

Sample	Equation		
	Linear	Logarithmic	Polynomial
S1	y = -0.498x + 48; R² = 0.980	y = -19.4ln(x) + 94.56; R² = 0.871	y = -0.000x² - 0.456x + 47.16; R² = 0.980
S2	y = -0.473x + 48.73; R² = 0.962	y = -17.8ln(x) + 90.86; R² = 0.804	y = -0.002x² - 0.19x + 43.06; R² = 0.980
S3	y = -0.404x + 38.06; R² = 0.985	y = -16.3ln(x) + 78.07; R² = 0.940	y = 0.001x² - 0.571x + 41.4; R² = 0.994

V. ACKNOWLEDGEMENT

The author appreciates Prof. O.A. Agbede for supervising the project from which this paper is written.

REFERENCES

[1] B.M. Das, *Soil mechanics* (California: Brooks/Cole publishers, 1990).

[2] G.M. Ayininuola, O.A. Agbede and S.O. Franklin, Influence of calcium sulphate on subsoil cohesion and angle of friction. *Journal of Applied Sciences Research*. 5(3), 2009, 297 – 304.

[3] C.A. Bareither, T.B. Edil, C.H. Benson and D.M. Mickelson, Geological and physical factors affecting the friction angle of compacted sands, *Journal of Geotechnical and Geoenvironmental Engineering*, 134 (10), 2008, 1476-1489.

[4] P.V. Lade, C.D. Liggio Jr. and J.A. Yamamuro, Effects of nonplastic fines on minimum and maximum void ratios of sand. *Geotechnical Testing Journal*, 21(4), 1998, 336–347.

[5] V.N. Georgiannou, J.B. Burland and D.W. Hight, The undrained behaviour of clayey sands in triaxil compression and extension. *Geotechnique*, 40 (3), 1990, 431 – 449.

[6] R. Salgado, P. Bandini and A. Karim, Shear strength and stiffness of silty sand. *Journal of Geotechnical and Geoenvironmental Engineering*, 126 (5), 2000, 451 – 462.

[7] S.A. Naeini and M.H. Baziar, Effect of fines content on steady state strength of mixed and layered samples of a sand. *Soil Dynamics and Earthquake Engineering*, 24 (3), 2004, 181 – 187.

[8] A.F. Cabalar, Effects of fines content on the behaviour of mixed samples of a sand. *Electronic Journal of Geotechnical Engineering*. 13 (D), 2008, 1-13.

[9] S. Wang, D. Chan and K.C. Lam, Experimental study of the effect of fines content on dynamic compaction grouting in completely decomposed granite of Hong Kong, *Construction and Building Materials*, 23, 2009, 1249–1264.

[10] N. Tatlisoz, C. Benson and T. Edil, Effect of fines on mechanical properties of soil-tyre chip mixtures, testing soil mixed with waste or recycled materials, ASTM STP 1275, Mark A. Wasemiller, Keith B. Hoddinott, Eds., (American Society for Testing and Materials, 1997).

[11] A.L. Ayodele, A study of the effect of fines content on the performance of soil as sub-base material for road construction. Unpublished M. Sc. Thesis. Obafemi Awolowo University, Ile-Ife, Nigeria, 2008.

[12] G.O. Adunoye, Study of relationship between fines content and cohesion of soil. *British Journal of Applied Science and Technology*. 4(4), 2014, 682 – 692.

[13] A.A. Bello, Unconfined compressive strength of compacted reddish brown tropical soil. *Pacific Journal of Science and Technology*. 12(1), 2011, 425-434.

[14] NAVFAC, Soil mechanics, design manual 7.01, Naval Facilities Engineering Command, Alexandria, Va, 1986.

[15] J. Schmertmann, Guidelines for cone penetration test performance and design. Rep. No. FHWA-TS-78-209, Federal Highway Administration, Washington, D.C, 1977.

[16] K. Terzaghi, R.B. Peck and G. Mesri, *Soil mechanics in engineering practice*, 3rd Ed. (Wiley, New York, 1996).

[17] G.O. Adunoye and O.A. Agbede, Statistical modelling of the relationship between bearing capacity and fines content of soil using square footing. *Civil and Environmental Research*. 3(2), 2013, 75 – 81.

[18] BS 1377, Methods of test for soils for civil engineering properties, London, UK: British Standard Institution, 1990.

[19] Multiquip Inc., Soil compaction handbook, 2004, http://www.concrete-catalog.com/soil_compaction.html. Accessed on 25 January 2008.

[20] F.C. Ugbe, Effect of multicyclic compaction on cohesion in lateritic soils, *Archives of Applied Science Research*, 3 (3), 2011, 115-121.

[21] Anonymous, Regression analysis. Available: http://www.statgraphics.com/regression analysis.htm. Accessed on 30 September 2013.

American Journal of Engineering Research (AJER)
e-ISSN : 2320-0847 p-ISSN : 2320-0936
Volume-03, Issue-03, pp-22-29
www.ajer.org

Research Paper Open Access

Exploitation of Artificial Neural Networks Approach To Predict The Thermal Conductivity of Food Products In Nigeria

[1] Ajasa,A.A., [2]Akinyemi,L.A, [3]Shoewu,O.O and [4]Adenowo, A.A.
Department of Electronic and Computer Engineering,
Lagos State University, Epe Campus, Epe, Lagos, Nigeria.

Abstract: - The application of neural networks in predicting the thermal conductivity of food (bakery) products as a function of moisture content, temperature and apparent density is presented herein. Bread, bread dough, cake, and whole-wheat dough were among some of the bakery products considered in this work. After several configurations had been considered and evaluated in the development of the ANN model, the results of this work showed that the optimal ANN model was a network with 8 neurons in each of the 2 hidden layers. Consequently, this optimal model was capable of predicting the thermal conductivity values of the considered bakery products for a wide range of conditions with MRE of **4.878 X 10^{-2} %**, MAE of **0.0054 W/mK** and SE of **0.0015 W/mK**. In addition, the simplest ANN model was found to be a network with 1 hidden layer and 10 neurons, and it predicted thermal conductivity values with MRE of **3.388 X 10^{-2} %**, MAE of **0.0034 W/mK** and SE of **0.0011 W/mK.** The MRE, MAE and SE are the estimated errors between the predicted and desired (or targeted) thermal conductivity values of the bakery products for both the optimal ANN and simplest ANN models. These errors are approximately equal to zero (i.e., 0 W/mK) and could, therefore, be regarded as a good result for the prediction. Since the simplest ANN model had the least values of all three errors (MRE, MAE and SE) when compared with other configurations, including the optimal ANN model, it is, however, regarded as the best ANN model and is thus,recommended.

Keywords: - *thermo-physical properties of biological products, thermal conductivity of bakery products, back-propagation, artificial neural network, mean absolute error, mean relative error, standard error*

I. INTRODUCTION

In a typical baking process, bakery products undergo physical, chemical and biochemical changes that cumulatively result in expansion of bulk volume, evaporation of water, formation of a porous structure, denaturation of protein, gelatinization of starch, formation of crust and browning reactions respectively. During such processes, ovens powered by gas, electricity, firewood, charcoal, or microwaves are used for generating the required heat.

Accordingly, heat is transferred mainly by convection from the heating media, and by radiation from oven walls to the product surface and then by conduction to the geometric centre. At the same time, moisture diffuses outward to the product surface [1, 2, 13].

The problem of interest in the design of bakery ovens is concerned with the promotion of the required rate of heat transfer with the minimum possible surface area and temperature difference. And from the engineer's point of view, it is usually sufficient to know the total quantities of energy emitted and absorbed by the material at various temperatures [18]. As such, it is frequently necessary to establish the rate at which heat will be conducted through a solid if a known temperature difference exists across the solid. For such purposes, and especially if the process varies with time, sophisticated mathematical techniques are required to establish this, the phenomenon being known as transient-heat conduction. A knowledge of the product properties, including thermal conductivity as a function of processing conditions is needed in order to predict the temperature and water distribution in the product during baking [2, 3, 15]. The temperature and moisture distribution within the porous product can be predicted using diffusion equations of heat and water.

II. LITERATURE REVIEW

Neural networks have been trained to perform complex functions in various fields including pattern recognition, identification, classification, speech, vision, and control systems. Today, neural networks can be trained to solve problems that are difficult for conventional computers or human beings. Commonly, neural networks are adjusted (or trained) so that a particular input leads to a specific target output. Typically, many such input/target pairs are needed to train a neural network.

Linko and Zhu also stated that of all the various modelling approaches of predicting the thermal conductivity of a wide range of foods, including bakery products, the neural network-based models have proven to be excellent. Among the major benefits of using ANN are excellent management of uncertainties, noisy data and non-linear relationships. Neural network modelling has generated increasing acceptance and is an interesting method in the estimation, prediction and control of bioprocesses [5, 6].

Review of past work showed that Ruan et al. applied ANN modelling to predict the rheological properties of dough in 1995 [6]. Fang et al. also applied the ANN modelling to predict the physical properties of ground wheat in 1998 [7, 9, 10, 11] while Hussain and Rahman, in 1999, predicted the thermal conductivity of fruits and vegetables with the application of ANN modelling [8]. Similarly, ANN modelling was applied by Myhara et al. in 1998 for the prediction of isotherms of dates [9], Ni and Gunasekaran in 1998 [10] and Xie and Xiong in 1999 [16] also applied ANN modelling differently for the prediction of food quality. Recently, Sablani and Shayya in 2001 applied ANN modelling for the prediction of heat penetration parameters in Stumbo's method of thermal process calculations [17].

Rahman's model [21] (data considered only above 0°C) predicted thermal conductivity with mean relative errors of 24.3 and 81.6%, respectively. This model was able to predict thermal conductivity with a mean relative error of 12.6% and a mean absolute error of 0.081 W/mK. The model can be incorporated in heat transfer calculations during food processing where moisture, temperature and apparent porosity dependent thermal conductivity values are required.

In Shyam et al's work,the optimal ANN model was found to be a network with 6 neurons in each of the 2-hidden layers. This optimal model was capable of predicting the thermal conductivity values of various bakery products (such as bread, bread dough, French bread, yellow cake, tortilla chip, whole wheat dough, baked chapati and cup cake) for a wide range of conditions with a mean relative error of 10%, a mean absolute error of less than 0.02 W/m K and a standard error of about 0.003 W/m K. The simplest ANN model, which had 1-hidden layer and 2 neurons, predicted thermal conductivity values with a mean relative error of less than 15%. [20, 21, 22] All these work were successfully carried out with satisfactory results obtained using ANN modelling.

In predicting thermal properties of a material at desired conditions, several modelling approaches have been proposed and none of them was found suitable for use over a wide range of foods. According to Murakami and Okos (1989) the most promising approach is based on chemical composition, temperature and physical characteristics [4]. More recently, Baik et al. in 2001 reviewed common and new measurement techniques, prediction models and published data on thermo-physical properties of bakery products [19]. The series model of specific heat, density and thermal diffusivity has been successfully applied to many food materials including porous materials such as baking products. However, for the prediction of thermal conductivity of porous food, there is still some theoretical argument for the use of the structural models [4]. Murakami and Okos (1989) evaluated nine different structural models with specific types of porous foods and found that parallel and perpendicular models showed 12–97% and 18–61% standard errors respectively.

Among the models, Keey's model was found to be the best prediction model for porous grains and powders. The model produced standard errors of <28% for full fat dry milk and <10% for other food materials. In addition, all structural models neglect interactions between components, phase transition and distillation heat transfer, which may be significant in the baking process [1]. Hence, most thermal conductivity models reported are usually empirical rather than theoretical.

III. MATERIALS AND METHODS

3.1 MATERIALS

Depending on the specific type of bakery product to be produced and associated production process, a wide variety of raw materials are available to the baker. In addition to the basic Raw materials (flour, water, salt and yeast) various other ingredients can be used. The ingredients used have an influence on the characteristics or technological aspect of the dough.

FLOUR

Flour account for the main portion of the raw materials involved in baked product production and the thermal conductivity of flour need to be considered while applying the neural network. Flour used is mainly

those extracted from two basic cereals – wheat and rye. Flour from other grains which do not contain gluten-forming proteins is usually blended with wheat flour for the production of bakery products. The quality of flour is basically dependent on its intended use. The flour quality depends on the following factors:

- Wheat variety
- Growing conditions
- Grain storage
- Flour production technique
- Flour storage

Table 1 Example of a requirement profile for various baking flours (REF)

	Patent Flour	gluten % Flour	High-Ash Flour	whole-Grain Flour
Moisture %	**13.0-15.0**	**13.0-15.0**	**13.0-15.0**	**11.0-13.0**
Ash % DM	**0.38-0.60**	**0.64-0.78**	**1.05-1.15**	**1.75-1.95**
Protein %	**12.0-14.0**	**13.5-15.0**	**14.0-15.5**	**13.5-15.0**
Wet gluten %	**28.0-33.0**	**31.0-35.0**	**32.0-36.0**	**29.0-33.0**
Falling N umber sec	**320-410**	**300-390**	**280-380**	**300-380**
Sedimentation ml	**38-45**	**38-43**	**25-30**	**NIL**
Water Absorption %	**60-64**	**61-65**	**65-70**	**66-71**
Weakening FU	**20-70**	**60-90**	**60-90**	**60-90**
Dough energy cm^2	**90-130**	**80-110**	**55-85**	**60-90**
Max. viscosity AU	**500-1000**	**350-800**	**300-550**	**250-500**

Average patent flour (first grade) is made up of the following:

- Carbohydrates: 73.5%. This includes starch: 71%, soluble sugars 2.4% and cellulose 0.1%.
- Proteins: 11.0 % :This includes gluten-forming proteins 10% & water soluble proteins 1%
- Water :14%
- Fat : 1.0%
- Minerals: 0.5 %

In terms of quantity carbohydrates accounts for the greatest portion in flour which incidentally forms the greater part of bakery products. Starch essentially fulfills the following functions: 1) a source of nutrient for yeast after enzymatic degradation, 2) absorption of free dough water during gelatinization, 3) contribution to crust, crumb and coloration formation.

The content of soluble sugar substances in wheat flour amounts to approximately 1.5 – 3%. The main soluble sugar substances are glucose, maltose and dextrin. They are dissolved during dough production in the available dough liquid. Glucose and Maltose are available as yeast food while Dextrin cannot be fermented by yeasts

Data were obtained at 25°C on thermal conductivities of slurries of starch in a carbon tetrachloride-ethyl benzene mixture having a density equal to that of the starch. The thermal conductivity of granular ordinary corn starch was estimated to be 0.125 B.t.u.-foot per hour-$foot^{2-0}$ F by calculation and by extrapolation from the slurry data. The thermal conductivities of granular corn starches decreased with increasing amylose content.
Thermal properties (thermal conductivity and diffusivity) of gluten and glutenin were measured in the temperature range 60-175°typically used in extrusion processing. Thermal conductivity and diffusivity of gluten decreased with increasing temperature and increased with increasing moisture content. Thermal conductivity and diffusivity of glutenin increased with temperature and moisture content. Thermal conductivity of gluten was 0.06-0.35 W/m-C and glutenin was 0.29-0.49 W/m-C for the temperature range 60-175°and moisture content range of 0-30%.

3.2 METHODS

(i) Mathematical Modelling For Thermal Conductivity Of Bakery Products

Although, the exact mechanism of heat conduction in solids is not entirely understood, it is believed, however, to be partially due to the motion of free electrons in the solid matter, which transports energy if a temperature difference is applied (Refer to Fig.1) and the conceptual representation of Oven dynamics during typical baking process as depicted in figure 2 below .

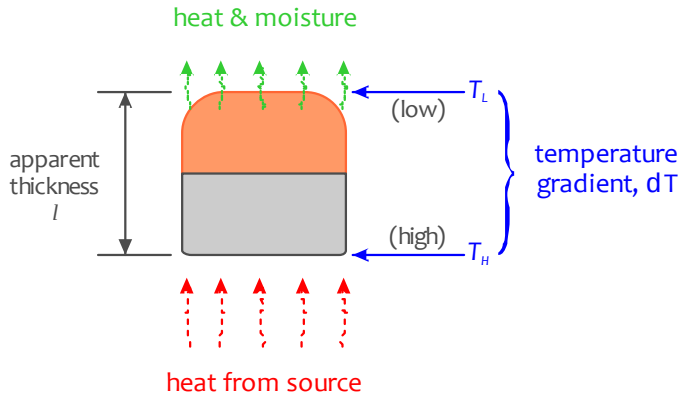

Fig. 1: Conceptualisation of thermal conductivity of a bakery product

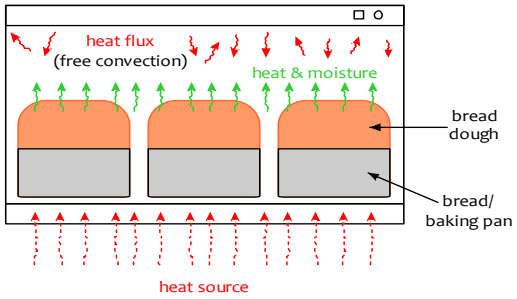

Fig. 2: Conceptual representation of Oven dynamics during typical Baking process

From Fourier's law of heat conduction, the rate at which such heat is conducted through a body per unit cross-sectional area is said to be proportional to the negative of the temperature gradient existing in the body [18]. In other words,

$$Q \propto -\nabla T \qquad (1)$$

The proportionality factor is called the thermal conductivity of the material. By definition, it is the ability of the material to conduct heat and thus, a measure of the rate at which heat flows through a material between points at different temperatures, measured in watts per meter per degree.

As a property, the thermal conductivity expresses the heat flux, Q (W/m^2) that will flow through the material if a certain temperature gradient, ΔT (K/m) exists across the material. That is, it is the heat flow per unit area per unit time when the temperature decreases by one degree in unit distance. Thus,

$$Q = -kA\frac{\Delta T}{\Delta x} \qquad (2)$$

or $$Q = -kA\frac{T_H - T_L}{l} \qquad (3)$$

where Q = heat flux, k = thermal conductivity, A = cross-sectional area, T_H = temperature at hot end, T_L = temperature at cold end, and l = thickness of material respectively, and the negative sign indicates that the heat flow is positive in the direction of temperature fall.

(ii) TRAINING THE ANN MODEL USING BACK PROPAGATION ALGORITHM

The back-propagation algorithm was utilized in model training. A hyperbolic-tangent transfer function was also used in all cases. Properly trained back-propagation networks tend to give reasonable answers when presented with unfamiliar inputs that have never been seen earlier. Typically, a new input leads to an output similar to the correct output for input vectors used in training that are similar to those being presented. This generalization properly makes it possible to train a network on a representative set of input/target pairs and get good results without training the network on all possible input/output pairs.

The back-propagation algorithm uses the supervised training technique where the network weights and biases are initialized randomly at the beginning of the training phase. For a given set of inputs to the network, the response to each neuron in the output layer is calculated and compared with the corresponding desired output response. The errors associated with desired output response are adjusted in the way that reduces these errors in each neuron from the output to the input layer.
In order to avoid the potential problem of over-training or memorization while employing the back-propagation algorithm, the option of saving the best result is adopted during the selected number of training cycles of 2,000.

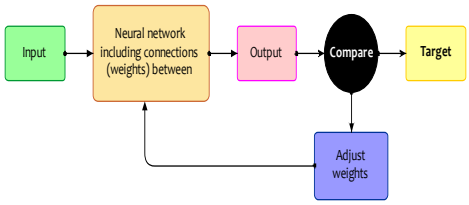

Fig. 3: Adjusting (or training) of a Neural network

(iii) OPTIMAL CONFIGURATION OF ANN MODEL FOR BAKERY PRODUCTS
Upon using the mean relative error (MRE), mean absolute error (MAE) and standard error (SE) as standard criteria, the performances of the various ANN configurations were compared. The mathematical representation of these error parameters are as defined in equations 1 to 3 as follow [11, 14]:

$$\text{MAE} = \frac{1}{n}\left[\sum_{i=1}^{n}(K_D - K_P)\right] \qquad (4)$$

$$\text{MRE} = \frac{1}{n}\left[\sum_{i=1}^{n}(K_D - K_P)/K_D\right] \qquad (5)$$

$$\text{SE} = \left[\frac{\sqrt{\sum_{i=1}^{n}(K_D - K_P)^2}}{n-1}\right] \qquad (6)$$

where n is the number of data points, K_D and K_P are the desired and predicted values of thermal conductivity respectively.

The optimum configuration of the network was chosen by selecting the lower value from the different configuration of the network. It was evidently based upon minimizing the difference between the neural network predicted values and the desired outputs. The datasets of 52 cases obtained from other literature [1] were divided into two sets. The first set consisted of 36 (~70%) cases for training/testing and 16 (~30%) cases for validation (simulation), chosen randomly from the set of 52 cases.

IV. SIMULATION AND RESULTS

4.1 SIMULATION

Computer simulation of ANN was employed for the purpose of this work using the MATLAB version 7.0.4.365 (R14) Service Pack 2 commercial software package with embedded neural network add-in toolbox.
Several ANN models were simulated (or trained) using the thermo-physical properties datasets of Table 1. The feed-forward network structure with input, output and hidden layers were also used and the generalized network structures are as shown in Fig. 5 and Fig. 6 respectively.

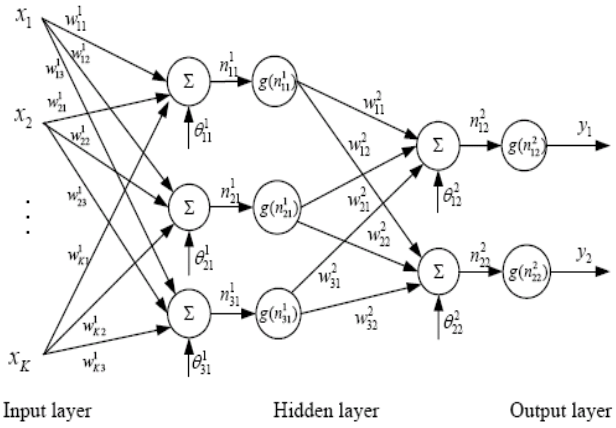

Fig. 5: Generalized multilayer neural network

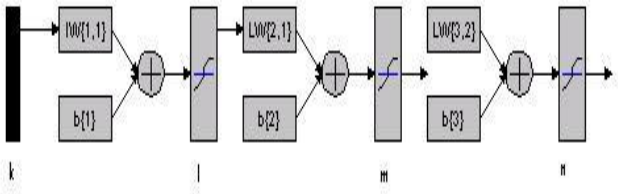

Fig. 6: Generalized multilayer neural network obtained with MATLAB

For the purpose of this work, the input layer consisted of 3 neurons which corresponded to a product's moisture content, temperature and apparent density respectively, while the output layer had 1 neuron representing the thermal conductivity. The number of hidden layers and neurons within each hidden layer can be varied based on the complexity of the problem and dataset. Moreover, the number of hidden layers was varied from 1 to 2. The neurons within each of these layers were varied from 2 to 16 with increments of 2. This resulted in a total of 16 networks.

4.2 RESULTS OF SIMULATION

Once a given ANN configuration was trained using the input data, its performance was evaluated using the same dataset. The analysis was repeated several times. The ANN configuration (out of 16) that minimized the three error measures: MRE, MAR and SE, was selected as the optimum. The error measures associated with different ANN configurations for prediction of thermal conductivity are presented in Table 4.1. The optimal ANN configuration included 2-hidden layers with 8 neurons in each layer. The MAE, MRE and SE for this optimal configuration were 0.0054W/mK, 4.8776 X 10^{-4} W/mK (4.8776 X 10^{-2} %) and 0.0015 W/mK respectively (shown highlighted below).

Table 2: Error parameters in the prediction of thermal conductivity with different neural network configurations

No. of hidden layers	**No. of neurons in each hidden layer**	**MRE** (%)	**MAE** (W/mK)	**SE** (W/mK)
1	2	0.17	0.0199	0.0046
1	4	4.2	0.2212	0.0970
1	6	0.035077	0.0038	0.0011
1	8	0.18	0.0191	0.0050
1	**10**	**0.03388**	**0.0034**	**0.0011**
1	12	0.26	0.0297	0.0073
1	14	0.090897	0.0149	0.0041
1	16	0.12	0.0115	0.0038
2	2	0.24	0.0298	0.0075
2	4	0.41	0.0641	0.0125
2	6	0.37	0.0606	0.0121
2	**8**	**0.048776**	**0.0054**	**0.0015**
2	10	0.29	0.0441	0.0106
2	12	0.22	0.0382	0.0095
2	14	0.17	0.0166	0.0047
2	16	0.22	0.0323	0.0072

Table 3: Error prediction for 1 hidden layer with their corresponding neurons

No. of neurons in each hidden layers	MRE (% x10^{-2})	MAE (W/mK x10^{-3})	SE (W/mK x10^{-4})
2	17	19.9	46
4	420	221.2	970
6	3.5	3.8	11
8	18	19.1	50
10	***3.4***	***3.4***	***11***
12	26	29.7	73
14	9.1	14.9	41
16	12	11.5	38

Table 4: Error prediction for 2 hidden layers with their corresponding neurons

No. of neurons in each hidden layers	MRE (% x10^{-2})	MAE (W/mK x10^{-3})	SE (W/mK x10^{-4})
2	24	29.80	75
4	41	64.10	125
6	37	60.60	121
8	***4.88***	***5.40***	***15***
10	29	44.10	106
12	22	38.20	95
14	17	16.60	47
16	22	32.30	72

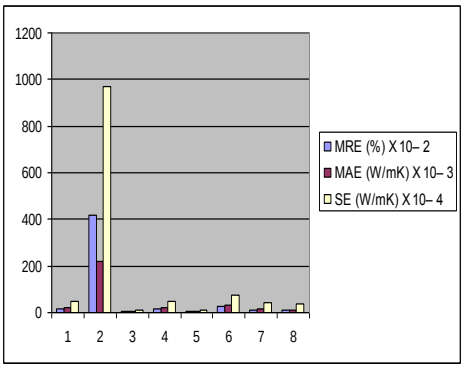

Fig *7: Corresponding chart showing the error values for 1-hidden layer*

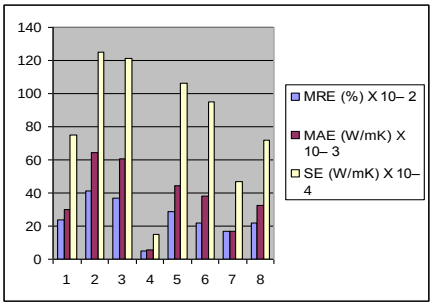

Fig. 8: Corresponding chart showing the error values for 2-hidden layers

4.3 DISCUSSION OF RESULTS

Herein, the thermal conductivity of the bakery products was modelled by simulation. As a result, both the predicted and targeted/desired thermal conductivity values are plotted separately against each of the three dependent variables as a function of moisture content (%), temperature (^{o}C) and apparent density (kg/m^{3}). The corresponding curves were obtained for the optimal ANN configuration; 2-hidden layers with 8 neurons, and the simplest ANN configuration; 1-hidden layer with 10 neurons .

For each of the corresponding diagrams, there was a considerable and first-rate agreement between the predicted and desired/targeted values of thermal conductivities for different parameters of MAE,MRE and SE.

It can be concluded that the predicted thermal conductivity is good, efficient and credible prediction for thermal conductivity of bakery products

V. CONCLUSION

In this paper, an ANN model was developed for calculating the thermal conductivity of a variety of bakery products under a wide range of conditions of moisture content, temperature and apparent density. The optimal model consisted of 2-hidden layers with eight neurons in each hidden layer, and was able to produce thermal conductivity values with a MAE of 54 X 10^{-4}W/mK, MRE of 4.878 X10^{-4}W/mK and a SE of 15 X 10^{-4}W/mK (see Table 3). However, the simplest ANN model has 1-hidden layer with 10 neurons. This also showed a good prediction with a MRE of about 3.388 X 10^{-4} W/mK, MAE of 34 X 10^{-4} W/mK and SE of 11 X10^{-4} W/mK (see Table 4).

From these values, it can be deduced and concluded that the simplest ANN model (with 1-hidden layer and 10 neurons), when compared with the optimal ANN model (with 2-hidden layers and 8 neurons in each hidden layer) has smaller mean relative error,smaller mean absolute error and lesser standard error. Therefore, this model performs better accordingly.

REFERENCES

[1] **Baik**, O. D., Marcotte, M., Sablani, S. S., and Castaigne, F. (2001): *Thermal and physical properties of Bakery products. Critical Review in Food Science and Nutrition*. CRC Press LLC

[2] Rask, C. (1989): *Thermal properties of dough and bakery products: A review of published data*. Journal of Food Engineering, 9, 167–193

[3] Sablani, S. S., Marcotte, M., Baik, O. D., and Castaigne, F. (1998): *Modelling of simultaneous heat and water transport in the baking process. Lebensmittel* Wissenchaft and Technologie, 31, Germany; 201–209

[4] Murakami, E. G., and Okos, M. R. (1989): *Measurement and Prediction of thermal properties of foods*. In R. P. Singh, and A. G. Medina (Eds.), Food Properties. Computer-aided Engineering of Food Processing System (pp. 3–48). Norwell, MA: Kluwer Academic Publishers

[5] Linko, P., and Zhu. Y. H. (1991): *Neural network programming in bioprocess variable estimation and state prediction.* Journal of Biotechnology, 21(3), 253–270

[6] Ruan, R., Almaer, S., & Zhang, J. (1995): *Prediction of dough rheological properties using neural networks*. Cereal Chemistry, 72(3), 308–311

[7] Fang, Q., Bilby, G., Haque, E., Hanna, M. A., and Spillman, C. K. (1998): *Neural network modelling of physical properties of ground wheat*. Cereal Chemistry, 75(2), 251–253

[8] Hussain, A. M., and Rahman, M. S. (1999): *Thermal conductivity prediction of fruits and vegetables using neural networks*. International Journal of Food Properties, 2(2

[9] Myhara, R. M., Sablani, S. S., Al-Alawi, S. M., and Taylor, M. S. (1998): *Water sorption isotherms of dates: Modelling using GAB equation and artificial neural network approaches*. Lebensmittel Wissenschaft und Technologies, 31(7/8), Germany; 699–706

[10] Ni, H., and Gunasekaran, S. (1998): *Food quality prediction with neural networks*. Food Technology, 52(10), 60–65

[11] Bishop, M. C. (1994): *Neural networks and their applications*. Review in Scientific Instruments, 64(6), 1803–1831

[12] Sweat, V. E. (1985): *Thermal properties of low and intermediate moisture food.* ASHRAE Transaction, 91, 369–389

[13] Bakshi, S. A. and Yoon, J. (1984): *Thermophysical properties of bread rolls during baking.* Lebensmittel Wissenschaft und Technologie, 17, 90–93

[14] Hornik, K., Stinchombe, M. and White, H.(1989): *Multilayer feed-forward network and universal approximator.* Neural Network, 2, 359–366

[15] Baik, O. D., Marcotte, M., Sablani, S. S., and Castaigne, F. (1999): *Modelling the thermal properties of a cup cake during baking.* Journal of Food Science, 64, 295–299

[16] Xie, G. and Xiong, R. (1999): *Use of hyperbolic and neural network models in modelling quality changes of dry peas in long time cooking.* Journal of Food Engineering, 41, (3/4), 151–162

[17] Sablani, S. S. and Shayya, W. H. (2001): *Computerization of Stumbo's method of thermal process calculations using neural networks.* Journal of Food Engineering, 47, 233–240

[18] Rogers, G. F. C and Mayhew, Y. R. (1989): *Engineering Thermodynamics*. ELBS 3/e, 469–502

[19] Baik, O. D., Sablani, S. S. and Marcotte M. (2002): Journal of Food Engineering. Elsevier. Retrieved from sciencedirect.com/science/article/pii/S0260877401001194

[20] Baik, O. D., Marcotte, M., Sablani, S. S., and Castaigne, F. (2006): *Modelling the Thermal properties of a Cup cake during Baking.* Journal of Food Science Volume 64, Issue 2, 295–299. Article first published online: 20 JUL 2006 and retrieved from onlinelibrary.wiley.com/doi/10.1111/j.1365-2621.1999.tb15886.x/abstract

[21] Shyam Sablani, S and Shafiur Rahman, M. (2003), *Using neural networks to predict thermal conductivity of food as a function of moisture content, temperature and apparent porosity*. Food Research International. Elsevier. Volume 36, Issue 6, 2003, 617–623. Retrieved from sciencedirect.com/science/article/pii/S0963996903000127

[22] Christina Rask (1989), *Thermal properties of dough and bakery products: A review of published data*. Journal of Food Engineering. Volume 9, Issue 3, 1989, 167–193. Elsevier. Retrieved from sciencedirect.com/science/article/pii/0260877489900393

American Journal of Engineering Research (AJER)
e-ISSN : 2320-0847 p-ISSN : 2320-0936
Volume-03, Issue-03, pp-30-36
www.ajer.org

Research Paper Open Access

Growth and optical properties of organic GOA crystals

Dr.Jyotsna R Pandey[1]
[1](*Department of Physics, K.C. College,Churchgate,Mumbai/ University of Mumbai, India)*

Abstract: - A new organic NLO crystal GOA was synthesized by slow evaporation method .Glycine and oxalic acid were combined in 3 different molar ratios to form glycine oxalic acid (GOA)transparent crystals of sizes (2-6 cm) in 2 to 3 weeks time. The phase formation using XRD studies shows orthorhombic crystal structure. The UV visible studies shows wide transparency window between 188 nm to 700 nm suggesting the use of grown materials for non linear applications. The NLO studies using Nd:YAG laser shows appreciable conversion efficiency for sample with change in concentration of oxalic acid. The samples exhibited positive as well as negative photoconductivity at lower applied fields, with more resolution at higher applied fields>200 volts/cm, separation between the light and dark current have been observed.

Keywords: - *Glycine, Oxalic acid ,UV studies, NLO studies, Photoconductivity studies*

I. INTRODUCTION

Crystal growth is a vital and fundamental part of material sciences and engineering. In the field of molecular electronics the organic material are demanded because of their versatile functionalities. The intermolecular interactions in organic materials affect novel functionalities such as conducting, dielectric and optical properties. In organic materials charge transfer process i.e transfer of electron between donor and acceptor molecules play critical roles. New organic NLO crystals are being developed with the physic-chemical stability of organic crystals with good second harmonic generation efficiency by increasing the intermolecular interactions. The main importance of organic NLO materials is that they are used in optical devices because of their large optical nonlinearity, low cutoff wavelength, short response time and high threshold for laser power. The organic NLO crystals are synthesizes with non-localized π electron system to realize nonlinear susceptibility better than inorganic crystals [1-4].Organic NLO materials are the key elements for future photonic technologies.The main advantage of organic materials is that they can be modified and tuned with respect to their chemical structure and properties of materials according to our requirement i.e. they have large structural diversity[5-7].The nonlinear optical (NLO)properties of organic materials are currently of great interest for applications in the field of communication technologies. Owing to the tendency to replace classical electronic material with suitable organic compound, organic crystals have non-linearity optical coefficient larger than inorganic crystals. In the field of nonlinear optical crystal growth, amino acids playing a vital role. A number of natural amino acids exhibit the nonlinear optical properties because they have a donor NH_2 and acceptor COOH and also intermolecular charge transfer is possible[8-9]. Among the amino acids, glycine is the basic one. It has no asymmetric carbon and is optically inactive. The Hydropathy index of glycine is -0.4. The second harmonic generation (SHG) variation of glycine based compounds is due to the interaction of acceptor and donor groups. The interaction between the NH_2 group (which is donor) and the –COOH (which is acceptor) results in the variation of SHG efficiency. Glycine with oxalic acid forms the crystals of glycine oxalic acid (GOA).The different molar proportions of glycine and oxalic acid results in the formation of a series of GOA crystals. It is interesting to grow new GOA (Glycine oxalic acid) series of crystals having NLO Characteristics[10] Glycine oxalic acid (GOA) crystals have been successfully grown by slow evaporation of solution containing the stoichiometric ratios of its components. The amino acid glycine (NH_2CH_2COOH) is the only protein forming amino acid without centre of chirality's [11]. Grown crystals were characterized by various techniques. The present paper gives insight of comparative analysis of the crystals with respect to its structure and optical properties.

II. EXPERIMENT

2.1 Growth of GOA crystals

Analytical reagent grade (AR) samples of glycine (NH_2CH_2COOH) and Oxalic acid $(COOH)_2$ (anhydrous) were dissolved in double distilled water and used for growth of crystal by slow evaporation method at room temperature. Glycine and oxalic acid were taken in 3 different molar ratios, viz 3:1,2:1,1:1 and saturated so;tion were filtered using WHATMAN 110 µm filter paper. All the crystals were found to be stable, colorless and transparent (Fig1).The period of growth ranged from about 2 to 3 weeks.

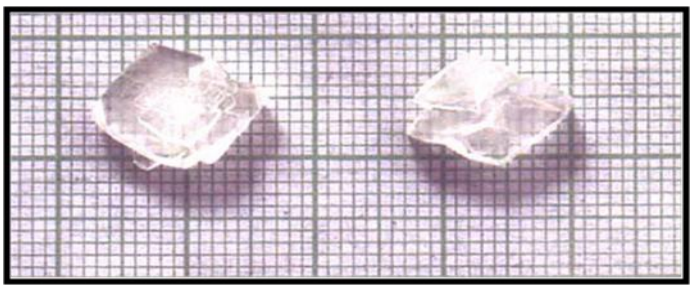

Figure 1 .Photograph of GOA series

III. RESULT AND DISCUSSION

3.1 Powder X-ray Diffraction Analysis

X-ray diffraction (XRD) is a well established technique for determine crystalline order in 3 dimensional solid. The crystals in powder X-ray diffraction technique exposed to characteristics X-ray (CuKα wavelength λ=1.5418A0) and output is obtained in the form of x-ray peaks where the Bragg's law is satisfied(fig2). The GOA crystals belong to orthorhombic symmetry. The cell parameters are dependent on the concentration of oxalic acid in the crystals (Table1).A software program was used to assign planes and determine the lattice parameters for all the grown crystals.

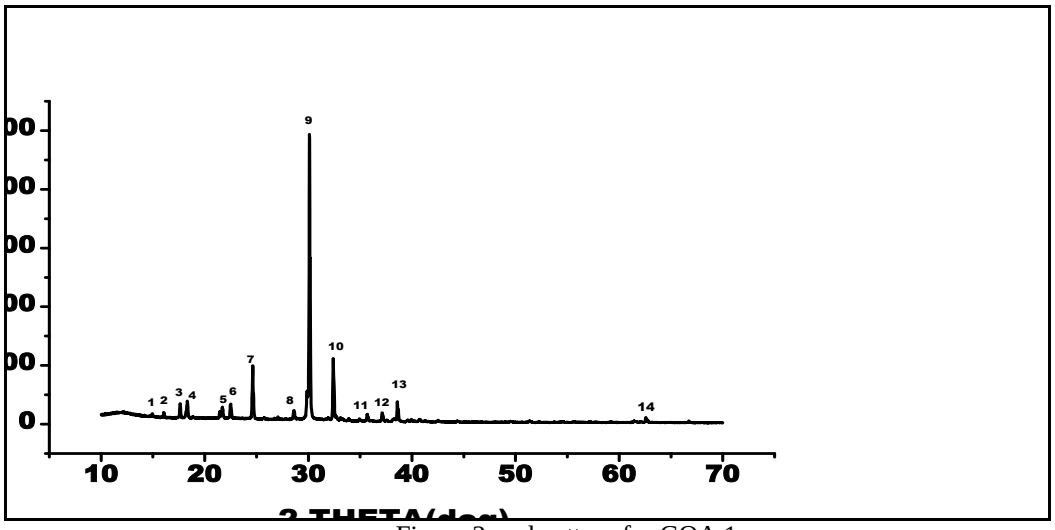

Figure 2 xrd pattern for GOA 1

Table 1 : X-Ray Diffraction - Lattice parameter values

Sample	a (A^0)	b (A^0)	c (A^0)	Volume	Structure
GOA 1	7.035	12.20	9.05	777.33	Orthorhombic
GOA2	9.02	10.01	14.50	1309.21	Orthorhombic
GOA3	17.50	23.10	26.43	10707.45	Orthorhombic

3.2 Ultra Violet Spectral studies

In UV spectral studies the optical transmittance window, the transparency and the lower cutoff wavelength is very important for the realization of SHG output in the range using diode laser. When the samples are transparent, an attempt is made to record the region in which they behave as nonlinear optical material. The ultra violet spectra were therefore recorded from 150nm to 700nm.If the maximum wavelength i.e. λ_{max} lies within this region, the existence of wide transparency window indicates material of NLO properties and which find applications in electronic industries[12-13].The spectral profiles showed that the samples are transparent within the region 190 nm to 700 nm (Fig 3 to5).The maximum cut-off wavelength of GOA (series) varies as the concentration of oxalic acid changes with respect to glycine, the λ_{max} value remains unchanged whereas the absorbance power is seen to decrease with increase in concentration of oxalic acid (figure 6). The effect of concentration of oxalic acid on λ_{max} and absorbance power are summarized in Table 2.

Table2-λmax and absorbance of GOA

Sample	Concentration of Oxalic acid (%)	Cutoff Wavelength ($\lambda_{max)\ nm}$	Absorbance
GOA 1	0.33	188.0	1.761
GOA 2	0.50	188.0	1.523
GOA 3	1.00	188.0	0.572

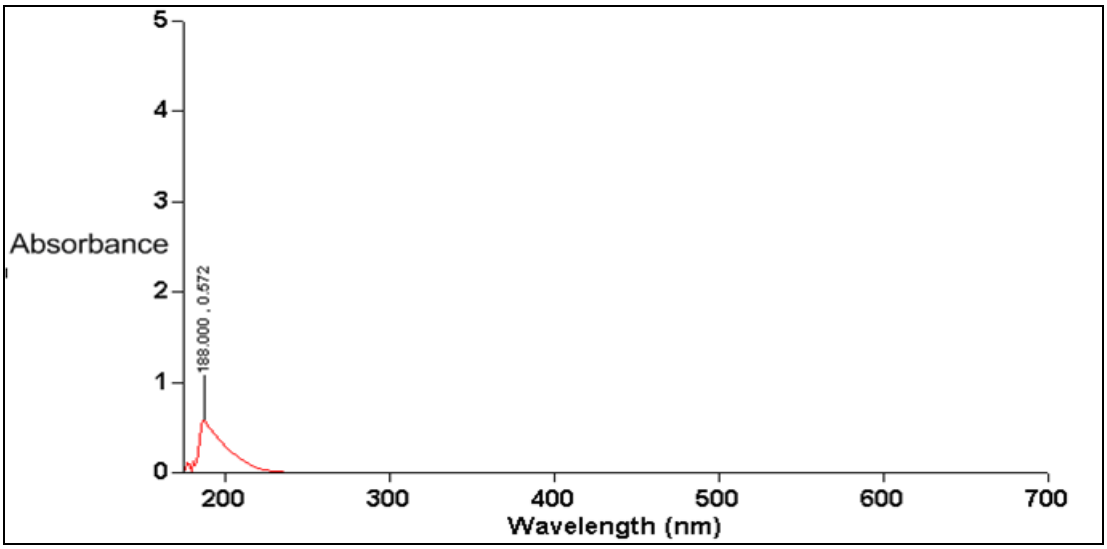

Figure3. UV spectrum for GOA 1

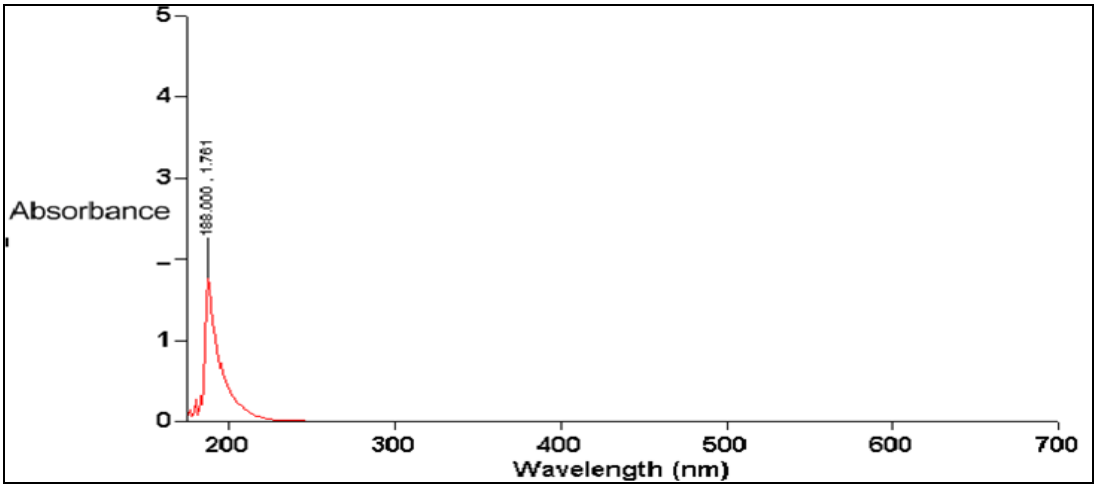

Figure 4. UV spectrum for GOA 2

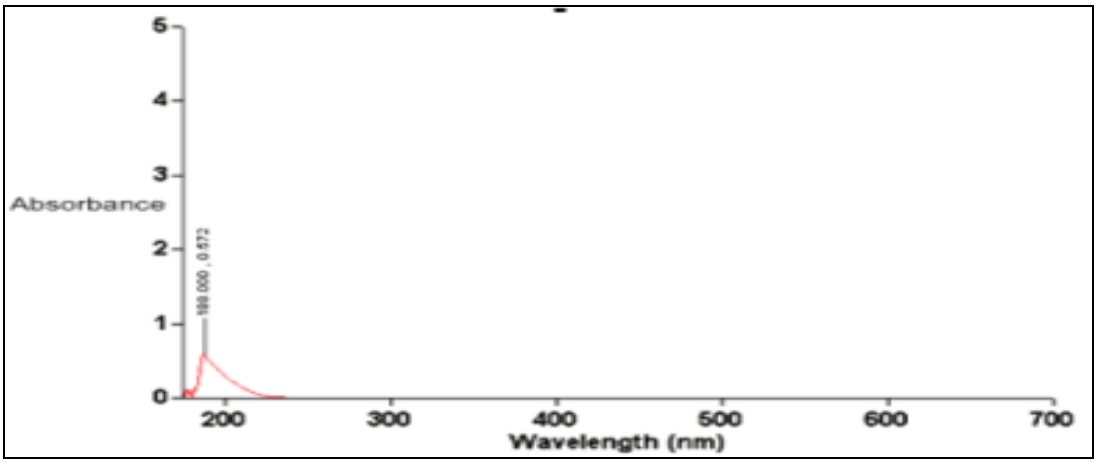

Figure5. UV spectrum for GOA 3

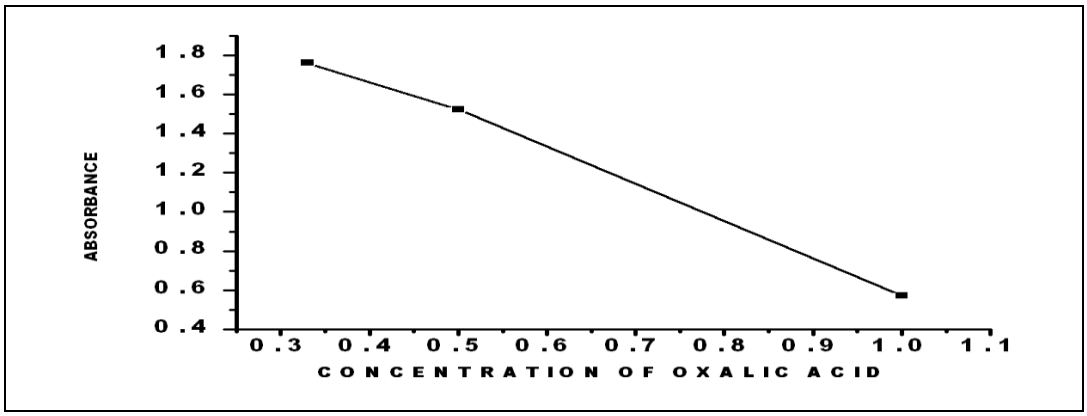

Figure6. Absorbance vs. Concentration of Oxalic acid for GOA (series)

3.3 Non linear optical studies

The first and most widely used technique for confirming the SHG from second order NLO materials is the Kurtz and Perry powder technique. The grown series of GOA crystals were illuminated with a wavelength (λ=1064 nm) of Nd:YAG laser with input enegy 1.35 mJ pulse and the corresponding second harmonic output power was recorded in terms of green light at 532 nm and collected by the photomultiplier tube. The SHG signals generated in the crystalline sample was radiation (λ=532 nm) from the crystals [14-17].It is found that as the concentration of oxalic acid increases,the conversion efficiency decreses,shown in table 3.From the study of conversion efficiency it is found that the GOA 1has maximum efficiency (Fig 7).

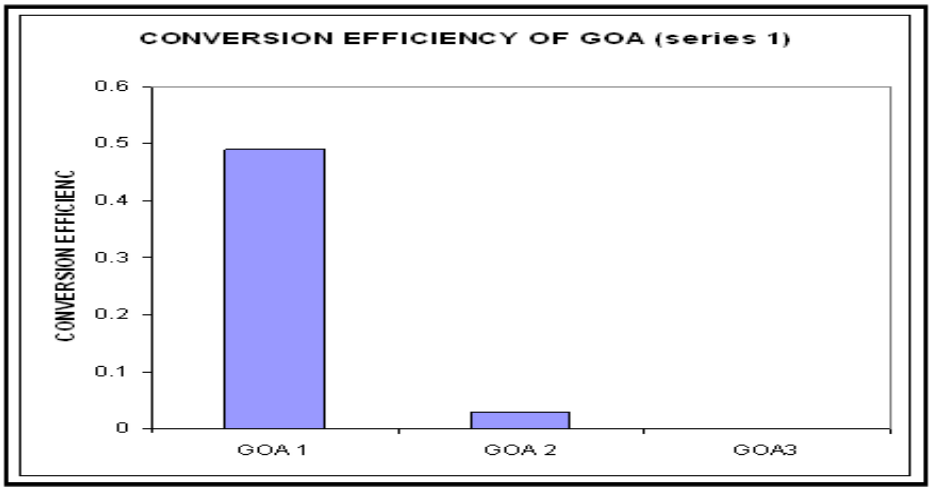

Figure 7. Conversion efficiency of GOA 1

Table3. Second Harmonic Generation conversion Efficiency of GOA (Series)

Sample	Concentration of oxalic acid	Conversion efficiency in(%)	Signal
GOA 1	0.33	0.49	27 mv
GOA 2	0.50	.03	1.7mv
GOA 3	1.0	---	0 mv
KDP	-----	---	55 mv

3.4 Photoconductivity studies

Photoconductivity is an optical phenomenon in which a material becomes more conductive due to the absorption of electromagnetic radiation such as visible light, UV light or gamma radiation. When there is no illumination a photoconductive sample has a conductance that depends on its dimension and temperature. In most cases the greater the radiant energy of a specific wavelength strikes the Surface, the higher the conductance of sample becomes up to a certain maximum. The sample shows positive as well as negative photoconductive nature. Cleaned and polished surface of the crystals have been exposed to light by using a filament lamp having iodine vapour.[18-19]. The changes in conductivity of sample in the presence and absence of light (dark current) can be recorded. The variations in photocurrent (I_P) and dark current (I_d) were determined.The enhancement of field depends on conductivity of the sample. On illumination due to absorption of photons, more of charge carriers are generated. The photoconductivity measurements were carried out on polished and silver plated samples of the grown GOA (series) samples by fixing it on microscope slide. The samples were connected in series with DC power supply and a digital picoammeter MODEL DPM111.The samples were illuminated by radiation from 100 watt lamp and photocurrent was recorded. For dark current measurement the samples were covered with a black cloth and voltage was varied in steps of 0 to 300 volts/cm. The figures 8 to 10 shows that the dark current is found to be less than the light bright current for GOA1 and GOA2 showing positive photoconductivity whereas for GOA 3 the negative photoconductivity has been recorded. As the concentration of oxalic acid decreases with respect to glycine the sample becomes negative photoconductive.

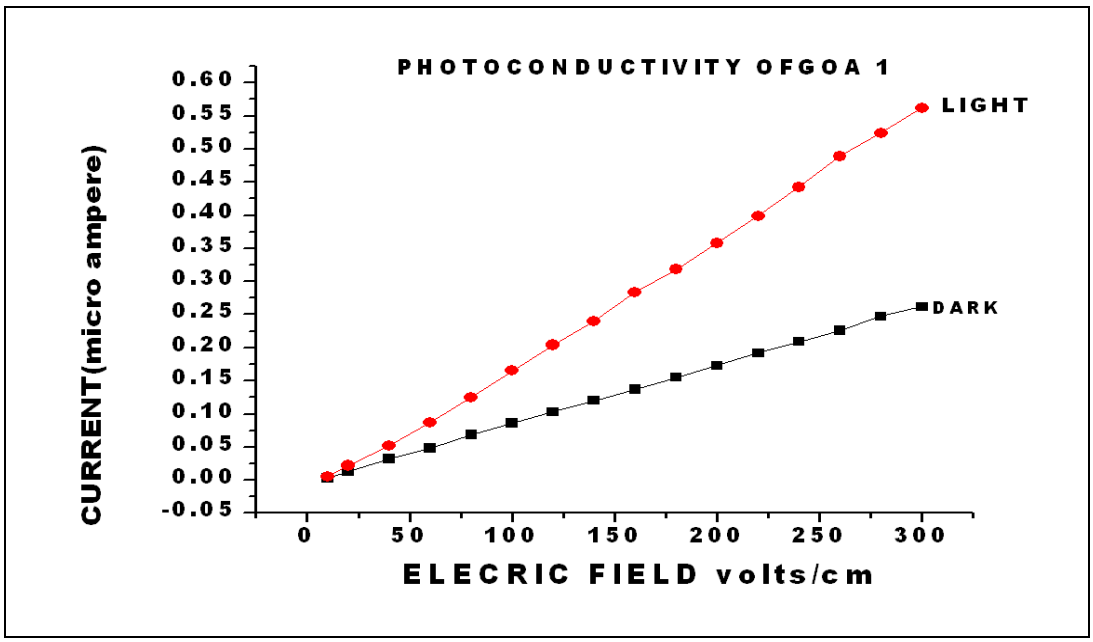

Figure8.Variation of Current with electric field forGOA1

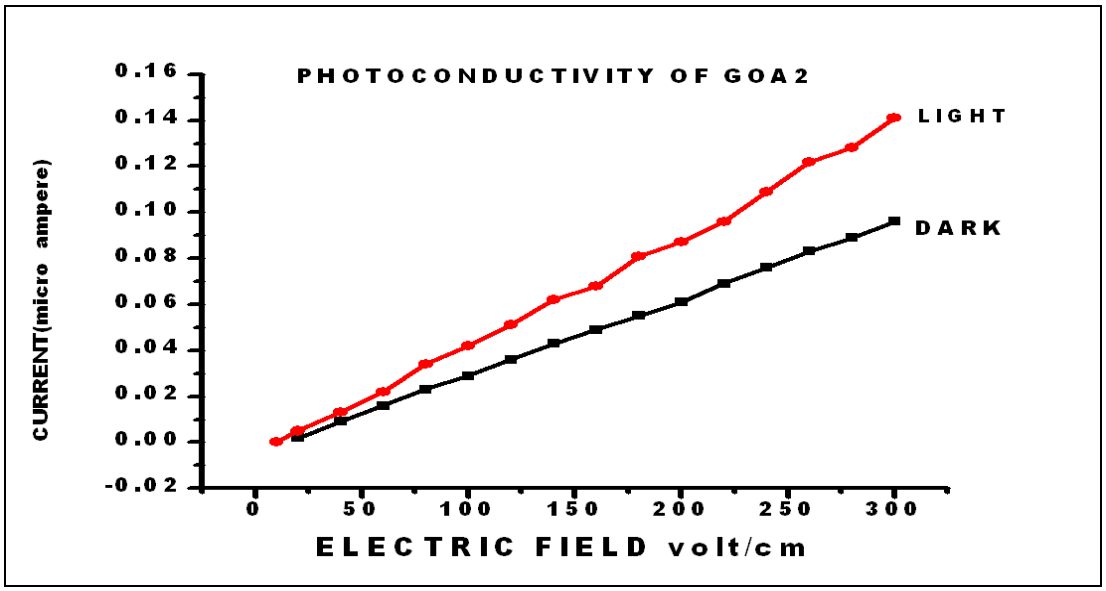

Figure9.Variation of Current with electric field forGOA2

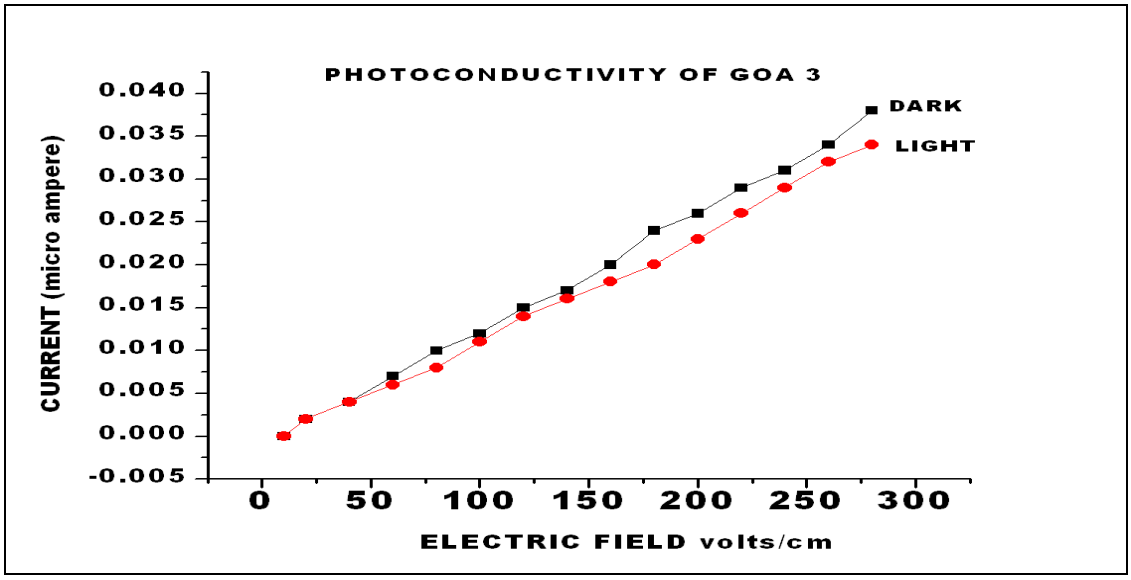

Figure10.Variation of Current with electric field forGOA3

IV. CONCLUSION

New organic GOA (glycine oxalic acid) crystals of appreciable sizes were grown from solution method in 2-3 weeks time.XRD studies reveals orhothrohmbic crystal structure. The cell parameters are dependent on the concentration of oxalic acid in the crystals. The UV visible studies shows wide transparency window between 188 nm to 700 nm suggesting the use of grown materials for non linear optical applications. The NLO studies using Nd:YAG laser shows appreciable conversion efficiency for different concentration of oxalic acid as the concentration of oxalic acid increases, the conversion efficiency decreases. The samples exhibited positive as well as negative photoconductivity at lower applied fields, with more resolution at higher applied fields>200 volts/cm, we can observe the separation between the light and dark current. As the concentration of oxalic acid decreases with respect to glycine the sample becomes negative photoconductive.

REFERENCES

[1] M. Narayan Bhatt and S.M. Dharamprakash, Effect of solvents on the growth morphology and physical characteristics of nonlinear optical γ-glycine crystals, *Journal of crystal growth* ,2002, 242-245

[2] S.Dhanuskodi and K.Vasantha, Growth and characterization of nonlinear single crystals of L-alaninium oxalate, *Crystal .Res. Technol, 3(9),* 2004, 259-261

[3] J B Brice, Crystal Growth Process (John Wiley Halsted Press New York, 1968)

[4] A W Vere, Crystal Growth –Principles and Progress (Glasgow publication New York 1987)

[5] A Wooster, Experimental Crystal Growth (Plenum press New York,1957)

[6] Jyotsna pandey, Growth and electrical properties of new organic GOA crystal, *IOSR Journal of Engineering, 2(9),* 2012, 49-53

[7] EnricoFermi, Degiorgio V and Flytzanis C, Nonlinear Optical Materials Principles and Applications, (International School of Physics 1995)

[8] T.Baraniraj and P.Philominathan, Growth, thermal, Mechanical and Dielectric studies of glycine doped potassium acid Phthalate single crystal, *Journal of Minerals and Materials characterization and Enginerring, ,10(9),* 2011, 805-815

[9] J. B Cohen , practical organic chemistry (Macmillan London1930)

[10] C,Sekar and R.Parimaladevi, Effect of silver nitrate on growth, optical, spectral, thermal and mechanical properties of γ-glycine single crystal, *Journal of optoelectronics and Biomedical materials, 1(2)* ,2009,215-225

[11] T Balakrishnan and K Ramamurthi, Structural, Thermal and optical properties of a semiorganic nonlinear optical single crystal-glycine zink sulphate, *Spectrochimica Acta Part A 12,* 2007,54

[12] S Gao, W Chen , G Wang and J Chen, Effect of second –phase particle morphology on grain growth kinetics, *Journal of crystal growth, 297,* 2006, 360- 361

[13] R RameshBabu, N Vijayan, R Gopalkrishanan and P Ramasamy, Growth and characterization of L-lysine monohydrochloride dehydrate (L-LMHCl) single crystal, *Crystal Res.Technol , 41,* 2006, 405-408

[14] T.Thaila and S.Kumararaman, Growth and characterization of glycine magnesium chloride crystals for NLO applications, *Archives of applied science Reserch ,4(3)* ,2012,1495-1501

[15] J Dyer, Applications of Absorption Spectroscopy of organic compounds (PHI New Delhi,1994)

[16] J Ramajothi, S Dhanuskodi and A.Mehmet, Crystal growth, thermal and optical studies on a semiorganic nonlinear optical material for blue-green laser generation, *Spectro.Chim.Acta Part A, 1,* 2007, 30-38

[17] S A MartinBrittoDhas and S Natrajan, Growth and characterization of two New NLO materials from the amino acid family:L-Histidine nitrate and L-cysteins tartarate monohydrate, *optics communication, 281,* 2008, 457-462

[18] S Palaniawamy and N. Balasundram, Effect of PH on the growth and characterization of glycine sodium chloride (GSC) single crystal , *Rasayan J.chem , 1(4),* 2008, 782-787

[19] V N Joshi , Photoconductivity (Marcel Dekker New York1992)

American Journal of Engineering Research (AJER)
e-ISSN : 2320-0847 p-ISSN : 2320-0936
Volume-03, Issue-03, pp-37-47
www.ajer.org

Research Paper Open Access

Image Segmentation using bi directional of neural network

HimadriNath Moulick[1], Moumita Ghosh[2], Dr. Chandan Koner[3]
[1]*CSE, Aryabhatta Institute of Engg& Management, Durgapur, PIN-713148, India*
[2]*CSE,University Institute Of Technology,(The University Of Burdwan) Pin -712104,India*
[3]*Dr. B.C. Roy Engineering College, Durgapur,Pin-713206, India*

Abstract: **-** Now a days image processing methods are widely used in medical science, to improve critical disease detection and fast treatment for recovery. Mainly this mechanism detects the disease as soon aspossible and also find out the exact point of disorder and calculate the growth of this disease,especially in Squamous cell carcinoma in lower lip. Actinic keratosis which is 1/4 inch in diameter, isa pink or flesh coloured rough spot is one of the most important cause of squamous cell carcinoma,which is mainly grown in sun-exposed area. It is usually grow slowly and affects epidermis layer todermis layer. Our proposed method focuses on five different modules. These methods are including inImage Acquisition module and respective Pre-processing , Segmentation , Filtering Phase and Edge Detection modules.

Keywords: - *Image Clipping, Smoothing , Enhancement, Thresholding, Histogram Analysis*

I. INTRODUCTION

Image processing [3] is any form of signal processing for which the input is an image, such as photographs; the output of image processing can be either an Image or a set of characteristics or parameters related to the image. Most image processing techniques involve treating the image as array, or a matrix, or a square pixel arranged in column and row. In 8 bits grayscale image each pixel has assigned intensity from 0 to 255.Gray scale image is what people normally call black and white image, but the name emphasize that such an image also include many shades of gray.A normal grayscale image has 8 bit color depth=256 grayscales. Where as a true color image has 24 bit color depth=8 x 8 x 8 bits=256 x 256 x256= 16 million colors Digital image processing is the use of computer algorithms to perform image processing on digital images. It allows a much wider range of algorithms to be applied to the input data, and can avoid problems such as the build-up of noise and signal distortion during processing.

Digital image processing methods were introduced in 1920, when people were interested in transmitting picture information across the Atlantic Ocean. The various steps required for any digital image processing applications are listed

Below:-

I. Image acquisition
II. Preprocessing
III. Segmentation
IV. Representation and feature extraction
V. Recognition and interpretation

An image is digitized to convert it to a form, which can be stored in a computer's memory or on some form of storage media such as a hard disk or CD-ROM. This digitization procedure can be done by a scanner, or by a video camera connected to a frame grabber board in a computer. Once the image has been digitized, it can be operated upon by various image-processing operations.

Image defects which could be caused by the digitization process or by faults in theImaging set-up (for example, bad lighting) can be corrected using Image Enhancement techniques. Once the image is in good condition, the Measurement Extraction operations can be used to obtain useful information from the image.Image processing involves processing or altering an existing image in a desired manner. The first step is obtaining an image in a readable format. This is much easier today than five years back. Once the image is in a readable format, image processing software needs to read it so it can be processed and written back to a file. An image consists of a two-dimensional array of numbers. The color or gray shade displayed for a given picture element (pixel) depends on the number stored in the array for that pixel. It is a binary image since each pixel is either 0 or 1. People can distinguish about 40 shades of gray, so a 256 shade image looks like a photograph. This project concentrates on gray scale images and also color images. The most complex type of image is color. Color images are similar to gray scale except hat there are three bands, or channels, corresponding to the colors red, green, and blue. All though there is so many color model, but the RGB is the popular one Thus, each pixel has three values associated with it.It use additive color mixer and is a basic color model used in television and any other miduam that projects color with light.RGB color model also used in computer and for web graphics but it cannot be used for print production.the secondary color of RGB is cyan, magenta and yellow. A color scanner uses red, green, and blue filters to produce those values. Images are available via the Internet, scanners, and digital cameras. Any picture shown on the Internet can be downloaded by pressing the right mouse button when the pointer is on the image. This brings the image to the PC usually in a JPEG format. Your software packages can convert that to correct resolution. Image scanners permit putting common photographs into computer files.

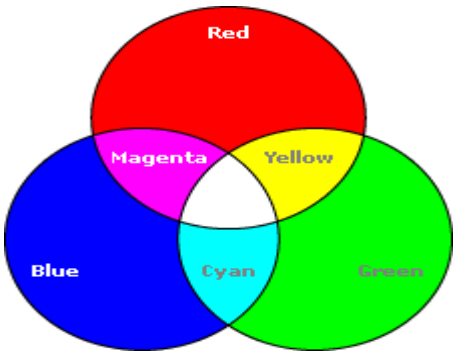

II. DIGITAL IMAGEREPRESENTATION

The term monochrome or simply, refers to a two-dimensional intensity function *f(x,y),*where x and y denote spatial coordinates and the value of f at any point (x,y) is proportional to the brightness (or the gray level)of the image at that point. Sometimes viewing an image functioning perspective with the third axis being brightness is useful. In this way as series of active peaks in regions with numerous changes in brightness levels and smoother regions or plateaus where the brightness levels varied little or were constant. Using the convention of assigning proportionately higher values to brighter areas would make the height of the components in the plot proportional to the corresponding brightness of the image. A digital image [5] is an image f(x,y) that has been discretized both in spatial coordinates and brightness. A digital image can be considered a matrix whose row and column indices identify a point in the image and the corresponding matrix element value identifies the gray level at the point .the elements of the digital array are called image elements, picture elements, pixels or pels, with the last two being commonly used abbreviations of "picture elements".Although the size of a digital image varies with the application, demonstrate the many advantages of selecting square arrays with sizes and number of gray levels that are integer powers of 2. For example, a typical size comparable in quality to a monochrome image is a 512 *512 array with 128 gray levels.

15	0	0	0	0	15
15	3	3	3	3	15
15	3	0	0	3	15
15	3	0	0	3	15
15	3	0	0	3	15
15	3	3	3	3	15
15	0	0	0	0	15

The above zoomed picture is a 6 X7 picture and its pixel value is written in a matrix form.
Here, x=7 and y=6.Then we can find f (2, 2) =3, f (4, 3) =0 and so on.
1 Simple image model

The term image [3] refers to a two-dimensional light-intensity function, denoted by *f(x, y)*, where the value or amplitude of f at spatial coordinates(x, y) gives the intensity (brightness) of the image at that point. As light is a form of energy *f*(x, y) must be nonzero and finite that is,

$0<f(x, y)<\infty$. ----------(1)

The basic nature of f(x, y) may be characterized by two components:

(1) The amount of source light incident on scene being viewed.

The amount light reflected by the objects in scene. Appropriately, they are called the illumination and reflectance components, and are denoted by i(x, y) and r(x, y), respectively. The functions i(x, y) and r(x, y) are combine as a product to form f(x, y):

$f(x, y) = i(x, y)r(x, y)$ ----------(2)

where

$0<i(x, y)<\infty$----------(3)

and

$0<r(x, y)<1$----------(4)

Equation (4) indicates is bounded by 0 (total absorption) and 1 (total reflectance). The nature of i(x, y) is determined by the light source, and r(x, y) is determined by the characteristics of the objects in a scene. The values given in Equations (3) and (4) are theoretic bounds. The following average numerical figures illustrate some typical ranges of i(x, y). On a clear day, the sun may produce in excess of 9000 foot-candles of illumination on the surface of the earth. The figure decreases to less than 1000 foot-candles on cloudy day. On a clear evening, a full moon yields about 0.01 foot-candle of illumination. The typical illumination level in a commercial office is about 100 foot-candles. Similarly the following are some typical values of r(x, y): 0.01 for black velvet, 0.65 for stainless steel, 0.80 for flat-white wall paint, 0.90 for silver plated metal, and 0.93 for snow.

The intensity of a monochrome image f at coordinates (x, y) the gray level (l) of the image of the point. From equations (2) through (4), it is evident that l lies in the range

$L_{min} \leq l \leq L_{max}$

The only requirement on $L_{min} = i_{min}r_{min}$ and $L_{max} = i_{max}r_{max}$. Using the preceding values of illumination and reflectance, the values $L_{min}=0.005$ and $L_{max}=100$ for indoor image processing applications may be expected.The internal $[L_{min}, L_{max}]$ is called the gray scale. This interval numerically to the interval [0, L], where l=0 is considered black and l=L is considered white in the scale. All intermediate values are shades of gray varying continuously from black to white.

III. IMAGE PROCESSING

Digital image processing [7] encompasses a broad range of hardware, software and theoretical underpinnings and it will be helpful to use a 'theme'.An application that is rather easy to conceptualize without any prior knowledge of imaging concepts is the use of image processing techniques for automatically reading the address on pieces of mail. The overall objective is to produce a result from a problem domain by means of image processing. The problem domain consists of pieces of mail, and the objective is to read the address on each piece. Thus the desired output in this case is a stream of alphanumeric characters.

Step1: The first step in the process is image acquisition-that is, to acquire a digital image. To do so requires an imaging sensor and the capability to digitalize the signal produced by the sensor. The imaging sensor could also be a line-scan camera that produces a single image line at a time.

Step2: The next step deals with preprocessing that image. The key function of preprocessing is to improve the image in ways that increase the chances for success of the other process. Preprocessing typically deals with technique for enhancing contrast, removing noise, and isolating regions whose texture indicate a likelihood of alphanumeric information.

Step3: The next step deals with segmentation. Segmentation partitions an input image into its constituent parts or objects. In general autonomous segmentation is one of the most difficult tasks in digital image processing. On the one hand, a rugged segmentation procedure brings the process a long way toward successful solution of an imaging problem. On the other hand weak or erratic segmentation algorithms almost always guarantee eventual failure. In the terms of character recognition, the key role of segmentation is to extract individual characters and words from the background. The output of the raw pixel data, constituting either the boundary of a region or all the points in the region itself. In either case, converting the data to a form suitable for computer processing is necessary. The first decision that must be made is whether the data should be represented as a boundary or as complete region. Boundary representation is appropriate when the focus is on external shape characteristics, such as corners and inflections. Regional representation is appropriate is on internal properties, such as texture or skeletal shape. In some applications however, these representations coexist. This situation occurs in character

recognition applications, which often require algorithms based on boundary shape as well as skeletons other internal properties.

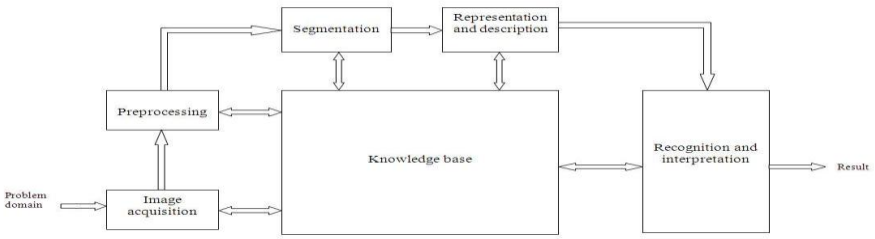

Fig : Fundamental Steps in Digital Image Processing [7]

Step4: Choosing a representation is only part of the solution for transforming raw data into a form suitable for subsequent computer processing. A method must also be specified for describing the data for features of interest are highlighted. *Description*, also called *feature selection*, deals with extracting features that result in some quantitative information of interest or features that are basic for differentiating one class of objects from another.
Step5: The last stage is recognition and interpretation. Recognition is the process that assigns a label to an object based on the information provided by its descriptors. Interpretations involve assigning meaning to an ensemble of recognized objects.

IV. IMAGE SEGMENTATION

Segmentation [4] refers to the process of partitioning a digital image into multiple region (set of pixels). Each of the pixels in a region are similar with respect to some characteristic such as color, intensity, texture. Adjacent regions are different with respect to the same.

1 Gradient operator

This is a part of image segmentation [4]. Through the gradient operator the edge can be detected and make it smooth.For estimating image gradients from the input image or a smoothed version of it, different gradient operators can be applied. The simplest approach is to use central differences:[4]

$$L_x(x,y) = -1/2 \cdot L(x-1,y) + 0 \cdot L(x,y) + 1/2 \cdot L(x+1,y).$$

$$L_y(x,y) = -1/2 \cdot L(x,y-1) + 0 \cdot L(x,y) + 1/2 \cdot L(x,y+1).$$

2 Edge Detection

There are many methods for edge detection, but most of them can be grouped into two categories, search-based and zero-crossing based. The search-based methods detect edges by first computing a measure of edge strength, usually a first-order derivative expression such as the gradient magnitude, and then searching for local directional maxima of the gradient magnitude using a computed estimate of the local orientation of the edge, usually the gradient direction. The zero-crossing based methods search for zero crossings in a second-order derivative expression computed from the image in order to find edges, usually the zero-crossings of the Laplacian or the zero crossings of a non-linear differential expression, as will be described in the section on differential edge detection following below. As a pre-processing step to edge detection, a smoothing stage, typically Gaussian smoothing, is almost always applied.The well-known and earlier Sobel operator is based on the following filters: [4]

$$L_x = \begin{bmatrix} -1 & 0 & +1 \\ -2 & 0 & +2 \\ -1 & 0 & +1 \end{bmatrix} * L \quad \text{and} \quad L_y = \begin{bmatrix} +1 & +2 & +1 \\ 0 & 0 & 0 \\ -1 & -2 & -1 \end{bmatrix} * L$$

Given such estimates of first- order derivatives, the gradient magnitude is thencomputed as:

$$|\nabla L| = \sqrt{L_x^2 + L_y^2}$$

While the gradient orientation can be estimated as

$$\theta = \text{atan2}(L_y, L_x)$$

3 Point Detection

The detection of isolated points in an image is straightforward. Using the mask shown in next Fig, we say that a point has been detected at the location on which the mask is centered if

$R > T$ …… (1)

Where T is a nonnegative threshold and R is given by the equation below [7]

$R=W_1Z_1 + W_2Z_2+ W_3Z_3+.....+ W_9Z_9$

Where Z_i is the gray level of the pixel associated with mask coefficient W_i.Basically, all that this formulation does is measure the weighted differences between the center point and its neighbors. The idea is that the gray level of an isolated point will be quite different from the gray level of its neighbors.

4 Region–oriented segmentation

The objective of segmentation is to partition an image into regions. We approach this problem by finding boundaries between regions based on intensity discontinuities, whereas earlier segmentation was accomplished via thresholds based on the distribution of pixel properties, such as intensity or color. Here we discussed segmentation techniques that are based on finding the regions directly.

Basic formulation:

Let R represent the entire image region. We may view segmentation as a process that partitions R into n sub-regions, R_1, R_2 …R_n, such that

a. $\sum_{i=0}^{n} R_i = R$,

b. $R_i$is a connected region, i = 1,2,…….n,

c. $R_i \cap R_j = \emptyset$ for all i and j, $i \neq j$,

d. $P(R_i)$ = TRUE for i = 1,2,…….,n, and

e. $P(R_i \cup R_j)$ = FALSE for $i \neq j$,

Where $P(R_i)$ is a logical predicate over the points in set $R_i$and Øis the null set. Condition (a) indicates that the segmentation must be complete; that is, every pixel must be in a region. The second condition requires that points in a region must be connected. Condition (c) indicates that the regions must be disjoint. Condition (d) deals with the properties that must be satisfied by the by the pixels in a segmented region- for example $P(R_i)$ =TRUE if all pixels in R_i have the same intensity. Finally, condition (e) indicates that regions R_i and R_j are different in the sense of predicate P.

V. NEURAL NETWORK CONCEPT

Neural Network [2] which are simplified models of biological neuron system, is a massively parallel distributed processing system made up of highly interconnected neural computing elements that have the ability to learn and thereby acquire knowledge and make it available for use.The structural constituents of human brain termed neurons are entity which performs computation such as cognition, logical inference, pattern recognition and so on. Hence the technology, which has been built on a simplified imitation of computing by neuron of a brain, has been termed as Artificial Neural Network.A human brain develops with time; this common parlance is known as experience. Technically this involves the development of neuron to adapt to their surrounding environment by updating their weight factors.

1. BASIC MODEL OF ARTIFICIAL NEURAL NETWORK[8]

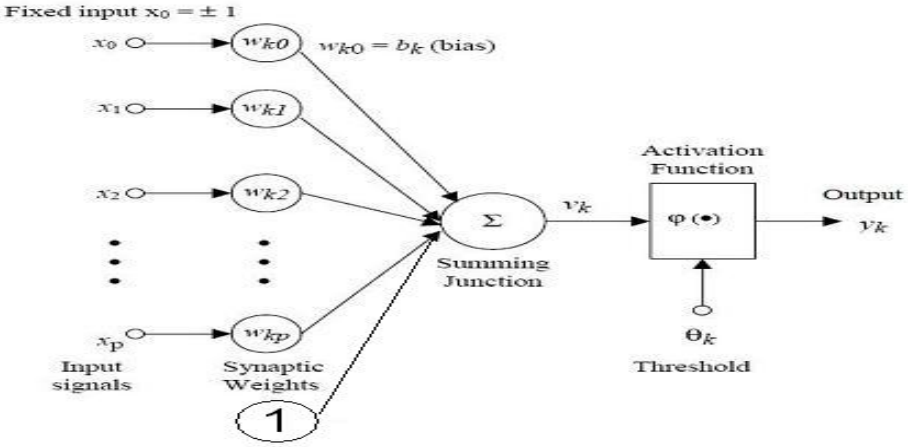

Here x1, x2, x3….xn are the input to artificial neuron.w1,w2,w3,w4…wn are the corresponding weights attached to the input links. One biased input has been considered having weight –k.
So the output can be calculated as bellow..

Vk=Wk1.X1+Wk2.X2+Wk3.X3-k

$$Vk = \sum_{i=1}^{n} Xi.Wki - k$$

Now the activation function wll be applied on it.

$$Vk' = f \sum_{i=1}^{n} Xi.Wki - k$$

Activation Transfer Function: This function represent the transfer characteristic of individual neuron.It determines the behavior of the incident inputs using dutiable learning algorithem.
Interconnection topology:This refers the mode of interconnection of the neuron in different layers of neural network.As in the biological neuron axon synopsis interconnection act as the storage junction similarly the interconnection if artificial neural network is characterized by weight factors which ascertain their activation level.
Learning Algorithem:There are two types of learning one is feedforward manner and another is feedback manner where a loop exist.In feedback algorithem information can be moved in backward direction or to the previous layers.

2.OPERATION MODES:

The operation modes of neural network can be classified into two main categories viz,supervisedans unsupervised learning.
Supervised learning: This architecture implies the use of some prior knowledge base to guide the learning phase. This knowledge base puts forward to the neural network a training set of input-output patterns and an input – output relationship. The neural network is then supervised to embed an approximation function in its operation.
Unsuprvised learning: This is an adaptive learning paradigm, which present the neural network with an input and allow it to self-organize the topological configuration depending on the distribution of the input data by means of prototype of input vector presented.

VI. RESULT

Gray Scale Image
Lena Image :-
Input Image :-

No.	Grey Scale Boundaries	Correlation
1.	{0, 21, 65, 106, 138, 167, 227, 255}	0.8970
2.	{0, 41, 80, 123, 158, 201, 240, 255}	0.8846
3.	{0, 38, 71, 113, 135, 168, 209, 255}	0.9068
4.	{0, 47, 80, 111, 146, 168, 212, 255}	0.9053
5.	{0, 47, 61, 111, 120, 169, 172, 255}	0.8605
6.	{0, 47, 53, 117, 119, 167, 172, 255}	0.7994
7.	{0, 48, 55, 121, 135, 185, 195, 255}	0.8051
8.	{0, 53, 55, 119, 121, 170, 186, 255}	0.7878

The output images are shown in the figure 6.4.1 and 6.4.2. figure 6.4.1 (a) represents the output image corresponding the set of serial no 1. Figure 6.4.1(b) represents the output image corresponding the set of serial

no 2 and so on. Similerly figure 6.4.2 (a) represents the output image corresponding the set of serial no 5 and figure 6.4.2 (b) represents the output image corresponding the set of serial no 1 and so on.
Baboon Image :-

Input Image :-

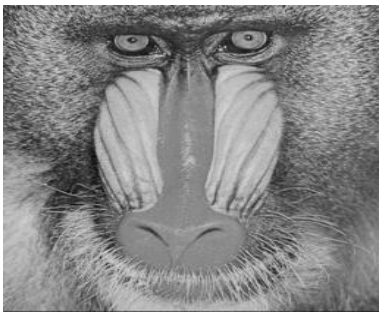

No.	Grey Scale Boundaries	Correlation
1.	{0, 68, 91, 112, 141, 169, 190, 255}	0.7570
2.	{0, 66, 84, 116, 143, 166, 189, 255}	0.7537
3.	{0, 65, 104, 128, 152, 168, 191, 255}	0.7720
4.	{0, 40, 78, 114, 140, 164, 191, 255}	0.7543
5.	{0, 82, 90, 125, 133, 163, 169, 255}	0.6919
6.	{0, 81, 82, 124, 126, 159, 162, 255}	0.6464
7.	{0, 76, 82, 108, 114, 147, 150, 255}	0.6754
8.	{0, 85, 86, 125, 132, 164, 173, 255}	0.6673

The output images are shown in the figure 6.4.3 and 6.4.4. figure 6.4.3 (a) represents the output image corresponding the set of serial no 1. Figure 6.4.3(b) represents the output image corresponding the set of serial no 2 and so on. Similerly figure 6.4.4 (a) represents the output image corresponding the set of serial no 5 and figure 6.4.5 (b) represents the output image corresponding the set of serial no 1 and so on.

RGB Image:-
Lena Image:-
Input Image:

No	Bounderies	Correleation
1.	R={43, 89, 156, 160, 172, 213, 237, 255}	0.9052
	G={0, 34, 67, 110, 151, 155, 187, 255}	
	B ={32, 67, 91, 107, 126, 164, 186, 238}	
2.	R={43, 70, 120, 130, 150, 170, 190, 255	0.9035
	G={0, 20, 140, 180, 190, 210, 230, 255}	
	B ={32, 45, 77, 85, 115, 145, 175, 238}	
3.	R={43, 104, 129, 134, 155, 165, 183, 255}	0.9041
	G={0, 13, 57, 147, 160, 207, 221, 255}	
	B={32, 66, 89, 118, 143, 167, 190, 238}	
	R={43, 121, 129, 144, 196, 214, 233, 255}	

4.	G={0, 30, 51, 120, 134, 138, 204, 255}	0.9082
	B ={32, 65, 77, 101, 123, 154, 187, 238}	
5.	R={43, 80, 90, 110, 120, 190, 200, 255}	0.9111
	G={0, 30, 75, 80, 100, 160, 220, 255}	
	B ={32, 50, 70, 90, 110, 150, 170, 238}	
6.	R={43, 96, 109, 128, 141, 153, 206, 255}	0.9055
	G={0, 51, 61, 116, 141, 176, 186, 255}	
	B={32, 70, 81, 94, 120, 153, 181, 238}	
7.	R={43, 70, 108, 116, 126, 151, 165, 255}	0.9046
	G={0, 41, 111, 157, 166, 180, 200, 255}	
	B={32, 53, 74, 88, 128, 145, 162, 238}	
8.	R={43, 58, 72, 140, 172, 210, 232, 255}	0.8947
	G={0, 15, 48, 110, 142, 178, 220, 255}	
	B={32, 55, 87, 112, 136, 140, 215, 238}	

The output images are shown in the figure 6.4.5 and 6.4.6. figure 6.4.5 (a) represents the output imagecorresponding the set of serial no 1. Figure 6.4.5(b) represents the output image corresponding the set of serial no 2 and so on. Similerly figure 6.4.6 (a) represents the output image corresponding the set of serial no 5 and figure 6.4.6 (b) represents the output image corresponding the set of serial no 1 and so on.

Baboon Image:-

Input Image:-

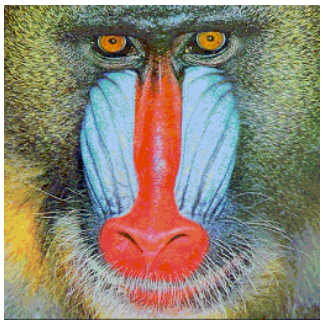

No	Bounderies	Correlation
1.	R={0, 17, 52, 73, 83, 116, 204, 255}	0.8579
	G={0, 27, 102, 152, 153, 180, 254, 255}	
	B ={0, 48, 89, 117, 136, 177, 230, 255}	
2.	R={0, 82, 85, 159, 163, 210, 214, 255}	0.8541
	G={0, 84, 96, 114, 163, 194, 207, 255}	
	B={0, 30, 69, 100, 124, 153, 211, 255}	
3.	R={0, 94, 106, 146, 173, 186, 203, 255}	0.8481
	G={0, 39, 69, 74, 88, 111, 147, 255}	
	B={0, 52, 75, 90, 127, 162, 219, 255}	
4.	R={0, 50, 60, 90, 100, 110, 150, 255}	0.8044
	G={0, 60, 110, 160, 170, 185, 200, 255}	
	B ={0, 10, 20, 60, 80, 150, 220, 255}	
5.	R={0, 57, 59, 79, 100, 244, 251, 255}	0.7875
	G={0, 15, 41, 108, 169, 178, 196, 255}	
	B={0, 47, 51, 111, 115, 221, 233, 255}	
6.	R={0, 91, 106, 125, 142, 143, 170, 255}	0.8631
	G={0, 52, 54, 75, 83, 86, 167, 255}	
	B={0, 52, 70,90, 126, 160, 223, 255}	
7.	R={0, 45, 55, 75, 95, 225, 245, 255}	0.7897
	G={0, 10, 35, 95, 155, 175, 195, 255}	
	B={0, 35, 45, 105, 110, 215, 230, 255}	
	R={0, 78, 110, 134, 186, 210, 233, 255}	

8.	G={0, 42, 68, 92, 120, 162, 240, 255}	0.8715
	B={0, 65, 114, 148, 167, 195, 230, 255}	

The output images are shown in the figure 6.4.7 and 6.4.8. figure 6.4.7 (a) represents the output image corresponding the set of serial no 1. Figure 6.4.7(b) represents the output image corresponding the set of serial no 2 and so on. Similerly figure 6.4.8 (a) represents the output image corresponding the set of serial no 5 and figure 6.4.8 (b) represents the output image corresponding the set of serial no 1 and so on.

Figure 6.4.1: Out put of gray Lena Images (1)

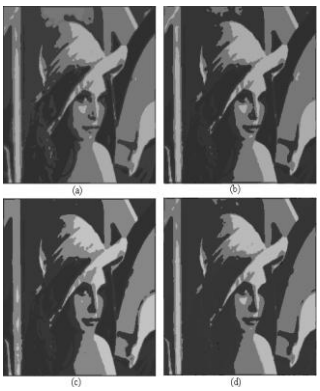

Figure 6.4.2: Out put of gray Lena Images (2)

Figure 6.4.5: Out put of color Lena Images (1)

Figure 6.4.6: Out put of color Lena Images (2)

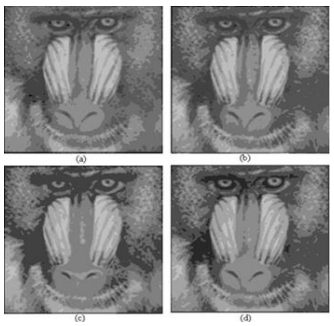

Figure 6.4.3: Out put of gray baboon Images (1)

Figure 6.4.4: Out put of gray Baboon Images (2)

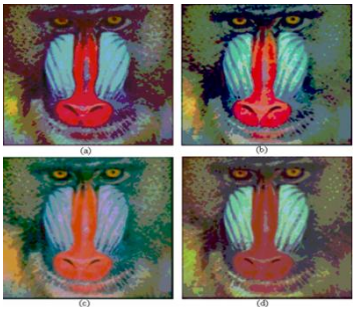

Figure 6.4.6: Out put of color Baboon Images (1)

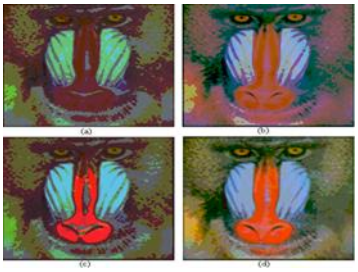

Figure 6.4.6: Out put of color Baboon Images (2)

VII. CONCLUSION

The neural network has not been used for the first time to segment an image. Previously image segmentation has been done using the MLSONN architecture. Many other algorithms are there for this purpose. The MLSONN architecture has some draw backs. As in this architecture in the back propagation part there is a recurrent loop connecting the output layer to the input layer which basically increase the complexity. This project work has been done based on the research that find the new BDSONN architecture in which the output is feed backed to hidden layer instead of input layer. It reduces so many computation burdens as much possible. That is the main advantage of this architecture that has been implemented in this project using the language Visual Basic 6.In the coming future BDSONN architecture will be widely used to perform image segmentation in the world. So the goal of our project is to put a look on this research and try to visualize our thought in this concern and this resource should be helpful.

VIII. REFERENCES

[1] A Self Supervised Bi-directional Neural Network(BDSONN) Architecture for Object Extraction Guided by Beta Activation Function and Adaptive Fuzzy Context Sensitive Thresholding.

[2] Siddhartha Bhattacharyya, ParamarthaDutta, UjjjwalMaulik and Prashanta Kumar Nandi: " A Self Supervised Bi-directional Neural Network(BDSONN) Architecture for Object Extraction Guided by Beta Activation Function and Adaptive Fuzzy Context Sensitive Thresholding" http://www.waset.org/journals/ijece/v1/v1-8-77.pdf

[3] Fundamentals of neural networks a classroom approach-by Satish Kumar

[4] Linda G. Shapiro and George C. Stockman (2001): "Computer Vision", , New Jersey, Prentice-Hall, ISBN 0-13-030796-3

[5] Dzung L. Pham, ChenyangXu, and Jerry L. Prince (2000): "Current Methods in Medical Image Segmentation", *Annual Review of Biomedical Engineering*, volume 2

[6] Chen C.H., Pau L.F., Wang P.S.P.The Handbook of Pattern Recognition and Computer Vision (2nd Edition). – World Scientific Publishing Co., 1998. – 1004 p.

[7] Vovk, O.L. (2006), "A new approach to visual similar image colors extraction". Journal of Automation and Information Sciences 6: 100-105.

[8] Ron Ohlander, Keith Price, and D. Raj Reddy (1978): "Picture Segmentation Using a Recursive Region Splitting Method", *Computer Graphics and Image Processing*, volume 8

[9] Neural Network Fuzzy ligic and Genetics algorithem ,synthesisans applications-by S.Rajasekaram and G.A VijayalakshmiPai

[10] S. Bhattacharyya, P. Dutta, and U. Maulik, Self organizing neural network (SONN) based grayscale object extractor with a multilevel sigmoidal (MUSIG) activation function, Foundations Comput. Dec. Sci. 33(2) (2008), pp. 131–165.

[11] Neural Networks:evaluation,topologies,learning algorithms and applications by Siddhartha Bhattacharyya.

[12] Roger L. Claypoole, Jr , Geoffrey M. Davis, WimSweldens ,"Nonlinear Wavelet Transforms for Image Coding via Lifting" , IEEE Transactions on Image Processing, vol. 12, NO. 12, Dec 2003.

[13] David Salomon, "Data Compression, Complete Reference", Springer-Verlag New York, Inc, ISBN 0-387-40697-2.

[14] Eddie Batista de Lima Filho, Eduardo A. B. da Silva MuriloBresciani de Carvalho, and Frederico Silva Pinagé "Universal Image Compression Using Multiscale Recurrent Patterns With Adaptive Probability Model", IEEE Transactions on Image Processing, vol. 17, NO. 4, Apr 2008.

[15] Ingo Bauermann, and Eckehard Steinbach, "RDTC Optimized Compression of Image-Based Scene Representations (Part I): Modeling and Theoretical Analysis" , IEEE Transactions on Image Processing, vol. 17, NO. 5, May 2008.

[16] Roman Kazinnik, ShaiDekel, and NiraDyn , "Low Bit-Rate Image Coding Using Adaptive Geometric Piecewise Polynomial Approximation", IEEE Transactions on Image Processing, vol. 16, NO. 9, Sep 2007.

[17] Bidgood, D. & Horii, S. (1992). Introduction to the ACR-NEMA DICOM standard.*RadioGraphics*, Vol. 12, (May 1992), pp. (345-355)

[18] Delbeke, D.; Coleman, R.E.; Guiberteau M.J.; Brown, M.L.; Royal, H.D.; Siegel, B.A.; Townsend, D.W.; Berland, L.L.; Parker, J.A.; Zubal, G. & Cronin, V. (2006).

[19] Procedure Guideline for SPECT/CT Imaging 1.0.*The Journal of Nuclear Medicine*, Vol. 47, No. 7, (July 2006), pp. (1227-1234).
[20] Gonzalez, R.; Woods, R., &Eddins, S. (2009) *Digital Image Processing using MATLAB*, (second edition), Gatesmark Publishing, ISBN 9780982085400, United States of America
[21] Lehmann, T.M.; Gönner, C. & Spitzer, K. (1999). Survey: Interpolation Methods in Medical Image Processing. *IEEE Transactions on Medical Imaging*, Vol.18, No.11, (November 1999), pp. (1049-1075), ISSN S0278-0062(99)10280-5
[22] Lyra, M.; Sotiropoulos, M.; Lagopati, N. &Gavrilleli, M. (2010a). Quantification of Myocardial Perfusion in 3D SPECT images – Stress/Rest volume differences, Imaging Systems and Techniques (IST), 2010 IEEE International Conference on 1-2 July 2010, pp 31 – 35, Thessaloniki, DOI: 10.1109/IST.2010.5548486
[23] Lyra, M.; Striligas, J.; Gavrilleli, M. &Lagopati, N. (2010b). Volume Quantification of I-123 DaTSCAN Imaging by MatLab for the Differentiation and Grading of Parkinsonism and Essential Tremor, *International Conference on Science and Social Research*, Kuala
[24] Lumpur, Malaysia, December 5-7, 2010. http://edas.info/p8295 Li, G. & Miller, R.W. (2010). Volumetric Image Registration of Multi-modality Images of CT
[25] .MRI and PET, Biomedical Imaging, Youxin Mao (Ed.), ISBN: 978-953-307-071-1, InTech, Available from: http://www.intechopen.com/articles/show/title/volumetric-image-registrationof- multi-modality-images-of-ct-mri-and-pet
[26] O¨ Gorman, L.; Sammon, M. &Seul M. (2008). *Practicals Algorithms for image analysis*, (second edition), Cambridge University Press, 978- 0-521-88411-2, United States of America Nailon, W.H. (2010). Texture Analysis Methods for Medical Image Characterisation, Biomedical Imaging, Youxin Mao (Ed.), ISBN: 978-953-307- 071-1, InTech, Available from: http://www.intechopen.com/articles/show/title/texture analysis-methodsfor.
[27] medical-image-characterisationMathWorks Inc. (2009) *MATLAB User's Guide*. The MathWorks Inc., United States of America
[28] erutka K. (2010). Tips and Tricks for Programming in Matlab, Matlab - Modelling, Programming and Simulations, Emilson Pereira Leite (Ed.), ISBN: 978-953-307-125- 1, InTech, Available from: http://www.intechopen.com/articles/show/title/tipsandtricks- for-programming-in-matlab.
[29]]Toprak, A. &Guler, I. (2006).Suppression of Impulse Noise in Medical Images with the Use of Fuzzy Adaptive Median Filter.*Journal of Medical Systems*, Vol. 30, (November 2006), pp. (465-471).

American Journal of Engineering Research (AJER)
e-ISSN : 2320-0847 p-ISSN : 2320-0936
Volume-03, Issue-03, pp-48-50
www.ajer.org

Research Paper Open Access

Removal of Organic Based Oil and Grease from Food Service Facility Effluent Using a Laterite Column

H. Ajith Hebbar[1], K.S.Jayantha[2]
[1]*Research Scholar, Department of Civil Engineering, Malnad College of Engineering, Hassan, India*
[2]*Professor, Department of Civil Engineering, Malnad College of Engineering, Hassan, India*

Abstract: **-** The effluents from food service facilities like restaurants, hostels and cafeteria typically contain floating cooked oil, ghee, and other fatty materials which are of organic in origin. Conventionally, before allowing this effluent to treatment plant or sewer, grease traps and skimming devices are used to separate these floating organic matters. If these are not effectively separated, these may clog sewers or interfere with biological treatment system. But these conventional methods need frequent maintenance and may not be cost effective. Alternatively, in this experimental work, an attempt was made to remove floating oil and grease using adsorption by passing the wastewater through a Laterite grain column. A real scale study unit was set up at the effluent point of a restaurant. The Various parameters like height of the column, grain size, and flow rate were monitored during the experiment. The results showed that the oil and grease could be removed up to an extent of 97.6% proving that Laterite has good adsorption potential.

Keywords: **-** *Flow rate, Laterite column, Laterite grain, Oil and grease removal efficiency.*

I. INTRODUCTION

Oil, grease and fatty materials are the main culprits of nuisance in the wastewater if not removed early from the point of source. The main sources of hydrocarbon based oil and grease are effluents from vehicle garages and service stations. Further, effluents from restaurants, hostels and cafeteria are the main sources of organic based oil and grease. The kitchen wastewater from a food service facility contains mainly cooked fatty oils, butter and ghee. If oil and grease laden wastewater is disposed to water bodies, it floats and spreads rapidly and forms thin film on the water surface, preventing the oxygen transfer from the atmosphere. This leads to low dissolved oxygen levels in the water due to microbial oxidative attack on hydrocarbon molecules. Further oil and grease is toxic to some aquatic organisms. Moreover, these can clog sewer pipes and pumping system in the treatment plants. If present in excess it may interfere with aerobic and anaerobic biological process, leading to decreased wastewater treatment efficiency. Present day techniques to remove oil and grease are to use skimming tanks, oil and grease traps and interceptors in treatment plants which need frequent cleaning of pipes and sometimes replacement of pipe system, thus resulting in increased maintenance and inspection cost. With these points in view, an alternate method was developed to remove oil and grease from wastewater using adsorption technique [1], [2], [3] and [4]. Easily and cheaply available Laterite grains were used as adsorbent material [5]. A column study using Laterite grains was made by setting up a real scale experimental unit at the effluent point of a restaurant.

II. MATERIALS AND METHOD

The Laterite stones from a quarry were crushed in to two size ranges 16mm-10 mm and 10mm-4mm. In Phase I of the experiment, the study was done on grains 16mm-10 mm size range. These grains were filled in a vertically positioned polyvinylchloride pipe of diameter 2 inch (0.05meter) fitted with taps at an equal interval of 0.7 meter from top, as shown in Fig.1. The experimental setup was sized to suit the effluent point of the restaurant. Wastewater from the restaurant was collected in a tank and passed through the pipe containing laterite grains. An additional tank containing same wastewater was used to maintain a constant head and constant flow rate of wastewater. When the flow came into contact with the adsorbent in the pipe and stabilized, the samples were collected from different taps provided and tested for oil and grease contents. Trials were

conducted for flow rates of 0.25 liters per sec (LPS), 0.5 LPS and 0.75 LPS. In Phase II, the same procedure was repeated for grain size range of 10mm-4mm and samples were tested. Results were compared to the initial concentration of oil and grease in the effluent and percentage removal of oil and grease was evaluated.

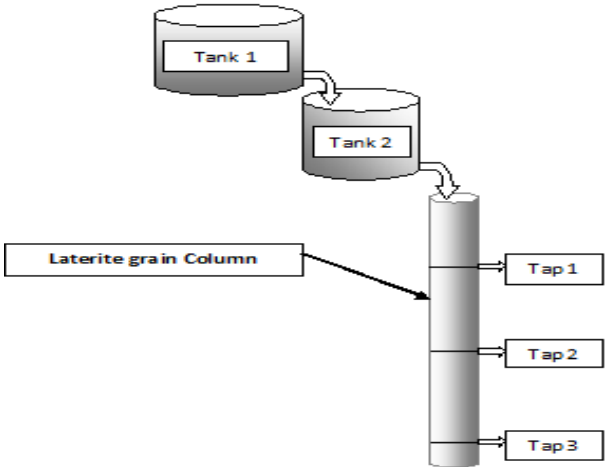

Figure 1: Schematic View of the Experimental Setup.

III. RESULTS AND DISCUSSION

The results obtained from the Phase I and Phase II are tabulated in Table 1 and Table 2.

Table 1: Oil and grease removal efficiency of Phase I

Phase I Grain size : *16mm-10 mm*		**Initial oil and grease Concentration (mg/L)**	**Final oil and grease Concentration (mg/L)**			**Oil and grease removal efficiency (%)**		
			Tap 1	Tap 2	Tap 3	Tap 1	Tap 2	Tap 3
Flow Rate (LPS)	0.25	45.6	8.9	6.2	3.6	80.3	86.4	92.1
	0.5	45.6	10.4	8.2	5.2	77.2	82.1	88.6
	0.75	45.6	13.3	10.7	8.3	70.8	76.5	81.7

Table 2: Oil and grease removal efficiency of Phase II

Phase II Grain size : *10mm-4 mm*		**Initial oil and grease Concentration (mg/L)**	**Final oil and grease Concentration (mg/L)**			**Oil and grease removal efficiency (%)**		
			Tap 1	Tap 2	Tap 3	Tap 1	Tap 2	Tap 3
Flow Rate (LPS)	0.25	51.6	8.9	4.3	1.2	82.8	91.7	97.6
	0.5	51.6	10.8	7.5	4.5	79	85.5	91.3
	0.75	51.6	13.9	11.4	7.8	73.1	77.9	84.8

From the results of Table 1 and Table 2 it is evident that the efficiency of oil and grease removal for a given tap position was highest for slowest flow rate and it started decreasing with increase in the flow rate, as shown in Fig.2. This was due to the fact that for slower flow rate more contact time with adsorbent was available. Further, for a given flow rate, efficiency was highest for Tap 3 position as shown in Fig.3. This was because the Tap 3 position needed a longer travel distance. The maximum efficiency in the Phase I was 97.6% for the flow rate of 0.25 LPS and in Phase II it was 92.1% for the same flow rate. This higher efficiency in Phase II was due to the usage of smaller sized grains in more numbers and hence more adsorption.

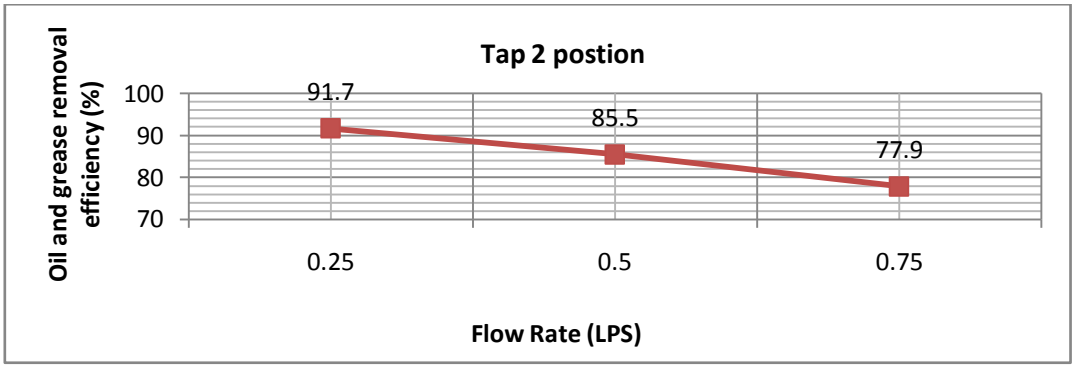

Figure 2: Variation of Oil and grease removal efficiency with Flow Rate

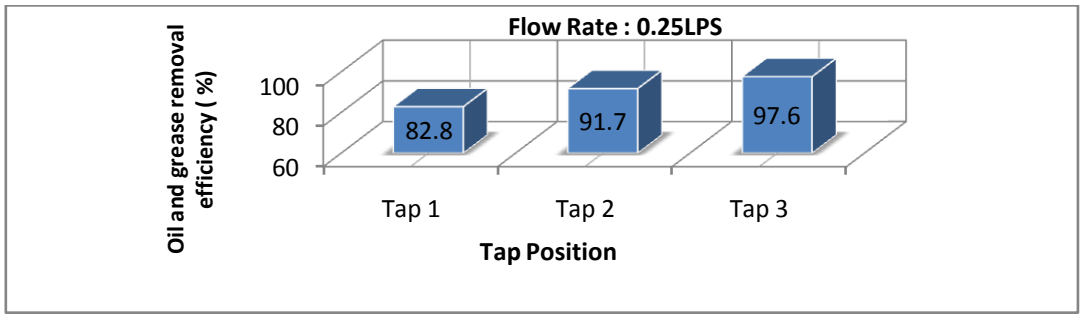

Figure 3: Variation of Oil and grease removal efficiency with Tap Position

IV. CONCLUSION

Based on the results obtained in the different stages of this experiment, it is quite evident that Laterite is a powerful adsorbing medium. For smaller grain sizes, the efficiency of the adsorbent found to be high. Further the adsorbent performed better for slower flow rates and higher distance of travel in the column. In the places where Laterite is cheaply and easily available, initial expenses of installation of the unit are low as compared to other systems. This can be adopted as pretreatment method in biological treatment plants. However further investigations may be necessary on performance of adsorbent for continuous wastewater flow and its reuse potential.

REFERENCES

[1] Abdul Latif Ahmad, Suzylawati Ismail, Norliza Ibrahim, Subhash Bhatia , Removal of suspended solids and residual oil from palm oil mill effluent, *Journal of Chemical Technology & Biotechnology, 78 (2),* 2003, 971–978.

[2] A. Sherry Mueller, R. Byung, E.Kim, E. James ,Anderson, Abizer Gaslightwala, J. Michael Szafranski and A. William Gaines, Removal of Oil and Grease and Chemical Oxygen Demand from Oily Automotive Wastewater by Adsorption after Chemical De-emulsification, *Pract. Periodical of Haz., Toxic, and Radioactive Waste Mgmt., 7(4)* , 2003, 156-162.

[3] K.S.Jayantha, G.R. Ranjana, H.R. Sheela, Modang Ritu and Y.S.Shivananni, Defluoridation studies using Laterite material, *J. Environmental Science and Engineering, 46 (3),* 2004, 282-288..

[4] A.L.Ahmad , S.Sumathi , B.H. Hameed , Residual oil and suspended solid removal using natural adsorbents chitosan, bentonite and activated carbon: A comparative study, *Chemical Engineering Journal , 108 (2),* 2004, 179-185.

[5] K.S. Jayantha, Santhosh Ingalagi, Shwetha, Sushma, B.S. Prashant., Oil and Grease Removal Using Laterite Column: A Case Study, *Proceedings of the International Conference on Business, Environment, International Competitiveness and Sustainable Development of the Asia Pacific Economics,* Malaysia, 2007, 103.

American Journal of Engineering Research (AJER)
e-ISSN : 2320-0847 p-ISSN : 2320-0936
Volume-03, Issue-03, pp-51-55
www.ajer.org

Research Paper Open Access

I- Continuous Functions in Ideal Bitopological Spaces

Mandira Kar, S. S. Thakur, S. S. Rana, J. K. Maitra
Department of Mathematics St. Aloysius College, Jabalpur (M.P.) 482001 India
Department of Applied Mathematics Government Engineering College, Jabalpur (M.P.) 482011 India
Department of Mathematics & Computer Science Rani Durgawati Vishwavidyalaya Jabalpur (M.P.) 482011 India
Department of Mathematics & Computer Science Rani Durgawati Vishwavidyalaya Jabalpur (M.P.) 482011 India

Abstract: - In this paper we introduce and study the concepts of (i,j)-**I**- continuous, (i,j)-**I**- open and (i,j)-**I**- closed functions in Ideal Bitopological Spaces.
AMS Mathematics Subject Classification (2000): 54A10, 54A05, 54E55

Key words and phrases: - *Ideal Bitopological spaces, (i,j)- **I**- open and (i,j)- **I**- closed sets, (i,j)- **I**- continuous and (i,j)- precontinuous functions.*

I. INTRODUCTION

In 1961 Kelly introduced the concept of bitopological spaces as an extension of topological spaces. A bitopological space (X, τ_1, τ_2) is a nonempty set X equipped with two topologies τ_1 and τ_2 [4]. The notion of ideal in topological spaces was studied by Kuratowski [5] and Vaidyanathaswamy [10]. An ideal **I** on a topological space (X, τ) is a nonempty collection of subsets of *X* which satisfies the conditions ***(i)*** $A \in \mathbf{I}$ and $B \subset A$ then $B \in \mathbf{I}$ and ***(ii)*** $A \in \mathbf{I}$ and $B \in \mathbf{I}$ then $A \cup B \in \mathbf{I}$. An ideal topological space is a topological space (X, τ) with an ideal **I** on X, and is denoted by $(X, \tau, \mathbf{I})$. Given an ideal topological space $(X, \tau, \mathbf{I})$ if $\mathcal{P}(X)$ is the set of all subsets of X, a set operator, $(.)^*: \mathcal{P}(X) \to \mathcal{P}(X)$ is called the local function $A^*(\tau, \mathbf{I})$ (in short A^*) [10] of A with respect to the topology τ and ideal **I** defined as $A^* = \{x \in X : U \cap A \notin \mathbf{I}, \forall\ U \in \tau$, where $x \in U\}$. A Kuratowski closure operator Cl* (.) for a topology τ^* $(\tau, \mathbf{I})$, called the *-topology, finer than τ, is defined by $Cl^*(A) = A \cup A^*$ [10].The collection $\{V \cap J : V \in \tau$ and $J \in \mathbf{I}\}$ is a basis for τ^* [9]. A subset A of X is called **I**-open if $A \subseteq int(A^*)$ and **I**- closed if its complement is open. A subset A of X is called *-dense in itself, (resp. τ^*- closed, *- perfect) if $A \subseteq A^*$ (resp. $A^* \subseteq A$, $A = A^*$) [2]. A subset A of X is called preopen [8] if $A \subseteq int(Cl(A))$. The complement of a preopen set is called preclosed. Every**I**- open set is preopen, but the converse may not be true.

II. PRELIMINARIES

Definition 2.1: [6] A function $f:(X, \tau) \to (Y, \sigma)$ is said to be precontinuous if the inverse image of every open set in Y is preopen in X

Definition 2.2: [7] A function $f: (X, \tau, \mathbf{I}) \to (Y, \sigma)$ is said to be **I** - continuous if for every $V \in \sigma$, $f^{-1}(V)$ is **I**-open in X

Definition 2.3: [1] A function $f: (X, \tau_1, \tau_2) \to (Y, \sigma_1, \sigma_2)$ is said to be pairwise continuous if inverse image of every σ_i- open (resp. σ_j- open) set in Y is τ_i- open (resp. τ_j- open) in X

Definition 2.4: [3] An ideal bitopological space is a quadruple $(X, \tau_1, \tau_2, \mathbf{I})$ where **I** is an ideal defined on a bitopological space (X, τ_1, τ_2)

Throughout this paper, A^{τ_i} {resp. $A^{\tau_j^*}$} denote the local function of a subset A of X with respect topology τ_i {resp. τj} and τi - Cl(A) (resp. τj - Cl(A)) and τ_i - int(A) {resp. τj - int(A)} denote the closure and interior of A with respect to topology τ_i (resp. τj}

Definition 2.5: [3] A subset A of an ideal bitopological space (X, τ_1, τ_2, I) is called (i,j)- preopen if $A \subseteq \tau_i$ - int (τ_j- Cl(A)) where ; i, j=1, 2, $i \neq j$

Definition 2.6: [3] A subset A of an ideal bitopological space (X, τ_1, τ_2, I) is called (i,j) **I** - open if $A \subseteq \tau_i$ - int($A^{\tau_j^*}$) where; i, j=1, 2, $i \neq j$

III. (I,J) -I-CONTINUOUS FUNCTIONS

Definition 3.1: A function f: $(X, \tau_1, \tau_2, I) \to (Y, \sigma_1, \sigma_2)$ is said to be (i,j)-**I** - continuous if $f^{-1}(V)$ is (i,j)-**I** - open in X for every σ_i -open set V in Y; i, j=1, 2, $i \neq j$

Definition 3.2: A function f: $(X, \tau_1, \tau_2, I) \to (Y, \sigma_1, \sigma_2)$ is said to be (i,j)- precontinuous if $f^{-1}(V)$ is (i,j)- preopen in X for every σ_i -open V in Y; i, j=1, 2, $i \neq j$.

Remark 3.1: Every (i,j)-**I** - continuous function is (i,j)- precontinuous but the converse is not true. For,

Example 3.1: Let X = {a, b, c, d} with topologies τ_1 ={X, ϕ, {a, c},{a, b, c}, {b}}; τ_2 = {X, ϕ, {a, b}, {a, b, d}, {d}} and **I** = {ϕ, {a}} be an ideal on X. Let Y = {p, q, r, s} with topologies σ_1 = {Y, ϕ, {p, r}, {p, q, r}, {q}}; σ_2 = {Y, ϕ, {p, q}, {p, q, s}, {s}}. Then f: $(X, \tau_1, \tau_2, I) \to (Y, \sigma_1, \sigma_2)$ defined by f(a) = p, f(b) = q, f(c) = r, f(d) = s is (1,2)- precontinuous but not (1,2)-**I**- continuous because (p, r) is open and f^{-1}(p, r) is (1,2)- preopen but not (1,2)-**I**- open.

Definition 3.3: A function f: $(X, \tau_1, \tau_2, I) \to (Y, \sigma_1, \sigma_2)$ is said to be pairwise **I**- continuous if $f^{-1}(V)$ is τ_i-**I**- open (resp. τ_j-**I**- open) in X for every σ_i- open (resp. σ_j- open) set V in Y

Remark 3.2: The concepts of pairwise **I**- continuity and (i,j)-**I**- continuity are independent.

Example 3.2: Let X = {a, b, c, d} with topologies τ_1 ={X, ϕ, {a, c}, {a, b, c}, {b}}; τ_2 = {X, ϕ, {a, b}, {a, b, d}, {d}} and **I** = {ϕ, {a}} be an ideal on X. Let Y = {p, q, r, s} with topologies σ_1 = {Y, ϕ, {p, r}, {p, q, r}, {q}} σ_2 ={Y, ϕ, {p, q}, {p, q, s}, {s}}. Then f: $(X, \tau_1, \tau_2, I \to (Y, \sigma_1, \sigma_2)$ defined by f(a) = p, f(b) = q, f(c) = r, f(d) = s is pairwise **I**- continuous but not (1,2)-**I**- continuous, because (p, r) is open , f^{-1}(p, r) is τ_1-**I**- open, but not (1,2)-**I**- open in X.

Example 3.3: Let X = {a, b, c, d} with topologies τ_1 = {X, ϕ, {a, c}, {a, b, c}, {b}}; τ_2 = {X, ϕ, {a, b}, {a, b, d}, {d}} and **I** = {ϕ, {a}} be an ideal on X. Let Y = {p, q, r, s} with topologies σ_1 ={Y, ϕ, {p, r}, {p, q, r}, {q}} σ_2 ={Y, ϕ, {p, q}, {p, q, s}, {s}}. Then f: $(X, \tau_1, \tau_2, I) \to (Y, \sigma_1, \sigma_2)$ defined by f(a) = p, f(b) = q, f(c) = r, f(d) = s is (1,2)-**I**- continuous but not pairwise **I**- continuous because (p, q, r) is open in Y, f^{-1}(p, q, r) is (1,2)-**I**- open but not τ_i-**I**- open in X.

Theorem 3.1: For a function f: $(X, \tau_1, \tau_2, I) \to (Y, \sigma_1, \sigma_2)$ the following conditions are equivalent:

(a) f is (i,j)-**I**- continuous.

(b) For each $x \in X$ and each $V \in \sigma_i$ containing f(x), there exists an (i,j)-**I**- open set W in X such that $x \in W$ and $f(W) \subset V$.

(c) For each $x \in X$ and each $V \in \sigma_i$ containing f(x), $(f^{-1}(V))^{\tau_j^*}$ is a τ^i- neighborhood of x

Proof:

(a) $\Rightarrow$ ***(b)*** $V \in \sigma_i$ containing f(x). Hence by ***(a)***, $f^{-1}(V)$ is (i,j)- **I**- open set in X containing x. Put $W = f^{-1}(V)$ then $x \in W$ and $f(W) \subset V$.

(b) $\Rightarrow$ ***(c)*** Since $V \in \sigma_i$ containing f(x), then by ***(b),*** there exists an (i,j)- **I**- open set W in X containing x s.t. $f(W) \subset V$. So, $x \in W \subseteq (\tau_i\text{-}(\text{int}(W)))^{\tau_j^*} \subseteq (\tau_i\text{-}\text{int}(f^{-1}(V)))^{\tau_j^*} \subseteq (f^{-1}(V))^{\tau_j^*}$. Hence $(f^{-1}(V))^{\tau_j^*}$) is a τ_i - neighborhood of x.

(c) $\Rightarrow$(***a)*** Obvious.

Theorem 3.2: For a function f: $(X, \tau_1, \tau_2, I) \to (Y, \sigma_1, \sigma_2)$ the following conditions are equivalent:

(a) f is (i,j)- **I**- continuous

(b) The inverse image of each σ_j- closed set in Y is (i,j)- **I**- closed in X.

(c) τ_i - int $f^{-1}(M)^{\tau_j^*} \subset \tau_i$ - $(f^{-1}(M^{\sigma_i^*})$, for each σ_i^*-dense-in-itself subset M of Y.

(d) τ_i - **f**(int(U))$^{\tau_j^*} \subset \tau_i$ - **f**$(U)^{\tau_j^*}$, for each U $\subset$ X, and for each σ_i^*- perfect subset of Y.

Proof:

(a) $\Rightarrow$ ***(b)*** Let M $\subset$ Y be σ_i- closed in Y, then Y\M is σ_i open in Y, then by ***(a)***, f^{-1}(Y\M) = X\f^{-1}(M) is (i,j)- **I**- open in X. Thus, f^{-1}(M) is (i,j)-**I**- closed in X.

(b) $\Rightarrow$ ***(c)*** Let M $\subset$ Y be σ_i- closed in Y, Since $M^{\sigma_i^*}$ is also σ_i- closed in Y, then by ***(b)*** $f^{-1}(M^{\sigma_i^*})$ is (i,j)- **I**- closed in X. Next, by using Theorem 2.4 [6], τ_i - int $f^{-1}(M^{\sigma_i^*})^{\tau_j^*} \subset f^{-1}(M^{\sigma_i^*})$ and since $M^{\sigma_i^*}$ is σ_i^*- dense in itself, τ_i - int $f^{-1}(M)^{\tau_j^*} \subset \tau_i$ - int $f^{-1}(M^{\sigma_i^*})^{\tau_j^*} \subset (f^{-1}(M^{\sigma_i^*})$.

(c) $\Rightarrow$ ***(d)*** Let U $\subset$ X and W = f(U), then by ***(c)***, τ_i - int$(U)^{\tau_j^*} \subset \tau_i$ - int $f^{-1}(W)^{\tau_j^*} \subset \tau_i$ - int $f^{-1}(W^{\sigma_i^*})^{\tau_j^*} \subset (f^{-1}(W)^{\tau_j^*}$ (because $W^{\sigma_i^*}$ is perfect). Hence, τ_i - f(int $(U)^{\tau_j^*} \subset \tau_i$ - $(W)^{\tau_j^*} = \tau_i$ - f$(U)^{\tau_j^*}$.

(d) $\Rightarrow$ ***(a)*** Let V ϵ σ_i ,W = Y\V, and U $\subset$ f^{-1}(W), then f(U) $\subset$ W and by ***(d)***, τ_i - **f**(int(U))$^{\tau_j^*} \subset \tau_i$ - **f** $(U)^{\tau_j^*} \subset \tau_i$ - $(W)^{\tau_j^*}$ = W (because W is σ_i^*- perfect). Thus, τ_i - (int(f^{-1}(W)))$^{\tau_j^*} = \tau_i$ - (int(U))$^{\tau_j^*} \subset f^{-1}$(W), and therefore, f^{-1}(Y\V) is (i,j)-**I**- closed. Hence, f^{-1}(V) is (i,j)-**I**- open in X and f is (i,j)-**I**- continuous.

Theorem 3.4: Let f: (X, τ_1, τ_2, **I**) $\rightarrow$ (Y, σ_1, σ_2) is (i,j)- **I**- continuous and U ϵ $\tau_1 \cap \tau_2$. Then the restriction f\U is (i,j)-**I**- continuous.

Proof:

Let V ϵ σ_i . Then, τ_i - $f^{-1}(V)^{\tau_j^*} \subseteq \tau_i$ - int$(f^{-1}(V))^{\tau_j^*}$ and so U $\cap$ τ_i - $f^{-1}(V)^{\tau_j^*} \subseteq$ U $\cap$ τ_i - int$(f^{-1}(V))^{\tau_j^*}$ Thus $(f\backslash U)^{-1}(V) \subseteq$ U $\cap$ τ_i - int$(f^{-1}(V))^{\tau_j^*}$. Since U ϵ τ_i, we get $(f\backslash U)^{-1}(V) = \tau_i$ - int(U $\cap$ $(f^{-1}(V))^{\tau_j^*}$ [5] $\subseteq \tau_i$ - int(U $\cap$ $f^{-1}(V))^{\tau_j^*} = \tau_i$ - int$((f\backslash U)^{-1}(V))^{\tau_j^*}$. Hence $(f\backslash U)^{-1}(V)$ is (i,j)**I**- open and f\U is (i,j)- **I**- continuous.

Theorem 3.5: For a function f: (X, τ_1, τ_2, **I**) $\rightarrow$ (Y, σ_1, σ_2) and $\{U_\alpha: \alpha \in \Delta\}$ be a biopen cover of X. If the restriction function $f\backslash U_\alpha$ is (i,j)- **I** - continuous, for each $\alpha \in \Delta$, then f is (i,j)- **I**- continuous.

Proof:

Similar to Theorem 1.4

Theorems that follow are immediate and their obvious proofs have been omitted

Theorem 3.6: Let f: (X, τ_1, τ_2, **I**) $\rightarrow$ (Y, σ_1, σ_2) is (i,j)- **I**- continuous and a biopen function, then the inverse image of each open set in Y, which is (i,j)**I**- open set in X is also (i,j)- preopen in X.

Theorem 3.7: Let f: (X, τ_1, τ_2, **I**) $\rightarrow$ (Y, σ_1, σ_2) is (i,j)- **I**- continuous and τ_i- $f^{-1}(V^{\tau_j^*}) \subset \tau_i$ - $(f^{-1}(V))^{\tau_j^*}$, for each V ϵ $\sigma_i \subset$ Y. Then the inverse image of each (i,j)- **I**- open set is (i,j)- **I**- open.

Remark 3.3: Composition of two (i,j)- **I**- continuous functions need not be (i,j)- **I**- continuous, in general, as shown by the following example.

Example 3.4: Let X = {a, b, c} with topologies τ_1 = {X, ϕ, {a}}, τ_2 = {X, ϕ}, and **I** = {ϕ, {c}} be an ideal on X; Y = {a, b, c, d} with topologies σ_1 = {Y, ϕ, {a, c}} σ_2 = {Y, ϕ} and **J** = {ϕ, {a}} be an ideal on Y; Z = {a, b, c} η_1 = {Z, ϕ, {c}, {b, c}} η_2 = {Z, ϕ}. Let f: (X, τ_1, τ_2, **I**) $\rightarrow$ (Y, σ_1, σ_2, **J**) be the identity function and let g: (Y, σ_1, σ_2, **J**) $\rightarrow$ (Z, η_1, η_2) be defined as g(a) = a, g(b) = g(d) = b, g(c) = c. It is clear that both f and g are (i,j)-**I**- continuous but the composition function g*o*f is not (i,j)**I**- continuous, because {c} is open, but $(gof)^{-1}$ {c} = {c}is not (i,j)-**I**- open.

Theorem 3.8: For the functions f: (X, τ_1, τ_2, **I**) $\rightarrow$ (Y, σ_1, σ_2) and g: (Y, σ_1, σ_2, **J**) $\rightarrow$ (Z, η_1, η_2) if f is (i,j)-**I**- continuous and g is pairwise continuous then g*o*f is (i,j)-**I**- continuous,.

Proof: Obvious.

IV. (I,J) I- OPEN AND (I,J) I- CLOSED FUNCTION

Definition 4.1: A function f: (X,τ_1,τ_2) $\rightarrow$ (Y,σ_1,σ_2, **J**); i, j = 1, 2, i $\neq$ j is called (i,j)-**I**- open function (resp. (i,j)-**I**- closed function) if for each U ϵ τ_i (resp. U ϵ τ_i^c), f(U) is an (i,j)**I**- open set in Y (resp. (i,j)-**I**- closed set in Y

Remark 4.1: (i,j)-**I-** open (resp. (i,j)-**I-** closed) function ⇒ preopen (resp. preclosed) function but the converse is not true.

Example 4.1: Let X = Y = {a, b, c} with topologies τ_1 ={X, ϕ, {b}, {a, b}, {b, c}} τ_2 = {X, ϕ} the discrete topology; σ_1 = {Y, ϕ, {a}, {a, b}}; σ_2 = {Y, ϕ} the discrete topology and **J** = {ϕ, {a}, {b}, {a, b}} an ideal on Y. Then the identity function f: (X, τ_1, τ_2) → (Y, σ_1, σ_2, **J**) is preopen but not (1,2)-**I-** open, because {b} is open, but f(b) is a (2,1)-**I-** preopen set but not a (2,1)-**I-** open set.

Remark 4.2: The concepts of (i,j)-**I-** open functions and pairwise open functions are independent concepts

Example 4.2: Let X = Y = {a, b, c, d} with topologies τ_1 = {X, ϕ, {a, b}, {a, b, d}} τ_2 the discrete topology; σ_1 = {Y, ϕ, {a, b}, {a, b, c}}; σ_2 the discrete topology and **J** = {ϕ, {c}, {d}, {c, d}} an ideal on Y. Then the identity function f: (X, τ_1, τ_2) → (Y, σ_1, σ_2, **J**) is a (1,2)**I-** open function but not pairwise open function.

Example 4.3: Let X = Y = {a, b, c}; τ_1 ={X, ϕ, {a}}; σ_1 = {Y, ϕ, {a}, {a, b}}; τ_2 and σ_2 the respective discrete topologies on X and Y and **J** = {ϕ, {a}} an ideal on Y. Then the identity function f: (X, τ_1, τ_2) → (Y, σ_1, σ_2, **J**) is an open function but not a (1,2)-**I-** open function because, {a} is open, but f(a) = a is σ_2 open but not a (1,2)-**I-** open.

Theorems that follow are immediate and their proofs obvious from the definitions

Theorem 4.1: Let f: (X, τ_1, τ_2) → (Y, σ_1, σ_2, **J)** be a function. Then the following are equivalent:

a) f is a (i,j)-**I-** open function.

b) For each x ∈ X and each neighborhood U of x, there exists an (i,j)-**I-** open set W ⊂ Y containing f(x) such that W ⊂ f(U)

Theorem 4.2: Let f: (X, τ_1, τ_2) → (Y, σ_1, σ_2, **J**) be an (i,j)**I-** open function (resp. (i,j)-**I-** closed function) if W ⊂ Y, and F ⊂ X is a closed (resp. open) set containing f^{-1}(W), then there exists an (i,j)**I-** closed (resp. (i,j)-**I-** open) set H containing W such that f^{-1}(H) ⊂ F

Theorem 4.3: If function f: (X, τ_1, τ_2) → (Y, σ_1, σ_2, **J**) is (i,j)-**I-** open, then τ_i- $f^{-1}(\text{int}(B))^{\sigma_i^*} \subset \tau_i$- $(f^{-1}(B)^{\sigma_i^*}$ such that f^{-1}(B) is σ_i^* dense-in-itself, for every B ⊂ Y

Theorem 4.4: For any one-one onto function f: (X, τ_1, τ_2) → (Y, σ_1, σ_2, **J**) the following are equivalent:

a) f^{-1} (Y, σ_1, σ_2, **J**) → (X, τ_1, τ_2) is (i,j)-**I-** continuous

b) f is (i,j)-**I-** closed

Theorem 4.5: If function f: (X, τ_1, τ_2) → (Y, σ_1, σ_2, **J**) is (i,j)-**I-** open and for each A ⊂ X, σ_i- $f(A)^{\tau_j^*} \subset \sigma_i$- $[f(A)]^{\tau_j^*}$, then the image of each (i,j)-**I-** open set is (i,j)-**I-** open.

Theorem 4.6: Let function f: (X, τ_1, τ_2) → (Y, σ_1, σ_2, **J**) and g: (Y, σ_1, σ_2) → (Z, η_1, η_2, **K)** be two functions, where **I**, **J** and **K** are ideals on X, Y and Z respectively, then

a) If f is open and g is (i,j)-**I-** open then g*o*f is (i,j)-**I-** open

b) f is (i,j)-**I-** open if g*o*f is open; g is one-one and (i,j)-**I-** continuous

c) If f and g are (i,j)-**I-** open; f is surjective and $g(V)^{\sigma_i^*} \subset [g(V)]^{\sigma_i^*}$ for each V ⊂ Y, then g*o*f is (i,j)-**I-** open

REFERENCES

[1] Dontchev J., On pre-I -open sets and a decomposition of O- continuity, Banyan Math J; 2, (1996)

[2] Hayashi E., Topologies defined by local properties, Math. Ann; 156, (1964), 205-215

[3] Kar M. and Thakur S.S., Pair-wise open sets in Ideal Bitopological Spaces, Int. J of Math. Sc. and Appln; Vol. 2(2) (2012) 839-842

[4] Kelly J.C., Bitopological Spaces, Proc. London Math. Soc.; 13, (1963), 71-89

[5] Kuratowski K., Topology, Vol.1, Academic Press New York; (1966)

[6] Mashhour A.S., Monsef M.E. Abd El and Deeb S.N. El., On precontinuous and weak precontinuous mappings, Proc. Math and Phys. Soc. Egypt; 53, (1982), 47-53

[7] Monsef M.E. Abd El; Lashien E.F and Nasef A.A; On I- open sets and I- continuous functions, Kyungpook Math. J.; 32(1), (1992), 21-30
[8] Noiri T; Hyperconnectedness and preopen sets, Rev. Roumania Math. Pure Appl.; 29 (1984), 329-334
[9] Samuel P; A topology formed from a given topology and ideal, J. London Math. Soc.; 2(10), (1975), 409-416
[10] Vaidyanathaswamy R; The localization theory in set topology, Proc. Indian Acad. Sci.; 20, (1945), 51-61

American Journal of Engineering Research (AJER)
e-ISSN : 2320-0847 p-ISSN : 2320-0936
Volume-03, Issue-03, pp-56-64
www.ajer.org

Research Paper Open Access

An Approach To Design A Controlled Multi-logic Function Generator By Using COG Reversible Logic Gates

Shefali Mamataj[1], Biswajit Das[2]
[1](Department of ECE, Murshidabad College of Engineering and Technology, India)
[2](Department of CSE , Murshidabad College of Engineering and Technology ,India)

***Abstract*: -** In today's world everyday a new technology which is faster, smaller and more complex than its predecessor is being developed. Reversible computation is a research area characterized by having only computational models that is both forward and backward deterministic. Reversible Logic is gaining significant consideration as the potential logic design style for implementation in modern nanotechnology and quantum computing with minimal impact on physical entropy. It has become very popular over the last few years since reversible logic circuits dramatically reduce energy loss. It consumes less power by recovering bit loss from its unique input-output mapping. This paper represents the implementation of conventional Boolean functions for basic digital gate by using COG reversible gate. This paper also represents a multi logic function generator circuit for generating multiple logical function simultaneously using COG gates. And also represents a controlled multi logic function generator circuit for generating any specified output in a controlled way.

Keywords: - *Reversible logic, Basic Reversible Gates, Boolean Function, Logical Operation, Garbage, Constant input , Quantum cost .*

I. INTRODUCTION

Modern digital circuits offer a great deal of computation. As technology evolves and many more transistors can fit in a given area, the concern for power dissipation as heat arises. Reversible logic was first related to energy when gates in 1973.It was Landauer states that information loss due to function irreversibility leads to energy dissipation in 1961who stated that there is small amount of heat dissipation the circuit due to loss of one bit of information and it would be equal to kTln2 where 'k' is Boltzman constant and T is the temperature [1]. This principle is further supported by Bennett that zero energy dissipation can be achieved only when the circuit contains reversible proved by Bennett that the energy kTln2 would not be dissipate from the circuit if input can be extracted from output and it would be possible if and only if reversible gates are used[2]. According to Moore's law the numbers of transistors will double every 18 months. Thus energy conservative devices are the need of the day. The amount of energy dissipated in a system bears a direct relationship to the number of bits erased during computation. Reversible circuits are those circuits that do not lose information A circuit will be reversible if input vector can be specifically retrieved from output vectors and here is one to one correspondence between input and output [3]. Younis and Knight [4] showed that some reversible circuits can be made asymptotically energy-lossless if their delay is allowed to be arbitrarily large. A reversible logic circuit should have the following features [5]: Use minimum number of reversible gates, Use minimum number of garbage outputs, Use minimum constant inputs.

II. REVERSIBLE LOGIC

A. Definition

Some of the basic Definitions [6] Pertaining to Reversible Logic are
Definition 1: Reversible Logic Function

A reversible logic function is a function which maps each input vector to a unique output vector. A function is said reversible if, given its output, it is always possible to determine back its input, which is the case when there is a one-to-one relationship between input and output states.

Definition 2: Reversible Logic Gate
A reversible logic gate is a device which performs such a one to one mapping. If a reversible logic gate has N inputs, then to perform one to one mapping, the number of outputs should also be N. Then this device is said to be an NxN reversible logic gate. The inputs are denoted by I_1 I_2 I_3 ... I_N and the outputs are denoted by O_1O_2 $O_3...O_N$.
Definition 3: Garbage
These are the outputs that are not used in the synthesis of a function. These may appear to be redundant but are very essential for preserving the reversibility of a gate. It is denoted by GO.
Definition 4: Constant Inputs
These are the inputs that have to be maintained at either a constant 0 or at constant 1 in order to generate a given logical expression using the reversible logic gates. It is abbreviated as CI.
Definition 5: Quantum Cost
This refers to the cost of the circuit in terms of the cost of a primitive gate. It is computed knowing the number of primitive reversible logic gates (1x1 or 2x2) required to realize the circuit. It is denoted as QC.

Definition 6: Gate Count
This refers to the number of gates that are present in the given reversible logic circuit. It is denoted by GC. Another parameter that can be defined in relation to the gate count is the flexibility, which can be defined as the ability of a reversible logic gate in realizing more functions. Higher the flexibility of a gate, lesser is the number of gates that are needed to implement a given function, lesser is the gate count.
Definition 7: Hardware Complexity
The hardware complexity [7] is measured by counting the number of AND operations, number of EX-OR operations and number of OR operations.
Let α = No. of EX-OR operation, β = No. of AND operations , δ = No. of NOT operations
Then the total hardware complexity T is given as sum of EX-OR, AND and NOT operations..

B. Reversible Logic Gate

The important basic reversible logic gates are, Feynman gate [8] which is the only 2x2 reversible gate which is as shown in the figure.1a and it is used most popularly by the designers for fan-out purposes. There is also a double Feynman gate [9],Fredkin gate [10] and Toffoli gate [11],New Gate[12] , Peres gate[13] , all of which can be used to realize important combinational functions and all are 3x3 reversible gates and are as shown in the figure.1b to figure.1e .

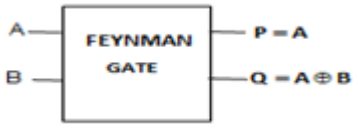

Fig 1a.Feyman gate-

Fig 1b.Fredkin gate-

Fig 1c. Toffoli gate-

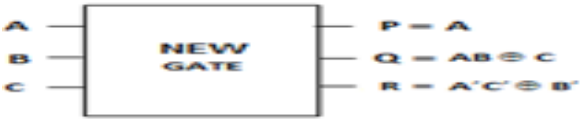

Fig 1d. Newi gate-

Fig 1e. Peres gate-

C. COG reversible gate

A 3X3 reversible gate COG (Controlled Operation Gate) logic already had been proposed [14] shown in Figure 3. The Truth table for the corresponding gate is shown in Table I also .The closer look at the Truth Table reveals that the input pattern corresponding to a specific output pattern can be uniquely determined and thereby maintaining that there is a one-to-one correspondence between the input vector and the output vector. In this gate the input vector is given by IV= (A, B, C) and the corresponding output vector is OV= (P, Q, R)

.

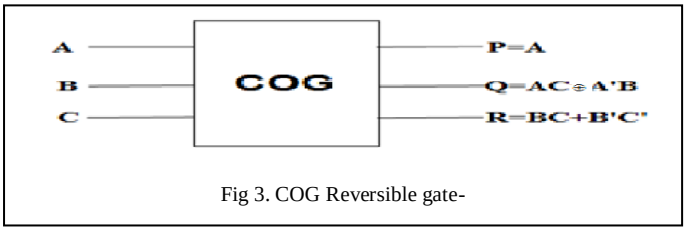

Fig 3. COG Reversible gate-

TableI. Truth table of COG Reversible gate

INPUTS			OUTPUTS		
A	**B**	**C**	**P**	**Q**	**R**
0	0	0	0	1	0
0	0	1	0	0	0
0	1	0	0	0	1
0	1	1	0	1	1
1	0	0	1	1	0
1	0	1	1	0	1
1	1	0	1	0	0
1	1	1	1	1	1

III. IMPLEMENTATION OF CONVENTIONAL BOOLEAN FUNCTION FOR BASIC DIGITAL GATES

We can implement the conventional digital gates by using the COG reversible gate. We can implement the AND, NOT,NAND, NOR, EXOR, EXNOR, OR and COPYING operation which are shown in fig 4a to 4f.In figure 4a We can see that by making the inputs A=A,B=0 and C=B of COG gate we will get AND, NOT & COPYING operation from the output lines. In this way we can get all the operation by setting the input values as per the requirement.

Fig 4a.Implementation of AND,NOT & COPYING gate by COG Reversible gates

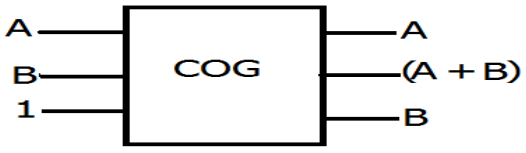

Fig 4b.Implementation of OR & COPYING gate by COG Reversible gates

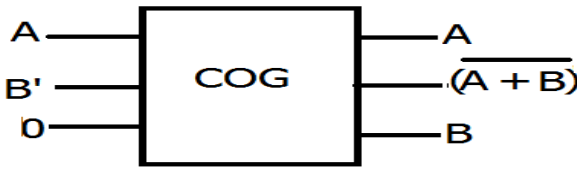

Fig 4c.Implementation of NOR & COPYING gate by COG Reversible gates

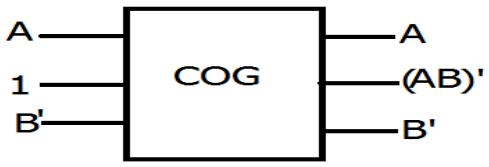

Fig 4d.Implementation of NAND,NOT & COPYING gate by COG Reversible gates

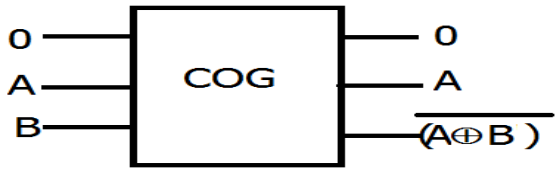

Fig 4e.Implementation of EXNOR & COPYING gate by COG Reversible gates

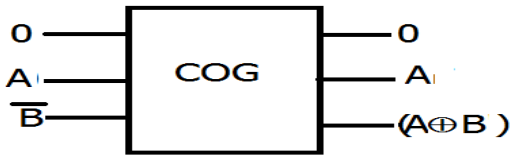

Fig 4f.Implementation of EXOR & COPYING gate by COG Reversible gates

IV. IMPLEMENTATION OF MULTI-LOGIC FUNCTION GENERATOR

A. Multi logic function generator for generating 8 functions

We have implemented a Multi-Logic Function Generator by using COG gates shown in figure 5.For this we have used seven COG reversible gates and one FEYNMAN gate. There are total eight operations at the output .In this way we can generate multiple logical function from this function generator. If two variables A and B are taken. Then the functions which are available AND operation(AB),NOR operation(A+B)',OR operation(A+B), NAND operation(AB)',EX NOR operation(A⊕B)',EXOR operation(A ⊕B),Copying operation(A),NOT operation operation(B')

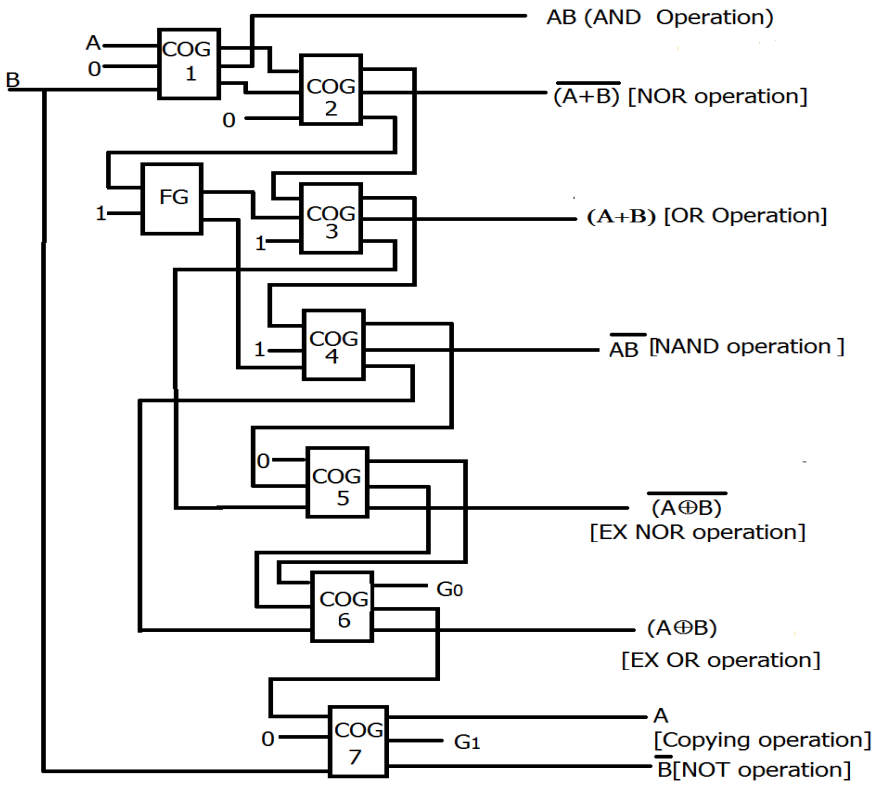

Fig 5.Implementation of MULTI –LOGIC FUNCTION GENERATOR by using COG Reversible gate for generating 8 functions

B. Multi logic function generator for generating 16 functions

We have implemented a Multi-Logic Function Generator by using COG gates shown in figure 6.For this we have used twelve COG reversible gates .There are total sixteen operations at the output .In this way we can generate multiple logical functions from this function generator. If two variables A and B are taken. Then the functions which are available at the output are AND operation(AB),NOR operation(A+B)',OR operation (A+B), NAND operation (AB)',EX-NOR operation (A⊕B)',EXOR operation(A⊕B), Transfer operation (A),

Transfer operation(B), Complement of B operation (B'),Complement of A operation(A'),A inhibits B(AB'), B inhibits A(A'B),B implies A(A+B'),A implies B(A'+B),Identity operation(1),Null operation(0).

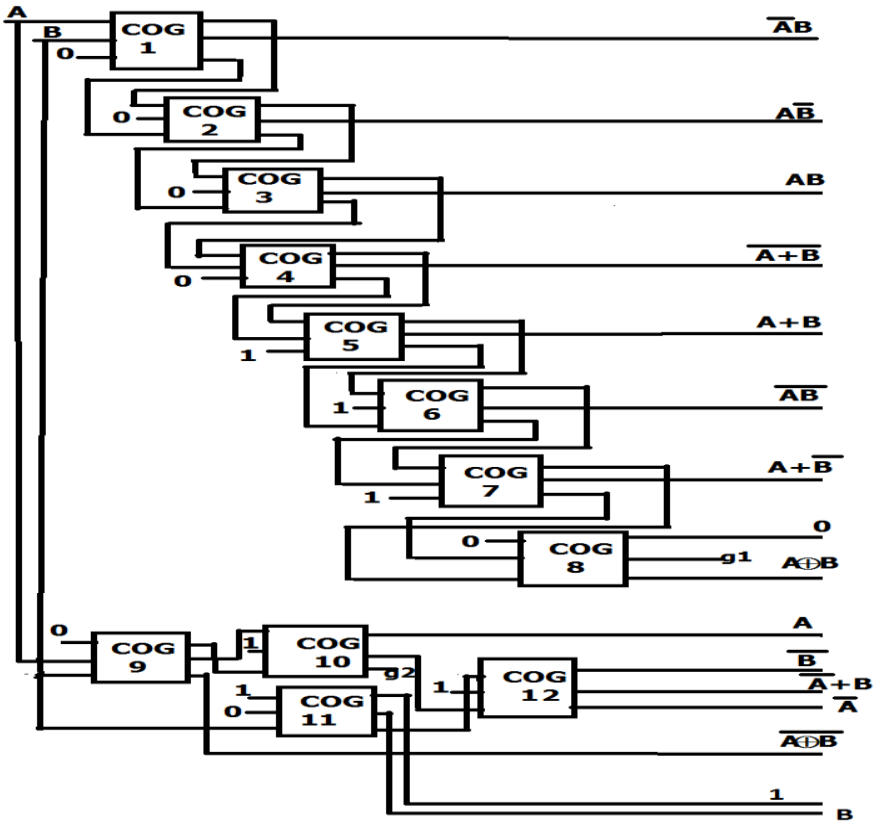

Fig 6.Implementation of MULTI –LOGIC FUNCTION GENERATOR by using COG Reversible gate for generating 16 functions

V. DESIGN OF COMBINATIONAL CIRCUIT

we can design many combinational circuit by using the reversible gates COG, one of these circuit is multiplexer. We can implement 8x1 MUX which is shown in fig7.Generally we use multiplexer for multiplexing one channel out of many channels. For this we have used seven COG reversible gates. There are three selection linesS_3,S_2,S_1 which can be used for channelizing the required input lines. There are total eight input lines I_0,I_1,I_2,I_3,I_4,I_5,I_6,I_7.Out of which we will get any one at the output depending on the selection lines value. There are 10 garbage output.

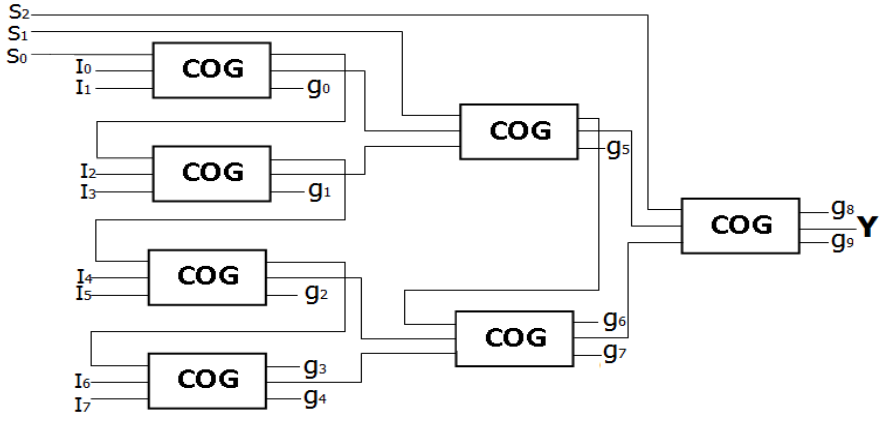

Fig 7.Implementation of 8x1 Multiplexer by COG Reversible gates

We can also implement 16x1 MUX shown in figure 8. For this we have used 15 COG reversible gates. There are four selection lines S_4,S_3,S_2,S_1 which can be used for channelizing the required input lines. There are total sixteen input lines $I_0,I_1,I_2,I_3,I_4,I_5,I_6,I_7I_8,I_9,I_{10},I_{11},I_{12},I_{13},I_{14}I_{15}$.Out of which we will get any one at the output depending on the selection lines value. There are 19 garbage outputs .

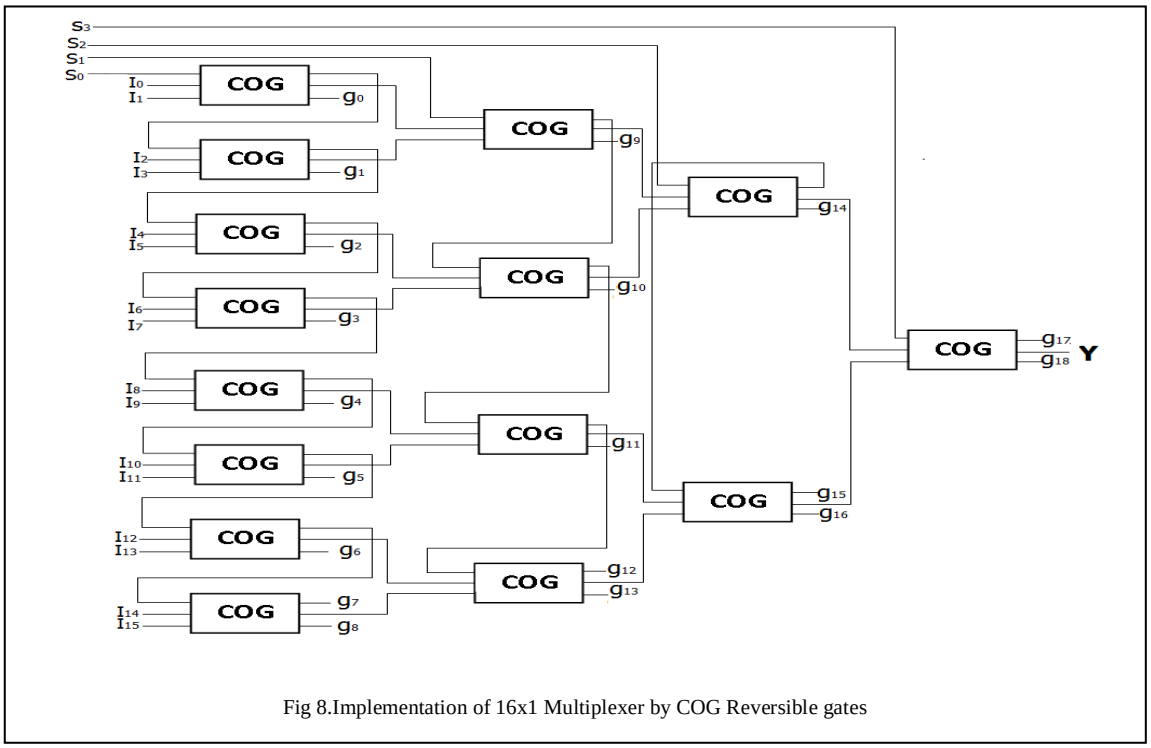

Fig 8.Implementation of 16x1 Multiplexer by COG Reversible gates

VI. IMPLEMENTATION OF PROPOSED CONTROLLED MULTI-LOGIC FUNCTION GENERATOR

A. Controlled Multi logic function generator for generating 8 functions

We have cascaded the function generator with the 8x1 multiplexer to get the controlled output shown in figure 9.Depending upon the value of the selection lines we will get the logical function at the output of the multiplexer which has already been specified.

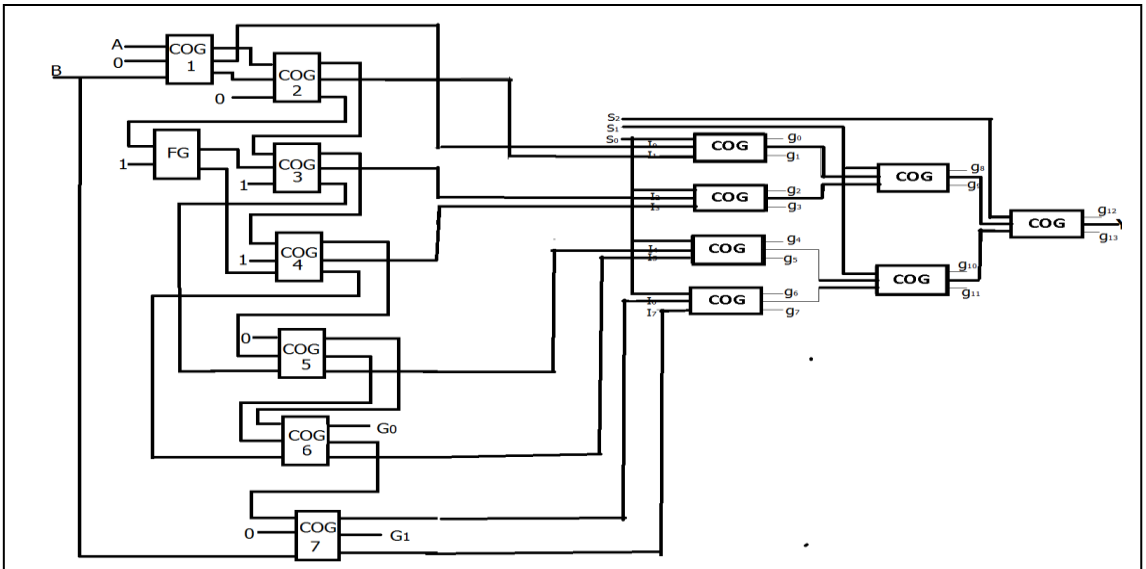

Fig 9.Implementation of controlled multi logic function generator using 8x1 Multiplexer by COG Reversible gates

So we can get the controlled behavior at the output of the circuit depending upon the values of S3, S2, and S1shown in TableII.
Table II.Variation at Output of 8x1 MUX

S3 S2 S1	Boolean function	Name of the function	Output Y of 8x1 MUX
0 0 0	(AB)	AND operation	I_0
0 0 1	(A+B)'	NOR operation	I_1
0 1 0	(A+B)	OR operation	I_2
0 1 1	(AB)'	NAND operation	I_3
1 0 0	(A⊕B)'	EX NOR operation	I_4
1 0 1	(A ⊕B)	EXOR operation	I_5
1 1 0	(A)	Copying operation	I_6
1 1 1	(B')	NOT operation	I_7

B. Controlled Multi logic function generator for generating 16 functions

We have also cascaded the function generator of 16 functions with the 16x1 multiplexer to get the controlled output shown in figure 10.Depending upon the value of the selection lines we will get the logical function at the output of the multiplexer which has already been specified by the selection values.

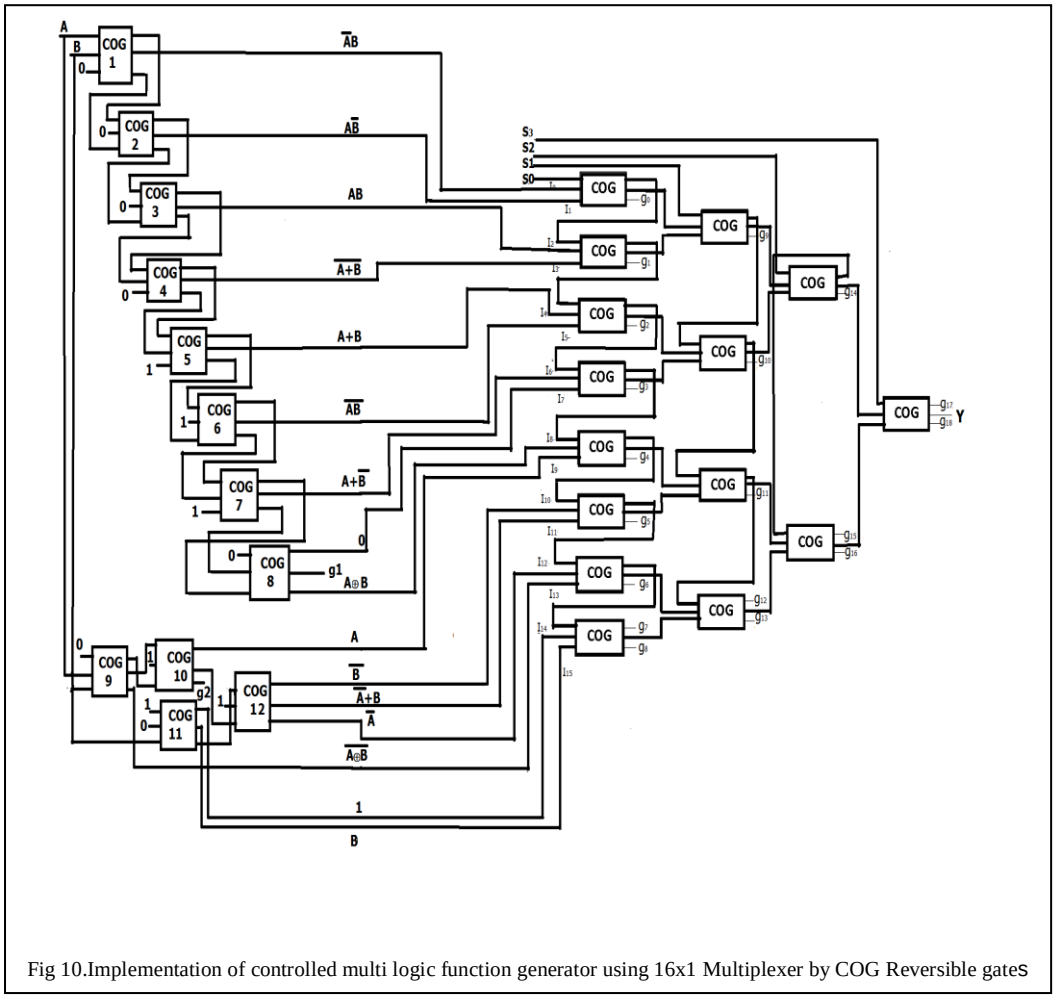

Fig 10.Implementation of controlled multi logic function generator using 16x1 Multiplexer by COG Reversible gateS

So we can get the controlled behavior at the output of the circuit depending upon the values ofS4, S3, S2, and S1shown in Table III.

Table III. Variation at Output of 16x1 MUX

S4 S3 S2 S1	Boolean function	Name of the function	Output Y of 16x1 MUX
0 0 0 0	A'B	B inhibits A	I_0
0 0 0 1	AB'	A inhibits B	I_1
0 0 1 0	AB	AND	I_2
0 0 1 1	(A+B)'	NOR	I_3
0 1 0 0	(A+B)	OR	I_4
0 1 0 1	(AB)'	NAND	I_5
0 1 1 0	A+B'	B implies A	I_6
0 1 1 1	0	Null	I_7
1 0 0 0	(A⊕ B)	EX OR	I_8
1 0 0 1	A	Transfer A	I_9
1 0 1 0	B'	Complement of B	I_{10}
1 0 1 1	A'+B	A implies B	I_{11}
1 1 0 0	A'	Complement of A	I_{12}
1 1 0 1	(A⊕ B)'	EX NOR	I_{13}
1 1 1 0	1	Identity	I_{14}
1 1 1 1	B	Transfer B	I_{15}

VII. COMPARISONS RESULTS

We have compared the proposed function generators in terms of number of gates,constant input ,garbage output and and hardware complexity shown in Table IV .

Parameters to be campared	Function Generator of 8 Functions		Function Generator of 16 Functions	
	Without Controlled Circuit	With Controlled Circuit	Without Controlled Circuit	With Controlled Circuit
Number of gates	8	15	12	27
Constant input	7	7	13	13
Garbage output	2	12	2	21
Hardware complexity	15α+14ß+14 δ	29α+28ß+28 δ	24 α+24ß+24 δ	54α+54ß+54 δ

VIII. CONCLUSIONS

We have compared the function generators in terms of number of gates, constant input, garbage output and hardware complexity shown in table IV. These proposed function generators can produce different logical functions. The 8 multi logic functions generator generates 8 logical functions whereas the 16multi logic function generator generates 16 functions. Most of the other function generator in the literature aim at producing only the main functions such as AND,OR,EX-OR and EX-NOR and use these functions to produce the remaining functions The distinguishing feature of these designs are that all the functions are produced within a single unit and the user can choose any one of the particular functions by the help of control unit .These Function generators can be efficiently used in the designing of ALU.As a future work there is vast application of these proposed designs and we would like to implement these design using quantum dot cellular automata.

IX. ACKNOWLEDGEMENTS

The authors wish to thank ECE Department and CSE Department of Murshidabad College of Engineering and Technology, Berhampore for supporting this work.

REFERENCES

[1] R.Landauer,-Irreversibility and Heat Generation in the Computational Process, IBM Journal of Research and Development , 5, pp. 183-191,1961 .

[2] C.H.Bennett, Logical Reversibility of Computation‖, IBM J.Research and Development, pp. 525-532, November 1973 .

[3] Pradeep singla and Naveen kr. Malik " A Cost - Effective Design of Reversible programmable logic array "International Journal Of Computer Application , volume 41 – no. 15, march- 2012.

[4] S.Younis and T. Knight, "Asymptotically Zero Energy Split Level Charge Recovery Logic, "Workshop on Low Power Design, June1994.
[5] Perkowski, M. and P. Kerntopf, "Reversible Logic. Invited tutorial" Proc. EURO-MICRO,Warsaw, Poland ,Sept 2001.
[6] Rakshith Saligram and Rakshith T R "Novel Code Converter employing Reversible Logic" Intl. Journal of Computer Applications, Vol 52, No. 18, Aug 2012.
[7] Md. Saiful Islam et.al" Synthesis of fault tolerant Reversible logic" IEEE 2009.
[8] R.Feynman, "Quantum Mechanical Computers", Optical News, pp. 11-20, 1985
[9] B.Parhami; "Fault Tolerant Reversible Circuits" Proc. 40th Asilomar Conf. Signals, Systems, and Computers, Pacific Grove,CA, Oct.2006.
[10] Fredkin, T. Toffoli, "Conservative Logic", International Journal of Theory. Physics, 21,pp.219-253, 1982.
[11] T.Toffoli.,"Reversible Computing", Tech memo MIT/LCS/TM - 151,MIT Lab for Computer Science (1980).
[12] Md. M. H Azad Khan, "Design of Full-adder With Reversible Gates", International Conference on Computer and Informa tion Technology, Dhaka,Bangladesh,pp.515-519,2002.
[13] Peres, A.. Reversible logic and quantum computers, Physical Review: A, 32 (6): 3266- 3276, 1985
[14] Shefali Mamataj, Biswajit Das, Anurima Rahaman "An Ease implementation of 4-bit Arithmetic Circuit for 8 Operation by using a new reversible COG gate"International Journal of Advanced Research in Electrical, Electronics and Instrumen tation EngineeringVol. 3, Issue 1, January 2014.

American Journal of Engineering Research (AJER)
e-ISSN : 2320-0847 p-ISSN : 2320-0936
Volume-03, Issue-03, pp-65-74
www.ajer.org

Research Paper Open Access

Concept of Hydrodynamic Load Calculation on Fixed Jacket Offshore Structures – An Overview of Vertically Mounted Cylinder

Aliyu Baba
(Department of Civil Engineering, Modibbo Adama University of Technology Yola, Adamawa State, Nigeria)

Abstract: - This paper focuses on the analysis of hydrodynamic loads on fixed offshore structures (vertical cylinder) that are operating in shallow water and are often subjected to huge wave loading. For the purpose of this study, linear (Airy) wave theory was adopted together with the application of (21) in the load computation. The loads for six different sea states were computed using spread sheet for the following values of time interval t = 0, T/4, T/2.

Keywords: *– Airy wave theory, Fixed Jacket Offshore Structure, Morrison equation, Vertically Mounted Cylinder*

I. INTRODUCTION

Hydrodynamic wave loading on fixed offshore structures has been an issue of concern to the offshore oil and gas industry. The analysis, design and construction of offshore structures are arguably one of the most demanding sets of tasks faced by the engineering profession. Over and above the usual conditions and situations met by land-based structures, offshore structures have the added complication of being placed in an ocean environment where hydrodynamic interaction effects and dynamic response become major considerations in their design. In general, wave and current can be found together in different forms in the ocean. The existence of waves and currents and their interaction play a significant role in most ocean dynamic processes and are important for ocean engineers.

In addition, the range of possible design solutions, such as: Tension Leg Platform (TLP) deep water designs; the more traditional jacket and jack-up oil rigs; and the large number of sized gravity-style offshore platforms themselves, pose their own peculiar demands in terms of hydrodynamic loading effects, foundation support conditions and character of the dynamic response of not only the structure itself but also of the riser systems for oil extraction adopted by them. Invariably, non-linearity in the description of hydrodynamic loading characteristics of the structure-fluid interaction and in the associated structural response can assume importance and need be addressed. Access to specialist modelling software is often required to be able to do so [1].

1.1 Basics of Offshore Engineering

A basic understanding of a number of key subject areas is essential to an engineer likely to be involved in the design of offshore structures, [2], [3], [4] and [5].
These subject areas, though not mutually exclusive, would include;

- Hydrodynamics
- Structural dynamics
- Advanced structural analysis techniques
- Statistics of extreme among others.

1.2 Hydrodynamics

Hydrodynamics is concerned with the study of water in motion. In the context of an offshore environment, the water of concern is the ocean. Its motion, (the kinematics of the water particles) stems from a number of sources

including slowly varying currents from the effects of the tides and from local thermal influences and oscillatory motion from wave activity that is normally wind-generated [1].

The characteristics of currents and waves, themselves would be very much site dependent, with extreme values of principal interest to the LFRD approach used for offshore structure design, associated with the statistics of the climatic condition of the site interest [6].

The topology of the ocean bottom also has influence on the water particle kinematics as the water depth changes from deeper to shallower conditions, [7]. This influence is referred to as the "shoaling effect", which assumes significant importance to the field of coastal engineering. For so called deep water conditions (where the depth of water exceeds half the wavelength of the longest waves of interest), the influence of the water bottom topology on the water particle kinematics is considered negligible, removing an otherwise potential complication to the description of the hydrodynamics of offshore structures in such deep water environment.

II. METHODOLOGY AND MATERIALS

The jacket structure used for this study (Fig. 5) is a HD accommodation platform to be operated in shallow water and is similar to all fixed jacket offshore structures. The part of the structure under water was discretized in to (264) beam elements. The water depth for the HD field is approximately 25.3m. The loads were computed using spread sheet. See TABLE I for the most probable wave heights and time periods for different sea states.

3.1 Wave Theories

All wave theories obey some form of wave equation in which the dependent variable depends on physical phenomena and boundary conditions [8]. In general, the wave equation and the boundary conditions may be linear and non linear.

3.1.1 Airy Wave Theory

The surface elevation of an Airy wave amplitude ζ_a, at any instance of time t and horizontal position x in the direction of travel of the wave, is denoted by η(x,t) and is given by:

$$\eta(x,t) = \zeta_a \cos(kx - \omega t) \quad \text{"equation 1"}$$

where wave number k = 2π/L in which L represents the wavelength (see fig. 1) and circular frequency ω = 2π/T in which T represents the period of the wave. The celerity, or speed, of the wave C is given by L/T or ω/k, and the crest to trough wave height, H is given by $2\zeta_a$. The along wave u(x, t) and vertical v(x, t) water particle velocities in an Airy wave at position z measured from the Mean Water Level (MWL) in depth water h are given by:

$$u(x,t) = \frac{\omega\zeta_a \cosh[k(z+h)]}{\sinh(kh)} \cos(kx - \omega t) \quad \text{"equation 2"}$$

$$v(x,t) = \frac{\omega\zeta_a \sinh[k(z+h)]}{\sinh(kh)} \sin(kx - \omega t) \quad \text{"equation 3"}$$

The dispersion relationship relates wave number k to circular frequency ω (as these are not independent), via:

$$\omega^2 = gk\tanh(kh) \quad \text{"equation 4"}$$

where g is the acceleration due to gravity (9.8 m/s^2). The along wave acceleration $\dot{u}(x, t)$ is given by the time derivative of (2) as:

$$\dot{u}(x,t) = \frac{\omega^2\zeta_a \cosh[k(z+h)]}{\sinh(kh)} \sin(kx - \omega t) \quad \text{"equation5a"}$$

while the vertical velocity $\dot{v}(x, t)$ is given by the time derivative of (3) as:

$$\dot{v}(x,t) = -\frac{\omega^2\zeta_a \sinh[k(z+h)]}{\sinh(kh)} \cos(kx - \omega t) \quad \text{"equation 5b"}$$

It should be noted here that wave amplitude, $a = \zeta_a$, is considered small (in fact negligible) in comparison to water depth h in the derivation of Airy wave theory.

For deep water conditions, kh > π, (2) to (5) can be approximated to:

$$u(x,t) = \omega\zeta_a e^{kz} \cos(kx - \omega t) \quad \text{"equation 6"}$$

$$v(x,t) = \omega\zeta_a e^{kz} \sin(kx - \omega t) \quad \text{"equation 7"}$$

$$\omega^2 = gk \quad \text{"equation 8"}$$

$$\dot{v}(x,t) = \omega^2\zeta_a e^{kz} \sin(kx - \omega t) \quad \text{"equation 9"}$$

This would imply that the elliptical orbits of the water particles associated with the general Airy wave description in (2) and (3), would reduce to circular orbits in deep water conditions as implied by (6) and (7).

3.1.2 Stoke's Second Order Wave Theory

Stokes employed perturbation techniques to solve the wave boundary value problem and developed a theory for finite amplitude wave that he carried to the second order. In this theory, all the wave characteristics (velocity potential, celerity, surface profile, particle kinetics….e.tc) are formulated in terms of a power series in successively higher orders of the wave steepness (H/L).

A condition of this theory is that (H/d) should be small so that the theory is applicable only in deep water and a portion of the immediate depth range.

For engineering applications, the second-order and possibly the fifth-order theories are the most commonly used [9].

Stoke's wave expansion method is formally valid under the conditions [10]:

H/d << (kd)2 for kd < 1 and H/L << 1.

Stoke's wave theory is considered most nearly valid in water where the relative depth (D/L) is greater than about (1/10) [11]. Stoke's theory would be adequate for describing water waves at any depth of water. In shallow water, the connective terms become relatively large, the series convergence is slow and erratic and a large number of terms are required to achieve a uniform accuracy [12].

The fluid particle velocities are then given by;

$$v_x = \frac{\pi H}{T}\frac{\cosh[k(z+h)]}{\sinh(kh)}\cos(k(kx-\omega t)) + \frac{3(\pi H)^2}{4TL}\frac{\cosh[2k(z+h)]}{\sinh^4(kh)}\cos 2(kx-\omega t) \quad \text{“equation 9a”}$$

$$v_z = \frac{\pi H}{T}\frac{\sinh[k(z+h)]}{\sinh(kh)}\sin(k(kx-\omega t)) + \frac{3(\pi H)^2}{4TL}\frac{\sinh[2k(z+h)]}{\sinh^4(kh)}\sin 2(kx-\omega t) \quad \text{“equation 9b”}$$

The fluid particle accelerations are then given by;

$$a_x = 2\frac{\pi^2 H}{r^2}\frac{\cosh[k(z+h)]}{\sinh(kh)}\sin(kx-\omega t) + \frac{3\pi^3 H^2}{T^2 L}\frac{\cosh[2k(z+h)]}{\sinh^4(kh)}\sin 2(kx-\omega t) \quad \text{“equation 10a”}$$

$$a_z = 2\frac{\pi^2 H}{r^2}\frac{\sinh[k(z+h)]}{\sinh(kh)}\cos(kx-\omega t) + \frac{3\pi^3 H^2}{T^2 L}\frac{\sinh[2k(z+h)]}{\sinh^4(kh)}\cos 2(kx-\omega t) \quad \text{“equation 10b”}$$

These velocities and accelerations in (9) and (10) are used in Morison's equation to calculate load vectors of hydrodynamic loading by using Stoke's wave theory after being transformed from global coordinates for each member of the offshore structure.

3.2 Morison's Equation

The along wave or in-line force per unit length acting on the submerged section of a rigid vertical surface-piercing cylinder, *F* (z, t), from the interaction of the wave kinematics at position *z* from the MWL, (see Fig. 2), is given by Morison's equation. This equation is originally developed to compute hydrodynamic forces acting on a cylinder at a right angle to the steady flow, and is given by:

$$F(z,t) = \rho\,\pi\frac{D^2}{4}C_m\,a(z,t) + \frac{1}{2}\rho\,D\,C_d\,V|V|(z,t) \quad \text{“equation 11”}$$

in this (11), it is assumed that the wave force is acting on the vertical distance (z, t) of the cylinder due to the velocity (v) and acceleration (a) of the water particles, where (ρ) is the density of water, (D) is the cylinder diameter, (C_m) and (C_d) are inertia and drag coefficients, F_D and F_I are drag force and inertia force [13].

$$F_D = \frac{1}{2}\rho\,D\,C_d\,V|V|(z,t) \quad \text{“equation 12”}$$

$$F_I = \rho\,\pi\frac{D^2}{4}C_m\,a(z,t) \quad \text{“equation 13”}$$

These coefficients are found to be dependent upon Reynold's number, *Re*, Keulegan Carpenter number, KC, and the β parameter, Viz;

$$KC = \frac{u_m}{D}T;\ \beta = \frac{Re}{KC} \quad \text{“equation 14”}$$

Where u_m = the maximum along wave water particle velocity. It is found that for KC < 10, inertia forces progressively dominate; for 10 < KC < 20 both inertia and drag force components are significant and for KC > 20, drag force progressively dominates [1].

Various methods exist for the calculation of the hydrodynamic loads on an arbitrary oriented cylinder by using Morison's equation. The method adopted here assumes that only the components of water particles and accelerations normal to the member produce [14].

To formulate the hydrodynamic load vector F_w, consider the single, bottom mounted cylindrical member (as shown in Fig. 2). The forces are found by the well known semi-empirical Morison's formula (11). It also represents the load exerted on a vertical cylinder, assuming that the total force on an object in the wave is the sum of drag and inertia force components. This assumption (introduced by Morison) takes the drag term as a function of velocity and the inertia force as a function of acceleration [15], [16] and [17], so that:

$$F_n = \rho \pi \frac{D^2}{4} C_m v_n' - (C_m - 1) \rho \pi \frac{D^2}{4} u_n'' + \frac{1}{2} \rho D C_d (v_n - u_n') |(v_n - u_n')| \quad \text{"equation 15a"}$$

This can be simplified to:

$$F_n = \rho \pi \frac{D^2}{4} C_m v_n' + \frac{1}{2} \rho D C_d (v_n) . |(v_n)| \quad \text{"equation15b"}$$

Where:

F_n = nodal hydrodynamic force normal to the cylinder, D = Outer diameter of cylinder, ρ = Sea water density. C_d = Drag coefficient (= 1.05). v_n' = water particle acceleration. C_m = Inertia coefficient (= 1.2). v_n = water particle velocity. u_n' = Structural velocity. u_n'' = Structural acceleration.

(15b) neglects the non-linear terms of drag coefficient [2] and [18] water particle velocity and acceleration can be evaluated by potential velocity computed from wave theories; the absolute value of velocity is needed to preserve the sign variation of the force.

3.2.1 Global and Local System

The kinematics of cross-flow with resultant velocity (see Fig. 3) is;

$$[U_L] = [t][U_g] \quad \text{"equation 16"}$$

$$W_n = \sqrt{u' + w'} \quad \text{"equation 17"}$$

is determined using wave theory applied in the global system and then transferred to the local system using transformation matrix (see Fig. 4).

Application of Morison's equation leads to:

$$F_L = \rho \pi \frac{D^2}{4} C_m \frac{du}{dt} + \frac{1}{2} \rho D C_d (w_n) . |(w_n)| \quad \text{"equation 18"}$$

The components of the forces in the local axis system then become;

$$\begin{bmatrix} f_y' \\ f_z' \end{bmatrix} = \frac{1}{2} \rho D C_d (w_n) |(w_n)| \begin{bmatrix} u' \\ w' \end{bmatrix} + \rho \pi \frac{D^2}{4} C_m \begin{bmatrix} u'' \\ w'' \end{bmatrix} \quad \text{"equation 19"}$$

To get the local forces, we need to get the matrices as follows;

$$T = \begin{array}{c|ccc} & X & Y & Z \\ x' & 0 & 0 & 1 \\ y' & 0 & 1 & 0 \\ z' & -1 & 0 & 0 \end{array} \quad ; \qquad T^{-1} = \begin{array}{c|ccc} & X & Y & Z \\ x' & 0 & 0 & -1 \\ y' & 0 & 1 & 0 \\ z' & 1 & 0 & 0 \end{array}$$

Therefore, the local forces are given as:-

$$\begin{bmatrix} f_x' \\ f_y' \\ f_z' \end{bmatrix} = \frac{1}{2} \rho D C_d (w_n) |(w_n)| [T] \begin{bmatrix} u' \\ v' \\ w' \end{bmatrix} + \rho \pi \frac{D^2}{4} C_m \begin{bmatrix} u'' \\ v'' \\ w'' \end{bmatrix} \quad \text{"equation 20"}$$

The local forces are then transferred in to global forces by the transpose matrix.

$$F_w = \begin{bmatrix} F_x \\ F_y \\ F_z \end{bmatrix} = [T]^{-1} \begin{bmatrix} 0 \\ f_y' \\ f_z' \end{bmatrix} \quad \text{"equation 21"}$$

III. RESULTS

The loads for six different sea states were computed using spread sheet for the following values of time intervals, t = 0, T/4, T/2. The magnitudes of these forces are presented graphically in Figures 6, 7, 8, 9, 10 and 11when x= 0 and x = 16m.

IV. CONCLUSION

The results for this work are thus;

1. The hydrodynamic force is directly proportional to the depth *z* and is minimum at *z = 0.*
2. For all the sea state, all the hydrodynamic forces follow the same directions as the direction of the wave propagation (as forces pushing the member) at time *t = T/2* and *t = 0* when distance *x = 0* and 16m respectively. (see Figures 8 and 9)
3. Also, all the hydrodynamic forces at time *t = 0, t = T/4* and *t = T/2* when distance *x = 0*, *= 0* and *x* = 16m respectively, are in direction (as forces pulling the member) similar to the direction of the wave propagation for all the sea states. (see Figures 6, 7 and 11)
4. In Figure 10, the hydrodynamic forces follow the same directions of the wave propagation (as both pushing and pulling forces) due to changes in sea states.
5. At constant time *t*, distance *x* and depth *z*, all the hydrodynamic forces are different for different sea state.

V. ACKNOWLEDGEMENT

This work was successful through the able guidance of Dr. H. S. Chan, School of Marine Science and Technology, Newcastle University, United Kingdom and (Name (s) of Reviewer(s)) for assistance in reviewing this paper.

REFERENCES

[1] Haritos, N, University of Melbourne, Australia, *Introduction to the Analysis and Design of Offshore Structures-An Overview, 2007.*
[2] Sarpakava, T and Isaacson, M, John Wiley and Sons, *Mechanics of Wave Forces on Offshore Structures*, 1981.
[3] Chakrabarti, S. K, Southampton, Computational Mechanics Publication, *Fluid Structure Interaction in Offshore Engineering*, (ed) 1987.
[4] Graff, W. J, Houston, Gulf Publishing Company, I*ntroduction to Offshore Structures – Design, fabrication, Installation*, 1981.
[5] DNV-OS-C101, General (LFRD Method), Det Norske Veritas, Norway, *Design of Offshore Steel Structures*, 2004.
[6] Nigam, N.C and Narayanan, S, New York, Springer-Verlag, *Applications of Random Vibrations*, 1994.
[7] Dean, R. G., and Dalrymple, R. A, New Jersey, world scientific, *Water waves Mechanics for engineers and Scientis*ts, 1991.
[8] Al-Salehy, S. M. S, *Dynamic Analysis of Offshore Structure Using Finite Element Method*, MSc Thesis, Basrah University, Iraq, 2002.
[9] Sorensen, R.M, Springer Science and Business Media, Inc, *Basic Coastal Engineering*, 2006.
[10] Iraninejid, B, *Dynamic Analysis of Fixed Offshore Platforms Subjected to Non-linear hydrodynamic Loading*, PhD Thesis, Illinois Institute of Technology, 1988.
[11] Patal, M, Buttler and Tanner Co., England, *Dynamics of Offshore Structures*, 1989.
[12] Muga, B. J, Edited by James F. Wilson, John Wily and Sons, *Deterministic Description of Offshore Waves-Dynamic of Offshore Structure*, 2003.
[13] Madhujit, M. and Sinha, S.K, Journal of the Ocean Engineering, *Modeling of Fixed Offshore Towers in Dynamic Analysis*, 15(6), 1988.
[14] Qian, J. and Wang, X, International Journal of computers and Structures, *Three –Dimensional Stochastic Response of Offshore Towers to Random Sea waves*, 43(2), 1992.
[15] Zienkiewicz, O.C., Lewis, R.W and Stagg, K.G, John Wiley and Sons, *Numerical Methods In Offshore Engineering*, 1978.
[16] Dean, R. G., and Dalrymple, R. A, Prentice – Hall, Inc., *Water waves Mechanics for Engineers and Scientis*ts, 1984.
[17] McCormic, M. E, John Wiley and Sons: New York, *Ocean Engineering Wave Mechanics*, 1973.
[18] Al-Jasim, S. A. J, *Dynamic Analysis of Offshore Template Structures with Soil Structure Interaction*, PhD Thesis: University of Basrah, Iraq, March, 2000.

Figures and Table

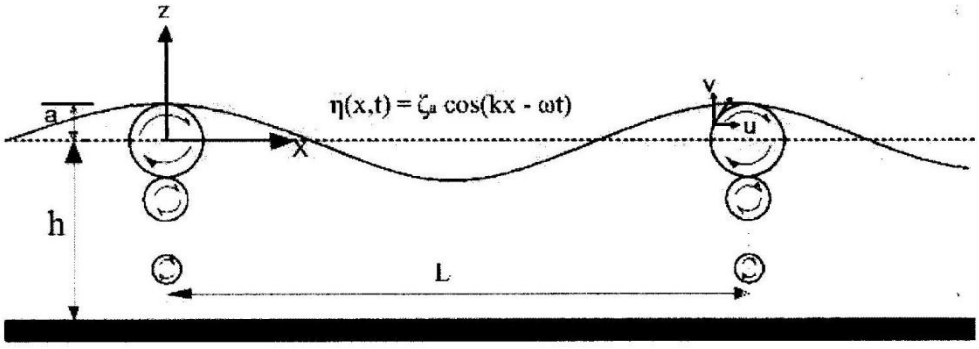

Figure 1: definition diagram for an airy wave [1]

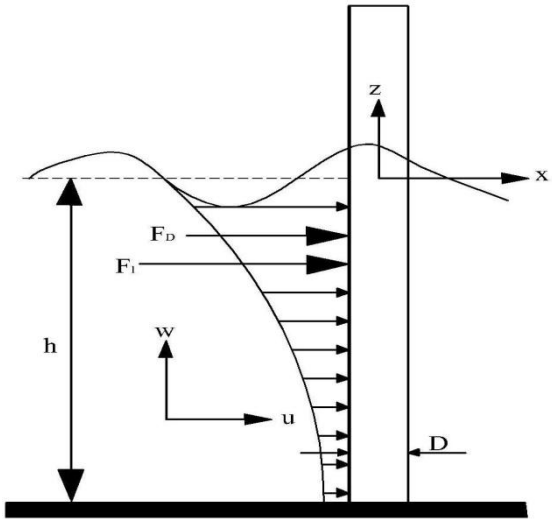

Figure 2: wave loading on a surface-piercing bottom mounted cylinder [1]

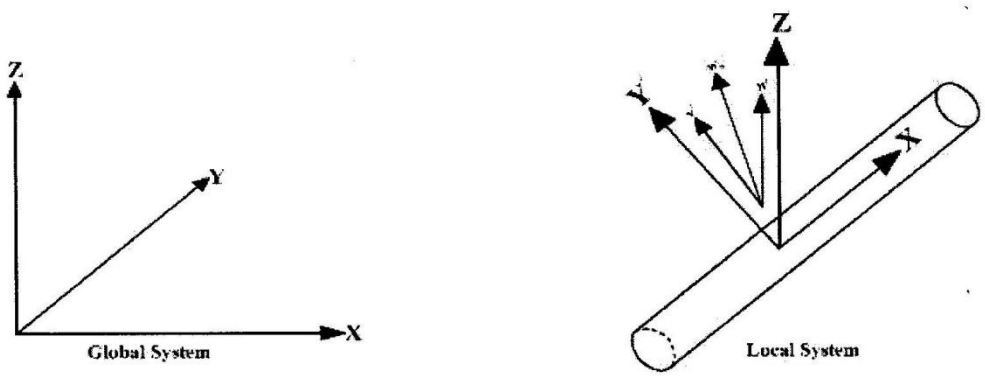

Figure 3: global and local system

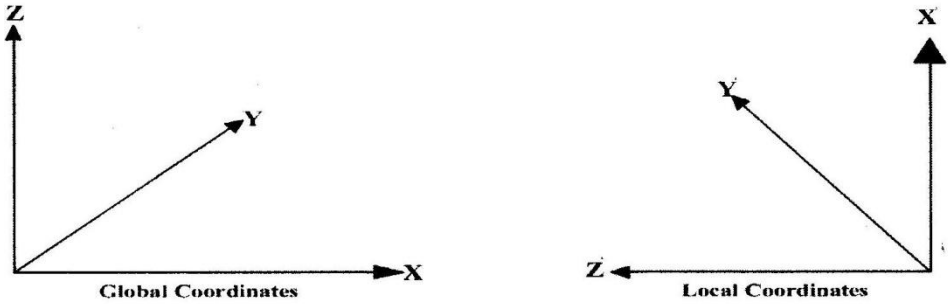

Figure 4: global and local coordinates

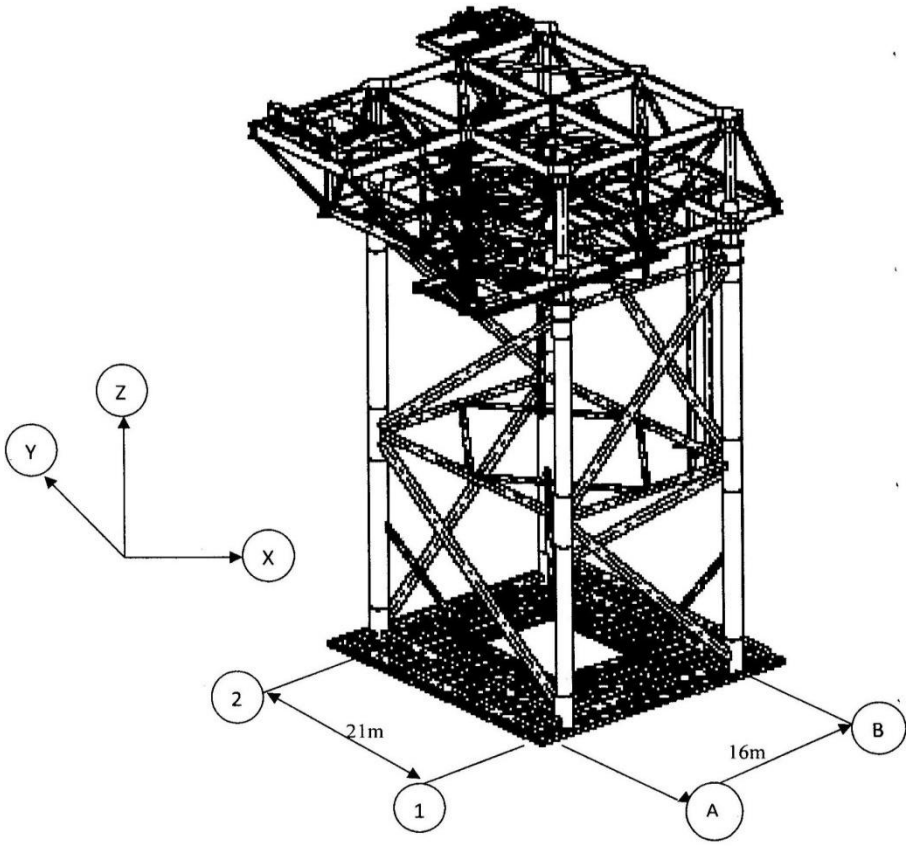

Figure 5: HD accommodation platform

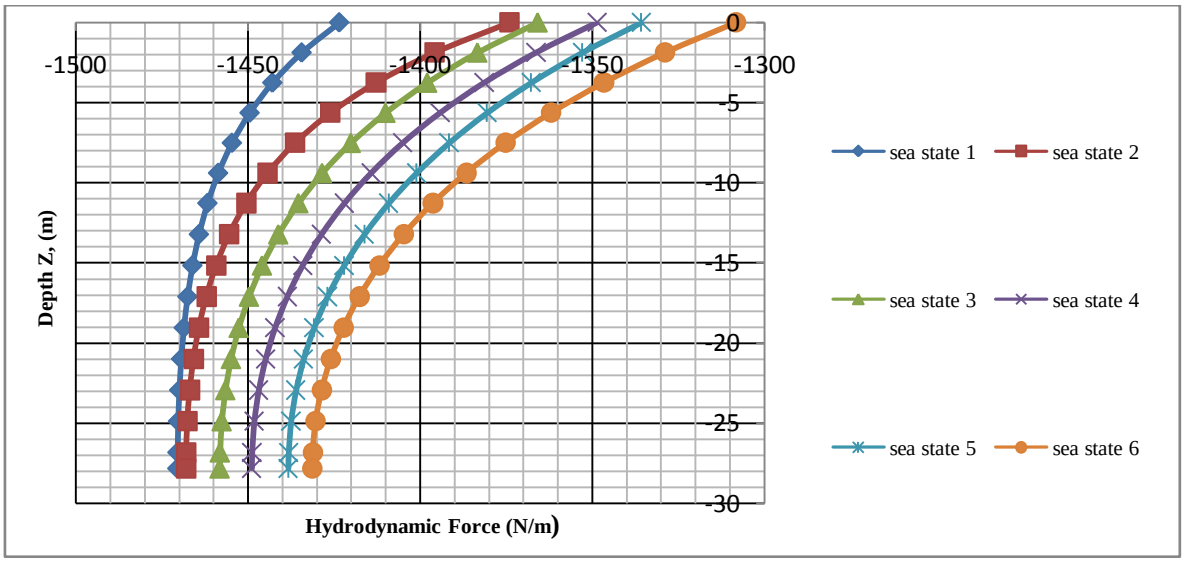

Figure 6: variation of hydrodynamic forces with depth (@ time t = 0 and distance x = 0)

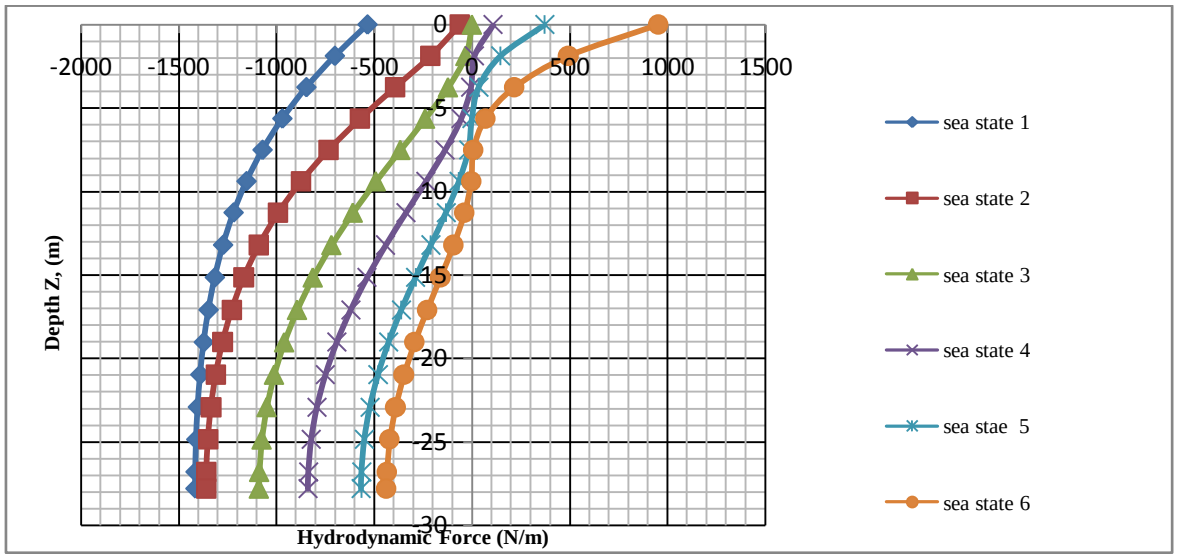

Figure 7: variation of hydrodynamic forces with depth (@ time t = T/4 and distance x = 0)

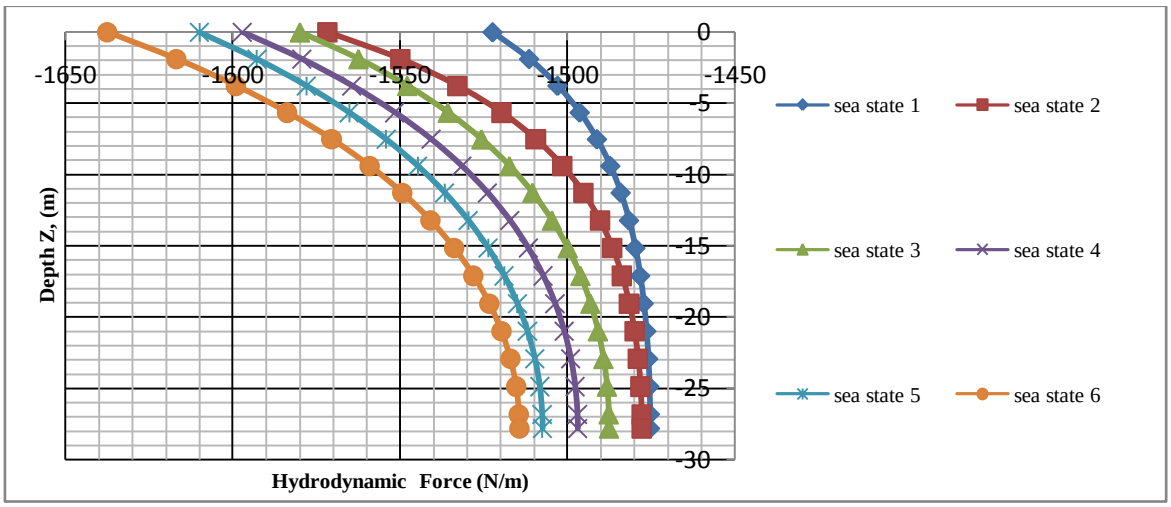

Figure 8: variation of hydrodynamic forces with depth (@ time t = T/2 and distance x = 0)

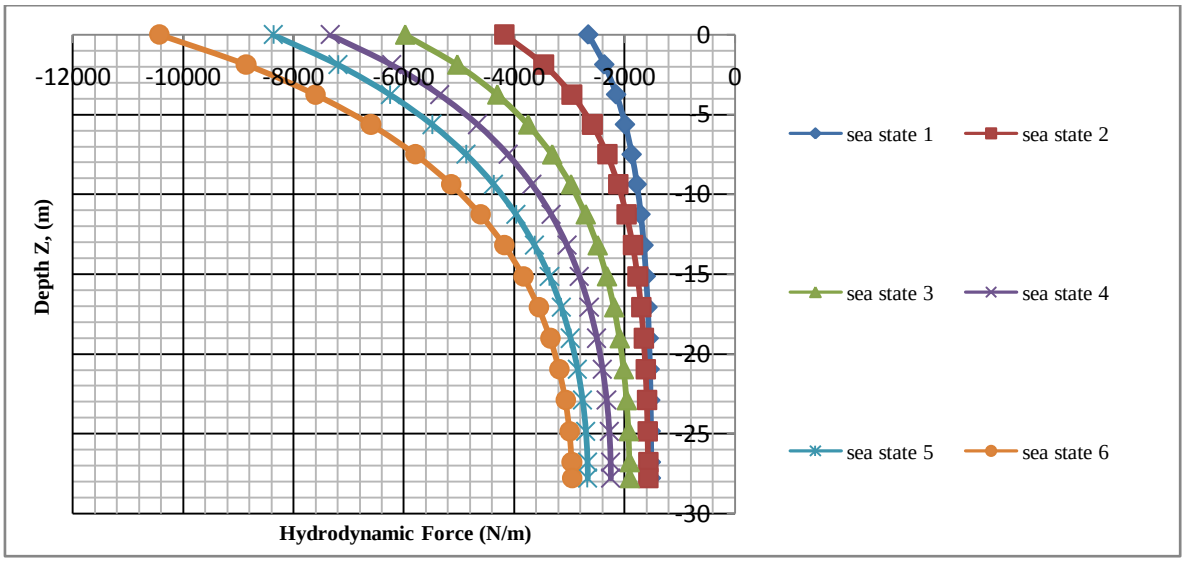

Figure 9: variation of hydrodynamic forces with depth (@ time t = 0 and distance x = 16m)

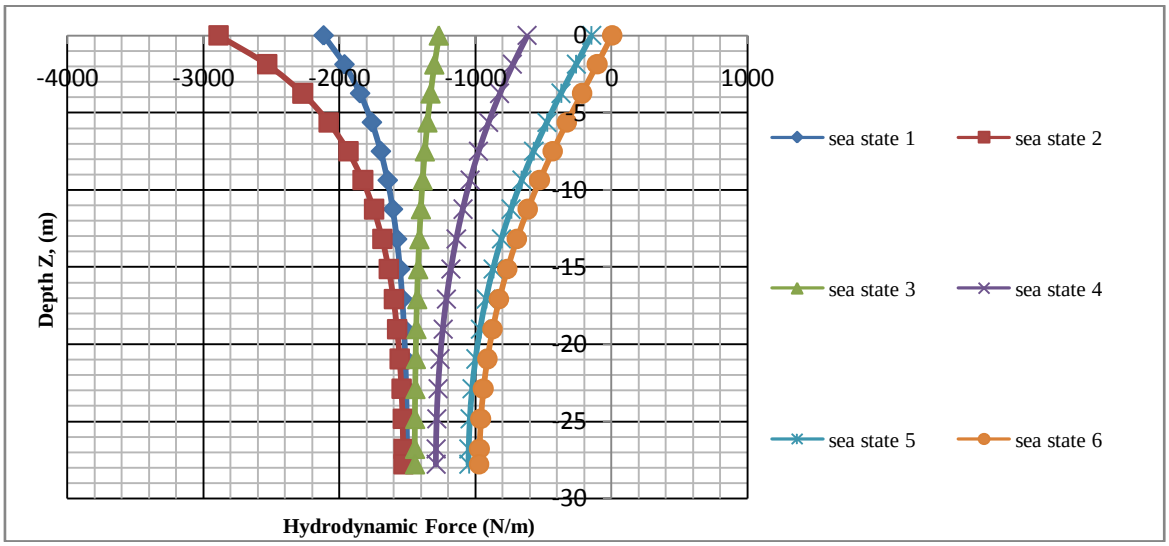

Figure 10: variation of hydrodynamic forces with depth (@ time t = T/4 and distance x = 16m)

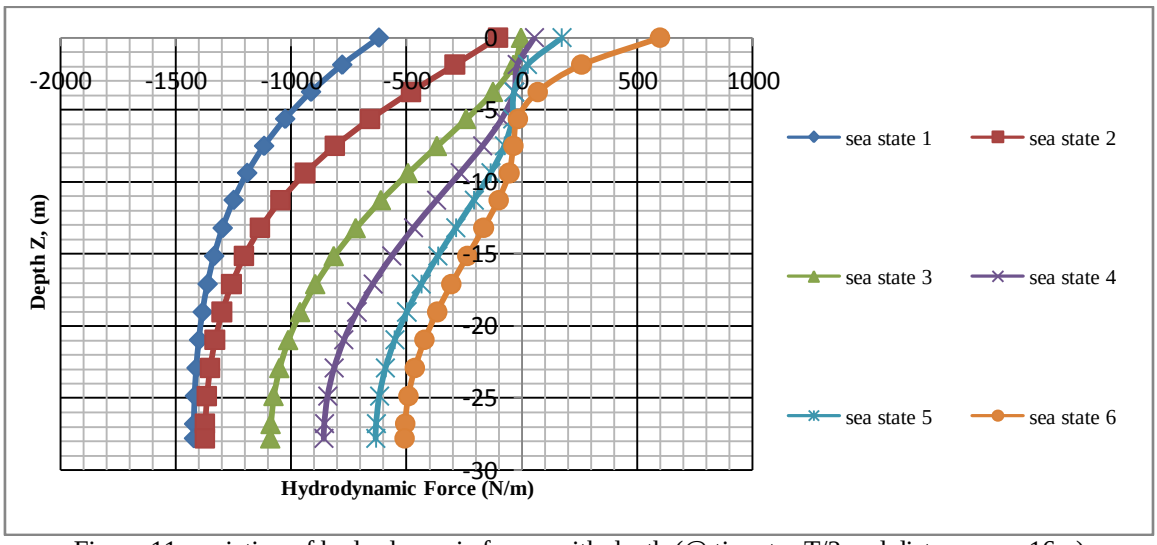

Figure 11: variation of hydrodynamic forces with depth (@ time t = T/2 and distance x = 16m)

Table I: Most Probable Wave Heights and Time Periods for Different Sea States (Area 59)

Sea State	Hs (m)	Tp (sec)	ζa (m)	t (sec)	k
1	1	5.5	0.5	4.125	0.133
2	2	5.5	1	4.125	0.133
3	3	6.5	1.5	4.875	0.0961
4	4	7	2	5.25	0.08371
5	5	7.5	2.5	5.625	0.0739
6	6	7.5	3	5.625	0.0739

American Journal of Engineering Research (AJER)
e-ISSN : 2320-0847 p-ISSN : 2320-0936
Volume-03, Issue-03, pp-75-79
www.ajer.org

Research Paper Open Access

Quasi-Static transient Thermal Stresses in a Neumann's thin Solid cylinder with internal moving heat source

[1]D. T. Solanke, [2]M. H. Durge
[1]*Sudhakar Naik and Umashankar Khetan college Akola, Maharashtra State, India.*
[2]*Anand Niketan Collge, Warora, Maharashtra State, India.*

Abstract: **-** This paper concern with transient non-homogeneous thermoelastic problem with Neumann's boundary condition in thin solid cylinder of isotropic material of radius a and height h, occupying the space $0 \le r \le a, 0 \le z \le h, 0 \le \phi \le 2\pi$ having initial temperature $f(r,\phi,z)$ placed in an ambient temperature zero. The cylinder is subjected to the activity of moving heat source along circular trajectory of radius r_0, where $0 < r_0 < a$, around the centre of the cylinder with constant angular velocity ω. Heat conduction equation containing heat generation term is solved by applying integral transform technique and Green's theorem is adopted in deducing the solution of heat conduction equation. The solution is obtained in a series form of Bessel function and trigonometric function and derived thermal stresses.

Keywords: **-** *Neumann's solid thin cylinder, moving heat source, thermal stresses, Green's theorem.*

I. INTRODUCTION

During the second half of 20th century, non-isothermal problems of the theory of elasticity became increasingly important. This is due to their wide application in diverse fields. The high velocities of modern aircraft give rise to aerodynamic heating, which produces intense thermal stresses that reduce the strength of aircraft structure.

No one previously studied such type of thermal stresses with moving heat source in thin solid cylinder with Neumann's boundary condition. This is new contribution to the field of thermoelasticity. Recently D. T. solanke ,S. M. Durge have studied the thermal stresses, in thin solid cylinder with Dirichlet's boundary condition [4]. In this present paper we determine temperature, thermal stresses, in a Neumann's thin solid cylinder, determined by $0 \le r \le a, 0 \le z \le h, 0 \le \phi \le 2\pi$ with internal moving heat source. Heat conduction equation with heat generation term is solved by applying integral transform technique and Green's theorem. Solution is obtained in series form of Bessel function and trigonometric function. The direct problems is very important in view of its relevance to various industrial mechanics subjected to heating such as main shaft of lathe, turbines and the role of rolling mill for base of furnace boiler of thermal power plant, gas power plant and measurement of aerodynamic heating.

II. FORMULATION OF THE PROBLEM

Consider a thin solid cylinder of isotropic material of radius a and height h, occupying the space $0 \le r \le a, 0 \le z \le h, 0 \le \phi \le 2\pi$ having initial temperature $f(r,\phi,z)$ placed in an ambient temperature zero. The cylinder is subjected to the activity of moving heat source which changes its place along circular trajectory of radius r_0, where $0 < r_0 < a$, around the centre of the cylinder with constant angular velocity ω. The activity of moving heat source and its initial temperature of the cylinder may cause the generation of heat due to nuclear interaction that may be a function of position and time in the form $g(r,\phi,z,t)$. The temperature distribution of thin solid cylinder is described by the differential equation of heat heat conduction with heat generation term as in [3] on page no. 232 is given by

$$\nabla^2 T + \frac{1}{k} g = \frac{1}{\alpha} \frac{\partial T}{\partial t}$$

where ∇^2 is Laplacian operator in cylinder, $T = T(r, \phi, z)$ is temperature distribution, k is thermal conductivity of the material of the cylinder, $\alpha = \dfrac{k}{\rho c_p}$ is thermal diffusivity, ρ is density, c_p is specific heat of the material and g is volumetric energy generation in the cylinder.

Now consider an instantaneously moving heat source $g_s^{\,i}$ located at a point (r_0, ϕ', ξ) and releasing its energy spontaneously at time τ. Such volumetric heat source in cylindrical coordinates is given by

$$g(r, \phi, z, t) = g_s^{\,i} \frac{1}{2\pi r} \delta(r - r_0)\delta(\phi - \phi')\delta(z - \xi)\delta(t - \tau)$$

Hence above equation reduces to

$$\nabla^2 T + g_s^{\,i} \frac{1}{2\pi r} \delta(r - r_0)\delta(\phi - \phi')\delta(z - \xi)\delta(t - \tau) = \frac{1}{\alpha} \frac{\partial T}{\partial t} \quad (3.1)$$

$$\phi' = \omega t \quad (3.2)$$

With initial and boundary condition

$$\frac{\partial T}{\partial r} = 0 \quad \text{at} \quad r = a \quad (3.3)$$

$$\frac{\partial T}{\partial z} = 0 \quad \text{at} \quad z = 0 \quad (3.4)$$

$$\frac{\partial T}{\partial z} = 0 \quad \text{at} \quad z = h \quad (3.5)$$

$$T = f(r, \phi, z) \quad \text{at} \quad t = 0 \quad (3.6)$$

4. Formulation of thermoelastic Problem:

Let us introduce a thermal stress function χ related to component of stress in the cylindrical coordinates system as in [3]

$$\sigma_{rr} = \frac{1}{r} \frac{\partial \chi}{\partial r} + \frac{1}{r^2} \frac{\partial^2 \chi}{\partial r^2} \quad (4.1)$$

$$\sigma_{\phi\phi} = \frac{\partial^2 \chi}{\partial r^2} \quad (4.2)$$

$$\sigma_{r\phi} = -\frac{\partial}{\partial r}\left(\frac{1}{r} \frac{\partial \chi}{\partial \phi}\right) \quad (4.3)$$

The boundary condition for a traction free body are

$$\sigma_{rr} = 0, \sigma_{r\phi} = 0 \quad \text{at} \quad r = a \quad (4.4)$$

$$\text{Where} \quad \chi = \chi_c + \chi_p \quad (4.5)$$

Where χ_c is complementary solution and χ_p is particular solution and

$$\chi_c \text{ satisfies the equation } \nabla^4 \chi_c = 0 \quad (4.6)$$

χ_p satisfies the equation $\nabla^4 \chi_p = -\lambda E \nabla^2 \Gamma$ (4.7)

Where Γ is temperature change and $\Gamma = T - T_i$ T_i is initial temperature

$\nabla^2 = \frac{\partial^2}{\partial r^2} + \frac{1}{r}\frac{\partial}{\partial r} + \frac{1}{r^2}\frac{\partial^2}{\partial \phi^2}$ since cylinder is thin, z component is negligible

5.Solution:

We define integral transform of T by

$$\bar{T}(\beta_m, v, \alpha_n) = \int_{z=0}^{h}\int_{\phi=0}^{2\pi}\int_{r=0}^{a} T(r,\phi,z,t) r J_v(\beta_m r)\cos v(\phi-\phi')\cos\alpha_n z\, dr\, d\phi\, dz$$

(5.1)

$$T(r,\phi,z) = \frac{4}{\pi h}\sum_{m,v,n=0}^{\infty} \bar{T}\frac{\beta_m{}^2 Jv(\beta_m r)\cos v(\phi-\phi')\cos\alpha_n z}{(\beta_m{}^2 a^2 - v^2) J_v{}^2(\beta_m a)}$$

(5.2)

Where β_m is roots of transcendental equation $J_{v+1}(\beta_m a) = 0$ (5.3)

$v = 0,1,2,3,4,.....$

(5.4)

$$\alpha_n = \frac{p\pi}{h}\ , \qquad p = 0,1,2,3,4,.....$$ (5.5)

By taking integral transform of equation (3.1) and using following Green's theorem

$$\int_R \nabla^2 T \psi_k dv = \int_R T\nabla^2\psi_k dv + \sum_{i=1}^{N}\int_{s_i}\left[\psi_k\frac{\partial T}{\partial n_i} - T\frac{\partial \psi_k}{\partial n_i}\right] ds_i$$

(5.6)

Which yield as

$$\frac{d\bar{T}}{dt} + \alpha(\beta_m{}^2 + \alpha_n{}^2)\bar{T} = \frac{\alpha}{2\pi k} g_s{}^i Jv(\beta_m r_0)\cos(\alpha_n\xi)\delta(t-\tau)$$

(5.7)

This is linear differential equation of first order whose solution by applying initial condition (3.6) is

$$\bar{T} = \left[\bar{f}(\beta_m, v, \alpha_n) + \frac{\alpha}{2\pi k} g_s{}^i J_v(\beta_m r_0)\sin\alpha_n(\xi + \tfrac{h}{2}) e^{\alpha(\beta_m{}^2+\alpha_n{}^2)\tau}\right] e^{-\alpha(\beta_m{}^2+\alpha_n{}^2)t}$$

(5.8)

Taking inverse integral Transform we obtain

$$T = \frac{4}{\pi h}\sum_{m,n,v=0}^{\infty}\frac{\beta_m{}^2 J_v(\beta_m r)\cos v(\phi-\phi')\cos(\alpha_n z)}{(\beta_m{}^2 a^2 - v^2) J_v{}^2(\beta_m a)}\left[\bar{f}(\beta_m, v, \alpha_n) + \frac{\alpha}{2\pi k} g_s{}^i J_v(\beta_m r_0)\cos(\alpha_n\xi) e^{\alpha(\beta_m{}^2+\alpha_n{}^2)\tau}\right].$$
$$e^{-\alpha(\beta_m{}^2+\alpha_n{}^2)t}$$

(5.9)

$$\Gamma = \frac{4}{\pi h}\sum_{m,n,v=0}^{\infty}\frac{\beta_m{}^2 J_v(\beta_m r)\cos v(\phi-\phi')\cos(\alpha_n z)}{(\beta_m{}^2 a^2 - v^2) J_v{}^2(\beta_m a)}\left[\bar{f}(\beta_m, v, \alpha_n) + \frac{\alpha}{2\pi k} g_s{}^i J_v(\beta_m r_0)\cos(\alpha_n\xi) e^{\alpha(\beta_m{}^2+\alpha_n{}^2)\tau}\right].$$
$$[e^{-\alpha(\beta_m{}^2+\alpha_n{}^2)t} - 1]$$

(5.10)

III. SOLUTION OF THERMOELASTIC PROBLEM

Let suitable form of χ_c satisfying (4.6) is

$$\chi_c = (Ar^{v+2} + Br^{-v+2})\cos v(\phi-\phi') + (Cr^{v+2} + Dr^{-v+2})\sin v(\phi-\phi')$$

(6.1)

Let suitable form of χ_p satisfying (4.7) is

$$\chi_p = \frac{4\lambda E}{\pi h}\sum_{m,n,v=0}^{\infty}\frac{J_v(\beta_m r)\cos v(\phi-\phi')\cos(\alpha_n z)}{(\beta_m{}^2a^2-v^2)J_v{}^2(\beta_m a)}\left[\overline{f}(\beta_m,v,\alpha_n)+\frac{\alpha}{2\pi k}g_s{}^iJ_v(\beta_m r_0)\cos(\alpha_n\xi)e^{\alpha(\beta_m{}^2+\alpha_n{}^2)\tau}\right].$$
$$[e^{-\alpha(\beta_m{}^2+\alpha_n{}^2)t}-1]$$

(6.2)

$$\chi = \chi_c+\chi_p$$

$$\chi = \sum_{v=0}^{\infty}(Ar^{v+2}+Br^{-v+2})\cos v(\phi-\phi')+(Cr^{v+2}+Dr^{-v+2})\sin v(\phi-\phi')+$$
$$\frac{4\lambda E}{\pi h}\sum_{m,n,v=0}^{\infty}\frac{J_v(\beta_m r)\cos v(\phi-\phi')\cos(\alpha_n z)}{(\beta_m{}^2a^2-v^2)J_v{}^2(\beta_m a)}\left[\overline{f}(\beta_m,v,\alpha_n)+\frac{\alpha}{2\pi k}g_s{}^iJ_v(\beta_m r_0)\cos(\alpha_n\xi)e^{\alpha(\beta_m{}^2+\alpha_n{}^2)\tau}\right].$$
$$[e^{-\alpha(\beta_m{}^2+\alpha_n{}^2)t}-1]$$

(6.3)

$$\sigma_{rr} = \sum_{v=0}^{\infty}\left[A(2+v-v^2)r^v+B(2-v-v^2)r^{-v}\right]\cos v(\phi-\phi')+\left[C(2+v-v^2)r^v+D(2-v-v^2)r-v\right]\sin(\phi-\phi')+$$
$$\sum_{m,v,n=0}^{\infty}\frac{4\lambda E}{\pi h}\left[\frac{\beta_m}{r}J_{v-1}(\beta_m r)-\frac{v+v^2}{r^2}J_v(\beta_m r)\right]\frac{\cos v(\phi-\phi')\cos(\alpha_n z)}{(\beta_m{}^2a^2-v^2)J_v{}^2(\beta_m a)}.$$
$$\left[\overline{f}(\beta_m,v,\alpha_n)+\frac{\alpha}{2\pi k}g_s{}^iJ_v(\beta_m r_0)\cos(\alpha_n\xi)e^{\alpha(\beta_m{}^2+\alpha_n{}^2)\tau}\right].[e^{-\alpha(\beta_m{}^2+\alpha_n{}^2)t}-1]$$

(6.4)

$$\sigma_{\phi\phi} = \sum_{v=0}^{\infty}\left[A(v^2+3v+2)r^v+B(v^2-3v+2)r^{-v}\right]\cos v(\phi-\phi')+\left[C(v^2+3v+2)r^v+D(v^2-3v+2)r^{-v}\right]\sin v(\phi-\phi')+$$
$$\sum_{m,v,n=0}^{\infty}\frac{4\lambda E}{\pi h}\left[\frac{\beta_m}{r}J_{v+1}(\beta_m r)-\beta_m{}^2J_v(\beta_m r)\right]\frac{\cos v(\phi-\phi')\cos(\alpha_n z)}{(\beta_m{}^2a^2-v^2)J_v{}^2(\beta_m a)}.$$
$$\left[\overline{f}(\beta_m,v,\alpha_n)+\frac{\alpha}{2\pi k}g_s{}^iJ_v(\beta_m r_0)\cos(\alpha_n\xi)e^{\alpha(\beta_m{}^2+\alpha_n{}^2)\tau}\right].[e^{-\alpha(\beta_m{}^2+\alpha_n{}^2)t}-1]$$

(6.5)

$$\sigma_{r\phi} = \sum_{v=0}^{\infty}\left[A(v^2+v)r^v+B(v-v^2)r^{-v}\right]\sin(\phi-\phi')+\left[C(-v^2-v)r^v+D(v^2-v)r^{-v}\right]\cos(\phi-\phi')+$$
$$\sum_{m,v,n=0}^{\infty}\frac{4\lambda Ev}{\pi hr^2}\left[\beta_m rJ_{v-1}(\beta_m r)-(1+v)J_v(\beta_m r)\right]\frac{\sin v(\phi-\phi')\cos(\alpha_n z)}{(\beta_m{}^2a^2-v^2)J_v{}^2(\beta_m a)}.$$
$$\left[\overline{f}(\beta_m,v,\alpha_n)+\frac{\alpha}{2\pi k}g_s{}^iJ_v(\beta_m r_0)\cos(\alpha_n\xi)e^{\alpha(\beta_m{}^2+\alpha_n{}^2)\tau}\right].[e^{-\alpha(\beta_m{}^2+\alpha_n{}^2)t}-1]$$

(6.6)

Applying condition (4.4) to (6.4) and (6.6) we obtain

$$A = \frac{4\lambda E}{\pi h}\frac{a^{-v-2}}{2v}\left[2J_v(\beta_m a)-\beta_m aJ_{v-1}(\beta_m a)\right]\frac{\cos(\alpha_n z)}{(\beta_m{}^2a^2-v^2)J_v{}^2(\beta_m a)}$$
$$\left[\overline{f}(\beta_m,v,\alpha_n)+\frac{\alpha}{2\pi k}g_s{}^iJ_v(\beta_m r_0)\cos(\alpha_n\xi)e^{\alpha(\beta_m{}^2+\alpha_n{}^2)\tau}\right].[e^{-\alpha(\beta_m{}^2+\alpha_n{}^2)t}-1]$$

(6.7)

$$B = \frac{4\lambda E}{\pi h}a^{v-2}\left[\left(\frac{1+v-v^2-v^3}{v^3-v}\right)J_v(\beta_m a)+\frac{1}{2v}\beta_m aJ_{v-1}(\beta_m a)\right]\frac{\cos(\alpha_n z)}{(\beta_m{}^2a^2-v^2)J_v{}^2(\beta_m a)}$$

$$\left[\overline{f}(\beta_m,v,\alpha_n)+\frac{\alpha}{2\pi k}g_s{}^{i}J_v(\beta_m r_0)\cos(\alpha_n\xi)e^{\alpha(\beta_m{}^2+\alpha_n{}^2)\tau}\right].[e^{-\alpha(\beta_m{}^2+\alpha_n{}^2)t}-1]$$

(6.8)

$$C=D=0$$

(6.9)

Substituting above value in (6.4), (6.5) and (6.6) we obtain

$$\sigma_{rr}=\sum_{m,v,n=0}^{\infty}\frac{4\lambda E}{\pi h}\frac{\cos v(\phi-\phi')\cos(\alpha_n z)}{(\beta_m{}^2a^2-v^2)J_v{}^2(\beta_m a)}\left[\overline{f}(\beta_m,v,\alpha_n)+\frac{\alpha}{2\pi k}g_s{}^{i}J_v(\beta_m r_0)\cos(\alpha_n\xi)e^{\alpha(\beta_m{}^2+\alpha_n{}^2)\tau}\right].[e^{-\alpha(\beta_m{}^2+\alpha_n{}^2)t}-1].$$
$$\left\{(2+v-v^2)\frac{a^{-v-2}r^v}{2v}\left[2J_v(\beta_m a)-\beta_m aJ_{v-1}(\beta_m a)\right]+(2-v-v^2)a^{v-2}r^{-v}\left[\left(\frac{1+v-v^2-v^3}{v^3-v}\right)J_v(\beta_m a)+\frac{1}{2v}\beta_m aJ_{v-1}(\beta_m a)\right]+\right.$$
$$\left.+\left[\frac{\beta m}{r}J_{v-1}(\beta_m r)-\frac{v+v^2}{r^2}J_v(\beta_m r)\right]\right\}$$

(6.10)

$$\sigma_{\phi\phi}=\sum_{m,v,n=0}^{\infty}\frac{4\lambda E}{\pi h}\frac{\cos v(\phi-\phi')\cos(\alpha_n z)}{(\beta_m{}^2a^2-v^2)J_v{}^2(\beta_m a)}\left[\overline{f}(\beta_m,v,\alpha_n)+\frac{\alpha}{2\pi k}g_s{}^{i}J_v(\beta_m r_0)\cos(\alpha_n\xi)e^{\alpha(\beta_m{}^2+\alpha_n{}^2)\tau}\right].[e^{-\alpha(\beta_m{}^2+\alpha_n{}^2)t}-1].$$
$$\left\{(v^2+3v+2)\frac{a^{-v-2}r^v}{2v}\left[2J_v(\beta_m a)-\beta_m aJ_{v-1}(\beta_m a)\right]+(v^2-3v+2)a^{v-2}r^{-v}\left[\left(\frac{1+v-v^2-v^3}{v^3-v}\right)J_v(\beta_m a)+\frac{1}{2v}\beta_m aJ_{v-1}(\beta_m a)\right]+\right.$$
$$\left.+\left[\frac{\beta m}{r}J_{v+1}(\beta_m r)-\frac{v+v^2}{r^2}J_v(\beta_m r)\right]\right\}$$

(6.11)

$$\sigma_{r\phi}=\sum_{m,v,n=0}^{\infty}\frac{4\lambda E}{\pi h}\frac{\sin v(\phi-\phi')\cos(\alpha_n z)}{(\beta_m{}^2a^2-v^2)J_v{}^2(\beta_m a)}\left[\overline{f}(\beta_m,v,\alpha_n)+\frac{\alpha}{2\pi k}g_s{}^{i}J_v(\beta_m r_0)\cos(\alpha_n\xi)e^{\alpha(\beta_m{}^2+\alpha_n{}^2)\tau}\right].[e^{-\alpha(\beta_m{}^2+\alpha_n{}^2)t}-1].$$
$$\left\{(v+1)\frac{a^{-v-2}r^v}{2}\left[2J_v(\beta_m a)-\beta_m aJ_{v-1}(\beta_m a)\right]+(1-v)a^{v-2}r^{-v}\left[\left(\frac{1+v-v^2-v^3}{v^2-1}\right)J_v(\beta_m a)+\frac{1}{2}\beta_m aJ_{v-1}(\beta_m a)\right]+\right.$$
$$\left.+\left[v\beta_m rJ_{v-1}(\beta_m r)-(v+v^2)J_v(\beta_m r)\right]\right\}$$

(6.12)

IV. CONCLUSION

In this paper we determined the temperature distribution and thermal stresses in a Neumann's thin solid cylinder with moving heat source with analytical approach on the surface is established. By giving particular values to the parameter one can obtain their desired results by putting values of the parameters in the equations (5.9), (6.10), (6.11), (6.12)

REFEREWNCES

[1] I. N. Sneddon The use of integral transform, McGraw Hill, New York, 1972
[2] M. Necati Ozisik `Heat conduction, Second Edition, A Wiley-Interscience Publication John Wiley and
[3] Sons, inc. New-York.
[4] N. Noda, R. B. Hetnarski, Y. Tanigawa, Thermal Stresses, second edition, 2002
[5] D. T. Solanke M. H. Durge Quasi-Static transient Thermal Stresses in a Dirichlet's thin Solid cylinder with internal moving heat source

American Journal of Engineering Research (AJER)
e-ISSN : 2320-0847 p-ISSN : 2320-0936
Volume-03, Issue-03, pp-80-90
www.ajer.org

Research Paper Open Access

Influence Of Silicon Addition And Temperature On The Cyclic Oxidation Behaviour Of Sintered Hot Forged High Density Cu – 8.5% Al Alloy

[1] (Mrs.) S. K. Pandey, & [2] K. S. Pandey
[1] *Director, National Institute of Technology, Puducherry, Karaikal-609 605, India.*
[2] *Professor, Department of Metallurgical & Materials Engineering, National Institute of Technology, Tiruchirappalli-620 015, Tamil Nadu, India.*

***Abstract:* -** Cyclic oxidation experiments were carried out to generate experimental data for Cu–8.5%Al sintered hot forged high density parts when alloyed with silicon in air at elevated temperatures. Silicon contents were kept at 0.90 and 1.8 per cent respectively. Homogeneously blended powders of Cu-8.5%Al, Cu-8.5% Al–0.9% Si and Cu–8.5%Al–1.8% Si were used separately to prepare compacts of 1.1 initial aspect ratio with diameter being 19.0 mm in the density range of 85±1 per cent of theoretical by applying pressure in the range of 360±10 MPa and taking pre weighed powder blends. Compacts were sintered in an argon atmosphere at 1223 ±10K and forged to thin discs of 5mm thickness and oil quenched. Discs were machined to 2.10 ± 0.01 mm thickness with 25.0 ± 1 mm diameter. Thoroughly cleaned discs were subjected to cyclic oxidation studies at 573,673 and 773 K respectively. Weight gains were measured at an interval of 30 minutes and the oxidation studies were carried out upto the time till the last three readings showed no weight gains. Experimental data have been critically analyzed for various oxidation mechanisms and were found to conform to a semi-logarithmic equation of the form: $Wg = A_1 \log (A_2 t + A_3)$ where, 'A_1', A_2' and 'A_3' are empirically determined constants and Wg is the weight gain with't' representing time.

Keywords: - *Blended, cyclic, elevated, generate, high density, .mechanism, oxidation, weight gains*

I. INTRODUCTION

It is well established and universally accepted fact that almost all metals tend to form simple or complex oxides at elevated temperatures in air and other oxidizing environments. However, in industries, machinery components are often exposed to high temperature environments where they get oxidized. Thus, the study of oxidation behaviour of such materials is increasingly becoming important, and, therefore, there is an immense need to invent materials for which the oxidation rates are at the bare minimum. In addition to low rates of oxidation, they are expected to exhibit high strengths at elevated temperatures [1-9]. It is reported [10–14] that the oxidation resistance of aluminium bronze is superior to that of any other copper based alloys and that only a very thin oxide film is formed in air temperatures as high as 773K. Since these alloys have good creep strength and elevated temperature fatigue properties, they are considered to be applicable up to temperatures as high as 673K. Main examples in this field include turbo - compressor blades, electrical heating elements sheaths and valve sheets for high performance petrol engines and clamps for resistance – welding machines.

Data for the stabilities of metallic compounds indicate that practically no metal would remain completely unaffected in the presence of active gaseous environments. Periodic table supplements the above statement by the fact that most of the elements have strong affinity towards oxygen [15]. However, only the degree of affinity varies from element to element. This is the basic reason why most of the elements found in nature are combined with oxygen. Similarly, when the elements exposed in the oxidizing environments, right from room temperature to melting points and above get oxidized to such an extent that depends upon the temperature and time of exposure. The films formed on to the metal surface could be characterized as either thin or thick which in turn would decide, whether the film formed is absolutely protective (completely adherent and non – permeable), partially protective (mildly/ strongly adherent but porous) or non – protective (fragile and

porous). The formation of protective film largely depends upon various factors such as the rate of flow of oxygen or air in to the reaction chamber, time of exposure of the specimen, temperature at which the oxidation studies are conducted, surface finish of the specimens, pits or surface scratch or other tool marks on the specimen, therefore, the affinity of the metal to oxygen rich environment attacks on the exposed metal surface. Apart from the above, the other parameters such as the presence of impurity, addition of alloying elements and the crystal geometry of the metal do affect the oxidation behaviour of metals/alloys [1-9].

Thickness of the oxide film formed on the metal surface is an important factor to be considered. Based on the thickness of the oxide film, Mott proposed the theory of "Thin Film Formation", and Wagner proposed the theory of "Thick Film Formation". Generally, thin films are treated as protective provided they are uniform, continuous and strongly adherent on the surface. However, the thick film formation on the metal surface can result in multiple cracks due to the existence of differential stresses which are generated due to the differing thermal conductivities of the metal and its own oxide. Cracks in the oxide layer expose the interface of the virgin metal to the oxidizing environment beneath the oxide layer [16, 17]. This result in the growth of oxide layer inward and, thus, thickens the oxide film. In the event, the formed oxide layer is porous and is able to permeate oxygen through it, the oxidation process would continue and more and more metal would be oxidized. However, the growth of oxide layer below the first layer would definitely create tensile stresses at elevated temperatures of oxidation due to differential heat conducting capabilities and due to differing coefficients of expansion of the metal and its own oxides. It is, therefore, obvious for the residual stresses to accumulate and once this accumulation approached beyond a certain threshold value, the formed oxide layer would rupture Oxidation behaviour of dense copper products have been comprehensively investigated by various groups of investigators [15-20] and the mechanisms of oxidation have been well established [21-27]. But, the oxidation behaviour of copper based P/M products need to be investigated as the same bears a strong potential for industrial application. A single report on the same exists which is reported elsewhere [1]. Hence, the present investigation has been planed to generate experimental data as a most preliminary research work in this regard on Cu – 8.5% Al with and without the addition of Silicon produced via P/M route to almost 100% dense product.

II. EXPERIMENTAL DETAILS

II.1 Materials Required

Electrolytic grade of copper, aluminum, aluminium-silicon eutectic and reduced silicon powders, each in the particle size range of -150 +37 µm were procured from M/S The Metal Powder Company Limited, Thirumangalam, Madurai, Tamil Nadu, India. Purities of copper, aluminium and silicon powders were chemically analyzed and found to correspond to 99.93, 99.71 and 99.5% respectively. The basic characteristics of these powders are listed in Table 1 and sieve size analyses of all required powders are given in Table 2 respectively.

Table 1 Powder Characteristics of Copper, Aluminium, Al-Si Eutectic and Silicon Powders

Property	Copper	Aluminium	Al- Si Eutectic	Silicon
Flow rate , S/100g	Very sluggish	63	49	45
Apparent density, g/cc	1.396	1.055	1.310	0.618
Compressibility, g/cc at a pressure of 250±10MPa	7.892	2.613	2.11	2.101

Table 2 Sieve Size Analysis of Copper, Aluminium, Al-Si Eutectic and Silicon Powders

	Size µm	-150 +125	-125 +106	+106 +90	-90 +75	-75 +63	-63 +53	-53 +45	-45 +37
Copper	Wt. % Ret.	0.037	0.500	0.121	0.345	2.531	2.852	88.200	5.676
	Cum. Wt.% Ret.	0.037	0.870	0.991	1.336	3.867	6.119	94.319	99.995
Aluminium	Wt. % Ret.	1.310	8.345	25.140	3.521	25.518	16.180	14.9011	4.984
	Cum. Wt.% Ret.	1.310	9.655	34.795	38.316	63.834	80.041	95.005	99.989
Al-Si Eutectic	Wt. % Ret.	3.212	9.222	20.550	19.812	2.908	15.985	25.130	3.173
	Cum. Wt.% Ret.	3.212	12.434	32.984	52.786	55.704	71.689	96.189	99.992
Silicon	Wt. % Ret.	2.100	8.712	21.919	20.167	6.385	32.010	6.788	1.718
	Cum. Wt.% Ret.	2.100	10.812	32.831	52.998	59.383	91.393	98.181	99.899

II.2 Compact Preparation

Compacts of 27.5 mm diameter and 9.2mm height of Cu – 8.5%Al, Cu-8.5%Al – 0.9%Si and Cu-8.5%Al-1.8%Si homogeneously blended powders were separately prepared on a 1.0MN capacity hydraulic press using suitable die, punch and bottom insert assembly in a pressure range of 360±10MPa to yield the compact densities in the range of 85±1 per cent of theoretical by taking accurately pre-weighed powder blends for each compact.

II.3 Application of Indigenous Ceramic Coating

Indigenously developed [28] ceramic coating was applied over the entire surfaces of all the compacts and the coating was allowed to dry under ambient conditions for a period of 16 hours. These coated compacts were recoated in the direction of 90º to the previous coating and were allowed to dry once for again for a further period of 16 hours under the aforementioned conditions.

II.4 Sintering and Hot Upset Forging

Ceramic coated compacts were sintered in an electrically heated muffle furnace in the uniform temperature zone in the range of 1223±10K for the period of 100 minutes. Once sintering schedule was completed , the sintered performs of all compositions were hot upset forged to pre – determined height strain so as yield the final theoretical density to the tune of 99.7±0.1 per cent on a 1.0MN capacity friction screw press using the flat hot die assembly. Forged specimens were cooled in still air. Immediately after cleaning the forged discs, the density was measured using Archimedian principle and the same in all cases was found to be 99.7% plus. Procedure for obtaining the density is described elsewhere [29].

II.5 Specimen Preparation for Oxidation Studies

Oxidation studies demand the scratch free specimens as the presence of scratches changes the expected oxidation rates abruptly and thus the oxidation mechanisms get affected adversely. Hence, every possible attempt was made to prepare scratch free specimens. Disc shaped specimens of 14mm dia and 1.75 mm thick were carefully machined and ground to 5µm surface finish. Ground specimens were annealed at 573 K in an organ atmosphere for a period of 45 minutes and cooled to room temperature inside the furnace chamber itself in the stream of argon by switching off the furnaces. Prior to subjecting the specimens to oxidation studies, the entire specimen surfaces were thoroughly cleaned by acetone so as to remove grease and any other unwanted adhered impurities. Measurement of surface area and the weight of each specimen were carried out prior to subjecting them to cyclic oxidation studies.

II.6 Conducting Cyclic Oxidation Experiments

Cyclic oxidation studies were carried out for each of the prepared specimens and weight gains were recorded for a fixed period of exposure at a given temperature. Further experiments on oxidation were stopped once the last three consecutive readings remained consistently constant. Weight measurements were carried out by using Adair and Dutt model A-180 single pan electronic balance of sensitivity of 10^{-4} g [30]. Oxidation experiments were carried out in an electric muffle furnace where the temperature of oxidation was maintained with in the range of 573 ±10K, 673±10K and 773 ± 10K respectively. Thus, three specimens from each composition were exposed to oxidation studies at the above temperatures separately.

III. RESULTS AND DISCUSSION

Oxidation curves are plotted between (Wt. gain / area, i.e., g/m^2) and time in seconds for each composition and temperature of oxidation. Such oxidation curves can be described by a simple or inverse logarithmic, a cubic, a parabolic, a linear or an asymptotic equation/s. Among the above equations which one of them will be governing equation for the relation between weight gain and the time would mainly depend upon the oxide scale thickness formed on to the metal surface at a given time and temperature. However, the changeover from one mechanism to another mechanism is probable, and in such events, oxidation mechanism followed could be represented by two or more than two mechanisms. Hence, extra precautions must be taken while establishing the oxidation mechanism/s.

Experimental data on oxidation behaviour of Cu – 8.5%Al with and without the addition of Silicon (0.9% and 1.8) are plotted in fig. 1.In order to establish the exact nature of these curves, different plotting techniques have been attempted so as to establish the exact mechanism of oxidation for P/M products. The product densities centered on 99.7±0.1 per cent of theoretical which were subjected to cyclic oxidation studies. Basically, a change in oxidation rates with respect to time (t) might conform to one of the several rate mechanisms or combinations of them. It is, with this reference point, it becomes mandatory to develop different types of plots so that an appropriate rate equation can be arrived at. For example, the validity of parabolic rate equation is tested by plotting ($Wg^{2)}$ and time (t) and this must yield a straight line. However, double logarithmic

plots between weight gain (W_g) and time (t) are the most convenient technique to evaluate the exponent (m) of W_g which acquires the values of 1, 2 and 3 for linear, parabolic and cubic oxidation rates for equations of the form:

$$W_g^m = K_m t + Cm \text{ ---------- (1)}$$

Where, K_m and C_m are empirically determined constants. But, the scales in such plots get highly compressed with increasing values of 'W_g' and 't'. Due to this reason alone, such plots tend to demonstrate a linear relationship between $\log_{10}(W_g)$ and $\log_{10}(t)$, and, therefore, the changes in rate equations and mechanisms are not identified distinctly. Hence, such plots demand great care to be exercised while interpreting the rate equations from double logarithmic plots. Therefore, such plots must be drawn only to confirm the results obtained by other types of graphical representations. Such plots are extremely good to summarize data covering large temperature ranges and time intervals and not for establishing the oxidation mechanisms.

III.1 Characteristic Nature of Oxidation Curves

Oxidation data obtained at 573, 673 and 773K for Cu-8.5%Al, Cu-8.5%Al-0.9%Si and Cu-8.5%Al-1.8%Si

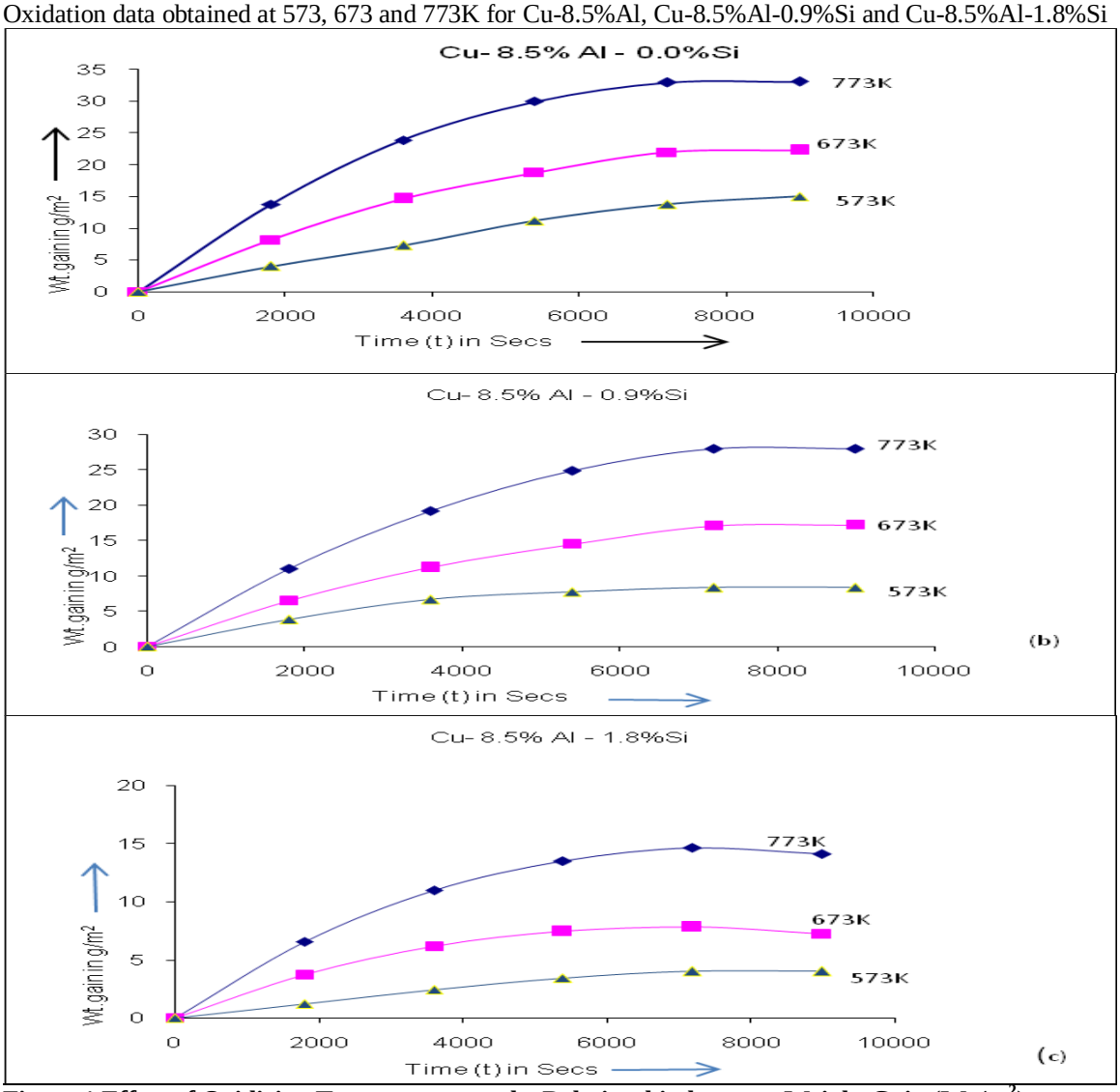

Figure 1 Effect of Oxidizing Temperature on the Relationship between Weight Gain (Wg/m^2) and Time (t) for Cu-8.5% Al With and Without Silicon Addition.

are plotted in figs. 1(a), 1(b) and 1(c) respectively. Curves in these plots are characteristically quite similar in nature to each other except the rates of oxidation at elevated temperatures had been quite pronounced. Since none of these curves conformed to straight line configuration and, therefore, oxidation rates did not conform to a linear mechanism.

III.3 Effect of Silicon Addition on Oxidation Behaviour:

Figs. 2(a), 2(b) and 2(c) are drawn between weight gain(g/m^2) and time (t in Secs) to exhibit the effect of silicon addition up to 1.8 per cent in Cu-8.5%Al alloy on oxidation behaviour. These figures drawn at 573, 673 and

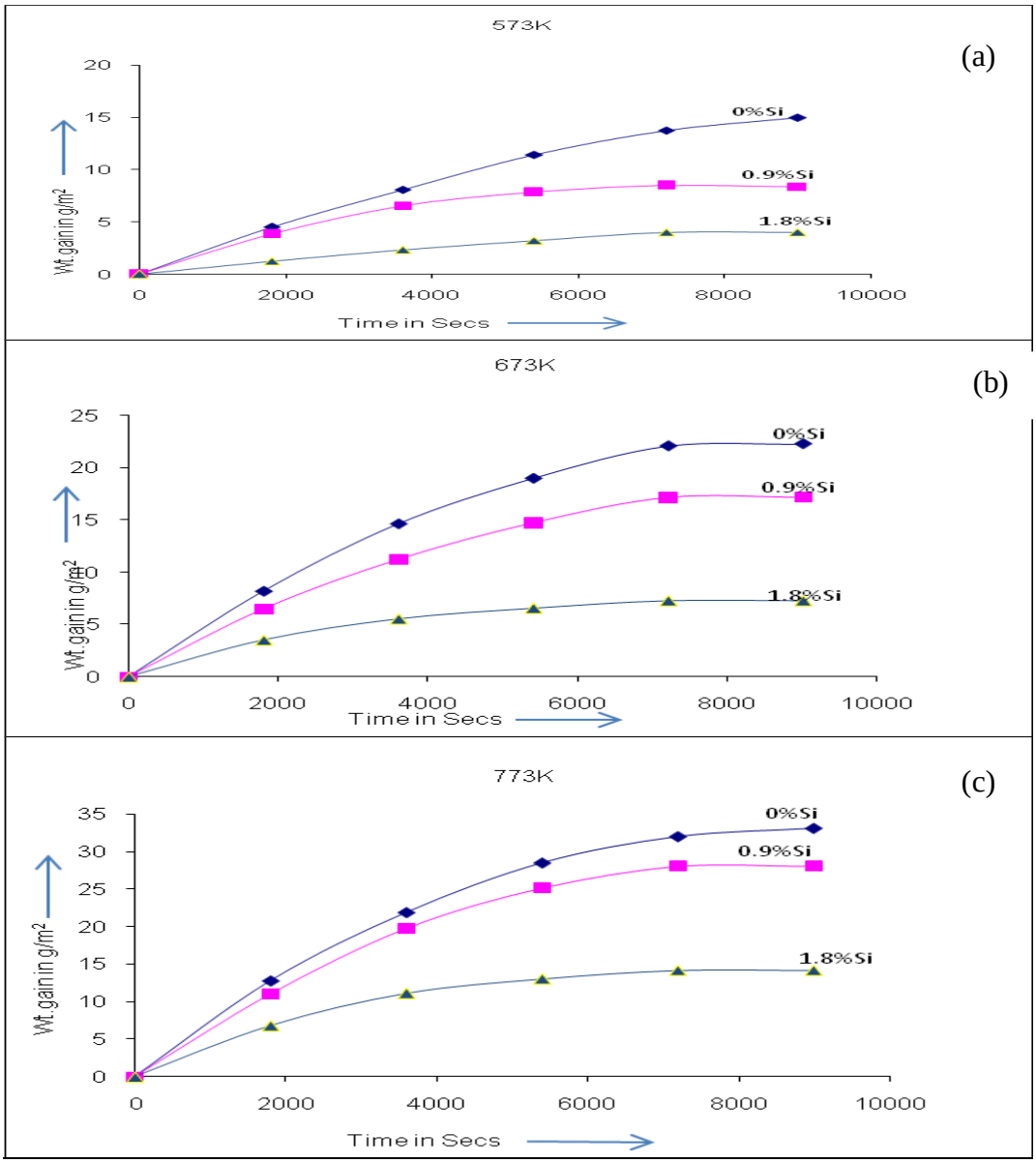

Figure 2 Effect of Silicon Addition on the Oxidation behaviour of Cu-8.5%Al Sintered Hot Forged (99.7%Th.Dense)

and 773K shows that the rate of oxidation was decreased as the silicon content was raised up to 1.8 per cent irrespective of the temperature of oxidation. However, the base alloy Cu-8.5%Al exhibited the least resistance to oxidation compared to the other alloys containing silicon. Presence of silicon in Cu-8.5%Al alloys promotes the formation of thin and smooth oxide layer which was found to be highly protective and quite adherent to specimen surfaces. This fact was evident on two grounds-firstly, the weight gain per unit area had been on lower side compared to the weight gain per unit area for Cu-8.5%Al alloys, and, secondly, the oxidation in later stages had proceeded in a very much reduced rate and finally the oxidation ceased for all practical purposes. Therefore, the oxidation studies carried out for a same length of time at any given tested temperature must have formed

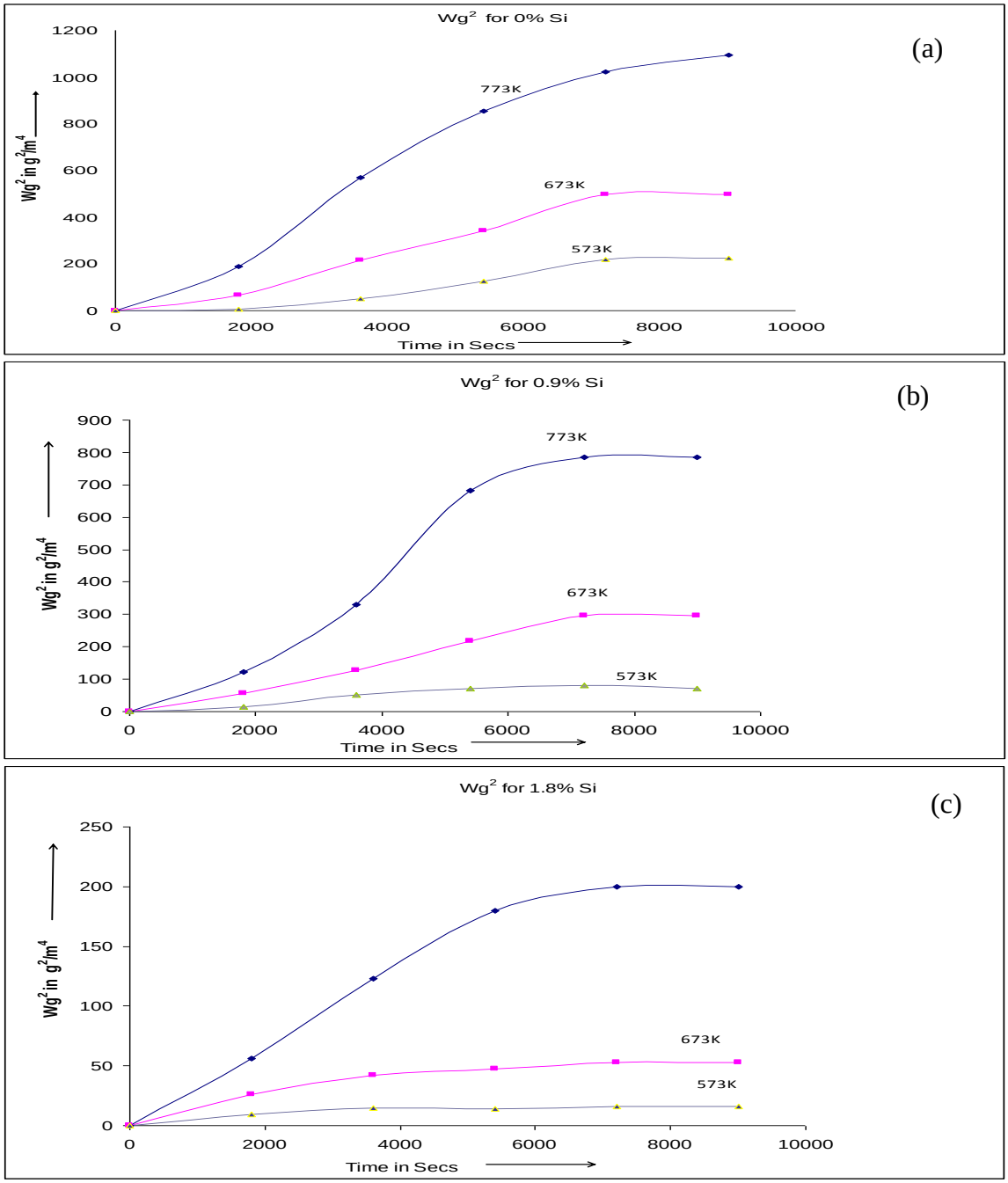

Figure 3 Relationship between weight gain square and time (t) for Cu-8.5%Al with or without silicon addition for sintered hot forged (close to Th. density) at different temperatures

lower amounts of oxides in case of silicon added Cu-8.5%Al alloys compared to no silicon contained Cu-8.5%Al alloys and hence providing a direct logical evidence that the oxide formed is thin layer protective and strongly adherent to the metal surface and hence, it is, established that the silicon addition in Cu-8.5%Al alloys is highly effective and beneficial induce oxidation resistance to the aforesaid alloys. These findings are in conformity with other research reports described elsewhere [15, 18].

Figs. 3(a), 3(b) and 3(c) are drawn between the square of weight gain per unit area as W_g^2 (g^2/m^4) and time‘t’ in seconds for all the three compositions and all the three temperatures of oxidation with or without the addition of silicon. Figs 3(a), 3(b) and 3(c) show the curves corresponding to Cu-8.5%Al, Cu-8.5%Al-0.9%Si and Cu-8.5%Al-1.8%Si respectively and none of the curves in these plots exhibit a linear behaviour and hence the oxidation mechanism could not be conformed to a parabolic rate law.

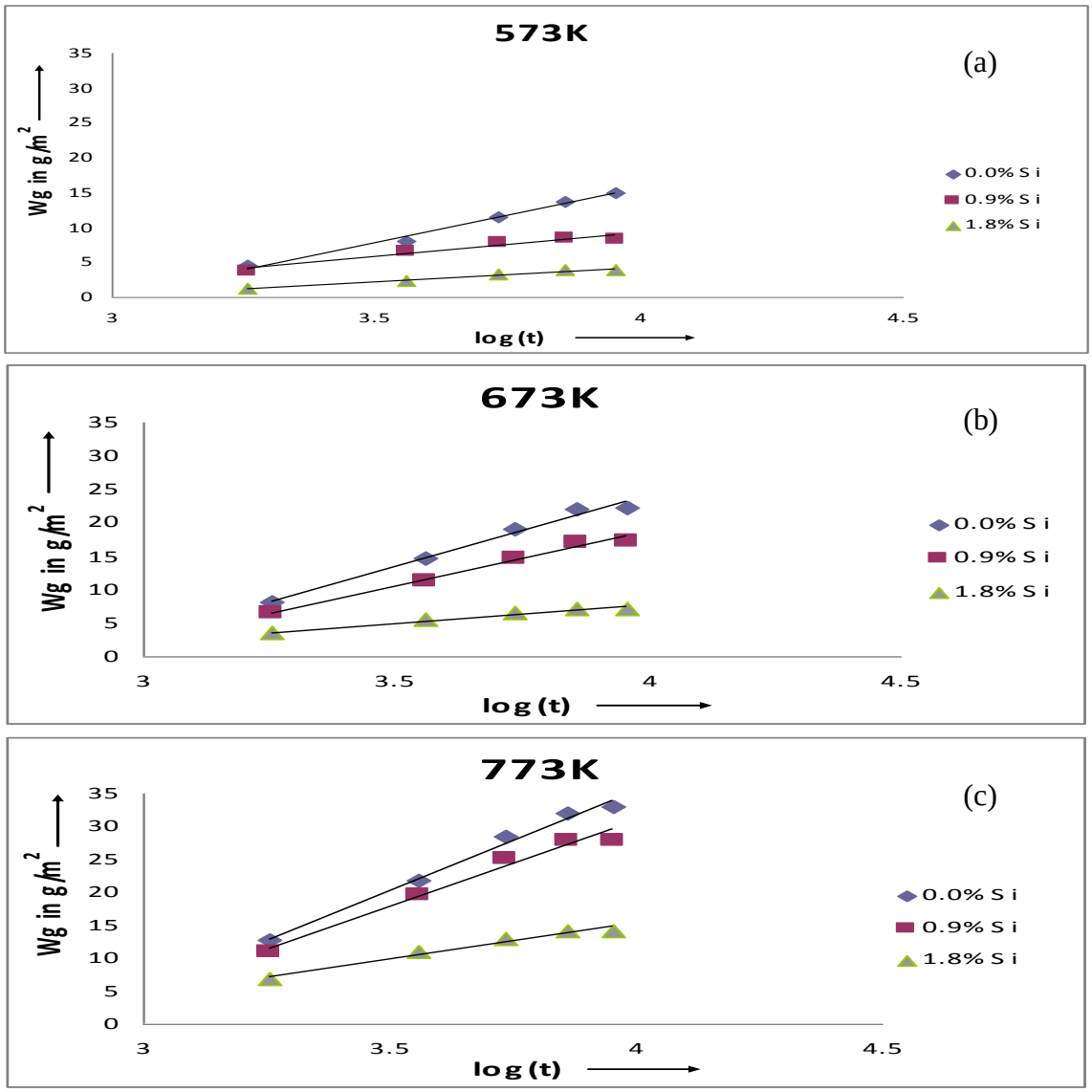

Figure 4 Relationships between Weight Gain Vs Log (t)

Fig. 4 has been drawn between weight gain (g/m^2) and $\log_{10}$ (t) for all the alloys investigated in the present study. The plots are drawn in figures 4(a),4(b) and 4(c) respectively. The curves drawn in these figures are found to be represented as straight lines in one segment. Thus, it is, obvious that the rate equation followed is well represented by the logarithmic nature of equation of the form.

$$W_g = A_1 \log_{10} (A_2 t + A_3) \text{ ---------- (2)}$$

Where, A_1, A_2 and A_3 are empirically determined constants. These constants are found to depend upon the compositions of the system and the temperatures of oxidation considered.

In the present investigation two significant methods have been employed to evaluate these constants, namely, A_1, A_2 and A_3 respectively.

III.4 Evaluation of Logarithmic Constants

Method-I

Since at time t = 0, $W_g = 0$, and, therefore, irrespective of the value of constant A_1, the constant $A_3 = 1$, so as to fulfill the conditions, i.e., $\log_{10} (1) = 0$. The calculated constants are reported in Table-II.

Table 3 Logarithmic Rate Constant by Using Method

Systems	Temp. of oxidation , K	Time Int. of Validity, S.	Rate Constants			$W_g(m)$ g/m^2	$W_g(c)$ g/m^2	% error
			A_1	A_2*10^{-3}	A_3			
Cu-8.5%Al 0.0%Si	573	0-9000	19.15	0.54754	1.0	15.0	14.85844	-0.944
	673	0-9000	21.429	1.0574	1.0	14.65	14.611	+0.278
	773	0-9000	28.125	1.7685	1.0	32	31.936	-0.200
Cu-8.5Al-0.9%Si	573	0-9000	6.48	2.58932	1.0	7.55	7.617775	-0.89765
	673	0-9000	15.0	10.0385	1.0	14.01	13.78553	-1.60
	773	0-9000	26.56	1.4988	1.0	28.01	28.46014	+1.610
Cu-8.5Al-1.8%Si	573	0-9000	4.687	0.9284	1.0	4.01	4.1509	+3.513
	673	0-9000	3.125	28.879	1.0	7.25	7.2494947	-0.00073
	773	0-9000	6.896	13.76	1.0	14.13	13.692223	-3.0982

W_g (m) = Measured Weight; W_g (c) = Calculated Weight, and, % error = $[(W_g(c)-W_g(m))/W_g(c)]*100$

Method-II

The characteristic curves are well represented by the logarithmic equation of the form:

$$W_g = A_1 \log_{10} (A_2 t + A_3) \text{ ---------- (2)}$$

It is, quite possible that in situations where A_3 cannot be taken to unity and also cannot be conveniently adjusted to this value, then the following approach is likely to lead to the evaluation of these constants A_1, A_2 and A_3 respectively. Now differentiating equation (2) w.r.t., time't', the following can be obtained.

$$\frac{d}{dt}(W_g) = (A_1 A_2) / (A_3 t + A_2) \text{ ---------- (3)}$$

Hence, $$[1/(\frac{d}{dt} W_g)] = (t/A_1) + (A_3/A_1A_2) \text{ ----------(4)}$$

Or, $$\{1/(\frac{d}{dt}(W_g))\} = Qt + R \text{ ---------- (5)}$$

Where, $Q = (1/A_1)$ and $R = (A_3/A_1A_2)$. However, the oxidation rates at various exposure times are possible to be determined from the empirical oxidation time curves. The reciprocals 1/ (d/dt) Wg of these oxidation rates can be plotted against the corresponding exposure times, t' and from these linear plots the values of 'Q' and 'R' are determined. Utilizing the values of 'Q' and 'R', the rate constant values of 'A_1', 'A_2' and 'A_3' are calculated. Several pairs of 'W_g' and time't' can be read from oxidation time curves and a value of A_3 is determined from each pair and is averaged out. Calculation of A_3 is done as under:

$$\log_{10}(K_3) = W_g Q + \log_{10}(Q/R+1) \text{ ---------- (6)}$$

From the mean value of A_3, A_2 is found out by:

$$A_2 = (Q/R)\, A_3 \text{ ---------- (7)}$$

Using the mean values of A_2 and A_3, A_1 can be empirically determined and same are reported in Table 4.

III.5 Determination of Rate Constants

Figs. 5(a), 5(b) and 5(c) are drawn between $[1/(dW_g/dt)]$ and time ,t for Cu-8.5%Al, Cu-8.5%Al-0.9%Si and Cu-8.5%Al-1.8%Si respectively. These plots are basically drawn to evaluate the desired constants, A_1, A_2 and A_3 slops

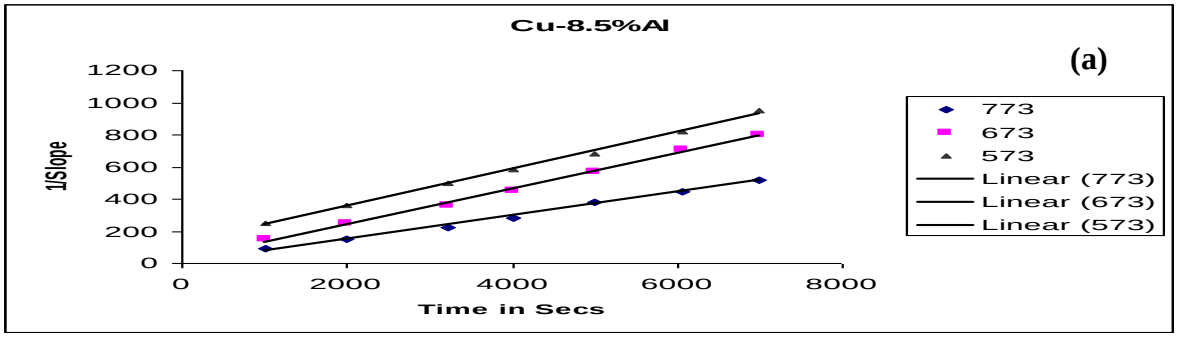

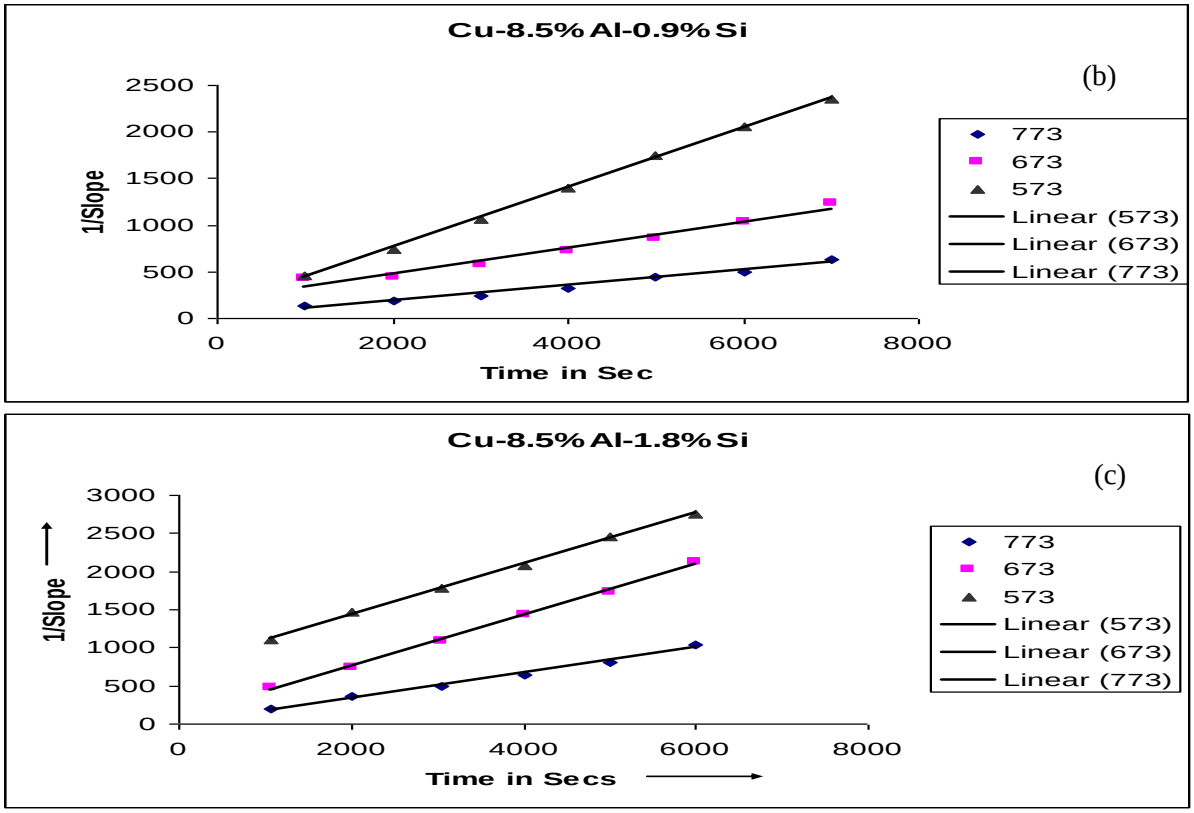

Figure 5 plots between slope inverse and time (t) during oxidizing of cu-8.5%Al alloys with and without silicon addition at different temperatures

of these lines provided different values of $1/A_1$ for a given composition and the temperature of oxidation where as the intercepts yielded the values of A_3/A_1A_2 and the values of A_3 was calculated from equation(6). The values of these constants A_1, A_2 and A_3 are listed in Table 4. Once an appropriate constant are fed into the logarithmic rate equation, the exact empirical relationships for each of these alloys can be obtained. However , the addition of silicon to Cu-8.5%Al alloys had the beneficial effects on oxidation mechanisms of sintered and hot forged high density copper based P/M alloys even in environments where oxidizing conditions prevail.

Comparing tables 3 and 4 carefully, it is found that method-I is quite sound compared to method-II in estimating the logarithmic rate constants, A_1, A_2 and A_3. This fact is validated by the fact that in couple of instances only, the error recorded was beyond 5% where as method-II involved errors in many cases beyond 5%. Therefore, method-I is found to be more appropriate in evaluating the logarithmic rate constants, i.e., A_1, A_2 and A_3 respectively.

Table 4 Logarithmic Rate Constants Using Method-II

System	Temperature of oxidation K	Time interval of validity in Sec	Rate constants			W_g(m)	W_g(c)	Maximum %error
			A_1	A_2*10^{-3}	A_3			
Cu-8.5%Al	573	0-9000	14.46	1.0299	0.4169	15.0	14.2566	-4.95
	673	0-9000	9.3023	16.67	7.4419	22.3	19.585	-12.174
	773	0-9000	9.524	112.08	295.00	27.5	28.378	+3.09
Cu-8.5%Al-0.9%Si	573	0-9000	12.372	0.76	0.477	7.55	8.177	+8.3
	673	0-9000	5.2165	108.34	2.8257	17.21	15.5988	-9.361
	773	0-9000	3.0147	$8.5x10^{7}$	$7.66x10^{6}$	28.01	26.50	-5.693
Cu-8.5%Al-1.8%Si	573	0-9000	6.579	0.62	0.36713	4.01	4.5	12
	673	0-9000	3.5334	11.5215	9.8931	7.25	6.9533	-4.09
	773	0-9000	3.2679	1198.3	3035.079	13.00	12.99	-0.0769

$W_g(m)$ = Measured weight in g/m^2
$W_g(c)$ = Calculated weight in g/m^2
%error = $[(W_g(m) - W_g(c)/ W_g(m)]*100$

IV. CONCLUSIONS

Based upon the experimental data, calculated parameters and various plots drawn assess the mechanism of oxidation of Cu-8.5%Al with and without silicon addition (maximum up to 1.8%), the following major findings have emerged:

1. Basic characteristic features of the oxidation curves for Cu-8.5%Al with and without silicon addition (0.0%, 0.9% and 1.8% are quite similar to each other in the temperature range of 573 to 773K. the rate of oxidation was found to increase initially, but in the final stages of oxidation, the oxidation has ceased as the oxide layers formed acted as protective and impermeable, and, hence, no oxidation.
2. Addition of silicon content (0.0% to 1.8%) in Cu-8.5%Al alloys was beneficial as the same offered as it formed strongly adherent, impermeable to oxygen and thus protective oxide layer over the alloy surfaces when exposed to elevated temperature in the air atmosphere.
3. None of the investigated systems exhibited linear or parabolic rate equations at any of the oxidizing temperatures, namely, 573, 673 and 773K respectively.
4. Experimental data obtained on oxidation behaviour of Cu-8.5%Al-1.8%Si alloy at all temperatures of oxidation conformed to the rate equation of the form; $W_g = A_1\log_{10}(A_2t+A_3)$ where , A_1, A_2 and A_3 are found to be logarithmic constant which are empirically determined. Further W_g is the weight gain at time‘t’. However, the oxidation mechanisms at all temperatures for Cu-8.5%Al and Cu-8.5%Al-0.9%Si though followed the semi-logarithmic rate equations and altered only after a certain length of time even through the mechanism remained represented by the semi-logarithmic rate equation.
5. Two different techniques of evaluating logarithmic rate constants were employed and it was established beyond any doubt that the first method was more effective compared to the second method because the error involved was well within the limits of ± 2.5% leaving aside exceptional cases where error percentage reached was beyond 5 per cent. However, the second method even though yielded errors on the higher side is recommended to be used when the first method virtually fails to accept the value of A_3 =1.0.

Summarizing the results and subsequent analysis, it is, established beyond any doubt that the Cu-8.5%Al-1.8%si alloy can be safely employed in air environment in the temperature range of 573K to 773K due to its highly protective, adherent and impermeable nature of the oxide layers formed on the alloy surface, and, hence, this alloy can be used as a component for equipment etc. which might be subjected in the above temperature range.

REFERENCES

[1] G.P.Maheswari, T.Srinivasa Rao and K.S.Pandey, “Oxidation Behaviour of Sintered Deformed Copper and Aluminium Admixed Copper Performs in Air”, Quarterly Int. J. of Powder Metall., Sci. and Technology, Vol.2, No.2, 1991, pp.43 – 52.

[2] S.K.Sridhar, R.Nagalakshmi and K.S.Pandey, “High Temperature Cyclic Oxidation of AISI 301 and 304 Stainless Steels in Air”, Engineering Today, Vol. 4, No. 1, January 2002, pp.16-19.

[3] O.Grinder and U.Ericson, “Low Temperature Oxidation of Inert Gas Atomized Steel Powder”, Mod. Dev. in Powder Metall., Ed. By Edward N. Aqua and Charles I. Whitman 1984, Vol.10, pp.295- 330.

[4] I.D.Kazarinova, V.A.Arlanmbekov and K.M.Gorbunova, “High Temperature Oxidation of Silicon”, - High Temperature Corrosion and Methods of Its Control – Part II, High Temperature Oxidation of Metals and Alloys, Ed. By A.V.Byalobzhe Skin, Yu. N.Golovanav, 1986, pp.77-89.

[5] P.Aravindan and K.S.Pandey, “Effect of Silicon Addition on the Oxidation Mechanism of Cu - 6.7%Al Sintered But Hot Forged Alloys in Air”, Adv. in Powder Metall., & Particulate Materials, 1998, Vol.3, Part – 9, pp. 9.79 – 9.94.

[6] Haroum Hindan and David P.Whittle, “Amelioration of Alloy Oxidation Behaviour of Minor Additions of Oxygen Active Elements”, Corrosion, Microstructure and Metallographic, Ed. By Derek O.Northwood, William E.White and Gearge F.Vander Voort, Microstructural Science, Vol.12, 1985, Proceedings of the 16th Annual Technical Meeting of Int. Metallographic Society, pp. 203 – 230.

[7] R.C.Lobb and H.E.Evans, “Truncation of the Distribution Function of Pit Depths during High Temperature Oxidation of a 20Cr Stainless Steel,” Plant Corrosion, Ed. by J.E. Struff and J.R.Nicholls, 1987, 275-288.

[8] V.F.Zelenskii and I.A. Petel’s guzov, “The Kinetics and Mechanism of Oxidation of Magnesium - Beryllium Alloys,’’ High Temperature Corrosion and Method of Its Control-Part II: High Temperature Oxidation of Metals and Alloys, Ed. by A.V. Byalobzhe Skii and Yu. N, Golovanov, 1986, pp. 35-46.

[9] S. K. Pandey and K.S. Pandey, "Oxidation Behaviour of Sintered High Density Cu-2.5 % Al Alloys," Engineering Today, Vol.4, No.1, Jan 2002, pp.12-15.
[10] P.J. Macken and A.A Smith, "The Aluminium Bronzes Properties and Production Process," Published by Copper Dev, Association, London School Edition, 1986, No.31.
[11] H.Okamoto, "Metal Hand Book Alloy and Phase Diagram", 1992.
[12] J.H. Cairns, "Technology of Heavy Non-Ferrous Metals and Alloys," Published by London George Newnes Limited, 1967, pp. 192-207.
[13] ASM Committee on Copper and Copper Alloys, "Introduction to Copper and Copper Alloys," Metals Hand Book, The Material Section, Vol.2, 1990, pp. 239-245.
[14] L.L. Shreir, "Copper and Copper Alloys." Corrosion, Vol.1, Metal/Environment Reactions, 1979, pp. 4.33-4.67.
[15] J.Sienko Michell and A. Robert Plane, "Chemistry," McGraw Hill Int. Book Company, Fifth Edition, 1984.
[16] T.N. Rohdin, J. of American Chemical Society, Vol.72, 1950. p. 5102.
[17] T.N. Rohdin, J. of American Chemical Society, Vol.73, 1951 p. 3143.
[18] D.P. White, D.J.Evan, D.B.Scully and G.C. Wood, Actamet, Vol.15, 1967 p.14.
[19] R.F. Tycote, J. of Metals, Vol.78, 1950, p. 259.
[20] R.F. Tylcote, J. of Institute of Metals, Vol.81, 1953, p. 681.
[21] A.Ronquist and H.Fischemeister, J. of Metals, Vol.89, 1960, p. 681.
[22] F.W.Young, J.V. Catchart and A.T. Gwathmey, Acta Metall., Vol.5, 1957, p. 574.
[23] E.A. Gulbransen and W.S. Wysong, J. of Physical Chemistry, Vol.51, 1947, p. 1087.
[24] H. Nishmma, J. of Minerals and Metall., Vol.9, 1938, p. 655.
[25] C.G. Wood and F.H. Science and Technology, Vol.3, 1987, p. 519.
[26] D.W. Bridge, J.P. Baur and W.M. Fassel, J. of Electrochemical Society, Vol.103, 1956, p. 475.
[27] W.E. Cambell and U.B. Thomas, Trans. Electrochemical Society, Vol.81, 1942, p. 305.
[28] K.S.Pandey, "Indigenously Developed Ceramic Coating," Regional Engg., College, Tiruchirappalli-620015, TamilNadu, India.
[29] K.H. Moyer, Int. J. on Powder Metall., and Powder Technology, Vol.15, 1979, p.33.
[30] Instruction Manual for Electronic Balances, Model A0-180, Adair Dutt and Co. (India) Pvt. Limited, Madras, India, 1987.

American Journal of Engineering Research (AJER)
e-ISSN : 2320-0847 p-ISSN : 2320-0936
Volume-03, Issue-03, pp-91-102
www.ajer.org

Research Paper Open Access

Cloud Computing for Technical and Online Organizations

Hagos Tesfahun Gebremichael[1] Dr.Vuda Sreenivasa Rao[2]
M.Sc. (Computer Science), School of Computing and Electrical Engineering, IOT, Bahir Dar University,Ethiopia[1].
Professor, School of Computing and Electrical Engineering, IOT, Bahir Dar University, Ethiopia, INDIA[2].

Abstract: - Cloud computing is a new computing model which is based on the grid computing, distributed computing, parallel computing and virtualization technologies define the shape of a new technology.It is the core technology of the next generation of network computing platform, especially in the field of education and online.Cloud computing as an exciting development in an educational Institute and online perspective.Cloud computing services are growing necessity for business organizations as well as for technicaleducational institutions.Students and administrative personnel have the opportunity to quickly and economically access various application platforms and resources through the web pages on-demand.Application of storage technology can significantly reduce the amount of cloud storage servers, thereby reducing system development costs, reduce the system caused by the server a single point of failure. Cloud storage services meet this demand by providing transparent and reliable storage solutions.In this paper shows that the cloud computing plays an important role in the fields of TechnicalEducational Institutions and Online.The research study shows that the cloud platform is valued for both students and instructors to achieve the course objective and the nature, benefits and cloud computing services, as a platform for Educational environment and online.

Keywords: - *Cloud Computing, Technical Educational Institutions and Online.*

I. INTRODUCTION

Technical education was acknowledged in time as one of the pillars of society development. Through the partnerships between universities, government and industry, researchers and students have proven their contribution to the transformation of society and the entire world economy (Lazowska et al., 2008). The tendency observed during the last few years within the higher education level (Mircea, 2010; Bozzelli, 2009), is the universities' transition to research universities and ongoing update of the IT (Information Technology) infrastructure as foundation for educational activities and Science research. With the evolution of technology, the number of services which migrate from traditional form to the online form grows as well. For these specific services, an adequate providing form must be found in the online environment, using the proper technologies, guaranteeing the access of large number of users, fast and secure payment services (Ivan et al., 2009).

Cloud Computing has got different meaning to people working in different areas of computer science. Cloudcomputing has become a highlight for the IT specialists in recent years. To implement this technology, great stepshad been taken. To develop this domain [1], the pledged profits have determined the companies to invest a bigamount of money for research. It is an internet depended service delivery technique that offers internet based services, computing and storage for users in all markets that contains financial health care and government.Cloud computing is a new and rising information technology that shifts the way IT architectural solutions are suggest by means of moving towards the theme of virtualization: of data storage, of local networks (infrastructure) as well as software [2-3].

Cloud Computing is a new model for hosting resources and provisioning of services to the consumers. It provides a convenient, on-demand access to a centralized shared pool of computing resources that can be deployed by a minimal management overhead and with a great efficiency.The term "Cloud Computing" sprang from the common practice of depicting the Internet in pictorial diagrams as a cloud Internet.Cloud Computing providers depend on the Internet as the intermediary communications medium leveraged to deliver their IT resources to their consumers on a pay-as-you-go basis. By using cloud computing consumers can be access

resources directly through the internet, from anywhere by using any internet devices, and at any time without any technical or physical concerns.

National Institute of Standards and Technology (NIST) defines Cloud Computing is on-demand access to a shared pool of computing resources. It is an all-inclusive solution in which all computing resources (hardware, software, networking, storage, and so on) are provided rapidly to the consumers.Cloud computing is a comprehensive solution that delivers IT as a service. Computers in the cloud are configured to work together and the various applications use the collective computing power as if they are running on a single system. Cloud computing is a centralized virtual software available in the server which provides all the required resource to the users where the user don't need to think about the location or a device. Just need to browse and have all that is required.The flexibility of cloud computing is a function of the allocation of resources on demand. This facilitates the use of the system's cumulative resources, negating the need to assign specific hardware to a task. Before cloud computing, websites and server-based applications were executed on a specific system. With the advent of cloud computing, resources are used as an aggregated virtual computer. This amalgamated configuration provides an environment where applications execute independently without regard for any particular configuration.Educational Institutions are under increasing pressure to deliver more for less and they need to find ways to offer rich, affordable services and tools. Cloud computing has the potential to provide computation and storage resources as services. Both the public as well as the private institutions can use the cloud computing to deliver better services with limited resources.

Cloud computing gets its name as a metaphor for the Internet. Typically, the Internet is represented in networkdiagrams as a cloud, as shown in Figure 1.

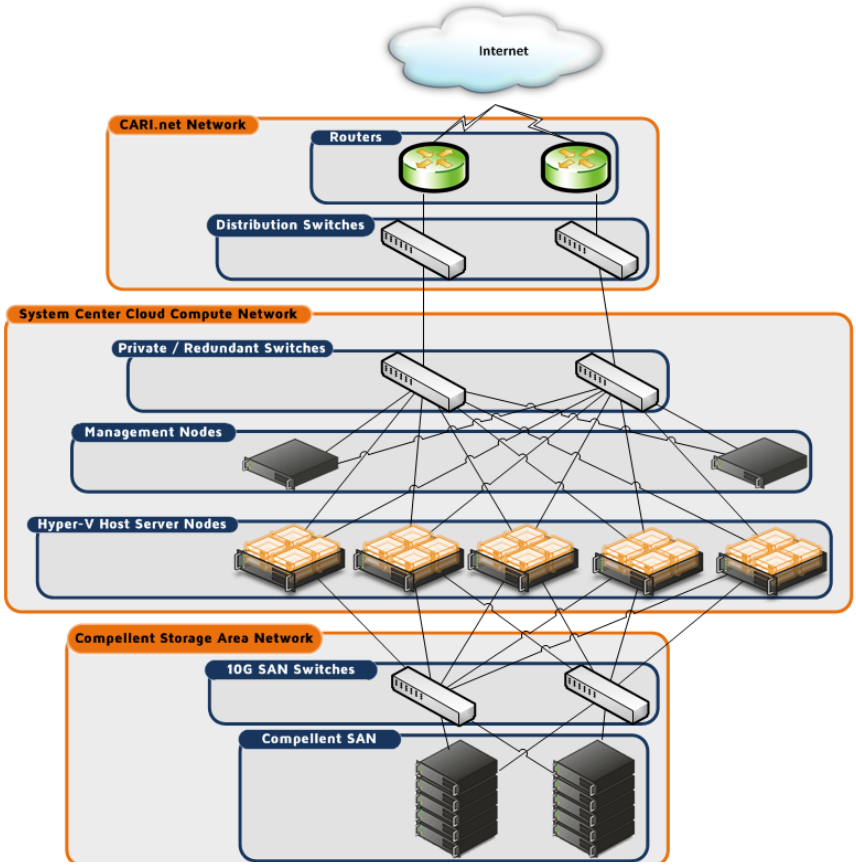

Figure 1: A cloud is used in network diagrams to depict the Internet.

There are eight fundamental elements that are vital to enabling the cloud concept to not just exist, but to grow to its fullest potential (see Figure 2). From the perspective of Rayport and Heyward (2009), it is essential to have the following conditions in the cloud environment:

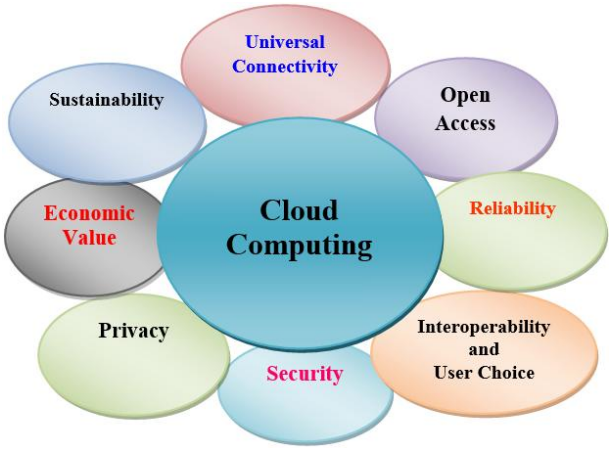

Figure 2: The 8 Fundamental Elements of Cloud Computing.

Universal connectivity—users must have near-ubiquitous access to the Internet.
Open access—users must have fair, non-discriminatory access to the Internet.
Reliability—the cloud must function at levels equal to or better than current stand-alone systems.
Interoperability and user choice—users must be able to move among cloud platforms.
Security—users' data must be safe.
Privacy—users' rights to their data must be clearly defined and protected.
Economic value—the cloud must deliver tangible savings and benefits.
Sustainability—the cloud must raise energy efficiency and reduce ecological impact.
Cloud uses virtualization as its key technology [4] .When end user submits their requirement a separate Virtual Machine is created to run their specific application. In a single host machine itself multiple Virtual Machines can be run to utilize theresources.

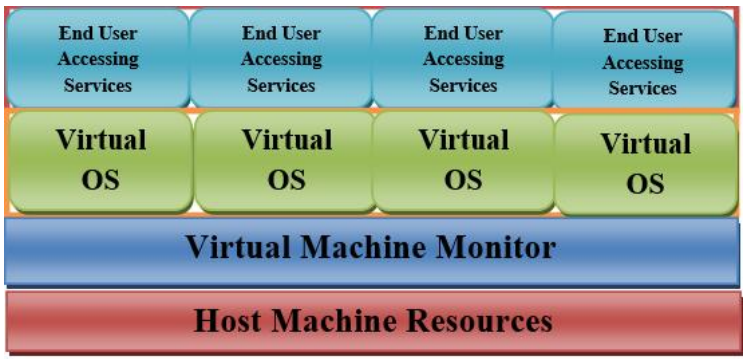

Figure. 3.Virtualization Technique.

Cloud storage is provided storage services, the network data stored in local storage service provider to provide online storage space. Furthermore, most of today's smart phones and tablet devices have good support for diverse networks and protocols. Thus, connectivity can be established between mobile participants via 4G, Wi-Fi, and Bluetooth. Physical machines may be dynamically allocated to virtual machines (VMs) which in turn may be migrated to other physical machines in case of machine faults. While this kind of flexibility increases availability and reduces cost, the highly dynamic nature in which VMs are allocated and migrated raises security concerns. Actually, Cloud computing is not a completely new concept. It has similar features as Grid computing that has been investigated for more than a dozen of years.

II. CLOUD COMPUTING BUILDING BLOCKS

The cloud computing model is comprised of a front-end and a back-end. These two elements are connected through a network, in most cases the Internet. The front end is the vehicle by which the user interacts with the system; the back end is the cloud itself. The front end is composed of a client computer, or the computer network of an enterprise, and the applications used to access the cloud. The back end provides the applications, computers, servers, and data storage that creates the cloud of services.

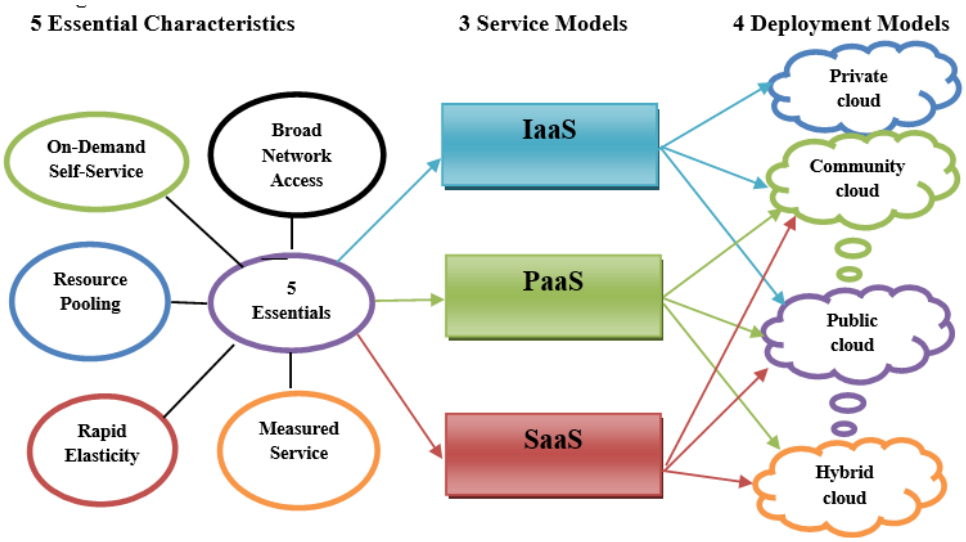

Figure 4: Cloud Computing Service Levels.

A.Essential Characteristics of Cloud Computing:

- *On-Demand Self-Service:* Customers can automatically provision computing capabilities and resources on their own when needed without necessitating any human intervention.
- *Broad Network Access:* Access and capabilities are available over the network through standard devices, such as cell phones, laptops, PDAs, etc.
- *Resource Pooling:* Resources such as network bandwidth, virtual machines, memory, processing power, storage capacity, etc. are pooled together to serve multiple customers using a multi-tenant model. That is, virtual and physical resources are dynamically assigned and reassigned based on need and customers' demands.
- *Rapid Elasticity:* Depending on demand, resources and capabilities can be quickly and automatically deployed and scaled at any quantity and at any time.
- *Measured Service:* Customer usage of the vendor's resources and services are automatically monitored controlled and reported offering a high level of transparency for the customer and vendor.

B.Service Models of Cloud Computing:

- *Software as a Service (SaaS):* The capability provided to the consumer is to use the provider's applications running on a cloud infrastructure. The applications are accessible from various client devices through either a thin client interface, such as a web browser (e.g., web-based email), or a program interface. The consumer does not manage or control the underlying cloud infrastructure including network, servers, operating systems, storage, or even individual application capabilities, with the possible exception of limited user -specific application configuration settings.
- *Platform as a Service (PaaS):* The capability provided to the consumer is to deploy onto the cloud infrastructure consumer-created or acquired applications created using programming languages, libraries, services, and tools supported by the provider.The consumer does not manage or control the underlying cloud infrastructure including network, servers, operating systems, or storage, but has control over the deployed applications and possibly configuration settings for the application-hosting environment.
- *Infrastructure as a Service (IaaS):* The capability provided to the consumer is to provision processing, storage, networks, and other fundamental computing resources where the consumer is able to deploy and run arbitrary software, which can include operating systems and applications. The consumer does not manage or control the underlying cloud infrastructure but has control over operating systems, storage, and deployed applications; and possibly limited control of select networking components (e.g., host firewalls).

C. Deployment Models Of Cloud Computing:

- *Private cloud:* The cloud infrastructure is provisioned for exclusive use by a single organizationcomprising multiple consumers (e.g., business units). It may be owned, managed, and operated by the organization, a third party, or some combination of them, and it may exist on or off premises.

- *Community cloud:* The cloud infrastructure is provisioned for exclusive use by a specific community of consumers from organizations that have shared concerns (e.g., mission , security requirements, policy, and compliance considerations). It may be owned, managed, and operated by one or more of the organizations in the community, a third party, or some combination of them, and it may exist on or off premises.
- *Public cloud:* The cloud infrastructure is provisioned for open use by the general public. It may be owned, managed, and operated by a business, academic, or government organization, or some combination of them. It exists on the premises of the cloud provider.
- *Hybrid cloud:* The cloud infrastructure is a composition of two or more distinct cloud infrastructures (private, community, or public) that remain unique entities, but are bound together by standardized or proprietary technology that enables data and application portability (e.g., cloud bursting for load balancing between clouds).

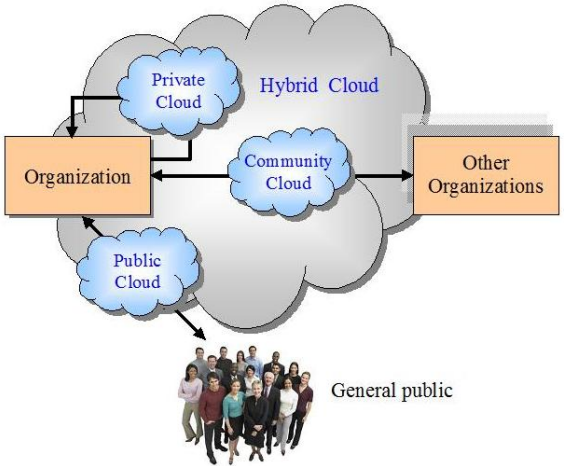

Figure 5: The cloud computing deployment models.

III. CLOUD COMPUTING CHALLENGES

Cloud computing has emerged as an important solution offering enterprises a potentially cost effective model to ease their computing needs and accomplish business objectives. Some features of cloud computing are:

- *Optimized Server Utilization:* As most enterprises typically underutilize their server computing resources, cloud computing will manage the server utilization to the optimum level.
- *On-Demand:*Cloud computing provides users with customized environments that are tailed to individual requirement. This feature is more user friendly than Grid computing where the application has usually to be adapted to the target architecture.
- *Dynamic Scalability:*Many enterprises include a reasonably large buffer from their average computing requirement, just to ensure that capacity is in place to satisfy peak demand. Cloud computing provides an extra processing buffer as needed at a low cost and without the capital investment or contingency fees to users.
- *Disaster Recovery:*It is a concern of enterprises about the resiliency of cloud computing, since data may be commingled and scattered around multiple servers and geographical areas. It may be possible that the data for a specific point of time cannot be identified. Unlike traditional hosting, the enterprise knows exactly where the location is of their data, to be rapidly retrieved in the event of disaster recovery. In the cloud computing model, the primary CSP(customer service provider) may outsource capabilities to third parties, who may also outsource the recovery process. This will become more complex when the primary CSP does not ultimately hold the data. The Cloud technology is currently still in the development phase. As the sensitive applications and data are moved into the cloud data centers, run on virtual computing resources in the form of virtual machine.

IV. THE BENEFITS OF CLOUD COMPUTING

As cloud computing begins to take hold,several major benefits have become evident:

Costs: The cloud promises to reducethe cost of acquiring, delivering, andmaintaining computing power, a benefitof particular importance in times offiscal uncertainty. By enabling agenciesto purchase only the

computing servicesneeded, instead of investing in complexand expensive IT infrastructures,agencies can drive down the costs ofdeveloping, testing, and maintainingnew and existing systems.

Access: The cloud promises universalaccess to high-powered computing andstorage resources for anyone with anetworkaccess device. By providing suchcapabilities, cloud computing helps tobolster an agency's continuity of operations(COOP) demands.

Scalability and Capacity: The cloud isan always-on computing resource thatenables users to tailor consumption totheir specific needs. Infinitely scalable,cloud computing allows IT infrastructuresto be expanded efficiently and expediently without the necessity of makingmajor capital investments. Capacity canbe added as resources are needed andcompleted in a very short period of time.Thus, agencies can avoid the latency,expense, and risk of purchasing hardwareand software that takes up datacenter space -- and can reduce thetraditional time required to scale up anapplication in support of the mission.Cloud computing allows agencies toeasily move in the other direction aswell, removing capacity, and thus expenses,as needed.

Resource Maximization: Cloud computingeases the burden on IT resourcesalready stretched thin, particularlyimportant for agencies facing shortagesof qualified IT professionals.

Collaboration: The cloud presents anenvironment where users can developsoftware-based services that enhancescollaboration and fosters greaterinformation sharing, not only within theagency, but also among other governmentand private entities.

Customization: Cloud computing offersa platform of tremendous potential forcreating and amending applications toaddress a diversity of tasks and challenges.Its inherent agility means thatspecific processes can be easily alteredto meet shifting agency needs, sincethose processes are typically changeableby making a configuration change,and not by driving redevelopment fromthe back-end systems (Heyward andRayport, 2009).

*Improve Accessibility:*You have access anytime, anywhere, making your life so much easier i.e. Google doc is an application of cloud computing provide the best way to others without cost.

V. CLOUD COMPUTING FOR TECHNICAL EDUCATION:

There was a time when, to use files (word processing files, spreadsheets, etc.) on different computers. Cloud computing is a new business model wrapped around new technologies like virtualization, SaaS and broadband internet. The safety, stability, and ease-of-use of cloud computing in education is resulting in widespread adoption in educational institutions of all sizes and types. Cloud computing entails using a network of remote servers hosted on the internet as opposed to a local server. This helps cut IT costs as well as simplifies content management processes for schools and educational systems. The results of a survey that have been completed in 2009 by Gartner analysts (Figure 6) about the IT trends (especially cloud computing) show that it is being used more in the areas of finance and business when compared to other sectors.

.

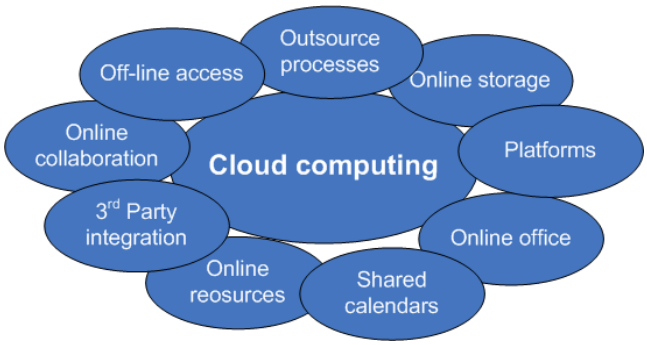

Figure. 6. Cloud computing usage.

*Back Up:*An important function of the Cloud is that it automatically saves content, making it impossible to lose or delete any valuable material. This means that even if a computer crashes, all documents and content will remain safe, saved, and accessible in the cloud.

*Storage:*The Cloud allows its users to store almost all types of content and data including music, documents, E-Books, applications, photos, and much more. We share the information of Attendance and Assignment in our Institute of students in Google doc and share all the information of students on doc via using an ERP Software and utilize the cloud resources

*Accessibility:*Any data stored in the Cloud can easily be accessed from almost any device including mobile devices such as phones or tablets. In our institute an URL provide to the students for accessing the data inside the campus or outside the campus.

*Collaboration:*The Cloud allows multiple users to work on and edit documents at the same time, it enables effortless sharing and transmission of ideas. It also provides the security to edit only those people who gain the right from admin. With this feature, group projects and/or collaborative lesson plans can be optimized for both teachers and students.
*Resource and Time Conscious:*With the availability of content online, it is no longer necessary for teachers to spend time and resources printing or copying lengthy documents or lesson plans. Now, students are able to access homework assignments, lesson notes, and other materials online like ERP Systems of education institute and parents also see the details of the students. Cloud can be used in underdeveloped or emerging countries creating a way of being able to teach children who would not ordinarily have access to education. Students and teachers can share their work without having to use paper. Using paper is costly both to the environment and in monetary terms and is therefore no longer a viable way to educate.
Assignments: The Cloud allows teachers to post assignments online. Students are able to access these assignments, complete them, and save them in a folder to be reviewed later.

VI. AN ARCHITECTURE OF CLOUD TECHNICAL EDUCATION

The model contains physical hardware layer, virtualizationlayer, education middleware layer, application programinterface layer, management system and securitycertification system, see Figure 7.

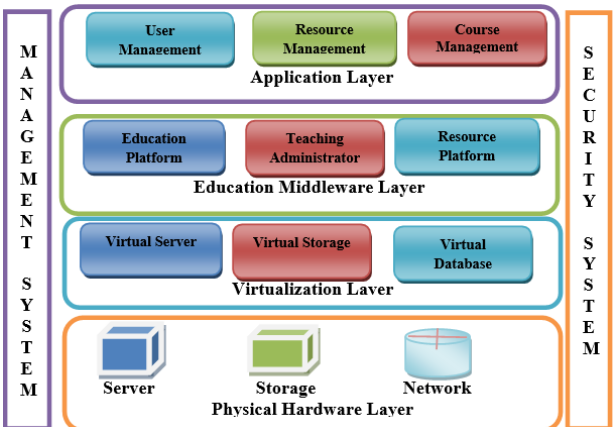

Figure 7. Architecture of Cloud Education model.

*Physical hardware layer*is a basic platformmodel, including servers, storage equipment's, And network equipment's.
*Virtualization layer*with the feature: dynamic configuration,distributed deployment, fee measurementrealizes the five characteristics of cloud computing.
The goal of virtualization layer is to break completelyinformation islands based on existing regionalthrough the distributed technology and virtualizationtechnology. This layer also consists of three parts: virtualservers, virtual storages, and virtual databases.
*Education middleware layer*is the core layer, because it is the basic business platform. This layer is different from existing, and all information attached to it on different computing node including ordinary file and database. So, all application systems on the middleware layer have
*Application program interface layer*can guarantee model's scalability. Because of the diversity of the existing application system and an application system cannot satisfy all the needs of customers. In this layer also provide the necessary interface beside, and still need to be able to provide hosting service.
*Management system*mainly watchers physical condition, virtualization software, hardware and software, open API. Management system can enhance the safety of the software platform.
*Security system*includes identity authentication and authorization, single point login, virtualization software and hardware access control and audit, the education middleware and open API access control.

VII. ADVANTAGES OF CLOUD COMPUTING IN ONLINE(E-COMMERCE)

For describing the different aspects of an online or E-commerce systems, digitally enabled commercial transactions between and among organizations and individuals.Cloud computing is now evolving like never before, with companies of all shapes and sizes adapting to this new technology. The figure 8 shows a high-level view on an E-commerce system's architecture. If used properly and to the extent necessary, working with data in the cloud can vastly benefit all types of businesses. Industry experts believe that this trend will only continue to

grow and develop even further in the coming few years. While cloud computing is undoubtedly beneficial for mid-size to large companies, it is not without its downsides, especially for smaller businesses.

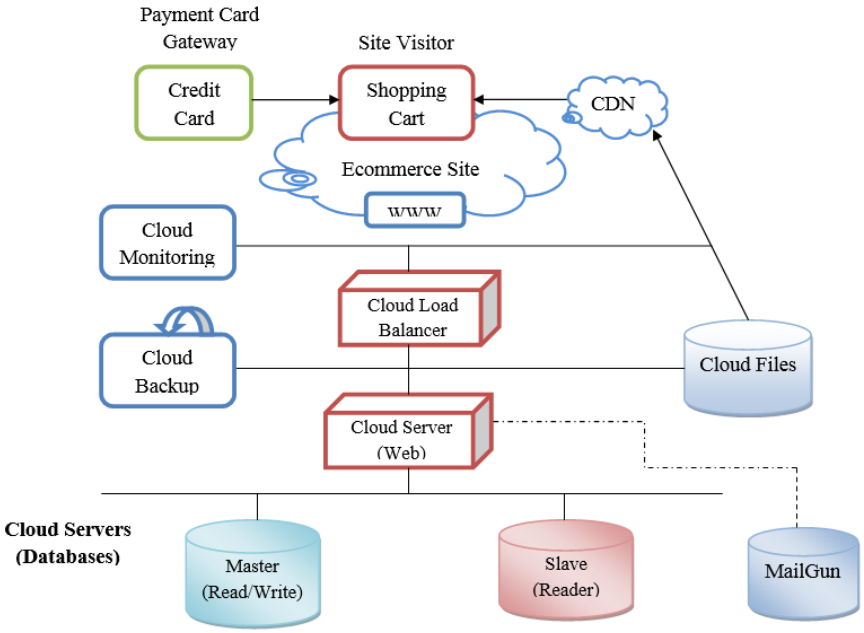

Figure. 8.E-Commerce system architecture.

*Unlimited accessibility:*Developing a business means being constantly connected With Cloud, you can manage your online shop from anywhere and at any time. A browser and an Internet connection are all it takes to process orders, interact with customers, schedule deliveries or generate invoices.
*Security and stability:*Security is one of the most important advantages of the Cloud technology. In the Cloud system, the data of each client is completely partitioned, so that none of the areas interferes with the others. The connection to the servers is secured according to the highest standards, making sure that you are the only one with access to your data. It's like having your own server, without paying considerable amounts of money.
*Full scalability:*Your business grows, so will your technical requirements. Unlike open source ecommerce solutions, which would normally require new investments for extending the technical infrastructure, a Cloud ecommerce system will always be ready to efficiently sustain your new volume of clients, orders, traffic and continuously growing product catalog.
*Minimal costs or No costs:*Cloud solution for E-Commerce, you don't need to worry about the initial investments. You don't need to buy your own server or pay for a separate hosting service. Depending on your business needs, you can always increase or limit the amount of resources you use and also optimize your costs thanks to the scalability of the system.
*Quick Deployment:*Lastly and most importantly, cloud computing gives you the advantage of quick deployment. Once you opt for this method of functioning, your entire system can be fully functional in a matter of a few minutes. Of course, the amount of time taken here will depend on the exact kind of technology that you need for your business.

VIII. PRIVACY AND SECURITY ISSUES

Security and privacy problems appear in technical and online because of operation mechanism and policy mechanism. The failure of security technology makes personal privacy be spread, diffused, aggrieved and scouted without permission. Loopholes in the law led to the network managers could store, amend, exchange, and sell personal information without punishment.We classify the privacy violation phenomenon of technical and online process during the information to be collected, used, saved, and deleted and so on.
*Security issues:*Some of the most serious threats are listed below:

- Deliberate software attacks (viruses, worms, macros, denial of service).
- Technical and human failures and errors (bugs, coding problems, accidents).
- Deliberate acts of espionage or trespass (unauthorized access and/or data collection).
- Deliberate acts of sabotage or vandalism (destruction of information or system).
- Technical hardware failures or errors (equipment failure).

- Deliberate acts of theft (illegal confiscation of equipment or information).
- Quality of Service deviations from service providers (power and WAN service issues).

The primary concern in technical and online is the security that can be summarized as following:

User Authorization and Authentication: The elementary feature of technical and online system is the reliable identification – recognition of the user as a genuine member of a user community because it is the basis for Access control to the online system. Authentication – verification of the user's identity. Authorization – permission to access specific resources.

Entry Points: There are many "entry points" in online system. A system can be attacked only through its "entry points". Designers can limit the security risks by reducing the number of entry points.

Dynamic Nature: The other challenge is the dynamic nature of these systems where there are dynamic sessions where any process may join or leave the group sessions at any time. Security is also concern with each particular member process, a strict session has to be maintained and the credentials are to be verified to control both at the session level and at the participant site.

Protection against Manipulation: One of the issues of E-Learning and online are manipulation from the side of the students the system must be secured against manipulation. There are many possible solutions where any manipulations can be protected by using the techniques of encryption, digital signatures, firewalls, etc.

Confidentiality: Confidentiality refers to the assurance that information and data are kept secret and private and are not disclosed to unauthorized persons, processes or devices.

Integrity: Integrity is that only authorized users are allowed to modify the contents which include creating, changing, appending and deleting data and metadata and the attacks on integrity are generally the attempts made to actively modify or destroy information in the E- Learning and online sites without proper authorization.

Availability: The E-Learning online material e-content, data (or metadata) are to be made available to the learner at the specified session when the user log on to the system for their session at the period of time, if the required material is not available the learner will lose interest and not get the at most use of ELearning system. Mainly there are two types of attacks via blocking attack and flooding attack, e.g.: Denial of Service, Node attacks, Line attacks, Network infrastructure attacks.

*Non-Repudiation:*Non-repudiation is the last step in information security where the learners have to be provided with technical and online services without any possible fraud such as when computer systems are broken in to or infected with Trojan horses or viruses, to deny the works or changes done by them in the system elimination of a refuted activity performed by a user.

IX. RESULT: USING CLOUD COMPUTING

Think of what you do on the web on a daily basis. You check your e-mail. You do your "social networking"—checking Facebook once, twice, 10 times a day, and now twittering. You post and view photos. You store files online, and yes, there can be real work done as well, creating documents, spreadsheets, and presentations entirely online.

The below figures shows the results of this research review work that how cloud used in educational,online and business system in present and future.

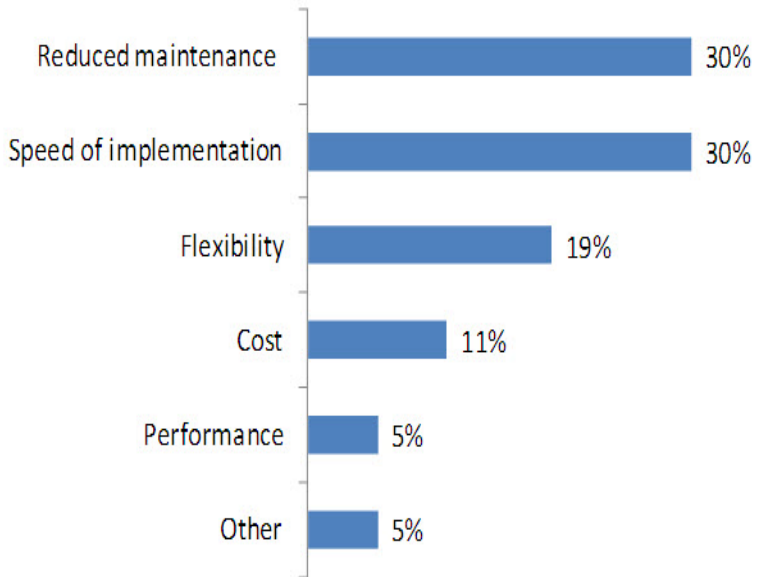

Figure 9: why cloud using in Technical, Online and Business.

Cloud Computing Activities by Different Age Cohorts:

Table 1: Internet users in each age group who do the following online activities (%)

Use of Internet-Based Cloud Activity.	Age				All Ages
	18-29	30-49	50-64	65+	
Use webmail services such as Hotmail, Gmail or Yahoo Mail.	77%	58%	44%	27%	56%
Store personal photos.	50%	34%	26%	19%	34%
Use online applications such as Google Documents or Adobe Photoshop Express.	39%	28%	25%	19%	29%
Store personal videos.	14%	6%	5%	2%	7%
Pay to store computer files online.	9%	4%	5%	4%	5%
Back up hard drive to an online site.	7%	5%	5%	4%	5%
Have done at least one activity.	87%	71%	59%	46%	-------
Have done at least two activities.	59%	39%	31%	21%	--------

Source: Adapted from Horrigan (2008).

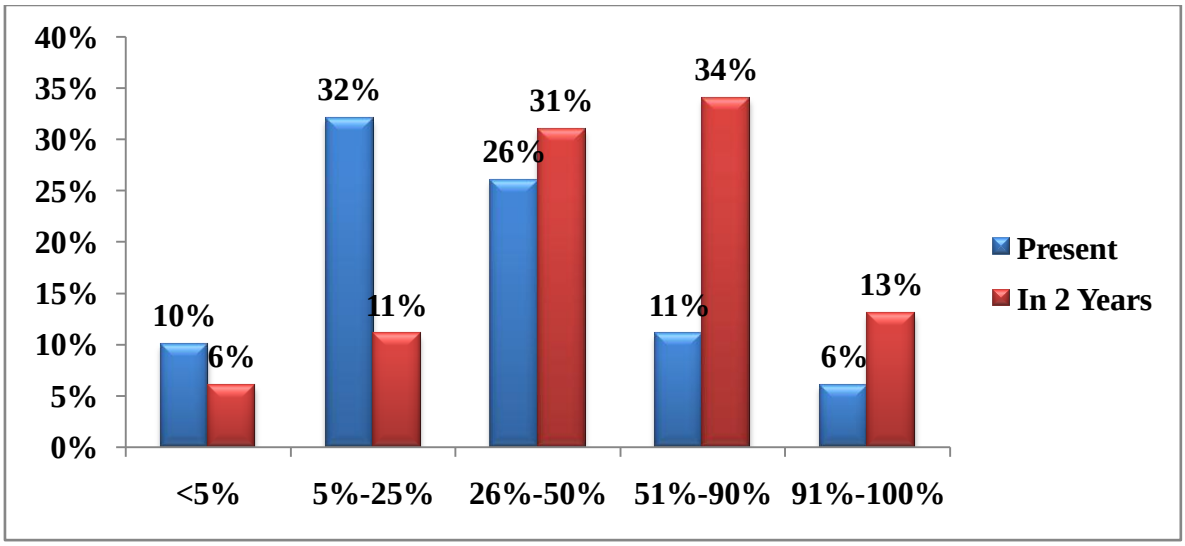

Figure 10: Cloud computing uses at present and next two years.

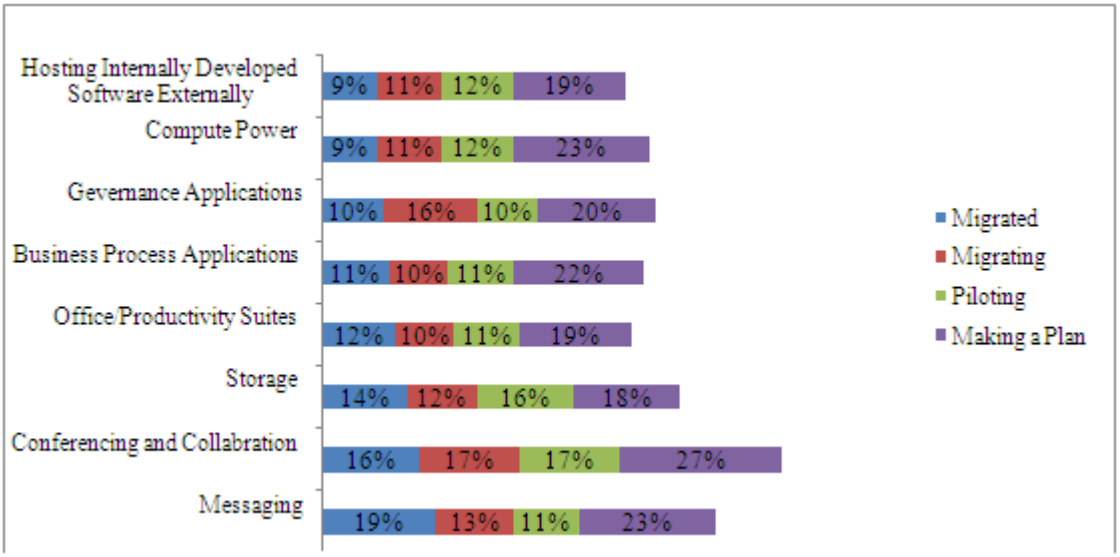

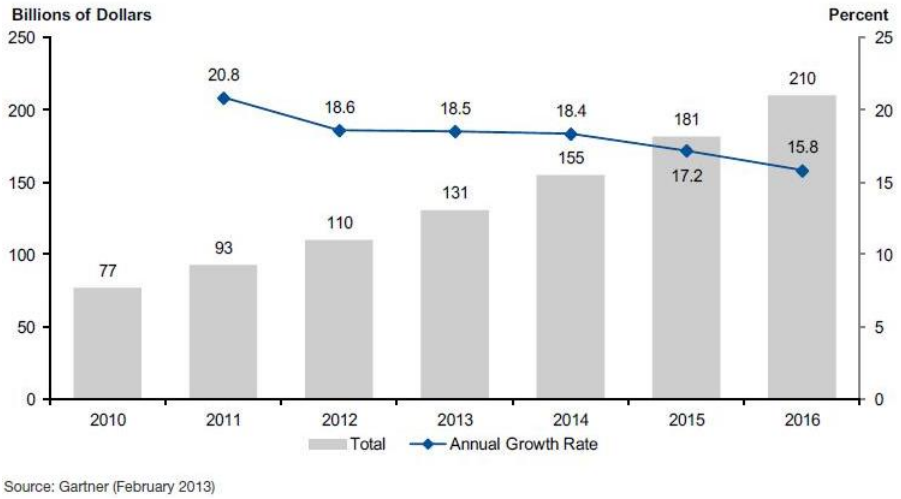

Figure 11: public cloud services market and Annual Growth Rate (2010-2016).

X. CONCLUSION

In this paper,benefits, challenges and security issues of could computing in educational organizational and online advantages provided by cloud, there is a great advantage for university IT staff to take them away the responsibility of the maintenance burden in the university and other online organization. Cloud provides instant global platforms, elimination of H/S capacities and licenses, reduced cost, simplified scalability marketing though cloud services. There will be an online survey to collect the required data for the use of cloud computing in the universities and other governmental or private institutions in the region the cloud computing services needed to deliver the majority of IT services needed by customers do not yet exist. Particularly new payment services with their user base help retailers to enter new markets.

REFERENCES

[1] Florin Ogigau-Neamtiu, "Cloud Computing Security Issues", International Journal of Application or Innovation in Engineering, Vol.1, no.2, pp.1-5, 2012.
[2] Leavitt N, 2009, "Is Cloud Computing Really Ready for Prime Time?" Computer, Vol. 42, pp. 15-20, 2009.
[3] Weinhardt C, Anandasivam A, Blau B, Stosser J, "Business Models in the Service World", IT Professional, vol. 11, pp. 28-33, 2009.
[4] Aymerich, F. M., Fenu, G., Surcis, S., & IEEE. (2008). An Approach to a Cloud Computing Network. 1st International Conference on theApplications of Digital Information and Web Technologies, Ostrava, Czech Republic, 120-125.
[5] Hosam F. El-Sofany, Abdulelah Al Tayeb, Khalid Alghatani, and Samir A. El-Seoud, "The Impact of Cloud Computing Technologies in E-learning", IJET – Volume 8, Special Issue 1: "ICL2012", January 2013.
[6] Ms. Shivani Goel, Dr. Ravi Kiran , Dr. Deepak Garg, "Impact of Cloud Computing on ERP implementations in Higher Education" (IJACSA) International Journal of Advanced Computer Science and Applications, Vol. 2, No. 6, 2011, pp-146 – 148.
[7] Anjali Jain, "Role of Cloud Computing in Higher Education", International Journal, Volume 3, Issue 7, July 2013.
[8] Alex Mu-Hsing Kuo and Alex Mu-Hsing Kuo,Opportunities and Challenges of Cloud Computing to Improve Health Care Services, JMIR.
[9] Marinela Mircea and Anca Ioana andreescu "Using Cloud Computing in Higher Education: A Strategy to Improve Agility in the Current Financial Crisis", IBIMA Publishing, Communications of theIBIMA.http://www.ibimapublishing.com/journals/CIBIMA/cibima.html, Vol. 2011 (2011), Article ID 875547, 15 pages, DOI: 10.5171/2011.875547.
[10] David C. Wyld, "Moving to the Cloud: An Introduction to Cloud Computing in Government".

AUTHORS BIBLIOGRAPHY

HagosTesfahun Gebremichael received his B.Sc. Degree in Computer Science from Bahir Dar University. Currently perusing M.Sc. in Computer Science, School of Computing and Electrical Engineering, IOT, Bahir Dar University, Ethiopia. His main research interest is Pattern Recognition and Cloud Computing.

Dr. Vuda Sreenivasa Rao received his M.Tech degree in computer science and engineering from Sathyabama University from 2007.He received PhD degree in computer science and engineering from Singhania University, Rajasthan, India from 2010. Currently working as Professor in School of Computing and Electrical Engineering, IOT, Bahir Dar University, Ethiopia. His main research interests are Data mining, Fuzzy logic, Mobile communication, cloud computing and Network Security. He has got 14 years of teaching experience. He has published 37 research papers in various international journals and one Springer international conference paper. He has Editor-in-Chief in 3 international journals and 126 Editorial Board / Reviewer Board memberships in various international journals. He has Technical committee member in various international Conferences. He is a life member of various professional societies like IEEE, ACM, MAIRCC, MCSI, SMIACSIT, MIAENG, MCSTA, MAPSMS, MSDIWC, SMSCIEI, SNMUACEE and MISTE.

American Journal of Engineering Research (AJER)
e-ISSN : 2320-0847 p-ISSN : 2320-0936
Volume-03, Issue-03, pp-103-112
www.ajer.org

Research Paper Open Access

A comparative study on march tests for SRAMS

Mrs. Princy.P, Dr. N.M Sivamangai
Research Scholar Department of Electronics & Communication Engineering Karunya University, Coimbatore, Tamilnadu, INDIA
Associate Professor Department of Electronics & Communication Engineering Karunya University, Coimbatore, Tamilnadu, INDIA

Abstract: - SRAMs are widely used in cache memories due to its infinite and very fast read/write operations. The ever increasing density of embedded memories on SoC's (System on Chips) gives rise to many defects and faults which cannot be identified during the fabrication process. The advantages of March tests for fault detection which make it acceptable for industries includes simplicity, high fault coverage and the linearity of test time with memory size.. High reliability is a major concern for memories if they are a part of control units implemented in hazardous environments. Even the occurrence of a single fault may lead to disasters.This emphasizes the importance of comparing and evaluating existing March tests considering all types of faults. All the traditional tests concentrates on the probability of occurrence of a fault rather than its mere occurrence This paper analysis the various types of faults in SRAMs(Static Random Access Memories), evaluates various dedicated March tests considering the percentage of fault detection.

Index Terms: - *SRAMs, static dynamic coupled, March tests.*

I. INTRODUCTION

A Comparative research on different existing march tests concentrating on faults in SRAMs is introduced in this paper. Advanced scaling techniques and shrinking dimensions in embedded memories cause new faults to appear in the core memory and its associated circuits. Due to the area, cost and time constraints for BIST(Built-in-Self Test) schemes in SoC's, the existing march tests concentrate on a particular classification of faults only. This paper compares the efficiency of different march tests to detect different fault models. March tests like SS [3] can detect different types of static single cell and double cell faults with a test length of 22N.March RAW and March RAW1 has a test length of 13N and 26N respectively. The former one detects dynamic single cell and later covers dynamic double cell faults. March AB , an improved version of March RAW detects whole set of dynamic faults detected by AB.It is also able to cover all static faults detected by March SS.March test BDN ,which is an extended modified version of March AB improves the fault coverage of AB, but maintains the same test complexity.

This paper is organized as follows: Section 2 deals with the basics and background. The classification of faults in SRAM's,definitions and notations, functional fault models and fault primitives are presented in Section 3..Section 4 deals with the results obtained after the comparative analysis of different well known march tests.

II. BASICS AND BACKGROUND

A.SRAM CELL

A 6T SRAM cell array is shown in figure [1]. This cell comprises of two inverters connected back to back, two access transistors, bit lines, word lines and associated circuitry. Defects and hence faults can occur either in the memory array or in the associated peripheral circuits.Faults differ according to the type of defect,

their location in the memory structure and also due to the way of performing read/ write operations. We can perform read/ write operations in SRAM cells with the activation of word lines and read/ write logic.

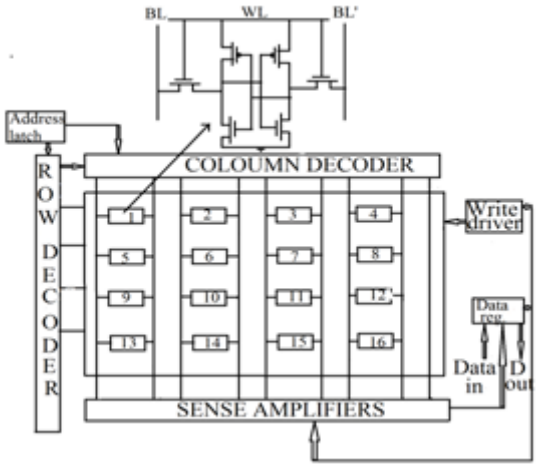

Fig1. SRAM Cell'

B.MARCH TESTS

As explained in [9], a March test is a test algorithm composed of a sequence of March elements which is usually denoted by a ' {...} ' bracket. Each March element [ME] is a sequence of operations applied sequentially on certain memory cell before proceeding to the next one, denoted by using ' (…) 'bracket.The ith operation can be defined as op_i where op_i ε {rd, wd}, 'rd' means read the contents of the memory cell and verify whether it is equal to 'd'.'wd' denotes write 'd'in a particular cell location, where 'd' ε {0, 1}.

C.FAULT NOTATIONS

The concept of functional fault primitives(FP),the compact notation used helps us to precisely define various functional fault models(FFM).For a given memory failure, a combination of S,F,R denoted as <S/F/R> (or <S/F/Rv>) represents FP for a single cell . <S_a; Sv/F/R> (S_a; Sv/F/$R_{a,v}$) represents the FP for two cells. ' S ' denotes the operation/value sensitizing the fault. S ϵ {0,1,0r0,0r1,1r0,1r1,0w0,0w1,1w0,1w1}.In the case of two cell FP's, S_a represents the operation (state) of the aggressor cell and S_v represents the operation(state) of the victim cell.' F' denotes the value of the faulty cell due to some sensitizing operation, where F Є{0,1 ↑,↓,?} whereby ↑(↓) represents an up(down) transition..R represents the logical value that appears at the output of the SRAM cell if the sensitizing operation is a read operation where .RЄ{0,1,?,-}.Here,'?' represents random or undefined logical value.A '-' in R represents that the output is not applicable in that case and the sensitizing operation does not contain a read operation.

III. FAULT CLASSIFICATION

Faults can be classified as simple static faults, static coupled faults, dynamic faults, dynamic coupled faults and faults associated with peripheral circuitry. Peripheral circuits of SRAMs includes address decoders, read/write control logic, sense amplifiers etc.

1) Simple static faults: Faults which cannot influence each other come under simple static faults.Static fauls are those FP's which can be sensitized by performing at most one operation. ***Case 1:***If the state of a cell is stuck at one, no operation is needed to sensitize the fault.***Case2:***If a read operation causes a cell to flip, one operation will be required to detect the fault.These faults can be classified as static faults.

a) State fault (SF): A cell is said to have a state fault, even if no operation is being performed on the cell, its logic value flips before it is accessed. No operation is needed for the sensitation of the fault.

b) Stuck at fault(SAF): A cell suffers from a stuck –at fault,if the contents of the cell remains stuck at a particular logical value irrespective of the operation performed on it.

*c) No-Access Fault(NF):*A cell suffers from a no access fault if the cell cannot be accessed.

d) Transition fault(TF): A cell suffers from a transition fault if the cell fails to undergo a transition while performing a write operation on the cell.

e) Write destructive fault(WDF): A cell is said to have write destructive fault if a non-transition write operation performed in a particular cell causes a transition of its contents.

TABLE 1 FAULT PRIMITIVES OF SINGLE CELL STATIC FAULTS x∈ {0, 1}

Type of fault	FFM		FP's
Simple static faults	State fault	SF	<0/1/->,<1/0/->
	Stuck-at-fault	SAF	<∀/1/->,<∀/0/->
	No access fault	NAF	{<0w1/0/->,<1w0/1/->,<rx/x/?>}
	Transition fault	TF	<0w1/0/->,<1w0/1/->
	Write destructive fault	WDF	<0w0/↑/->,<1w1/↓/->
	Read destructive fault	RDF	<r0/↑/1>,<r1/↓/0>
	Deceptive read destructive fault	DRDF	<r0/↑/1>,<r1/↓/1>
	Random read destructive fault	RRDF	<r0/↑/?>,<r1/↓/?>
	Incorrect read fault	IRF	<r0/0/1>,<r1/1/0>
	Random read fault	RRF	<r0/0/?>,<r1/1/?>
	Data retention fault	DRF	{<1T/↓/->,<0T/↑/>,<xT/?/->}
	Undefined state fault	USF	<1/?/->,<0/?/->
	Undefined read fault	URF	<rx/?/0>,<rx/?/1>,<rx/?/?>
	Undefined write fault	UWF	<0w0/?/->,<0w1/?/->, <1w0/?/->, <1w1/?/->

f) Read destructive fault(RDF): A cell has a read destructive fault if a read operation performed in a particular cell changes the logical value stored in the cell and returns an incorrect value at the output.

g) Decepive read destructive fault:(DRDF): A cell suffers from a deceptive read destructive fault if a read operation performed on the cell returns a correct value at the output but changes the data in the cell.

h) Random read destructive fault(RRDF); A cell has a random read destructive fault if a read operation performed on the memory cell changes the logical value stored in the cell and returns a random value as output.

i) Incorrect read fault(IRF): A cell is said to have an incorrect read fault if a read operation performed on the cell does not change the contents of the cell but returns a incorrect logical value at the output.

*j) Random read fault(RRF):*A cell suffers from a random read fault if a read operation performed on the cell retuns a random value at the output while keeping the correct value within the cell.

*k) Undefined State Fault(USF):*A cell suffers from an undefined state fault, if even if we are not performing any operation on the memory cell ,the contents of the cell flips to an undefined value ,before being accessed.

l) Undefined Write Fault(UWF): A cell has a undefined write fault,if a write operation performmed on the cell brings the cell to an undefined state.

*m) Undefined Read Fault(URF):*A cell is said to have an undefined read fault if a read operation performed on the memory cell brings the cell to an undefined state.

n) Data retention fault(DRF): A cell has a data retention fault if the contents of the cell changes after a certain time T,before it is being accessed.

*2) Static coupled faults:*Faults related to two cell operations come under static coupled faults.The classification of static coupled faults are as under.

a) State coupling fault(CFst):: Two cells suffers from a state coupling fault if we are not performing any operation on the victim cell or aggressor cell,.the victim cell is forced into a given logic state , only if the aggressor cell is in a logic state.

*b) Undefined State Coupling Fault(CFus):*Two cells are said to have an undefined state coupled fault if we are not performing any operation on the victim cell or aggressor cell,.the victim cell is forced into a given logic state , only if the aggressor cell is in a logic state.

c) Disturb coupling fault(CFds): Two cells are said to have a disturb coupling fault if the the contents of the victim cell flips on application of an operation(read,non-transition write,transition write) performed on the aggressor cell.

TABLE II TABLE OF DOUBLE CELL STATIC FAULTS

Type of fault	FFM		FP's
Static coupled faults	State coupling fault	CFst	<0;0/1/->,<1;0/1/->,<;0;1/0/->, <1;1/0/->
	Undefined state coupling fault	CFus	<0;0/?/->,<0;1/?/->,<1;0/?/->, <1;1/?/->
	Disturb coupling fault	CFds	<0w0;0/↑/->,<0w1;0/↑/->,<1w0;0/↑/>, <1w1;0/↑/>,<0w0;1/↓/->,<0w1;1/↓/->,<1w0;1/↓/->, <1w1;1/↓/->,<r0;0/↑/->, <r1;0/↑/->,<r0;1/↓/->,<r1;1/↓/->,
	Undefined Disturb coupling fault	CFud	<0w0;0/?/->,<0w1;0/?/->,<1w0;0/?/->,<1w1;0/?/->, <0w0;1/?/->,<0w1;1/?/->,<1w0;1/?/->,<1w1;1/?/->, <r0;0/?/->,<r1;0/?/->, <r0;1/?/->,<r1;1/?/->
	Idempotent coupling fault	CFid	<0w1;0/↑/->,<1w0;0/↑/->, <0w1;1/↓/->,<<1w0;1/↓/->
	Inversion coupling fault	CFin	{<0w1;0/↑/->,<0w1;1/↓/->}, {<1w0;0/↑/->,<1w0;1/↓/->}
	Transition coupling fault	CFtr	<0;0w1/0/->,<1;0w1/0/->, <0;1w0/1/->,<1;1w0/1/->
	Write disturb coupling fault	CFwd	<0;0w0/↑/->,<1;0w0/↑/->, <0;1w1/↓/->,<1;1w1/↓/->
	Read disturb coupling fault	CFrd	<0;r0/↑/1>,<1;r0/↑/1>, <0;r1/↓/0>,<1;r1/↓/0>
	Deceptive Read disturb coupling fault	CFdrd	<0;r0/↑/0>,<1;r0/↑/0>, <0;r1/↓/1>,<1;r1/↓/1>
	Random read destructive coupling fault	CFrrd	<0;r0/↑/?>,<1;r0/↑/?>, <0;r1/↓/?>,<1;r1/↓/?>
	Incorrect read disturb coupling fault	CFir	<0;r0/0/1>,<1;r0/0/1>, <0;r1/1/0>,<1;r1/1/0>
	Random Read coupling fault	CFrr	<0;r0/0/?>,<1;r0/0/?>, <0;r1/1/?>,<1;r1/1/?>
	Undefined Read coupling fault	CFur	<0;r0/?/0>,<1;r0/?/0>,<0;r0/?/1>,<1;r0/?/1>,<0;r0/?/?>, <1;r0/?/?>,<0;r1/?/0>,<1;r1/?/0>,<0;r1/?/1>, <1;r1/?/1>,<0;r1/?/?>,<1;r1/?/?>
	Undefined Write coupling fault	CFuw	<0;0w0/?/->,<1;0w0/?/->,<0;0w1/0/->,<1;0w1/0/->, <0;1w0/?/->,<1;1w0/?/->,<0;1w1/?/->, <1;1w1/?/->

*d) Undefined Disturb Coupling Fault(CFud):*Two cells are said to have an undefined disturb coupling fault if the victim cell is forced into an undefined state on application of an operation(read,non-transition write,transition write) performed on the aggressor cell.

e) Idempotent coupling fault(CFid): Two cells are said to have an iodempotent coupling fault if the contents of the victim cell flips on application of a transition write operation on the aggressor cell.

f) Inversion coupling fault(CFin): Two cells are said to have an inversion coupling fault if the contents of the victim cell gets inverted on application of a transition write operation on the aggressor cell.

g) Transition coupling fault(CFtr): Two cells are said to have a transition coupling fault if a logic value in the aggressor cell prevents a transition write operation on the victim cell.

h) h) Write destructive coupling fault(CFwd): Two cells are said to have a write distructive coupling fault, if the aggressor cell in a certain logic state ,a non-transition write operation performed on the victim cell results in a transition of the contents of the victim cell.

i) Read destructive coupling fault(CFrd):: Two cells are said to have a read destructive coupling fault, if the aggressor cell in a certain logic state,a read operation performed on the victim cell changes the contents of the victim cell and returns an incorrect value at the output.

j) Deceptive read disturb coupling fault(CFdrd):: Two cells are said to have a deceptive read destructive fault, if the aggressor cell in a certain logic state,a read operation performed on the victim cell changes the contents of the victim cell and returns a correct value at the output.

*k) Random Read Disturb Coupling Fault(CFrrd):*Two cells are said to have a random read disturb coupling fault if the aggressor cell in a certain logic state, a read operation performed on the victim cell changes the contents of the victim cell and returns a random value at the output

l) Incorrect read disturb coupling fault(CFir): Two cells are said to have an incorrect read disturb coupling fault if the aggressor cell in a certain logic state , a read operation performed on the victim cell does not changes the contents of the victim cell, but returns an incorrect value at the output.

m) Random read coupling fault:(CFrr): Two cells are said to have a random read coupling fault if the aggressor cell in a certain logic state, a read operation performed on the victim cell does not changes the contents of the victim cell and returns a random value at the output.

*n) Undefined Read Coupling Fault(CFur):*Two cells are said to have an undefined read coupling fault if the aggressor cell in a certain logic state, a read operation performed on the victim cell brings the victim cell to a undefined state.

o) Undefined Write Coupling Fault(CFuw): Two cells are said to have an undefined write coupling fault if the aggressor cell in a certain logic state, a write operation performed on the victim cell changes the victim cell to a undefined state.

3) Dynamic faults**:** Dynamic faults are those faults that can be sensitized by at least two sequential operations.For example,a dynamic read operation(i.e,a write operation immediately followed by a read operation) changes the logical value stored in the memory cell and returns an incorrect output .Then in this case we need two read operations to sensitize the fault.

a) Dynamic read disturb fault(dRDF): In the case of this fault, a write operation immediately followed by a read operation returns an incorrect output value and changes the data stored in the memory cell.

b) Dynamic deceptive read destructive fault(dDRDF): In the case of this fault, a write operation immediately followed by a read returns a correct output but changes the data stored in the memory cell.

c) Dynamic incorrect fault (dIRF): In the case of this fault, a write operation immediately followed by a read operation, returns an incorrect output but does not change the data stored in the memory cell.

TABLE III FAULT PRIMITIVES OF SINGLE CELL DYNAMIC FAULTS

Type of fault	FFM		FP's
Simple, dynamic fault	Dynamic read disturb fault	dRDF	<0w0r0/1/1>,<1w1r1/0/0>, <0w1r1/0/0>,<1w0r0/1/1>
	Dynamic Deceptive read disturb fault	dDRDF	<0w0r0/1/0>,<1w1r1/0/1>, <0w1r1/0/1>,<1w0r0/1/0>
	Dynamic incorrect read fault	dIRF	<0w0r0/0/1>,<1w1r1/1/0>, <0w1r1/1/0>,<1w0r0/0/1>

*3) Dynamic coupling faults:*The FP's of dynamic faults includes operations performed on the aggressor and victim cell.The classification of dynamic coupling faults are as under:

a) Dynamic Disturb Coupling Fault(dCFds): In the case of this fault,a write operation immediately followed by a read operation on the aggressor cell, causes the victim cell to flip.

*b) Dynamic Read Disturb Coupling Fault(dCFrd):*Two cells are said to have a dynamic read disturb coupling fault if the aggressor cell is in a given state, a write operation immediately followed by a read operation performed on the victim cell returns an incorrect output but changes the logical value stored in the memory .

*c) Dynamic Deceptive Read Disturb Coupling Fault(dCFdrd):*Two cells are said to have a dynamic deceptive read disturb coupling fault if the aggressor cell is in a given state, a write operation immediately followed by a read operation performed on the victim cell returns an correct output but changes the logical value stored in the memory

*d) Dynamic Incorrect Read Disturb Coupling Fault(dCFir):*Two cells are said to have a dynamic incorrect read disturb coupling fault if the aggressor cell is in a given state, a write operation immediately followed by a read operation performed on the victim cell returns an incorrect output but does not affect the logical value stored in the memory.

TABLE IV FAULT PRIMITIVES OF DOUBLE CELL DYNAMIC FAULTS

Dynamic coupled faults	**Dynamic disturb coupling fault**	**dCFds**	**<0w0r0,0/1/->,0w0r0,1/0/->,<1w1r1,1/0/->, <1w1r1,0/1/->,<0w1r1,0/1/->,<1w0r0,1/0/->, <0w1r1,1/0/->,<1w0r0,0/1/->,**
	Dynamic read disturb coupling fault	**dCFrd**	**<0,0w0r0/1/1/>,<1,0w0r0/1/1/>,<1,1w1r1/0/0/>, <0,1w1r1/0/0/>,<0,0w1r1/0/0/>,<1,0w1r1/0/1/>, <1,1w0r0/1/0/>,<0,1w0r0/1/0/>,**
	Dynamic deceptive read disturb coupling fault	**dCFdrd**	**<0,0w0r0/1/0>,<1,0w0r0/1/0>,<1,1w1r1/0/1>, <0,1w1r1/0/1>,<0,0w1r1/0/1>,<1,0w1r1/0/1>, <1,1w0r0/1/0>,<0,1w0r0/1/0>**
	Dynamic incorrect read disturb coupling fault	**dCFir**	**<0,0w0r0/0/1>,<1,0w0r0/0/1>,<1,1w1r1/1/0>, <0,1w1r1/1/0>,<0,0w1r1/1/0>,<1,0w1r1/1/0>, <1,1w0r0/0/1>,<0,1w0r0/0/1>**

IV. RESULTS AND DISCUSSIONS

TABLE V SIMPLE STATIC FAULT DETECTION OF VARIOUS MARCH TESTS

FFM's	A	Q	SS	C-	OP:C-	SR	iC	RAW	AB	BDN	Cd
SAF	*	*		*	*	*	*				
SOF											
SF			*						*	*	
TF	*	*	*	*	*	*	*		*	*	
RRF		*-			*-	*-					
RDF		*	*	*	*	*	*		*	*	
WDF			*						*	*	
DRF		*			*						
DRDF		*	*		*	*			*	*	
USF											
UWF											
URF											
NAF											
IRF		*	*	*	*	*	*		*	*	

The table V comprises fourteen different types of simple static faults. March Q is an efficient test which can detect nearly 50% of simple static faults.March SS ,AB and BDN detects 42.8% of simple static faults.March RAW concentrates on dynamic faults.iC detects the same set of faults detected by C-.OP.C- detects data retention faults, deceptive read destructive faults and a fraction of the random read faults, in addition to the faults detected by C-.Considering the complete set of fault models March Q and March OP.C- has the highest percentage of fault detection in the case of simple static faults.

TABLE VI STATIC COPLED FAULT DETECTION OF VARIOUS MARCH TESTS

FFM's	A	Q	SS	C-	OP.C-	SR	iC	RAW	AB	BDN	Cd
CFst	*	*	*	*	*	*	*		*	*	*
CFus											
CFin	*										*
Cfid	*										*
Cfds		*	*	*	*	*	*		*	*	
CFud											
CFwd			*						*	*	
CFtr		*	* -	*	*	*	*		*	*	
CFrd		*	*	*	*	*	*		*	*	
CFdrd			*						*	*	
CFir		*	*	*	*	*	*		*	*	
CFuw											
CFur											
CFrr											
CFrrd											

March A can detect SF, TF and a fraction of CFs.In the case of coupling faults, March Q detects 33.3 % of static coupled faults .(state coupling fault, disturb coupling fault,transition coupling fault, read disturb coupling fault,incorrect read disturb coupling fault.)March C-, March OP. C-, March SR and March iC- covers the same set of static coupled faults as detected by March Q.March SS has a better % (~ 46.66%) of fault detection when compared to the above mentioned tests. In addition to the faults detected by March C- it detects deceptive read disturb coupling fault and a fraction of write destructive coupling faults. Compared to all the tests mentioned in this paper, March AB and March BDN have the same percentage of fault coverage as March SS. (46.66%).

TABLE VII SIMPLE DYNAMIC FAULT DETECTION OF VARIOUS MARCH TESTS

FFM's	A	Q	SS	C-	OP.C-	SR	iC	RAW	AB	BDN	Cd
dRDF								*	*	*	
dDRF								*	*	*	
dIRF								*	*	*	
dDRF										*	

In the case of single cell dynamic faults, only March AB, March RAW, and March BDN can detect dynamic faults. All the other tests proposed in this paper either concentrates on simple static faults or double cell static faults. March AB and March RAW detects (75%) of single cell dynamic faults considered in this paper. They

detects dynamic read destructive fault, dynamic deceptive read destructive fault and dynamic incorrect read fault.Refering to the different march tests considered, March BDN has the highest fault coverage(100%).

TABLE VIII DYNAMIC COUPLED FAULT DETECTION OF VARIOUS MARCH TESTS

FFMs	A	Q	SS	C-	OP.C-	SR	iC	RAW	AB	BDN	Cd
dCFrd								*	*	*	
dCFdrd								*	*	*	
dCFir								*	*	*	
dCFds								*	*	*	

Among the different March tests considered, only March AB, March RAW, and March BDN can detect dynamic coupled faults. These tests have the same set of fault coverage(100 %).They are capable of detecting dynamic disturb coupling fault , dynamic read disturb coupling fault, dynamic deceptive read disturb coupling fault, dynamic incorrect read disturb fault.

Peripheral faults can occur anywhere in the associated circuits of SRAMs.They can occur in read/write logic,sense amplifier or in address decoder circuits.Another type of fault associated with memory is linked faults. These types of faults do influence each other. In this case, masking occurs i.e. the behavior of a particular fault can change the behavior of another one. Assume that we are performing an operation in cell $c_1$and let it changes the contents of the cell c_v. Now, an operation performed in cell c_2 causes a fault in the same cell but the effect of the fault is just opposite to that caused by c1.In other words, masking will occur in c_v, if we perform an operation in c1 followed by an operation in c_2. No fault will be visible since the fault effect in c1 is masked by that in. c_2.

TABLE IX PERIPHERAL FAULT DETECTION OF VARIOUS MARCH TESTS

FFMs	A	Q	SS	C-	OP.C-	SR	iC	RAW	AB	BDN	Cd
LRF											
ADOF	*			*	*		*			*	
R-AODF	*			*			*			*	
Slow WDF										*	
Bridging fault											
NPSF											
Sense amplifier recovery fault											
Write recovery fault											
Disturb fault											

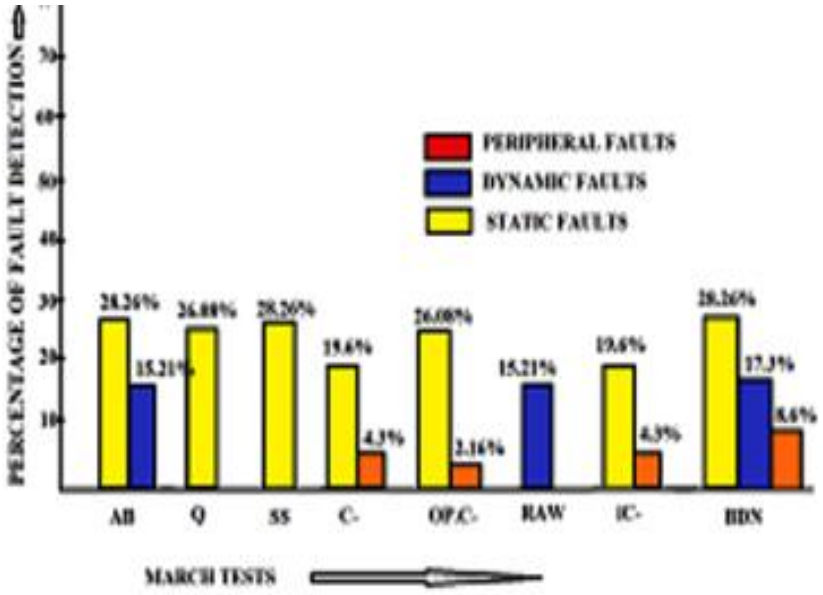

Fig2 PERCENTAGE OF FAULT DETECTION OF VARIOUS MARCH TESTS

V. CONCLUSION

Various March tests have been analyzed and evaluated in this paper. In the case of simple static faults, March Q has the higher percentage of simple static fault coverage. For static coupled faults, March SS, March AB, March BDN have the highest fault coverage when compared to other tests. In the case of simple dynamic faults, March BDN detects the maximum number of faults. When compared to other tests, March RAW, March AB and March BDN have the highest percentage of fault detection for dynamic coupled faults. It is seen that March BDN has the overall highest percentage of fault coverage when compared to all tests.

REFERENCES

[1] N.M Sivamangai, K. Gunavathi" Fault detection in SRAM cell using wavelet transform based transient current testing method"International Journel of latest trends in Software engineering (IJLTSE),Vol.1,No.1,pp20-27,2011

[2] A-W.Z.W. Hasan, I. Halin S. Shafie and M. Othman"An efficient diagnosis march based algorithm for coupling faults in SRAM" RSM2011 Proc., 2011, Kota Kinabalu, Malaysia

[3] Mansita,W.H.W Zuha,R.M. Sudek,A.H.Izhal "March based SRAM diagnostic algorithm for distinguishing stuck –at and transition fault,s"IEICE Electronics Express 2009,Volume 8, No. 15, 1091-1097

[4] March SS –A Test for All Static Simple SRAM faults Said Hamdioui,Ad J van de Goor,Mike Rodgers, Proceedings of the 2002 IEEE International Workshop on Memory Technology, Journel on Design and Testing (MTDT 2002)1087-4852A-M.I.

[5] Luigi Dilillo Bashir M. Al-Hashimi"March CRF: an Efficient Test for Complex Read Faults in SRAM Memories" Workshop on Design and Diagnostics of Electronic Circuits and Systems, Krakow, Poland April 11th . 13th, 2007

[6] March iC.An improved version of March C- for ADOF's detection, L. Dilillo P. Girard S. Pravossoudovitch A. VirazelJournal of Electronic Testing: Theory and Applications .

[7] Said Hamdioui1;2 Zaid Al-Ars2 Ad J. van de Goor2"Testing Static and Dynamic Faults in Random Access Memories" Jounel on electronic testing: Theory and Applications 19, 195–205, 2003

[8] Alberto Bosio, Giorgio Di Natale"March test BDN :A March test for dynamic faults CEAI, Vol.10, No. 2, pp. 3-9, 2008

[9] A.Benso,A.Bosio "March AB,March AB1 New March tests for unlinked Dynamic momory faults"IEEE International test conference

[10] D.S.Suk and Reddy'A march teest for functional faults in semiconductor random access memories"IEEE Transactions on computers,Vol.c-30,No.12,December 1981
[11] Mudappu Parvathi,N. Vasantha,K.Sathya Prasad"Modified March C- with concurrency in testing for Embedded memory alpplications"International jornel of VLSI Design &Communication systems,Vol.3,No.5, October 2012
[12] Luigi Dillilo,Patrick Girard,Arnaud Virazel"Dynamic Read destructive faults in Embedded-SRAMs";Analysis and march test solutionProceedings of IEEE(ETS'04)
[13] Nor azura zakaria, W.Z.W.Hazssan,R.M. Sidek "Fault detection with march test algorithm" Journel of theoretical and applied information technology 2005
[14] V.G.Mikitjuk,V.N. Yarmolik,A.J van de Goor" Ram testing algorithms for detection multiple linked faults" Proceedings of IEEE,(ED&TC'96)
[15] Said Hamdioui,Ad. J.van de Goor"March SS- A test for all static simple RAM faults"Proceedings of IEEE,MTDT 2002
[16] Said Hamdioui,Zaid Al Ars "Testing Static and Dynamic faults in random access memories"Proceedings of IEEE VLSI Test symposium

American Journal of Engineering Research (AJER)
e-ISSN : 2320-0847 p-ISSN : 2320-0936
Volume-03, Issue-03, pp-113-120
www.ajer.org

Research Paper Open Access

Experimental Investigation on Dynamic Viscosity and Rheology of Water-Crude Oil Two Phases FlowBehavior at Different Water Volume Fractions

Rasha Mohammed Abd, Abdurhman H. Nour, Ahmad Ziad Sulaiman
Chemical Engineering Program, Faculty of Chemical Engineering & Natural Resources, Universiti Malaysia Pahang, Lebuhraya Tun Razak, 26300 Gambang, Kuantan, Pahang, MALAYSIA.

Abstract: - Emulsionconsidered as a ruthless problem within the petroleum industry due to their various costly problems in terms of production loss and transport difficulties. In this study, the dynamic viscosity and rheological properties of water-oil two phase flow were investigated using emulsion and blending with lighter crude oil approaches at different water volume fractions. Water-in-oil emulsion stabilized by (1.5 vol.%) of Cocamide DEA was considered in the study. Two samples of crude oil were used: Heavy crude oil, and heavy-light blended crude oil at (60-40) vol.%. The dynamic viscosity was determined by Brokfeild Rotational Digital Viscometer Model LV/DV-III. Factors that affect the emulsion rheologyical properties: temperature, rotational speed, shear rate, shear stress, and water volume fractionwas inspected.Results showed that the water-in-heavy oil emulsion approach resulted in reducing the viscosity of original crude oil about (14%) and characterized the Non-Newtonian shear thinning "pseudo-plastic" behavior. On the other hand, the second approach of blending with (40 vol.%) of lighter crude oil showed that the viscosity and the density were significantlyreduced to (93.6 %), and (5.7%) at 30 ºC, respectively. However, water-in- blended crude oil emulsion followed the same behavior of the original crude oil emulsion under the same factors and conditions. Finally, the rheology studies of both approaches showed that temperature, shear rate,and water volume fraction have a great impact on the viscosity behavior of water-oil two phase flow.

Keywords: - *Emulsion, Dynamic Viscosity, Rheology, Flow Behavior.*

I. INTRODUCTION

Emulsions are a fine dispersion of two phases (water-in-oil or oil-in-water) with drop sizes usually in the micron range [1], [2], [3]. It has the ability to resist changes in its properties over time, the more stable the emulsion, the more slowly its properties changes [4]. In the petroleum industry, the formation of emulsion plays a significant role as the crude oil is often mixed with water that usually happen at the exit of the well bore. As the oil-water mixture passes over chokes and valves, mechanical input leads to the formation of water-in-oil (w/o) emulsions. This emulsion is considered as a ruthless problem within the petroleum industry due to their various costly problems in terms of production loss and transport difficulties [5]. To minimize the cost of emulsion, it is necessary to separate the produced water that can be settled and separated from the oil by gravity. In fact, natural emulsions are submitted to destabilization processes to separate the two phases to recover pure oil and pure water, while manufactured emulsions tend to stabilize its structure as long as possible [6]. Hence, a good knowledge of crude oil emulsions as well as the availability of methodologies to study emulsion is essential for enhancing the recovery processes at all oil production stages [7], [8], [9].

Since emulsion is a multiphase system, therefore the nature of the emulsion is depending on several factors; lift technique, shear energy, pressure cycle, thermal cycle, chemical demulsifier, and the water cuts during crude oil recovery process [10].Therefore, studying the rheological and physical properties of the emulsion is necessary to identify the factors that affecting the formation of emulsions. In 1977, the rheological properties of emulsions containing different amounts of crude oil at different temperatures were studied by Mao and Marsden [11]. The rheology of both o/w and w/o emulsions between 24°C to 82°C was described adequately by the power-law relationship. It was found that emulsions that having concentrations of the

dispersed phase up to 50% by volume behave like Newtonian fluids, whereas those having higher concentrations have flow behavior like Non-Newtonian fluids (pseudoplastic ones). Another rheological study has been done based on light crude oil and tap water emulsion. It was found that the emulsion characterized a Newtonian fluid where some of these emulsions showed the Non-Newtonian behavior if the volume fraction of the dispersed phase is high and near to the inversion point [12].Moreover, a study performed on the water-in-oil (w/o) emulsions that alreadyformed at the exit of the well bore in some heavy crude oil fields.It was found that in the dispersed pattern the viscosity of the mixtureincreases dramatically compared to that of the continuous oilphase, especially at high water volume fractions [13], [14]. The flow behavior of suchmixtures is further complicated by strong non-Newtonian characteristics [15].

This study focused on several points to understand the flow behavior of water-oil two phases in order to enhance the oil recovery at the oil field. The main point of this investigation is to determine the dynamic viscosity of the water-oil two phases, and to inspect their rheological propertiesat different water volume fractions. The study divided into three sections. Firstly, to characterize the crude oil samples. Second, to investigate the dynamic viscosity and the rheological properties of water-in-heavy oil emulsion. The third section is to study the viscosity behavior and the rheological properties of the blended crude oil emulsion to compare its flow ability with the original crude oil emulsion.Indeed, the rheological propertieswill be performed through observing the effects of temperature, shear stress, shear rate, and the water volume fraction data on the apparent dynamic viscosity for theprepared emulsion.

II. MATERIALS AND METHODS

2.1CRUDE OIL SAMPLES

Two types of heavy and light crude oil samples were collected from Petronas Refinery at Melaka, Malaysia for investigation. The heavy crude oil samplewas marked as crude oil A, whereas the sample of (60 vol.%)heavy crude oilblended with (40 vol.%) lighter crude oil was marked as crude oil B. The Physio-chemicalproperties and the chemical fractionation were carried out to identify the behavior of both crude oils before processing as shown in Tables (1) and (2).

2.2 COCAMIDE DEA

The non-ionic surfactant Cocamide Diethanolamine (Cocamide DEA) was used in this study as a natural emulsifying agent to stabilize the crude oil emulsions for the advantage of the recovery in the refinery is much easier compared to other agents. The Cocamide DEA concentration of (1.5 vol. %) was selected based on a previous stability screening studyas it gave a better stability for the prepared emulsion at the room temperature. The concentration (vol.%) is based on the total volume of the prepared emulsion.

2.3 EMULSION PREPARATION AND TESTING

3samples of water-in-crude oil emulsion at three fractions by volume of water and oil phases (50-50, 40-60, and 20-80) vol. % were prepared. In graduated beakers, 300 mL of emulsions was prepared by "agent-in oil method" through mixing the crude oil sample (continues phase) with (1.5 vol. %) of Cocamide DEA (surfactant agent) then the sample was sheared vigorously for 6 minutes. After that, water (dispersed phase) was added gradually and slowly to the mixing phase (oil and surfactant) then agitated for another 4 minutes. The preparation process was achieved using a standard three blade propeller at a range of rotational speeds from (1500- 1800) rpm at 30 ^{o}C. The prepared emulsions were examined by filter paper as well as by test tube methods to identify the type of the emulsion, whether it is a water-in-oil or an oil-in-water. Only w/o emulsion was selected for the study[16].

2.4 SARA METHOD OF ANALYSIS

To identify the crude oil fractions, SARA method of analysis was performed. The fractions that considered in this study include those in the categories of Asphaltenes, Aromatic, Resins, and Saturated compounds. The analytical design of the standardized ASTM (American Society for Testing and Materials) method, ASTM D2007, that employs open-column liquid chromatography [17], [18]was used to separate the crude oil into two major fractions; Asphaltenes and Maltenes(Aromatic, resins, and Saturated) compounds.

2.5 DETERMINATION OF THE APPARENT DYNAMIC VISCOSITY

The dynamic viscosity of the prepared emulsions was examined by Brokfeild Rotational Digital Viscometer Model LV/DV-III with UL adapter and spindle # 31. The Viscometer was connected with a water bath thermostat. Viscosity measurements were performed over a rotational speed range (50,100,150, and 250) rpm and temperatures range (30, 50, 70, and 90) ^{o}C.

2.6 SURFACE AND INTERFACIAL TENSION DETERMINATION

For measurements of the surface and the interfacial tension, a standard test method ASTM(American Society for Testing and Materials) was performed using Du Nouy Interfacial Tensiometer. The tensiometerequipped with 6-cm circumference platinum ring. In this method, the water was placed first in the sample boat for calibration. Then, the oil was added the water to form an emulsion as it's lighter than water. The platinum ring should be inserted in the water layer where the contact of the oil and this ring should be avoided. After 5 minutes, where the interfacial tension reaches to its equilibrium value, measurements were taken.

III. RESULTS AND DISCUSSION

3.1 CRUDE OIL PROPERTIES

Depend on the Physio-chemical propertiesand SARA Fractionation method, it was found that sample A behaves as heavy crude oil, whereas sample B behaves as medium crude oil, as shown in Tables 1, and 2.

Table1: Phsical Properties of The Crude Oil Samples

Crude oil	Crude A	Crude B
Density (g cm^{-3})	0.947	0.893
Viscosity (m·Pas)	298.7	19.1
Surface Tension at 20C (mNm^{-1})	28.98	27.33
Interfacial Tension at 20 ℃ (mNm^{-1})	25.83	21.07
API Gravity	17.13	26.12

Table II:SARA Fractionations of The Crude Oil Samples

Crude oil samples	Asphaltenes (wt.%)*	Saturated (wt.%)*	Aromatic (wt.%)*	Resins (wt.%)*	R/A ratio
A	12.2	48.7	34.6	4.5	0.37
B	7.6	61.4	27.2	3.8	0.51

* (wt. %) by dry basis

3.2 VISCOSITY BEHAVIOR FOR W/O EMULSION OF HEAVY CRUDE OIL

3.2.1 EFFECTS OF SHEAR RATE AND SHEAR STRESS ON VISCOSITY

The relation between shear rate and shear stress was plotted Fig. 1 to investigate their effects on the flow behavior of the water-in-heavy crude oil emulsion stabilized by (1.5 vol.%) of the Cocamide DEA at different water-oil two phasesratios (50-50, 40-60, and 20-80) vol.%, and temperatures (from 30 to 90) ℃. Itcan be observed that the shear stress increased gradually and significantly with the shear rate. Which indicates that all emulsions are following the Non-Newtonian behavior.

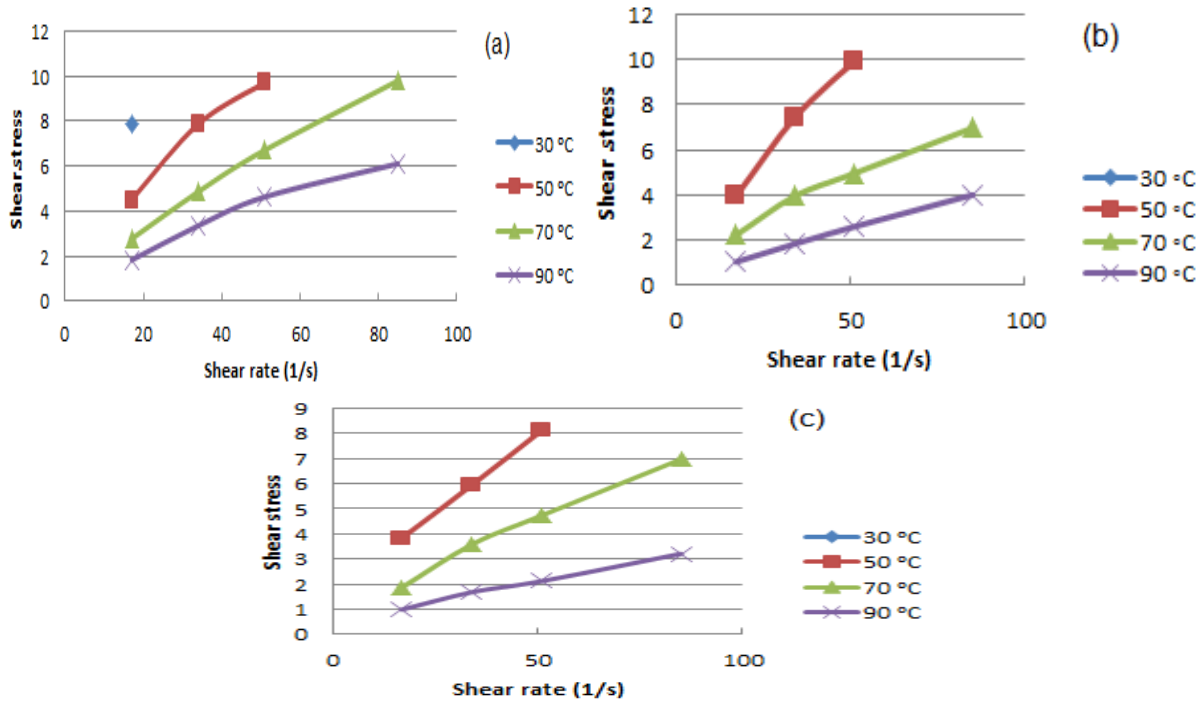

Figure 1: Effects of shear rate and shear stress on viscosity of: a) 50-50 vol.%, b) 40-60 vol.%, and c) 20-80 vol.% of water-in-heavy crude oil emulsion stabilized with (1.5vol.%) of DEA at different temperatures.

3.2.2 EFFECTS OF SHEAR RATE AND TEMPERATURE ON VISCOSITY

The behavior of the apparent viscosity for (50-50,40-60, and 20-80) vol.% of water-in heavy crude oil emulsion stabilized with (1.5 vol.%) of Cocamide DEA were investigated under the effects of shear rate at different temperatures as presented in Fig. 2. In general, over a wide range of shear rate (from 17 to 85) 1/s, the viscosity was significantly decreased as the shear rate increasedwhich means the prepared emulsions are depended on shear rate and following shear-thinning behavior (pseudo-plastic behavior). Thereasonfor this behavior is at the moment of spindle moving,the bonds of aggregated molecules in the sample are starting to destroyand deformed wherethe molecules oriented more parallel to the spindle surface. Thus, the resistance to the spindle rotation (shear rate)is less and therefore viscosity. As the shear rate increased, the aggregates may be more deformed and breaking down into individual flocs thus the viscosity is more reduced.

On the other hand,because temperature is one of the most obvious factors that can affect on the rheological behavior of the materials as some materials are quite sensitive to temperature and a relatively small variation will result in significant change in viscosity. Therefore, the effect of temperature on the w/o emulsion viscosity was investigated as shown in Fig.2. It was found that increase the temperaturegradually (from 30 to 90) ^{o}C resulted in considerable reduction in the dynamic viscosity which indicates that the w/o emulsion viscosity depended on temperature and it is a subject to temperature variations in the processing.

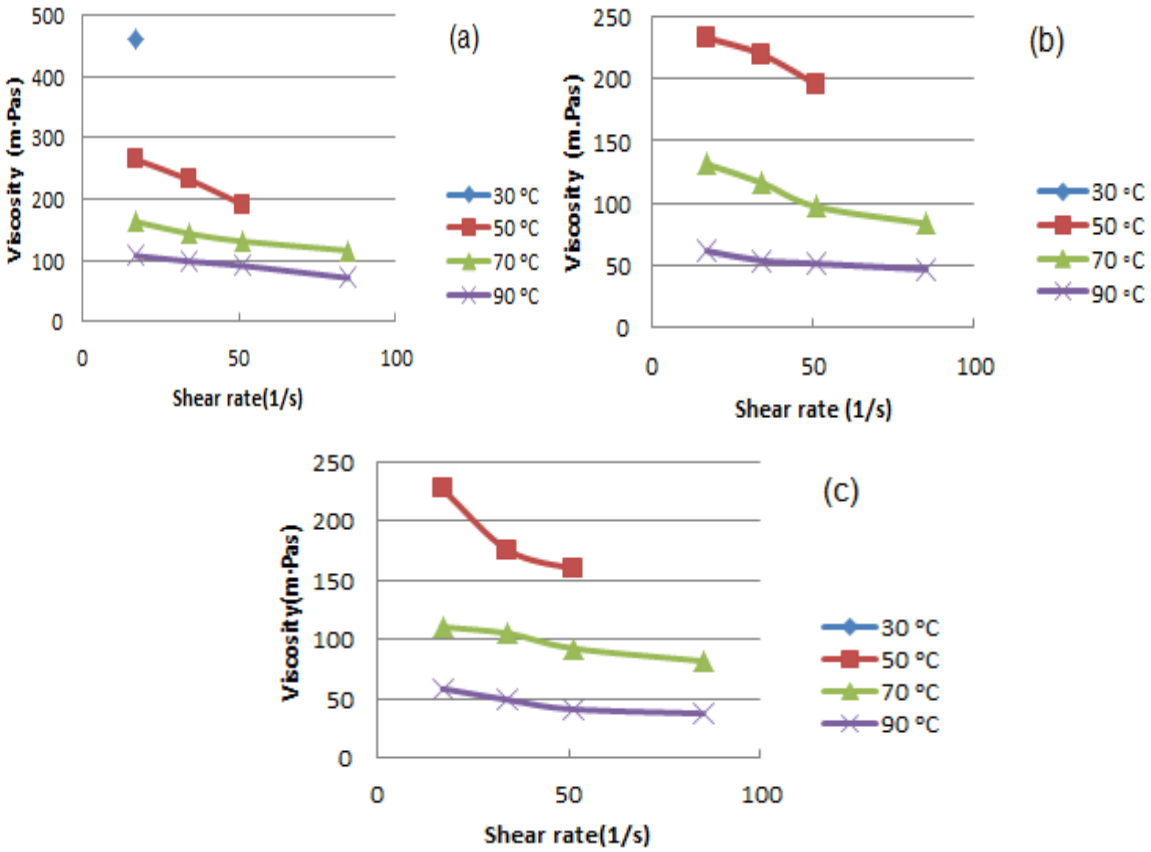

Figure 2: Effects of shear rate on the viscosity of: a) 50-50 vol.%, b) 40-60 vol.%, and c) 20-80 vol.% of water-in-heavy crude oil emulsion stabilized with (1.5 vol.%) of the DEAat different temperatures.

3.2.3 EFFECTS OF WATER VOLUME FRACTION ON VISCOSITY

The volume fraction of water (dispersed phase) found to have a significant effect on the emulsion viscosity behaviorof heavy crude oil emulsion as shown in Fig 3. In theFigure, data of (50-50, 40-60, and 20-80) vol.% w/o emulsion stabilized with (1.5 vol.%) of Cocamide DEA demonstrated the viscosity behavior at different rotational speeds (from 50 to 250) rpm and varied temperatures (from 30-90)^{o}C. It can be noted that reducing the volume fraction of the water (from50 to 40, then to 20)% resulted in significant reduction in the apparent viscosity (from 264.5 to 227.2) m·Pas at 50^{o}C,which is about (14%).Moreover, it can be noted

thatemulsion with50 % of the water volume fraction characterize higher elastic behavior andit needs a higher shear rate followed by emulsion with 40%, then 20 %.The reason behind increase the viscosity when thehigh volume fraction of the dispersed phase(water)was used is due to increase the number of the hydrogen bond that leads to increase the hydrodynamic forces and hence the viscosity [3], [16]. Thus,it needs a high shear rate to start the deformation.

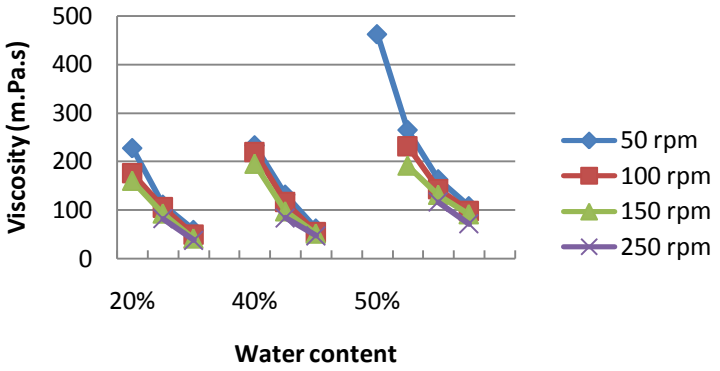

Figure 3: Effects of the water volume fractions on viscosity of heavy crude oil emulsions stabilized with (1.5 vol.%) of DEA at different rpm and temperatures.

3.3 VISCOSITY BEHAVIOR FOR W/O EMULSION OF HEAVY-LIGHT CRUDE OIL

The main task of blending the heavy crude oil with the lighter crude oil is to reduce the viscosity as well as the density and to enhance the flow-ability that could be desirable for the pipeline transportation.Observing the viscosity value for heavy and blended crude oil samples (Table 1), it can be highlighted that blending with (40 vol.%) of a light crude oil resulted in drop theviscosity (from 298.7 to 19.1) m·Pas at 30 °C, which is almost (93.6%)less than the original viscosity value. Moreover, the density of the original heavy crude oil were reduced (from 0.947 to 0.893) $g.m^{-3}$ at 30 °C, which is about (5.7 %) less than the original density.For that reason, it is important to investigate the factors that affect thewater- oil two phase flow behavior for the blended crude oil sample to provide a deep understanding of the emulsion system.

3.3.1 EFFECTS OF SHEAR RATE AND SHEAR STRESS ON VISCOSITY

The effects of the shear stress and shear rate data on viscosity of (50-50, 40-60, and 20-80) vol.% of water-in-blended crude oilemulsion using (1.5vol.%) of Cocamide DEA at different testing temperatures (from 30to 90) °C are shown in Fig. 4. The blended crude oil emulsion was found to follow the Non-Newtonian behavioras the shear stress increased significantly with the shear rate. Similarbehavior was noticed withw/o emulsion of the original crude oil.

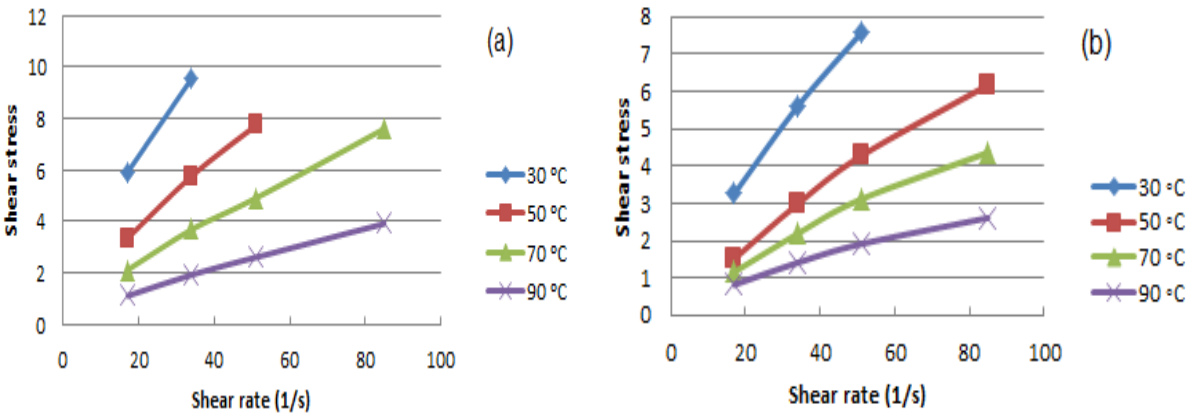

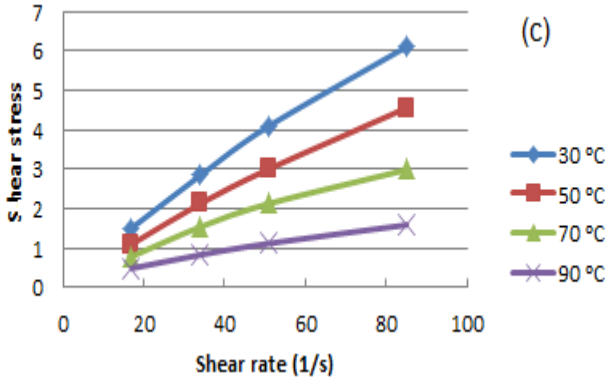

Figure 4: Effects of shear rate and shear stress on the viscosity of: a) 50-50 vol.%,b) 40-60 vol.%, and c) 20-80 vol.% of blended crude oil emulsion stabilized with (1.5 vol.%) DEA at different temperatures.

3.3.2 EFFECTS OF SHEAR RATE AND TEMPERATURE ON VISCOSITY

Fig. 5 represents the relationship between the apparent viscosity of the blend crude oil emulsion and the shear rate at different temperatures (from 30 to 90) °C. It can be noted thatat (50-50 vol. %) of w/o emulsion, the dynamic viscosity of blendedoil emulsionis about (347.9) m.Pas whichis less than the viscosity of the original crude oil emulsion(461.8) m.Pas at 30 °C, which is (24.2%) less than original oil emulsion. However, the viscosity of blended oil taken the same behavior ofthe heavy crude oil emulsionby following shear-thinning (pseudo-plastic) behavior in term of decreasing the emulsion viscosity with increasing the shear rate and the temperature which means the emulsion depended on shear rate and temperature.

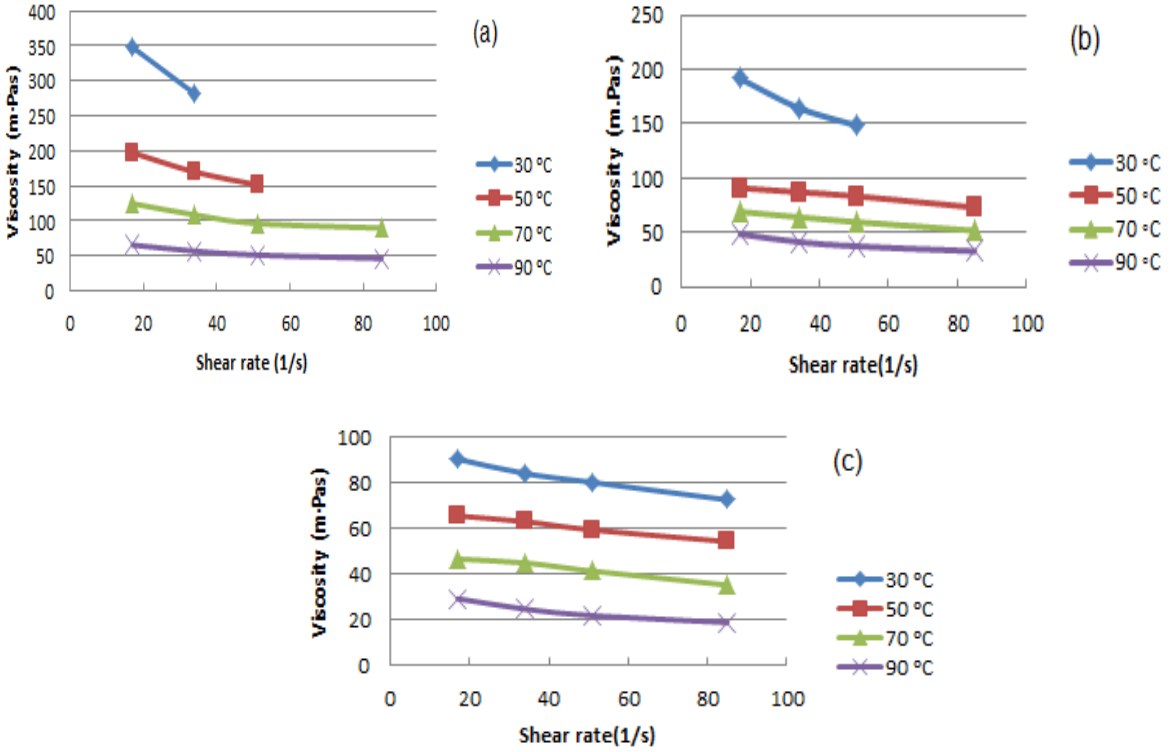

Figure 5: Effects of shear rate and temperature on the viscosity of:a) 50-50 vol.%, b) 40-60 vol.%, and c) 20-80 vol.% of blended crude oil emulsion stabilized with (1.5 vol.%) of DEA.

3.3.3EFFECTS OF WATER VOLUME FRACTION ON VISCOSITY

The effects of the water volume fractions(dispersed phase) on the viscosity of theblended crude oil emulsion stabilized with (1.5 vol.%) of Cocamide DEA over a range of rotational speeds (from 50-250)rpm and temperatures (from 30-90)°C are presented in Fig. 6. It was found that the volume fraction had a significant effect on the rheological properties of the flow behavior of w/o emulsion. This effect appears as the water fraction decreased from 50% to 40% and then to 20%,where the emulsion viscosity was decreased from (347.9,

191.8, to 90) m·Pas at 30 °C, respectively. Thus, emulsion with (50 vol.%) of water needs higher shear rate and characterize higher elastic behavior followed byan emulsion with (40 vol.%)of water, and thenthe emulsion with (20 vol.%) of water as shown in Fig.6 (a), (b), and (c), respectively.This behavior is similar to thebehaviorthat was indicated with the original crude oil emulsions.
Table 3 showed the effects of all approaches used in this study on the dynamic viscosity at low shear rate of 17 (1/s) and different temperatures.

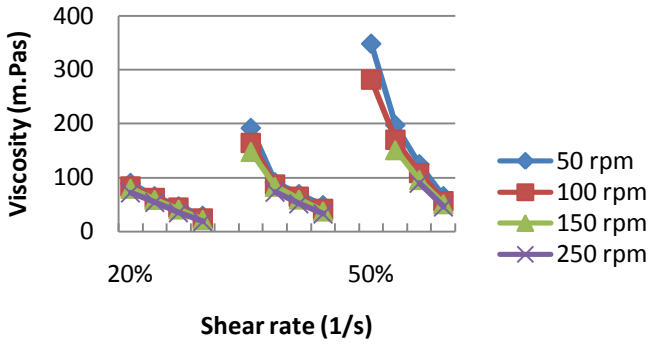

Figure 6: Effect of water volume fractions on the viscosity of the blend crude oil emulsion stabilized with (1.5 vol.%) of DEA at different rpm and temperature

TABLEIII:: VISCOSITY VALUES OF ALL APPROACHES USED IN THIS STUDY AT SHEAR RATE 17 (1/S)

Sample	30 ^{0}C	50 ^{0}C	70 ^{0}C	90 ^{0}C
Pure Heavy oil	298.7			
20-80% w/o emulsion		227.2	110.8	58.8
40-60% w/o emulsion		232.9	131.4	61.8
50-50% w/o emulsion	461.3	264.5	163	107.6
Pure Blended oil	19.1			
20-80% w/o emulsion	90	65.3	46.5	29.2
40-60% w/o emulsion	191.8	91.2	69.3	48.8
50-50% w/o emulsion	347.9	197.3	124.7	65.4

* Viscosity unitesare (m·Pas)

IV. CONCLUSIONS

The present study examinedthe viscosity behavior and the rheology properties of water-oil two phase flow at a different water volume fraction using Malaysian crude oil. Water-in- crude oil emulsion stabilized by (1.5 vol.%) of Cocamide DEA was investigated.A wide range of temperatures (from 30 to 90) °C, rotational speeds (from 50 to 250) rpm, and water volume fractions (20, 40, and 50) % were covered. Using the firstapproachto investigate the viscosity by forming a water-in-heavy crude oil emulsion containing different water volume fraction found that the emulsion flowed a Non-Newtian shear-thinning behavior (pseudo-plastic). Reducing the water volume fraction (from 50 to 20) % resulted in a viscosity reduction about (14%) of original viscosity and the emulsion characterized less elastic behavior that means better flow ability. The second approach of blending with (40 vol.%)lighter crude oil resulted inviscosity and density reduction to about(93.6 %), and (5.7%) at 30 °C, respectively. In addition, forming the water-in-blended crude oil emulsion resulted in more viscosity reduction to about (24.2%) compare to originalw/o emulsion. However, the blended oil emulsion is following the same behavior of the original crude oil emulsion under the same factors and conditions. Finally, the rheological investigation found that temperature, shear rate, and water volume fraction have a great impact on the viscosity behavior of water-oil two phase flow.

V. ACKNOWLEDGEMENTS

The authors would like to thank University Malaysia Pahang (UMP) for the support with the Research Grant "GRS 120319", and Pertronas for donating the crude oil.

REFERENCES

[1] S. J. Joblom ,*Encyclopedic hand book of emulsion technology*(New York:Marcel Dekker,2001).

[2] J. Bibette,F. Leal- Calderon, V. Schmitte, andP. Pouline,*Introduction in emulsion science-basic principles* (*Springers, 2002).*

[3] L. K. Sunil, Crude oil emulsions,in W. L. Larry and R. F. John (Ed.), *Petroleum Engineering Handbook :General Engineering, 1*(U.S. Texas, 2006)

[4] J. David Julian, and Mc. Clements, *Food emulsions: principles, practices, and techniques, 2nd Ed.*,2 ,2005 , 269.

[5] W. H. Shadi, T. G. Mamdouh, and E. Nabil, Heavy crude oil viscosity reduction and rheology for pipeline transportation, *J. Fuel, 89,* 2010, 1095–1100.

[6] D. Clausse, F. Gomez, C. Dalmazzone, and C. Nick, A method for the characterization of emulsions, thermogranulometry: Application to water-in-crude oil emulsion, *Journal of Colloid and Interface Science, 287,* 2005, 694–703.

[7] A.Ram, and D. Shah, Emulsion in tertiary oil recovery, in K. J. Lissant (Ed.),*Emulsion and emulsion technology, Surfactant science series, 6* (New York: Marcel Dekker, Inc,1984).

[8] H. K. Abdel-Al, A. Mohamed, and M.A. Fahim, *Petrolum and Gas Field ProcessingHandbook* (NewYork:Marcel Dekker, Inc. Basel, 2003).

[9] D. Langevin, S. Poteau, I. Hénaut, and J.F. Argillier, Crude Oil Emulsion Properties and their Application to Heavy Oil Transportation, *J.Oil & Gas Science and Technology – Rev. IFP,* 59, (5) , 2004, 511-521.

[10] W. S. Gar, and Z. Moshen, Emulsion resolution in electrostaticprocesses, *Energy & Fuels, 14,* 2000, 31-37.

[11] M. L. Mao, and S.S. Marsden, Stability of concentrated crude oil-in-water emulsions as a function of shear rate, temperature and oil concentration,*J. Can. Pet. Tech.* 1977, 54.

[12] D. Dou Dan, and J. Gong , Apparent viscosity prediction of non-Newtonian water-in-crude oil emulsions, *Journal of Petroleum Science and Engineering, 53,* 2006, 113–122

[13] E.EJohnsen., and H.P Rönningsen,Viscosity of 'live' water-in-crude-oil emulsions: experimental work and validation of correlations, *J. Pet. Sci. Eng., 38,* 2003, 23–36.

[14] M. A.. Farah, R. C.Oliveira, J.N. Caldas, Raand K. jagopal, Viscosity of water-in-oil emulsions: variation with temperature and water volume fraction, *J. Pet. Sci.Eng., 48,* 2005, 169–184.

[15] W. Wei, G. Jing , A. Panagiota,Investigation on heavy crude-water two phase flow and related flow characteristics, *International Journal of Multiphase Flow,37,* 2011, 1156–1164.

[16] A.N.Ilia Anisa, H. N. Abdurhman , and H. N. Azhary, Catastrophic and transitional phase inversion of w/o emulsion for heavy and light crude oil, *J. of Applied Science,10(23),* 2010,2076-3083.

[17] V. C. Laura, and F. Vazquez, Fractionation and Characterization of Mexican Crude Oils, *Energy & Fuels, 23,* 2009, 1603–1609

[18] C. K.Geoffrey, A. M. Annelie, P.R. Ryan, and G. M. Alan, Use of Saturates/Aromatics/Resins/Asphaltenes (SARA) Fractionation To Determine Matrix Effects in Crude Oil Analysis by Electrospray Ionization Fourier Transform Ion Cyclotron Resonance Mass Spectrometry, *J. Energy & Fuels, 20,* 2006, 668-672.

American Journal of Engineering Research (AJER)
e-ISSN : 2320-0847 p-ISSN : 2320-0936
Volume-03, Issue-03, pp-121-126
www.ajer.org

Research Paper Open Access

Development of a Networked Thumb Print-Based Staff Attendance Management System

Tolulope Awode [1], Oluwagbemiga Shoewu [2], Oluwabukola Mayowa Ishola [3], Segun O. Olatinwo [4]

[1] *Department of Computer Science and Engineering, Ladoke Akintola University of Technology, Ogbomoso, Nigeria.*
[2] *Department of Electronics and Computer Engineering, Lagos State University, Epe Campus, Nigeria*
[3] *Department of Computer Science, University of Lagos, Akoka, Lagos State, Nigeria.*
[4] *Department of Computer Engineering, Moshood Abiola Polytechnic, Abeokuta, Nigeria.*

Abstract: - This paper focuses on the development of a networked thumb print-based attendance management system. Now, more than ever, it has become necessary to give more thought to the methods of time and attendance management. The traditional time clock, manual attendance registering often no longer makes sense and simply does not meet the needs of the modern work environment. This system offers a comprehensive software solution that will streamline company's operations, and simplify timekeeping. Nowadays, the need of a solution for Time and Attendance in the modern company is a necessity. It is important to be able to manage and control the workers by means of a system of control of times and schedules.

Keywords: - *Staff attendance management, networked thumb print, Service Oriented Application*

I. INTRODUCTION

Centuries back, employees' attendances are captured by using attendance sheet. The attendance sheet is the paper used by the employer to take their employees' attendance. In the attendance sheet, the information needed are the employee's name, address and their signature. In this attendance, signature is really important because it is used to verify the employee's attendance. Time and attendance management is a system of monitoring employees' work hours for the entire company and the analysis of various human resource figures such as overtime allowance, meal allowance, transport allowance and even bonus that are often derived from employee working hours. For the management level personnel, such a system allows them to monitor employee performance automatically and thus allowing them to evaluate if there are any loopholes within the system. It also keeps track of employees within the organization by forcing them to be accountable for their absences – once again, better for the business than for the employee himself. That is why most bosses are eagerly engaging in implementing time and attendance management system into their standard operating procedures.

In manual attendance system all work is done on paper. The whole session attendance is stored in register and at the end of the session the reports are generated. Some of the problems encountered with manual attendance system are: less user friendly, difficulty in report generation, manual control, lots of paperwork, and time consuming. The proposed system is allows efficient control of attendance and punctuality of all employees. It empowers management with real-time employee information and labour data such as working times, absences, attendance, tardiness and more. The system can be set up in companies/ businesses as a technology demonstration project wherein employees and visitors of the organization are tracked. It is the key to proficient and successful time tracking and management in your workplace. It enables you to collect and organize your employees' time data simply and accurately. It represents the most state-of-the-art method of time management for today's businesses.

II. MATERIALS AND METHODS

Design Methodology Overview

This paper attempts to design and implement a networked thumbprint based attendance management system which requires that staff should register the attendance as soon as he/she gets to the office in the morning, and the Staff is expected to register at the end of the day's work. The proposed system is enhanced with advanced patented Biometric Technologies. It significantly simplifies the routine time management tasks and makes the procedures of registering the coming and leaving events quick, fool-proof and convenient.
The proposed system performs: recording of employees' arrival and departure events, accounting of work hours for each employee, department or company, automation of report, data export to .html, .xls, .xml, .pdf formats, storage and search of employees' biometric records in the database, creation of Company's Divisional Structure, monitoring of employees' activity, On-line notification to the Administration Officer on the presence of employees at their workplaces;

Application Requirements
The functional components employed by the proposed system are: fingerprint scanner, Griaule Fingerprint SDK, laptops, network, Service Oriented Application (SOA), Web Server, Back-End/Database, web camera

Application Components
The application components are subdivided into seven main components as shown in Figure 1.

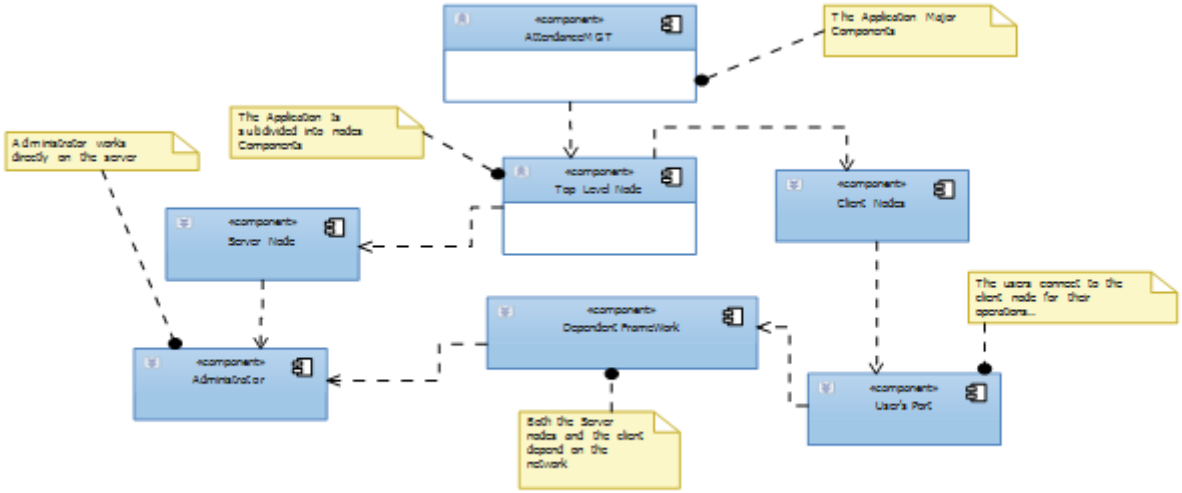

Figure 1: Application Components

Application Use Case
Figure 2 detailed the interaction between the application and the users (Administrators and the other users) also known as the actors can be explained in the diagram below:

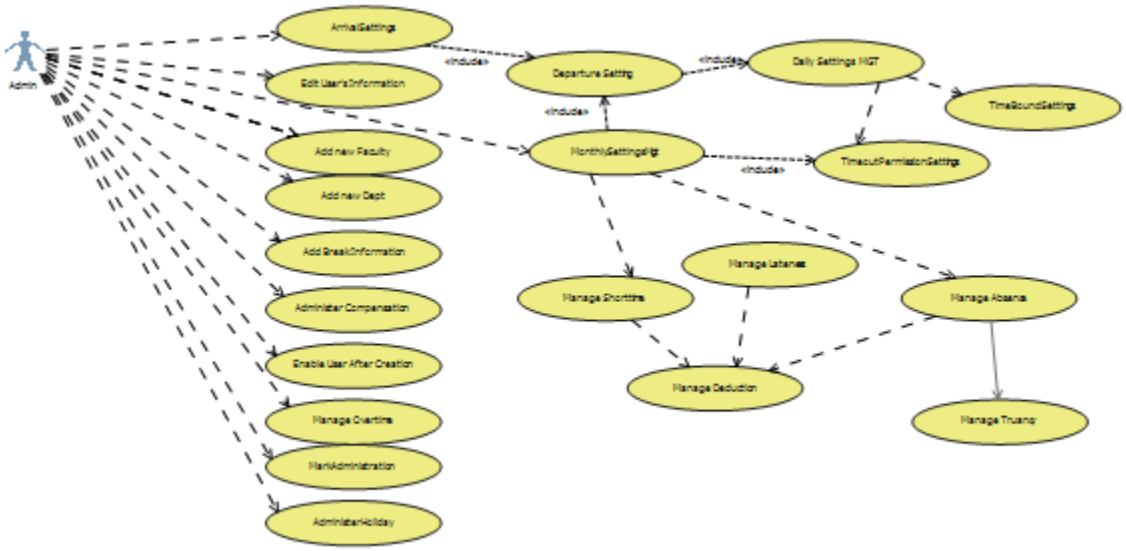

Figure 2: Application Use Case

The Administrator performs the following actions: manage users, manage attendance, manage deductions, manage faculty, manage departments, and manage reports

III. FINGERPRINT MATCHING ALGORITHM

Fingerprint Matching

Given a reference representation in database and an input representation extracted from an input image, the matching stage determines the similarity of two fingerprint features and decides whether they are of the same finger. In most Automated Fingerprint Identification Systems (AFIS), the representation of fingerprints is based on minutiae such as ridge ending and ridge bifurcation, with each minutia being characterized by its locations and orientation. With this representation, the matching problem is reduced to a point pattern matching problem. In the ideal case described by Jain, the matching can be accomplished by simply counting the number of spatially overlapping minutiae. But in practice, the sensing system maps the three-dimensional finger on to two dimensional images. Once the location, pressure and direction of impression change, the mapping will change accordingly, which inevitably leads to nonlinear deformation of fingerprint images. Two fingerprint images may have translation, rotation or even nonlinear deformation between them. If the time span between two impressions is long, the images may also change due to cuts on finger or skin disease. In most systems, fingerprint is represented with a set of minutiae which is called Template. The representation itself may be noisy due to presence of spurious minutiae and absence of genuine minutiae. Also, the properties of minutiae such as the location and orientation may be inaccurately estimated due to image degradation and imperfect reprocessing. Considering these, a good fingerprint matching algorithm should meet the following two criteria:

- Be robust to all kinds of possible deformation which are commonly observed in fingerprints and are hard to model.
- Be robust to small perturbation on minutiae and minutiae properties.

Several approaches have been proposed for point pattern matching, but these methods did not perform well because they did not make use of the extra information provided by fingerprint minutiae.

Fingerprint Matching Based on Error Propagation

After a fingerprint image is enhanced and thinned with image processing methods, the ridges associated with each minutia are tracked. The tracking procedure stops when the tracking length reaches a certain predefined threshold or another minutia is encountered on the ridge. The ridge sampling method is similar to that of Hong's. In order to overcome the ambiguity that orientation may cause, we use the direction of minutiae as x-coordinate in our sampling instead. Therefore, each ridge is represented by its direction and sampling values. And each minutia is repented by its type, position, direction as well as the ridges it resides (one ridge for an end and three ridges for a bifurcation). The matching algorithm is a three-step method:

- First, each minutiae in the reference template is matched with each minutiae in the input template and all resulting potential correspondences are used to find several most reliable one, the initial correspondences, using Hough transformation;
- Secondly, all minutiae surrounding the correspondence are matched and those minutiae pairs whose matching error are less than certain thresholds are added to the MatchedSet;
- Finally, we adjust the matching error of each unmatched minutia according to the information provided by the MatchedSet recursively until the number of elements in MatchedSet stops increasing. A conformation process which checks the consistency of the matching errors of elements in the MatchedSet is made to label and remove the mismatched minutiae after each iteration.

Correspondence Estimation

In the ideal case, the alignment of two point patterns can be precisely decided according to one correspondence. But in practice, we need more candidates to estimate correspondences robustly. To do this, we define two kinds of correspondences: End Correspondence and Bifurcation Correspondence. The similarity criteria are different in the two cases. Suppose that d and D (the reference and input features are denoted by lowercase and capital letters respectively) are the reference and input ridges respectively, d^i and D^i are the i_{th} points on the ridges, and the Similarity S of two ends is defined in Equation 1.

$$S = \frac{\sum_{i=0}^{L} \left(d^i - \mathrm{D}^i\right)^2}{L} \qquad (1)$$

d^i = Reference input in the i^{th} points on the ridges
D^i = Input ridges in the i^{th} points on the ridges
S =Similarity of two ends

L = Length of the shorter ridge.

Here, nonlinear penalty function is adopted to ignore small deformation and emphasize large deformation because our goal is to find the most consistent area (the region around the correspondence) of the two templates. The similarity measure of bifurcation is composed of two parts, namely the sum of the similarity scores of the three ridges and the matching error of direction.

Then the similarity measure of two bifurcations is defined in Equations 2 and 3.

$$S = \frac{\sum_{j=0}^{2} \frac{\sum_{i=0}^{L_j} \left(d^i_j - \mathrm{D}^i(k+j)\%3\right)^2}{L_j}}{4} \qquad (2)$$

d_0, d_1, d_2= reference ridges in the ith points on the ridges

D_0, D_1, D_2 = three input ridges in the ith points on the ridges

T_0,T_1,T_2 are the orientation of these ridges respectively.

k = point on the ridge % = modulo operation

S =Similarity of two ends

$$\Delta\theta = \min_{i=0}^{i=2}\left(\left|\theta_1 - \Theta_{(i+1)\%3} - \left(\theta_0 - \Theta_i\right)\right| + \left|\theta_2 - \Theta_{(i+2)\%3} - \left(\theta_0 - \Theta_i\right)\right|\right) \qquad (3)$$

k = point on the ridge % = modulo operation

Θ = ith input minutiae

θ = ith template minutiae

IV. RESULTS AND DISCUSSION

User Interface of the System Design

The Attendance Management System starts with the Administrator to preset the username and the password. Admin may also find it convenient to access the system with his private login password initially set by default to "admin". The admin can create a new staff with the following fields: staff Id, surname, other names, phone no, department and address, etc. The fingerprint of staff is registered into the database through finger print reader and also the passport of the staff.

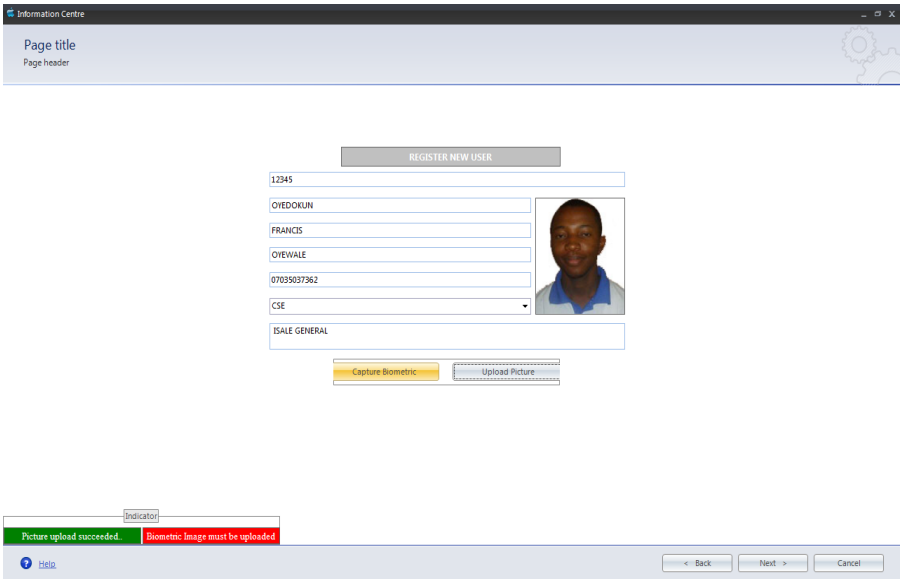

Figure 3: Registration Interface

Users Information

The interface below shows the information of all the Users as registered in the database:

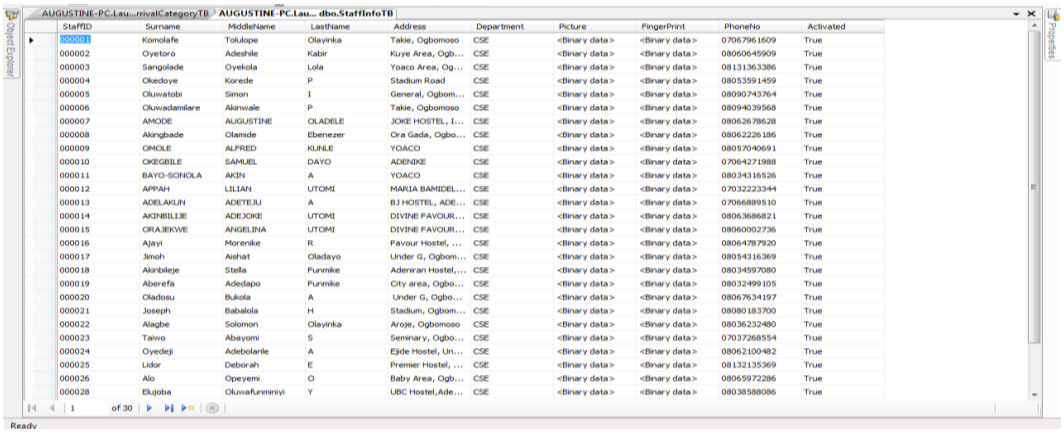

StaffID	Surname	MiddleName	LastName	Address	Department	Picture	FingerPrint	PhoneNo	Activated
000001	Komolafe	Tolulope	Olayinka	Takie, Ogbomoso	CSE	<Binary data>	<Binary data>	07067961609	True
000002	Oyetoro	Adeshile	Kabir	Kuye Area, Ogb...	CSE	<Binary data>	<Binary data>	08060645909	True
000003	Sangolade	Oyekola	Lola	Yoaco Area, Og...	CSE	<Binary data>	<Binary data>	08131363386	True
000004	Okedoye	Korede	P	Stadium Road	CSE	<Binary data>	<Binary data>	08053591459	True
000005	Oluwatobi	Simon	I	General, Ogbom...	CSE	<Binary data>	<Binary data>	08090743764	True
000006	Oluwadamilare	Akinwale	P	Takie, Ogbomoso	CSE	<Binary data>	<Binary data>	08094039568	True
000007	AMODE	AUGUSTINE	OLADELE	JOKE HOSTEL, I...	CSE	<Binary data>	<Binary data>	08062678628	True
000008	Akingbade	Olamide	Ebenezer	Ora Gada, Ogbo...	CSE	<Binary data>	<Binary data>	08062226186	True
000009	OMOLE	ALFRED	KUNLE	YOACO	CSE	<Binary data>	<Binary data>	08057040691	True
000010	OKEGBILE	SAMUEL	DAYO	ADENIKE	CSE	<Binary data>	<Binary data>	07064271988	True
000011	BAYO-SONOLA	AKIN	A	YOACO	CSE	<Binary data>	<Binary data>	08034316526	True
000012	APPAH	LILIAN	UTOMI	MARIA BAMIDEL...	CSE	<Binary data>	<Binary data>	07032223344	True
000013	ADELAKUN	ADETEJU	A	BJ HOSTEL, ADE...	CSE	<Binary data>	<Binary data>	07066889510	True
000014	AKINBILLIE	ADEJOKE	UTOMI	DIVINE FAVOUR...	CSE	<Binary data>	<Binary data>	08063686821	True
000015	ORAJEKWE	ANGELINA	UTOMI	DIVINE FAVOUR...	CSE	<Binary data>	<Binary data>	08060002736	True
000016	Ajayi	Morenike	R	Favour Hostel, ...	CSE	<Binary data>	<Binary data>	08064787920	True
000017	Jimoh	Aishat	Oladayo	Under G, Ogbom...	CSE	<Binary data>	<Binary data>	08054316369	True
000018	Akinbileje	Stella	Funmike	Aderiran Hostel,...	CSE	<Binary data>	<Binary data>	08034597080	True
000019	Aberefa	Adedapo	Funmike	City area, Ogbo...	CSE	<Binary data>	<Binary data>	08032499105	True
000020	Oladosu	Bukola	A	Under G, Ogbo...	CSE	<Binary data>	<Binary data>	08067634197	True
000021	Joseph	Babalola	H	Stadium, Ogbom...	CSE	<Binary data>	<Binary data>	08080183700	True
000022	Alagbe	Solomon	Olayinka	Aroje, Ogbomoso	CSE	<Binary data>	<Binary data>	08036232480	True
000023	Taiwo	Abayomi	S	Seminary, Ogbo...	CSE	<Binary data>	<Binary data>	07037268554	True
000024	Oyedeji	Adebolanle	A	Ejide Hostel, Un...	CSE	<Binary data>	<Binary data>	08062100482	True
000025	Lidor	Deborah	E	Premier Hostel, ...	CSE	<Binary data>	<Binary data>	08132135369	True
000026	Alo	Opeyemi	O	Baby Area, Ogb...	CSE	<Binary data>	<Binary data>	08065972286	True
000028	Elujoba	Oluwafunminiyi	Y	UBC Hostel,Ade...	CSE	<Binary data>	<Binary data>	08038588086	True

Figure 4: Attendance Record Showing Staff Information

The primary key linking each table containing the records were indicated with a small "key" icon in each of the tables linked. The backend was implemented using microsoft SQL server 2008.

Staffs' Attendance and Report

Figure 5 shows a staffs' attendance for a day. The time at which the User clocks in will be recorded into the database.

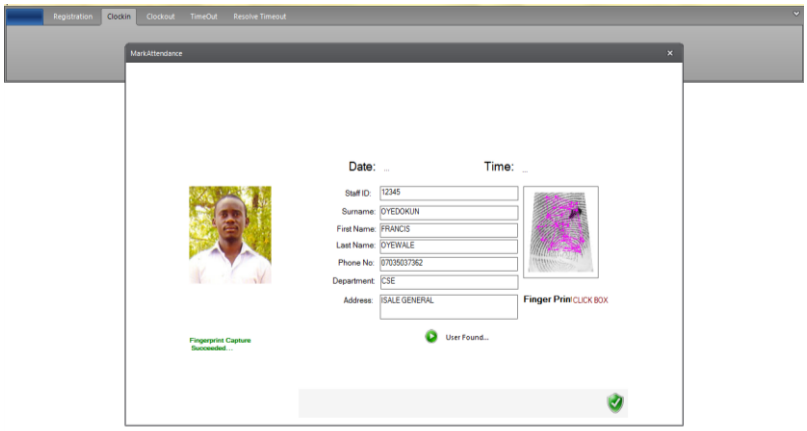

Figure 5: Daily Attendance Record

Attendance Management

The attendance of the Staff marked was documented and sectional reports based on the arrival list, departure list, all staff List, Truancy list, Lateness and Deduction based on the decision of the Administration.

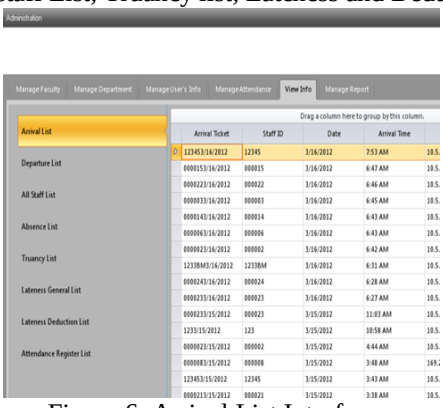

Figure 6: Arrival List Interface

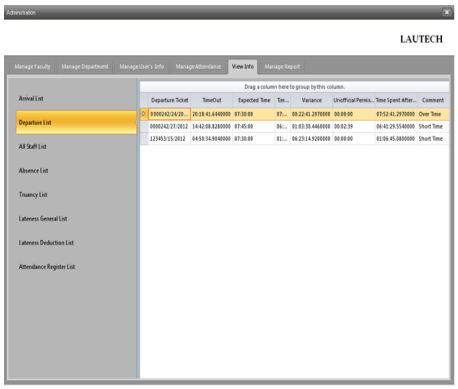

Figure 7: Departure List Interface

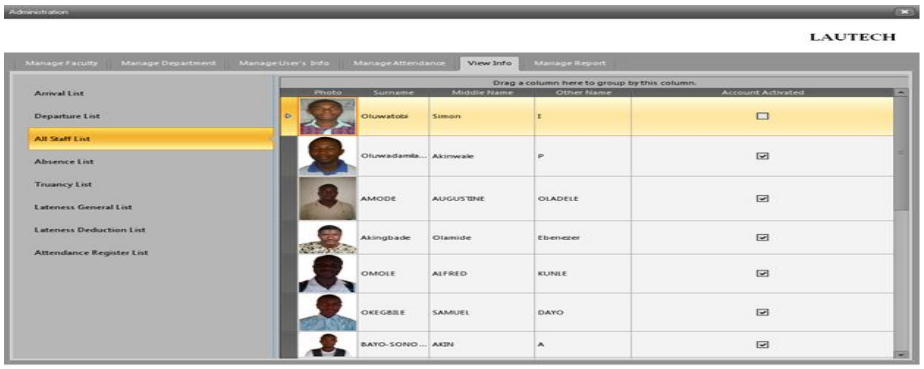

Figure 8: All Staff List Interface

V. CONCLUSION

Thumbprint based attendance system was aimed to address the shortcomings of existing means of taking attendance with a view of improving sanity and credibility of the education system in tertiary institutions and to keep the attendance of the staff for future reference. This also allows the implementation of the deduction on the staff that did not fulfill the basic requirement of marking their daily records. Employing the uniqueness and simplicity of thumbprints in the development ensured that the proposed aim of this work was achieved.

Recommendations

From the foregoing discussions, the following suggestions were made:

- The system could be used for attendance management system in an educational system but could also be adapted to benefit other similar areas such as industrial sector, banking sector, ministries among others.
- Also, staff may not prove their level of commitment to the work they employed for because many may come to mark attendance in the morning and leave the environs with the aim of coming back in the evening to sign out without doing any tangible work for the day. In lieu of this, it is recommended that the establishment should employ the use of access control database system that will only allow the employee (Staff) to open the door if and only if he signs out. This requires the use of fingerprint door.

REFERENCES

[1] AK Jain, A Ross and S Prabhakar. An introduction to biometric recognition, Circuits and Systems for Video Technology. IEEE Transactions. 2004; Vol. 14, Issue 1, p. 4 – 20.
[2] HP Cheong and H Park. Fingerprint classification using fast Fourier transform and nonlinear discriminant analysis Pattern Recognition. 2005; 38, 495 – 503.
[3] Digital Persona. Guide to Fingerprint Recognition, Inc. 720 Bay Road Redwood City, CA 94063 USA, Available at: http://www.digitalpersona.com, accessed November 2008.
[4] F Zhao, X Tang. Preprocessing and post-processing for skeleton-based fingerprint minutiae extraction, Pattern Recognition. 2007; 40(4): p. 1270-1281.
[5] Fingerprint Database (FVC2002). Available at: http://bias.csr.unibo.it/fvc2002, accessed July 2012.
[6] U Halici, LC Jain, A Erol. Introduction to Fingerprint Recognition, Intelligent Biometric Techniques in Fingerprint and Face Recognition, CRC Press. 1999.
[7] E. Hastings. A Survey of Thinning Methodologies, Pattern Analysis and Machine Intelligence, IEEE Transactions. 1992; Vol. 4, Issue 9, p. 869 - 885
[8] HC Lee and RE Gaensslen. Advances in Fingerprint Technology, Elsevier Science, New York, ISBN 0-444-01579-5. 2009.
[9] L Hong. Automatic Personal Identification Using Fingerprints. Ph.D. Thesis, ISBN: 0-599-07596-1. 1998.
[10] D Maltoni, D Maio, AK Jain, S Prabhaker. Handbook of Fingerprint Recognition. Springer, New York, USA. 2003
[11] K Manvjeet, M Singh, G Akshay, and SS Parvinder. Fingerprint Verification System using Minutiae Extraction Technique. World Academy of Sci. Eng. and Tech. 2008

American Journal of Engineering Research (AJER)
e-ISSN : 2320-0847 p-ISSN : 2320-0936
Volume-03, Issue-03, pp-127-131
www.ajer.org

Research Paper Open Access

Prioritization: A Means of Achieving Positive Rural Development In Nigeria.

Amadi; D.C.A; Zaku Sabo; Idiege D.A; Maiguru Abel; and Oluronke Sobola.
Department of Forestry and Wildlife Management, Federal University Wukari, Taraba State, Nigeria.

Abstract: **-** Rural developmen occupies a priority place in agenda of Nigeria's national development. However, the gap between scarce and stingy allocation of resources by Governments and rural people's needs calls for prioritization in the areas of investment with regards to rural development. This paper examined the priority areas for rural development in Nigeria. Data on the needs of rural dwellers were randomly collected in 2006, 2008 and 2010 respectively. The rural dwellers were interviewed in each of the years using questionnaire and oral discussions. The questionnaire centered on rural dwellers needs among many alternatives such as Irrigation Facility, Roads, Markets, Portable Water Supply, Clinics/Hospitals, Electricity, Loan, Schools/Education and farm inputs. Analysis of variance, (ANOVA using the general linear models procedure) was used in data analysis. Results show that majority of rural farmers' needs are in order of preference Potable Water Supply, Roads, Farm Inputs, Loan and Schools/Education. The implication is that future rural development projects and Programs if directed towards these areas will help to accelerate the improvement of rural dwellers welfare and help to reduce the number of rural to urban migrating, resulting in rural stability and integrated rural development.

Keywords: **-** *Priority areas, rural development, rural dwellers needs, investment.* *Amadi D.C.A (Ph.D.) A Senior Lecturer in Forestry and Rural Development In the Department of Forestry and Wildlife Mgt; Federal University Wukari, Taraba State Nigeria.*
Zaku Sabo (M.Sc.) A Lecturer 1 In the Department of Forestry and Wildlife Mgt; FederalUniversity Wukari, Taraba State Nigeria.
Maiguru Abel (M.Sc.) An Assistant Lecturer In the Department of Forestry and Wildlife Mgt; Federal University Wukari, Taraba State Nigeria.
Idiege D.I. (M.Sc.) An Assistant Lecturer In the Department of Forestry and Wildlife Mgt; Federal University Wukari, Taraba State Nigeria.
Oluronke Sobola (B.Tech) A Graduate Assistant In the Department of Forestry and Wildlife Mgt; Federal University Wukari, Taraba State Nigeria.

I. INTRODUCTION

According to (Ariyo 1991), rural development has been pushed to the top of agenda in Nigeria's national development plan. The possibility of misplaced priority in Nigeria's rural development effort in the context of different political inclinations is now the concern of many rural development experts, implementers and vanguards. The type of political, tribal and religious inclinations has helped to drag back the pace of development in Nigeria (Simpson1987). Hence in many parts of Africa and Nigeria in particular, many failed rural development projects abound, Signifying waste of scarce resources. Therefore, if we are to attract global assistance or government revenue for rural development, it is important that the priority needs of the rural area in question be first determined. Rural development project cited in any area without consulting the local people do not interest them (Oyalde, 1989, Awolola 1986). Development must meet the needs of the people to be appreciated and to make the people to take responsibility of the security and sustainability of such projects.

The enormous funds wasted on abandoned, unsustained or failed projects should not be repeated in the face of scarce resources and conflicting needs. According to Landis (2005), the enormous gap between needs and current spending suggest that: however, innovative the funding strategies devised, goals are unlikely to be

met when needs outstrip resources. Priority setting then becomes crucial. This paper therefore set out to determine the priority areas of need for development among rural dwellers in Nigeria.

In view of the gap between resources and needs, a number of strategies have been adopted since independent in Nigeria to address rural development. It has been viewed that agricultural development is synonymous with rural development because majority of most rural dwellers are small scale farmers. In an effort to reverse the slow growth of rural areas in Nigeria, the Federal Government established the Directorate for Food, Roads and Rural Infrastructure (DFRRI) in 1986, to among other things improve the quality of life and standard of living of the majority of people in rural areas. Ekpo and Olaniyi (1995) evaluated the achievements of DFRRI against its mandate and showed that by 1992, 85,592.82 km of feeder roads were completed. In rural electrification, DFRRI selected two model villages in every local government area of the country, and by 1992, 506 communities were supplied with electricity by DFRRI and 18,680 wells/boreholes were sunk. These achievements have not been due to the activities of DFRRI alone, the agency was able to mobilize rural communities towards self reliance in rural development projects. DFRRI was only responsible for 14.8 percent of the rural access roads constructed, while community efforts accounted for 30.2 percent of roads constructed or rehabilitated. In the area of water supply and health, DFRRI was merely responsible for 17.3 percent and 0.5 percent respectively communal efforts again accounted for the highest number of water project 28.0 percent and 11.4 percent of health projects. These achievements were possible because the projects dwelt on the priority areas of need of the local people and were therefore able to attract their interest and commitment. DFRRI project has long been abandoned, enshrining it on the list of abandoned rural development projects in Nigeria.

According to Ariyo (1991), the Federal and State governments have set up a number of institutions to undertake specific rural development activities on their behalf. The Agricultural Development Program (ADP) system is an example of institutions with specific mandate to develop the rural areas. The ADP system was introduced in Nigeria in the mid 1970s to help improve the traditional system of agricultural production and raise productivity, income and standard of living of small scale farmers. Moreover, the ADP system has been able to survive various governments with varying political inclinations (Eboh 1995), Ayichi (1995). Generally the ADPs in Nigeria has generally improved the agricultural extension service in Nigeria by reducing extension agent – farmer ratio from pre ADP level of 1:3000 to a national average of 1:800 (Patel 1989, Owona 1992). On crop output, Ayichi (1995) noted that crop output increased significantly due to the Programmes activities. The implication is that farmers income and welfare improved. Kwa (1992) reported that average income per hectare from various crops and returns to family labor / man day were over 200% above pre-project situation in most completed ADPs. This political survival of the program and her achievements informed the use of ADP farmers as respondents for this research.

II. METHODS

The study area is Adamawa State of Nigeria made up of 21 local government areas. According to the 1991 census, the state has a population of 2.102,053 people spread over 38,741 square kilometers. The landform type and climate conditions favor tropical agriculture. The major vegetation formations in the state are the Southern Guinea Savannah, Northern Guinea Savannah, and the Sudan savannah (Akosim *et al* 1999). The onset of rains is normally accompanied b strong devastating wind storms (Amadi and Adebayo 2005). The major food crops grown are mainly cereals, legumes and root crops, while the cash crops grown are mainly cotton, groundnut and sugar-cane (Sajo and Kadams 1999). Adamawa State has a very high concentration of wide variety of livestock. Almost all the traditional industries are agriculturally based and majority of the population are engaged in subsistence agriculture. With the provision of basic rural needs therefore, the rural farmers will be stabilized for sustained food production.

Data on the priority needs of rural dweller collected in 2006, 2008 and 2010 were used for this paper. The primary sources of data were through questionnaires, interviews and oral discussion. A total of 435 rural dwellers in Adamawa State of Nigeria were interviewed. The scope of the interview included age, occupation and priority needs of rural people. However, oral discussion with our respondents centered on their priority needs. The analyses of variance (ANOVA) were used in the data analysis.

III. RESULTS & DISCUSSION

Poverty is lack of basic human needs, such as adequate nutritious food, clothing, housing, clean water, and health services. Respondent's priority areas for rural development are shown in Table 1 and chart 1. Analysis of variance result (Table 2) shows that there is high significant difference in the priority needs of the rural population. This led to further analysis of mean performance to determine areas of significant difference (Table3). Most rural communities needed in order of priority: Portable water supply, good rural roads, farm inputs such as fertilizers, adequate loan facility, and education. In most rural settings in Nigeria, dwellers rely on local streams and tube wells as source of drinking water. Many water borne diseases abound and the rural poor

are sick and weak. Poverty is also expressed as the lack or degeneration of community resources such as inadequacy of water supply, roads, health centers, electricity, and industries (Francis *et al* 1996). Most rural roads are death traps making the evacuation of agricultural products and farm inputs costly. The rural poor meets small needs by drawing on slender reserves of cash, reduced consumption, barter or loans. Disasters such as crop failure, famine, burnt hut, accident, sickness, funeral and wedding expenses have to be met by becoming poorer. This often means selling or mortgaging assets such as land, livestock, tools, trees, jewelry, standing crops or future labor. This explains the need for access to loan facilities to rural farmers. In a simpler form, Akinbode (1988) explained rural development as the stage when people in the villages can turn on their taps and get water inside or near their houses, have medical facilities, schools, markets, transportation facilities, banks, electricity, shelter, clothing, balanced diet, recreational facilities, efficient sewage system, participation in decision making that effect their lives and the pride to remain in those villages.

IV. CONCLUSION

With regards to the importance attached to rural development in Nigeria, and the relative scarcity of resources for conflicting demands, it is now extremely important to identify priority areas of rural dwellers needs before investing resources in rural development projects. The era of abandoned projects due to poor feasibility studies and hasty uncoordinated implementation should be over. The conflict between government and rural dwellers in Nigeria on developmental matters will be greatly reduced if investment of resources in rural development is done by taking the priority needs of the rural people into consideration.

Tables and Figures

Table 1 Respondents Priority for rural Development.

Years	*Road*	*Water*	*Elect.*	*Educ.*	*F/input*	*Hosp.*	*Loan*	*Mkt.*	*Irriga.*	*Total*
1991	36	40	7	13	19	5	19	1	5	145
1997	35	37	9	8	21	7	21	1	6	145
2003	35	39	9	9	20	6	20	2	5	145
Total	106	116	25	30	60	18	60	4	16	435
Mean	35.2	28.7	8.33	10	20	6	20	1.33	5.3	-

Source Field Data 2010.

Table 2 Anova Mean value for Priority on rural development

SV	d f	MS
Priority	8	1.623.50**
Error	72	1.22
Total	80	

** Highly Significant (P=0.01)

Table 3 Table of mean performance for priority needs of the rural people

S/No.	Priority Area	Means Performance
1	Water	38.667
2	Roads	35.333
3	Farm Input	20.000
4	Loan	20.000
5	Education	10.000
6	Electricity	8.33
7	Hospital	6.00
8	Irrigation	5.333
9	Market	1.333

LSD = 1.0389
CV = 6.861
(P = 0.05)

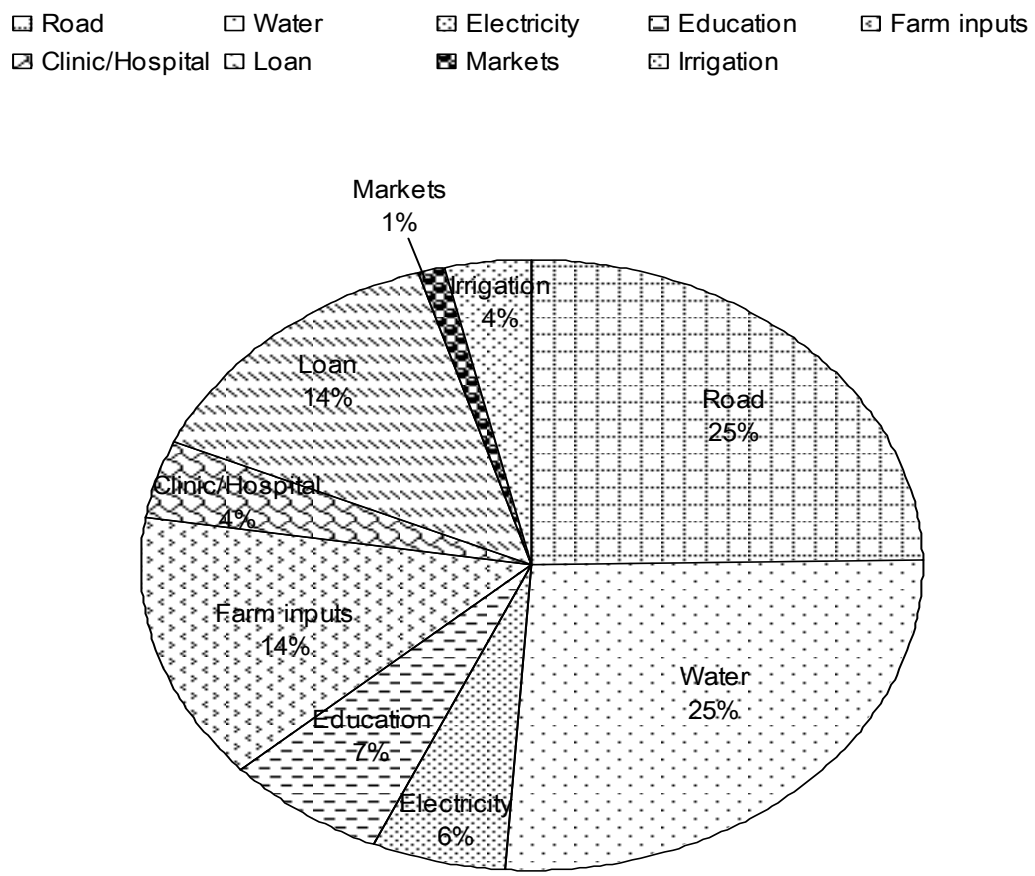

Chat 7: Respondents priority for rural development in the State

Fig. 1 Respondents' Priority for Rural Development.

REFERENCES

[1] *Akinbode, A. (1988). The Conceptual Framework for Rural Development In Developing Countries. Research for Development Vol.5 No.1 and 2 P.8-9.*

[2] Akosim C, Tella I.O., & Jatau D.F. (1999). *Vegetation and forest Reserves.* In Adamawa State in Maps, Yola: Dept. of Geography, F.U.T. Yola and Paraclete Publishers.Amadi D.C.A and Adebayo A.A (2005) *Effects of Agro forestry practices on crop Yield. A case Study of Gombi Local Government Area of Adamawa State.* Journal of Arid Agriculture, Vol. 15 of 2005. Faculty of Agriculture, University of Maiduguri.

[3] Ariyo J.A. (1991) *Rural Development Institutions: An overview of the Factors*

[4] *which influence their Effectiveness.* In Ariyo J.A (ed) *Perspectives on Environmental Management and Resource Development in Nigeria.* Department of Geography, ABU Zaria. Occasional Paper ISSN 8065-4698. pp 55-61.

[5] Awolola A.D. (1986). *Edecational problems in Development Programmes* Rural Development in Nigeria Vol. 2 No. 2.

[6] Ayichi, D (1995). *Models of Rural Development in Nigeria with special focus on the ADPs* . In Eboh E.C, Okoye C.U. & Ayichi D. (Eds) *Rural Development in Nigeria.* Enugu: Auto Century Publishing Company.

[7] Eboh E.C (1995). *Sustainable Development, The theory implications for Rural*

[8] *Nigeria.* In Eboh E.C., Okoye C.U & Ayichi D. *Rural Development in Nigeria.* Enugu: Auto Century Publishing Co. Ltd

[9] Ekpo A.H. & Olaniyi O. (1995). *Rural Development in Nigeria. Analysis of the impact of the Directorate for Foods, Roads and Rural infrastructure. (DFRRI)* In Eboh E.C., Okoye C.U. & Ayichi D. *Rural Development in Nigeria.* Enugu: Auto Century Publishing Co. Ltd.
[10] Francis P; Akinwumi J.A Ngwu P. Nkom S.A. Odibi J. Olomajeye J.A.
[11] Okumadewa F. & Shebu D.J. (1996). *Community and Local Development in Nigeria* Washington D.C: World Bank
[12] Kwa, A.R (1992). *The Impact of ADP on the Nigerian Farmers* Paper Presented at a Symposium Organized During the 1992 Agricultural Show, Kaduna.
[13] Landis Mackeller (2005) *Priorities in Global Assistance for Health, ADIS and*
[14] *Population.* In Population and Development Review Vol. 31 No. 2 pp 293-300
[15] *Owona, S. (1992). Implementation of the ADP System in Nigeria: The World Bank Experience. Paper Presented at the 1992 ADP Show Kaduna.*
[16] *Oyaide, O.F.J (1989). The Challenge of Rural Development in Nigeria. Federal Agricultural Development Unit (FACU) Occasional Paper No 7.*
[17] *Patel, A.U. (1989). Agricultural Extension in Nigeria. Past, Present and prospects Occassional Paper No. 5 Ibadan FACU*
[18] Sajo & Kadams (1999*) Food and Cash Crops*. In Adebayo A.A & Tukur A.L (Eds), *Adamawa State In Maps*. Yola: Department of Geography, F.U.T Yola and Paraclete Publishers Nigeria.
[19] Simpson, E.S (1987). *The Developing World. An Introduction* U.K: Longman Group p 190.

American Journal of Engineering Research (AJER)
e-ISSN : 2320-0847 p-ISSN : 2320-0936
Volume-03, Issue-03, pp-132-137
www.ajer.org

Research Paper Open Access

The Use of Super Absorbent Polymer as a Sealing Agent in Plain Concrete

Mohammad Daoud[1], Moayyad Al-Nasra[2]
[1](*Department of Civil Engineering, Zarqa University, Jordan)*
[2](*Department of Engineering Technology, West Virginia University Institute of Technology, Montgomery, West Virginia)*

Abstract: - The super absorbent polymer (SAP) has the ability to absorb relatively large amount of water and convert it into gel at the same time the volume increases proportionally. These properties are found to be very useful and effective in plain concrete. Also the use of super absorbent polymer in concrete is proven to have many positive effects on the properties of concrete in its both stages; fresh concrete and hardened concrete. This study focuses on the water tightness properties of plain concrete with time. The study includes short term and long term effect of the super absorbent polymer on the water sealing properties. There are also many advantages of the use of the super absorbent polymer in plain concrete including providing internal water source. This internal water source acts as internal curing agent after the final setting of concrete. At the same time the SAP releases water at relatively slower rate at the fresh concrete stage. The SAP also provides additional voids in the concrete mass. These voids affect the concrete strength negatively at the same time improve the concrete performance by improving the concrete workability and consistency, reducing the concrete susceptibility to freezing thawing cycle, and improving concrete stability.

Keywords: - *Concrete Curing, Concrete Strength, Sealant, Super Absorbent Polymer, Water Tightness*

I. INTRODUCTION

The SAP absorbs water and converts it into gel, then releases it slowly with time, at the same time the gel volume increases proportionally. This property is very useful when it comes to watering plants over time. The expansion in volume has the tendency to clog the water pathways in the concrete mass, and consequently improving its water tightness properties. The use of SAP is proven to be very effective as a sealant in plain concrete if sufficient amount is used. This study focuses on the long term effect as well as the short term effect of the use of the SAP in plain concrete. Several samples were prepared with different SAP content. The content of SAP is measured as a percentage of the Portland cement used by weight. The amount of water added to the fresh concrete is one of the most important key factors that affect the concrete properties, including water tightness durability and strength. The water is an essential ingredient needed for the hydration process in the fresh concrete and for the curing process in the hardened concrete at its early stages. Excessive amount of water added in the fresh concrete improves the concrete workability in general, reduces the concrete strength, and increases the drying shrinkage of the hardened concrete. Different admixtures were used to reduce the amount of water demand in the fresh concrete without jeopardizing the workability. Water reducer admixtures were used extensively in the ready mix plants. The most common admixture used nowadays is the superplasticier which is water reducer and at the same time retarder. The water gel created in the fresh concrete by the use of SAP provides cushioning and lubrication in the concrete mass which in turn improves the concrete workability as well as concrete stability.

Jensen (2013) used superabsorbent polymers in concrete. His study focused on the strength and shrinkage of concrete. He concluded that the shrinkage of concrete due to loss of water to the surroundings is the cause of cracking both in the plastic and in the hardened stage. This type of cracking can effectively mitigated by slowing down the water loss. The superabsorbent polymers use in concrete has the potential to reduce concrete cracking. Jensen and Hensen (2001) studied the autogenous shrinkage phenomena in concrete.

They concluded that the autogenous shrinkage may lead to cracking and affect concrete strength and durability, which is also, can be considered as technological challenge of high performance concrete. Addition of superabsorbent polymer in the ultra-high-performance concrete can be used to control the autogenous shrinkage. They also conducted tests that show that the shrinkage reduction due to superabsorbent polymer is related to a corresponding increase in the internal relative humidity of the cement paste. In addition, the use of superabsorbent polymer in concrete resulted in a reduction or elimination of stress buildup and related cracking during restrained hardening of these high-performance cementitious systems (Jensen and Hensen 2002).

Al-Nasra (2013) studied the use of Sodium Polyacrylates as SAP in concrete. His study focused on determining the optimum amount of SAP to be added to the concrete in order to maximize the strength and durability of concrete. Al-Nasra concluded in his study that the optimum amount of SAP is 0.11 percent of cement by weight, which he showed to be the most effective amount to be used in concrete.

The use of superabsorbent polymer in concrete is also useful in frequent freeing-thawing cycle environment, by providing the concrete frost protection. The superabsorbent polymers particles shrinks during the hydration process leaving voids in the concrete similar to the voids created by adding air entrainment agent to the concrete. The air bubbles left in the concrete are critical to absorb the hydraulic pressure due the water freezing. Water expands upon freezing about ten percent in volume generating hydraulic pressure in the concrete that has the potential to cause the concrete to crack. Providing voids in the concrete absorb the hydraulic pressure and provide addition space for the water to expand. The same can be said about the osmotic pressure in the concrete. The osmotic pressure is usually generated due to the difference in salt concentration in the water. This difference in salt concentration can be created by adding deicer to the concrete top surface, for the purpose of melting the ice on the concrete. Also these voids can be useful to absorb other kinds of internal pressures in concrete including alkali reactivity pressure.

Snoeck et al (2012) studied the use of superabsorbent polymers as a crack sealing and crack healing mechanism in cementitious materials. Their research focused on the use of the superabsorbent polymer to seal concrete cracks. As concrete cracks due to its low tensile strength and as harmful unfriendly chemicals may migrate into these cracks, the durability of concrete is endangered if no proper treatment or manual repair is applied. The first stage focused on hindering the fluid flow by swelling of superabsorbent polymers after they are exposed to a humid environment. The sealing capacity was measured by means of water permeability tests and through visualization of permeability tests by neutron radiography. They also concluded that the use of superabsorbent polymers is able to seal cracks and thus allow a recovery in water-tightness as a decrease in permeability is noticed. The second stage focused on healing of small cracks by the use of fiber reinforced cementitious materials that have the ability to restore the mechanical properties. These mechanical properties were analyzed by four-point-bending tests and the crack closure was microscopically monitored. Cracks close through the combination of further hydration of unhydrated cement particles, precipitation of calcium carbonate and activation of the pozzolanic reaction of fly ash. Also they concluded that the desorption of superabsorbent polymers triggers healing in the vicinity of crack faces and cracks up to 130 μm were able to close completely in wet/dry cycles due to the precipitation of calcium carbonate.

The process of curing involves maintaining satisfactory moisture content and temperature after concrete is placed in order to hydrate the cement particles and produce the desired hardened concrete properties. Proper curing can improve strength, durability, abrasion resistance, resistance to freeze-thaw cycles, deicer scaling resistance and reduce concrete shrinkage. Traditionally, concrete has been cured externally either through the use of water curing or sealed curing. Curing either supplies additional moisture from the original mixing water or minimizes moisture loss from the concrete. Water may be bonded directly on the concrete surface or may use other methods like wet burlap bags or fogging near the surface of the concrete to prevent evaporation of water from the fresh concrete. Sealed curing is accomplished by applying some sort of sealant to the surface of concrete in order to prevent moisture loss. Internal curing can be divided into two categories. The first category is internal water curing in which an internal curing agent stores water during mixing which is gradually released as hydration processes. The second category is internal sealing which is very similar to external sealed curing in that its goal is to prevent the loss of moisture from the concrete (RILEM, 2007).

II. SUPER ABSORBENT POLYMNER

The super absorbent polymer used in this study is Sodium Polyacrylate, also known as water-lock, which is a sodium salt of polyacrylic acid with the chemical formula $[-CH_2-CH(COONa)-]_n$ and broad application in consumer products. It has the ability to absorb as much as 200 to 300 times its mass in water. Sodium polyacrylate is anionic polyelectrolytes with negatively charged carboxylic groups in the main chain. Figure 1, shows the composition of the sodium polyacrylate.

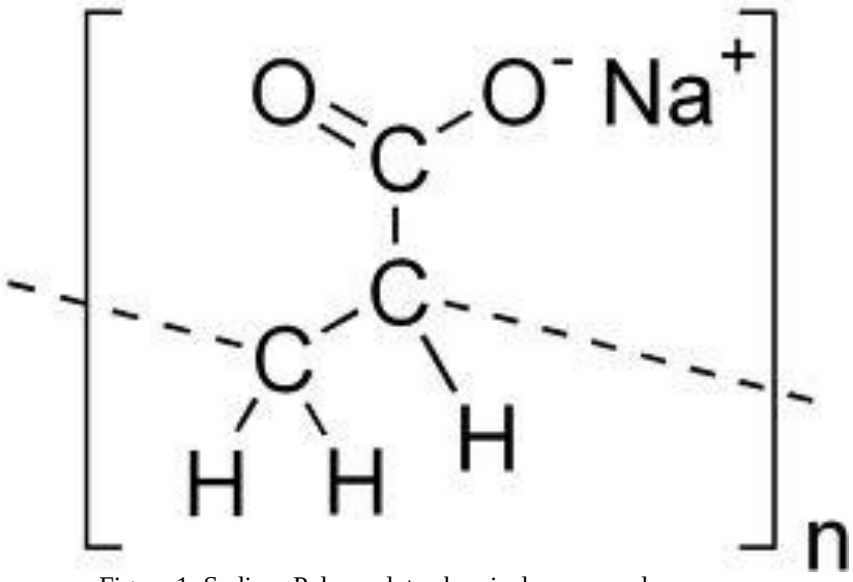

Figure 1: Sodium Polyacrylate chemical compound.

Sodium polyacrylate is a chemical polymer that is widely used in a variety of consumer products for its ability to absorb several hundred times its mass in water. Sodium polyacrylate is made up of multiple chains of acrylate compounds that possess a positive anionic charge, which attracts water-based molecules to combine with it, making sodium polyacrylate a super-absorbent compound. Sodium polyacrylate is used extensively in the agricultural industry and is infused in the soil of many potted plants to help them retain moisture, behaving as a type of water reservoir. Florists commonly use sodium polyacrylate to help keep flowers fresh.

III. WATER FLOW TEST

The use of SAP in plain concrete alters several properties of concrete. There is an optimum amount of SAP that can be added to the plain concrete in order to improve its strength, and durability. In the other hand, adding more of SAP in the plain concrete improves the water tightness property of concrete. Also it is relevant to mention that the concrete plasticity improves with the increase amount of SAP in plain concrete. The color and texture of the concrete mixed with SAP will change too. The shiny water surface of the fresh concrete seemed to disappear when using the SAP due to transforming the excess water in fresh concrete into gel.

Several samples were prepared with different amount of SAP added to the plain concrete expressed in terms of percentage of the Portland cement by weight. Table 1 shows the mix design of the three samples used in this study. The samples are labeled as P for plain concrete sample with no SAP added to the mix, S1 sample has 0.2% of SAP, and S2 sample has 0.5% of SAP by weight of Portland cement. The water cement ratio (W/C) is kept constant for all samples used.

Table 1: Ingredients used

Sample ID	Sand (gm)	Cement (gm)	SAP (gm)	W/C
P	200	100	0.0	0.45
S1	200	100	0.2	0.45
S2	200	100	0.5	0.45

Figure 2 shows the dimension of the samples used in this study. Special mold is used to make the test samples. The samples are of cylindrical shape of 35 mm base diameter and 10 mm height. Figure 3 shows a typical sample ready to be tested. A sealant is applied at the perimeter of the concrete samples in order to prevent any leak, and force the water to go through only the concrete sample under pressure.

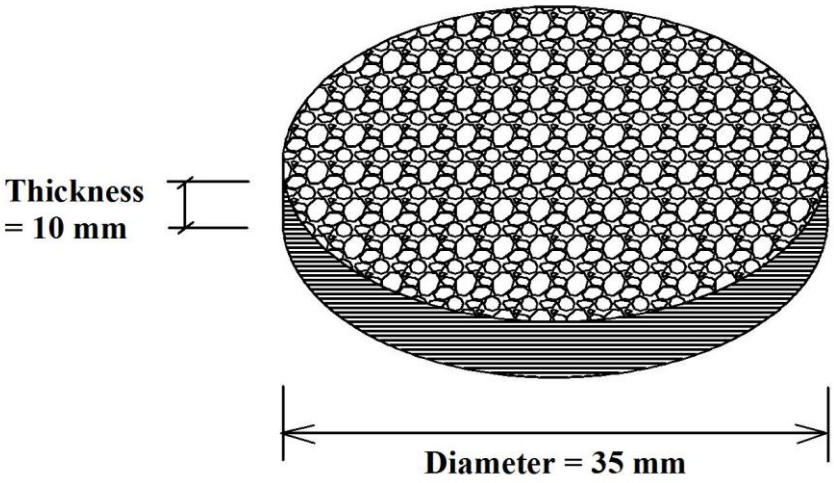

Figure 2: Size of samples used.

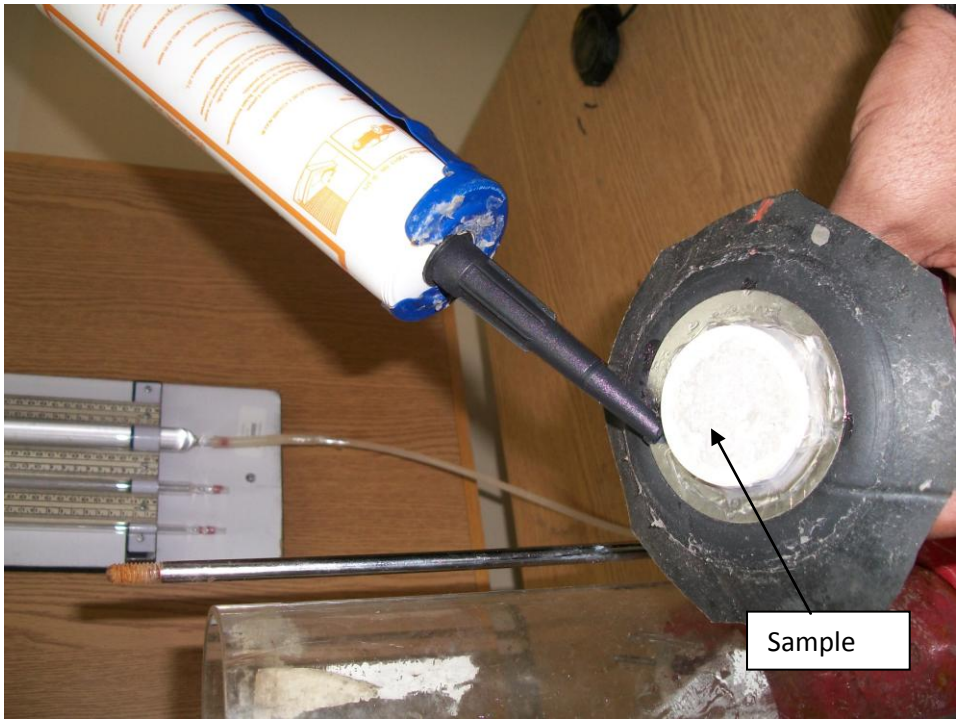

Figure 3: Preparing samples for the test.

The samples are subjected to a water pressure that varied from 180 cm of water to 170 cm. The average water pressure is 175 cm. The time it takes for the water pressure to drop from 180 cm to 170 cm is measured and recorded. The amount of water that flows through the samples will be constant of about 31 cm^3 during the drop of the water pressure by 10 cm. The discharge though the sample can be calculated using the following formula:

$Q=V/t$

Where;

Q= water flow rate in cm^3/min

V= volume of water passing through the sample in cm^3

t = the measured time that takes the pressure to drop from 180 cm to 170 cm, discharging a total of about 31 cm^3 of water. Thus

The water flow rate = 31.42 cm^3/ the measured time (min)

Figure 4 shows the experimental set up. The samples are confined in a chamber and tight sealed at the perimeter.

Figure 4: Test set up.

IV. TEST RESULTS

The samples were tested under an average water pressure of 175 cm. The time it took for the water to flow through the concrete layer is recorded at a total of 31.42 cm^3 of water flow. The test continued for several days and weeks. Figure 5 shows the flow rates of the three samples tested. This figure shows the flow rate results for a short term duration of 2 hours or less. As can be seen in Fig. 5 that the flow rate decreases with time for the samples prepared with SAP, while the plain concrete sample has the tendency to stabilize at a constant rate of flow.

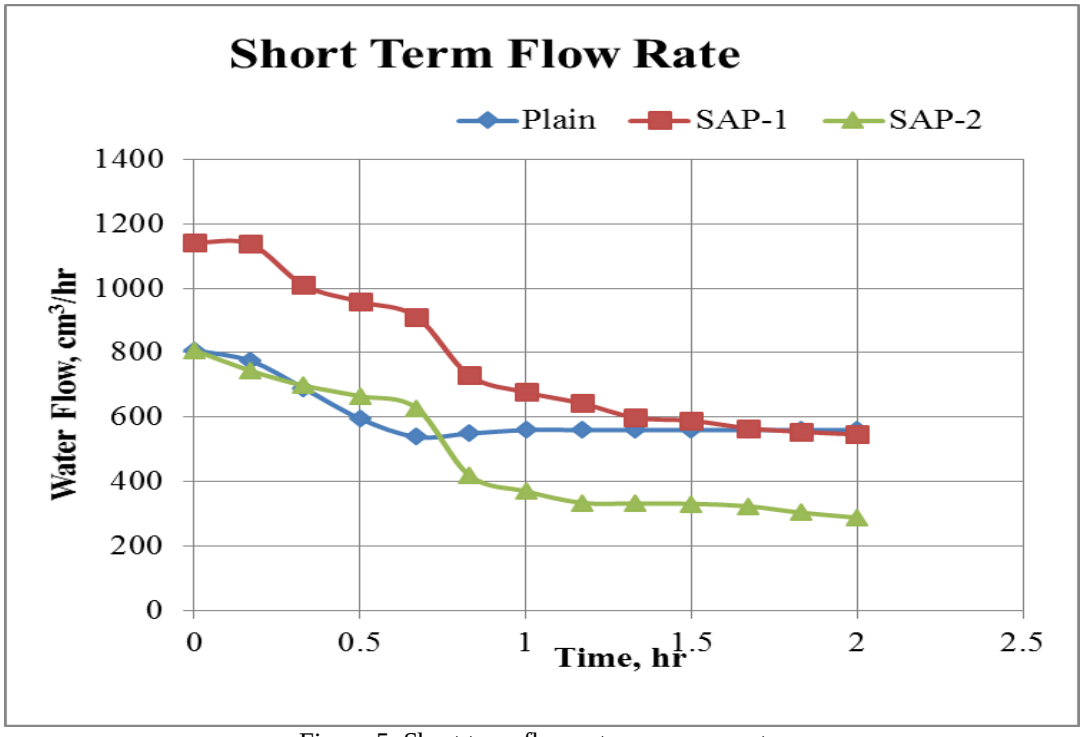

Figure 5: Short term flow rate measurements.

The results obtained for the short term flow study lead to the conclusion that the flow rate is related to the time. Long term study was conducted to focus on the effect of time on the flow rate. Figure 6 shows the results of the long term results. Figure 6 shows that the plain concrete sample has constant flow rate and that the flow rate is not affect by the time. The other samples showed a different trend. The flow rate decreases substantially with time, making it easier to seal the concrete with time. Also one may observe that the increase in the amount of SAP used decreases the flow rate. This long term study is also conducted at the same conditions of the short term study.

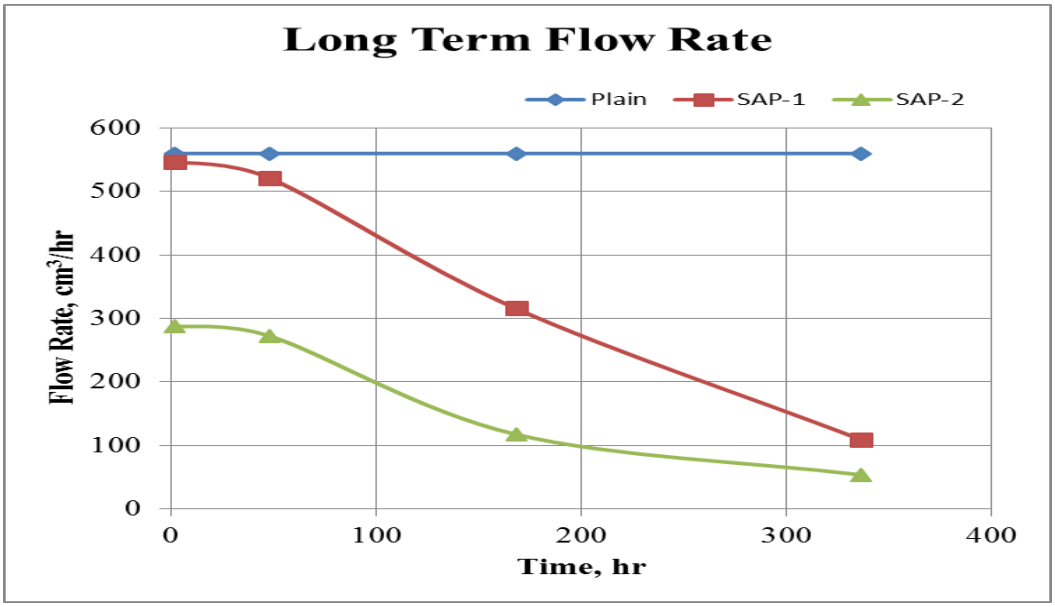

Figure 6: Long term study of water flow rate

V. CONCLUSION

The use of sodium polyacrylate as super absorbent polymer in concrete has promising potential to improve several properties of concrete including the water tightness. This property is very useful to prevent water leaks through the concrete mass making it a self-sealing concrete. This property improves with time if subjected to moisture for a properly designed concrete with adequate amount of SAP. The adequate amount of SAP to be used to prevent future water leak though the concrete mass is yet to be determined. Also the water pressure is another factor that plays a significant role in the water flow rate calculation. The increase in the water pressure increases the flow rate. Also the increase in the amount of SAP used in the concrete mix decreases the flow rate. Several other properties of concrete can be altered by using SAP as an admixture which in turn converts the liquid water into gel.

REFERENCES

[1] Jensen, M, "Use of superabsorbent polymers in concrete," Concrete International, Vol. 35, No. 1, January 1, 2013, pages 48-52.

[2] Jensen, O., and Hensen, "Autogenous deformation and RH-Change in prospective," Cement and Concrete Research, Vol. 31, No. 12, Dec. 2001, pages 1859-1865.

[3] Jensen, O., and Hensen, "Water-Entrained cement-based materials: Experimental observations," Cement and Concrete Research, Vol. 32, No. 6, June 2002, pages 973-978.

[4] Al-Nasra, Moayyad, "Optimizing the Use of Sodium Polyacrylate in Plain Concrete," International Journal of Engineering Research and Applications (IJERA) ISSN: 2248-9622 www.ijera.com, Vol. 3, Issue 3, May-Jun 2013, pages 1058-1062.

[5] Snoeck, Didier, Van Tittelboom, Kim, De Belie, Nele, Steuperaert, Stijin and Peter Dubruel, Peter, "The use of superabsorbent polymers as a crack sealing and crack healing mechanism in cementitious materials," 3rd International conference on Concrete Repair, Rehabilitation and Retrofitting (ICCRRR - 2012), Cape Town, South Africa, pages 152 – 157, ISBN:9780415899529.

[6] RILEM. Internal Curing of Concrete - State-of-the-Art Report of RILEM Technical Committee 196-ICC. State of the Art Report, RILEM Publications SARL, 2007.

American Journal of Engineering Research (AJER)
e-ISSN : 2320-0847 p-ISSN : 2320-0936
Volume-03, Issue-03, pp-138-143
www.ajer.org

Research Paper Open Access

Design of Pseudomorphic High Electron Mobility Transistor Based Ultra Wideband Amplifier Using Stepped Impedance Stub Matching

Aayush Aneja[1], Mithilesh Kumar[2]
[1](M.Tech., Electronics Deptt, University College Of Engineering, RTU, Kota)
[2](Professor, Electronics Deptt., University College Of Engineering, RTU, Kota)

Abstract: **-** In this paper, the design of an ultra wideband low noise amplifier using pseudomorphic high electron mobility transistor is described. The amplifier achieves a flat gain across the bandwidth and has minimized input and output return loss. The circuit also has a very low noise which is less than 2 dB. A detailed design is carried for low noise amplifier and simulated on serenade simulation tool. The amplifier is fabricated on RT duroid substrate (ε_r=2.2) and the results of simulated and fabricated amplifier have been compared. Impedance matching is achieved using a stepped impedance stub. The amplifier also consumes very low power for operation.

Keywords: *– High Electron Mobility Transistor, Stepped Impedance Stub, Ultra Wideband*

I. INTRODUCTION

The introduction of the paper should explain the nature of the problem, previous work, purpose, and the contribution of the paper. The contents of each section may be provided to understand easily about the paper. Ultra wideband amplifier technology is a short range communication technology that uses low power and operates in 3.1 to 10.6 GHz band. UWB is able to transmit more data in a given period of time than the more traditional technologies such as WLAN, Bluetooth etc. The potential data rate over a given RF link is proportional to the bandwidth of the channel and the logarithm of the signal-to-noise ratio (Shannon's Law) [1]. UWB can transmit and receive wireless signals at rates in excess of several hundred of Mbits per second, while consuming a small amount of power without interfering with existing communications signals. UWB application is not limited to wireless; the technology is used for medical imaging, automotive radars, and security systems applications.

Microwave amplifiers are a necessary building block in designing of any microwave transmitter, receiver or trans-receiver circuit. Microwave amplifiers require matched termination rather than open or short circuited termination that is characterized by S- parameters. S- Parameters can be used to express many electrical properties such as gain, return loss, Voltage standing wave ratio (VSWR), reflection coefficient and amplifier stability.

Previous work on ultra wideband amplifier show different technologies that are used for its design and implementation. A low noise amplifier was designed using a reactive feedback technique in 0.13µm CMOS technology . The idea was to use reactive feedback to reduce the noise levels and stabilizing the gain. The amplifier was designed using a cascode gain cell, input filter and output buffer and a negative feedback was applied to that.[2]. In [3], a low noise amplifier in common-gate configuration was designed. In this the reactive matching was extended to wideband matching using butterworth filter. Another low noise amplifier in 130 nm CMOS was made using current reuse technique and worked in 3 to 5 GHz band. The authors used LC band pass filter for input matching of the amplifier.[4] Letter on ultra wideband high gain GaN power amplifier is studied. The letter proposed a three stage power amplifier with feedback design for better gain and output. The GaN HEMTs which require low power have been used to design the amplifier[5]. Since, the GaN HEMTs have high voltage and high power density capabilities; therefore, they are used in designing of power amplifiers [6]. An ultra wideband amplifier was designed using an ERA- 1 amplifier and study was based on the designing of

UWB amplifier using MMIC. The source amplifier used roll off and power supply circuit to get low noise [7]. For Our designed amplifier, The source is matched to load using stepped impedance stub. The amplifier thus designed is simulated in serenade and fabricated on RT duroid substrate with dielectric constant of 2.2.

II. AMPLIFIER DESIGN

An Ultra-wideband (UWB) low-noise amplifier (LNA) is usually the first stage of an UWB receiver. As approved by the FCC, the UWB receiver has a 3.1-10.6 GHz frequency range and so our UWB LNA design will focus on this bandwidth. The UWB LNA is designed to amplify the weak incoming RF signal without adding significantly to the noise level. To meet this requirement, the noise figure of a UWB receiver should normally be less than 7 dB.

The amplifier is designed using the concepts of two port network. The schematic of the amplifier and the designed structure is shown in figure 1 (a) & 1(b).

The first step in designing of the amplifier is choosing a perfect active device that has a good wideband working range. For the designed amplifier, NE3201S01 which is a pseudomorphic Hetero-Junction FET that uses the junction between Si-doped AIGaAs and undoped InGaAs to create very high mobility electrons. It has a gate length Lg ≤ 0.20µm and gate width Wg = 160 µm.

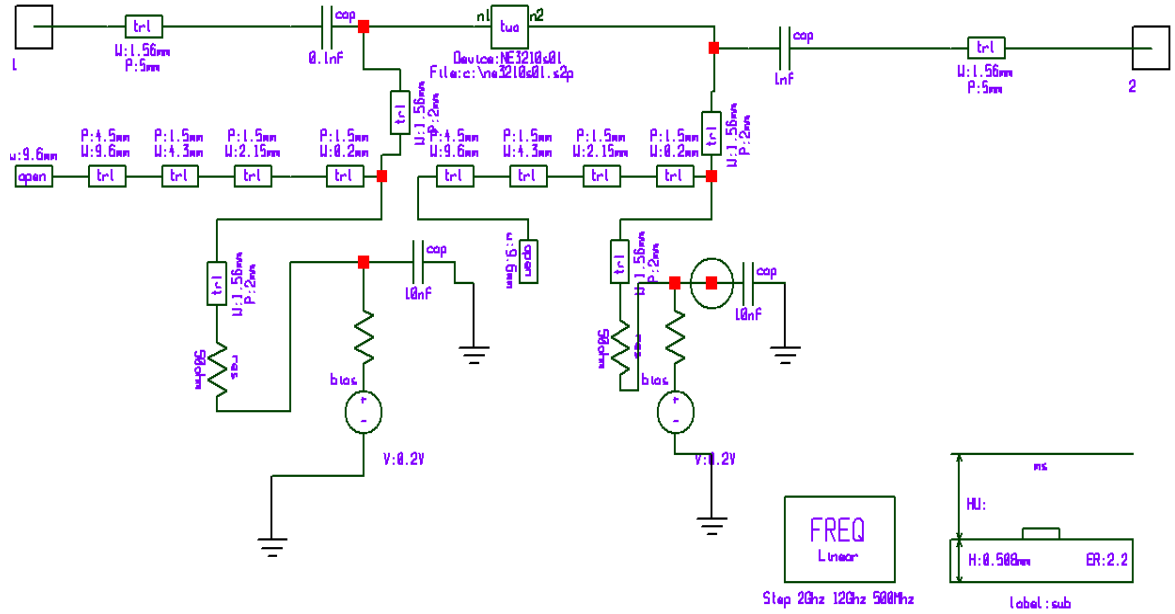

Fig. 1(a) Ultra wideband amplifier design using pHEMT

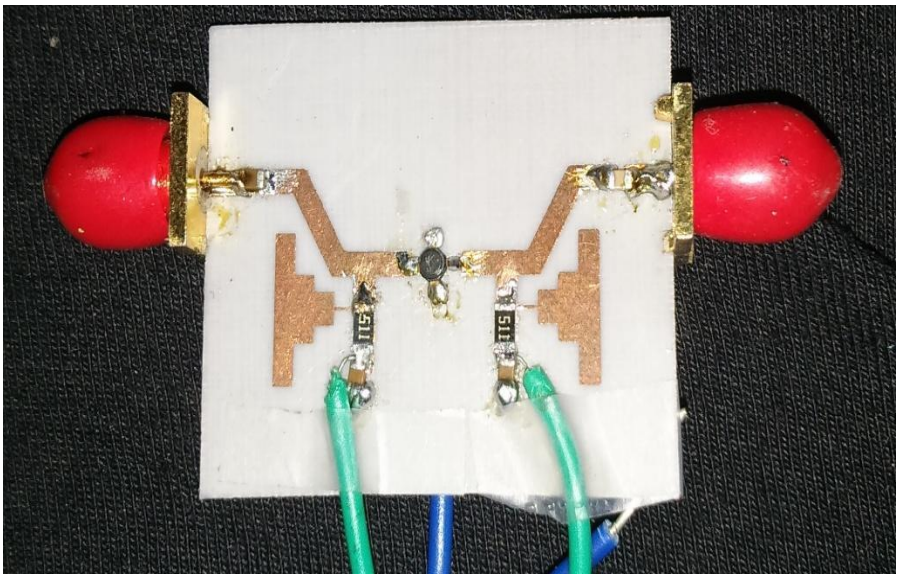

Fig. 1 (b) Fabricated Ultra wideband amplifier using step impedance stub matching technique

At the input of the amplifier, a DC blocking capacitor is chosen for the frequency of operation. This technique helps to isolate the DC bias settings of the two coupled circuits.The next step in designing of the amplifier is designing a bias network. The designed amplifier uses potential divider bias for its operation. [8]
Maximum gain will be realized when these sections provide a conjugate match between the amplifier source or load impedance and the transistor. Because most transistors exhibit a significant impedance mismatch (large |S11| and |S22|), the resulting frequency response may be narrowband.. maximum power transfer from the input matching network to the transistor will occur when $\Gamma_s = \Gamma_{in}^*$ and $\Gamma_L = \Gamma_{out}^*$ [9]. With the assumption of lossless matching sections, these conditions will maximize the overall transducer gain. this maximum gain will be given by

$$G_p = \frac{1}{1-|\Gamma_s|^2}|S_{21}|^2 \frac{1-|\Gamma_L|^2}{|1-S_{22}\Gamma_L|^2} \quad (1)$$

In the circuit schematic shown in Figure 6.1, the input matching network is designed using a stepped impedance stubs. A classical wideband amplifier topology is designed using quarter-wavelength stub, in which λ/4 length shunt stubs are used. while λ/4 connecting lines are used for coupling. The different sections of the stub are designed by calculating the stub widths for L and C in different sections of a wideband filter.
For impedance matching of a wideband amplifier, a band pass filter is applied and the matching circuit is designed by using a stepped impedance band pass filter with stubs of lengths λ/4. Besides stability and gain, another important design consideration for a microwave amplifier is its noise figure.

$$F = F_{min} + \frac{R_N}{G_S}|Y_s - Y_{opt}|^2. \quad (2)$$

where the following definitions apply:
$Y_S = G_S + j\,B_S$ = source admittance presented to transistor.
Y_{opt} = optimum source admittance that results in minimum noise figure.
F_{min} = minimum noise figure of transistor, attained when *YS* = *Y*opt.
R_N = equivalent noise resistance of transistor.
G_S = real part of source admittance.

III. RESULTS AND DISCUSSIONS

The ultra-wideband low-noise amplifier design should optimize the overall performance according to the following criteria:
• wide bandwidth from 3.1 to 10.6 GHz (7.5 GHz frequency range),
• high and flat gain through 3.1-10.6 GHz bandwidth,
• low noise figure over the entire bandwidth,
• high linearity through the entire bandwidth,
• low input and output return loss through the whole bandwidth, and
• low DC power consumption.
An ultra wideband amplifier working in frequency range of 3.1 to 10.6 GHz has been designed and fabricated and the results of simulation and measured results have been recorded and compared. The amplifier achieves flat gain across the bandwidth and attains a maximum of over 9 dB in the band. Fig. 2 Shows the simulated and measured gain of UWB amplifier.

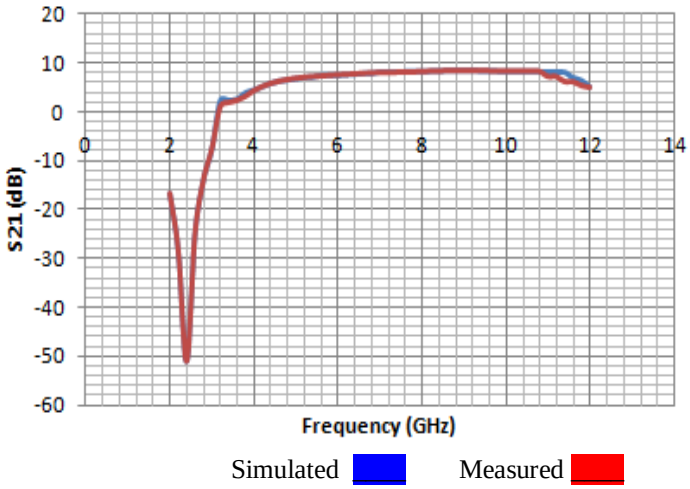

Fig. 2 Simulated and measured gain of UWB amplifier.

Because of the better input match, both simulated nad measured input reflection coefficients are less than -10 dB in the whole of bandwidth. The input reflection coefficent S_{11} of the amplfier is shown in Fig. 3.

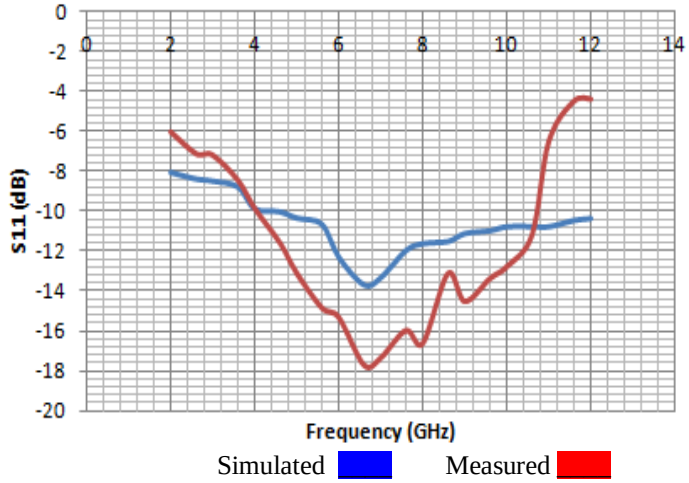

Fig. 3 Simulated and Measured Input reflection coefficient of the amplilfier

The designed ultra wideband amplifier has a good output reflection coefficient which is below -10dB in the whole of UWB range. The circuit also has a good reverse isolation that achieves a minimum of -39 dB in th band of interest. The measured and simulated output reflection ceofficient and reverse isolation of the amplifier is shown in Fig. 4 and 5 respectively.

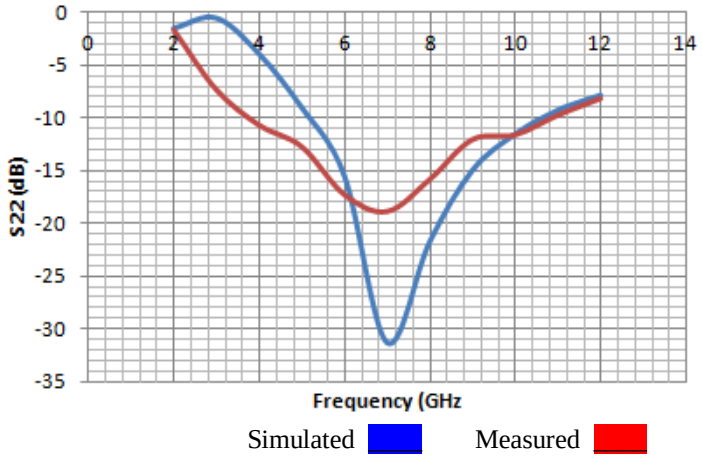

Fig. 4 Simulated and measured output reflection coefficient of the UWB amplifier.

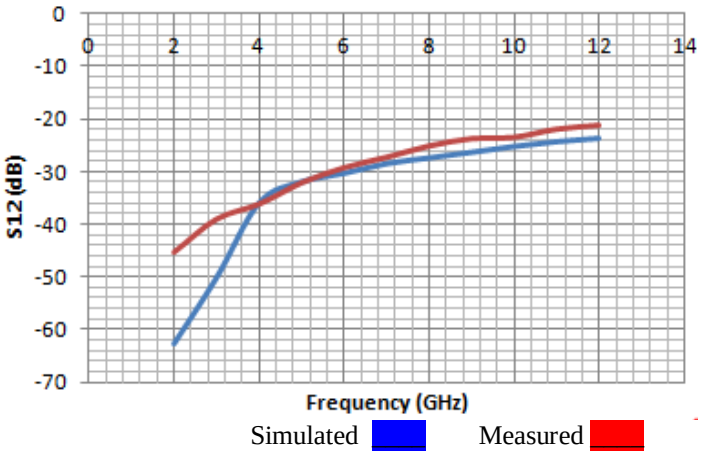

Fig. 5 Simulated and measured reverse isolation of the UWB amplifier.

In RF front-end circuit designs, the noise is caused by the small current and voltage fluctuations that are generated within the devices themselves. Noise figure in amplifiers must be controlled at the initial stage, since for a higher noise figure, the further stages of the amplifier if added will amplify noise to a larger extent and hence the performance can degrade. The ultra wideband amplifier design discussed in this paper has a very low noise figure across the whole bandwidth from 3.1 to 10.6 GHz and is shown in Fig. 6.

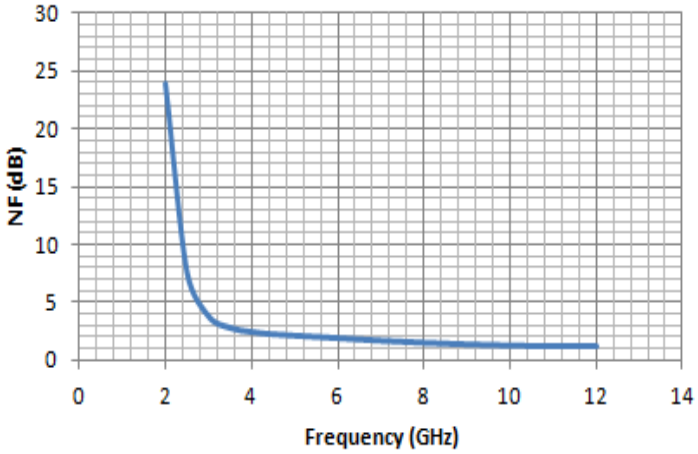

Fig. 6 Simulated Noise figure of the Ultra Wideband amplifier

The power consumption of an LNA can be defined as:

$P = I_D V_{DD,}$

Where I_D is the DC current of the amplifier circuit and V_{DD} is the Supply voltage. The power consumption of the amplifier is only 10 mW, which is quite low.

IV. CONCLUSION

A low power Ultra wideband amplifier has been designed using NEC3210S01 as the active device and applying step impedance stub matching technique for reducing return losses. Voltage divider bias is used for biasing of the transistor. The transistor has input and reflection coefficients which are less than -10dB in across the bandwidth. The amplifier also has a low noise figure, which is less than 2dB. The amplifier is simulated and fabricated using MIC fabrication technique and simulated and fabricated amplifier results have been studied and compared.

Table I Comparison with other works

Parameter	This work	In [3]	In[7]
Frequency	3.1-10.6	3-10	4-9.3
S_{21}(dB)	>8Db	6.1-7.8	7.1
S_{11}(dB)	< -10	<-9	< -10
S_{22}(dB)	<-10	< -10	< -10
S_{12}(dB)	<-25dB	<-30dB	<-18dB
NF (dB)	2-3	4-5	-
Power(mw)	10	7.2	-

REFERENCES

[1]. "Enabling high – speed wireless personal area networks", White Paper, Ultra wideband Technology, Intel Corporation , 2005, Printed in USA.

[2]. Micheal T. Rhea and John R. Long, " A 1.2 V Reactive feedback 3.1 to 10.6 GHz Low Noise Amplifier in 0.13µm CMOS" , IEEE Journal of Solid State Circuits, Vol. 42, No. 5, May 2007, pp1023-1033.

[3]. Yao Huang Kao and Chia Hung Hsieh, " Design of Low Noise Amplifier in Common-Gate Configuration for Ultra-Wideband Applications", IEEE proceedings of Asia-Pacific Microwave Conference, Dec 2007, pp 1-4.

[4]. Muhammad Khurram and S.M. Rezaul Hasan , " A 3-5 GHz Current- Reuse g_m – Boosted CG LNA for Ultrawideband in 130 nm CMOS", IEEE Transactions on Very Large Scale Integration (VLSI) Systems, Vol. 20, No. 3, March 2012, pp 400- 409.

[5]. Song Lin and Murat Eron, " Ultra Wideband High Gain GaN Power Amplifier", IEEE Radio and Wireless Symposium, January 2010, pp 10-14.
[6]. Y. Kamo, T. Kunii, H. Takeuchi, Y. Yamamoto, M. Totsuka, S. Miyakuni, T. Oku, T. Nanjo, H. Chiba, T. Oishi, Y. Abe, Y. Tsuyama, R. Shirahana, H. Ohtsuka, K. Iyomasa, K. Yamanaka, M. Hieda, M. Nakayama, H. Matsuoka, Y. Tarui, T. shikawa, T. Takagi, K. Marumoto and Y. Matsuda, "C-Band 140 W AlGaN/GaN HEMT with Cat-CVD Technique", 2005 IEEE MTT-S Int. Microwave Symp. Dig. WE1E-4, June 2005.
[7]. Jan VANCL, Vrastilov SOKOL, Petr CERNY, Zbynek SKVOR , " The UWB amplifier 3.1 -10.6 GHz ", IEEE 14th International Conference on Microwave Techniques, Prague, COMITE 2008, Aprill 2008, pp 1-4.
[8]. Aayush Aneja, M.Kumar, "Design of Ultra Wideband Amplifier Using Single Hetro Junction Bipolar Transistor For Wirelss Applications", IEEE 5th International Conference on Computational Intelligence and Communication Networks(CICN), Sep. 2013, pp 442-445.
[9]. David M. Pozar , " Microwave Engineering", Third Edition, John Wiley & Sons Publications, November 2011, 4th Edition, ISBN-13- 978-0-470-63155-3.

American Journal of Engineering Research (AJER)
e-ISSN : 2320-0847 p-ISSN : 2320-0936
Volume-03, Issue-03, pp-144-149
www.ajer.org

Research Paper Open Access

Eucalyptus Biodiesel; an Environmental friendly fuel for Compression Ignition Engines

N. S Senthur[1], T. S Ravikumar[2], Cijil. B. John[3]
[1,2,3](Hindustan Institute of Technology & Science, Chennai, Tamil Nadu, India)

Abstract: - Fossil fuels have always been the most important source of energy for the world. But in view of the energy crisis faced by the world today due to fossil fuel depletion, it is time for us to shift our attention to other renewable sources which could be used as fuel alternatives. This paper examines the suitability of Eucalyptus oil as a source of biodiesel, for use in Compression Ignition Engines. Biodiesel was produced from pure Eucalyptus oil by the process of Transesterification and the fuel properties were studied. In the next phase, a single cylinder direct injection diesel engine was used to test the blends of eucalyptus biodiesel with neat diesel fuel in various ratios (10%, 20% and 30% by volume). The various performance and emission characteristics of the engine for each of the fuel blends were analyzed for all operating conditions of the engine. Results showed that the use of biodiesel blends resulted in a significant reduction in the HC and CO emissions with a performance almost equivalent to diesel fuel at almost all loads. However, an increase in the NOx emissions was noticed while raising the biodiesel content in the fuel blend, which could be reduced by suitable engine optimisation techniques.

Keywords: - *Alternate fuels - biodiesel –eucalyptus oil - performance and emission –transesterification.*

I. INTRODUCTION

Depletion of fossil fuels, environmental concerns caused by increased emissions and the steep hike in the price of petroleum products have become one of the most serious problems faced by the world today. Fossil fuels have always been the main source of energy for the power production and transportation sectors of the world. The fact that the fossil fuel reserves are getting depleted day by day is leaving the world at stake. It is time for us to pay serious attention to finding other renewable fuel sources which could be used as alternative fuels to the conventional fuels – petrol and diesel.

An alternative fuel to petrol or diesel must be technically feasible, economically competitive, environmental friendly and abundantly available [1]. There are many sources of alternative fuels like Ethanol, Natural Gas, Hydrogen, HHO etc., but the most suitable alternative to conventional fuels – mainly diesel – is Biodiesel. Biodiesel refers to a vegetable oil or animal fat based diesel fuel consisting of long chain alkyl (methyl, ethyl, or propyl) esters [2]. Biodiesels are produced from vegetable oils by a process known as transesterification. Transesterification involves the reaction of the vegetable oil with an alcohol, in the presence of a catalyst, to form Esters and glycerol. These esters are referred to as biodiesels and they can be used in Compression Ignition engines either as a sole fuel (neat biodiesel) or by blending with petro-diesel in various proportions [3,4].

Numerous biodiesels, which are extracted from different vegetable oil sources, have been tried as alternative to diesel fuel for several years. Previous researches in this field showed that the use of biodiesels resulted in a performance comparable to diesel fuel with added benefit of lower emissions. Biodiesels are also expected to reduce the engine wear in diesel engines as they are found to have better lubrication properties than petro-diesel [5]. In the present work, Eucalyptus oil was selected as the source of biodiesel and the various

characteristics wereanalyzed. The eucalyptus tree is a non-edible species capable of growing in all climatic conditions. Eucalyptus oil was derived mainly from the leaves and barks of the tree and is available throughout the year [6].

Once the pure eucalyptus oil has been extracted, it was converted into biodiesel by the process of transesterification. The physico-chemical properties of the biodiesel thus obtained were analyzed and compared with those of petro-diesel to find its suitability for use in diesel engines. Eucalyptus biodiesel was then blended with petro-diesel mainly in three blend ratios E10, E20 E30 (10%, 20% and 30% by vol.). The engine tests were carried out on a single cylinder direct injection diesel engine at loads varying from zero (no load) to full load. The results of engine performance and emission characteristics were thus determined and discussed.

II. PREPARATION OF BIODIESEL AND ITS CHARACTERIZATION

Transesterification of vegetable oils is, so far, the best known and the most widely accepted method for the production of biodiesel. It is the chemical reaction between a triglyceride and an alcohol in the presence of a catalyst [7]. Even though several other techniques are available for biodiesel preparation, transesterification is the best method as the physical characteristics of the (m)ethyl esters produced closely resemble those of petro-diesel and the production process is relatively simple[8].

In the preparation of Eucalyptus biodiesel, ethyl transesterification was adopted. Ethanol was used as the alcohol in the preparation of eucalyptus biodiesel. Pure eucalyptus oil was taken in a reaction flask. The proportions were 500 ml pure eucalyptus oil, 100 ml ethanol and 5g NaOH pellets as the catalyst. The pellets of NaOH were dissolved in ethanol solution taken in a beaker. Once all the NaOH pellets were completely dissolved, the solution could be called Sodium Ethoxide solution. The solution thus obtained was then added to the pure eucalyptus oil in the beaker and it was heated and stirred thoroughly for about an hour at 55^{o}-65^{o}. The stirring process was characterized by a change in the color of the mixture from clear yellow to reddish yellow. The solution obtained was then poured in an inverted flask and allowed to settle down for nearly 24 hours. Then glycerol would be settle at the bottom of the flask as a dark brown colored liquid and ethyl esters (coarse biodiesel) would be formed at the top. The glycerol was removed and the coarse biodiesel was heated above 100^{0}C to remove any untreated ethanol. The NaOH impurities were removed by washing with water. The cleaned biodiesel thus obtained was the ethyl ester of Eucalyptus oil, simply known as Eucalyptus biodiesel.

The various physico-chemical properties of the obtained biodiesel were studied so as to find its suitability for use in diesel engines. The closeness in properties of the proposed biodiesel with petro-diesel shows that it could be used as an alternative with reasonable performance. Table 1 shows the various properties of the tested fuels.

Table 1. Properties of fuels

Property	Petro-diesel	Eucalyptus biodiesel
Calorific Value	43.2 MJ/Kg	42.5 MJ/Kg
Density (15^{0} C)	0.845	0.908
Viscosity (40^{0} C) cSt	1.57	1.85
Flash point (^{0}C)	56	32
Fire point (^{0}C)	65	42
Cetane Index	50	48

It is quite obvious from the table that eucalyptus biodiesel shows similarities in properties to petro-diesel and is hence evaluated to be a fuel alternative to diesel.

III. EXPERIMENTAL SETUP AND PROCEDURES

The performance and emission tests were performed on a constant speed, single cylinder, directinjection diesel engine. The detailed specifications of the engine used for the test are given below. All the performance and emission tests were conducted at a constant speed of 1500 rpm.

Table 2. Test engine specifications

Engine	Kirloskar TV1
Type	Single cylinder, Direct Injection, 4S
Bore * Stroke	87.5mm*110mm
Cubic Capacity	0.661 cc
Compression Ratio	17.5 :1
Rated power	3.5 kW @ 1500rpm
Injection Timing	23^{o} BTDC
Type of cooling	Water cooled

Figure 1 shows the experimental setup. The engine was coupled to a rheostat load bank with electrical loading. A DC generator with electrical load bank was used for loading purposes. The rheostat connected in series to the circuit controls the load on the engine by controlling the voltage. Carbon monoxide, Unburned Hydrocarbons and Nitrogen oxide emissions in the engine exhaust were measured by using a Crypton Five gas analyzer and the smoke density was measured using the AVL smoke meter.

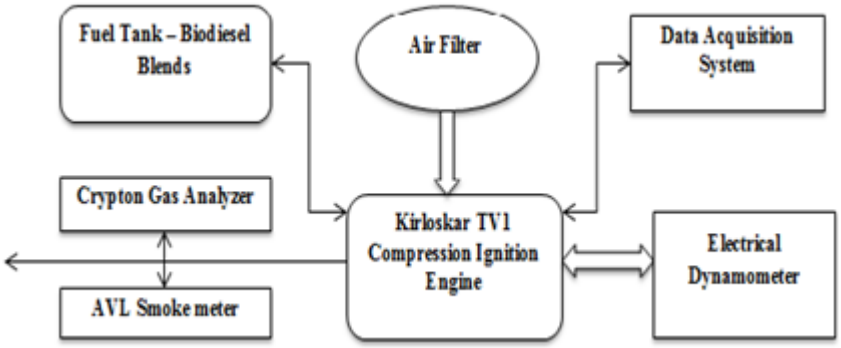

Figure 1. Experimental setup

The engine was started with neat diesel as fuel and was allowed to warm up for a few minutes. The performance and emission characteristics of the engine were noted using diesel as the reference fuel. The fuel was then switched to E10 [10% biodiesel + 90% diesel] and the characteristics were noted. The same procedure was repeated for the other blends [E20, E30] also. Once the tests were completed and all the required readings were taken, the engine was again switched to pure diesel fuel so as to avoid any future startup problems. The various performance and emission characteristics were obtained in this procedure.

IV. RESULTS AND DISCUSSIONS

The experiments were conducted at an injection pressure of 200 bar, compression ratio 17.5:1 and a standard injection timing 23^{o} BTDC.

Performance Characteristics

Brake thermal Efficiency (BTE) indicates the efficiency of the engine to convert the chemical energy of the fuel into useful output power. The variation in BTE with respect to power output at various loads for diesel and

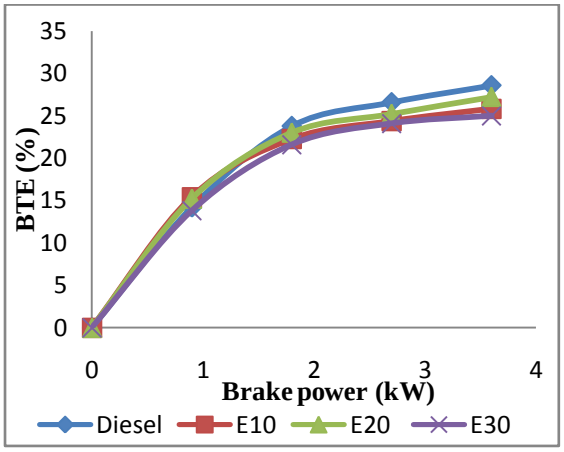

Figure 2. Variation of BTE with power output

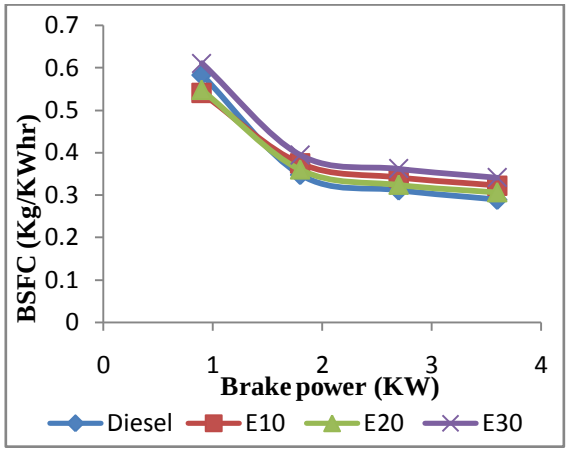

Figure 3. Variation of BSFC with power output

biodiesel blends is shown in the figure 2. It can be seen that the BTE increases with an increase in the load on the engine, as a result of the increase in the brake power. The highest BTE was recorded for petrodiesel (28.5%) at the rated power output. E20 fuel blend resulted in a reduction in the maximum BTE by a marginal 4.8%. It can be seen that the BTE of biodiesel blends is lower than that of diesel. Also, as the biodiesel content in the blend increases, the BTE decreases. This may be due to the lower heating values leading to a slower burning process when compared to diesel.

The fuel consumption characteristics of the engine are represented by the term Brake Specific Fuel Consumption (BSFC). BSFC is defined as the ratio of the total fuel consumption of the engine to the brake power produced by the engine. Figure 2 represents the variation of BSFC for diesel and the various biodiesel blends at different power outputs and loads on the engine. Similar to BTE, BSFC also depends mainly on the calorific value and viscosity of the fuel blend. BSFC of the engine is also inversely proportional to the BTE. Since the BTE is highest for diesel fuel, the lowest BSFC is also recorded by diesel fuel when compared to biodiesel blends. The reason for the increase in fuel consumption of biodiesel blends is that when the biodiesel content in the blend increases, the overall heating value of the blend reduces. Therefore, increased fuel consumption is required to maintain the same speed and power output of the engine. BSFC decreases as the power output of the engine increases.

EMISSION CHARACTERISTICS

Carbon monoxide (CO) is an important emission occurring in an engine. CO emissions take place due to the incomplete combustion of the fuel, mainly due to lack of oxygen atoms for effective combustion to occur. Another reason for CO emissions is the lack of time for effective combustion to occur. The variation in CO emission for diesel, neat biodiesel and the various blends at various loads of the engine are shown in figure 4. It can be seen that there is a significant reduction in the CO emissions while using biodiesel blends when compared to petrodiesel. The reason for the reduced CO emissions is the more effective and complete combustion taking place due to the increased number of oxygen atoms in the biodiesel. The availability of sufficient oxygen atoms causes most of the CO to be oxidized and converted to CO_2 but the complete conversion of CO to CO_2 is never possible.

Hydrocarbons (HC) are another prominent parameter in the emission characteristics of a diesel engine. Similar to CO emissions, HC emission also occurs when the fuel molecules fail to burn completely inside the engine. The variations in HC emission for diesel fuel, neat biodiesel, and the various blends at varying loads on the engine are shown in figure 5. The figure shows that the HC emissions of biodiesel blends are much lower than those of diesel fuel. It can also be seen that the lowest HC emissions were recorded by E30 blend. As the biodiesel content in the fuel blend increases, the HC emissions decrease. The reduction in HC emissions while using biodiesel as the fuel can be attributed to the efficient and more complete combustion taking place due to the presence of greater number of oxygen atoms in the biodiesel fuel blends. It was found from the investigation that the use of E30 fuel blend resulted in a reduction of HC emission by about 32.5% while the use of E20 blend

resulted in a reduction of nearly 25% when compared to petroleum diesel.

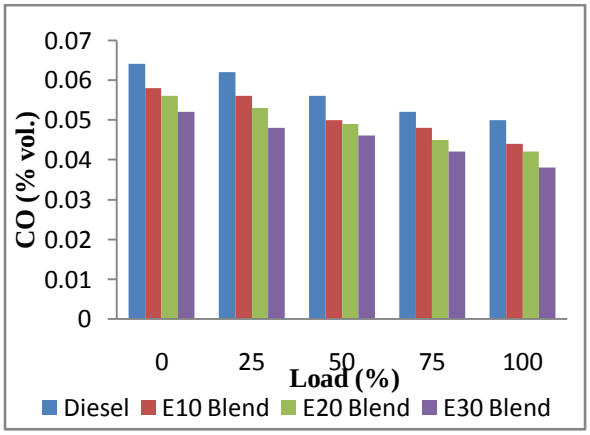

Figure 4. CO emissions at various engine loads

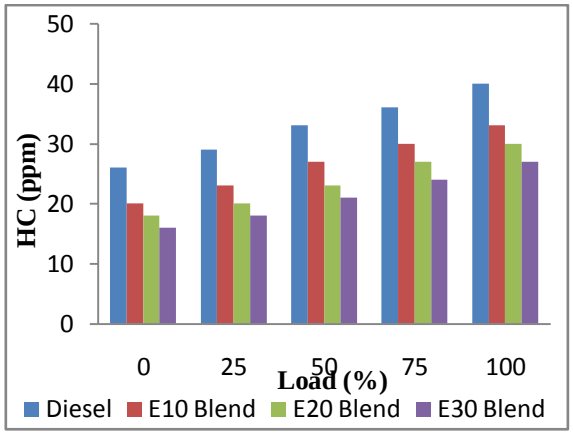

Figure 5. HC emissions at various engine loads

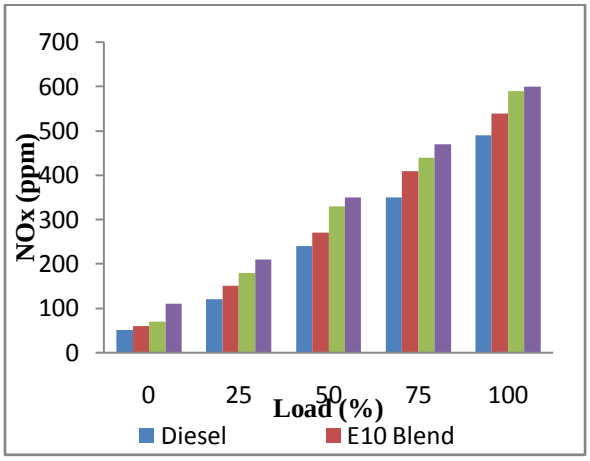

Figure 6.NOx emissions at various engine loads

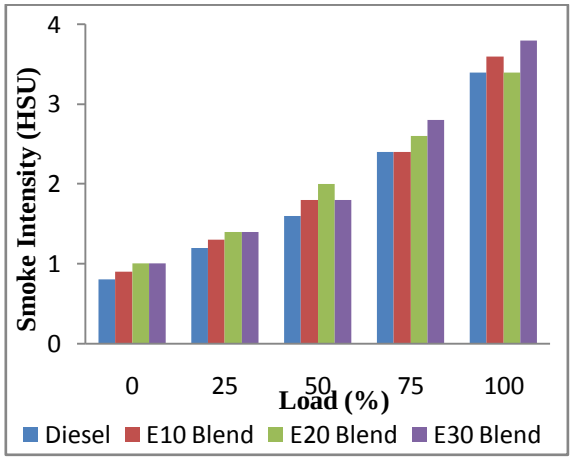

Figure 7 Smoke intensity at various engine loads

The variations of NOx emissions for diesel and biodiesel blends for various engine loads are shown in the figure 6. NOx emission from an engine increases with increase in power output of the engine. The NOx emission from an engine depends upon the maximum combustion temperature and the availability of oxygen. When the combustion temperature inside the engine exceeds a particular limit, atomic nitrogen combines with free oxygen to form oxides of nitrogen (NOx). Since the combustion temperature is higher and the oxygen concentration is greater for biodiesel, it can be seen that the NOx emissions of biodiesel and its blends are higher than those of diesel at all loads on the engine.

Smoke, defined as the visible products of combustion, is due to the poor combustion of the fuel in the engine. The three main operating conditions under which smoke is heavily produced in an engine are acceleration, overloading and during full load operation of the engine. Under these conditions more fuel is burned in the engine and the combustion chamber temperatures become very high. As a result of this extremely high temperature, the fuel molecules undergo thermal cracking leading to soot formation. Figure 7 shows the smoke intensity of the tested diesel and biodiesel fuel blends with respect to various loads on the engine. It can be seen that E30 fuel blend recorded the highest smoke intensity when compared to diesel while E20 fuel blend recorded almost the same smoke intensity as that of diesel fuel, especially at high engine loads. The smokeintensity at lower engine loads is almost the same for diesel and biodiesel blends. The increase in smoke intensity of E30 fuel blend at higher engine loads may be because of the higher viscosity of the fuel blend resulting in a poor atomization, thereby leading to increased smoke production.

V. CONCLUSION

This research aims at determining the suitability of Eucalyptus biodiesel as an alternative fuel for use in Compression Ignition Engines. In this experimental analysis, biodiesel was produced from pure eucalyptus oil by the process of transesterification. The prepared biodiesel was then blended with petrodiesel in three proportions (10%, 20% and 30% by vol.) and then tested in a single cylinder direct injection diesel engine to obtain the performance and emission characteristics. The similarities of various physico–chemical properties of eucalyptus biodiesel with diesel show its suitability for use as an alternative fuel. Following are the main conclusions drawn from this experimental investigation.

- The BSFC increases with increase of biodiesel content in the fuel blend due to decrease in calorific value of the blend.
- The BTE of biodiesel blends are found to be slightly lower than that of diesel at all loads and power outputs of the engine mainly due to the reduced heating value of the blend.
- A significant reduction in the HC and CO emissions was noted whereas NO_x emissions and Smoke intensity recorded an increase while using biodiesel blends as the fuel.

In general, Eucalyptus biodiesel in lower blend ratios was found to be good alternative to be used in direct injection diesel engines. E20 (20% biodiesel + 80% diesel) could be used as a very good alternative fuel with optimum engine performance and reduced emissions.

VI. ACKNOWLEDGEMENTS

The authors would like to thank the Sophisticated and Analytical Instrument Facility (SAIF) at IITM and ITA Lab Private Limited, Chennai, for their valuable assistance in the testing of the fuel properties.

REFERENCES

[1] Ayhan Demirbas, Progress and recent trends in biodiesel fuels, *Energy Conversion and Management*, 50 (2009), 14-34.

[2] S.P. Singh, Dipti Singh, Biodiesel production through the use of different sources and characterization of oils and their esters as the substitute of diesel: A review, *Renewable and Sustainable Energy Reviews*, 14 (2010), 200-216.

[3] Amar Pandhare, Atul Padalkar, Investigations on Performance and Emission Characteristics of Diesel Engine with Biodiesel (Jatropha Oil) and Its Blends, *Hindawi Publishing Corporation - Journal of Renewable Energy*, Research Article, 2013, 1-11.

[4] A.S Ramadhas, S. Jayaraj, C. Muraleedharan, Use of vegetable oils as I.C Engine fuels – a review, *Journal of Renewable Energy*, 29(5), 2004, 727-742.

[5] M. Prabhahar, R. Murali Manohar, S. Sendilvelan, Performance and emission characteristics of a diesel engine with various injection pressures using biodiesel,*Indian Journal of Science and Technology*, 5(6), 2012, 2880-2884.

[6] Lyes Tarabet, Khaled Loubar, Mohand Said Lounici, Samir Hanchi, Mohand Tazerout, Eucalyptus Biodiesel as an Alternative to Diesel Fuel: Preparation and Tests on DI Diesel Engine, *Hindawi Publishing Corporation - Journal of Biomedicine and Biotechnology*, Research Article,2012, 1-8.

[7] Pradeep Kumar A.R, Annamalai. K, Premkartikkumar. SR, Experimental Investigation on Emission parameters of Transesterified Adelfa oil (Methyl ester of Nerium Oil), *International Journal of ChemTech Research*, 5(4), 2013, 1664-1670.

[8] A.S Ramadhas, S. Jayaraj, C. Muraleedharan, Biodiesel production from high FFA rubber seed oil, *Fuels*, 84 (2005), 335-340.

American Journal of Engineering Research (AJER)
e-ISSN : 2320-0847 p-ISSN : 2320-0936
Volume-03, Issue-03, pp-150-154
www.ajer.org

Research Paper Open Access

Comparative study of Self Compacting Concrete mixes containing Fly Ash and Rice Husk Ash

B.H.V. Pai[1], M. Nandy[2], A. Krishnamoorthy[3], P.K.Sarkar[4], Philip George[5]
[1]*AssociateProfessor, Dept. of Civil Engg.,Manipal Institute of Technology, Manipal, India*
[2]*Professor, Chemical Sciences Division, Saha Institute of Nuclear Physics, Kolkata, India*
[3]*Professor, Dept. of Civil Engg.,Manipal Institute of Technology, Manipal, India*
[4]*Distinguished Fellow, Manipal Centre for Natural Sciences, Manipal, India*
[5]*P.G.Student, Dept. of Civil Engg.,Manipal Institute of Technology, Manipal, India*

Abstract: **-** Self-compacting concrete (SCC) is a type of concrete that can flow under its own weight and completely fill the form work, without vibration effect, and at the same time cohesive enough to be handled without bleeding. It ensures proper filling and good structural performances of restricted areas and heavily reinforced structural members. SCC usually requires a large content of binder and chemical admixtures. This work outlines the preliminary results of a research project aimed at producing and comparing SCCs incorporating Fly ash (FA) and Rice husk ash (RHA)as supplementary cementing materials in terms of their properties like compressive strength, split tensile strength and flexural strength.

Keywords: *-Self-compacting concrete, Fly ash, Rice husk ash,Compressive strength, Flexural strength, Split tensile strength.*

I. INTRODUCTION

Self-Compacting Concrete (SCC) was developed in Japan during the later part of the 1980's to be mainly used for highly congested reinforced structures in seismic regions. Recently, this concrete has gained wide use in many countries for different applications and structural configurations. The use of SCC has many advantages, such as: reducing the construction time and labor cost, eliminating the need for vibration, reducing the noise pollution, and also improving the filling capacity of highly congested structural members.

SCC consists of the same components as conventionally vibrated concrete, which are cement, aggregates and water, with the addition of chemical and mineral admixtures in different proportions .The first point to be considered when designing SCC is to restrict the volume of the coarse aggregate so as to avoid the possibility of blockage on passing through spaces between steel bars. This reduction necessitates the use of a higher volume of cement which increases the cost besides resulting in temperature rise. So cement should be replaced by high volume of mineral admixture like fly ash or rice husk ash.

Fly ash (FA) is a beneficial mineral admixture for concrete. Research shows that adding FA to normal concrete, as a partial replacement of cement (less than 35 %), will benefit both the fresh and hardened states. In the fresh state, the fly ash improves workability. This is due to the smooth, spherical shape of the fly ash particle. The tiny spheres act as a form of ball bearing that aids the flow of the concrete. In the hardened state, fly ash contributes in a number of ways, including strength and durability [1, 2].

Rice husk ash (RHA)has been used as a highly reactive pozzolanic material to improve the microstructure of the interfacial transition zone between the cement paste and the aggregate in SCC. Research shows that the utilization of rice husk ash in SCC mix produced desired results, reduced cost, and also provided an environment friendly disposal of the otherwise agro-industry waste product [3, 4].

For concrete to be self-compacting it should have filling ability, passing ability and resistance against segregation. Self-compactability is obtained by limiting the coarse aggregate content and using lower water–powder ratio together with the addition of super plasticizers.

II. EXPERIMENTAL PROGRAMME

2.1.Materials:

2.1.1 Cement:

All types of cement complying with Indian standards are suitable for SCC. The cement used in this experiment is the 43 grade Ordinary Portland Cement [5].

Table 1: Test results on cement

Test		Test Results
Normal consistency		30%
Specific gravity		3.15
28-days Compressive Strength (MPa)		45.79
Setting Time(minutes)	Initial	62
	Final	190

2.1.2 Fly ash (FA): FA is a by-product obtained from burning pulverized coal in electric power generating plants. The FA used in the present work had a specific gravity of 2.23, and a normal consistency of 45%.

2.1.3 Rice husk ash (RHA): RHA is produced by incinerating the husk of rice paddy. Rice husk is a by-product of rice milling industry. The RHA used in the present work had a specific gravity of2.13, and a normal consistency is 26%.

2.1.4 Aggregates: The fine aggregate(sand) can be finer than normal, as the material <150micron may help increase cohesion, there by resisting segregation. River sand was used as fine aggregate, and crushed stone with a maximum size of 12mm was used as coarse aggregate [6]. Table 2 shows the test results on aggregates.

Table 2: Test results on aggregates

Test	Test Results	
	Coarse Aggregate	Fine Aggregate
Bulk Density (kg/m^3)	1404	1500
Specific gravity	2.65	2.64

2.1.5 Super plasticizer (SP): This is a chemical compound used to increase the workability of the mix without adding more water.The super plasticizer used in this work is Cera Hyper plasticizer HRW 40.

2.1.6 Water: Potable water was used for mixing and curing.

2.2 The Mix Proportioning:

The process of mixture proportioning is one of the important tasks in achieving SCC properties. So far a mix design procedure to get the proportion of the ingredients in the SCC is not standardized. No method specifies the grade of concrete in SCC, except the Nan Su et al. method [7]. In this work, mix designing was carried out for M25 grade concrete, and the procedure is based on the method proposed by Nan Su et al. This method was preferred as it has the advantage of considering the strength of the SCC mix. Unlike other proportioning methods like the Okamura and EFNARC methods, it gives an indication of the target strength that will be obtained after 28days of curing. The water to powder ratio was varied so as to obtain SCC mixes of various strengths. The principal consideration of the proposed method is to fill the paste of binders into voids of the coarse aggregate piled loosely. The strength of SCC is provided by the aggregate binding by the paste at hardened state, while the workability aspect of SCC is provided by the binding paste at fresh state. Therefore, the amount of coarse and fine aggregates, binders, mixing water and SP will be the main factors influencing the properties of SCC[8]. The quantities of the SCC ingredients obtained are listed in Table 3.

Table 3.Quantities of SCC ingredientsin kg/m^3

Mix	Cement	FA	RHA	Coarse aggregate	Fine aggregate	Water	SP
FA based SCC	200	301.4	-	743	961	216.2	9
RHA based SCC	200	-	331.3	743	961	166.4	9.6

2.3 Tests conducted:

2.3.1 Fresh concrete tests: Once a satisfactory mix is arrived at, it is tested in the lab for properties like flowing ability, passing ability and blockage using Slump cone, L-Box, U-Box and V-funnel apparatus.The slump flow test is used to assess the horizontal free flow of SCC in the absence of obstructions, anditindicatesthe resistance to segregation, and filling ability of concrete. On lifting the slump cone filled with concrete the average diameter of spread of the concrete is measured. Also T50 time is taken in seconds from the instant the cone is lifted to the instant when the horizontal diameter of the flowreaches 500mm.

The flow ability of the fresh concrete can be tested with the V-funnel test, whereby the flow time is measured. The funnel is filled with about 12 liters of concrete and the time taken for it to flow through the apparatus is measured. Shorter flow time indicates greater flow ability.

L-box test assesses filling and passing ability of SCC, and serious lack of stability (segregation) can be detected visually. The vertical section of the L- Box is filled with concrete, and then the gate is lifted to let the concrete flow into the horizontal section. Blocking ratio, i.e. ratio of the height of the concrete at the end of the horizontal section (H_2) to height of concrete at beginning of horizontal section (H_1) is determined.

U-box test is used to measure the filling and passing ability of SCC. The apparatus consists of a U shape vessel that is divided by a middle wall into two compartments. The U-box test indicates the degree of compactability in terms of filling height i.e. H_1-H_2, the difference of height of concrete attained in the two compartments of U-box.

The mixes are checked for the SCC Acceptance Criteria laid down by the European Federation of Specialist Construction Chemicals and Concrete Systems (EFNARC) [9] listed in Table 4.

2.3.2 Hardened Concrete Tests:The tests on hardened concrete include compressive strength (cube size: 150mm side), split tensile strength (cylinder size: length 300mm and diameter 150mm), and flexural strength (prism size: 100x100x500mm) eachfor 7 days, 14 days and 28 daysofcuring [10] [11].

III. RESULTS AND DISCUSSIONS

3.1 Fresh concrete test results:

The results of slump flow, L-Box, U-Box, V-funnel tests are given in Table 4

Table 4. Test results of fresh SCC mixes

Test	Unit	Range(as per EFNARC)	Test Results		Remarks
			FA based SCC	RHA based SCC	
Slump flow	mm	650-800	740	710	Acceptable
T50 slump flow	sec	2-5	4	2.5	Acceptable
L- box (H_2/H_1)	-	0.8-1.0	0.9	0.86	Acceptable
U- box (H_1- H_2)	mm	0-30	25	21	Acceptable
V- funnel	sec	6-12	11	9	Acceptable

Both the fresh SCC mixes were tested for filling ability (slump flow by Abrams cone, and V- Funnel) and passing ability (L-box, U-box). All the test results satisfied the acceptance criteria for rheological properties of SCC as laid down by EFNARC, as seen from Table 4.

3.2 Hardened concrete test results:

Table 6: Tests results on Hardened SCC specimens

Strength (in MPa)		FA based SCC	RHA based SCC
Compressive strength	7 days	13.69	11.28
	14 days	19.55	12.95
	28 days	21.80	14.10
Split tensile Strength	7 days	0.85	0.74
	14 days	1.14	0.89
	28 days	1.29	1.14
Flexural Strength	7 days	2.54	2.27
	14 days	3.66	3.25
	28 days	4.84	3.77

The hardened properties like compressive strength, split tensile strength and flexural strength were checked and found that not all the test results were satisfactory. Fig. 1 through Fig. 3 show the graphical representation of the strengths against the age at loading for the different mixes. The low strength of RHA based

SCC maypossiblybe due to the high amount of RHA (62.35%), and the low strength of FA based SCC may possibly be due to the high amount of FA (60.11%) in the mixes.

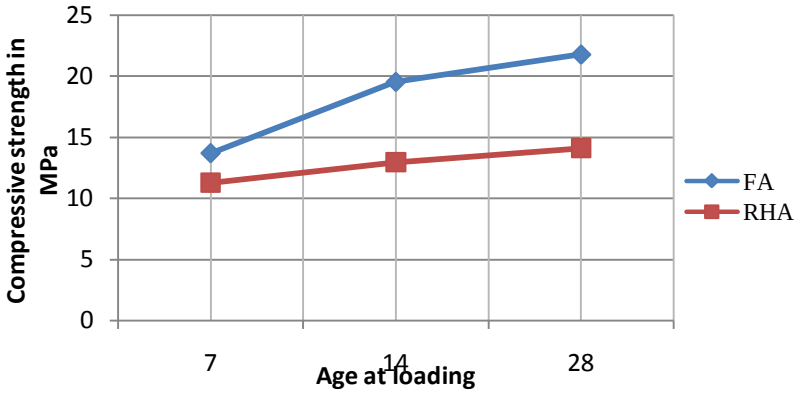

Fig 1. The variation in Compressive Strength with Age at loading

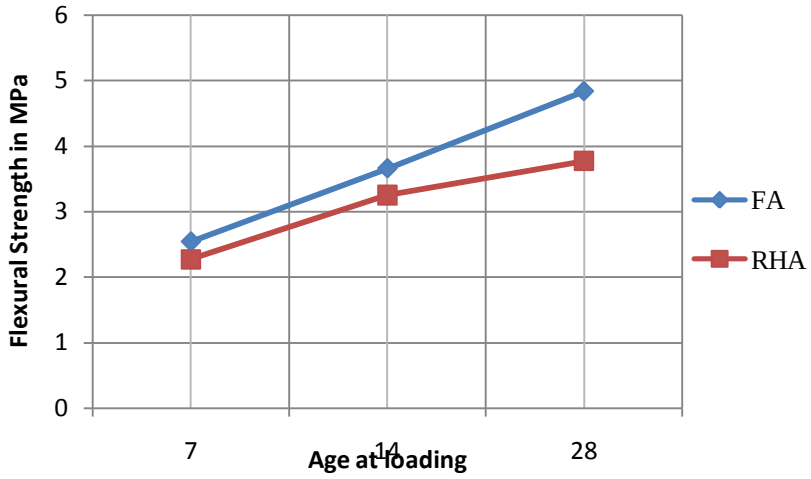

Fig 2. Variation in Flexural Strength with Age of loading

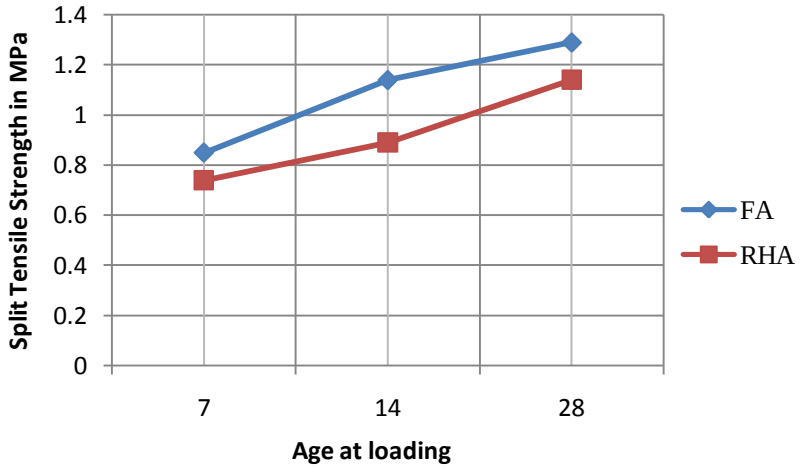

Fig 3. Variation in Split Tensile Strength with Age of loading

IV. CONCLUSIONS

The SCC mixes containing fly ash, and that containing rice husk ash as filler materials were tested for their fresh properties as per EFNARC guidelines. Both SCC mixes have satisfied all the acceptance criteria laid down by EFNARC.

The hardened properties like compressive strength, split tensile strength and flexural strength were checked and found that not all the test results were satisfactory. But acomparative study of the test results

shows that SCC containing FA has better compressive strength, split tensile strength and flexural strength than SCC containing RHA.

Past research has shown that the optimum level of cement replacement with RHA for normal concrete is30% [12]. The low strength of rice husk ash based SCC may be due to the high amount of rice husk ash (62.35% of total powder). Also, the optimum level of cement replacement with fly ash for normal concrete is 35% [2].The low strength of fly ash based SCC is possibly due to the high amount of fly ash (60.11% of total powder).

It isalsoobserved from the results that the calculated cement content (200kg/m^3) as per the Nan Su et al. method was not adequate to give the required strength to the mix. The quantity of cement content calculated was possibly not sufficient to bind all the ingredients in the mix. As a consequence, more trials with higher percentage of cement are required to attain the target strength.

V. ACKNOWLEDGEMENT

The equipment used in this work are fabricated using the funds received from the Board of Research in Nuclear Sciences (BRNS), Department of Atomic Energy, Government of India. The authors wish to gratefully acknowledge the help and support of the BRNS authorities in carrying out this work.

REFERENCES

[1]. N. Bouzoubaa, M. Lachemi, Self Compacting Concrete Incorporating High-Volumes of Class F Fly Ash: Preliminary Results, *Cement and Concrete Research, 31(3),* 2001, 413-420.
[2]. N. R. Gaywala, D. B Raijiwala, Self compacting Concrete: A concrete of next decade, *Journal of Engineering Research and Studies, 2(4),* 2011, 213-218.
[3]. A. Juma, E. Rama Sai, et al.,A Review on Experimental Behavior of Self Compaction Concrete Incorporated with Rice Husk Ash,*InternationalJournal of Science and Advanced Technology, 2(3*), 2012,75-80.
[4]. Safiuddin, J. S. West, K. A. Soudki, Hardened properties of self-consolidating high performance concrete including rice husk ash, *Cement and Concrete Composites, 32(9),* 2010,708-717.
[5]. IS: 8112- 1989.Specifications for 43 grade ordinary Portland cement. New Delhi, India: Bureau of Indian Standards.
[6]. IS: 383-1970. Specifications for coarse and fine aggregates from natural sources for concrete.New Delhi, India: Bureau of Indian Standards.
[7]. Nan Su, Kung-Chung Hsu, His-Wen Chai, A simple mix design method for self compacting concrete, *Cement and Concrete Research, 31,* 2001, 1799-1807.
[8]. Vilas V. Karjinni, B. A. Shrishail, Mixture proportion procedure for SCC, *Indian Concrete Journal, 83(6),* 2009, 35-41.
[9]. EFNARC, Specification and guidelines for Self Compacting Concrete,2002, website: *http://www.efnarc.org*
[10]. IS: 516-1959. Methods of tests for strength of concrete. New Delhi, India: Bureau of Indian Standards.
[11]. IS: 5816-1970. Methods of tests for splitting tensile strength of concrete cylinders. New Delhi, India: Bureau of Indian Standards.
[12]. K. Ganesan, K. Rajagopal, K. Thangavel, Rice husk ash blended cement: Assessment of optimum level of replacement for strength and permeability properties of concrete, *Construction and Building Materials, 22(8),* 2008, 1675-1683.

American Journal of Engineering Research (AJER)
e-ISSN : 2320-0847 p-ISSN : 2320-0936
Volume-03, Issue-03, pp-155-167
www.ajer.org

Research Paper Open Access

Development of the model of optimized parameters of quality of the raw water

Dragolav Ilic PH.D.[1], Slobodan Stefanovic Ph.D.[2], Nenad Janjic Mr[3], Damjan Stanojevic Msc.[4]

[1]*Public Utility Company "Water", Zajecar, Serbia*
[2,3,4] *Higher School of Applied Professional Studies, Vranje, Serbia*

Abstract: - The models can be mathematically relatively simple to analyze, but to be applicable and successful in the future, it is necessary to continuously update the input data, must be of good quality and it will reflect the change in raw water quality over time.

Keyword : *– drinking water, model, environmental aspects, optimization.*

I. INTRODUCTION

Water shortage affects many communities in the world and prevents their current and future development. Problems with water are increasingly associated with social, economic, environmental, legal and political issues at different levels of government, and often have an international dimension (Biswas, 2008). Re-use of water is one of the key elements to increase the availability of water, and to preserve the sustainable use of water resources (Figure 1.).

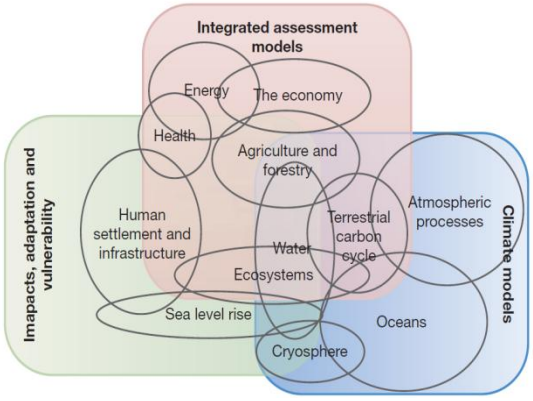

Source: Richard H. Moss, et al., The next generation of scenarios for climate change research and assessment, Nature, 2010

Figure 1. The next scenario for climate change research and assessment resources

The United Nations (UN) in 1977. organized the Conference about Water in Mar del Plata, Argentina, considered a turning point in the approach to water management (eg, Lee, 1992). The conference is a recognized global problem - the existing water management policies have been unsuccessful in achieving the goals of management (Heathcote, 1998).
Table 1., defines seven sustainability criteria for the planning of water.

Table 1. Sustainability criteria for water planning

Criteria	Characteristics
Criterion 1. Basic human needs for water	A basic water requirement will be guaranteed to all humans to maintain human health.
Criterion 2. Basic needs for water	A basic water requirement will be guaranteed to restore and maintain the health of ecosystems.
*Criterion 3.*Water quality standards	Water quality will be maintained to meet certain minimum standards. These standards will vary depending on location and how the water is to be used.
*Criterion 4.*Renewable water resources	Human actions will not impair the long-term renewability of freshwater stocks and flows.
*Criterion 5.*Data collection and availability	Data on water resources availability, use, and quality will be collected and made accessible to all parties.
*Criteria6 and 7.*Institutions, management and conflict resolution	Institutional mechanisms will be set up to prevent and resolve conflicts over water.
	Water planning and decision making will be democratic, ensuring representation of all affected parties and fostering direct participation of affected interests.

Source: Gleick, P.: *Water in crisis: Paths to sustainable water use*, Ecological Applications, 8(3), 1998, pp. 571–579

The World Summit on Sustainable Development in Johannesburg in 2002, countries have been invited "to develop a management strategy and efficient development and utilization of water resources by 2005 and to assist the developing countries" (Knezevic, B., 2005).
Developed an approach of integrated water resources management, which includes the management and development of water resources in a balanced and sustainable manner, taking into account social, economic and environmental factors and interests.
The idea of the concept of IWRM has been to every country, if it is to establish and achieve their national goals of sustainable development must ensure investment in water infrastructure (water intakes, transport pipelines, irrigation systems, hydroelectric plants, reservoirs, etc.). This approach involves integrated management of surface and groundwater, as well as the quantitative and qualitative characteristics of water resources.
In the developed countries of the EU (eg. France, Spain) was needed over 50 years to establish the current level of water management that is in line with the principles of integrated water resources management and the Water Framework Directive (Hassing and others, 2009).
In underdeveloped and developing countries, this process is much slower place (the result of many factors which slow down the reforms and the establishment of IWRM). Table 2 provides an overview of the developing countries that have adopted the IWRM concept.

Table 2. The records of the adoption and use of IWRM concept

Country	Documents
Angola	• the concept of IWRM and water efficiency roadmap - Ministry of Water and Energy (draft 2007)
Argentina	• IWRM Roadmap - Subsecretariat of Water Resources (2007)
Brazil	• National Water Policy (Law No. 9433) - The Government of Brazil (1997) • National Plan for Water Resources - Ministry of Environment (Ministry of Environment , SRH / MMA) , the National Water Council (National Water Council , CNRH) and the National Water Agency (National Water Agency , ANA) (2007)
Egypt	• National Plan for Water Resources - Ministry of Water Resources and Irrigation (2004)

Indonesia	• National Water Act 7/2004 - The Government of Indonesia (2004) • IWRM plan - Directorate General of Water Resources Ministry of Public Works (2006)
Jordan	• National Water Policy - Ministry of Water and Irrigation • National Strategy for Water - Ministry of Water and Irrigation (2003) • National Master Plan - Ministry of Water and Irrigation (2004)
China	• National Water Act - (2002) • Law on Prevention and Control of Water Pollution - (1996) • Act on the national flood control - (1997) • National legislation on water and soil conservation (1991) • IWRM plan - The planning process began in 2002 and is still ongoing.
Colombia	• National Development Plan 2006-10 - Department of National Planning (2006)
Serbia	• National Water Policy • National Water Act - Ministry of Agriculture, Forestry and Water Management (1991) • Environmental Protection Act - Ministry of Agriculture, Forestry and Water Management (2004) - WATER Master Plan - Ministry of Agriculture, Forestry and Water Management (2002)
Syria	• National Water Policy - The Government of Syria • National Water Act (No. 31) - The government of Syria (2005) • IWRM and Water Management Plan effectiveness - partially implemented
Honduras	• IWRM Action Plan - Water Platform of Honduras (2006)
Croatia	• Water Act (OG 107/95, 150/05) - The Ministry of Agriculture, Forestry and Water Management • Law on Financing Water (Fig. 107/95, 19/96, 88/98, 150/05) - The Ministry of Agriculture, Forestry and Water Management • National Environmental Strategy to National Action Plan (NEAP) (OG 46/02) - The Ministry of Agriculture, Forestry and Water Management • the concept of IWRM and Water Efficiency Plan

Source: Report of UN-Water, Status Report on Integrated Water Resources Management and Water Efficiency Plans, Prepared for the 16th session of the Commission on Sustainable Development - May 2008.

II. INTEGRATED WATER RESOURCES MANAGEMENT

The aim of the introduction of integrated management of water resources, to achieve the economic benefits and social gains from the use of water resources. [1]

Integrated water resources management can be considered in terms of two basic categories (GWP, 2004):

• natural structure - determined by the availability and quality of water

• social composition, ie. human factor - determine the use of water resources, production of waste water and pollution of water resources.

In addition to the integration over the general sector policy, IWRM requires integration among sub-sectors - the "needs" of water management such as water supply, quality, environmental protection, water control, irrigation,

[1]Integrated water resources management is achieved by:
Economic efficiency, equity in the available water (access to sufficient quantities of good quality water is a fundamental human right that must be universally recognized) and environmental sustainability (use of water resources must be done in a manner that does not jeopardize their use by future generations).

flood control, navigation, hydropower, and recreation (Figure 2. shows this correlation).

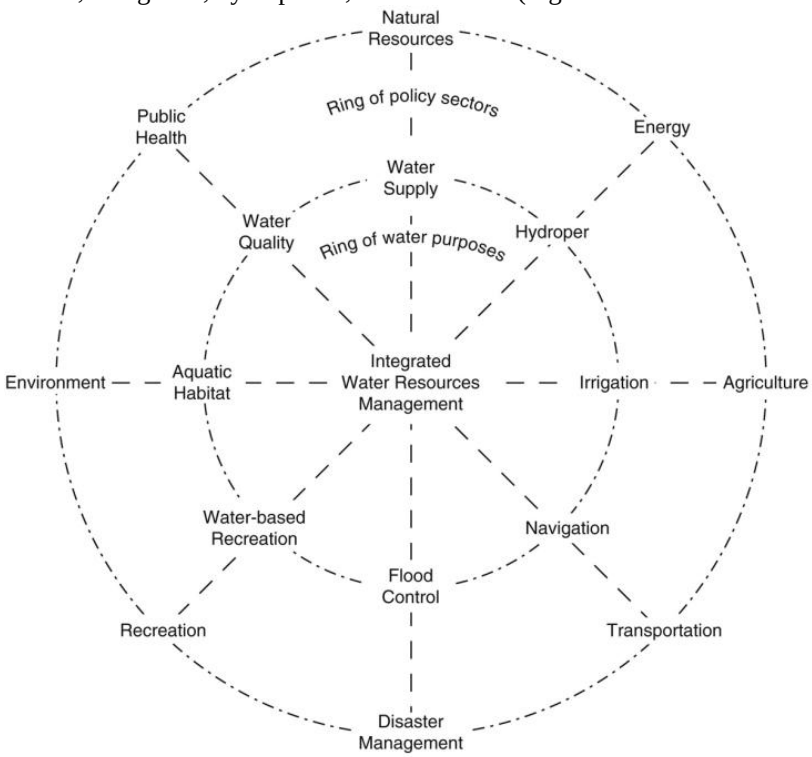

Figure 2. Integrated water management by sector

Source: Grigg, N. S.; *Integrated water resources management: balancing views and improving practice*, Water International,Vol. 33, No. 3, September 2008, pp. 284.

When integrated water resources management is crucial management of the entire space (not just water) as the hydrological cycle, ie. movement of water depends on the composition of the water - land - air - vegetation. Management of water resources is mainly oriented so. "Blue water". The drainage area to manage all water resources, including water used by vegetation so. "Green water" ("get lost" in the process of evaporation and transpiration).

To supply systems to meet the consumer must gradually change their priorities: instead of expanding and opening new sources, it is necessary to reduce losses in the network (internal reserves) and the irrational use of water by consumers. In this way, increasing the economic efficiency of water supply (Prodanovic, 2003). The concept of water changes from water supply system that meets the consumer (demand driven consumption) the system begins to operate water consumption (demand managed consumption).

In the process of implementation of EU directives on water management in Serbia must be made in the reorganization of the water sector through changes in the management of water resources:[2]

• Integration of social interests, public and private organizations in the field of production, protection and regulation of water requires a new organization of water management.

Coordinates the activities of various institutions to the achievement of the aims of sustainable water management. It is necessary to establish institutional mechanisms to ensure integration and cooperation between different water users, stakeholders and the public.

- *• Access management at the river basin (catchment area) must be installed in the water legislation.*

[2]Basic principles of reorganization and institutional strengthening are: organization of water management at the river basin (catchment area), legislative support, the provision of financial resources, exchange of information on water quality and quantity. Access control at the level of the river basin (catchment area) must be installed in the water legislation (the basis for the organization of water management, planning, management and decision-making, integration and coordination of activities, funding, implementation of management decisions, licensing, inspection activities, enforcement of penal provisions and other activities) . Muskatirovic, J.: Implementation of the policy of integrated management of water resources in Serbia, Institute for Water Resources "Jaroslav Cherni", Belgrade, http://www.jcerni.co.yu/srpski/projekti/mon4.pdf.

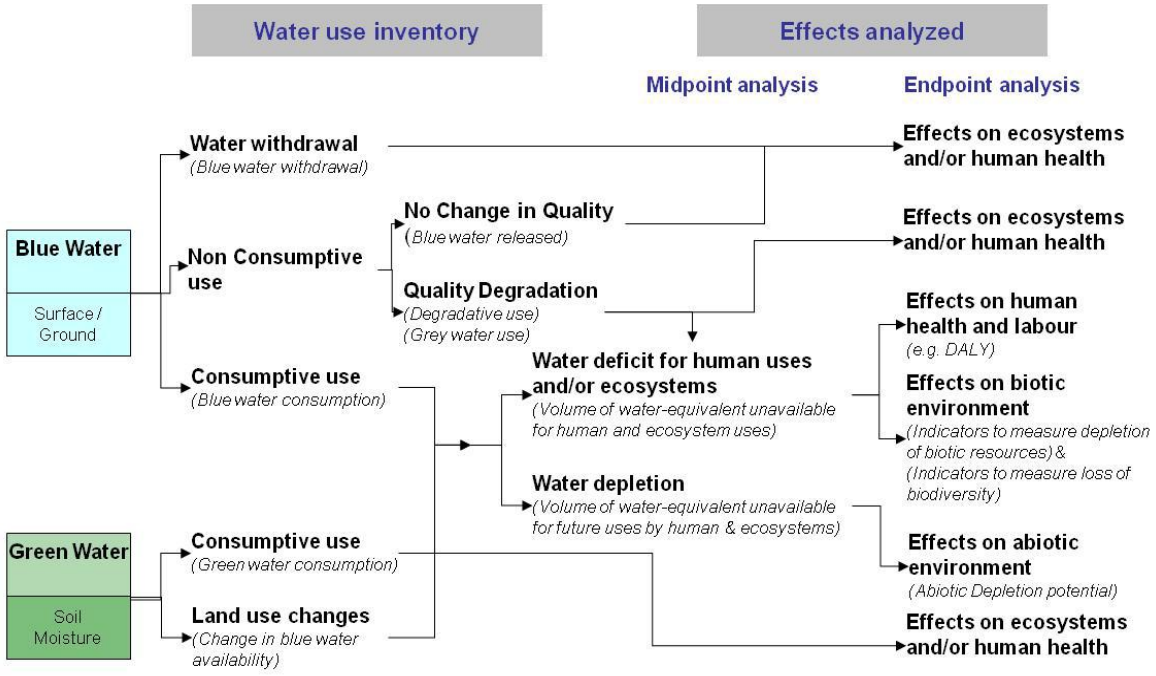

Figure 3. Use of the water and the effects of it

Source: Sonia Yeh, GouriMishra, and Jacob Teter, Institute of Transportation Studies University of California, Davis, Presentation to LCFS Sustainability Workshop, December 15, 2010

Such legislation is the basis for the organization of water management, planning, management and decision-making, integration and coordination of activities, funding, implementation of management decisions, licensing, inspection activities, enforcement of penal provisions and other activities.

- *• Providing funding for water use based on the principles of sustainable development requires a new water treatment as a resource*.

To policy development companies comply with policies to protect water and ecosystems, water has become an economic category. With the introduction of the economic cost of water and collection of water services can provide secure sources of financing, as well as the continuous flow of funds for water supply, drainage and water treatment (eg, protection from the harmful effects of construction of water infrastructure, environmental protection, etc.).

- *• Develop awareness of the water as a natural resource*.

It is necessary to establish public awareness on sustainable use and protection of water and ensuring meaningful participation of all sections of the population in decision-making processes in the field of water.[3]

III. BASIC POSTULATES OF MODEL

The quality of water in artificial lakes is a key characteristic that changes over time. Because often talks about the process of aging reservoirs, which must be taken into account at all stages of the design and operation of the system, so that these processes under control. In addition to the environmental and aesthetic impact on the environment, the waters with the highest quality water enriched or degraded - if the process of eutrophication out of control, water quality affects the purpose of accumulation.For example, uncontrolled growth of phytoplankton and algae creates serious problems at treatment plants, a negative impact, and in cases where the reservoirs used for recreation and tourism. Increased amounts of gases that result from the anaerobic decomposition of organic matter (CH_4, H_2S, NH_3, and other). Alter the taste and smell of the water, which prevents the use of the reservoir for recreational and tourism purposes and degrades the environment. The figure shows the impact of human activities and the need for water resources management.

Although a very important aspect of water quality and its modeling is only in recent decades intensely developed and implemented. The main reason for this is the complexity of the dynamics of physical, chemical and biological processes in the lake ecosystems, which can only at this stage of development of science and technology can be adequately reviewed and a mathematical model.The second, equally important reason, have

[3]*Questionnaire to measure attitudes and knowledge of the Water Framework Directive, the Ministry of Agriculture, Forestry and Water Management / Directorate of Water*

limited opportunities autopurification water and their last decades more intense pollution, which follow the increasingly stringent requirements in terms of quality of supplied water (hydro- reservoirs, 2003).

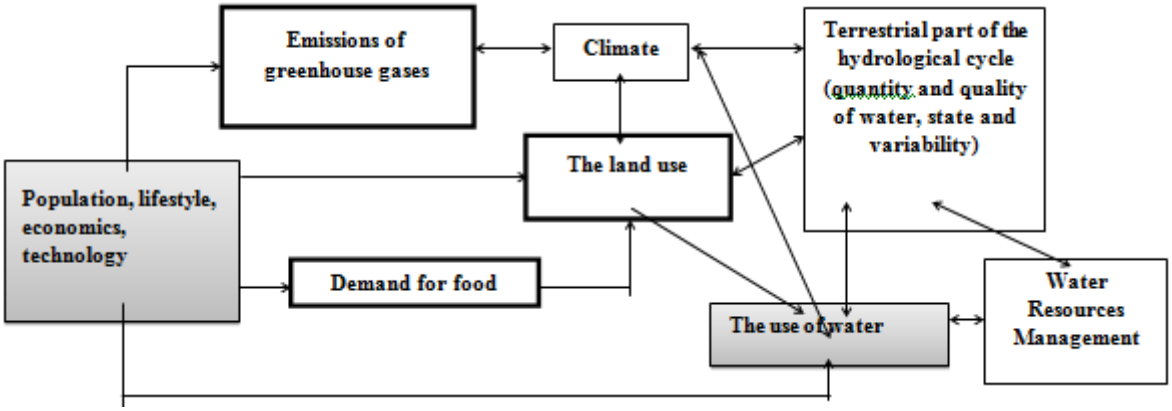

Figure 4. The impact of human activities and the need for water resources management
Source: Oki, 2005.

Lakes are among the first aquatic ecosystems that are generally modeled. The achieved accuracy of simulations of hydrodynamic phenomena in the lake in previous models can be considered satisfactory and the results of simulations of inert chemical components (Blumberg, 1998). Results of the simulation of behavior of nutrients and dissolved oxygen in the lake water are less precise (DiToro, 1980). All known experience, primarily eutrophication models, show that one of the same model still need to be modified on a case-by-case basis, and every lake ecosystem has its own specific features. The phenomenon that is very important for a lake to another to not be.It is possible to construct a large model that would in itself involve a large number of features and phenomena, but that requires a large amount of data required for its calibration. After data collection is the most costly phase of the formation of the lake ecosystem model that is often a limiting factor in its creation.When speaking about the differences in the application of the same model in different lake systems, the main reason is the large variation in chemical and biological processes. With relatively simple assumptions, the physical processes are more easily adapted solutions, while the practice has shown that biological processes are difficult to adapt to using the available mathematical „tools“ (Sekulic, 2004).
The first step in developing the model is that the available data on the quality of raw water well examined and systematized the analysis of available time, place and type of parameters.
The next step is to start work on the model.

Modeling should be understood as a process in which alternating gather information, develop model and study the behavior of the system, check the agreement of the results with the observations, the observed differences, gather new information and suggestions, the model improves, and there is a new round of analysis, etc.. Figure 5. presents the model selection - is very important problem definition, model selection, simulation and application, and Figure 5.shows application of the model through a process of monitoring, management and development.
In time the model becomes more reliable and better describes the real system, and the participants in this business and how to acquire and useful knowledge. Any other approach is wrong and does not give good results, an attempt to create a model once in its final form fails or leads to long delays and expenditure of time and resources (Obradovic, 1999).

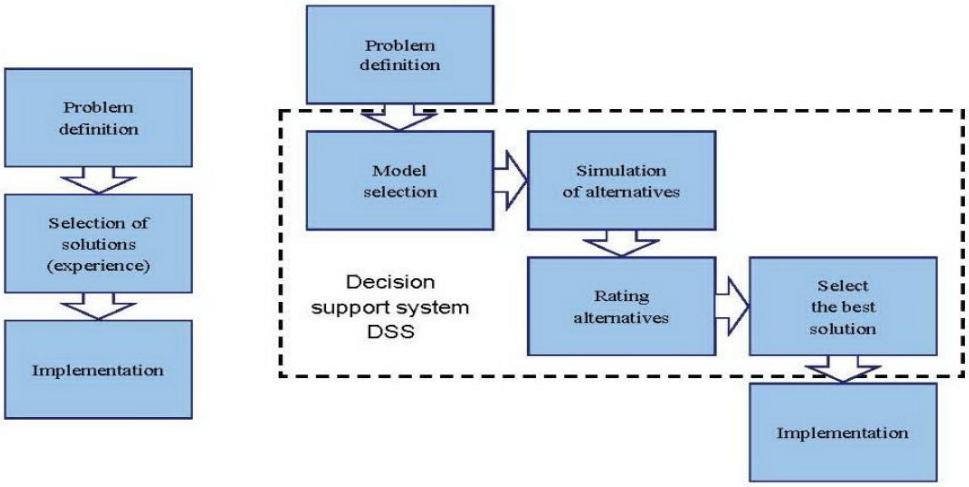

Figure 5. Display selection model
Source: Milicevic, D., Milenkovic, S., Potic., O. FACTA UNIVERSITATIS Series: Architecture and Civil Engineering, Vol. 8, No 2, 2010, pp. 250

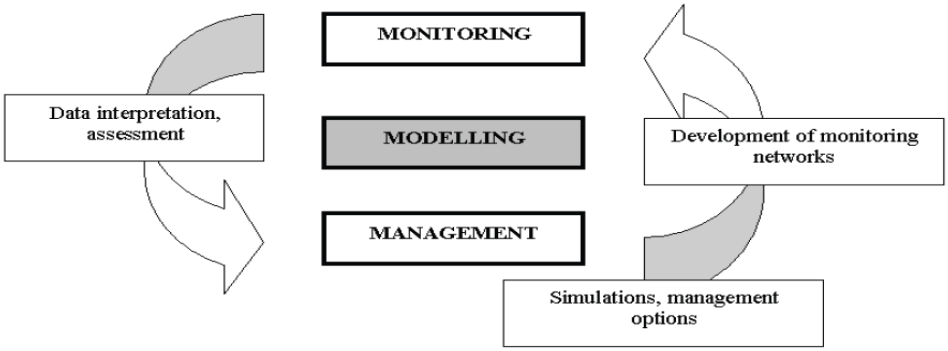

Figure 6. Application of the model - the process of monitoring, management and development
Source: Milicevic, D., Milenkovic, S., Potic., O. FACTA UNIVERSITATIS Series: Architecture and Civil Engineering, Vol. 8, No 2, 2010, pp. 250

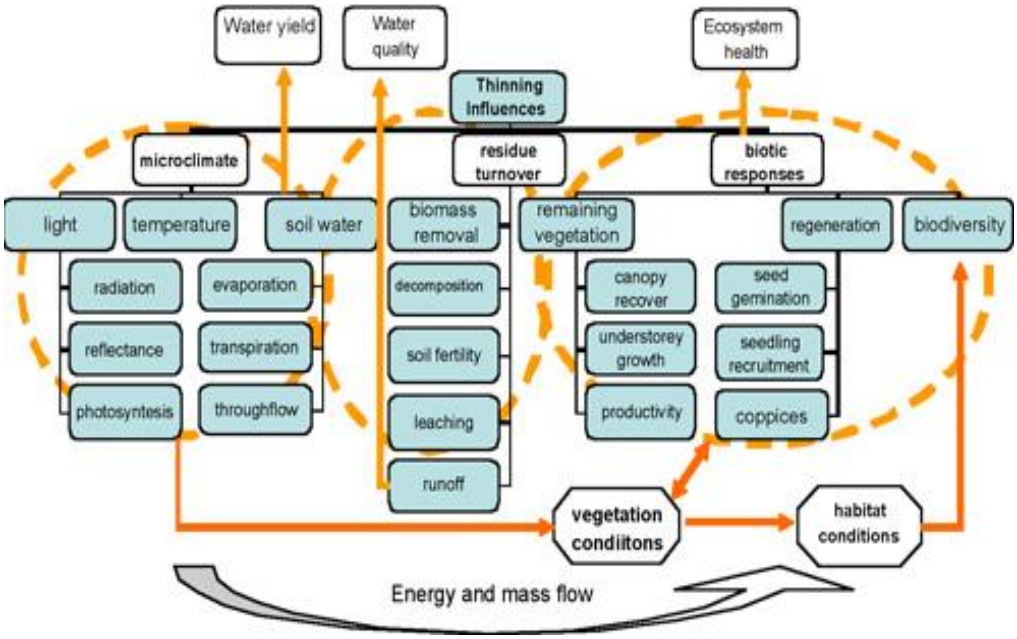

Figure 7. Schematic effects on water yield, water quality and ecosystems

Ecosystem response may be driven by changes in microenvironment and energy (light, organic matter) and mass (water and nutrients) flow.

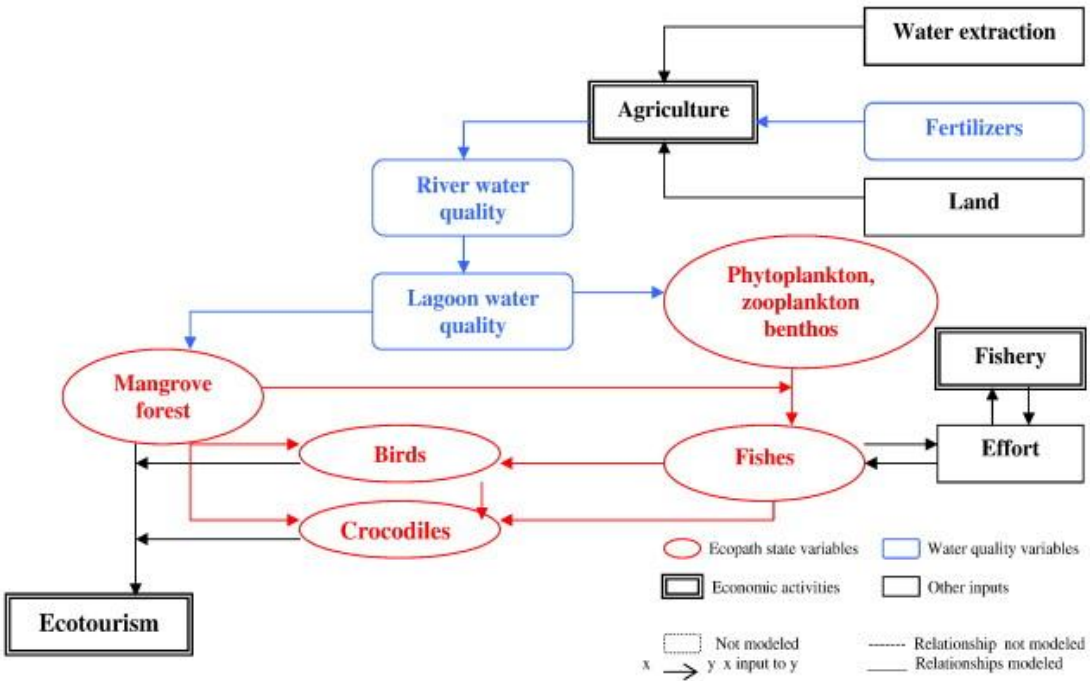

Figure 8. Scheme ecological-economic model

Source; V.S. Avila-Foucat, An *ecological–economic model for catchment management: The case of Tonameca, Oaxaca, México*, Ecological Economics, Volume 68, Issues 8–9, 15 June 2009, Pages 2224–223

Aquatic ecosystems have some specific features that complicate the design and development of their model and quite different from similar processes in other engineering disciplines. Description of processes in aquatic ecosystems requires a large, interconnected system of algebraic and differential equations, and often requires an interdisciplinary approach. Many processes, especially in the lower layers of the water mass, are poorly understood, and as a rule, collection of data for a better understanding of them is a very expensive process. Some parameters or conditions of aquatic ecosystems, such as temperature or the concentration of some of the inorganic compounds, can be adequately described using the continuum mechanical laws. However, other conditions and parameters, for example, change the number of populations in an ecosystem, are discrete, movable and resizable so unacceptable to the standard model's techniques.Timeframe phenomena that occur in aquatic ecosystems measured by years or even decades so that their validity is not practical for some shorter intervals. In many scenarios, the possible occurrence of, for example. spillovers or large inflow of water system models can not help or they result unusable.

Massive fund of various information from time series of different concentrations of the compounds, the weather conditions to geographical data about aquatic ecosystems are necessary to create and test the model, or get a satisfactory solution. They are very rare cases that the model designers are very familiar with both of the two dominant phenomena in any aquatic ecosystem - hydrodynamics and ecology. Therefore, there are very few models that equally, or well enough describe both phenomena (Sekulic and other, 2004).

In assessing the impact of impoundment on water quality, it is necessary to reliably determine the temperature regime in the reservoir. Hydrodynamic characteristics of the flow and temperature distribution in terms of stratification significantly affect other quality parameters (primarily in dissolved oxygen, biological oxygen demand (BOD).

The dilemma exists in the choice of model type, ie, whether you choose a model that relies on describing the hydrodynamic flow or so called. "Ecological " model. In the hydrodynamic model, simulates a small number of parameters, but to observe their interplay (interaction) through the analyzed period. When "environmental model, it is possible to simulate a larger number of parameters which are observed independently of each other (no interaction). When deciding on the choice of the model, an important factor in the decision are the parameters that we know (9.).

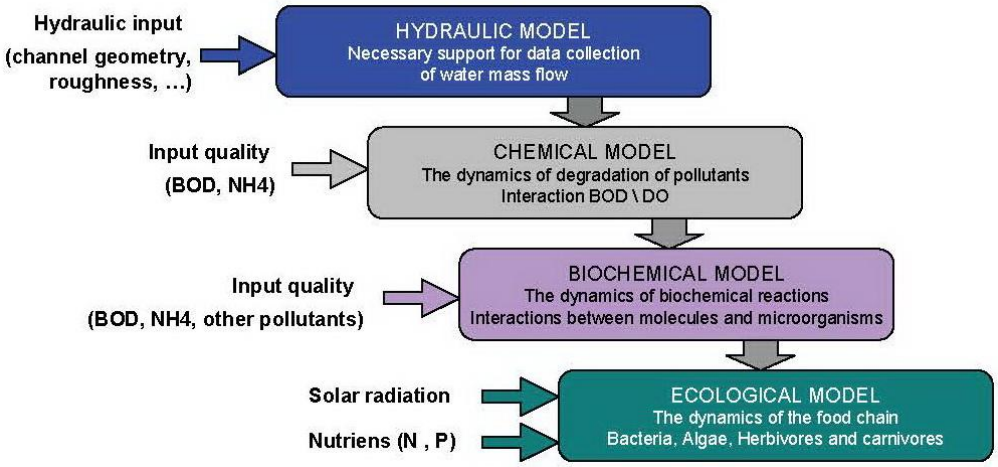

Figure 9. The structure of the model based on the quality of water
Source: Milićevic, D., Milenkovic, S., Potic., O. FACTA UNIVERSITATIS Series: Architecture and Civil Engineering, Vol. 8, No 2, 2010, pp. 252

Thus, the crucial point for the selection of the mathematical model is a good knowledge of the real system being modeled and processes which are dominant. With this in mind, decided to ecological type of model that will analyze the following parameters:

a) Microbiological parameters: total coliforms as a notification (MPN) in 100 ml of water, the total number of air mesophilic bacteria were incubated 48h/37^{o}C in 1 ml of water.

b) Biological parameters: enzyme phosphatase activity mmol/s/dm^{3} pNP (30°C), saprobic index, chlorophyll Chl "a", oligotrophic bacteria, heterotrophic bacteria by Khola, the degree of self-purification O/H

c) Physico-chemical parameters: temperature, turbidity, organic matter as KMnO4 consumption, total organic matter in the water, iron, manganese, oxygen, ammonia, nitrite, nitrate, phosphorus, chloride, the rest of the fumes, electrical conductivity.

The new solution (model) must be connected in a well designed functional unit, which can precisely manage ("Precision Process Technology") - the integration of the production phase in the logical production units to enable them to precisely manage for maximum use of natural resources, auxiliary materials, energy, etc. . Realization of these principles of action, the selected process technology will be fully integrated into the principles of sustainable development (10).

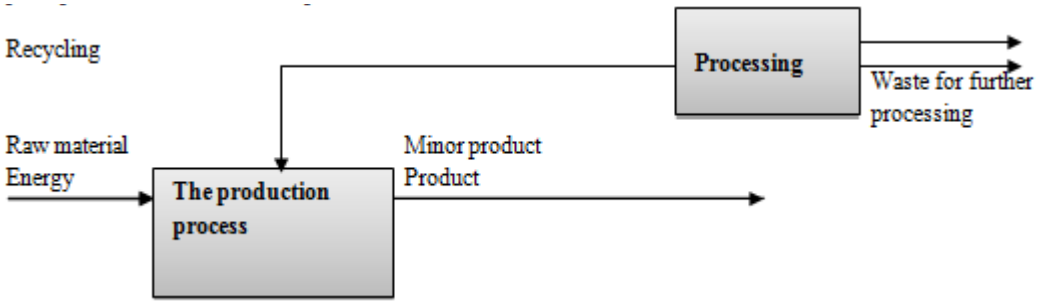

Figure 10. The general scheme of "closed" ("clean") process technology

IV. SELECTION OF CONTROL POINTS IN THE SYSTEM

The content and concentration of a large number of water quality parameters during treatment and distribution depend on many factors - the implementation of the Water Framework Directive (Figure 11.).

Setting goals monitoring parameters that indicate of water quality are divided into two groups:

1. The parameters in which the concentrations of specific concentration of the substantially water inlet and uncertain, which vary in the course of distribution: e.g. arsenic, cyanide, fluoride, hardness, pesticides, sodium, selenium, sulfates, total soluble matter.
2. The parameters that may vary in concentration in distribution of: parameters that may participate in the reactions (which change the concentration) within the distribution system, but where the distribution of concentration in highly dependent on the concentration at the entrance of the system: for example,

aluminum, the residuals of disinfectants and disinfection by-products, iron, manganese, fluoride, color, turbidity, odor, taste, pH, characteristics for which the distribution system is the main source: eg. corrosion products (cadmium, chromium, lead, zinc, copper).

The frequency of sampling depends on the key characteristics of their variability, the aesthetic characteristics and the impact on human health. For microbiological parameters, sampling and analysis are much more common.A sufficient number of parameters must be collected during a representative period information to be provided to these programs can be statistically processed, and the significant changes in the trends identified, treatment options as compared to the recommendations monitored. The required number of samples depends on the desired level of precision with a known degree of confidence. (Dalmatia, B., Agbaba, J.2006.)

The accuracy of any laboratory analysis depends on the sampling method. The sample must be characteristic of the tested water (and the test parameters) otherwise the result is of no consequence. Sampling must be done professionally, in a prescribed manner.

Sampling points should provide data that are sufficiently representative of the quality of the water when it comes. To establish these points, short-term research monitoring is necessary.

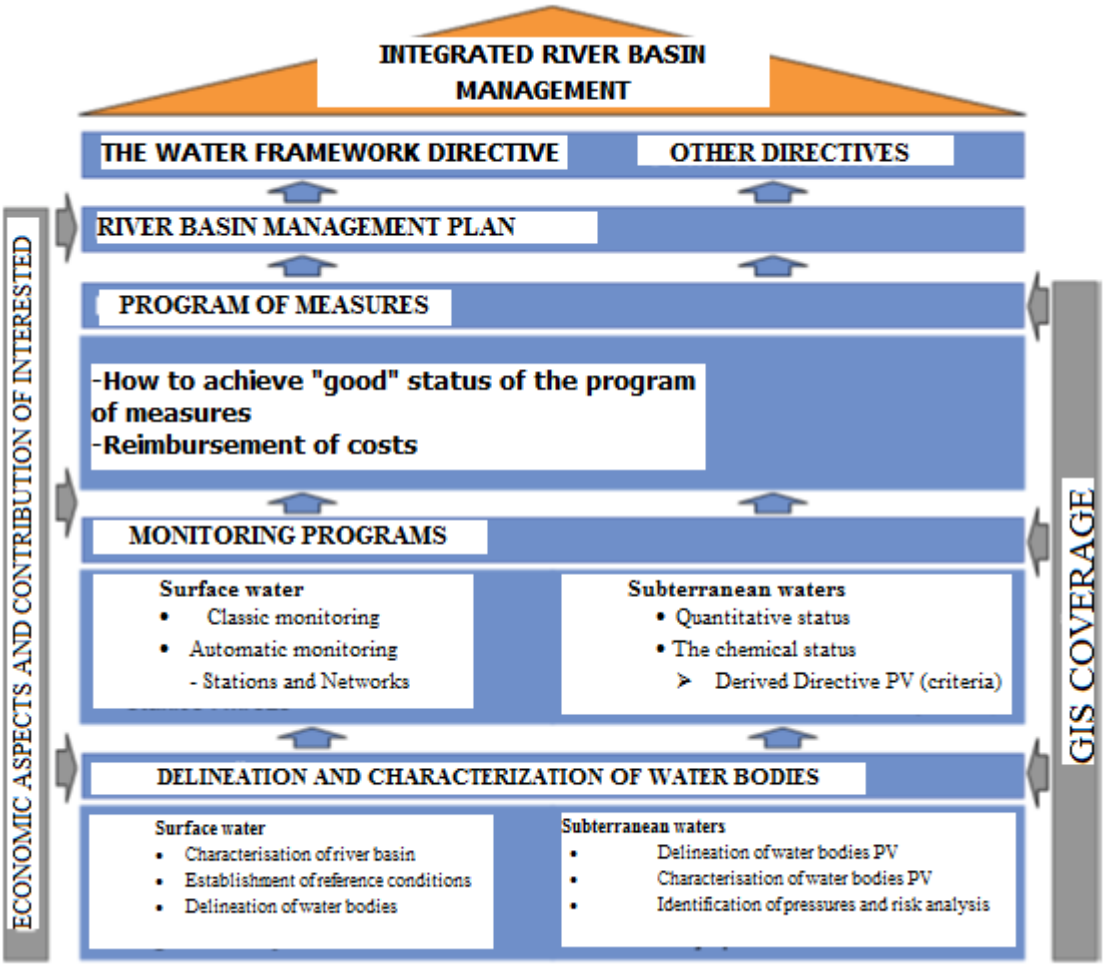

Figure 11. The implementation of the Water Framework Directive
Source: Milicevic, D., Milenkovic, S., Potic.,O. - FACTA UNIVERSITATIS
Series: Architecture and Civil Engineering, Vol. 8, No 2, 2010, pp. 249

In addition to official control, it is necessary that the manufacturer (and supplier) performs its own control, which includes the systematic control: the source, ie. the raw water, the purification process for optimal production, produced and delivered water at representative points.

Sampling points are: Raw water (source) device for the treatment of (process control, no performance monitoring), Treated (treated) water inlet water in the distribution system, tank, representative composite and/or random samples of points of distribution system, Points that represent the quality of water available to consumers, Consumer taps for specific research (eg., corrosion products or verification of distribution sampling points), Point at which previous research has shown satisfactory quality.

Place of sampling in the distribution system should be set up to enable the monitoring of residual disinfectants and determine the microbiological quality of water. For routine bacteriological tests, the sampling should be taken of the relevant precautions, including all national safety requirements.
Distribution systems can be open, closed and mixed. Supply can be from multiple sources (wells). At the same time, the source can be both surface and ground water, and water that has undergone processing or directly from the source without treatment except disinfection, pumped into the distribution network.

Depending on the distribution system, the WHO proposes a sampling.

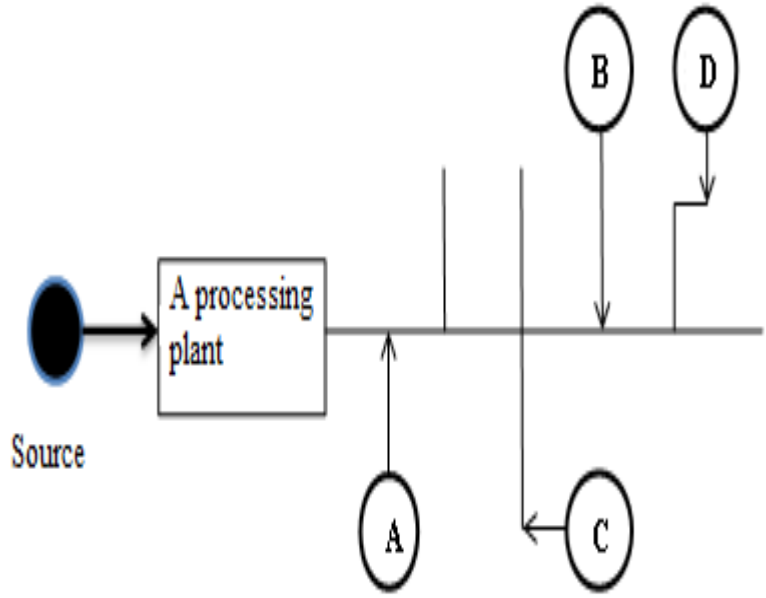

Figure 12. Open distribution system
Source: WHO, 1983

A - Sampling clean water after the treatment plant, is used to verify the effectiveness of the system and to show the input water quality in the distribution system; B - Is the sample of water from the central water pipe; C - Represents the water sample in one of the branches of the central water pipe; D - Represents a sample of water at the end of the system.

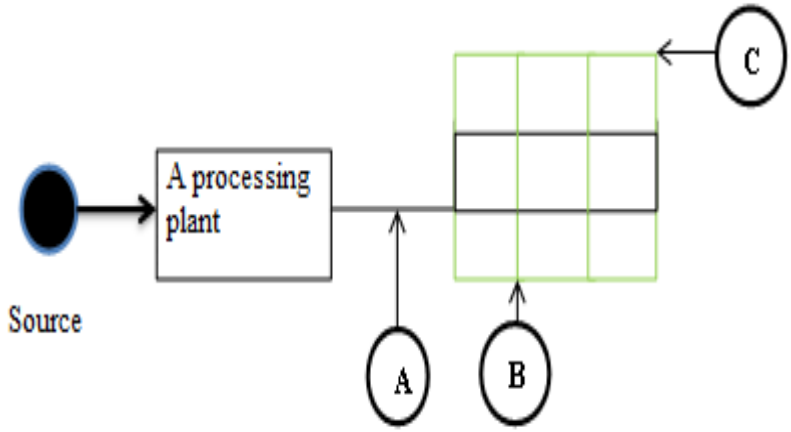

Figure 13. Closed distribution system
Source: WHO, 1983

A - Sampling clean water after the treatment plant, is used to verify the effectiveness of the system and to show the input water quality in the distribution system; B - Represents the water sample in one of the branches of the central water pipe; C - Represents the water sample at the end of the system.

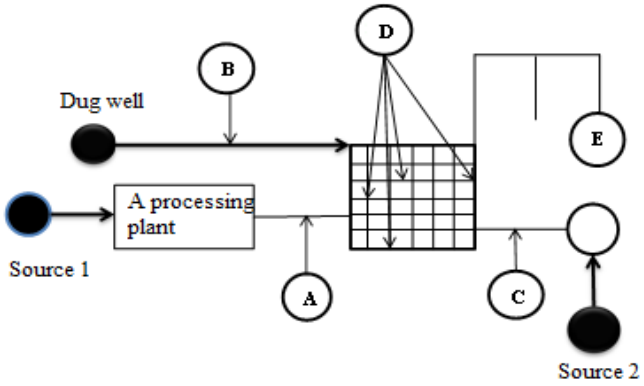

Figure 14. Mixed distribution system
Source: WHO, 1983

In this case there are three sources of water, and the system has a "closed" distribution zone and other "open" type. A - Sampling clean water after the treatment plant, is used to verify the effectiveness of the system and to show the input water quality in the distribution system; B - Is the quality of well water that enters the system; C - The point is the quality of the water after passing through the reservoir, (in some cases, it is also important to take samples before the tank); D - Point represents the water in the main system (the similar point in the network should have the same value; E - Is the quality of the water in an open system (in this simple case, the samples are taken from secondary branches and at the end of the system).

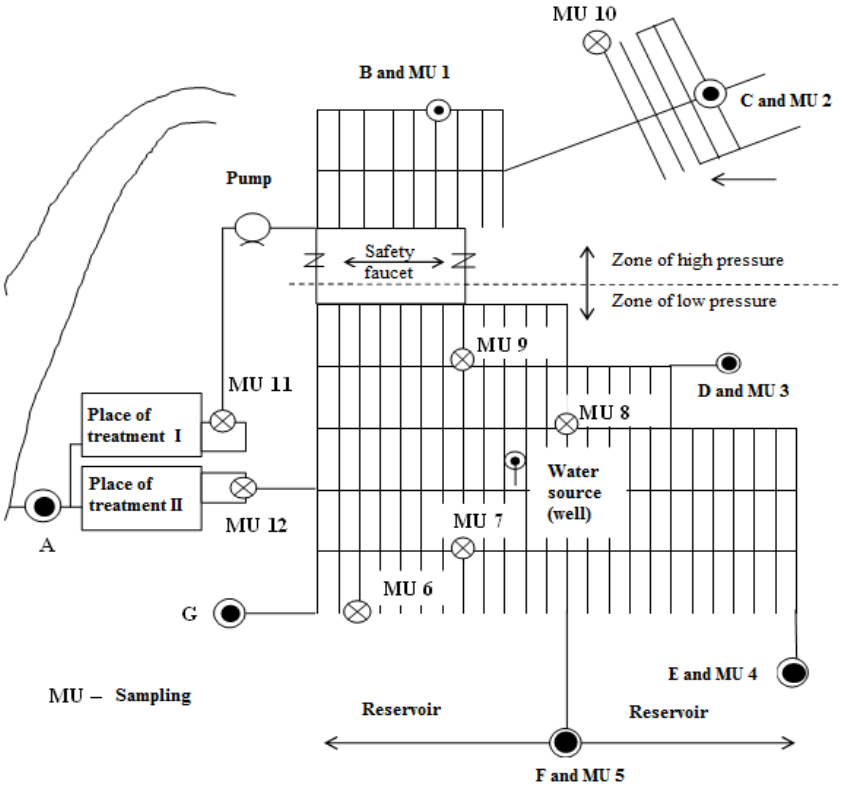

Figure 15. The combined system of branches and loops
Source:B. Dalmatia 2000.

Sampling "A" is the entrance to the distribution system. Sampling "B" main tube, position "C" is a "dead spot" water main. Places "D" and "E" are in the branches and the "deadlock" branch. Samples taken from the position of "B" and "E" requires a complete analysis. Place "F" is under the influence of the water tank. Point "G" is a "dead spot". The numbers are marked for sampling of the distribution system.

V. CONCLUSION

A key aspect of model selection parameter optimization of the quality of the raw water is a good knowledge of the real system being modeled. With this in mind, we decided to use environmentally friendly type of model. Based on the research results presented ecological models, it is concluded that the presented models have great potential and that with further updates can turn into a very good tool for the prediction quality of the raw water and an estimate of funds required in the process of obtaining drinking water.

REFERENCES

Journal Papers:

[1] D. ILIC, S.KOSTIC-NIKOLIC, S.STEFANOVIC, SUSTAINABLE MANAGING OF WATER RESOURCES IN URBAN AREA WITH SUBURBS, Lucrarea trimisă redacţieiMetalurgia International a fost acceptată spre publicare în numărul din 2013., ISSN 1582 – 2214, "METALURGIA INTERNATIONAL" is introduced in THOMSON SCIENTIFIC MASTER JOURNAL LIST, letter M, position 440. vol. 18 SPECIAL ISSUE NO. 8, str. 278 – 284 (2013).

[2] D. ILIC, S. KOSTIC - NIKOLIC, S. STEFANOVIC, MATHEMATICAL MODELING IN THE CONSUMPTION OF RAW FOR WATER TREATMENT. "METALURGIA INTERNATIONAL" is introduced in THOMSON SCIENTIFIC MASTER JOURNAL LIST, letter M, position 440., vol. 18 Special Issue no. 4, str. 298 – 306 (2013).

[3] S. Stefanović, D. Ilić, WATER - A COMMON HERITAGE WHOSE VALUE WE HAVE TO KNOW, International Journal of technical – Technological and Biotechnical Sciences, Number 1, UDS 62, ISSN 2217-2424, str. 49-58., Zrenjnin.

Books:

[4] S. Stefanović, R. Cvejić, D, Ilić, EKOLOŠKI ASPEKTI VODE, Tiraž: 120 primeraka, Izdavač: TQM Centar, Zrenjanin, 2010. ISBN 978 – 86 – 88065 – 11 – 5 Narodna biblioteka Srbije.

[5] *Richard H. Moss, et al., The next generation of scenarios for climate change research and assessment, Nature, 2010.*

[6] Gleick, P.: *Water in crisis: Paths to sustainable water use*, Ecological Applications, 8(3), 1998, pp. 571–579.

[7] Report of UN-Water, Status Report on Integrated Water Resources Management and Water Efficiency Plans, Prepared for the 16th session of the Commission on Sustainable Development - May 2008.

[8] Grigg, N. S.; *Integrated water resources management: balancing views and improving practice*, Water International,Vol. 33, No. 3, September 2008, pp. 284.

[9] Sonia Yeh, GouriMishra, and Jacob Teter, Institute of Transportation Studies University of California, Davis, Presentation to LCFS Sustainability Workshop, December 15, 2010.

[10] Milićević, D., Milenković, S., Potić., O. FACTA UNIVERSITATIS, Series: Architecture and Civil Engineering, Vol. 8, No 2, 2010, pp. 250.

[11] V.S. Avila-Foucat, An *ecological–economic model for catchment management: The case of Tonameca, Oaxaca, México*, Ecological Economics, Volume 68, Issues 8–9, 15 June 2009, Pages 2224–223.

[12] Milićević, D., Milenković, S., Potić., O. FACTA UNIVERSITATIS, Series: Architecture and Civil Engineering, Vol. 8, No 2, 2010, pp. 252.

[13] *Милићевић, Д., Миленковић, С., Потић., О. - FACTA UNIVERSITATIS,* Series: Architecture and Civil Engineering, Vol. 8, No 2, 2010, pp. 249.

Theses:

[14] D. Ilic, МОДЕЛОВАЊЕ ВОДНИХ СИСТЕМА И ОПТИМИЗАЦИЈА ПАРАМЕТАРА КВАЛИТЕТА СИРОВЕ ВОДЕ У ПРОЦЕСУ ПРЕРАДЕ ВОДЕ ЗА ПИЋЕ, Doktorska disertacija, Fakultet za poslovne studije, Beograd, 2013.

Proceedings Papers:

[15] Далмација, Б., Агбаба, Ј.2006.

[16] WHO, 1983.

[17] Продановић, 2003.

[18] Lee, 1992.

[19] Секулић, 2004.

[20] Кнежевић, Б., 2005.

[21] GWP, 2004.

American Journal of Engineering Research (AJER)
e-ISSN : 2320-0847 p-ISSN : 2320-0936
Volume-03, Issue-03, pp-168-180
www.ajer.org

Research Paper Open Access

Motherhood Means Delivering Child?... *(A new theory on "Thaimai")*

M.Arulmani, V.R.Hema Latha,
[1.]*B.E. (Engineer)* [2.]*M.A., M.Sc., M.Phil. (Biologist)*

Abstract: - This scientific research article focus that the word "**Thaimai**" shall be considered as a prehistoric **Tamil word** refers to "**Yield**" ("**E**") and concerned with origin of life and matters in the early universe. The word "**THAI-e**" shall be considered as the "**HEART**" of creator (or) **GOD**. "**MAI-e**" shall be considered as the "**SPIRIT**" emitted from the heart. "**THAIMAI**" shall mean "**CREATION**". The spirit shall also be called as "**J-RADIATION**".

(i)

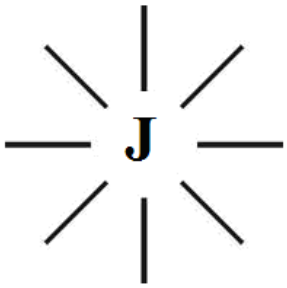

(THAI-e)

(ii)

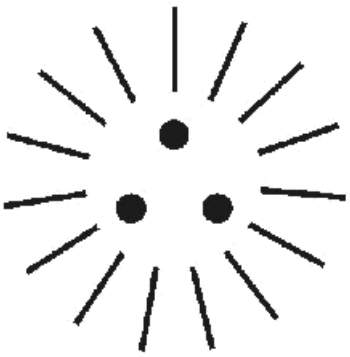

(MAI-e)

This research further focus that in the **early universe** all the life and matters shall be considered created initially by the creator and subsequently undergone three major genetic changes called as "**Three species of matters**" due to growth of different radiation level. Every initially created matter shall be considered like Individual "**TEAR DROP**" emanated from "**THAI-e**" and having their own "**genetic structure and genetic value**". Every "RAY" emanated from "HEART" shall be considered representing individual "**family name**" of

initially created matters. In prehistoric Tamil HEART shall mean "**KAN-MAI**", "**KANMANI**". RAY shall mean "**E-MAI**"

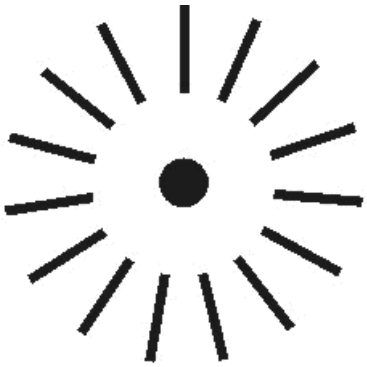

(E-MAI)

"Nanmai, Theemai, Karumai, Venmai, Ezhimai, Perumai, Varumai, Valimai, Porumai, Poramai, Madamai, Makimai etc. shall be considered as each "TEAR DROP" representing "GENE" of every matter".

Key Words: -

a)	Philosophy of	"**COSMIC EYE**"	e)	Philosophy of	"**ALL-E FAMILY**"
b)	Philosophy of	"**TEAR DROP**"	f)	Philosophy of	"**3G MOTHER**"
c)	Philosophy of	"**E-MAI**"	g)	Philosophy of	"**KANNI-e**"
d)	Philosophy of	"**AKKI-E FAMILY**"	h)	Philosophy of	"**E-LANGUAGE**"
			i)	Philosophy of	"**WHITE INK**"

I. INTRODUCTION

In global level human culture "**Motherhood**" is proudly considered as "**successfully delivering the child after marriage**". After the marriage the woman who are not able to deliver child due to various scientific, environmental reasons are very much "**ill-treated**" and in the society and called as "**Barren Lady**". In **cinema**, **pattimantram** also the fact of "**Woman become mother**" after delivering child is sometime strongly supported.

It is focused that today across the globe, many "**CINEMA STARS**", "**PATTIMANTRAM STARS**" are throwing away their "**Newly born Infant**" in the Bush, garbage (Kuppaithottil) and proudly forecasting message with stiff nick about "**Thaimai**" (motherhood). Whereas still some "**HELPING HANDS**" in the society save the thrown away **Godly product** and cherishing their life through "**ORPHANAGE**".

MOTHER HAS TO NECESSARILY DELIVER CHILD?...

The philosophy English word "**Mother**" has in depth meaning. Mother shall mean "**KANNI-e**" the source of matters of the Universe created through every "**TEAR DROP**" by "**Universal law**". KANNI-e shall be considered as the 1st Generation name for heart; **KANNEER** shall be considered as the 1st Generation name for **particle**.

(i)

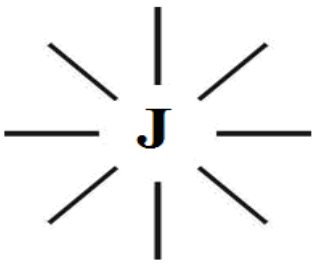

(KANNI-e)

(ii)

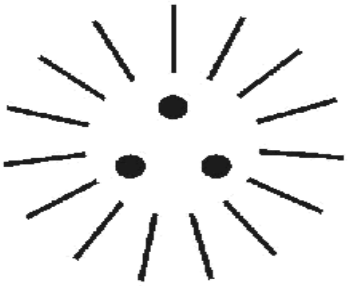

(KANNEER)

(iii)

(THAI-e)

The philosophy of "**MOTHER**" shall be defined within the following scope.
1) Mother shall mean "Heart" of **GOD**
2) Mother hood shall mean "Creations" of GOD
3) Mother hood shall mean creation rather than delivering jackfruit like baby.

*"The philosophy of International woman's day, mother's day, might be derived from the philosophy of "Kanni-e". Kanni-e shall mean "**BARREN CREATOR**". Kanni-e shall mean "**Transformer**".*

II. PREVIOUS PUBLICATION:

The philosophy of origin of first life and human, the philosophy of model Cosmo Universe, the philosophy of fundamental neutrino particles have already been published in various international journals mentioned below. Hence this article shall be considered as **extended version** of the previous articles already published by the same author.

[1] Cosmo Super Star – IJSRP, April issue, 2013
[2] Super Scientist of Climate control – IJSER, May issue, 2013
[3] AKKIE MARS CODE – IJSER, June issue, 2013
[4] KARITHIRI (Dark flame) The Centromere of Cosmo Universe – IJIRD, May issue, 2013
[5] MA-AYYAN of MARS – IJIRD, June issue, 2013
[6] MARS TRIBE – IJSER, June issue, 2013
[7] MARS MATHEMATICS – IJERD, June issue, 2013
[8] MARS (EZHEM) The mother of All Planets – IJSER, June issue, 2013
[9] The Mystery of Crop Circle – IJOART, May issue, 2013
[10] Origin of First Language – IJIRD, June issue, 2013
[11] MARS TRISOMY HUMAN – IJOART, June issue, 2013
[12] MARS ANGEL – IJSTR, June issue, 2013
[13] Three principles of Akkie Management (AJIBM, August issue, 2013)
[14] Prehistoric Triphthong Alphabet (IJIRD, July issue, 2013)
[15] Prehistoric Akkie Music (IJST, July issue, 2013)

[16] Barack Obama is Tamil Based Indian? (IJSER, August issue, 2013)
[17] Philosophy of MARS Radiation (IJSER, August 2013)
[18] Etymology of word **"J"** (IJSER, September 2013)
[19] NOAH is Dravidian? (IJOART, August 2013)
[20] Philosophy of Dark Cell (Soul)? (IJSER, September 2013)
[21] Darwin Sir is Wrong?! (IJSER, October issue, 2013)
[22] Prehistoric Pyramids are RF Antenna?!... (IJSER, October issue, 2013)
[23] HUMAN IS A ROAM FREE CELL PHONE?!... (IJIRD, September issue, 2013)
[24] NEUTRINOS EXIST IN EARTH ATMOSPHERE?!... (IJERD, October issue, 2013)
[25] EARLY UNIVERSE WAS HIGHLY FROZEN?!... (IJOART, October issue, 2013)
[26] UNIVERSE IS LIKE SPACE SHIP?!... (AJER, October issue, 2013)
[27] ANCIENT EGYPT IS DRAVIDA NAD?!... (IJSER, November issue, 2013)
[28] ROSETTA STONE IS PREHISTORIC "THAMEE STONE" ?!... (IJSER, November issue, 2013)
[29] The Supernatural "CNO" HUMAN?... (IJOART, December issue, 2013)
[30] 3G HUMAN ANCESTOR?... (AJER, December issue, 2013)
[31] 3G Evolution?... (IJIRD, December issue, 2013)
[32] God Created Human?... (IJERD, December issue, 2013)
[33] Prehistoric "J" – Element?... (IJSER, January issue, 2014)
[34] 3G Mobile phone Induces Cancer?... (IJERD, December issue, 2013)
[35] "J" Shall Mean "JOULE"?... (IRJES, December issue, 2013)
[36] "J"- HOUSE IS A HEAVEN?... (IJIRD, January issue, 2014)
[37] The Supersonic JET FLIGHT-2014?... (IJSER, January issue, 2014)
[38] "J"-RADIATION IS MOTHER OF HYDROGEN?... (AJER, January issue, 2014)
[39] PEACE BEGINS WITH "J"?... (IJERD, January issue, 2014)
[40] THE VIRGIN LIGHT?... (IJCRAR, January issue 2014)
[41] THE VEILED MOTHER?... (IJERD, January issue 2014)
[42] GOD HAS NO LUNGS?... (IJERD, February issue 2014)
[43] Matters are made of Light or Atom?!... (IJERD, February issue 2014)
[44] THE NUCLEAR "MUKKULAM"?... (IJSER, February issue 2014)
[45] WHITE REVOLUTION 2014-15?... (IJERD, February issue 2014)
[46] STAR TWINKLES!?... (IJERD, March issue 2014)
[47] "E-LANKA" THE TAMIL CONTINENT?... (IJERD, March issue 2014)
[48] HELLO NAMESTE?... (IJSER, March issue 2014)

III. HYPOTHESIS:

a) Philosophy of creation?...

It is hypothesized that "**GOD**" shall be considered as the "**Creator**" of the Universe and all the matters. GOD is considered as the source of Infinite level of "**Dark Assets**" (SPIRIT) in the form of **Dark matter, Dark energy** and during the course of time GOD Transformed the dark assets into "**White Tear Drops**" (souls) through "White hole". The white hole shall be considered as the Integral part of "**narrow duct**" called tear duct and convergent device called "**Cosmic eye**". The cosmic eye is considered as the source of Accelerating force "**J-RADIATION**" which transforms dark assets into **WHITE TEARS.** In prehistoric tamil every tear drop shall be called as "**E-MAI**" representing each gene of matter origin. E-MAI shall also mean **WHITE INK.**

(i)

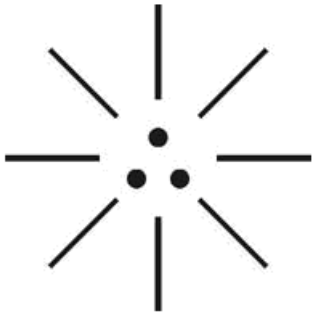

(COSMIC EYE)

(ii)

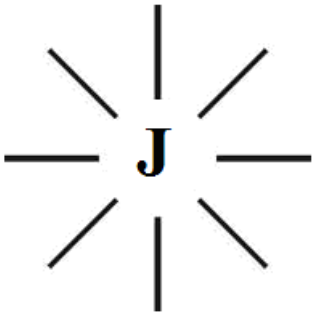

(WHITE INK)

*"**TEAR**" shall be considered as produced by "**HEART**" rather than "**EYE**".*

- Author

b) Philosophy of "All-e" family?...

It is hypothesized that the name of creator shall be called as "**All-e**" and billions or created matters (**Natural matters**) shall be considered belong to "**All-e family**" under three domain.

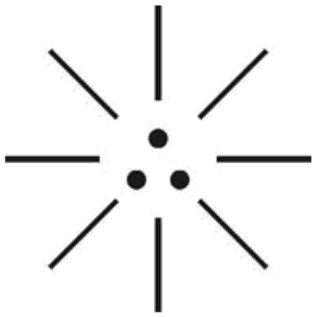

(THREE DOMAIN)

Some of the hypothetical families are cited below:
1) "**Akki-e**" – Fundamental **particle** family
2) "**Nee-e**" – Fundamental **radiation** family
3) "**All-e**" - Fundamental **human** family
4) "**Ape-e**" – Fundamental **monkey** family
5) "**Age-e**" - Fundamental **plant** family

c) Philosophy of Tear?...

It is hypothesized that each "**Tear drop**" shall be considered containing three-in-one fundamental particles **Photon, Electron, Proton** (**Natural particles**) having well defined genetic structure.

(i)

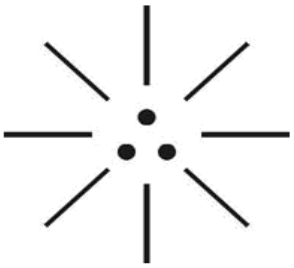

(AKKI-e)

(ii)

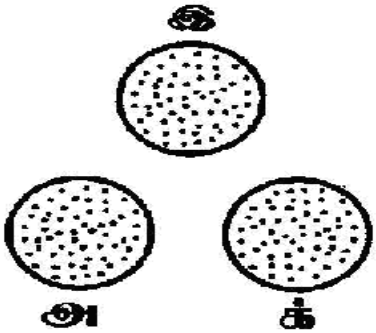

(TEAR DROPS)

i) Right dot – **Proton** (Functional logic)
ii) Left dot – **Electron** (Structural logic)
iii) Centre dot – **Photon** (Sequence logic)

d) Philosophy of (NEE-e) Nuclear family?...

It is hypothesized that the fundamental "**J-Radiation**" shall be considered pertain to "**All-e**" family. Thousands of various other cosmic radiations and coloured lights shall be considered "**Species**" or sub-families to All-e family. '**J-Radiation**" shall also be called as "**VIRGIN LIGHT**".

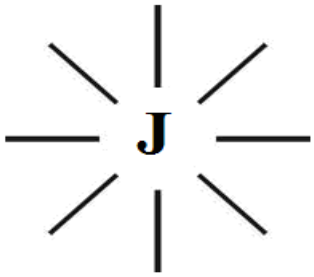

(VIRGIN CREATION)

e) Philosophy of Akki-e family?...

It is hypothesized that photon, Electron, proton shall be considered as the three-in-one fundamental particles called J-particles (or) white particles (or) God particles having **zero mass**.

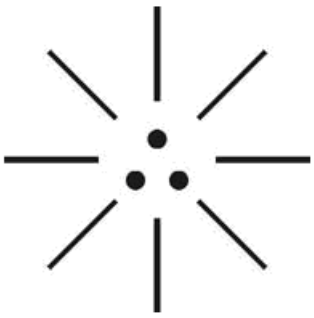

(AKKI-e)

In Akki-e family, the three fundamental particles shall be considered as the Three-in-one members of the family as described below:

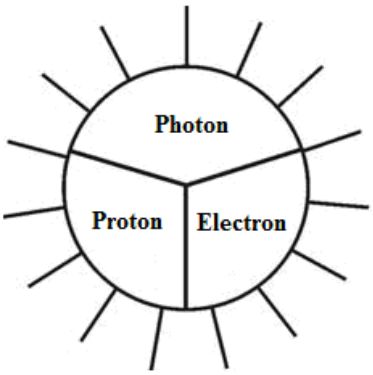

(AKKI-e Family)

i) **FATHER** - "Photon"
ii) **MOTHER** – "Electron"
iii) **INFANT** – "Proton"

In prehistoric **Tamil culture** the members of Alli-e family shall be considered derived from Akki-e family called by name as below:

i) Photon - "**Ay-e**"
ii) Electron - "**Mai-e**"
iii) Proton - "**Thai-e**"

f) Philosophy of three species family?...

It is hypothesized that in the expanding universe three human species families shall be considered evolved from Alli-e family due to impact of evolution of three radiation family.

During three nuclear, geological periods the members of the Alli-e family shall be considered undergone major genetic changes such as in structure, mass, colour of the particles and considered called by different names as described below:

Generation	**Father**	**Mother**	**Infant**
Origin	Ali-e	Mai-e	Thai-e
Ist generation	Ayy-e	Anni-e	Chei-e
2nd generation	Achi-en Achi-e	Koli-e	
3rd generation	Ary-en	Ary-e	Maki-e

Further the cosmic Tamil equivalents in prehistoric Tamil shall be indicated as below:

Sl.No.	**Tamil origin**	**English equivalents**
1)	Kanni-e	Cosmic eye
2)	Kantam	Galaxy, continent
3)	Kanneer	Tear drop, particle
4)	E-mai	Eye lash, white ink
5)	Mari-e	Rain drop
6)	Kanmani	Dark assets
7)	Vellimani	White assets
8)	Mukkil	White cloud
9)	Mathuram	Matter, honey
10)	Ezhem (Athi-e)	Heart (single chamber)
11)	Ethi-e	Heart (three chamber)
12)	Ary-e	Heart (four chamber)

g) Philosophy of 3G matters?...

It is hypothesized that various matters such as Human blood, Tear. Urine, Hormone, Honey, Rain, Acid shall be considered as "**Natural products**". Billions of other matters shall be considered as species matters.

(i)

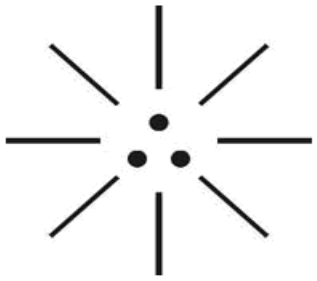

(NATURAL TEAR DROP)

(ii)

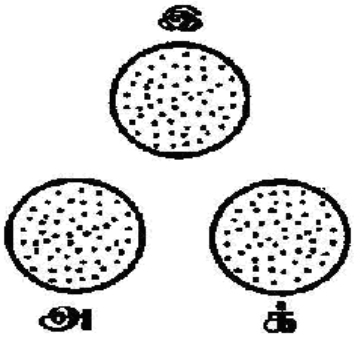

(3G TEAR DROPS)

Ocean shall be considered as the Accumulated blue tears, green tears, red tears of "Kanni-e". While snow "dew drop" (White Ocean) shall be considered as "white tears" of Kanni-e.

h) Philosophy of model cosmo universe?...

It is hypothesized that the whole cosmo universe shall be considered as the closed "**TRIPOD**" container shape having Three-in-one regions of different characteristics In prehistoric tamil the cosmo universe shall be called as "Akki – Ezhem" (Akki-e)

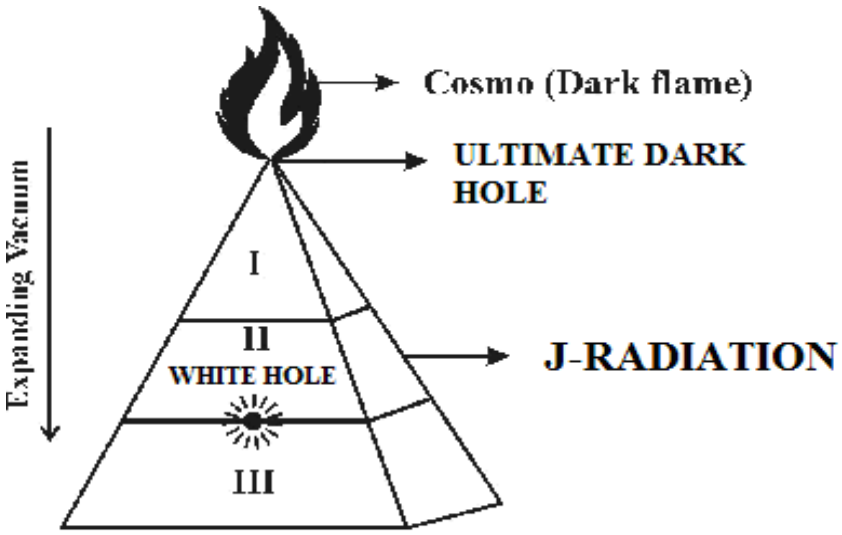

(AKKI-EZHEM)

i) Philosophy of White ink?...

Case study shows that Global research is going on about origin of language and whether the language is originated from "**FATHER**" or "**MOTHER**". Universally language is called as "**mother language**", "**mother tongue**" of the respective country.

It is hypothesized that in the early Universe the first language shall be called as "**EZHEM**". EZHEM shall be considered as "**Heart Language**" (E-LANGUAGE) rather than pronounced by **tongue, lips**. The heart language shall be considered as the language derived from fundamental particles **PHOTON, ELECTRON, PROTON**. The heart language shall also be called as white language or "**J-Language**" written with "**White ink**" (Secret alphabet).

It is further hypothesized that in the early Universe the 1st Generation human population might have had only "**white eye iris**" and they could not distinguish language written by **BLUE INK, GREEN INK, RED INK.** It is focused that every "**HUMAN HEART BEAT**" shall be considered as **natural pulse language** consists of "**J-CODE**" written in "**white ink**".

(i)

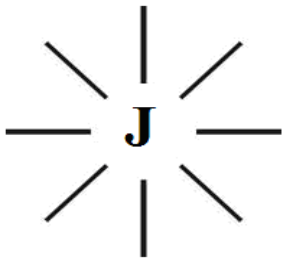

(WHITE INK)

(ii)

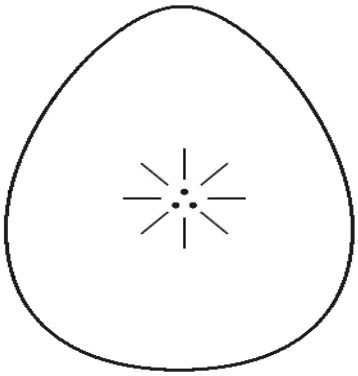

(HUMAN HEART PULSE)

The Philosophy of Chinese language Tai-Chinese, KJANGE, and other 3rd Generation computer programming languages such as B-Language, C-Language, D-Language might be derived from the Philosophy of "J-LANGUAGE". The etymology of English word "Etymology", "Language" might be derived from the Philosophy of "EZHEM", ETHI-e.

2. Hypothetical Narration

a) Philosophy of Human family?...

In human family Father, Mother, Infant are considered as the integral part of family. It is hypothesized that the philosophy or human family might be derived from the philosophy of "**Akki-e, family**". It is further focused that in Akki-e family the members of the family shall be always considered united and never be separated.

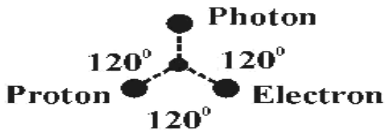

(AKKI-e FAMILY)

i) Father is like Photon (Ay-e)
ii) Mother is like Electron (Mai-e)
iii) Infant is like Proton (Thai-e)

b) Philosophy of English word mother?...

It is focused that the philosophy of English word "**Mother**" might be derived from the philosophy of prehistoric Tamil placities "**Muthu**" (**MU-ETHI-e**). MU-ETHI-e shall mean THREE-IN-ONE particles **PHOTON, ELECTRON, PROTON**.

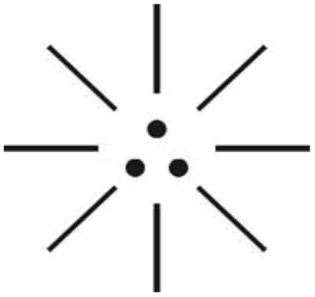

(MU)

c) Philosophy of MAGI?...

Case study shows that the English word '**Magi**" refers to three Wisemen guided by star in **Greek/Hebrew** belief. It is hypothesized that the philosophy of "Magi" shall be considered associated with **AKKI-e**. MAGI shall mean "**MA-AKKI-e**" (**SUN, EARTH, MOON**). It is focused that the mathematical constant i, e, π shall be considered as closely associated with characteristics of SUN, EARTH, MOON in the Universe.

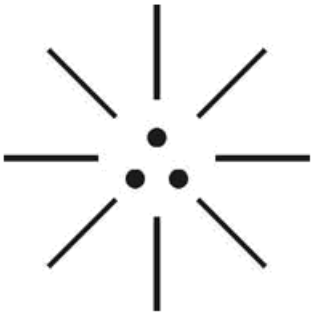

(MA-AKKI-e)

d) Etymology of English word Maid, Maiden Name?...

It is hypothesized that the philosophy, the etymology of English words MAID (MAI-D), MAIDEN NAME might be derived from the philosophy of prehistoric Tamil phonetics "**MAI**". MAI shall mean "**Electron**" (Mother).

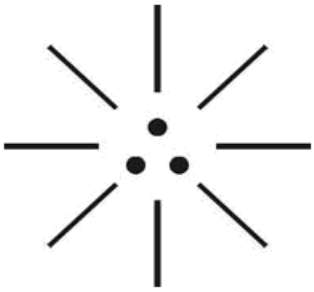

(AKKI-e)

e) Philosophy of Human Heart Pulse?...

It is hypothesized that the energy for human heart function one the human heart pulse shall be considered derived from the AkkI-e shall be considered like "**INFANT**" and associated with Universal mother "**KANNI – e**".

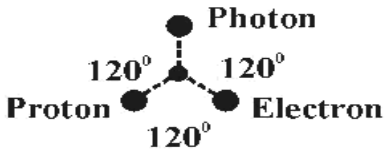

(KANNI-e)

f) Philosophy of English word MAYA, MAYAVATHI?...

It is focused that the philosophy of INDO based name MAYA, MAYAM, MAYAN, MAYAVATHI might be derived from the philosophy of prehistoric Tamil phonetics "**MAI**". Similarly the Philosophy of name MATHAJEE, GURUJEE might be derived from the Philosophy of "**CHEI-e**". "BANNERJEE" shall mean "**KANNI-e**". Further the Tamil word "**KAN-MAI**" shall mean a huge reservoir having "**stock**" of **TEARS** (**KANEER**).

g) Philosophy of word CANE, CANON, CANAAN, CANNY?…

It is focused that the philosophy of English word CANE, CANON, CANNAN, CANNY shall be considered derived from the philosophy of "**KANNI – e**".

h) Philosophy of α, β, γ radiation?…

It is focused that **α, β, γ** shall be considered as the three distinguished families of Radiation in three generation derived from "**AKKI – e Family**".

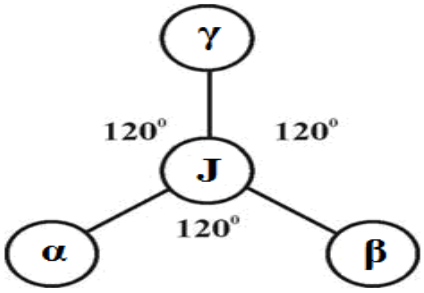

(3G RADIATION)

IV. CONCLUSION

It is focused that the philosophy of "**Thaimai**", "**Motherhood**" shall be considered as the act of symmetry of **Akkli-e particles** of "**Mother Universe**" (Region III of cosmos Universe) rather than getting the credit and "**title**" of Mother hood by delivering Jackfruit like baby in conventional Human Family. The philosophy of "**Thaimai**" shall means effort for PEACE & SUPER SYMMETRY for sustainability of **balanced Life** rather than give birth to child in broad sense.

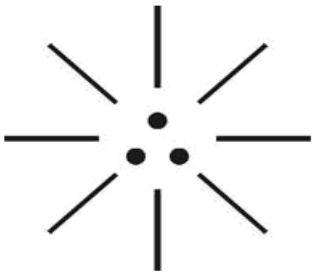

(SUPER SYMMETRY PEACE)

MOTHER TERESA IS WOMAN OR MOTHER?...

Mother Teresa (Full name: ANJEZE GONXHE BOJAXHIU) born in August 26, 1910, at SKOPJE, Republic of MACEDONIA, have become "**CITIZEN OF INDIA**" and dedicated her entire life at Calcutta, India for poor, depressed and suppressed population. She was awarded with Nobel peace prize, Bharat Ratna and other many multiple international awards and finally died on **05.09.1997** at Calcutta.

It is speculated by the author that she might have had **colour blindness** and could not distinguish whether blue, green, red, Hindu, Christian, Muslim and does not have **caste identity** with either **prefix or suffix** with name. It is further focused that the Philosophy of English word "**TERESA**" shall be considered as derived from prehistoric Tamil phonetic "**THIRI-e**". THIRI-e shall mean virgin light, Erai, Allah, Annai, Ammu, Ammoo, Amma, Amen.

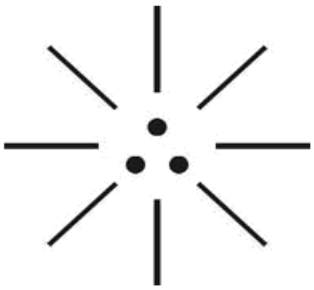

(THAI-e)

(KANNI-e)

(KOLKATTA MOTHER)

"PEACE BEGINS WITH A SMILE" – Mother Teresa

REFERENCE

[1] Intensive Internet "e-book" study through, Google search and wikipedia
[2] M.Arulmani, "3G Akkanna Man", Annai Publications, Cholapuram, 2011
[3] M. Arulmani; V.R. Hemalatha, "Tamil the Law of Universe", Annai Publications, Cholapuram, 2012
[4] Harold Koontz, Heinz Weihriah, "Essentials of management", Tata McGraw-Hill publications, 2005
[5] M. Arulmani; V.R. Hemalatha, "First Music and First Music Alphabet", Annai Publications, Cholapuram, 2012
[6] King James Version, "Holy Bible"
[7] S.A. Perumal, "Human Evolution History"
[8] "English Dictionary", Oxford Publications
[9] Sho. Devaneyapavanar, "Tamil first mother language", Chennai, 2009
[10] Tamilannal, "Tholkoppiar", Chennai, 2007
[11] "Tamil to English Dictionary", Suravin Publication, 2009
[12] "Text Material for E5 to E6 upgradaton", BSNL Publication, 2012
[13] A. Nakkiran, "Dravidian mother", Chennai, 2007
[14] Dr. M. Karunanidhi, "Thirukkural Translation", 2010
[15] "Manorama Tell me why periodicals", M.M. Publication Ltd., Kottayam, 2009
[16] V.R. Hemalatha, "A Global level peace tourism to Veilankanni", Annai Publications, Cholapuram, 2007
[17] Prof. Ganapathi Pillai, "Sri Lankan Tamil History", 2004
[18] Dr. K.K. Pillai, "South Indian History", 2006
[19] M. Varadharajan, "Language History", Chennai, 2009
[20] Fr. Y.S. Yagoo, "Western Sun", 2008
[21] Gopal Chettiar, "Adi Dravidian Origin History", 2004
[22] M. Arulmani; V.R. Hemalatha, "Ezhem Nadu My Dream" - (2 Parts), Annai Publications, Cholapuram, 2010
[23] M. Arulmani; V.R. Hemalatha, "The Super Scientist of Climate Control", Annai Publications, Cholapuram, 2013, pp 1-3

American Journal of Engineering Research (AJER)
e-ISSN : 2320-0847 p-ISSN : 2320-0936
Volume-03, Issue-03, pp-181-187
www.ajer.org

Research Paper Open Access

Software Theft Detection Using Birthmark Alg.

Dheeraj Kumar[1], Ms. Prince Marry[2]
[1]*PG Scholar (M.E. /CSE),* [2]*Faculty of computer science*
Department of Computer Science Sathyabhama University, Chennai, Tamil Nadu

Abstract: - Due to rapid development 0f internet technologies java script has become an important part of the software development process. Though the copy of java script program can be easily done and poses a serious threat to the intellectual property theft. In order to help protect and prove the ownership of the source code there are two technique such as software watermarking and software code obfuscation technique are being used. However watermarking needs extra effort to implement to prove ownership of the source code and it has been found that it can be defaced by a deliberate attempt, whereas code obfuscation makes the code hard to be understand by a human but does not prevent it from being copied. In this paper our attempt is to implement a considerably new technique called software birthmark to which takes the security of codes to another level. Birthmark technique is defined as the intrinsic characteristic of a source code and does not require any additional effort to implement. In order to implement birthmark we extend two recent birthmark that extract the birthmark at runtime.

Keywords: - *code theft detection, software birthmark, Software protection, Software code obfuscation.*

I. INTRODUCTION

Today I won't be wrong if i would say that we live in the era of information technology and due to the existence of web 2.0 and HTML5 it is more relevant to say that everything wat we can imagine can be done with the help of virtual environment i.e, internet. It has been found under various studies being conducted that today java script is proving to be one of the most popular programming language and will continued to be so. According to a survey conducted by Evans Data in the year 2008, it has been found that over 60% of the developers uses java script and that has outraged all scripting languages use, including Java[1]. However the codes of java script programs can be obtained very easily as it is an interpreted language and almost all browsers provide handful of methods to obtain the source code of the web page. This makes it very difficult to protest intellectual property right of the software developer.

Software security has already been a topic of interest for the computer scientist an will continue to be so. In order to protect and prove ownership of the software code their is a earliest and most popular technique being used called watermarking technique. It is an well-known and easiest technique used to detect software piracy. In this approach watermark is embedded into the source program which proves the ownership just like a signature [2]-[5]. However it has been found by studies that water marking can be defeated by a fairly deliberate attempt of a hacker [4]. However it requires an extra effort from the developer to embed watermark in the software prior to the release. Due to these reasons many developers avoid using watermarking and use code obfuscation technique before the release of their product. This technique is used to obfuscate codes which makes it difficult to understand by human in other words the original code is encrypted. code obfuscation is actually a semantics-preserving transformation of source code which makes it difficult to understand and reverse engineer [5]. Though it does not prevent the pirates from copying of the code.

There is another technique available which is relatively less popular but i believe is more powerful and handy for the software theft detection. This technique is called as birthmark. The term birthmark was first used by a computer scientist Derrick Grover in 1989. He explained birthmark as the intrinsic characteristic occurring in a program by chance which could be used to aid program identification. It was first used by IBM to sue the pirates for their PC-AT ROM by showing the register push and pooped pattern. As it is clear from the definition birthmark does not require any code being added to the program it depends solely on the intrinsic

characteristic of a program to determine similarity between two programs [6]-[13]. It was shown in [7] that a birthmark could be used to identify software theft even if watermark transformation is destroyed. According to Wang et al.[6] birthmark is unique characteristic a program possesses. To identify the software theft first the birthmark of the protected code is extracted and then the suspected program is compared against the birthmark if the search is found match then the suspected program has the high possibility that it is a copy of the original program. Birthmark can be looked under two categories i.e. static and dynamic birthmark. Static birthmark can be extracted from the syntactic structure of the program [10],[12],[13]. Whereas dynamic birthmark is extracted from the dynamic behaviour of the program at run-time [6]-[9],[11]. As we know that the technique like code obfuscation semantic-preserving transformation which only modifies the syntactic structure of a program but not the dynamic behaviour of the program, hence birthmark is more efficient and robust with respect to them.

However we know that birthmark is a better technique for securing software codes but still there is certain variations found in the to improve its performance. Earlier dynamic birthmarks made use of the complete control flow trace, the API call trace, or the system call trace obtained during the execution of the program [6]-[9],[11]. Birthmark based on these factors exhibits certain flaw such as birthmark based on control flow trace may still be exposed to the obfuscate attack as loop transformation. Similarly birthmark based on API call trace may suffer may suffer from the problem of not having enough system call to make unique identification. Recently, another technique to identify birthmark on the basis of run-time heap has been proposed [14],[15]. However evaluation of these birthmark is based on small number of tiny programs. Moreover birthmark comparison algorithm proposed in [14] does not scale up well and limits the size of birthmark. The graph isomorphism algorithm used in [15]makes birthmark vulnerable to reference injection attack.

This paper proposes a redesigned heap graph based birthmark algorithm for java script as well as the design code such as HTML, and JSP to make it a scalable and robust technique to detect software theft.

II. RELATED WORKS

There are many works has already been carried out on this topic in order to help insure and improve the performance of the birthmark selected. The works related to this topic are:

A. *Dynamic Path Based Software Water [4],this paper is mainly focused on the watermarking technique to provide security to the software codes. According to this paper the watermarking is done by inserting certain bit stream into the software code to make it identifiable but this paper has also introduced about the short falls of the watermarking technique and described how it can be destroyed by deliberate attempt of the attacker. This paper introduces path-based watermarking, which is a new approach to software watermarking based on the dynamic branching behaviour of a program. Experimental results, using both Java byte code and IA-32 native code, indicate that even relatively large watermarks can be embedded into programs at reasonable cost.*

B. *Detecting Software Theft via Whole Program [7],According to this paper Every rule of the grammar is constructed by a non-terminal and a series of symbols which the non-terminal represents. To create DAG, a node is added for every unique symbol. For every rule an edge is added from the non-terminal to each of the symbols it represents. The DAG is the Whole Program path.. The WPP birthmark is built i similar manner as The WPP with the exception of the DAG in the stage. As our interest lies in regularity only hence we eliminate all terminal nodes in the DAG. It is the internal nodes which will be more difficult to modify through program transformation.*

C. *A Dynamic Birthmark for Java[8], this paper deals with the issues related with the creation of birthmark for java codes. As we know that java has been a widely accepted language used for coding by most prominent companies. same has been the reason for the concern for them as they believe code as the important resource of their organisation and consider code as a core asset. A birthmark can help them to detect code theft by identifying intrinsic properties of a program. Two programs with the same birthmark are likely to share a common origin. Birth marking works in particular for code that was not protected by tamper-resistant copyright notices that otherwise could prove ownership. We propose a dynamic birthmark for Java that observes how a program Uses objects provided by the Java Standard API. Such a birthmark is difficult to foil because it captures the observable semantics of a program. In an evaluation, our API Birthmark reliably identified XML parsers and PNG readers before and after obfuscating them with state-of-the-art obfuscation tools. These rendered existing birthmarks ineffective, such as the Whole-Program-Path Birthmark by Myles and Collberg.*

D. *Dynamic Software Birthmarks to Detect the Theft of Windows Applications [11], This paper introduces dynamic software birthmarks which can be obtained while execution of Windows applications. Birthmarks are unique and native characteristics of software. For a pair of software p and q, if q has the same birthmarks as p's, q is suspected as a copy of p. security analyse of this paper shows that the proposed birthmark possess good result against different types of program transformation attacks.*

There are many other works being carried out in order to enhance and increase the robustness and performance of the birthmark algorithm.

III. EXISTING SYSTEM

For the purpose of insuring the integrity and security of the software codes mainly there are two techniques being used such as software watermarking and code obfuscation. Where as another relatively new technique being used and has become a matter of huge research among the computer scientist is birthmark. Software birthmark algorithm is getting huge acceptance and still a lot of work is still required to be carried out to make it more robust.

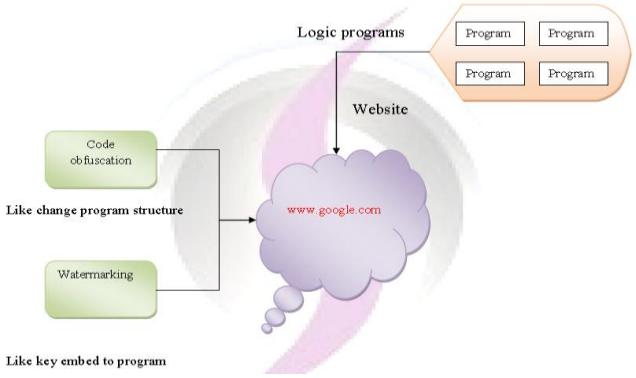

Fig 2. Existing system with watermarking and code obfuscate algorithms.

The problem existed with the existing system was that there were no guarantee that the system was full proof and and requires extra effort in order to implement.

IV. PROPOSED SYSTEM

Here in this paper we propose a relatively new technique called birthmark technique. Here in our proposed system we extend two types of birthmark i.e., static and dynamic birthmark.

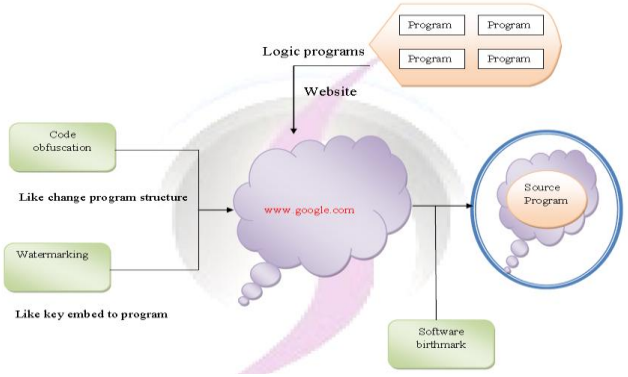

Fig 1. Proposed system with birthmark algorithm used.

A. Software birthmark:

It is a group of unique characteristics obtained from a program. software birthmark can be divided into two categories: static birthmark and dynamic birthmark.

Definition 1: Dynamic Birthmark: dynamic birthmark is defined as the unique characteristics obtained by chance by a program at runtime.

Let two a and b be two program components and let I be an input given to the programs a and b. Now let f(a, I) be the dynamic birthmark of program a if and only if the two of the conditions are satisfied:

1) f(a, I) comes out only when p is executed with input I.
2) Program a is copy of b if a=>f(a, I) = f(b,I).

B. Subgraph Monomorphism:

Definition 2: A graph monomorphism from a graph G=(N,E) to a graph G' = (N', E') is a bijective function f(N) -> N' such that (u,v) belongs to E=>(f(u),f(v)) belongs to E'.

V. V. **SYSTEM DESIGN**

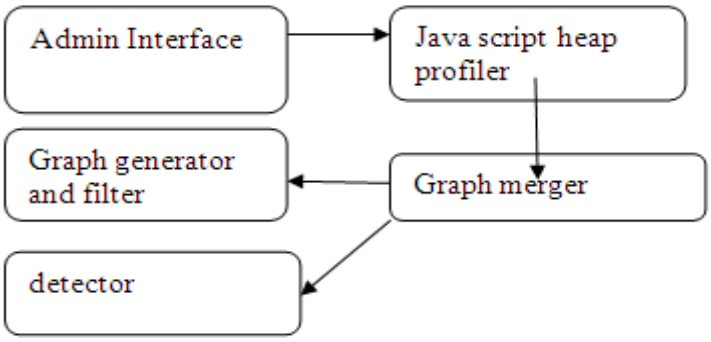

Fig 3. System design with modules.

Fig 3 shows the complete design module of our proposed system. It outlines the steps that original program and the suspected program undergoes in our system.

A. Admin Interface Design: in our proposed system admin interface module is one of the important part. It gives interface to the user and also provides primary level security by checking the authenticity of the user. Admin interface design is basically used as the normal user login authentication purpose. It also provides the admin and normal user access to the teo separate windows with the relevant capability.

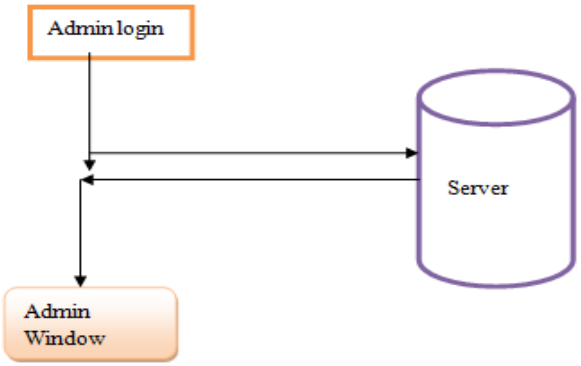

Fig. 4 Admin Interface Design.

B. ***Java Script Heap Profiler:***

Java script heap profiler in our paper is another module where the java script codes are stored. Being an interpreted language we know that java script allows for the creation of objects at anytime. And on the other shide we know that java script heap keeps changing due to the creation of object and garbage collection but abter some time it has been found that hai peap of the java script becomes constant.

Therefore to exploit full benefit of the behaviour of the heap , we try to obtainevery object that occurs in the heap.there for we use java heap profiler in our system.

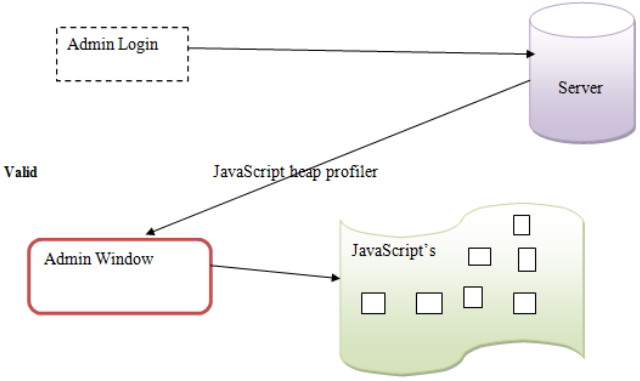

Fig 5. Java Script Heap Profiler

The fig5 shows the structure and the worke flow of the java script heap profiler module.

C. Graph Generator And Filter:

Graph generator and filter is another important module in our system which is mainly used for providing the security of the code.infact graph generator and filter is a module where code obfuscation is implemented to make the software pirates difficult to understand the code. Here symentic preserving transformation is being used which transforms the original code with the encrypted code but it does not have any effect on the runtime behaviour of the program.

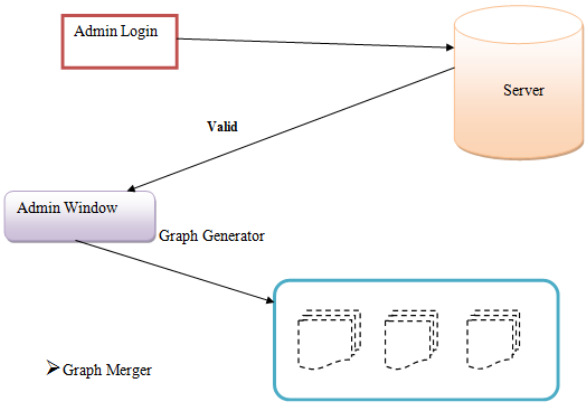

Fig6. Graph Generator And Filter.

We perform a death first search traversal of and print out the heap graph with nodes and edges that pass a filter. We describe such a filter in details as follows.

Objects in the V8 JavaScript heap are divided by six categories: *INTERNAL*, *ARRAY*, *STRING*, *OBJECT*, *CODE*, and *CLOSURE*. We need not to include in our heap graph objects which comes under *INTERNAL*, *ARRAY*, *STRING*, and *CODE* categories. Because the design decision are as follows: *INTERNAL* objects are virtual objects fand are used for housekeeping purpose which can not be accessed from the program code. *Array* objects, represent an array of elements objects. Though, our observation says that arrays are actually represented by an object of the type *OBJECT* with name "*Array*" and the references from the array are coming out from that object. Hence, *ARRAY* objects are also not included. *STRING* and *CODE* objects, we do not find any reference coming out of them. Hence, they are excluded as well. To count up, we only include *OBJECT* and *CLOSURE* objects in our heap graph.

References between objects in the V8 JavaScript heap are divided into 4 categories: *CONTEXT_VARIABLE*, *ELEMENT*, *PROPERTY*, and *INTERNAL*. We do not include references that belongs to *CONTEXT_VARIABLE* and *INTERNAL* categories. The reasons behind this design decision are as follows: *CONTEXT_VARIABLE* is a variable in a function context, accessible by its name from inside a function closure.Therefore, it is not accessible by objects outside that function and it is automatically created by V8 for housekeeping purpose. *INTERNAL* references are properties added by the JavaScript virtual machine. They are not accessible from JavaScript code. Therefore, we only include in our heap graph *ELEMENT* and *PROPERTY* references. *ELEMENT* references are regular properties with numeric indices, accessed via [] (brackets) notation and *PROPERTY* references are regular properties with names, accessed via the . (dot) operator, or via [] (brackets) notation. There are some objects created by the JavaScript engine that exist not just for one program. For example, the *HTML Document* object can be found in the heap graphs of all the JavaScript programs we studied. Therefore, we need to filter such objects out as they dilute the uniqueness of the heap graph. Basically, the filtered objects include objects created to represent the DOM tree and function closure objects for JavaScript built-in functions.

D. Graph Merger:

Graph merger is another module in our system which is basically implemented in order to show verify the result of the project. Graph merger is the module which is basically used in another application such as in the suspected program which is used to reconstruct the original code from the obfuscated code which is obtained as the output of the graph merger and filter. unique ID is assigned to every object in the JavaScript heap by the V8 JavaScript engine. However, the ID of an object is fixed even after the multiple dumps and therefore, can be used to identify the object. The Graph Generator and Filter also uses every node in the heap graph with its object

ID. Hence, we can tell whether or not two nodes in two heap
graphs points to the same object. The graph merger takes multiple heap graphs as input and which is basically the output from graph generator and outputs a one single graph that includes all the nodes and edges appearing in the input heap graphs. The algorithm of graph merger is shown in
Algorithm 1.
Algorithm 1 Calculate single graph of a set of labeled
connected graphs
Require: connected graphs , labeling
function where and is a positive integer
Ensure: is connected and is a superimposition of
graphs in G with labeling function where
and is a positive integer
for all where **do**
if where **then**
Combine mapping and
end if
end for
In short, it merges all all the graphs one by one by
taking the union of the nodes and edges of the two graphs
being merged. In order to make the resulting single graph also connected, we need to ensure that there should be at least
one object in common (with the same object ID) in two graphs
before merging them.

E. Detector:

The detector takes the sub graph from the original program and the entire heap graph of the suspected program as inputs and checks whether the selected sub graph of the original program can be found in the heap graph of the suspected program. Similar to the the sub graph selector, it takes sub graph of the objects under the Window objects from the suspected program and uses sub graph monomorphism to check whether the sub graph of the original program is present in suspected program. Once there is a match found, the detector raises an alert and reports where the match is found.

VI. CONCLUSION

In order to discuss the performance of the work carried out in this paper we created two prototype of the java application and we checked the result on about 200 wesites and found much improved results whith almost zero false-positive output. We believe that the system proposed is best to our knowledge and can be implement to be used with effective results.

VII. FUTURE WORK

In this section we want to discuss the sections we wish we could do something better in order to improve the results.
1). *Improved Graph Selector:* Currently, we are using the largest object subgraph as the birthmark of our program. As of now we do not know if there exists a good way then this to do it. One primary idea can be of using frequent subgraph mining which gives the frequent subgraph which appears in all the heap graphs we extracted from the program. This can make the birthmark more lively and effective of the program. Though, the running time
of frequent subgraph mining on large graphs is slow and there should be some performance tuning in order for it to be practical.
2) Faster Detector: Due to the theoretical running time limit of graph monomorphism algorithm we used in our detector, we need to limit the size of the heap graphs in order to control the running time of the detector.
3) Implementation in design codes: currently in our prototype we implement birthmark on the java script codes but we believe that the design codes such as JSP,HTML are equally important.

REFERENCES

[1] E. Data, JavaScript Dominates EMEA Development Jan. 2008 [Online]. Available: http://www.evansdata.com/press/viewRelease. php?pressID=127
[2] C. Collberg and C. Thomborson, "Software watermarking: Models and dynamic embeddings," in *Proc. Symp. Principles of Programming Languages (POPL'99)*, 1999, pp. 311–324.

[3] A. Monden, H. Iida, K. I.Matsumoto, K. Inoue, and K. Torii, "Watermarking java programs," in *Proc. Int. Symp. Future Software Technol.*, Nanjing, China, 1999.
[4] C. Collberg, E. Carter, S. Debray, A. Huntwork, J. Kececioglu, C. Linn, and M. Stepp, "Dynamic path-based software watermarking," in *Proc. ACM SIGPLAN 2004 Conf. Programming Language Design and Implementation (PLDI '04)*, New York, 2004, pp. 107–118, ACM.
[5] C. Collberg, C. Thomborson, and D. Low, A Taxonomy of Obfuscating Transformations Tech. Rep. 148, Jul. 1997 [Online]. Available: http://www.cs.auckland.ac.nz/~collberg/Research/Publications/ Collberg ThomborsonLow97a/index.html
[6] X. Wang,Y.-C. Jhi, S. Zhu, and P. Liu, "Behavior based software theft detection," in *Proc. 16th ACM Conf. Comput. and Commun. Security (CCS '09)*, New York, 2009, pp. 280–290, ACM.
[7] G.Myles and C. Collberg, "Detecting software theft via whole program path birthmarks," in *Proc. Inf. Security 7th Int. Conf. (ISC 2004)*, Palo Alto, CA, Sep. 27–29, 2004, pp. 404–415.
[8] D. Schuler, V. Dallmeier, and C. Lindig, "A dynamic birthmark for java," in *Proc. 22nd IEEE/ACM Int. Conf. Automated Software Eng. (ASE '07)*, New York, 2007, pp. 274–283, ACM.
[9] H. Tamada, K. Okamoto, M. Nakamura, A. Monden, and K. I. Matsumoto, Design and Evaluation of Dynamic Software Birthmarks based on API Calls, Nara Institute of Science and Technology, Tech. Rep., 2007.
[10] H. Tamada, M. Nakamura, and A. Monden, "Design and evaluation of birthmarks for detecting theft of java programs," in *Proc. IASTED Int. Conf. Software Eng.*, 2004, pp. 569–575.
[11] H. Tamada, K. Okamoto, M. Nakamura, and A. Monden, "Dynamic software birthmarks to detect the theft of windows applications," in *Proc. Int. Symp. Future Software Technol.*, Xian, China, 2004.
[12] G. Myles and C. Collberg, " -gram based software birthmarks," in *Proc. 2005 ACM Symp. Appl. Computing (SAC '05)*, New York, 2005, pp. 314–318, ACM.
[13] H. Tamada, K. Okamoto, M. Nakamura, A. Monden, and K. I. Matsumoto, Detecting the Theft of Programs using Birthmarks, Graduate School of Information Science, Nara Institute of Science and Technology, Tech. Rep., 2003.
[14] P. Chan, L. Hui, and S. Yiu, "Jsbirth: Dynamic JavaScript birthmark based on the run-time heap," in *Proc. 2011 IEEE 35th Annu. Comput. Software and Applicat. Conf. (COMPSAC)*, Jul. 2011, pp. 407–412.
[15] P. P. F. Chan, L. C. K. Hui, and S.M. Yiu, "Dynamic software birthmark for java based on heap memory analysis," in *Proc. 12th IFIP TC 6/TC 11 Int. Conf. Commun. and Multimedia Security (CMS'11)*, Berlin, Heidelberg, 2011, pp. 94–106, Springer-Verlag.
[16] P. C. Team, Prototype JavaScript Framework [Online]. Available: http://prototypejs.org/
[17] V. Proietti, Mootools JavaScript Framework [Online]. Available: http://mootools.net/
[18] Google Chromium Project [Online]. Available: http://code.google. com/chromium/
[19] Google v8 JavaScript Engine [Online]. Available: http://code.google.com/p/v8/
[20] VFLib [Online]. Available: http://www-masu.ist.osaka-u.ac.jp/~kakugawa/ VFlib/
[21] Content Scripts [Online]. Available: http://code.google.com/chrome/ extensions/content_scripts.html
[22] Jasob 3 [Online]. Available: http://www.jasob.com/
[23] L. Cordella, P. Foggia, C. Sansone, and M. Vento, "Performance evaluation of the vf graph matching algorithm," in *Proc. Int. Conf. Image Anal. and Processing*, 1999, pp. 1172–1177.
[24] M. Sosonkin, G. Naumovich, and N. Memon, "Obfuscation of design intent in object-oriented applications," in *Proc. 3rd ACM Workshop on Digital Rights Manage. (DRM '03)*, New York, 2003, pp. 142–153, ACM.

American Journal of Engineering Research (AJER)
e-ISSN : 2320-0847 p-ISSN : 2320-0936
Volume-03, Issue-03, pp-188-196
www.ajer.org

Research Paper Open Access

Inline Array Jet Impingement Cooling Using Al_2O_3 / Water Nanofluid In A Plate Finned Electronic Heat Sink

R. Reji Kumar [1], Nigussie Mulugeta[2]
[1,2]*Department of Mechanical Engineering Bahirdar University, Bahirdar, Ethiopia.*

Abstract: - Jet impingement cooling is a technique used for cooling the electronic systems. In this work, heat transfer and pressure drop characteristics of deionized water and Al_2O_3/water nanofluid in an electronic heat sink having aluminium plate fins and provision for jet impingement cooling have been studied. A novel heat sink contains two rows of plate fins of size 29mm x 24mm x 0.56mm. A thin plate having 110 holes of diameter 2.5 mm is used to produce number of jets. The plate is kept inside the heat sink in such a way that H/d_n is 5.2 mm and adjacent jet spacing is 2mm. The overall dimension of the heat sink is 60x60x 65 mm. For this work we prepared a Al_2O_3/water nanofluid by dispersing specified quantity of nanoparticles in to deionized water by using a ultrasonic bath. Experiments were conducted under constant heat flux condition and the volume flow rate of the fluid was in the range of 1.315 to 2.778. It is found from the results that the nanofluid removes heat better than water in the jet impingement cooling with very low rise in pressure drop.

***Keywords*: -** *Jet impingement, Nanofluid, Heat transfer, Pressure drop, Heat sink*

I. INTRODUCTION

The electronic systems of today are embedded with large number of minute circuits which makes it more compact and faster in processing speed. Thus it consumes a large amount of power, as a result the heat flux generated is high. These heat fluxes should be dissipated in a proper manner completely as fast as possible. Otherwise the heat thus generated will harm and affect the performance of the system and even may damage it. Conventionally we use forced air and water cooling technique, but this cannot satisfy the increasing cooling requirement in the future. So in order to increase the cooling requirement and miniature the heat exchangers research on nanofluid is still going on from the past decade. The reason behind to keep an eye on this investigation is that it is the next generation heat transfer fluid. The heat transfer capabilities of these nanofluids are higher than that of their base fluid.

Nanofluid is a fluid containing nano sized particles known as nano particle. These fluids are engineered colloidal suspensions of nano particles in a base fluid. The nano particle is defined as a smallest object that behaves as a whole unit in terms of transport and properties. Nano fluids have novel properties that make them potentially useful in many application in heat transfer, including micro electronics fuel cells, pharmaceutical processes, hybrid powered engines, engine cooling /vehicle thermal management, domestic refrigerator chiller, heat exchanger, nuclear reactor coolant in grinding, machining, in space technology , defense and ships and in boiler flue gas temperature requisition they exhibit enhanced thermal conductivity and convective heat transfer coefficient compared to the base fluid.In analysis such as computational fluid dynamics (CFD), nanofluids can be assumed to be a single phase fluid, classical theory of single fluids can be applied, where physical properties of nanofluid is taken as a function of properties of both constituent and their concentrations. There are many different types of nanofluids that can be made by using different nano particles and base fluid combinations. Some of the most common nanoparticles used are Alumina Oxide (Al_2O_3), Copper Oxide (CuO), Zinc Oxide (ZrO_2), and SilicaOxide (SiO_2). The most common base fluids used for nanofluids are de-ionized water, oil and ethylene glycol.

All nanofluids follow a basic preparation technique. Once the desired weight or volume fraction has been determined, the nanoparticles are added into the base fluid and mixed. Mixing is usually done by ultrasonication to avoid settling of the particles. The amount of time spent mixing the nanofluids depends on the many factors such as the ratio of base to nanoparticles, how long the experiment will last, and the weight or

volume fraction used. It's been shown that nanofluids in general have better heat transfer properties than the base fluid alone, specifically better thermal conductivity and heat transfer coefficient. These heat transfer properties theoretically should make nanofluids ideal for phase change heat transfer processes. These enhancements have been researched using experiments such as the transient hot wire method, pool boiling, spray cooling and impinging jet.

The transient hot wire method is a transient dynamic technique where the temperature rise of a sample is measured at a defined distance from a heat source. The hot wire is assumed to have a uniform heat output along its length and the thermal conductivity of the sample can be calculated from the temperature change of the sample over a known time interval. Pool boiling is the process in which vapor is created at the liquid-surface interface by a surface heated above the saturation temperature of the bulk fluid. The motion of the vapor and the surrounding fluid near the heated surface is due to buoyancy forces. As vapor escapes the surface, liquid comes in to fill the void and this process removes heat from the heated surface. Another method that utilizes the impingement of a working fluid onto a heated surface is spray cooling. During spray cooling the pressure difference between the nozzle and the environment is sufficient to create droplets of the working fluid and those droplets impinge the surface to remove heat.

Impinging jet research is another way to study the effects that nanoparticles have on the heat transfer coefficients of the base fluids. A nozzle is used to spray a jet of fluid onto a heated surface to enhance the heat transfer coefficients for convective heating, cooling or drying.

Jet impingement technique is one of the passive methods of convective heat transfer. The jet impingement cooling can be classified into two types. The first type is the submerged jet and the second type is the free surface jet.

In submerged jets, the jet from the nozzle gets injected into the same fluid at the same state. In free surface jet, the jet from the nozzle passes through gaseous atmosphere before impinging the target zone. This investigation work deals with free surface jet impingement cooling. Here arrays of numerous jets are made to impinge a heat sink which has large number of plate fins. The convective heat transfer in this type of cooling is based on the jet impingement velocity, adjacent jet distance to jet diameter (S/d_n), number of jets (n), distance between two rows of jet, jet diameter(d_n), target distance to jet diameter (H/d_n), Reynolds number (R_e),Prandle number (P_r) and physical geometry of heat sink. It is to be noted that the heat extracted by the working fluid should be uniform because temperature non uniformities in the heat sink make it to suffer mechanical stress which leads to permanent or temporary damages. The damage is bending of heat transferring surface makes air to fill which reduces the heat transferring capability very much. Thus the performance of the electrical system is affected due to less heat dissipation. So the temperature uniformity is a vital factor which should be considered while designing a jet impingement cooling with heat sink.

II. LITERATURE REVIEW

The term nanofluid was proposed by Choi in 1995 of Argonne National Laboratory, U.S.A [1]. He stated that "Fluid with nanoparticles suspended in them are called nanofluids". Later many researches are conducted on the properties of nanofluid and to enhance the heat transfer rate using these fluids and it is still going on. Xiang-Qi Wang et al [2] have prepared a paper which gives on overview of the recent developments in the study on heat transfer using nanofluids. This paper obviously shows the various investigations on thermal conductivity, viscosity, convective heat transfer and boiling heat transfer. This also provides clear information about the theoretical investigation of mechanisms of nanofluids, thermal conductivity and numerical investigations. Womac et al [3] have correlated equations for confined submerged and free surface jet impingement cooling with jet diameter 0.513mm, arrays of 2×2 and 3×3 with various jet to jet spacing. He found that by decreasing the distance of jet to jet spacing the heat transfer rate can be enhanced for free surface jets he also explains that the heat transfer can be enhanced by increasing the velocity of jet by raising the volumetric flow rate keeping the d_n and N as constant. He pointed out that the heat transfer doesn't depend on jet to target spacing ranges on $5 \leq H/d_n \leq 10$. In case of confined submerged liquid jet arrays. There is no serious effect in heat transfer coefficient for jet to target spacing lies on $2 \leq H/d_n \leq 4$. D.Y Lee and K.Vafoi [4] performed comparative studies of jet impingement and micro channel cooling. Obviously, the result showed jet impingement cooling is for longer target and micro channel for smaller target. Fabbri and Dhir [5] made an investigation on free surface micro jet arrays using water and FC40 as working fluid. They selected the jet diameter ranges $65\mu_m \leq d_n \leq 250\mu_m$and the Reynolds number ranges $73 < R_e d_n < 3813$. The investigation shows heat transfer coefficient increases with increase in R_e and P_r as well as in S/d_n. The result was that the heat transfer can be enhanced using micro jet arrays than using a convectional jet arrays. It was found that a maximum heat transfer can be obtained by using an optimum of $75\mu_m$ jet diameter with 5mm as jet interspacing distance.

B.Sagot et al [6] investigated experimentally the jet impingement heat transfer using air on a flat plate maintained at a constant wall temperature. The result reveals that the average Nusselt number (N_u) at constant wall temperature condition is a function of jets Reynolds number (R_{ej}), geometrical parameters (R/D, H/D) and

dimensionless viscosity ratio (μ_j/μ_ω). Brain P.Whelon et al [7] conducted on experiment for determining the nozzle geometry effects in liquid array impingement heat transfer. He used a square array of 45 jets of fixed 1mm diameter, fixed jet interspacing of 5mm and six different nozzle geometries were investigated. Here the jet is made to impinge a circular copper surface with a nominal heat flux of 25.66W/cm^2 and its diameter is 31.5mm. The result shows that by chamfering and contouring the nozzle inlet and outlet increases the heat transfer coefficient, at the same time reduces the pressure drop across the nozzle. AkhileshP. Rallabandi et al [8] have conducted an experiment on heat transfer and pressure loss using jet impingement and channel flow method. He used copper plate as test section with inline and staggered rib condition. The result shows the use of inline rib causes 50% to 90% increase in heat transfer in jet impingement as well as in channel flow method.
Terri B.Hoberg et al [9] have proved heat transfer co-efficient of about 900W/m^{2}k can be achieved using a compact staggered array pattern over an area of 8.5cm^2 with an inter jet spacing of 2.34 jet diameters. Jerome Barrae et al [10] made on experimental study of a new hybrid jet impingement / micro channel cooling scheme for improving the temperature uniformity of the heat sink. In this micro channels of depth 0.5mm and width varies from 3.5mm to 0.5mm is used. The result showed that this geometry enhances the heat transfer coefficient as well as uniform distribution of temperature over the surface of heat sink. Paisarn Naphonand Somachai Wongwises [11] have done on experimental investigation on jet impingement heat transfer for central processing unit of PC. They used deionized water as their working fluid and fabricated a rectangular fin heat sink in copper. The experiment was tested with channels of three different widths and the result showed reduction in processor temperature than other cooling methods. Mangosh Chaudhari et al [12] made on experiment on multiple orifice synthetic jet for improving the impingement heat transfer. He conducted experiments for different configuration with a center orifice surrounded by multiple satellite orifices. The result showed that upto 30% more heat transfer coefficient is obtained in multiple orifice synthetic jet compared to single orifice jet. S.Suresh, et al [13] have presented the effect of AL_20_3-Cu /water hybrid nanofluid in heat transfer which is carried out in a straight horizontal copper tube of 1000 mm long, 10mm ID and 12mm OD test section with constant heat flux. The result shows that the heat transfer performance is amplified with an average increase in Nusselt number of 10.94% also the convective heat transfer coefficient increases with increasing Reynolds number, but there is an average increase in friction factor of about 16.97% compared to water.

The current study is to determine the effectiveness of alumina nanofluids for dissipating heat from a plate finned heat sink using a inline array jet impingement cooling scheme. The data collected is compared to de-ionized water at the same volume flow rate and distance from the surface. A mass concentrations of 0.1% alumina nanofluids will be compared with de-ionized water to establish a relationship for heat transfer coefficients, interface temperature and pressure drop with volume flow rate. Other parameters can have an effect on the effectiveness of jet impingement cooling, such as the flow temperature at the inlet of the flow regime. Therefore, for the effective investigation of heat transfer study in alumina-water nanofluids the inlet flow temperature is recorded initially before heating takes place and it should be maintained constant till the end of the experiment.

III. SPECIFICATIONS

3.1 Specification of alumina particles

- Size of the particle - 50nm
- Shape of the particle - near spherical
- Density - 3800 kg/m^3
- Thermal conductivity - 40 W/mK
- Specific heat - 773 J/kgK

3.2 Specification of Al_2O_3/water nanofluid

- Density - 1002.8 kg/m^3
- Thermal conductivity - 0.6148 W/mK
- Specific heat - 4174.06 J/kgK

IV. EXPERIMENTAL SETUP AND PROCEDURE

4. 1. Preparation of nanofluid

The preparation of nanofluid includes the production of nano sized particles and dispersing it into the base fluid. The two techniques used to produce nanofluids are single-step method and two-step method. For the preparation of aluminium oxide particles two-step method is more suitable. In the current study aluminium oxide of 0.1% mass concentration is used and the reason for choosing alumina is that it's widely known thermal properties and easy dispersion. The aluminium oxide nanoparticles are purchased from a commercial trader. The

properties of the nanofluid are average particle size = 50nm, density = 3800kg/m^3, thermal conductivity = 40 W/mK, specific heat 773 J/kgK. The required volume fraction of 0.1% was prepared by dispersing the specified quantity in de-ionized water using an ultrasonic bath and sonication was done for 6 hours. This ultrasonic vibrator generates ultrasonic pulses in the power 180 W at 40 KHz. The stability of dispersion is determined by measuring its pH value and it is found around 5.5, which is far from iso-electrical point. Thus the Al_2O_3 nanoparticle in water is more stable. The visual inspection after 10 days showed Al_2O_3 nanoparticles maintained good dispersion with water.

The density of the nanofluid was determined from Pak and Cho equation[14].

$$\rho_{nf} = \rho[1+k_p\emptyset] \quad (1)$$

The specific heat of the nanofluid was determined from Xuan and Roetzel's equation [15].

$$C_{pnf} = Cp\left[\frac{1+kc\emptyset}{1+kp\emptyset}\right] \quad (2)$$

The thermal conductivity of the nanofluid was determined from Maxwell equation [16].

$$k_{nf} = k[1+k_k\emptyset] \quad (3)$$

The thermo physical properties of the nanofluid are density = 1002.8 kg/m^3, specific heat = 4801.68 J/kgK and thermal conductivity = 0.6148 W/mK.

4.2. Fabrication of test block

Fabrication of test block starts with shearing the sheet metal and bending it into the required cubical shape. Here a sheet metal of aluminium with a thickness of 1mm is used to fabricate the cover of the test block. The dimension of the heat sink is 60mm×60mm×42mm. It is also made up of aluminium. The heat sink has plate fins with a central flow channel.

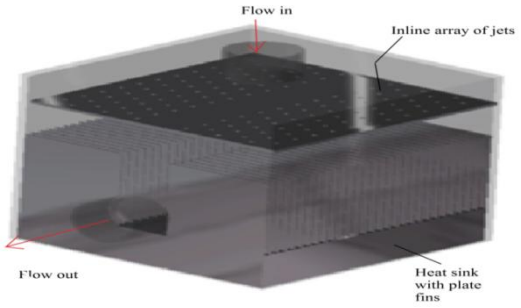

Figure.4.1. Test block

The dimension of the plate fin is 29mm x 12mm x0.56mm. Its thickness is assumed to be negligible. The total number of fins used is 56 and they are arranged in the form of 28 rows and 2 columns with a central flow channel. The fin to fin spacing is about 1.64mm and the channel width is 12mm. The central flow channel helps for the quick excitation of working fluid in order to prevent pool formation. A perforated plate with inline array pattern of jets are kept above the heat sink at a distance of 13mm, the inlet is provided at the top of the test block and two outlets are provided of either side of the central flow channel. The diameter of the inlet and outlet pipe is 13.5mm. The test block is sealed with epoxy compound to prevent the leakage losses.

4.3. Fabrication of heating block

The heating block is a solid aluminiun block. The dimensions of the heating block are 60mm x 60mm x 80mm. A central hole of 5mm diameter is drilled at the center of the heating block. Inside this a heating coil of 150 W is inserted as a tight press fit without any clearance. Another two holes of 2mm diameter on either side of the central hole is drilled to insert the thermocouple. Teflon is coated around the thermocouple to prevent the heat losses around the sides. The heating block is well insulated using polyurethane foam and styrofoam. As these insulating materials have very low thermal conductivity and the heat losses through the side walls can be neglected. Thus one dimensional heat transfer can be obtained in the heating block.

4.4. Acquisition system

The acquisition system is to get data for the heat transfer studies from the heat sensing devices. The acquisition system includes a data logger with a computer system and a temperature display devices. The computer system as a display element is connected to a data logger using a USB connector. This data logger gets data about the fluid flow temperature at the inlet and outlet of the regime. The flow temperature is sensed

by a RTDs and the leads are connected to the data logger. Based on the difference in temperature its resistance value changes, the corresponding change is converted into electrical signal in the data logger.

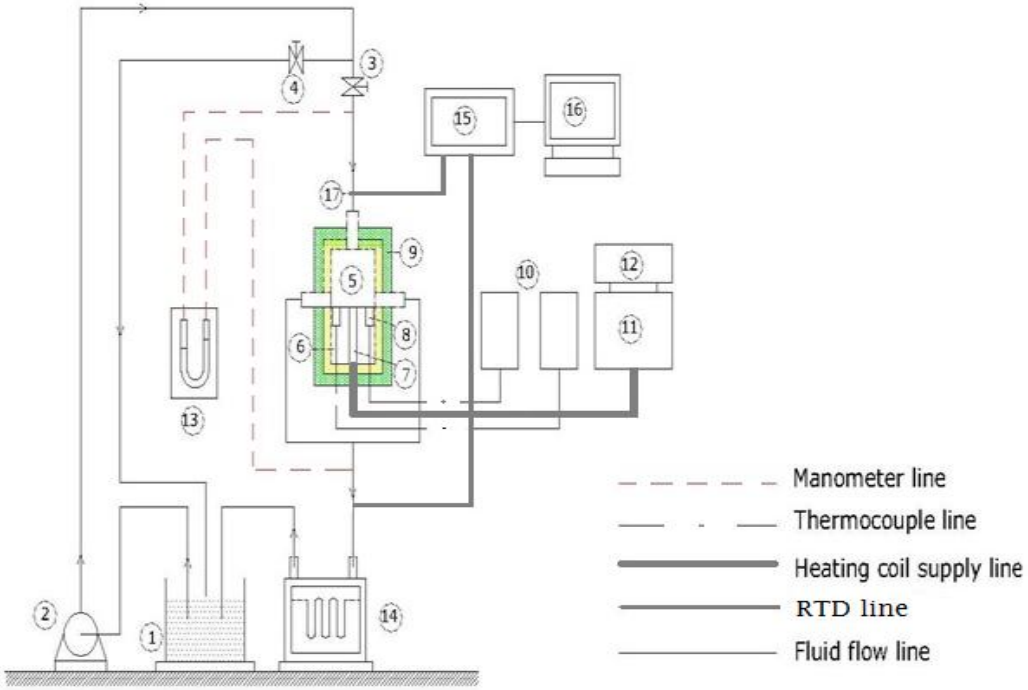

1.Storage tank
2.Circulating pump
3.Flow control valve
4.Bypass valve
5.Test block
6.Heating block
7.Heating coil
8.Thermocouple
9.Insulator
10.Digital temperature display device
11. Auto Transformer
12.Power supply
13.U-Tube manometer
14.Radiator
15.Data logger
16.Computer system
17. RTD

Figure.4.2. Experimental setup

The thermocouple is used to determine the interface temperature. The thermocouple used here is of k-type. The material combination in k-type thermocouple is alumal and chrome. The end leads of the thermocouple are connected to the digital temperature display devices. When there is a change in temperature a small current in the range of milli amps flows through this thermocouple and its value is displayed in the display devices.

4.5.Experimental procedure

Both the test block and heating block are well insulated using polyethylene and neoprene foam mixture and also with styrofoam. A thermal compound is applied at the interface of the heating block and the test block. The inlet and outlet temperatures of the working fluid are measured using RTDs. Data acquisition system such as data logger and digital temperature display devices are used to visualize the temperature obtained. The inlet line is connected to a peristaltic pump and exit to the storage tank through a radiator. The pressure drop between the inlet and exit is measured using U-tube manometer. Power of about 120 watts is supplied to the heating coil through an auto transformer.

After inspecting all the connection switch on the pump. Initially a blow down is done to remove all the dust and impurities then measure the temperature of the fluid. This temperature is taken as inlet temperature of the working fluid forever. Switch on the auto-transformer to energize the heating coil. After stability prevails for a certain volume flow rate, the interface temperature and fluid inlet and outlet flow temperatures are measured and noted from the data acquisition systems. The corresponding pressure drop value is also measured for every change in mass flow rate by noting the difference in mercury level in the manometer limb. The experiment is repeated by changing the mass flow rate for about five times. Calculate the heat transfer coefficient, Nusselt number and pressure drop using the formulae listed in the data reduction part to find out the effectiveness of the jet impingement cooling using alumina nanofluid.

V. THEORETICAL CONSIDERATION

Total heat $Q = Q_{in} - Q_{loss}$ (4)

Where

Q_{in} = Input heat supplied by cartridge heater

Q_{loss} = heat loss from the heated and water blocks assembly

Heat flux,

$$q'' = \frac{Q}{A} \quad (5)$$

A = Exposed heat transfer area of the water block.

The average of the measured interface temperatures (T_i), bulk mean temperature of the inlet and outlet fluids and heat flux are used to calculate the heat transfer coefficient of the water block as given in Eqn (6). The interface temperature is calculated as the average of the two temperatures measured at the interface of two different locations of the heater and water block.

$$h_w = \frac{q''}{(Ti - Tfm)} \quad (6)$$

Where T_{fm} is the bulk mean temperature of the fluid.

Reynolds number is calculated using the following equation.

$$Re = \frac{4m}{\pi \mu Di} \quad (7)$$

The Nusselt number is then calculated as,

$$N_u = \frac{hDi}{k} \quad (8)$$

Pumping power $= \dot{V} \Delta p$ (9)

VI. TABULATION

Table .6.1 Tabulation for de-ionized water

Sl. No	VFR (lpm)	$T_{i\,1}$ ^0C	$T_{i\,2}$ ^0C	$T_{i\,avg}$ ^0C	$T_{f\,in}$ ^0C	$T_{f\,out}$ ^0C	T_{fm} ^0C	h (w/m^{2}k)	Nu	Δp (Pascal)
1	1.315	44.6	42	43.3	32.6	33.1	32.85	57.3854277	1.26379	1200.74
2	1.614	43.9	41.4	42.65	32.6	33.4	33	122.036111	2.687582	1467.576
3	1.944	43.8	41	42.4	32.6	33.6	33.1	190.649411	4.198641	2001.24
4	2.454	43	40.1	41.55	32.7	33.8	33.25	296.627429	6.532578	2801.736
5	2.778	42.7	39.6	41.15	32.7	33.9	33.3	387.316489	8.529808	3335.4

Table.6.2 Tabulation for nanofluid

Sl. No	VFR (lpm)	$T_{i\,1}$ ^0C	$T_{i\,2}$ ^0C	$T_{i\,avg}$ ^0C	$T_{f\,in}$ ^0C	$T_{f\,out}$ ^0C	T_{fm} ^0C	h (w/m^{2}k)	Nu	Δp (Pascal)
1	1.315	43.4	40.5	41.95	32	32.6	32.3	74.3408586	1.632403	1280
2	1.614	42.7	39.9	41.3	32	33	32.5	166.762632	3.661834	1520
3	1.944	42.5	39.6	41.05	32	33.4	32.7	296.357351	6.507522	2115
4	2.454	42.3	39.4	40.85	32.1	33.6	32.85	418.363428	9.186575	2890
5	2.778	42.2	39.3	40.75	32.1	33.7	32.9	514.825866	11.30473	3389.5

VII. RESULTS AND DISCUSSION

Experiments are conducted with deionized water and Al_2O_3/water nanofluid and their results are presented for heat transfer coefficients, interface temperature and pressure drop with volume flow rate. The volume flow rate was given in the range from 1.315 LPM to 2.78 LPM. An array of inline jets were tested with d_n = 2.5 mm, H/d_n = 13 mm and S/d_n = 5 mm.

7.1 Convective heat transfer coefficient

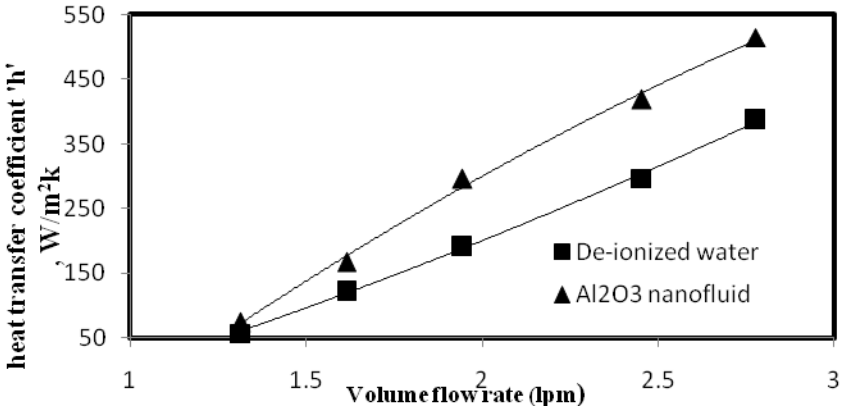

Figure.7.1. Volume flow rate V_s Heat transfer coefficient

Fig. 6.1.Shows the effect of convective heat transfer coefficient on volume flow rate. The heat transfer rate between the solid and the fluid depends upon the convective heat transfer coefficient. It is very important to study the heat transfer coefficient for determining the heat transfer rate. The convective heat transfer coefficient 'h' gradually increases with increasing volume flow rate and it is high for Al_2O_3 /water nanofluid compared to deionized water. Here upto32.92% increase in convective heat transfer coefficient is obtained frorn a nanofluid compared to water at a heat input of 120W. This is because the thermal conductivity of the nanofluid is higher than that of water. Thus the heat transfer rate is high in Al_2O_3/water nanofluid.

7.2 Interface temperature

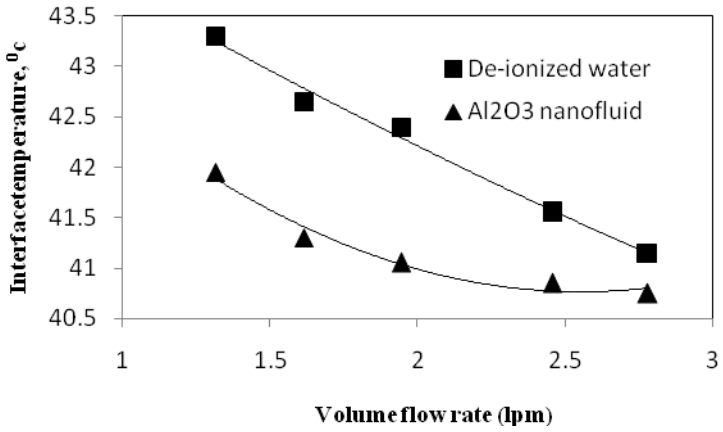

Fig. 7.2. Volume flow rate V_s Interface temperature

Fig.7.2. shows the change in interface temperature with respect to volume flow rate. Interface temperature is the temperature maintained between the heat sink and the heater block at its contacting surface. The interface temperature is reduced as far as possible for better performance of the electronic application. The interface temperature gradually decreases with increase in volume flow rate. The interface temperature maintained between the heated block and the heat sink is less for Al_2O_3/water nanofluid compared to water. It was found that about 0.4^0C decrease in interface temperature in nanofluid to water. This is because the heat transfer rate is high in Al_2O_3 /water nanofluid than water at constant volume flow rate. Consequently the surface temperature T_s gets reduced due to high heat transferring capability of nanofluid and corresponding increase in volume flow rate.

7.3 Pressure drop characteristics

Fig. 7.3.shows change in pressure drop with respect to volume flow rate. Pressure drop is the difference in pressure occurring between the entry and the exit of the test section. The pressure drop is caused due to the

frictional forces in liquid and these frictional forces increases the pump work. So the pressure drop plays a vital role in the fluid flow studies in the test regime. The pressure drop increases with increase in volume flow rate. It is obvious that pressure drop in Al_2O_3/water nanofluid is greater compared to water. This is because the density of the nanofluid is high compared to the density of water. It was found that about 6.6% pressure rise in nanofluid compared to water. The nozzle act as a restriction for the flow and thus a pressure difference is created at the inlet and exit of the nozzle in the test section. At high volume flow rate, there is no significant difference in pressure for deionized water and dilute Al_2O_3/water nanofluid. The figure shows a non linear rise in pressure drop with corresponding increase in volume flow rate.

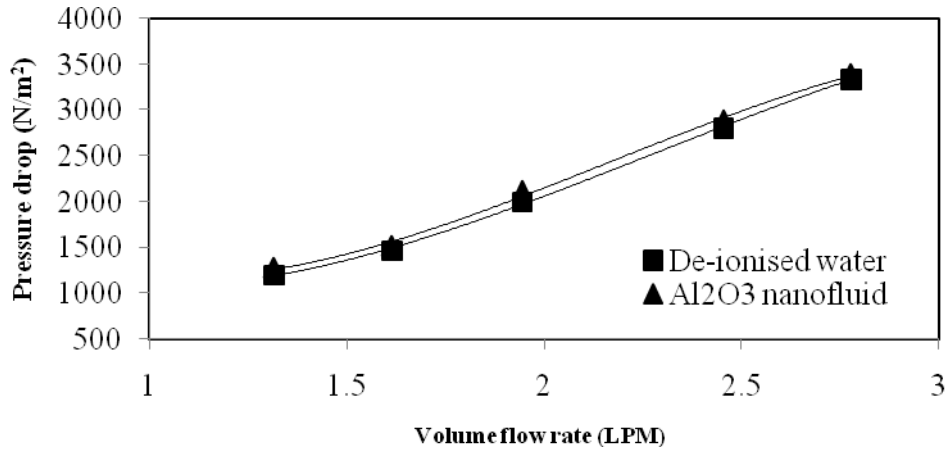

Figure. 7.3. Volume flow rate V_s Pressure drop

VIII. CONCLUSION

In jet impingement cooling the heat transfer coefficient, interface temperature, pressure drop characteristics in a rectangular plate heat sink with inline array jets are experimentally investigated. De-ionized water and Al_2O_3/water nanofluid are used as working fluid and it was found that Al2O3/water nanofluid is the best medium for the heat transfer enhancement compared to water. Jet impingement cooling scheme is compact in nature and hence used for high power density applications. The geometry of the heat sink, rectangular plate fins with a central channel along with uniformly distributed nozzles for jets makes the working fluid to spread uniformly over the entire flow regime to reduce the temperature non uniformity and pool formation.

Result of the study reveals that adding nano particles to the de-ionized water increases the heat transfer rate. About 32.92% increase in heat transfer coefficient is achieved when 0.1% volume concentration of Al_2O_3 nano particles is dispersed in de-ionized water. The interface temperature between the test block and the heater block is reduced by 0.4^0C inAl_2O_3/water nanofluid. Thus the nanofluid gives a better performance when compared to water. But in case of pressure drop it is higher in nanofluid due to its high density. Around 6.6% hike in pressure is found in Al_2O_3/water nanofluid. In low volume concentration there is no significant difference. This reveals that the pumping power required for nanofluid increases with corresponding increase in volume fraction of nano particle.

REFERENCES

[1] S.U.S Choi, Enhancing thermal conductivity of fluids with nanoparticles , Developments and applications of Non-Newtanian Flows, FED-vol 231/MD-vol. 66, 1995, pp. 99-105.

[2] Xiang-Qi Wang, Arun S. Mujumdar, Heat transfer characteristics of nanofluids a review, International Journal of Thermal Sciences 46 (2007) 1-19.

[3] D.J.Womac, F.P.Incropera, S.Ramadhyani, Correlating equation for impingement cooling of small heat sources with multiple circular jets, Journal of Heat Transfer 116(1994) 482-486.

[4] D.Y.Lee and K.Vafoi, Comparative analysis of jet impingement and micro channel cooling for high heat flux applications, International Journal of Heat and Mass Transfer 42 (1999) 1555-1568.

[5] M.Fabbri, V.K.Dhir, Optimized heat transfer for high power electronic cooling using arrays of microjets, Journal of Heat Transfer 127 (2005) 760-769.

[6] B.Sagot, G.Antonini, A.Christgen, F.Buron, Jet impingement heat transfer on a flat plate at a constant wall temperature, International Journal of Thermal Sciences 47 (2008) 1610-1619.

[7] Brain P.Whelan, A.J.Robinson, Nozzle geometry effects in liquid jet array impingement, Applied Thermal Engineering 29 (2009) 2211-2221.
[8] AkhileshP.Rallabandi, Dong-Ho Rhee, Zhihong Gao Je-Chin Han, Heat transfer enhancement in rectangular channels, with axial ribs or porous foam under through flow, International Journal of Heat and Mass Transfer 53 (2010) 4663-4671.
[9] Terri B Hoberg, Andrew J.Onstad, John K.Eaton, Heat transfer measurements for jet impingement arrays with local extraction, International Journal of Heat and Fluid flow 31 (2010) 400-467.
[10] Jerome Barrau, Daniel Chemisana, Joan Rosell, LounesTadrist, M.Ibanez, An experimental study of new hybrid jet impingement / micro-channel cooling scheme, Applied Thermal Engineering 30 (2010) 2058-2066.
[11] Paisarn Naphon and Somachai Wongwises, Investigation on the jet impingement heat transfer for the central processing unit of personal computers, International Communications in Heat and Mass Transfer 37 (2010) 822-826.
[12] Mangesh Chaudhari, BhalchandraPuranik, AmitAgarwal, Multiple orifice synthetic jet for improvement in impingement heat transfer, International Journal of Heat and Mass Transfer 54 (2011) 2056-2065.
[13] S.Suresh, K.P.Venkitaraj, P.Selvakumar, M.Chandrasekar, Effect of Al_20_3-Cu/water hybrid nanofluid in heat transfer, ETF 7607.
[14] B.C. Pak, Y. Cho, Hydrodynamic and heat transfer study of dispersed fluids with submicron metallic oxide particle, Experimental Heat Transfer 11 (1998) 151–170.
[15] Y. Xuan, W. Roetzel, Conceptions for heat transfer correlation of nanofluids, International Journal of Heat and Mass Transfer 43 (2000) 3701 3707.
[16] J.C. Maxwell, Treatise on Electricity and Magnetism, Dover, New York., 1954.

LIST OF SYMBOLS

Symbol	Description	Unit
Nomenclature		
A	Exposed heat transfer area	m^2
C_p	Specific heat	J/Kg k
d_n	Jet diameter, m	m
H	Jet to target spacing	m
D	Diameter	m
n	Number of jets	
k	Thermal conductivity	W/m K
h	Heat transfer coefficient	w/m^2 k
Q	Heat transfer	W
Re	Reynolds number	
Nu	Nusselt number	
Pr	Prandtl number	
q"	Actual heat flux	W/m2
m	Mass flow rate	Kg/s
T	Temperature	° C
v	Velocity	m/s
T_i	Average interface temperature	^{0}c
T_{fm}	Bulk mean temperature	^{0}c
Δp	Pressure difference	N/m^2
Greek symbols		
Ø	Volume concentration	
μ	Dynamic viscosity	Kg/ms
ρ	Density	kg/m^3

American Journal of Engineering Research (AJER)
e-ISSN : 2320-0847 p-ISSN : 2320-0936
Volume-03, Issue-03, pp-197-204
www.ajer.org

Research Paper Open Access

Assessment of heavy metal pollution in flooded soil of kudenda, Kaduna state. Nigeria.

M. Bashir[1], Y I Zakari[1], I G E Ibeanu[2] and U Sadiq[1]
[1]*Department of physics, Ahmadu Bello University Zaria, Kaduna state. Nigeria*
[2]*Centre for energy research and training (CERT) Zaria, Kaduna state. Nigeria.*

Abstract: - Assessment of heavy metal pollutant: As, Cr, Cu, Fe, Mn and Ni was conducted in the flooded soil of kudenda area (latitude 10.480^0N and 10.481^0 N and longitude 7.394^0E and 7.395^0E) in Kaduna state, Nigeria, using contamination factor (CF) and pollution load index (PLI). Samples were taken in each of the grid area at depth 0-<5, 5-<25, 25-<50, 50-100cm and were analyzed using Energy Dispersive X-Ray Fluorescence (EDXRF). The concentrations of all the metals were found to increase to a maximum concentration at a depth of 25-<50cm then decreased. The study area was observed to be contaminated with As (maximum 2.07), Cr (maximum 2.83), Cu (maximum 2.24), Fe (maximum 1.44), Mn (maximum 1.85) and Ni (maximum 2.20) in all the sampled points and depth except 50-100cm depth. The pollution load indices (PLI) were found to be high but decrease (1.54-0.95) with increase in depth (0-100cm) indicating that the study area was polluted by all the observed heavy metals (PLI>1).

Keywords: - *Heavy metals, Pollution, CF, PLI, EDXRF*

I. INTRODUCTION

Pollution of the natural environment by heavy metals is a universal problem because these metals are indestructible and most of them have toxic effects on living organisms, when permissible concentration levels are exceeded (Mmolawa *et al.*,2011). Heavy metals are either naturally or through anthropogenic sources introduced into river water. Metals that are naturally introduced into the river come primarily from sources such as rock weathering, soil erosion, and the dissolution of water-soluble salts. Naturally occurring metals (especially the trace metals) move through aquatic environments independent of human activities and usually without any detrimental effects (Garbarino *et al.*, 1995 & Opuene *et al.*, 2008). Anthropogenic pollutants are discharged from industrial, domestic and agricultural wastewater into river water system (Ho *et al.*, 2001 & Priju *et al.*, 2007). Sediment served as sinks for most of the metals in aqueous phase (Klavins, *et al.*, 1995). The concentrations of heavy metals in soils are varied according to the rate of particle sedimentation, the rate of heavy metals deposition, the particle size and the presence or absence of organic matter in the soils (Saloman *et al.*,1987).The assessment of sediment enrichment with elements can be carried out in many ways; The most common ones are the index of geo-accumulation (I-geo) and pollution load index (PLI). The I-geo has been utilized as a measure of pollution in freshwater sediment (Singh *et al.*,1997), while pollution load index (PLI) represents the number of times by which the heavy metals concentrations in the sediment exceeds the background concentration, and give a summative indication of the overall level of heavy metal toxicity in a particular sample (Priju *et al.*,2006),this index is a quick tool used to compare the pollution status of different places (Adebowale *et al.*,2009), this type of measure has however been defined by some authors in several ways, for example, as the numerical sum of eight specific contamination factors (Hakason, 1980), whereas, Abrahim (2005) assessed the site quality as the arithmetic mean of the analyzed pollutants. In this study, the authors found it appropriate to express the PLI as the geometric mean of the studied pollutants since this method tends to reduce the outliers, which might bias the reported results.

Several analytical techniques have been extensively employed for environmental pollution monitoring, such as: instrumental Neutron activation analysis (INAA)(Coskun *et al.,2006,*Steinnes, 2000 and IAEA,2001), X-Ray Fluorescence analysis (XRF) (Cojocaru *et al.,2006* and Ene, *et al.,2009*), Particle-Induced X-ray Emission (PIXE)(Ene *et al.,2009* and Ene *et al.,2010*), Atomic Absorption Spectrometry (AAS)(Daud *et*

al.,2009, Popescu *et al., 2009* and Al-khashman,2009) and Inductively Coupled Plasma Spectrometry-Atomic Emission Spectroscopy (ICP-AES) (Popescu *et al.*,2009). The EDXRF analysis of environmental samples has the advantage of being a rapid and inexpensive method with a simple sample preparation procedure (Ene *et al.,2010* and EPA, 2006). Quantitative and qualitative analyses by XRF techniques are performed without chemical digestion and a great number of elements can be determined simultaneously in a short time (Ene *et al.,2009*).

The objective of the present work was to use EDXRF to: (i) assess heavy metals concentration and contamination of environment by As, Cr, Cu, Fe, Mn and Ni using control soils obtained 3km away from the sampling area and (ii) assess soil contamination of study area using contamination factor (CF) and pollution load index (PLI).

II. MATERIALS AND METHODS

2.1 Study area: (Description and sampling techniques)

The study area is 60m^2 of the kudenda area of Kaduna state, Nigeria, where the flooding of river Kaduna occurred in 2012. The area is bounded by latitude 10.480^{0}N, 10.481^0 N and longitude 7.394^{0}E, 7.395^{0}E. The site was divided into 9grid points (mesh) of 20m^2 each labeled A-I with A-C, D-F and G-I parallel to the river bank but separated by 20m from each other and A-G, B-H and C-I perpendicular to the river bank and 60m away. Samples were collected at the middle of each grid from depths of 0-<5, 5-<25, 25-<50 and 50-100cm using hand auger. Control samples were collected at a distance of 3km away from the river bank. After removal of stones and vegetable matter, each soil sample was packed into its own secure water-tight polyethene bag to prevent cross contamination.

2.2 Sample preparation and analysis

Samples were each placed in an oven for drying at a temperature of 30^{o}C until a constant weight was reached ensuring complete removal of any residual moisture. The dried samples were pulverized into a fine powder and passed through a standard mesh (500µm). The samples were homogenized and an average of 0.5g of each of the sample was measured and pelletized at 10tons with the aid of hydraulic press (13mm dice). Each of the pellet was then irradiated in a sample chamber with X-Ray for 1000 seconds to acquire the sample spectral and each peak made up of the spectral was visually investigated to determine the elements contained in the samples by qualitative interpretation method. The quantitative interpretation was done with the aid of software called AMPTEK to obtain the concentrations of each metal.

2.3 Assessment of metal contamination

2.3.1 Contamination factor (CF)

The level of contamination of soil by metal is expressed in terms of a contamination factor (CF) calculated as:

$$\mathrm{CF} = \frac{\mathrm{C_m\ Sample}}{\mathrm{C_m\ Background}} \qquad (1)$$

C_m Sample = metal concentration in Sample

C_m Background = metal concentration in background or control Sample

Where the contamination factor CF < 1 refers to low contamination; 1 ≤ CF < 3 means moderate contamination; 3 ≤ CF ≤ 6 indicates considerable contamination and CF > 6 indicates very high contamination.

2.3.2 The Pollution Load Index (PLI)

The Pollution Load Index (PLI) is obtained as contamination Factors (CF), this CF is the quotient obtained by dividing the concentration of each metal with its control value. The PLI of the place are calculated by obtaining the n-root from the n-CFs that was obtained for all the metals. Generally pollution load index (PLI) as developed by Tomlinson *et al* (Tomlinson *et al.*,1980), is as follows:

$$\mathrm{PLI} = \sqrt[n]{(\mathrm{CF_1} \times \mathrm{CF_2} \times \mathrm{CF_3} \times \ldots\ldots \times \mathrm{CF_n})} \qquad (2)$$

Where,

CF = contamination factor, n = number of metals

The PLI value of > 1 is polluted, whereas <1 indicates no pollution (Harikumar *et al.*,2009*).*

III. RESULTS AND DISCUSSION

3.1 Heavy metal concentrations in soils

Fig 1(a-f) are plots of the observed elemental concentration of each grid point A-I and for each grid is a variation with depth 0-100cm in the plotted range shown, it can be observed that mean heavy metal

concentrations (in ppm) in the sampled soils ranged from (14 to 41) As, (40 to 211) Cr, (15 to 63) Cu, (4713 to 21219) Fe, (173 to 930) Mn and (83 to 231) Ni.

Also Fig 1(a-f) displays the elemental concentration in each of the grid sampled area A-I as depicted for each of the elements; As, Cr, Cu, Fe, Mn and Ni, and an observed pattern is displayed consistent with all the grid points A-I analyzed. For each of the grid points A-I the metal concentration vary with sampling depths (0-100cm) with an observed increase in concentration to a depth point of 25-<50cm then decreases. This may probably be indication of soil filtration effect.

The elements are observed to accumulate at different concentrations at each of the grid points. Fig 1(a) indicates a maximum accumulation of As at the centre grid point E. Similarly fig 1(f) also has its maximum concentration of Ni at the same centre grid point. Meanwhile fig 1(d and e) had Fe and Mn accumulation to concentrate maximally at grid point B but only Cr fig 1(b)have maximum concentration at grid point C and Fig 1(c) for Cu also indicate maximum concentration at grid point A maybe due to its density when compared to the other metals. It could be observed that along the same profile is deposited the other heavy metals Fe, Mn at grid point B and Cr at grid point C.

3.2 Contamination Factor (CF)

Using equation 1, contamination factor of various metals within each grid sampled area A-I with depths were calculated and presented in table 1. At depth 0-<5, 5-<25 and 25-<50cm most of the grid points were observed to be moderately contaminated with As, Cu, Cr, Mn and Ni but Fe is observed with most of the grid points to indicate low contamination. Whereas, at 50-100cm depth most of the grid points were observed to be moderately contaminated with Ni but As, Cu, Cr, Fe and Mn were observed with most of the grid points to indicate low contamination.

3.3 Pollution Load Index (PLI)

To effectively know the measure of degree of overall contamination, the pollution load index (PLI) was calculated using equation 2 for each grid sampled area A-I with depth and presented in table 1.

Based on the results presented in table 1, it was observed that at depth 0-<5, 5-<25 and 25-<50cm all the grid sampled points were polluted (>1) except grid point D at depth 25-50cm which is unpolluted (<1) and at depth 50-100cm all the grid sampled point were unpolluted (<1) except grid point C and I which were polluted (>1).

Fig 2 is a plot of the variation of pollution load index with depth. According to fig 2 the pollution load index (PLI) decreases (1.54-0.95) with depth (0-100cm) which confirm that the study area is facing probable environmental pollution especially with dangerous heavy metals (As, Cu, Cr, Mn and Ni) which could be as a result of increased rate of non-treated industrial waste discharged into river Kaduna and deposited in the area due the flood activity.

IV. CONCLUSION

A study of the flood profile using the elemental concentrations at the site indicates most of the toxic element to accumulate at a depth 25-<50cm. this could be due to the common source of the metals and to have the same grain size hence filtered to the same depth into the soil.

Anthropogenically impacted and control soils of the study area were assessed using contamination factors and pollution load index for As, Cu, Cr, Fe, Mn and Ni. The contamination factors were observed generally to indicate low to moderate contamination by heavy metals across the grid points and depths; the background soil was higher than that of the study area for some of the element and grid points which could be attributed to human activity such as sewage deposit.

The measure of degree of overall contamination (PLI) at the sampled grid area indicate strong signs of pollution deterioration by the six measured metals at depth 0-<5, 5-<25 and 25-<50cm and no overall contamination at 50-100cm depth. The pollution load index (PLI) (1.54-0.95) vary with depth(0-100cm) which confirm that the study area is facing probable environmental pollution especially with dangerous heavy metals which result from increased rate of non-treated industrial waste discharged into river Kaduna and deposited at the river bank due to flood activity.

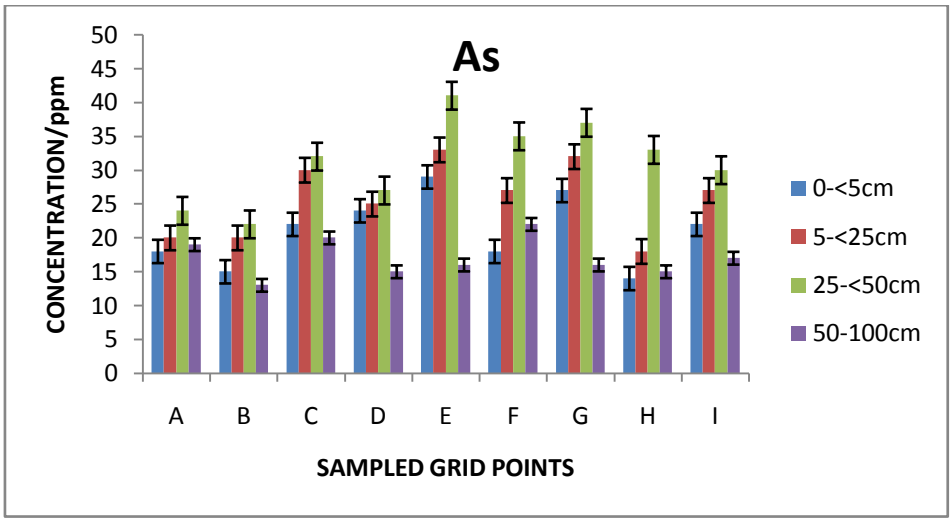

Fig 1(a): Concentration of As of Sampled grid points

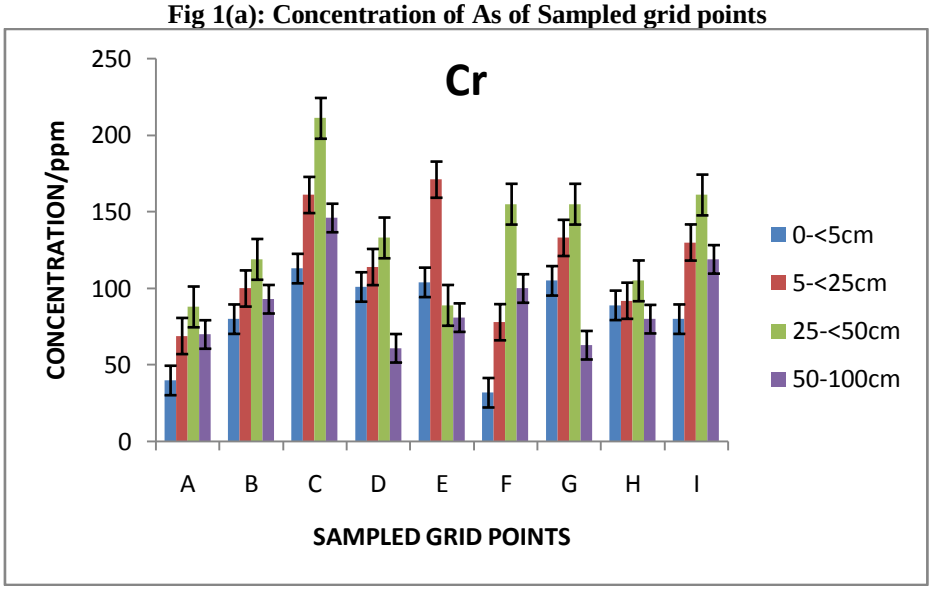

Fig 1(b): Concentration of Cr of Sampled grid points

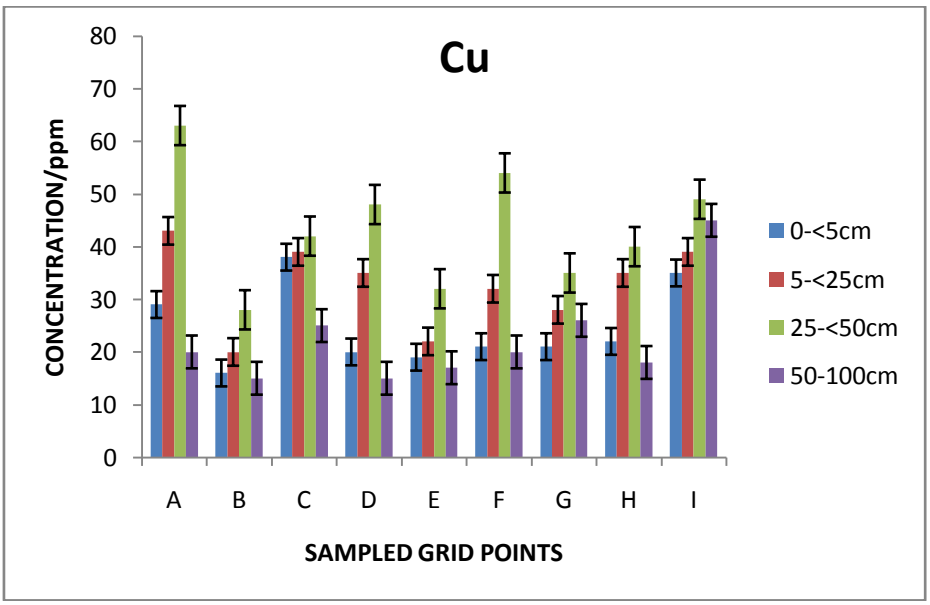

Fig 1(c): Concentration of Cu of Sampled grid points

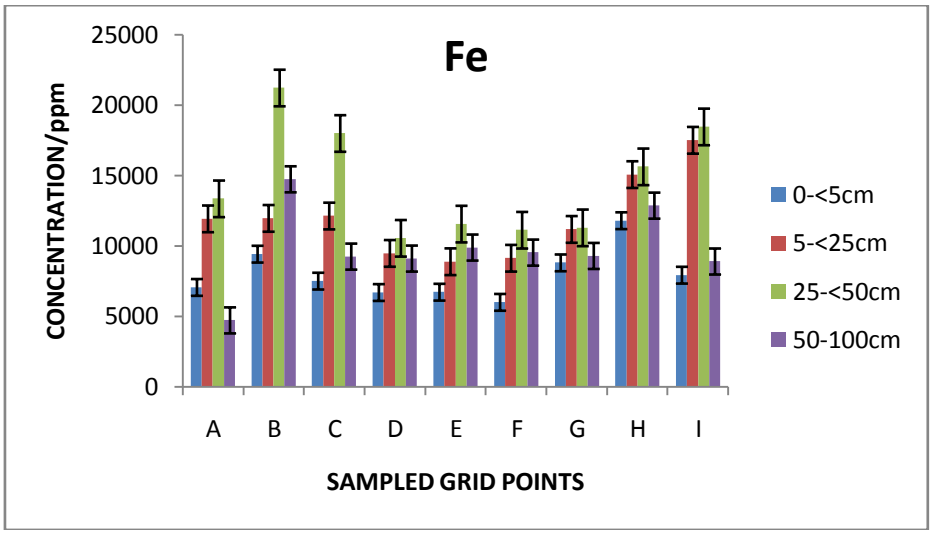

Fig 1(d): Concentration of Fe of Sampled grid points

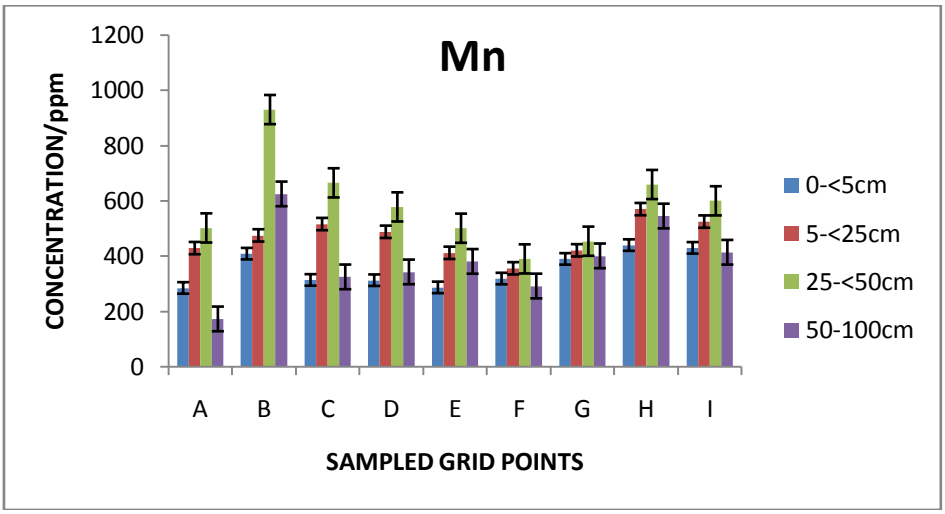

Fig 1(e): Concentration of Mn of Sampled grid points

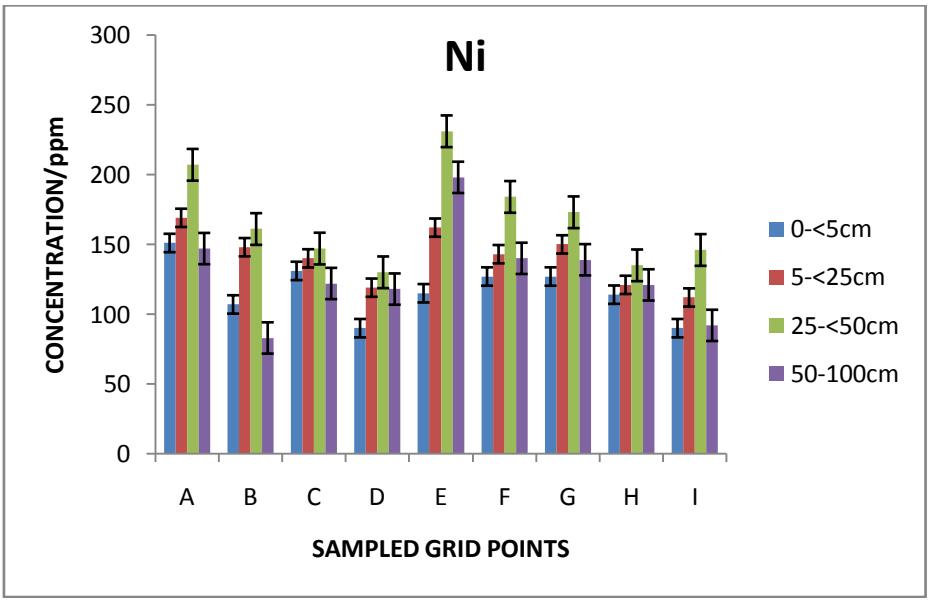

Fig 1(f): Concentration of Ni of Sampled grid points

Table (1): Contamination factor (CF) and Pollution Load Index (PLI) for the sampled area.

Location/Depth	CF As	CF Cu	CF Cr	CF Fe	CF Mn	CF Ni	PLI
0-<5cm							
A	1.29	1.71	1.00	0.78	1.00	1.70	1.20
B	1.07	0.94	2.00	1.04	1.44	1.20	1.24
C	1.57	2.24	2.83	0.83	1.11	1.47	1.54
D	1.71	1.18	2.53	0.74	1.10	1.01	1.27
E	2.07	1.12	2.60	0.74	1.01	1.29	1.34
F	1.29	1.24	0.80	0.66	1.12	1.43	1.05
G	1.93	1.24	2.63	0.98	1.37	1.43	1.51
H	1.00	1.29	2.23	1.31	1.55	1.28	1.40
I	1.57	2.06	2.00	0.88	1.51	1.01	1.43
5-<25cm							
A	1.11	1.54	0.96	0.86	1.08	1.40	1.13
B	1.11	0.71	1.39	0.86	1.19	1.22	1.06
C	1.67	1.39	2.24	0.87	1.29	1.16	1.38
D	1.39	1.25	1.58	0.68	1.22	0.98	1.15
E	1.83	0.79	2.38	0.64	1.03	1.34	1.20
F	1.50	1.14	1.08	0.66	0.89	1.18	1.04
G	1.78	1.00	1.85	0.80	1.06	1.24	1.23
H	1.00	1.25	1.28	1.08	1.43	1.00	1.16
I	1.50	1.39	1.81	1.26	1.32	0.93	1.34
25-<50cm							
A	1.00	1.75	0.79	0.81	1.00	1.48	1.09
B	0.92	0.78	1.07	1.30	1.85	1.15	1.13
C	1.33	1.17	1.90	1.10	1.32	1.05	1.28
D	1.13	1.33	1.20	0.64	1.15	0.21	0.81
E	1.71	0.89	0.80	0.71	0.99	1.65	1.06
F	1.46	1.50	1.40	0.68	0.77	1.31	1.13
G	1.54	0.97	1.40	0.69	0.90	1.24	1.08
H	1.38	1.11	0.95	0.95	1.31	0.96	1.10
I	1.25	1.36	1.45	1.13	1.19	1.04	1.23
50-100cm							
A	0.95	0.83	0.75	0.46	0.37	1.63	0.74
B	0.65	0.63	1.00	1.44	1.34	0.92	0.95
C	1.00	1.04	1.57	0.90	0.69	1.36	1.06
D	0.75	0.63	0.66	0.89	0.73	1.31	0.80
E	0.80	0.71	0.87	0.97	0.81	2.20	0.97
F	1.10	0.83	1.08	0.93	0.62	1.56	0.98
G	0.80	1.08	0.68	0.91	0.86	1.54	0.94
H	0.75	0.75	0.86	1.26	1.16	1.34	0.99
I	0.85	1.88	1.28	0.87	0.88	1.02	1.08

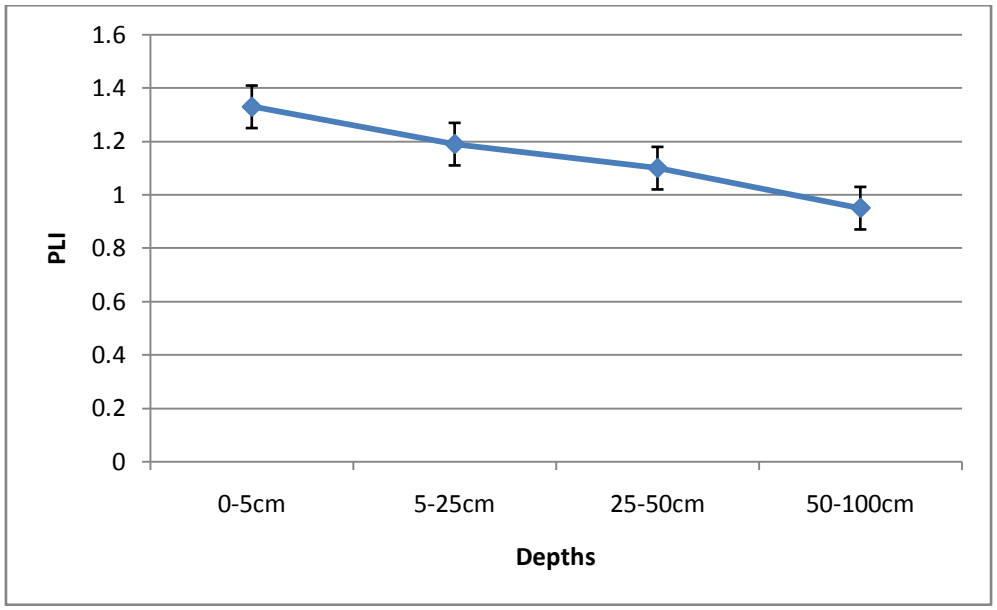

Fig.(2): Variation of pollution load index (PLI) with depth

REFERENCES

[1] Abrahim G.M.S (2005): Holocene sediments of tamaki Estuary. Characterisation and impact of recent human activity on an urban estuary in Aukland, Newzealand. PhD thesis, University of Aukland, Aukland, Newzealand, p.36.

[2] Adebowale K.O., Agunbide F.O.and Olu-owolabi B. (2009): Trace metal concentration, site variations and partitioning pattern in water and bottom sediments from costal area: a case study of Ondo coast, Nigeria, Environmental Research Journal, vol. 3, No. 2, pp. 46-59.

[3] Al-khashman O. A. and Shawabkeh R. A. (2009): Metal distribution in urban soil around steel industry beside Queen Alta Airport. Jordan Environ. Geochem. Health 31,717

[4] Cojocaru V., Pantelica A., Pincovschi E. and Georgescu I.I. (2006): EDXRF versus INAA in pollution control of soil; Journal of Radioanal Nuclear Chemistry 268(1),7

[5] Coskun M., Steinnes E., Frontasyeva M. V., Sjobakk T. E. and Demkina S. (2006): Heavy metal pollution of surface soil in the three region, Turkey. Environmental Monitoring Assessment 119,545

[6] Daud M., Wasim M., Khalid N., Zaidi J. H.and Iqbal J. (2009): Assessment of elemental pollution in soil of Islamabad city using instrumental neutron activation analysis and atomic absorption spectrometry techniques. Radiochim, Acta 97,117

[7] Ene A, Stihi C., Popescu I. V., Gheboianu A., Bosneaga A. and Bancuta I. (2009): Comparative studies on heavy metal content of soils using AAS and EDXRF atomic spectrometric techniques, Ann Dunarea de Jos University. Galati, Fasc.II. 32(2), 51

[8] Ene A., Popescu I. V.and Stihi C. (2009): Applications of proton-induced X-ray emission technique in material and environmental science. Ovidius Univ. Ann. Chem. 20(1), 35

[9] Ene A., Popescu I. V., Stihi C., Gheboianu A., Pantelica A.and Petre C. (2010): PIXE analysis of multielemental samples. Rom. Jurn. Phys. 55(7-8),806

[10] EPA/540/R-06/004 February (2006): Innovative Technology Verification Report, Niton XLt 700 Series XRF Analyzer, XRF Technologies for measuring Trace Elements in soil and sediment, United States Environmental Protection Agency.

[11] Garbarino, J.R., Hayes, H.C., Roth, D.A., Antweiler, R.C., Brinton,T.I. And Taylor, H.E. (1995): Heavy Metals in the Mississippi River. (In R.H. Meade (Ed.) Contaminants in the Mississippi River, U.S. Geological Survey Circular 1133.

[12] Hakason L. (1980): Ecological risk index for aquatic pollution control, a sedimentological approach. Water resources, 14; 975-1001

[13] Harikumar P. S., Nasir U. P. and Mujeebu Rahma M. P. (2009): Distribution of heavy metals in the core sediments of a tropical wetland system; International Journal of Environmental Science and Technology, vol. 6, pp. 225-232.

[14] Ho, K.C. And Hui, K.C.C. (2001): Chemical contamination of the east river (Dongjiang) and its implication on sustainable development in the Pear River delta. Environmental International, **26**, 303-308.

[15] IAEA-TECDOC-1215 (2001): Use of research reactors for neutron activation analysis, Appendix II.IAEA, Vienna
[16] Klavins, M., Briede, A., Klavins, I. and Rodinov, V. (1995): Metals in sediment of lakes in Latvia. Environmental International, **21(4),** 451-458.
[17] Mmolawa K. B., Likuku A. S. and Gaboutioeloe G. K. (2011): Assessment of heavy metal pollution in soils along major roadside areas in Botswana. African Journal of Environmental Science and Technology, vol 5 (3), pp. 186-196.
[18] Opuene, K., Okafor, E.C. And Agbozu, I.E. (2008): Partitioning characteristics of heavy metals in a non-tidal freshwater ecosystem. International Journal of Environmental Resources. **2(3),** 285-290.
[19] Popescu I. V., Frontasyeva M., Stihi C., Cimpoca Gh. V., Radulescu C., Gheboianu A., Oros C., Vlaicu Gh., Petre M., Bancuta I. and Dulama I. (2010): Nuclear and nuclear related analytical methods applied in environmental research. Romanian Journal of physics 55(7-8), 821
[20] Popescu I. V., Stihi C., Cimpoca Gh. V., Dima G., Vlaicu Gh., Gheboianu A., Bancuta I., Ghisa V. and State G. (2009): Environmental Samples Analysis by Atomic Absorption Spectrometry (AAS) and Inductively Coupled Plasm- Optical Emission Spectrometry ICP-AES), Rom. Journ. Phys. 54(7-8), 741
[21] Priju C. P and Narayana A.C. (2006): Spatial and temporal variability of trace element concentrations in tropical lagoon, southwest coast of india; Environmental implications. Journal of coastal Research, vol. 39, pp. 1053-1057
[22] Priju, C.P. And Narayana, A.C. (2007): Heavy and Trace metals in Vembanad lake sediments. International Journal of Environmental Resources. 1(4)**,** 280-289.
[23] Saloman W. N., Rooij H.and Bril J. (1987): sediment as a source for contaminants; Hydrobiologia, vol. 149, pp. 13-30.
[24] Singh M., Ansari A.A., Muller G. and Singh I.B. (1997): Heavy metals in freshly deposited sediments of the Gomati river a tributary of the Ganga river, effect of human activities; Environmental Geology, vol. 29, pp. 246-252.
[25] Steinnes E. (2000): Neutron activation techniques in environmental studies. Journal of Radioanal. Nuclear Chemistry 243,235
[26] Tomlinson D. L., Wilson J. G., Harris C. R. and Jeffney D. W. (1980): problems in the assessment of heavy metal levels in estuaries and the formation of pollution index, Helgol. Wiss. Meeresunters, vol. 33, pp.566-572
[27] Wakida F. T.D., Lara-Ruiz E. J. and Temores P. (2008): Heavy metals in sediments of the tecate River, Mexico, Environmental Geology, vol. 54, pp.637-642.

American Journal of Engineering Research (AJER)
e-ISSN : 2320-0847 p-ISSN : 2320-0936
Volume-03, Issue-03, pp-205-211
www.ajer.org

Research Paper Open Access

Effect of Superplasticizer on Fresh and Hardened Properties of Self-Compacting Concrete Containing Fly Ash

S. M. Dumne
Lecturer, Department of Applied Mechanics, Government Polytechnic, Nashik, Maharashtra, INDIA

Abstract: - The use of mineral and chemical admixtures in concrete is a common solution to achieve full compaction particularly where reinforcement congestion and shortage of skilled workers. The past researchers have been underscored the use of mineral and chemical admixtures imparts the desirable properties to concrete in both fresh and hardened state. This paper has been made an attempt to study the influence of superplasticizer dose of 0.25, 0.30 and 0.35percentage on performance of Self-Compacting Concrete containing 10% fly ash of cement content. The experimental tests for fresh and hardened properties of Self-Compacting Concrete for three mixes of M_{20} grade are studied and the results are compared with normal vibrated concrete. The tests considered for study are, slump test, compaction factor test, unit weight and compressive strength test The results show that for the constant water cement ratio, increase of superplasticizer dose in Self-Compacting Concrete leads to gain of good self compaction ability in addition to marginal reduction in unit weight. Moreover, there is also slightly increase in compressive strength than that of normal concrete mix.

Keywords: *- Compressive strength, Fly ash, Normal concrete, Self-Compacting Concrete, Superplasticizer, Unit weight, Workability*

I. INTRODUCTION

The concrete performance plays a vital role in the development of infrastructures including commercial, industrial, residential, military structures etc. In recent past, there is wide use of reinforced concrete not only for medium structures but also for long span heavy loaded structures. To some circumstances, there is more congestion of reinforcement's which causes in difficulty for its full compaction but there is shortage of skilled workers, resulting to adverse effects on properties and quality of concrete. In order to obtain workable concrete without strength loss, minerals and chemical admixtures are added in fresh mix of normal concrete, known as Self-Compacting Concrete (SCC). During further study, it is noticed that Self-Compacting Concrete is also referred as Self-Consolidating Concrete or High-Performance Concrete. The SCC concept was first introduced into scientific world in Japan in 1980 by Professor Hajime Okamura from Tokyo University. The Self-Compacted Concrete is a kind of concrete with excellent deformability and good segregation resistance which is able to flow under its own weight and self compacted into every corner of a formwork as a results it offers rapid rate of concrete placement [1]. The Self-Compacting Concrete is often produced with lesser water-cement ratio yielding early strength and hence faster use of structures. Moreover, elimination of vibrating equipment improves the environment at site in addition to reducing noise and vibrations. Further, to ensure high filling ability and flow without blockage, Self-Compacting Concrete should have lesser coarse aggregate contents and hence high cement content which can increase the cost and temperature during hydration [2] which leads to possible effect on other properties such as creep and shrinkage. In recent past, to enhance the properties of fresh and harden concrete, an addition like fly-ash is often partially incorporated in place of cement. Further, the use of fly ash in concrete is well established and widely applicable because it is not only economical from cost but it also improves the fresh and hardened properties of concrete [3]. Its typical usage is about 10-25% replacement to the cement which helps to maintain the viscosity of concrete resulting to in blockage risk and decreases the superplasticizer requirements. Therefore, to extend the concept of Self-Compacting Concrete, cement is partially replaced by fly ash due to its sustainability and reduced cost. The exhaustive study [4] have been underscored that initial cost of Self-Compacting Concrete mix get increases due to addition of Polycarboxylic ether based superplasticizer but the same shall be compensated by the production cost efficiency

such as reduction in placing time, vibrator use and its maintenance, formwork cost, worker safety in addition to the achievement of filling ability, passing ability and segregation resistance. The optimized composition of SCC was prepared with silica fume (0-20% of cement weight) and superplasticizer (0.20-0.50% of cement weight) then each composition is tested by slump cone, L-box and V-funnel apparatus to meet the requirements of SCC [5]. The performance of Self-Compacting Concrete containing minerals through experimental study illustrated that an addition of mineral and chemical admixtures not only modify the properties of wet concrete in-flow and filling ability but also retain/enhance the properties of harden concrete like strength and durability. It is also observed that when mineral admixtures used in SCC, can reduce the amount of normal range (plasticizer) and high range (superplasticizer) admixtures which are necessary to achieve the fluidity but its requirements is depends on their participle size, shape and surface characteristics [6].

The general objective of this paper is to evaluate the performance of Self-Compacting Concrete containing 10% percent cement replacement with fly ash in addition to varying dose of superplasticizer. In this study, it is decided not being reduced the percentage of coarse aggregates in mix against the addition of superplasticizer in order to achieve the self compact ability without losing its strength. The specific objectives are (i) effect of superplasticizer on workability and strength of Self-Compacting Concrete containing fly ash through various tests (ii) interpretation of test results obtained from the normal and various SCC mix (iii) based on experimental results, superiority of SCC mix containing fly ash and superplasticizer with respect to normal mix has been established in terms of workability, unit weight and compressive strength.

II. MATERIALS USED AND PROPERTIES

The materials used for study are cement, fly ash, superplasticizer, fine and coarse aggregates. This type of concrete involves many factors that affect the deformability and segregation such as water- cement ratio and numerous properties of aggregates that is, volume, size distribution, void content, fine to coarse aggregate ratio, surface properties and density. Further, few tests of our interest are conducted as per codal provisions on concrete materials to determine their properties and suitability for the tests under consideration.

2.1. Cement

Cement is one of the important concrete components that bind the concrete ingredients all together. In order to achieve more workable mix, an increased paste is required to achieve the required deformability. The various tests are conducted on an Ordinary Portland Cement (OPC) of 43 grade confirming to IS: 8112-1989 [7] to know the physical properties such as fineness= 4%, normal consistency= 28%, initial setting time= 70min, final setting time= 265min, specific gravity= 3.15, compressive strength at 7 days= 22.45 N/mm^2 and compressive strength at 28 days= 48.88 N/mm^2.

2.2. Fly Ash

The most often fillers used to increase the viscosity of Self-Compacting Concrete is the fly ash, obtained from the Eklahare thermal power plant Nashik (Maharashtra, India). This fly ash is used as partial replacement to cement in concrete as mineral admixture for reducing heat of hydration, permeability and bleeding. Further, incorporation of fly ash also eliminates the need of viscosity-enhancing chemical admixtures and may improve the rheological property and reduce thermally-induced cracks in concrete. Further, reducing the cement content is one of the economical benefits besides the use of fly reduces the environmental pollution. However, there are some disadvantages to use the fly ash regarding the reduced air-entraining ability and early strength due to the influence of residual carbon in fly ash. In this work, 10% cement content required for normal mix is replaced by fly ash for all trial mixes of Self-Compacting Concrete. The test results obtained from the laboratory of thermal power plant Nashik are, fineness ROS # 350 (45 MIC) = 16.37%, specific surface by Blaine's permeability method= 371 m^2/kg, moisture content= 0.28%, soundness by autoclave expansion= 0.03% and compressive strength at 28 days= 44.23N/mm^2.

2.3. Fine and Coarse aggregates

The fine aggregates with well-graded, spherical shape and low absorption are advantageous to self-compacting concrete. The fine aggregates are used from locally available river confirming to grading zone II of IS code [8] whereas crushed stones having nominal size 12.5mm as coarse aggregates confirming to IS 383-1970 are used for conducting the various tests. To investigate the properties and suitability of aggregates for its intended application, the tests are conducted as (1) sieve analysis and fineness modulus (2) specific gravity (3) water absorption (4) silt content. The test results obtained in laboratory for fine aggregates are, fineness modulus= 3.20, specific gravity= 2.63, water absorption = 2.23 % and silt content= 2.33 % whereas for coarse aggregates, fineness modulus= 7.12, specific gravity= 2.78, water absorption= 0.37 % and silt content= 0.30 %.

2.4. Superplasticizer (SP)

When cement mixes with water, cement particles always flocculate and agglomerate then electrostatic attractive forces are generated by the electric charge on particle surface as a results large amount of free water being trapped in flocks, leads to reduce the homogeneity of concrete. The water reducing agents or workability agents such as plasticizer and superplasticizer among which superplasticizer is more consistence and viscous even at low w/c ratio. Further, to achieve high filling ability, it is necessary to reduce inter-particle friction among solid particles in concrete by using superplasticizer and reducing coarse aggregate contents. The incorporation of a superplasticizer not only reduces the inter-particle friction but also maintain the deformation capacity and viscosity. The locally available admixture that is, CONPLAST SP 430 G8 used as a superplasticizer with density 1.2 kg/l, specific gravity= 2.10 at 30^{o}C, air entrainment = 1% (approximately) and blackish in colour. For all the mixes, an addition of superplasticizer about 0.25, 0.30 and 0.35 percent of cement content is used.

III. CONCRETE MIX PROPORTION

For the performance analysis, three design mixes of M_{20} concrete grade with same water cement ratio 0.55 in which 10% replacement of cement with fly ash in addition to varying superplasticizer dose of 0.25, 0.30 and 0.35 percentage of cement content required for mix of normal concrete are prepared. These mixes are casted in standard cement concrete cubes and tested in the Applied Mechanics Department, Government Polytechnic Nashik. These three mixes of SCC are abbreviated as A1, A2, and A3 for further discussion and interpretation with respect to normal concrete (compacted artificially without addition of fly ash and superplasticizer) being designated as A. The design proportion obtained for normal concrete mix using IS code practice for concrete mix design [9] and are re-adjusted the same proportion for various Self-Compacting Concrete mixes corresponding to use of 10% fly ash are mentioned in following table 1.

Table 1 Mix proportion for various trials mixes of M_{20} concrete grade

Trial mix	Water		Cement		Fly ash		Fine aggregate		Coarse aggregate		Superplasticize	
	Proportion	Quantity (Liters)	Proportion	Quantity (Kg)	Proportion	Quantity (Kg)	Proportion	Quantity (Kg)	Proportion	Quantity (Kg)	Proportion	Quantity (Liters)
A	0.55	191.4	1	348	--	--	1.61	558	3.47	1207	--	--
A_1	0.55	191.4	1	313.2	0.11	34.80	1.78	558	3.85	1207	0.0027	0.87
A_2	0.55	191.4	1	313.2	0.11	34.80	1.78	558	3.85	1207	0.0033	1.04
A_3	0.55	191.4	1	313.2	0.11	34.80	1.78	558	3.85	1207	0.0038	1.22

IV. EXPERIMENTAL RESULTS AND DISCUSSION (LITERS)

The proposed study has undertaken the various tests on mix are, slump, compaction factor, unit weight and compressive strength at 7th and 28th days. The complete mixing operation is performed manually using drinkable water and table vibrator is used while casting mix of normal concrete only. After casting the mix in cube mould for 24 hours then the same is cured in normal water of curing tank having room temperature.

4.1. Workability test

The workability test includes slump test as shown in Fig. 1 and compaction factor test are conducted as per special code of practices [10] in order to produce homogeneous and workable mix. From the observations shown in table 2, it is noted that slump value and compaction factor are, 120 mm and 0.92 respectively for normal concrete mix whereas for mix containing 0.35% superplasticizer along with 10% fly ash, the slump value and compaction factor as 285 mm 1.12 which is very high. The results of both tests reflects that fluidity or workability of Self-Compacting Concrete is a function of increase in percentage of superplasticizer with 10% fly ash of cement content for same water-cement ratio of 0.55. Once an acceptable workability achieved then concrete cubes casted and hardened cubes after 28 days of curing is shown in Fig. 2.

Figure 1 Slump cone test

Figure 2 Cement concrete cubes in wet and dry state

From the Fig. 3 as shown below, it is observed that workability in terms of slump and compaction factor of SCC mix increases corresponding to increase in superplasticizer dose along with constant 10% fly ash.

Table 2 Workability test results for various concrete mixes

Concrete mix	% age Fly ash	% age Superplasticizer	Workability test	
			Slump (mm)	Compaction factor
A	0	0	120	0.92
A_1	10	0.25	150	0.99
A_2	10	0.30	200	1.03
A_3	10	0.35	285	1.12

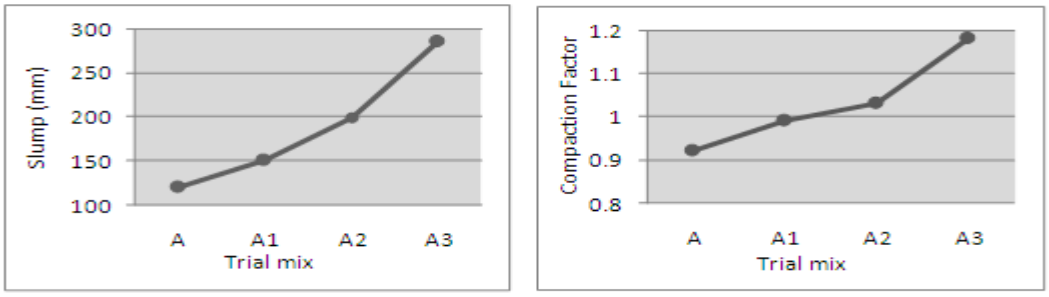

Figure 3 Comparison of compressive strength of various mixes at 7th and 28th days

4.2. Unit weight

The quantities of concrete ingredients required for one meter cubic of normal concrete are estimated to a proportion of 1: 1.61: 3.47 that is, Cement= 348 kg, F.A. = 558 kg, C.A = 1200 kg and Water= 191.6 liters with water cement ratio 0.55 then quantities of concrete ingredients required for three cubes of concrete are, Cement= 4.77 Kg, F.A= 7.67 Kg, C.A. = 16.55 Kg and Water= 2.2 liters respectively. After confirming workability to the normal mix then convert the normal mix to Self-Compacting Concrete mix in which 10% cement content is replaced by fly ash in addition to some varying percentage of superplasticizer. The properties of normal concrete mix of ingredients are re-adjusted to fulfill the required quantities of ingredients as per original proportion. Three mixes are prepared corresponding to additions of superplasticizer dose to 0.25, 0.30 and 0.35 percentage of cement content required for normal mix and are casted in laboratory. Further, weight of each concrete cubes are taken after 7 and 28 days of curing are noted in table 3 as below

Table 3 Unit weight of normal concrete and various SCC mixes

Specimen	% age Fly ash	% age Superplasticizer in %age	Av. unit Wt. (Kg)		Percentage reduction	
			7 days	28 days	7 days	28 days
A	0	0	8.341	8.441	---	---
A_1	10	0.25	8.145	8.245	2.350	2.322
A_2	10	0.30	7.879	7.879	5.538	6.658
A_3	10	0.35	7.717	7.617	7.481	9.761

From the Fig. 4, one can conclude that increase in superplasticizer with 10% fly ash in the SSC mix leads to reduce in weight of mix, resulting to reduction in total dead weight of structures. Hence, using concrete with lower density can result in significant benefit to light weight structures and better thermal insulation than ordinary concrete but use of lower density concrete permits the construction with low load-bearing structures.

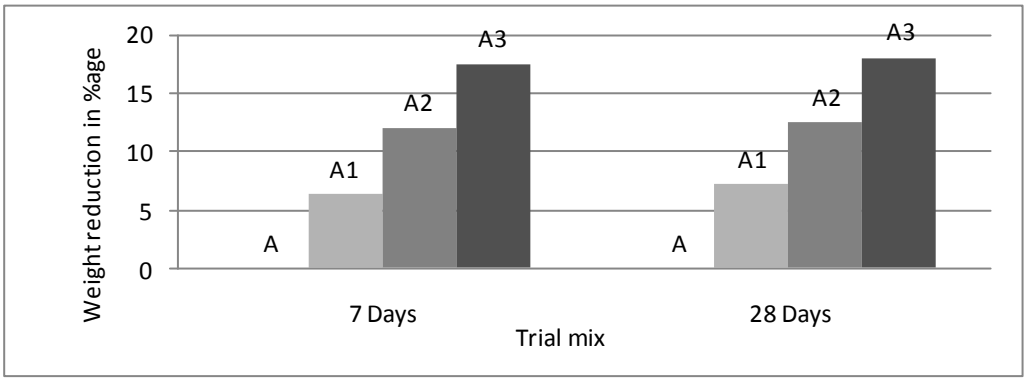

Figure 4 Variation of reduction in unit weight with various concrete mixes

4.3. Compressive strength

For each trial mix, three concrete cubes are casted for both normal as well as three trial mixes of Self-Compacting Concrete are tested to know the average compressive strength at 7 and 28 days of standard curing in the Laboratory of Government Polytechnic Nashik and results are mentioned in table 4.

Table 4 Compressive strength of various concrete mixes at 7 and 28 days

Specimen	% age Fly ash	% age Superplasticizer	Actual Comp. Strength (MPa)		Av. Compressive Strength (MPa)		% age Strength Gain	
			7 days	28 days	7 days	28 days	7 days	28 days
A	--	0	19.00	27.11	19.90	27.11	----	----
			22.00	27.32				
			18.60	26.89				
A_1	10	0.25	22.00	29.11	21.95	28.96	06.28	07.12
			22.44	29.32				
			21.55	28.42				
A_2	10	0.30	22.36	31.56	22.29	30.48	12.01	12.43
			22.25	29.11				
			22.29	30.21				
A_3	10	0.35	23.12	32.00	23.37	31.98	17.43	18.01
			22.98	31.52				
			24.45	32.67				

The observations from table 4 show that compressive strength of Self-Compacting Concrete contains fly ash and superplasticizer is increases relatively faster upto 7 days thereafter its rate becomes slower for same water-cement ratio. Overall, on can conclude that superplasticizer dose increases the compressive strength of concrete mix at both 7^{th} and 28^{th} days of curing.

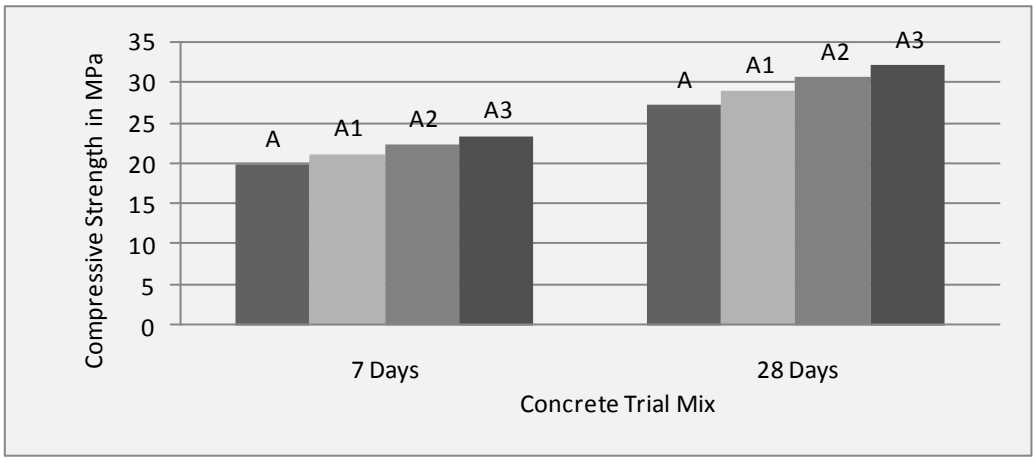

Trial concrete mix

Figure 5 Compressive strength of various trials concrete mixes at 7th and 28th days

From the Fig. 5, it has been observed that consistent increase in compressive strength could attributed due to addition of superplasticizer in concrete containing 10% fly ash with constant water-cement ratio. Further, one can say that compressive strength increases rather than decreases though there is increase in workability of mix. Similarly, from the scenario of graph shown in figure 6, one can comment that rapid in strength gain takes place up to its 7 days of curing later on its gaining rate getting flatter with increase in curing period of various Self-Compacting Concrete mixes.

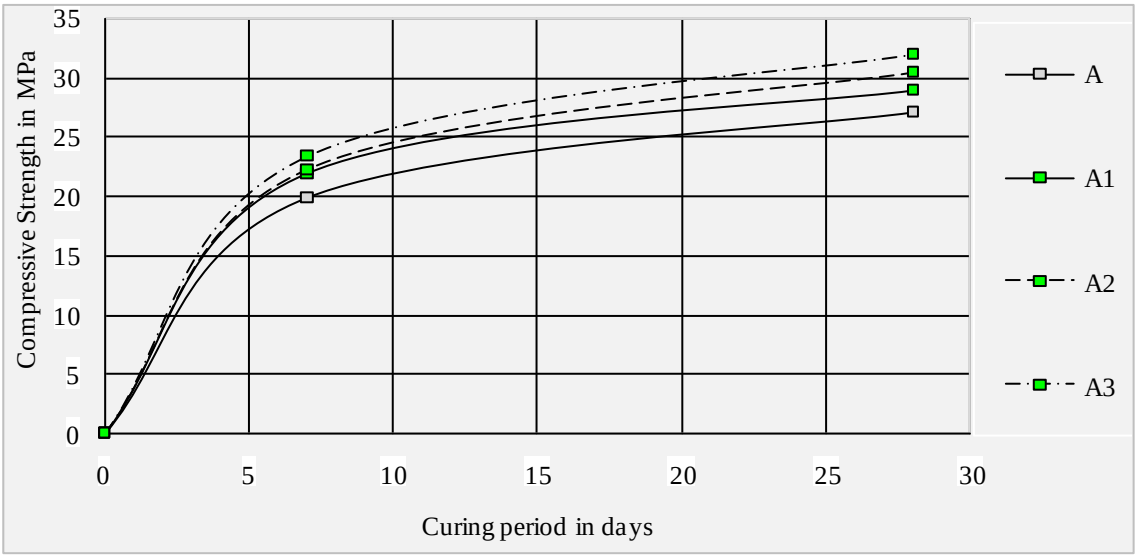

Figure 6 variation of compressive strength of concrete mix

V. CONCLUSION

The general objective is to evaluate the workability, unit weight and compressive strength of concrete mix with 10% replacement of cement content by fly ash in addition to varying doses of superplasticizer. From the test results, following conclusions are

1. Use of supplementary cementious materials that is, fly ash with an aim to achieve better workability with the saving in cementious material.
2. From the slump and compaction factor tests, it is observed that concrete containing fly ash and superplasticizer yields good workable mix in addition to increase in compressive strength marginally.
3. Addition of superplasticizer along with 10% fly ash of cement content accelerates the compressive strength of Self-Compacting.
4. Self-Compacting Concrete not only establishes the uniform and homogenous mix but also gives marginal reduction in weight of hardened mix of concrete.

5. From the present study, one can support to the comments made by previous researchers about saving of time in construction and also environment friendly user because of no compaction and vibrations resulting to no noise creation.
6. The scope of study in future is to assess the workability of mix using L-box test for the requirement of properties like passing, filling and flow ability whereas V-funnel test employed to know the property of viscosity. Further, hardened properties of SCC could be assessed for other test like flexural strength, split tensile strength and water absorption test as per Indian standards.

VI. ACKNOWLEDGEMENTS

The author would like to express gratitude to the Principal, Government Polytechnic Nashik for providing facility of conducting various tests in the laboratories and furthermore, I would like to extend thanks to my colleagues and students of third year Civil Engineering for their continuous support during experimental work.

REFERENCES

[1] K.C. Panda and P.K. Bal, *Properties of Self-compacting concrete using recycled concrete aggregate, Procedia Engineering, 51, 2013, 159-164.*
[2] H.J.H. Brouwers and H.J. Radix, Self-Compacting Concrete: Theoretical and Experimental study, *Elsevier, Cement and Concrete Research, 35, 2005, 2116-2136*
[3] J.M. Khati, Performance of Self-Compacting Concrete containing fly ash, *Construction and Building Materials, 2, No. 9, 2008, 1963-1971.*
[4] C. Jayashree, S. Manu and G. Ravindra, Cement-superplasticizer compatibility-issue and challenges, *The Indian Concrete Journal, 85, No. 7, 2011, 48-58.*
[5] D. Rahario, A. Subakti and Tavio, Mixed concrete optimization using fly ash, silica fume and iron slag on the SCCs compressive strength, *Procedia Engineering, 54 2013, 827-839.*
[6] P. Ramanathan, I. Baskar, P. Muthupriya and R. Venkatasubramani, Performance of Self-Compacting Concrete containing different mineral admixtures, *KSCE Journal of Civil Engineering, 12(2), 2013, 465-472.*
[7] IS 8112, Ordinary Portland Cement 43 grade, *1989, May 2006*
[8] IS 383, Indian standard specification for coarse and fine aggregates from natural sources for concrete (second revision), *Bureau of Indian Standards, Manak Bhavan, 9 Bahadur Shah Zafar Marg, New Delhi 110 002, 1970.*
[9] IS 10262, (Reaffirmed 1999), Recommended Guidelines for Concrete Mix Design, *Bureau of Indian Standards, Manak Bahavan, 9 Bahadur Shah Zafar Marg, New Delhi 110 002, 1982.*
[10] SP 23, Handbook of concrete mixes (based on Indian standards), *Bureau of Indian Standards, Manak Bhavan 9 Bahadur Shah Zafar Marg, New Delhi 110 002, 1982.*

American Journal of Engineering Research (AJER)
e-ISSN : 2320-0847 p-ISSN : 2320-0936
Volume-03, Issue-03, pp-212-218
www.ajer.org

Research Paper Open Access

Dynamic Response of Tray to Tray Temperature to Sudden Changes in Reflux Flow Rate in a Binary Distillation Column

Zekieni R. Yelebe, Seigha I. Fetepigi and Revelation J. Samuel
Department of Chemical/Petroleum Engineering, Niger Delta University,Bayelsa State Nigeria

Abstract: - This paper focusses on the strategic steps in the design, operation and response of tray to tray temperature in a binary distillation column to changes in the reflux flow rate. The temperature profile of a distillation column is an important parameter in the determination of the column performance. A model for the tray dynamics in distillation column is developed and used to determine the temperature profile of a binary distillation column that have been subjected to sudden changes in reflux flow rate. These equations were forward tested and the results obtained were compared with those from literature and was discovered that the percentage error ranges from 0–10.Thus, thebinary distillation column equations presented in this paper for the response of tray to tray temperature due to sudden changes in reflux flow rate can be used to predict the tray to tray temperature in multi-component distillation column that result from sudden changes in the reflux flow rate in such column. Hence, the developed model is suitable for the prediction of tray to tray temperature changes in any distillation column due to changes in reflux flow rate.

Keywords: - *binary, distillation, reflux, temperature, transfer function*

I. INTRODUCTION

Distillation is probably the most widely used separation process in the chemical and allied industries [1]. It is applicable in almost all separation of liquid mixtures into their various components such as rectification of alcohols, which has been practiced since antiquity and fractionation of crude oil. In processing industries, the demand for purer products coupled with the need for greater efficiency has encouraged continuous research into the principles and techniques governing the operation of the distillation unit [1].

The operation of the distillation column is governed by the principles of mass and energy balances in separating liquid mixtures into various components using their bubble point as a major criterion in determining the purity of separation [2]. The temperature profile of a distillation column may deviate from that of the designed temperature profile either by alteration in feed composition, reboiler flow rate or reflux flow rate. When these changes occur it is expected that the temperature profile (i.e. tray to tray temperature) of the column changes also. In this paper, we shall concentrate on the disturbance of reflux flow rate and its effect on tray to tray temperature in the binary distillation column.

The temperature profile of a distillation column is a measure of performance of the column [3], a means for monitoring these changes in tray to tray temperature is essential. Furthermore, for petroleum refinery (multi-component) column operation where side streams are withdrawn at a particular tray temperature, a monitoring of tray to tray temperature may enable (without leading necessarily to a shut-down of the column) the operator determine which trays now hold the new temperature (due to sudden change in reflux flow rate) from which side streams can be withdrawn [4], [5]. When such sudden change occurs (and remains constant for a while), the dynamics of operation of the column changes too. In this paper, we will track these changes in the dynamics of tray to tray temperature using the principles of mass and energy balance, and Taylor series expansion in linearizing non-linear terms.

Distillation columns are designed with a larger range in capacity than any other type of processing equipment with, single column 0.3-10m in diameter and a height of about 3-75m [6]. Designers and process control operators are aimed at achieving the desired product quality at minimum cost and also to provide constant purity of product even though there may be varieties in feed composition (especially in crude oils) and

alteration in reboiler and reflux flow rate [7]. A distillation unit is normally considered with its associated control systems and it is often operated in association with several other separate units.

The operations of a distillation column is governed by the principles of mass and energy balances in the separation of liquid mixtures into various components using their bubble point as a major parameter in the separation process [8]. The temperature profile of the distillation column is an important parameter in the determination of the column performance; therefore a means for monitoring and controlling the temperature profile is very essential [9]. However, the temperature profile of a distillation column may vary from that of the designed temperature profile either by modification and/or disturbance(s) in feed composition, reboiler flow rate and/or reflux flow rate [10]. When these sudden changes occur, it is expected that the temperature profile (tray to tray temperature) of the column changes also. In this paper, we shall consider the disturbance of reflux flow rate (only), and its effect on tray to tray temperature in the binary distillation column.

This paper shows the strategic steps in the design, operation and response of a binary distillation column to changes in the reflux flow rate. The column comprises of 25 trays or plates, a reflux drum, a condenser and a reboiler. The thirteenth tray is considered as the feed tray. In such distillation column, when there is sudden change in reflux flow rate its results in a change in tray to tray temperature, then, the methods proposed in this paper may be used for quick estimate of the tray temperature, so as to determine the new tray to which side stream can be withdrawn. Therefore, binary distillation column equations presented here for the response of tray to tray temperature due to sudden changes in reflux flow rate can be used to predict the tray to tray temperature in multi-component distillation column that result from sudden changes in the reflux flow rate in such column.

II. MODEL DEVELOPMENT

In this paper, a mathematical model for the dynamic response of tray to tray temperature to sudden changes in reflux flow rate in a binary distillation column is developed and perturbations equations are analysed.

Let us consider the Fig. 1 to develop a mathematical model to describe the dynamics of a single tray in the distillation column.

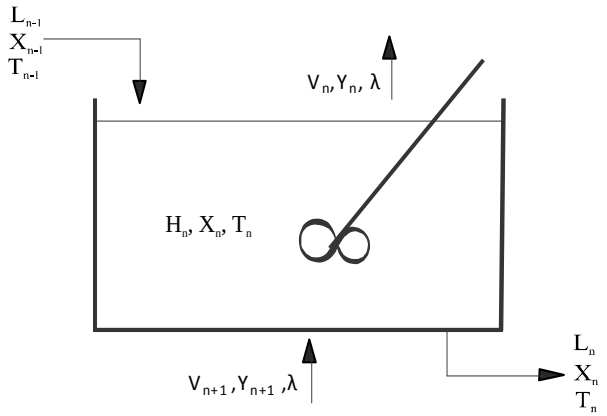

Fig. 1: A continuously stirred tank heater as a tray in the column

Where

H_n = volume of liquid hold-up in moles in tray n

L_{n-1} = the molar flow rate of liquid in to tray n from tray n-1.

X_{n-1} = mole fraction of the more volatile components in L_{n-1}

T_{n-1} = temperature of liquid L_{n-1}

V_n = molar flow rate of vapour exiting tray n

Y_n = mole fraction of the more volatile component in V_n

λ = latent heat of vaporization

L_n = molar flow rate of liquid out of tray n

X_n = mole fraction of the more volatile components in L_n

T_n= temperature of liquid L_n

V_{n+1} = molar flow rate of vapour in to tray n from tray n+1

Y_{n+1} = mole fraction of the more volatile component in V_{n+1}

2.1 MODEL ASSUMPTIONS

Some basic assumptions are considered to simplify the mathematical model of the dynamic response of the tray to tray temperature in a binary distillation column as follow:

1. Liquid hold-up in each plate is constant. Regardless of whether sudden changes occur, the rate at which liquid enters the tray will be the same as the rate at which liquid leaves the tray. Thus ensuring that liquid hold-up is constant.
2. Total pressure and temperature are uniform throughout the entire binary distillation column.
3. The binary distillation column is perfectly insulated. This is to ensure that there is no heat loss or gain between the column and its surroundings, thus enabling the distillation column operate adiabatically.
4. The feed is introduced as a saturated liquid. If the volume of liquid in the reboiler changes as a result of sudden changes in the reflux flow rate, it is expected that the controller action on the reboiler would responds fast enough so as to the supply of the heat necessary to cause the number of moles of vapour travelling from the stripping section to the rectifying section to remain constant from tray to tray. Thus, Equimolar overflow and Equimolar vaporization.
5. Hold-up of vapour in any tray in the binary distillation column is relatively small compared to liquid hold-up, and thus can be neglected.
6. Vapour bubbles through the liquid hold-up on each tray at a rate that is fast enough to enhance thorough agitation of the liquid hold-up. As a result, each tray together with its hold-up may be considered as a continuously stirred tank heater in which heat is supplied by the vapour releasing its heat of condensation to the liquid hold-up, and into which liquid flows in and out at the same rate.
7. All heats of solution are negligible.

2.2 MODEL DEVELOPMENT

The unsteady state energy balance consideration yields:

$$L_{n-1}X_{n-1}T_{n-1}C_p + V_{n+1}Y_{n+1}\lambda - L_{n-1}X_nT_nC_p - V_nY_n\lambda = \frac{d}{dt}H_nX_nT_nC_p \quad (1)$$

Based on equimolar vaporization and equimolar overflow, equation 1 can be written as:

$$L_{n-1}X_{n-1}T_{n-1}C_p + V\lambda(Y_{n+1}+Y_n) - L_{n-1}X_nT_nC_p = \frac{d}{dt}H_nX_nT_nC_p \quad (2)$$

The steady state energy balance equation is then:

$$\overline{L}_{n-1}\overline{X}_{n-1}\overline{T}_{n-1}C_p + V\lambda(Y_{n+1}+Y_n) - \overline{L}_{n-1}\overline{X}_n\overline{T}_nC_p = 0 \quad (3)$$

It is important to note that non-linear terms $L_{n-1}X_{n-1}T_{n-1}$, $L_{n-1}X_nT_n$ appear in equation2. Using a Taylor series expansion to linearize these non-linear terms yields the following two expressions after neglecting terms of higher powers:

$$L_{n-1}X_{n-1}T_{n-1} = \overline{L}_{n-1}\overline{X}n_{-1}\overline{T}_{n-1} + \overline{L}_{n-1}\overline{X}_{n-1}(T_{n-1}-\overline{T}_{n-1}) + \overline{L}_{n-1}\overline{T}_{n-1}(X_{n-1}-\overline{X}_{n-1}) + \overline{T}_{n-1}\overline{X}_{n-1}(L_{n-1}-\overline{L}_{n-1}) \quad (4)$$

A similar linearization gives,

$$L_{n-1}X_nT_n = \overline{L}_{n-1}\overline{X}_n\overline{T}_n + \overline{L}_{n-1}\overline{X}_n(T_n-\overline{T}_n) + \overline{L}_{n-1}\overline{T}_n(X_n-\overline{X}_n) + \overline{T}_n\overline{X}_n(L_{n-1}-\overline{L}_{n-1}) \quad (5)$$

Substituting equations 4 and 5 into 2, dividing through by C_p and subtracting the steady state energy balance equation yields the following linearized unsteady state energy balance equation:

$$\overline{X}_{n-1}\overline{T}_{n-1}L_{n-1} + \overline{L}_{n-1}\overline{T}_{n-1}X_{n-1} + \overline{L}_{n-1}\overline{X}_{n-1}T_{n-1} - 3\overline{X}_{n-1}\overline{T}_{n-1}\overline{L}_{n-1} - \overline{X}_n\overline{T}_nL_{n-1} - \overline{L}_{n-1}\overline{X}_nT_n - \overline{T}_n\overline{L}_{n-1}X_n + 3\overline{X}_n\overline{T}_n\overline{L}_{n-1}$$
$$= \overline{H}n\frac{d}{dt}X_nT_n \quad (6)$$

Introducing the perturbation variables

$$L_{n-1} = \overline{L}_{n-1} + \Delta L_{n-1} \quad (i)$$
$$X_{n-1} = \overline{X}_{n-1} + \Delta X_{n-1} \quad (ii)$$
$$T_{n-1} = \overline{T}_{n-1} + \Delta T_n \quad (iii)$$
$$X_n = \overline{X}_n + \Delta X_n \quad (iv)$$
$$T_n = \overline{T}_n + \Delta T_n \quad (v)$$

into the linearized unsteady state energy balance equation yields the equation of perturbations

$$\overline{X}_{n-1}\overline{T}_{n-1}\Delta L_{n-1} + \overline{L}_{n-1}\overline{X}_{n-1}\Delta T_{n-1} + \overline{T}_{n-1}\overline{L}_{n-1}\Delta X_{n-1} - \overline{X}_n\overline{T}_n\Delta L_{n-1} - \overline{L}_{n-1}\overline{X}_n\Delta T_n - \overline{T}_n\overline{L}_{n-1}\Delta X_n = \overline{H}_n\frac{d}{dt}(\overline{X}_n\Delta T_n + \overline{T}_n\Delta X_n) \quad (7)$$

The consequence that a change in reflux would have on composition is obtained by setting $\Delta T_n = 0$ in equation 7. Likewise the effect of a change in reflux on temperature is obtained by setting $\Delta X_n = 0$ in equation 7. In this way equation 7 is uncoupled so as to get two equations of perturbation:

$$\frac{\overline{H}_n}{\overline{L}_{n-1}}\frac{d}{dt}\Delta X_n + \Delta X_n = \frac{\overline{X}_{n-1}}{\overline{T}_n}\Delta T_{n-1} + \frac{\overline{T}_{n-1}}{\overline{T}_n}\Delta X_{n-1} + \frac{\overline{X}_{n-1}\overline{T}_{n-1}-\overline{X}_n\overline{T}_n}{\overline{L}_{n-1}\overline{X}_n}\Delta L_{n-1} \quad (8)$$

$$\frac{\overline{H}_n}{\overline{L}_{n-1}}\frac{d}{dt}\Delta T_n + \Delta T_n = \frac{\overline{X}_{n-1}}{\overline{X}_n}\Delta T_{n-1} + \frac{\overline{T}_{n-1}}{\overline{X}_n}\Delta X_{n-1} + \frac{\overline{X}_{n-1}\overline{T}_{n-1}-\overline{X}_n\overline{T}_n}{\overline{L}_{n-1}\overline{T}_n}\Delta L_{n-1} \quad (9)$$

Let $\tau = \frac{\overline{H}_n}{\overline{L}_{n-1}}$ defined the time constant for the consequence of change in reflux on temperature. This same time constant gives the consequence of change in reflux on composition. Thus, equations 8 and 9 can be written as:

$$\tau\frac{d}{dt}\Delta X_n + \Delta X_n = \frac{\overline{X}_{n-1}}{\overline{T}_n}\Delta T_{n-1} + \frac{\overline{T}_{n-1}}{\overline{T}_n}\Delta X_{n-1} + \frac{\overline{X}_{n-1}\overline{T}_{n-1}-\overline{X}_n\overline{T}_n}{\overline{L}_{n-1}\overline{T}_n}\Delta L_{n-1} \quad (10)$$

$$\tau\frac{d}{dt}\Delta T_n + \Delta T_n = \frac{\overline{X}_{n-1}}{\overline{X}_n}\Delta T_{n-1} + \frac{\overline{T}_{n-1}}{\overline{X}_n}\Delta X_{n-1} + \frac{\overline{X}_{n-1}\overline{T}_{n-1}-\overline{X}_n\overline{T}_n}{\overline{L}_{n-1}\overline{X}_n}\Delta L_{n-1} \quad (11)$$

2.3 SOLUTION TO PERTURBATION EQUATIONS

Equations 10 and 11 are the equations of perturbation that are solved using Laplace transformation to obtain transfer functions that relates changes in temperature and changes in composition to changes in reflux. Also, it is important to note that sudden changes in reflux do not have any effect on mole fraction and temperature of liquid hold-up in the reflux drum and consequently the reflux temperature remains constant and so does reflux composition. Therefore ΔT_0 and ΔX_0 are negligible. Furthermore, based on the assumptions that these sudden changes in reflux does not change with time, so that, $\Delta L_{n-1} = \Delta R$.

On tray n = 1, equation 10 yields:

$$\tau\frac{d}{dt}\Delta X_1 + \Delta X_1 = \left(\frac{\overline{X}_0\overline{T}_0-\overline{X}_1\overline{T}_1}{\overline{L}_0\overline{T}_1}\right)\Delta R$$

whose Laplace transformation yields the transfer function:

$$\frac{\Delta X_1(S)}{\Delta R(s)} = \left(\frac{\overline{X}_0\overline{T}_0-\overline{X}_1\overline{T}_1}{\overline{L}_0\overline{T}_1}\right)\frac{1}{\tau S+1} \quad (12)$$

Likewise substituting n = 1 into equation 11 yields:

$$\tau\frac{d}{dt}\Delta T_1 + \Delta T_1 = \left(\frac{\overline{X}_0\overline{T}_0-\overline{X}_1\overline{T}_1}{\overline{L}_0\overline{X}_1}\right)\Delta R$$

whose Laplace transformation yields:

$$\frac{\Delta T_1(S)}{\Delta R(s)} = \left(\frac{\overline{X}_0\overline{T}_0-\overline{X}_1\overline{T}_1}{\overline{L}_0\overline{X}_1}\right)\frac{1}{\tau S+1} \quad (13)$$

On tray 2, equation 10 yields:

$$\tau\frac{d}{dt}\Delta X_2 + \Delta X_2 = \frac{\overline{X}_1}{\overline{T}_2}\Delta T_1 + \frac{\overline{T}_1}{\overline{T}_2}\Delta X_1 + \frac{\overline{X}_1\overline{T}_1-\overline{X}_2\overline{T}_2}{\overline{L}_1\overline{T}_2}\Delta R$$

on Laplace transformation it yields:

$$\Delta X_2(S)(\tau S+1) = \frac{\overline{X}_1}{\overline{T}_2}\Delta T_1(S) + \frac{\overline{T}_1}{\overline{T}_2}\Delta X_1(S) + \frac{\overline{X}_1\overline{T}_1-\overline{X}_2\overline{T}_2}{\overline{L}_1\overline{T}_2}\Delta R(S) \quad (14)$$

Substituting equations 12 and 13 into 14 and simplifying gives:

$$\frac{\Delta X_2(S)}{\Delta R(S)} = \frac{\overline{X}_1\overline{T}_1-\overline{X}_2\overline{T}_2}{\overline{L}_1\overline{T}_2}\frac{1}{(\tau S+1)} + 2\left(\frac{\overline{X}_0\overline{T}_0-\overline{X}_1\overline{T}_1}{\overline{L}_0\overline{T}_2}\right)\frac{1}{(\tau S+1)^2} \quad (15)$$

Likewise putting n = 2 into equation 11 gives

$$\tau\frac{d}{dt}\Delta T_2 + \Delta T_2 = \frac{\overline{X}_1}{\overline{X}_2}\Delta T_1 + \frac{\overline{T}_1}{\overline{X}_2}\Delta X_1 + \frac{\overline{X}_1\overline{T}_1-\overline{X}_2\overline{T}_2}{\overline{L}_1\overline{X}_2}\Delta R$$

applying Laplace transform gives

$$(\tau S+1)\Delta T_2(S) = \frac{\overline{X}_1}{\overline{X}_2}\Delta T_1(S) + \frac{\overline{T}_1}{\overline{X}_2}\Delta X_1(S) + \frac{\overline{X}_1\overline{T}_1-\overline{X}_2\overline{T}_2}{\overline{L}_1\overline{X}_2}\Delta R(S) \quad (16)$$

Substituting equations 12 and 13 into 16 yields:

$$\frac{\Delta T_2(S)}{\Delta R(S)} = \frac{\overline{X}_1\overline{T}_1-\overline{X}_2\overline{T}_2}{\overline{L}_1\overline{X}_2}\frac{1}{(\tau S+1)} + 2\left(\frac{\overline{X}_0\overline{T}_0-\overline{X}_1\overline{T}_1}{\overline{L}_0\overline{X}_2}\right)\frac{1}{(\tau S+1)^2} \quad (17)$$

On tray 3, equation 10 yields:

$$\tau\frac{d}{dt}\Delta X_3 + \Delta X_3 = \frac{\overline{X}_2}{\overline{T}_3}\Delta T_2 + \frac{\overline{T}_2}{\overline{T}_3}\Delta X_2 + \frac{\overline{X}_2\overline{T}_2-\overline{X}_3\overline{T}_3}{\overline{L}_2\overline{T}_3}\Delta R$$

upon Laplace transform yields:

$$(\tau S+1)\Delta X_3(S) = \frac{\overline{X}_2}{\overline{T}_3}\Delta T_2(s) + \frac{\overline{T}_2}{\overline{T}_3}\Delta X_2(s) + \frac{\overline{X}_2\overline{T}_2-\overline{X}_3\overline{T}_3}{\overline{L}_2\overline{T}_3}\Delta R(s) \quad (18)$$

Substituting equations 15 and 17 into 18 and simplifying gives:

$$\frac{\Delta X_3(S)}{\Delta R(S)} = \left(\frac{\overline{X}_2\overline{T}_2-\overline{X}_3\overline{T}_3}{\overline{L}_2\overline{T}_3}\right)\frac{1}{\tau S+1} + 2\left(\frac{\overline{X}_1\overline{T}_1-\overline{X}_2\overline{T}_2}{\overline{L}_1\overline{T}_3}\right)\frac{1}{(\tau S+1)^2} + 4\left(\frac{\overline{X}_0\overline{T}_0-\overline{X}_1\overline{T}_1}{\overline{L}_0\overline{T}_3}\right)\frac{1}{(\tau S+1)^3} \quad (19)$$

Also on tray 3, equation 11 yields:

$$\tau\frac{d}{dt}\Delta T_3 + \Delta T_3 = \frac{\overline{X}_2}{\overline{X}_3}\Delta T_2 + \frac{\overline{T}_2}{\overline{X}_3}\Delta X_2 + \frac{\overline{X}_2\overline{T}_2-\overline{X}_3\overline{T}_3}{\overline{L}_2\overline{X}_3}\Delta R$$

upon Laplace transform yields:

$$(\tau S+1)\,\Delta T_3(s) = \frac{\overline{X}_2}{\overline{X}_3}\,\Delta T_2(s) + \frac{\overline{T}_2}{\overline{X}_3}\,\Delta X_2(s) + \frac{\overline{X}_2\overline{T}_2-\overline{X}_3\overline{T}_3}{\overline{L}_2\overline{X}_3}\,\Delta R(s) \quad (20)$$

Substituting equations 15 and 17 into 20 and simplifying gives:

$$\frac{\Delta T_3(S)}{\Delta R(S)} = \left(\frac{\overline{X}_2\overline{T}_2-\overline{X}_3\overline{T}_3}{\overline{L}_2\overline{X}_3}\right)\frac{1}{\tau S+1} + 2\left(\frac{\overline{X}_1\overline{T}_1-\overline{X}_2\overline{T}_2}{\overline{L}_1\overline{X}_3}\right)\frac{1}{(\tau S+1)^2} + 4\left(\frac{\overline{X}_0\overline{T}_0-\overline{X}_1\overline{T}_1}{\overline{L}_0\overline{X}_3}\right)\frac{1}{(\tau S+1)^3} \quad (21)$$

In like manner $\Delta X_4(S)$, $\Delta T_4(S)$, $\Delta X_5(S)$, and $\Delta T_5(S)$ are solved to yield the following four equations:

$$\frac{\Delta X_4(S)}{\Delta R(S)} = \left(\frac{\overline{X}_3\overline{T}_3-\overline{X}_4\overline{T}_4}{\overline{L}_3\overline{T}_4}\right)\frac{1}{\tau S+1} + 2\left(\frac{\overline{X}_2\overline{T}_2-\overline{X}_3\overline{T}_3}{\overline{L}_2\overline{T}_4}\right)\frac{1}{(\tau S+1)^2} + 4\left(\frac{\overline{X}_1\overline{T}_1-\overline{X}_2\overline{T}_2}{\overline{L}_1\overline{T}_4}\right)\frac{1}{(\tau S+1)^3} + 8\left(\frac{\overline{X}_0\overline{T}_0-\overline{X}_1\overline{T}_1}{\overline{L}_1\overline{T}_4}\right)\frac{1}{(\tau S+1)^4} \quad (22)$$

$$\frac{\Delta T_4(S)}{\Delta R(S)} = \left(\frac{\overline{X}_3\overline{T}_3-\overline{X}_4\overline{T}_4}{\overline{L}_3\overline{X}_4}\right)\frac{1}{\tau S+1} + 2\left(\frac{\overline{X}_2\overline{T}_2-\overline{X}_3\overline{T}_3}{\overline{L}_2\overline{X}_4}\right)\frac{1}{(\tau S+1)^2} + 4\left(\frac{\overline{X}_1\overline{T}_1-\overline{X}_2\overline{T}_2}{\overline{L}_1\overline{X}_4}\right)\frac{1}{(\tau S+1)^3} + 8\left(\frac{\overline{X}_0\overline{T}_0-\overline{X}_1\overline{T}_1}{\overline{L}_1\overline{X}_4}\right)\frac{1}{(\tau S+1)^4} \quad (23)$$

$$\frac{\Delta X_5(S)}{\Delta R(S)} = \left(\frac{\overline{X}_4\overline{T}_4-\overline{X}_5\overline{T}_5}{\overline{L}_4\overline{T}_5}\right)\frac{1}{\tau S+1} + 2\left(\frac{\overline{X}_3\overline{T}_3-\overline{X}_4\overline{T}_4}{\overline{L}_2\overline{T}_5}\right)\frac{1}{(\tau S+1)^2} + 4\left(\frac{\overline{X}_2\overline{T}_2-\overline{X}_3\overline{T}_3}{\overline{L}_2\overline{T}_5}\right)\frac{1}{(\tau S+1)^3} + 8\left(\frac{\overline{X}_1\overline{T}_1-\overline{X}_2\overline{T}_2}{\overline{L}_1\overline{T}_5}\right)\frac{1}{(\tau S+1)^4} + 16\left(\frac{\overline{X}_0\overline{T}_0-\overline{X}_1\overline{T}_1}{\overline{L}_0\overline{T}_5}\right)\frac{1}{(\tau S+1)^5} \quad (24)$$

$$\frac{\Delta T_5(S)}{\Delta R(S)} = \left(\frac{\overline{X}_4\overline{T}_4-\overline{X}_5\overline{T}_5}{\overline{L}_4\overline{X}_5}\right)\frac{1}{\tau S+1} + 2\left(\frac{\overline{X}_3\overline{T}_3-\overline{X}_4\overline{T}_4}{\overline{L}_2\overline{X}_5}\right)\frac{1}{(\tau S+1)^2} + 4\left(\frac{\overline{X}_2\overline{T}_2-\overline{X}_3\overline{T}_3}{\overline{L}_2\overline{X}_5}\right)\frac{1}{(\tau S+1)^3} + 8\left(\frac{\overline{X}_1\overline{T}_1-\overline{X}_2\overline{T}_2}{\overline{L}_1\overline{X}_5}\right)\frac{1}{(\tau S+1)^4} + 16\left(\frac{\overline{X}_0\overline{T}_0-\overline{X}_1\overline{T}_1}{\overline{L}_0\overline{X}_5}\right)\frac{1}{(\tau S+1)^5} \quad (25)$$

In order to calculate the temperature changes, these S-space transfer functions for the changes in temperature as a consequence of reflux changes (only) are transformed to real time space using inverse Laplace transform.

III. RESULTS AND DISCUSSION

The transfer functions were transformed to real time space equations and the solution for the tray to tray temperature changes of the distillation column are calculated.The real time equations obtained are used in conjunction with data obtained from [14], to predict the tray by tray temperatures for the distillation column due to sudden changes in reflux from 40.5 lbmol /100 lbmol of feed to 33.5 lbmol /100 lbmol. Thus, the S-space transfer functions that were obtained in the previous section are converted into real time space using the inverse Laplace transformation techniques, assuming that transient effects due to a change in reflux have arrived at a new steady state; we let $t \to \infty$ in real time space solution. The results are presented and discussed in following figures.

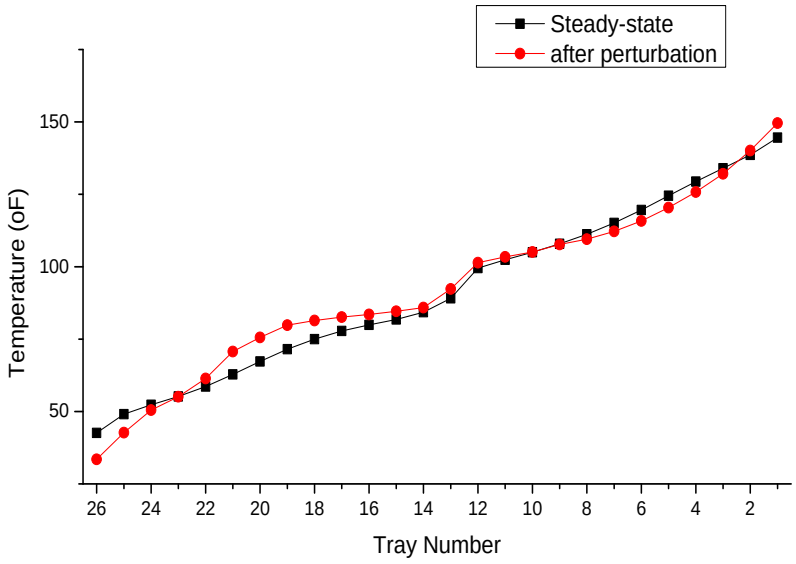

Fig. 2: Tray to tray temperature profile down the column

Fig. 2 shows the tray to tray dynamic temperature profile down the column to a sudden change in reflux flow rate. The steady-state temperature profile of the column increases at uniform rate from top to bottom. The sudden change of reflux flow rate from 40 lbmol/100 lbmol to 33.5 lbmol/100 lbmol introduced a perturbation to the temperature profile. As such, the sudden decrease in temperature below the steady-state temperature in the top three trays was observed, this may be as a result of the introduction of a colder reflux temperature into the column. The temperature then increases in the seventh tray above the steady-state temperatures until the feed tray where its falls back to the steady-state temperature. This temperature profile of the distillation column is an important parameter in the determination of the column performance; therefore a means for monitoring and controlling the temperature profile is very essential.

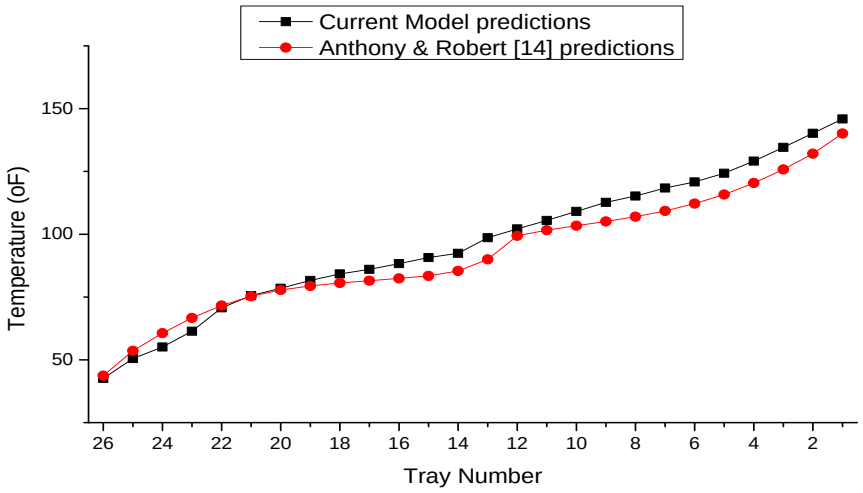

Fig. 3: Tray to tray temperature profile down the column

Fig. 3 shows a comparison of the predicted results of the current model with those predicted by Anthony & Robert [14] for the same operating conditions. Both predictions were similar, although the current model predicted lower temperatures for the first four trays and slightly higher temperatures down the column. This tray to tray dynamic temperature response is essential for the prediction of side stream to which new temperature of the required range now falls.

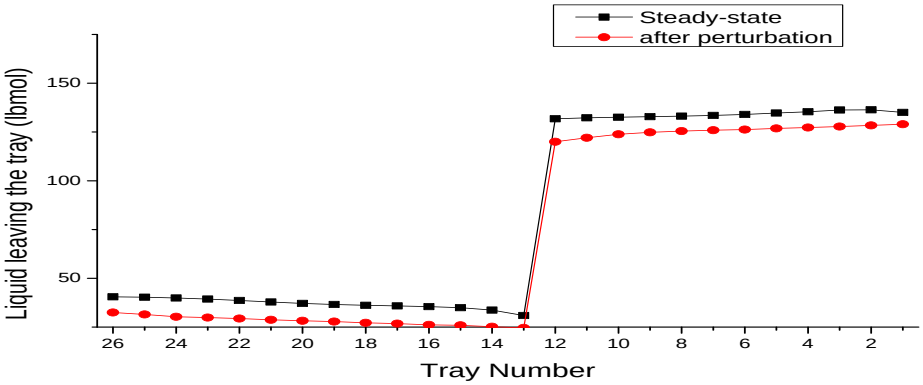

Fig. 4: Liquid hold-up from tray to tray down the column

Fig. 4 shows the level of liquid in the column from tray to tray. The liquid hold-up is lower above the feed tray and rises rapidly above at the feed tray showing the introduction of more liquid into the column. The level of liquid at steady-state is higher compared with the one after perturbation because of the reduction in the reflux. Hence, the current model shows high percentage reliability and applicability for the prediction of tray to tray temperature changes in a distillation column due to changes in reflux flow rate.

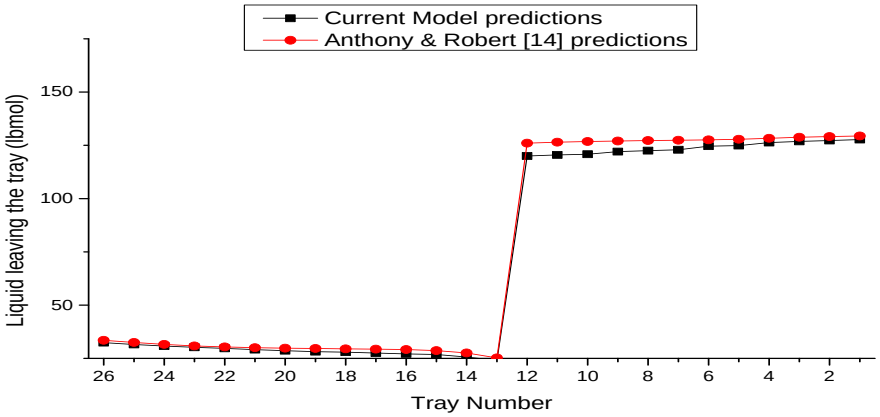

Fig. 5: Liquid hold-up from tray to tray down the column

Fig. 5 shows the liquid hold-up predictions down the column after perturbation comparing those of Anthony & Robert [14] and the current model. The liquid hold-up is lower above the feed tray and rises rapidly above at the feed tray showing the introduction of more liquid into the column. Similar observations were shown in both cases with lesser liquid-hold predicted by the current model. Hence, the current model shows high percentage reliability and applicability for the prediction of tray to tray temperature changes in a distillation column due to changes in reflux flow rate.

IV. CONCLUSION

This paper becomes applicable when quick estimates for changes in temperature due to sudden change in reflux flow rate are required for a distillation column, then it is recommended that the method discussed in this paper can be used since the errors predicted in this paper falls within the users allowable tolerances (0% - 10%). Thus, this paper may be relevant in multi-component distillation column operations were side streams are withdrawn from trays that are at particular temperature. In such distillation column, a sudden change in reflux flow rate causes a change in tray to tray temperature, then the methods proposed in this paper may be used for quick estimate of the tray temperature, so as to determine the new tray to which side stream can be withdrawn. Therefore, binary distillation column equations presented in this paper for the response of tray to tray temperature due to sudden changes in reflux flow rate can be used to predict the tray to tray temperature in multi-component distillation column that result from sudden changes in the reflux flow rate in such column.

V. REFERENCES

[1] J.M. Coulson and J.F. Richardson, *Particle Technology and Separation Process*, volume 1, 5th edition, Butterworth-Heinemann, 2002, pp 493-515

[2] W.L. Nelson, *Petroleum Refinery Engineering*, 4th edition, McGraw Hill, 1969, pp 502-505

[3] Perry H. Robert, *Chemical Engineering Handbook*, 7th edition, McGraw Hill, New York, 1997

[4] Donald R. Coughanowr, *Process Systems Analysis and Control*, second edition, McGraw Hill, 1991, pp 321, 328-333

[5] Yang Wen-jel and Masubuchi Masami, *Dynamics for Process and system control*, Gordon and Beach, New York, 1985, 207-213.

[6] J.M. Coulson and J.F. Richardson, *Chemical Engineering Design*, volume 6, 4th edition, Butterworth-Heinemann, 2005

[7] Samuel H. Maron and Carl F. Prutton, *Principles of Physical Chemistry*, 4th edition, Mac Millan Company, 1965, pp 143.

[8] Fouad M. Khoury, Simulate Absorbers by Successive Iteration, *Chemical Engineering*, McGraw Hill, Vol. 87, (26), December 1980

[9] William L. Luyben, "*Process Model, Simulation and Control for Chemical Engineers*", 2nd edition McGraw Hill, 1774

[10] Alan S. Foust, Leonard A. Wenzel, Curtis W. Clump, Louis Maus, and Bryce L. Andersen, "*Principle of Unit Operation*", John Wiley & Son, Inc. 1960, 20-27.

[11] Thomas W. Weber, *Introduction to Process Dynamics*, John Wiley and Sons, 1973

[12] Robert E. Treybal, *Mass Transfer Operation*, 2nd edition, McGraw Hill, 1968

[13] Mc Cabe, Smith and Harritt, *Unit Operation of Chemical Engineering*, McGraw Hill, 2001

[14] Anthony L. Hines and Robert N. Maddox, *Mass Transfer Fundamental and Application*, Prentice Hall Inc, 1985, pp 368-372.

American Journal of Engineering Research (AJER)
e-ISSN : 2320-0847 p-ISSN : 2320-0936
Volume-03, Issue-03, pp-219-224
www.ajer.org

Research Paper Open Access

Face Feature Extraction for Recognition Using Radon Transform

Justice Kwame Appati[1], Gabriel Obed Fosu[1], Gideon Kwadzo Gogovi[1]
[1]*Department of Mathematics, Kwame Nkrumah University of Science and Technology, Kumasi, Ghana*

Abstract : **-** Face recognition for some time now has been a challenging exercise especially when it comes to recognizing faces with different pose. This perhaps is due to the use of inappropriate descriptors during the feature extraction stage. In this paper, a thorough examination of the Radon Transform as a face signature descriptor was investigated on one of the standard database. The global features were rather considered by constructing a Gray Level Co-occurrences Matrices (GLCMs). Correlation, Energy, Homogeneity and Contrast are computed from each image to form the feature vector for recognition. We showed that, the transformed face signatures are robust and invariant to the different pose. With the statistical features extracted, face training classes are optimally broken up through the use of Support Vector Machine (SVM) whiles recognition rate for test face images are computed based on the L1 norm.

Keywords: *- Radon Transform; SVM; Correlation; Face Recognition*

I. INTRODUCTION

In recent years, extensive research has been conducted on Face Recognition Systems. However, irrespective of all excellent work achieved, there still exist some problems unhandled fully especially when it comes to databases containing individuals presenting their faces with different poses.

In 1997, Etemad and Chellappa [1], in their Linear Discriminant Analysis (LDA) algorithm, made an objective evaluation of the significance of features extracted for identifying a unique face from a database. This LDA of faces provides a small set of features that carries the most relevant information for classification purposes. These features were obtained through eigenvector analysis of scatter matrices with the objective of maximizing between-class variations and minimizing within-class variations. The algorithm uses a projection based feature extraction procedure and an automatic classification scheme for face recognition. A slightly different method, called the evolutionary pursuit method for face recognition was described by Liu and Wechsler [2]. Their method processes images in a lower dimensional whitened PCA subspace. Directed but random rotations of the basis vectors in this subspace are searched by Genetic Algorithm, where evolution is driven by a fitness function defined in terms of performance accuracy and class separation. From thence, many face representation approaches have been introduced including subspace based holistic features and local appearance features [3]. Typical holistic features include the well-known principal component analysis (PCA) [4-5] and independent component analysis (ICA) [6].

In 2003, Zhao et al [7] made a great progress on database images with small variation in facial pose and lighting. In their study, Principal Component Analysis (PCA) was use as their face descriptor. Following their work, Moon and Jonathon [8] implemented a generic modular Principal Component Analysis (PCA) algorithm where numerous design decisions were stated. Experiment was made by using different approach to the illumination normalization in order to study its effects on performance. Moreover, variation in the number of eigenvectors to represent a face image as well as similarity measure in the face classification proceeds.

This study investigates the problem of feature extraction in face recognition to achieve high performance in the face recognition system. Face Recognition method based on Radon Transform which provides directional information in face image as a feature extraction descriptor and SVM as a classifier was achieved by testing it on Face94 Database.

II. PRELIMINARY DEFINITIONS

Some definitions of the features extracted from a face image *P(i,j)* for performance analysis and the proposed RTFR model using SVM are discussed.

2.1 Energy

It is the sum of squared elements in the GLCMs. The range for GLCMs is given by [0, 1]. Energy is 1 for constant image [9].

$$Energy = \sum_{i=1}^{N}\sum_{j=1}^{N}(P(i,j))^2 \qquad (1)$$

2.2 Contrast

It is the measure of the intensity contrast between a pixel and its neighbour over the whole face image. The range for GLCMs is given by [0, (size (GLCMs, 1) - 1)^2]. Contrast is zero for constant image [9].

$$Contrast = \sum_{i=1}^{N}\sum_{j=1}^{N}(|i-j|)^2 P(i,j) \qquad (2)$$

2.3 Homogeneity

It is a value that measures the closeness of the distribution of elements in the GLCMs to the diagonal. The range for GLCMs is [0, 1]. Homogeneity is 1 for diagonal GLCMs. [9]

$$Homogeneity = \sum_{i=1}^{N}\sum_{j=1}^{N}\frac{P(i,j)}{(1+(i-j))} \qquad (3)$$

2.4 Correlation

It is a measure of how correlated a pixel is to its neighbour over the whole image. The range for GLCMs is given by [-1, 1]. Correlation is 1 or -1 for a perfectly positively or negatively correlated image. Correlation is NaN (not a number) for a constant image. [9]

$$Correlation = \sum_{i=1}^{N}\sum_{j=1}^{M}\frac{(i-\mu_i)(j-\mu_j)P(i,j)}{\delta_i\delta_j} \qquad (4)$$

whereμ is the mean and δ is the variance.

III. MODEL

3.1Radon Transform

Radon transform computed at different angles along with the estimated facial pixel motion gives a spatio-temporal representation of the expression, are efficiently tackled. The motion vector at position *(x, y)* can be expressed as:

$$\hat{v}_k(x,y) = a_k(x,y)e^{j\phi_k(x,y)} \qquad (5)$$

The discrete Radon transform of the motion vector magnitude, at angle θ is then given by:

$$R(\theta) = \sum_{u=-\infty}^{\infty} a_k(x,y)\,|_{x=t\cos\theta-u\sin\theta,\,y=t\sin\theta+u\cos\theta} \qquad (6)$$

As it can be seen from this equation, using Radon transform we estimate the spatial distribution of the energy of perturbation. An attempt to compute the direction of the facial parts motion, although useful, requires extremely accurate optical flow estimation as well as global facial feature tracking.

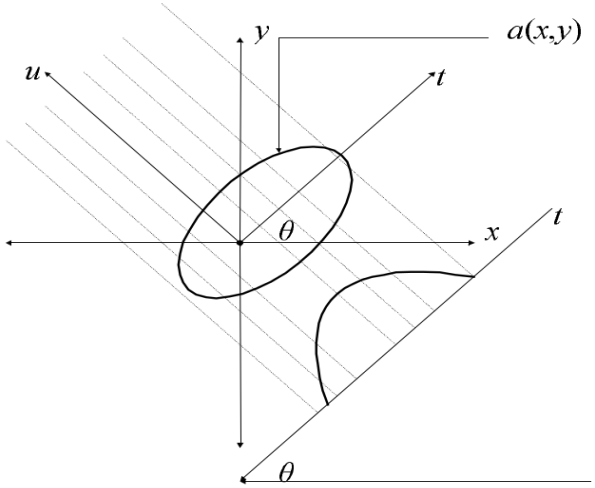

Fig. 1. Concept of the Radon Transform

The projections on the Radon Transform on angles give the face signatures and are used to characterize the expressions.

3.2 Support Vector Machine Classification (SVM)

SVM is class of maximum margin classifier for pattern recognition between two classes. It works by finding the decision surface that has maximum distance to the closest points in the training set which are termed support vectors. Assume training set of points $x_i \in R^n$ belongs to one of the two classes identified by the label $y_i \in \{-1, 1\}$ and also assuming that the data is linearly separable, then the goal of maximum classification is to separate the two classes by a hyperplane such that the distance to the support vectors is maximized. This hyperplane is referred to as the optimal separating hyperplane and has the form:

$$f(x) = \sum_{i=1}^{\ell} \alpha_i y_i x_i \bullet x + b \qquad (7)$$

The coefficients α_i and the b in *Eqn (7)* are the solutions of a quadratic programming problem. Classification of new data point x is performed by computing the sign of the right side of *Eqn (7)*. In the following we will use

$$d(x) = \frac{\sum_{i=1}^{\ell} \alpha_i y_i x_i \bullet x + b}{\left\| \sum_{i=1}^{\ell} \alpha_i y_i x_i \right\|} \qquad (8)$$

to perform multi-class classification. The sign of d is the classification result for x and $|d|$ is the distance from x to the hyper-plane. The further away the point is from the decision surface, the more reliable the classification result.

In multi-class classification, there are two basic strategies for solving q-class problems with the SVM:

In one-vs-all approach, q SVM is trained and each of the SVM separates a single class from all remaining classes.In the pairwise approach, $q(q - 1)/2$ machines are trained and each SVM separates a pair of classes. However, regarding the training effort, the one-vs-all approach is preferable since only q SVM has to be trained compared to $q(q - 1)/2$ SVM.

3.3 Feature Vectors

The Radon transform is used to extract the image intensity along the radial line oriented at a specific angle. Out of this face signature, the Gray-Level Co-occurrence Matrix is computed from which the following statistical features are extracted; Correlation, Contrast, Energy and Homogeneity which are concatenated in row to form the unique feature vector for a particular face image.

3.4 Matching

The final feature vector of the test face image is determined and compared with the trained feature vector. The Euclidean Distance is then computed between trained face database and the test face data. The image matched index which recorded the list Euclidean Distance is selected with the assumption that, it is the

correct index for the test image. This is then verified with the original index of the test image. If the indices are the same then a match is recorded otherwise miss-match.

$$\|X - A\|_2 = \sqrt{\sum_{i=1}^{n} (x_i - a_i)^2} \qquad (9)$$

where:
X is the feature vector of the trained image.
A is the feature vector of the test image
$n$is the number of elements in the feature vector
$x_i$is the element of the trained feature vector
$a_i$is the element of the test feature vector

IV. ANALYSIS AND DISCUSSION

Facial images used for this study were taken from Faces94 database which is composed of 152 individuals with 20 been female, 112 male and 20 male staff kept in separate directories. These separate directories were merged into one to achieve the different lighting effect. The subjects were sited at approximately the same distance from the camera and were asked to speak while a sequence of twenty images was taken and this was to introduce moderate and natural facial expression variation. Each facial image was taken at a resolution of 180 × 200 pixels in the portrait format on a plain green background and index 1 to 20 prefixed with a counter. In all, a total of 3040 images were created which make up the database for the study.

Fig. 2. Sample of face image from Database

Table 1. Algorithm for the RTFR

1. Read face image from the database.
2. Convert image from color space to gray scale.
3. Compute the intensity map of each face image in the database by applying the Radon Transform on it.
4. For each intensity image map computed, calculate the Gray-Level Co-occurrence Matrix
5. The global statistical feature, that is: Correlation, Energy, Contract and Homogeneity are established from the Gray-Level Co-occurrence Matrix.
6. A concatenation of these four features forms the final feature vector per face image.
7. Dataset containing feature vector is now divided in to training and test set for performance analysis
8. SVM is applied to compute the recognition rate

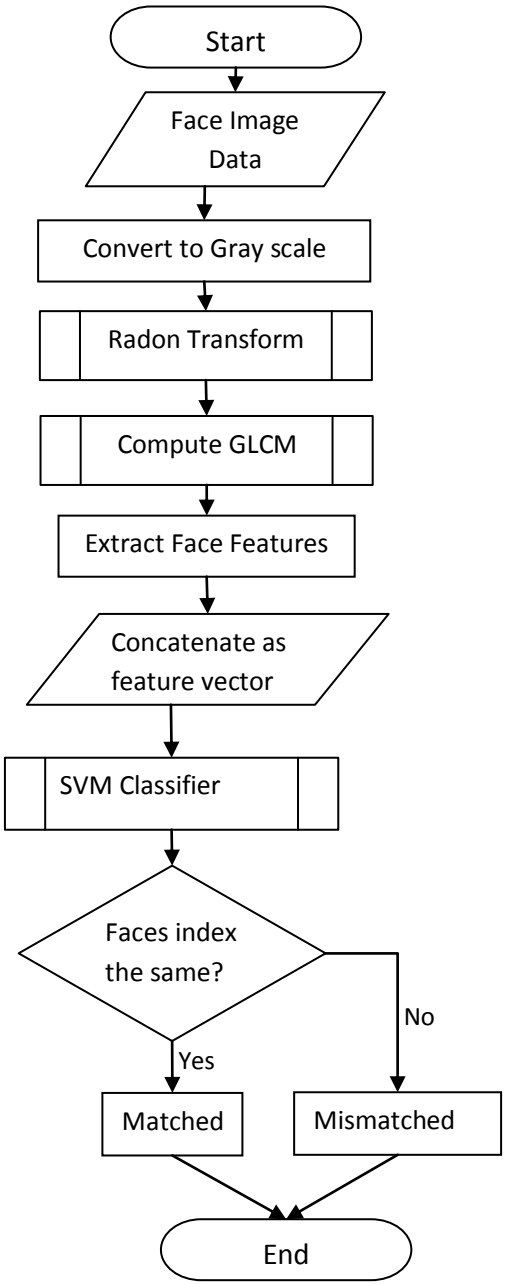

Fig. 3. Block Diagram of RTFR

This proposed algorithm accept face image as input and returns a verified face image from the trained dataset as output. The objective of this design is to extract the least features from a face image which is global and spacio-temporal in nature so as the make face recognition invariant to pose.

The performance of our proposed method (RTFR) was revealed by testing it on the face94 database. Before this performance was carried out, the feature vector containing 12,160 features with four features for each face image was partitioned into two disjoint set that is the trained features and the test features. At the end of the partition, the test data has 2,432 features whiles the trained date has 9,728 features resulting in 608 and 2432 face images for test and train respectively. Each face feature in the test data is matched against all the face features in the train dataset while the Euclidean distance is taken. Out of the many distance taken, the minimum distance is selected along with it image index. At the end of all these processes, the recognition rate was computed which gave 97% accuracy.

V. CONCLUSION

In this paper, we observed that our Radon Transform based feature extraction for face recognition (RTFR) yielded a good recognition rate though only four features were extracted from the face for recognition purpose. This may be due to the fact that the Radon transforms extract features that are highly correlated therefore throwing away the less relevant intensity values. This act as a feature reduction method since only face projections are of interest to us for further reduction and hence makes feature storage easier for computation aside the good performance rate recorded.

REFERENCES

[1] K. Etemad and R. Chellappa, *"Discriminant Analysis for Recognition of Human Face Images",* Proc. First Int. Conf. on Audio and Video Based Biometric Person Authentication, Crans Montana, Switzerland, Lecture Notes In Computer Science; Vol.1206, August 1997, pp.127 - 1422

[2] C. Liu and H. Wechsler, *"Face Recognition usingEvolutionary Pursuit",* Proc. Fifth European Conf. on Computer Vision, ECCV, Freiburg, Germany, Vol II, 02-06 June 1998, pp.596-612.

[3] S. Z. Li and A. K. Jain, *"Handbook of Face Recognition"*,New York,Springer-Verlag, 2005

[4] M. A. Turk and A.P. Pentland, *"Face Recognition usingeigenfaces"*, Proc. IEEE Computer Society Conf. Comput. vs. Pattern Recognition, June 1991 pp. 586-591.

[5] P. Belhumeur. J. Hespanha and D. Kriegman, *"Eigenfacesvs. fisherfaces: recognition using class specific linear projection",* IEEE Trans. On Pattern Analysis and Machine Intelligence, vol. 26, no. 9, Sept. 2004, pp.1222-1228

[6] P. Conor, *"Independent component analysis a new concept",* Signal Processing, vol. 36,1994, pp. 287-314.

[7] W. Zhao, R. Chellappa, P. J. Phillips, *"A. Rosenfeld, FaceRecognition: A Literature Survey"*, ACM Computing Surveys, Vol. 35, No. 4, 2003, pp.399-458.

[8] H. Moon, P Jonathon Phillips, *"Computational andPerformance Aspects of PCA Based Face Recognition Algorithms"*, Perception 30(3), 2001, pp.303 – 321

[9] D. R. Shashi Kumar, K. B. Raja, R. K. Chhotaray, and S.Pattanaik, "DWT Based Fingerprint Recognition using Non Minutiae Features", International Journal of Computer Science Issues, vol 8(2), 2011, pp. 257-265.

American Journal of Engineering Research (AJER)
e-ISSN : 2320-0847 p-ISSN : 2320-0936
Volume-03, Issue-03, pp-225-229
www.ajer.org

Research Paper Open Access

Threshold based Bit Error Rate Optimization in Four Wave Mixing Optical WDM Systems

Karamjeet Kaur

Abstract: - Optical communication is communication at a distance using light to carry information which can be performed visually or by using electronic devices. The trend toward higher bit rates in light-wave communication has interest in dispersion-shifted fibre to reduce dispersion penalties. At an equivalent time optical amplifiers have exaggerated interest in wavelength multiplexing. This paper describes optical communication systems where we discuss different optical multiplexing schemes. The effect of channel power depletion due to generation of Four Wave Mixing waves and the effect of FWM cross talk on the performance of a WDM receiver has been studied in this paper. The main focus is to minimize Bit Error Rate to increase the QoS of the optical WDM system.

I. INTRODUCTION

Since the mid 90's, optical fibers have been used for point to point communication at a very high speed. Fiber-optic communication is a method of transmitting information from one place to another by sending light through an optical fiber. Fiber-optic communication systems have revolutionized the telecommunications industry and played a major role in the advent of the information age. Often the optical fiber offers much higher speed than the speed of electronic signal processing at both ends of the fiber. Because of its advantages over electrical transmission the use of optical fiber has largely replaced copper wire communication in the developed world. The main benefits of fiber are it exceptionally low loss with allowing long distances between amplifiers and repeaters and its inherently high data-carrying capacity such that thousands of electrical links would be required to replace a single high bandwidth fiber. The another benefit of fiber is that even when run alongside each other for long distances and fiber cables experience effectively no crosstalk in contrast to some type of electrical transmission lines. Other main advantages of the optical fiber communication are the large capacity, high speed and high reliability by the use of the broadband of the optical fiber. Huge bandwidth of optical fiber communication system can be utilized to its maximum by using multiple access techniques.

OPTICAL wavelength division multiplexing (WDM) networks are very promising due to their large bandwidth with their large flexibility and the possibility to upgrade the existing optical fiber networks to WDM networks [2]. WDM has already been introduced in commercial systems. All-optical cross connects (OXC), however, have not yet been used for the routing of the signals in any of these commercial systems. A number of OXC topologies have been introduced but their use has so far been limited to field trials and usually with a small number of input–output fibers & wavelength channels. The practical systems have many signals and wavelength channels which influence each other and cause significant crosstalk in the optical cross connect that has probably prevented the use of OXC's in commercial systems. The crosstalk levels in OXC configurations presented so far are generally so high that they give rise to significant signal degradation and to an increased bit error probability. Because of the complexity of an OXC is different when sources of crosstalk exist and this makes it difficult to optimize the component parameters for minimum total crosstalk.

Optical communication is any form of telecommunication that uses light as a transmission medium. Optical communication system consists of a transmitter which encodes a message into an optical signal channel which carries the signal to its destination and a receiver which reproduces the message from the received optical signal. Optical communication systems are used to provide high-speed communication connections [1]. Optical communication is one of the newest and most advanced forms of communication by electromagnetic waves. It differs from radio and microwave communication only in the sense that the wavelengths employed are shorter or equivalently or the frequencies employed are higher. In another very real sense it differs markedly from these

older technologies because for the first time the wavelengths involved are much shorter than the dimensions of the devices which are used to transmit or receive and otherwise handle the signals.
The advantages of optical communication are threefold. First, the high frequency of the optical carrier (typically of the order of 300,000 GHz) permits much more information to be transmitted over a single channel than is possible with a conventional radio or microwave system. Second, the very short wavelength of the optical carrier (typically of the order of 1 micrometer permits the realization of very small, compact components. Third, the highest transparency for electromagnetic radiation yet achieved in any solid material is that of silica glass in the wavelength region 1–1.5 μm. This transparency is orders of magnitude higher than that of any other solid material in any other part of the spectrum [2]. Optical communication in the modern sense of the term dates from about 1960, when the advent of lasers and light-emitting diodes (LEDs) made practical the exploitation of the wide-bandwidth capabilities of the light wave.

II. OPTICAL MULTIPLEXING SCHEMES

2.1 Orthogonal frequency-division multiplexing (OFDM):

Orthogonal frequency-division multiplexing (OFDM) — It is identical to Coded OFDM (COFDM) and Discrete multi-tone modulation (DMT) — is a frequency-division multiplexing (FDM) scheme utilized as a digital multi-carrier modulation method.Large number of closely-spaced orthogonal sub-carriers are used to carry data. Data is divided into several parallel data streams or channels one for each sub-carrier. Every Sub-carrier is modulated with a conventional modulation scheme (such as quadrature amplitude modulation or phase-shift keying) at a low symbol rate maintaining total data rates similar to conventional single-carrier modulation schemes in the same bandwidth [11]. OFDM has developed a popular scheme for wideband digital communication, whether wireless or over copper wires, used in applications such as digital television and audio broadcasting, wireless networking and broadband internet access.

The primary advantage of OFDM over single-carrier schemes is its ability to cope with severe channel conditions — for example attenuation of high frequencies in a long copper wire and frequency-selective fading due to multipath — without equalization filters. The channel equalization is simplified because OFDM may be viewed as using many slowly-modulated narrowband signals rather than one rapidly-modulated wideband signal.The Low rate symbols makes the use of a guard interval between symbols affordable and making it possible to handle time-spreading and eliminate intersymbol interference (ISI). This mechanism also facilitates the design of Single Frequency Networks (SFNs), where several adjacent transmitters send the same signal simultaneously at the same frequency as the signals from multiple distant transmitters may be combined constructively rather than interfering as would typically occur in a traditional single-carrier system [13].

2.2 Wavelength division multiplexing (WDM)

In fiber-optic communications wavelength-division multiplexing (WDM) is a technology which multiplexes multiple optical carrier signals on a single optical fiber by using different wavelengths (colours) of laser light to carry different signals. This thing allows for a multiplication in capacity in addition to enabling bidirectional communications over one strand of fiber. It is a form of frequency division multiplexing (FDM) but is commonly called wavelength division multiplexing [12].
The term wavelength-division multiplexing is commonly applied to an optical carrier (which is typically described by its wavelength) on the other hand frequency-division multiplexing typically applies to a radio carrier (which is more often described by frequency).Since wavelength and frequency are inversely proportional and since radio and light are both forms of electromagnetic radiation the two terms are equivalent in this context.

A WDM system uses a multiplexer at the transmitter to join the signals together and a demultiplexer at the receiver to split them apart. By using the right type of fiber it is possible to have a device that does both simultaneously and can function as an optical add-drop multiplexer.

As explained before, WDM enables the utilization of a significant portion of the available fiber bandwidth by allowing many independent signals to be transmitted simultaneously on one fiber and each signal located at a different wavelength. The routing and detection of these signals can be accomplished independently with the wavelength determining the communication path by acting as the signature address of the origin destination or routing. The components are therefore required that are wavelength selective allowing for the transmission recovery or routing of specific wavelengths [6].

In a simple WDM system each laser must emit light at a different wavelength with all the lasers light multiplexed together onto a single optical fiber. Being transmitted through a high-bandwidth optical fiber combined optical signals must be demultiplexed at the receiving end by distributing the total optical power to each output port and then requiring that each receiver selectively recover only one wavelength by using a tunable optical filter. The laser is modulated at a given speed the total aggregate capacity being transmitted along the high-bandwidth fiber is the sum total of the bit rates of the individual lasers.The example of the

system capacity enhancement is the situation where ten 2.5-Gbps signals can be transmitted on one fiber and producing a system capacity of 25 Gbps.Wavelength-parallelism circumvents the problem of typical optoelectronic devices which do not have bandwidths exceeding a few gigahertz unless they are exotic and expensive.Speed requirements for the individual optoelectronic components are therefore relaxed even though a significant amount of total fiber bandwidth is still being utilized.

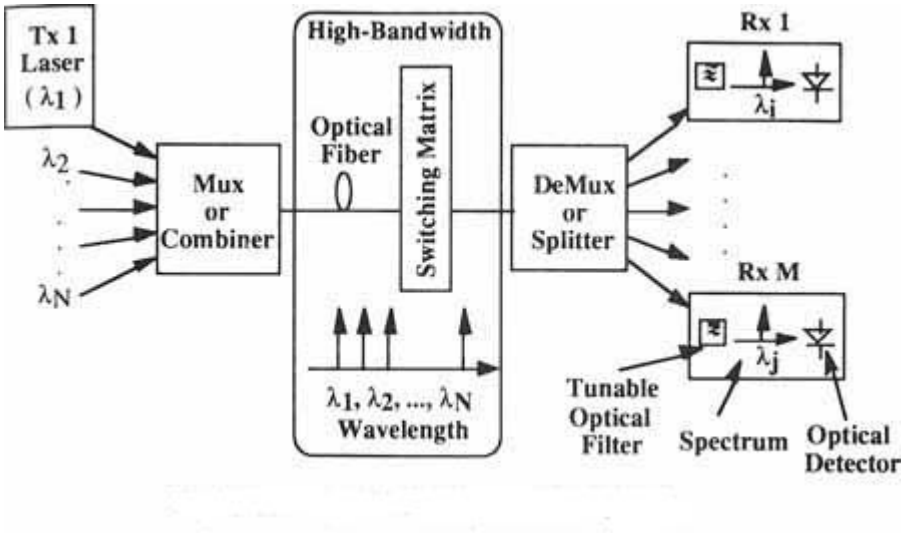

Fig 1: Simple WDM system

A single mode fibre can support many different wavelengths at the same time. If two different colored lasers (different wavelength, fibre chosen in a way that both are single mode) excite a mode in a fibre each and then both of them are multiplexed onto the same singlemode fibre, the fibre has now two first order modes with different wavelengths travelling in it [5]. This is not to be confused with a multimode fibre every color has several different modes! The different channels are independent of each other [4]. The wavelength also serves another purpose: As it is unique for every channel it can be seen as a kind of an address to route the signal. At the end of the fibre, the different wavelengths have to be separated from each other (demultiplexed) and then detected separately [5].
In each of the two different fibres, one channel at a different wavelength gets excited. All the other channels are still unused (in this example, there is only one other channel). Both signals then get multiplexed onto a single fibre (in this example, both available channels are now occupied). As a result, the capacity of the fibre can be doubled without having to increase the bitrate of a single channel.

Advantages of WDM
The wavelength division multiplexing has several advantages over the other presented approaches to increase the capacity of a link:
• It works with existing single mode communication fibre [4].
• It works with low speed equipment [5]
• Is transparent:It doesn't depend on the protocol that has to be transmitted [2].
• Is scalable: Instead of switching to a new technology it adds new channel to existing channels. The companies only have to pay for the bandwidth they actually need [4].
• It is easy for network providers to add additional capacity in a few days if customers need it.Companies using WDM an economical advantage. Parts of a fibre can be leased to a customer who then gets fast network access without having to share the connection with others.

2.3 DWDM System:
Dense wavelength division multiplexing or DWDM for short refers originally to optical signals multiplexed within the 1550 nm band so as to leverage the capabilities (and cost) of erbium doped fiber amplifiers (EDFAs), which are effective for wavelengths between approximately 1525-1565 nm (C band), or 1570-1610 nm (L band). EDFAs were originally developed to replace SONET/SDH optical-electrical-optical (OEO) regenerators which they have made practically obsolete. The EDFAs can amplify any optical signal in their operating range regardless of the modulated bit rate. In multi -wavelength signals so long as the EDFA has enough pump energy available to it so that it can amplify as many optical signals as can be multiplexed into its

amplification band (though signal densities are limited by choice of modulation format). The EDFAs therefore allow a single-channel optical link to be upgraded in bit rate by replacing only equipment at the ends of the link while retaining the existing EDFA or series of EDFAs through a long haul route. The single-wavelength links using EDFAs can similarly be upgraded to WDM links at reasonable cost.

Tasks in a DWDM / WDM Network

- Generating signals: The stable lightsource, with a narrow specific wavelength and the possibility of fast modulation [8].
- Combining signals: To merging all the different lightsources into one fibre [8].
- Transmission of signals: Controlling parameters as crosstalk and loss. Control over variables as channel spacing or input power. For long links: Amplification needed (flat gain amplifiers to amplify all used wavelengths together). It may further be necessary to remove or add certain wavelengths from the link, before they reach the end [8].
- To separating the received signals at the receiver end (demultiplexing) [8].
- Detecting the separated signals [8].

Combining / Separating: Multiplexer and Demultiplexer

Multiplexers and demultiplexers can either be active or passive devices. Passive devices use prisms, gratings or fixed filters whereas active designs work with tunable filters. The main challenge in designing a (de)multiplexer is to get a high channel separation and low cross talk [9]. The isolation between the channels should be at least 20 dB. This means, that each neighbouring channel gets damped by at least a factor of 100 when detecting the wanted channel [10].

III. FOUR WAVE MIXING

When a high power optical signal is launched into a fiber then the linearity of the optical response is lost. One such non-linear effect, which is due to the third order electric susceptibility, is called the optical Kerr effect. Optical fiber nonlinearities can lead to distortion, interference and excess attenuation of the optical signals which results in performance degradation. Most common nonlinear optical effect of importance in optical fiber communication systems results from the fiber non linear refractive index [13]. The nonlinearity in the refractive index is known as Kerr nonlinearities. Kerr nonlinearity gives rise to different effects, such as self-phase modulation (SPM), cross-phase modulation (CPM), and four-wave mixing (FWM). FWM may include lightpath BER fluctuations in dynamic networks that can affect the optical signal to noise ratio and quality of service in transparent networks under highly complex nonlinear effect and influence the frequency chirp and extinction ratio in the system. Four Wave Mixing (FWM) is one of the dominating degradation effects in wavelength –division multiplexing (WDM) systems with dense channel spacing and low chromatic dispersion on the fiber.

Applications of FWM

Multiwave mixing, especially four-wave mixing (FWM), is a fundamental process in nonlinear optics. Nonlinearity couples the underlying modes that generate new sum and difference frequencies from the original waves. In typical scenario, two pump waves interact with a signal wave that creates a daughter wave that is phase conjugated with the signal. Because dispersion creates issues of phase matching, FWM has proved useful in such applications as realtime holography, super-continuum generation, and soliton communication systems [11]. The most common configuration involves a self-focusing nonlinearity and a backward geometry in which the initial pump beams counter propagate to create a reflection grating. The focusing non-linearity has the advantage of intensity concentration, but higher intensity can lead to other non-linear effects, while the spatial (transverse) extent of interaction is limited by modulation instability. Furthermore, the backward geometry makes it difficult to cascade the wave mixing and follow the evolution of daughter waves.

IV. CONCLUSION

The effect of channel power depletion due to generation of FWM waves has been analyzed for intensity modulated WDM systems with unequal channel spacing. The channel power depletion is assumed to be a binomial random variable. Based on this model, the effect of FWM cross talk on the performance of a WDM receiver has been studied. The bit error rate and power penalty have been calculated in the worst case scenario, i.e., in the nondegenerate FWM case. It has been shown that the BER increases nonuniformly at rapid rates as the number of channels increases. If the channel number increases (four and above), more and more frequency components are generated by FWM and may coincide with the channel frequencies. These deteriorate the system performance and increase the BER. Receiver noise should also be minimized to get improved

performance through minimization of cross talk. The power penalty due to FWM cross talk has been shown as a function of input power for different numbers of channels. Power penalty first decreases with input power and ultimately becomes constant. For a fixed input power, as the channel number increases, the power penalty increases quite rapidly. This is because newly generated frequency components due to FWM increases with channel numbers. These frequencies may ultimately mix with other channels in the WDM system and deteriorate the system performance. The variation of the bit error rate with the detection threshold has also been calculated for different numbers of channels. The study on the optimum detection threshold has shown that as the number of channels decreases, the optimum detection threshold increases toward the ideal value. The minimum BER obtained using the optimum detection threshold decreases as power increases. This decrease in BER occurs due to a large signal-to-noise ratio at the destination. As the input power increases, the minimum BER occurs for a higher detection threshold.

REFERENCES

[1] Santu Sarkar and N. R. Das, "On the Optimum Detection Threshold for Minimum Bit Error Rate due to Four-Wave Mixing in a WDM System" J. OPT. COMMUN. NETW./VOL. 5, NO. 4/APRIL 2013

[2] N.Gopi, I.Muthumani, A.Sivanantha Raja, S.Selvendran, "Dispersion Compensation for WDMSignals with Polarization Insensitivity" International Conference on Information Communication and Embedded Systems (ICICES), pp. 840 – 844, 21-22 Feb. 2013

[3] S.Sugumarani, P.Arulmozhivarman, "Effect of Chromatic Dispersion on Four-WaveMixing in WDM systems and its suppression" International Conference on Emerging Trends in VLSI, Embedded System, Nano Electronics and Telecommunication System (ICEVENT), pp. 1 – 5, 7-9 Jan. 2013

[4] Priyanka Dalotra, Hardeep Singh "Effect of Chromatic Dispersion on FWM in Optical WDM Transmission System" International Journal of Advanced Research in Computer and Communication Engineering, Vol. 2, Issue 6, June 2013.

[5] V.Nidhya Vijay, S.Gandhimathi Usha, D.Shanmuga sundar, "EFFECTIVE FIBER OPTIC COMMUNICATION BY OPTICAL PHASE CONJUGATION FOR A MULTICHANNEL SYSTEM" International Journal Of Engineering And Computer Science, Volume 2 Issue 6 June 2013 Page No.2092-2097.

[6] Anupjeet Kaur, Kulwinder Singh, Bhawna Utreja, "Performance analysis of semiconductor optical amplifier using four wave mixing based wavelength Converter for all Optical networks" nternational Journal of Engineering Research and Applications (IJERA), Vol. 3, Issue 4, Jul-Aug 2013, pp.108-113

[7] Nahyan Al Mahmud, Bobby Barua, "Effects of Four Wave Mixing on an Optical WDM System by using Dispersion Shifted Fibre" International Journalof Engineering and Technology Volume 2 No. 7, July, 2012

[8] Laxman Tawade,Shantanu Jagdale, Premanand Kadbe, Shankar Deosarka "INVESTIGATION OF FWM EFFECT ON BER IN WDM OPTICAL COMMUNICATION SYSTEM WITH BINARY AND DUOBINARY MODULATION FORMAT" International Journal of Distributed and Parallel Systems (IJDPS) Vol.1, No.2, November 2010

[9] Shelly Garg, Keshav Dutt, Abhimanyu and 4Manisha, "Effect of Four Wave Mixing in WDM Optical Fiber Systems" http://icacct.apiit.edu.in/download/all%20chapters/CHAPTER-93.pdf.

[10] S Sugumaran, Neeraj Sharma, Sourabh Chitranshi, Nischya Thakur, P Arulmozhivarman, "Effect of Four-wave Mixing on WDM System and its Suppression Using Optimum Algorithms" International Journal of Engineering and Technology (IJET).

[11] M. S. Islam and S. P. Majumder, "Bit error rate and cross talk performance in optical cross connect with wavelength converter" OURNAL OF OPTICAL NETWORKING, Vol. 6, No. 3 / March 2007.

[12] H.S.Mruthyunjaya, G.Umesh, and M.Sathish Kumar, "Coding In WDM Systems to Counter Impacts of SRS and Channel Beat Noise" INTERNATIONAL JOURNAL OF MICROWAVE AND OPTICAL TECHNOLOGY, VOL. 1 , NO.2 ,AUGUST 2006

[13] Santos kumar Das, Tusar Ranjan Swain, Sarat Kumar Patra, "Impact of In-band Crosstalk & Crosstalk Aware Datapath Selection in WDM/DWDM Networks" IEEE –INTERNATIONAL CONFERENCE ON ADVANCES IN ENGINEERING, SCIENCE AND MANAGEMENT

American Journal of Engineering Research (AJER)
e-ISSN : 2320-0847 p-ISSN : 2320-0936
Volume-03, Issue-03, pp-230-237
www.ajer.org

Research Paper Open Access

An investigation into the influence of friction damper device on the performance of steel moment frames

Amir Shirkhani*, Naser Shabakhty, Seyed Roohollah Mousavi
Department of Civil Engineering, University of Sistan and Baluchestan, Zahedan, Iran
shirkhani_am@pgs.usb.ac.ir

ABSTRACT: - Friction damper device belongs to those passive control systems made according to friction mechanism. Since, friction is a great source of energy dissipation; it is used in structures in order to decrease the structure response against wind and earthquake load. In this paper, steel moment frames with 3, 7 and 12 stories equipped with the mentioned damper is investigated under seismic analysis. Finally, it is concluded that by adding dampers, the reduction percentage of roof displacement of frames will be decreased by increasing the number of stories. It is also concluded that 7 stories frame equipped with dampers has a better performance.

Keywords: - *Friction damper device, passive control systems, seismic analysis, roof displacement, energy dissipation.*

I. INTRODUCTION

Using the dampers or energy dissipation devices are one of the controlling methods of structures vibration under seismic loads. The applications of these devices in design the new buildings and retrofitting the existence buildings are possible [1]. Friction dampers are one of the passive control systems which have an increasing application in moment frames. These are lots of project of such dampers all over the world [2]. Friction damper is functioned according to friction mechanism among rigid materials. In fact, friction is a great mechanism of energy dissipation, employed in car brake systems successfully and extensively. A base metal selection of friction damper is of high importance. Since, there are different materials employed for slippery surfaces [3, 4, 5]. A new friction damper device was employed for the first time by Mualla in his PhD thesis [6]. Full scale experiments for three stories structure equipped with such damper on shaking table was done in Taiwan [7]. In order to increase the seismic capacity of existing structures, it is possible to use the friction damping system connected to high strength tendons [8]. Three steel moment frames with 3, 7 and 12 stories equipped by friction damper devices are investigated under nonlinear time history analysis in present study. The influence of dampers on seismic performance of frames is studied by comparing the parameters like base shear, displacement and energy dissipation of frames with and without dampers.

II. FRICTION DAMPER DEVICE

The components of friction damper device are central vertical plate, two lateral horizontal plates and two circle friction pads placed between the steel plates [9]; (Fig. 1).

Figure 1: Friction damper device [10].

A single story frame equipped with friction damper device is presented in Fig. 2. When a lateral external force excites a frame, the beam starts to displace horizontally. The damper will follow the horizontal movement of the frame because of the hinge connection, which transfer the forces to the damper parts. The bracing system and the frictional forces developed between the frictional surfaces of steel plates and friction pad materials will resist the horizontal movement. The central plate will start to move horizontally and rotate around the hinge. The clamping force in the bolt, which makes the damper parts stick to each other, and due to this introduces frictional forces. These frictional forces will rotate the horizontal plates within the same value of rotation and direction as the central plate dose, because they are higher than the applied forces. The damper will continue being in sticking phase until the applied forces in the damper exceed the frictional forces, at this slip moment, starts and the central plate rotates relatively to the friction pads, around the bolt [6].

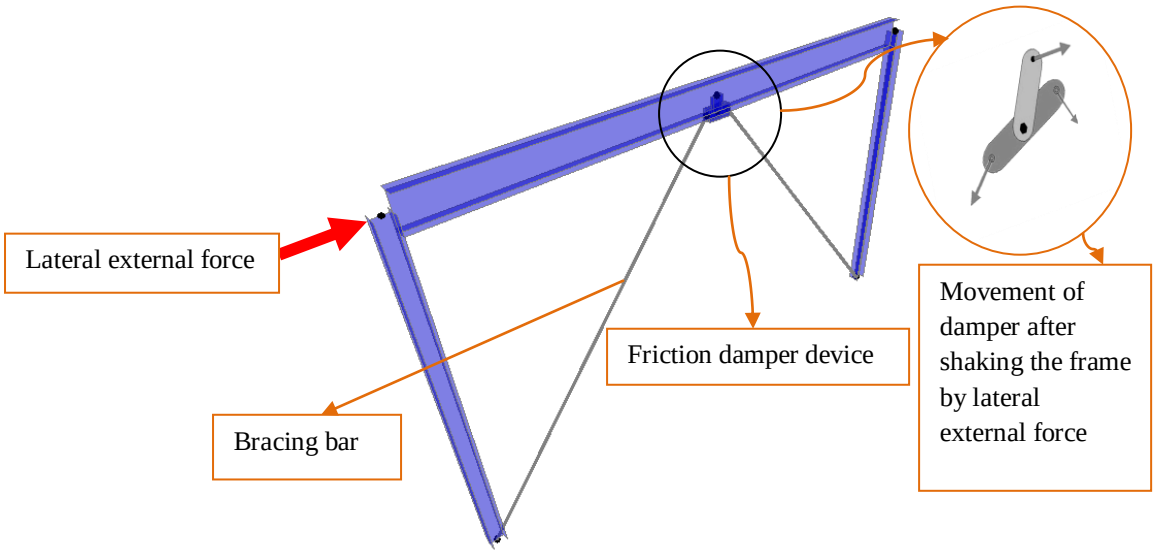

Figure 2: Frame equipped with friction damper device.

The horizontal plates also start to slip and rotate but in another direction because of the tensile forces in the bracing. In this sliding phase, the damper will dissipates energy by means of friction between the sliding surfaces. This phase will keep on and later will be changed to the sticking phase when the load reverses its direction [6]. To prevent the buckling of compression bar, the bars are pretensioned by F_p force according to equation 1.

$$F_p = \frac{M_f}{2h_a \cos v} \tag{1}$$

In which v is the bar slope angle with horizontal line. Therefore the cross-sectional area of bars is determined according to equation 2.

$$A_b = \frac{M_f}{\sigma_y h_a \cos v} \tag{2}$$

In which σ_y is the yielding stress of bracing bar. Friction damper has two phases: sticking and sliding phases. The stiffness of damping system in sticking phase is calculated according to equation 3.

$$k_{bd} = \frac{2EA_b}{l}\cos^2 v + \frac{2F_p}{L}\sin^2 v \tag{3}$$

Where E is elasticity module, A_b is bracing bar area, l is length of the bracing bar and L is length between the hinge which is existed on the top of the friction damper device and the end of bracing bar. The stiffness of damping system is ignored in sliding phase, as it is negligible [11].

III. MODEL VERIFICATION

To be sure the accuracy of modeling, the displacement results for a one story frame under El Centro earthquake excitation are compared with the results obtained by Mualla [9]. The response obtained by Mualla and Belev is shown in Fig. 3.a and the response of mentioned frame in the present study is given in Fig. 3.b.

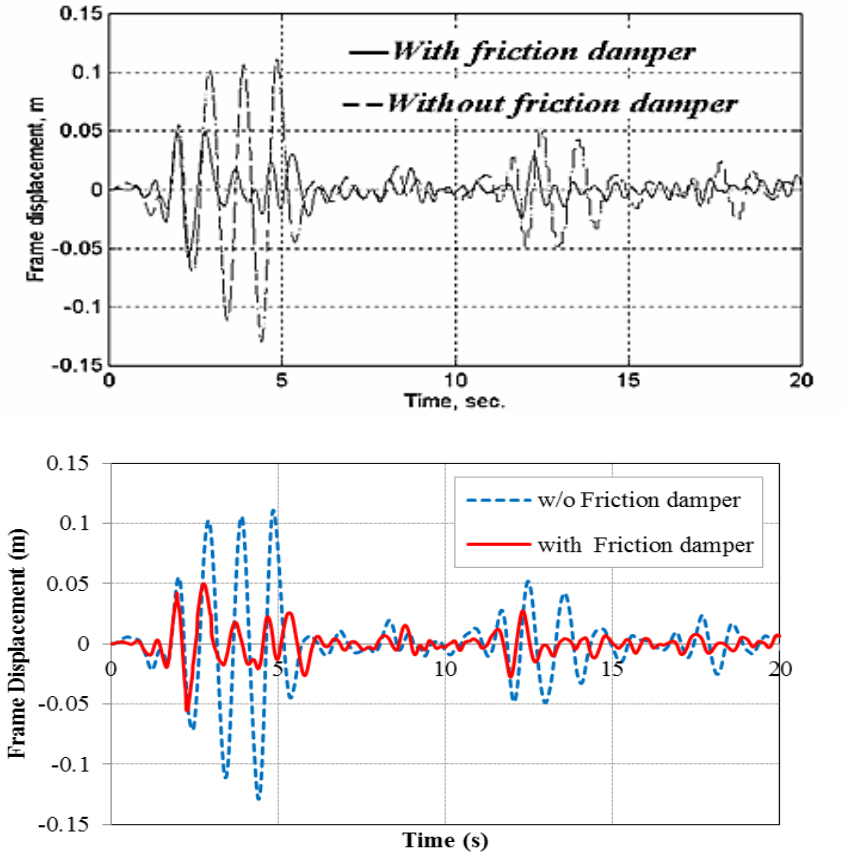

Figure 3: Displacement response: a) results by Mualla [9], b) results of this study.

These figures show that results are well-matched for Mualla and Belev model and that of the present study.

IV. DESIGN OF STEEL FRAMES

To investigate the performance of steel moment frames with and without friction damper devices, two-dimensional frames with 3, 7 and 12 stories are considered in this study. The length of each bay and height of each story in all frames are 5 m and 3.2 m, respectively. These frames are designed based on AISC ASD design code [12].The studied soil is type C of Standard ASCE/SEI 41-06 [13]. In the naming of frames, prefixes "MF" and "IVRMF" represent moment frames without and with friction damper device, respectively. For example "MF7s3b" represents moment frame with 7 stories and 3 bays. Dampers are installed in middle bay and total stories of frames. The specifications of the frames of the present study and the period of free vibration of frames with and without friction damper devices are presented in Tables 1 and 2, respectively.

Table 1: Specifications of the frames

Frames	Number of Stories	Weight (ton)	Design base shear (ton)
Mf3s3b	3	148.63	18.58
Mf7s3b	7	355.92	31.89
Mf12s3b	12	618.29	42.29

Table 2: The period of free vibration of frames with and without dampers

Frames	Period of free vibration (s)
MF3s3b	0.945
IVRMF3s3b	0.477
MF7s3b	1.422
IVRM7s3b	0.953
MF12s3b	2.018
IVRMF12s3b	1.539

V. GROUND MOTIONS

Seven ground motions are selected from a set of 20 used record in FEMA440 [14] which are recorded on soil type C. The characteristics of ground motions are shown in Table 3.

Table 3: Ground motions employed in this study [14]

Date	Earthquake name	Magnitude (Ms)	Station number	Component (deg)	PGA (g)	Abbreviation
06/28/92	Landers	7.5	12 149	0	0.171	LADSP000
10/17/89	Loma Prieta	7.1	58 065	0	0.512	LPSTG000
10/17/89	Loma Prieta	7.1	47 006	67	0.357	LPGIL067
10/17/89	Loma Prieta	7.1	58 135	360	0.450	LPLOB000
10/17/89	Loma Prieta	7.1	1 652	270	0.244	LPAND270
04/24/84	Morgan Hill	6.1	57 383	90	0.292	MHG06090
01/17/94	Northridge	6.8	24 278	360	0.514	NRORR360

According to ASCE/SEI 41-06, the ground motions be scaled such that the average of the ordinates of the 5% damped linear response spectra does not fall below the design spectrum for the period range $0.2T_i$–$1.5T_i$, where T_i is the fundamental period of vibration of each frame [15]. The response spectra of selected seven records and hazard level BSE-2 of ASCE/SEI 41-06 are presented in Fig. 4. The scale factors of seven records for frames with (IVRMF) and without (MF) friction damper devices are shown in Table 4.

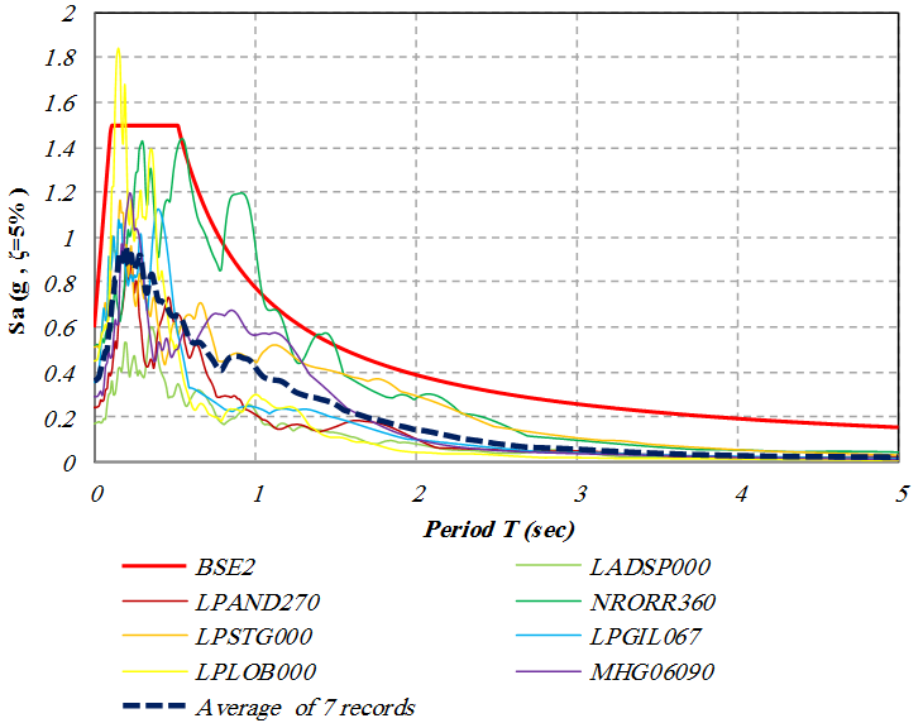

Figure 4: Response spectra of seven records and hazard level BSE-2 of ASCE/SEI 41-06.

Table 4: Scale factors of seven ground motions for frames with (IVRMF) and without dampers (MF)

Frames	LADSP 000	LPAND270	MHG 6090	LPGIL067	LPLOB000	LPSTG000	NRORR360
MF3s3b	3.98	2.98	1.75	2.62	2.73	1.85	1.09
IVRMF3s3b	3.87	2.49	2.22	2.14	2.11	2.02	1.32
MF7s3b	4.20	3.13	2.05	2.83	3.74	1.66	1.13
IVRM7s3b	3.98	2.99	1.75	2.62	2.74	1.84	1.09
MF12s3b	4.78	3.65	2.78	3.47	5.46	1.71	1.31
IVRMF12s3b	4.33	3.27	2.20	2.94	4.08	1.65	1.15

VI. SEISMIC ANALYSIS RESULTS

The frames are subjected to nonlinear time history analysis. The energy dissipated by friction damper device and its behavior (the hysteresis curve of moment-rotation) are investigated in the present study. A comparison of base shear history is made between MF7s3b and IVRMF7s3b frames under record LADSP000 (Fig. 5). According to the base shear history of mentioned frames, it is observed that by adding friction damper devices to MF7s3b frame, the maximum base shear will be decreased by 47.18%.

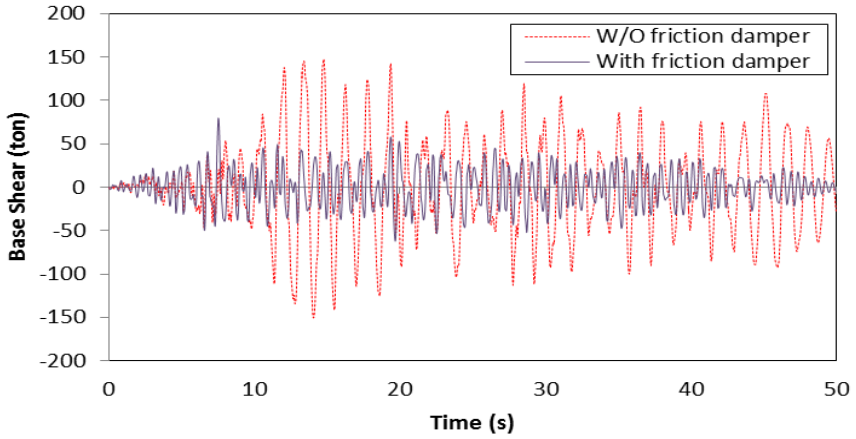

Figure 5: Comparison of base shear history between MF7s3b and IVRMF7s3b frames under record LADSP000.

A comparison of roof displacement history is made between MF7s3b and IVRMF7s3b frames under record NRORR360 (Fig. 6). According to the roof displacement history of mentioned frames, it is determined that by adding friction damper devices to MF7s3b frame, the maximum roof displacement will be decreased by 52.75%.

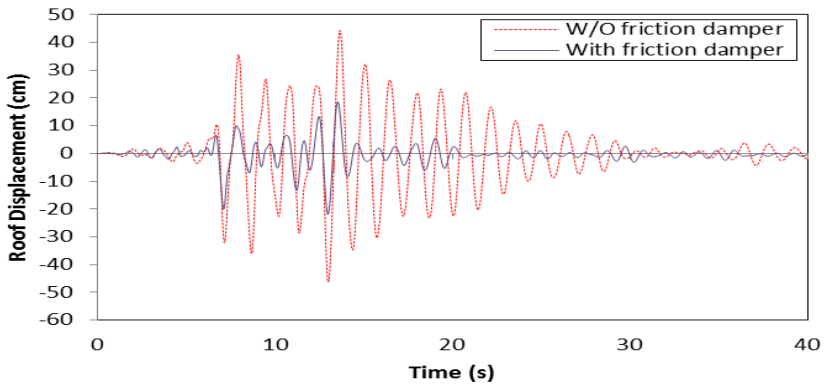

Figure 6: Comparison of roof displacement history between MF7s3b and IVRMF7s3b frames under record NRORR360.

The diagram of energy dissipated by damper in IVRMF3s3b frame under record NRORR360 is presented in Fig. 7. According to the diagram by adding dampers to MF3s3b frame, 47.61% of input energy will be dissipated.

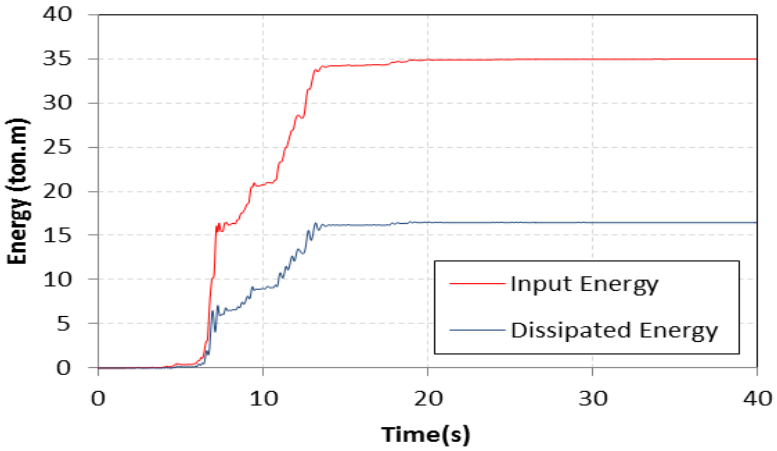

Figure 7: Energy dissipated by damper in IVRMF3s3b frame under record NRORR360.

The hysteresis cycle for the damper in fourth story of IVRMF7s3b frame under record NRORR360 is presented in Fig. 8. As it is obvious, there is an appropriate correspondence between the hysteresis cycle and the real behavior of damper. So, it can be said that the approximate rectangular hysteretic behavior of damper reveal that its performance in energy dissipation is suitable.

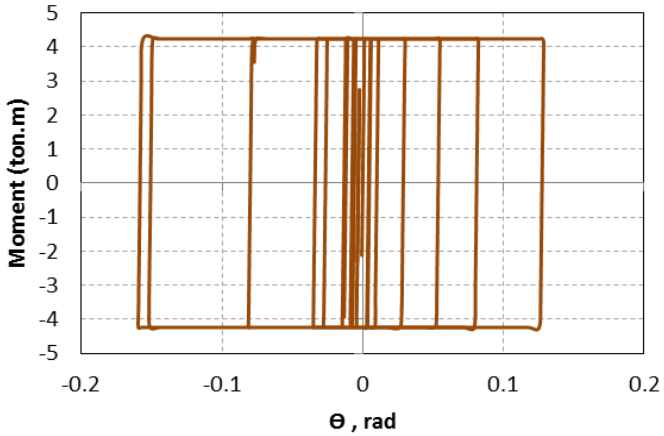

Figure 8: Hysteresis cycle for the damper in fourth story of IVRMF7s3b frame under record NRORR360.

After calculating the average of all the responses of analysis, the reduction percentage of parameters like base shear and roof displacement of frames by adding dampers and energy dissipated by dampers are determined. These items are shown in Table 5 to 7.

Table 5: Base shear of frames with and without dampers

Frame	Base shear of frames without dampers (ton)	Base shear of frames with dampers (ton)	Reduction of Base Shear (%)
MF3s3b	116.73	86.45	25.94
MF7s3b	171.49	122.07	28.82
MF12s3b	209.42	165.71	20.87

Table 6: Roof displacement of frames with and without dampers

Frame	Roof displacement of frames without dampers (cm)	Roof displacement of frames with dampers (cm)	Reduction of roof displacement (%)
MF3s3b	25.55	8.61	66.29
MF7s3b	40.68	19.95	50.96
MF12s3b	52.94	29.87	43.58

Table 7: Dissipated energy by dampers

Frame	Input energy for frames with dampers (ton.m)	Energy dissipated by dampers (ton.m)	Dissipated energy (%)
IVRMF3s3b	23.03	11.73	50.93
IVRMF7s3b	60.73	35.18	57.93
IVRMF12s3b	92.22	48.90	53.03

According to these tables, it is obvious that dampers have an appropriate performance in decreasing the roof displacement and base shear in steel moment frames. Energy dissipation is also done appropriately. As it is obvious, the maximum percentage of base shear reduction is occurred by adding dampers in 7 stories frame. By increasing the number of stories and increasing the free vibration period of structure, the reduction percentage of roof displacement will be decreased by adding dampers to the structure. The energy dissipated by dampers in 7 stories frame is more than other frames.

VII. CONCLUSION

As it is known, the free vibration period of structure will be decreased by adding friction damper devices. According to the results of the present study, it is obvious that, by increasing the number of stories and free vibration period of structure, reduction percentage of roof displacement will be decreased by adding dampers to the structure. The energy dissipated by damper in 7 stories frame is more than other frames. It reveals that 7 stories frame equipped with dampers has a better performance. It can be said that the friction damper device has a vital role in decreasing the displacement and base shear. According to the present study, this damper has a significant role in energy dissipation, since its hysteretic behavior is almost rectangular.

REFERENCES

[1] H. Adeli and H. Kim, Hybrid control of smart structures, *6th International Congress on Advances in Civil Engineering*, Istanbul, Turkey, 2004.

[2] A. Malhotra, D. Carson, P. Gopal, A.Braimah, G.D. Giovanni, and R. Pall, Friction dampers for seismic upgrade of st.Vincent hospital, Ottawa, *13th World Conference on Earthquake Engineering*, Vancouver, Canada, no 1952, 2004.

[3] L.D. Sarno and A.S. Elnashai, *Seismic retrofitting of steel and composite building structures*, Report, University of Illinois, 2002.

[4] M. Tehranizadeh and F. Khaleghian, A comparison of experimental results of friction damper with different sliding surface, *5th international conference of Seismology and Earthquake Engineering*, Tehran, Iran, 2008.

[5] F. Khaleghian and M. Tehranizadeh, Designing an new type of friction damper with brake lining , *Journal of Seismology and Earthquake Engineering, 9 (4),* 171-182.

[6] I.H. Mualla, *Experimental and computational evaluation of a novel friction damper device*, PhD thesis, Department of Structural Engineering and Materials, Technical University of Denmark, 2000.

[7] W. Liao, I. Mualla and C. Loh, Shaking table test of a friction damped frame structure, *The Structural Design of Tall and Special Buildings, 13,* 2004, 45–54.
[8] J. Kim, H. Choi and K.W. Min, Use of rotational friction dampers to enhance seismic and progressive collapse resisting capacity of structures, *The Structural Design of Tall and Special Buildings, 20,* 2011, 515-537.
[9] I.H. Mualla, Parameters influencing the behavior of a new friction damper device, Technical University of Denmark, 2800 Lyngby, Denmark, 1982.
[10] DAMPTECH earthquake protection presentation technical, http://WWW.DAMPTECH.COM, 2006.
[11] L. Nielsen and I.H. Mualla, *A friction damping system low order behavior and design*, Department of Civil Engineering DTU-bygning, R-0302002, 2002.
[12] American Institute of Steel, Allowable Stress Design Manual of Steel Construction, 9th ed. Chicago: AISC, 1989.
[13] ASCE standard ASCE/SEI 41-06. Seismic Rehabilitation of Existing Buildings, American Society of Civil Engineers, 2007.
[14] FEMA, Improvement of Nonlinear Static Seismic Analysis Procedures. FEMA-440, Federal Emergency Management Agency, Washington (DC), 2005.
[15] H.E. Estekanchi, H.T. Riahi and A. Vafai, Application of endurance time method in seismic assessment of steel frames, *Engineering Structures, 33,* 2011, 2535–2546.

American Journal of Engineering Research (AJER)
e-ISSN : 2320-0847 p-ISSN : 2320-0936
Volume-03, Issue-03, pp-238-244
www.ajer.org

Research Paper Open Access

Methods of quantifying operational risk in Banks : Theoretical approaches

Fatima Zahra El ARIF[1], Said HINTI[2]
1PhD student – Department of Economics and Management, Center of Doctoral Studies, Faculty of Economic Sciences, University Mohammed V-Souissi, Rabat, Morocco
2Professor Authority – Department of Economics and Management, Faculty of Economic Sciences. University Mohammed V-Souissi, Rabat, Morocco.

Abstract: - The definition of operational risk is a challenge. This risk has an atypical character as far as it concerns all the activities of the bank. It is also often difficult to estimate it independently of the other risks which characterizes the banking activity. Indeed, it is very difficult to determine the amount, the frequency, and the key factors behind this risk. Banks are still putting in place procedures of data collection and formalized approaches in this area. This is what we try to decipher. How then banks are they supposed to assess, predict and effectively manage operational risk, given the incredible diversity of dangers and threats now facing their business? How can they successfully respond to new constraints emanating from regulatory authorities while preserving their future profitability? These two questions are at the heart of the issues related to the measurement of operational risk, and are not without effect on the future ability of banks to manage this type of risk.

Keywords: - *Banks, Basel II, Methods of quantification, Operational Risk, Regulatory measure.*

I. INTRODUCTION

During this last years, we see a growing interest of financial institutions to identify losses associated with operational risk, and that, due to regulatory considerations on the one hand, and upon the occurrence of huge operating losses in the financial sector on the other hand. Let us quote examples of huge operating losses incurred in the financial sector : $ 2.4 billion attributable to subsequent proceedings Enron and a loss of $ 690 million caused by an unauthorized transaction Allied Irish Bank.

Add the case of the oldest bank in the United Kingdom (233 years), Barings, which went bankrupt as a result of unauthorized activities causing losses of $ 1.3 billion. These examples show the extent of this risk. They also provide a signal to alert financial institutions that must define, measure and manage it, to avoid any huge losses that may arise.

In addition to these significant losses, operational risk affects all activities and operations of financial institutions in different ways. Indeed, we find operational events attributable to persons, processes, systems and external events. However, the units are not affected in the same way by the operational risk. The impact varies depending on the nature of activities and the various stakeholders. Operational risk therefore becomes more and more large and its management becomes a necessity.

Aware of this big risk, regulators have launched a debate on the definition, identification, measurement and management of operational risk in June 1999. They thus introduce the pressure on banks to put in place a management framework specific to the operational risk management system (management system of risk, senior management). This framework allows, inter alia, the identification and measurement of the loss of an operational capital. One way to hedge exposure to operational risk is to hold capital to cover unexpected losses, as is the case for market risk and credit risk.

Several approaches of measures of operational risk capital have been proposed by the regulatory authorities, except that banks are encouraged to develop their own method, a method of measuring progress that will better reflect the level of operational risk. The development of such a method of measurement is in the

center of this article. We study various aspects of the quantification of the operational risk of the banking institutions, in order to develop a measure that reflects the actual exposure of a bank.

Thus, the objective of this paper is to propose a robust method for calculating the value at operational risk, which will be the most realistic and the most representative of the level of operational risk of a bank.

One of the approaches proposed in the agreement of Basel II for the quantification of the operational risk is the advanced approach [1]. The development of such an approach requires a large database. The data can come from different sources. In fact, the internal data is of great value to reflect the actual degree of exposure in front of operational risk. However, the historical collection is short and operational losses observed are far from being representative of losses which a bank could suffer. Indeed, the internal data of a bank does not include enough of rares losses with a high severity, especially as the process of collection of losses is still in its infancy.

II. THE REGULATORY MEASURE OF THE OPERATIONAL RISK UNDER BASEL II

The operational risk measurement corresponds to a value at risk [2], similar in its principle to that calculated in the areas of market risk and credit risk. It should therefore cover both the « expected loss » and « unexpected loss ». Yet, in theory, regulatory capital only cover unexpected losses and not average losses, the latter being intended to be covered by provisions or charged to current income. The Basel Committee proposes three different approaches to determine the regulatory capital charge for operational risk [3] :

– *Basic Indicator Approach or BIA*
– *Standardised Approach or SA*)
– *Advanced Measurement Approach* or *AMA*

As highlighted in the Committee, regardless of the approach, an institution must demonstrate that its operational risk measure meets a soundness standard comparable to that of the IRB (Internal Ratings Based Approach) for risk credit (corresponding to a holding period of one year and a confidence interval of 99.9%). Banks have the option to choose the one that seems the most suitable to the specificity of their activity, but also to their overall capacity of action. They should indeed ensure that they have all the means necessary for the implementation of the solution. The degree of sophistication of each of these three methods is indeed increasing.

II.1. General principle of the available approaches

Under the BIA approach, the calculation of required capital is from an indicator of exposure. The Basel Committee[1] proposes to retain 15% of the average banking net income (Gross Income or IM) over the last three years. The required capital (or capital requirement) K_{BIA} is then equal to:

$$K_{BIA} = \alpha \times GI$$

The coefficient α is set at 15%.

This standard method is imperfect and concerns mainly the small local banks who can not do better. If no eligibility criterion is required, it does not matter as long as the regulator allows banks operating in the international financial scene to use this approach so unrefined.

Unlike the BIA, banks using the AMA methods are allowed to calculate themselves their own regulatory capital from their own internal models. These banks must meet many requirements to use the advanced approach. In particular, certain qualitative criteria concerning the politics of risk of the bank must be respected (daily management, capital allocation to major units, reporting losses, integrated system, etc.). AMA methods lead to a requirement for regulatory capital a priori lower than in the case of the BIA approach , which clearly favors the bank. At first sight, the cost of implementation of the AMA may seem high. However, the marginal cost is not. Most qualitative criteria required to implement an AMA are indeed already validated, because laws (such as Sarbanes-Oxley, for example) or other regulatory procedures (regarding governance in particular) impose to respect them.

The standardized approach is between the BIA approach and AMA measures [4]. The required quality criteria are very similar to those of AMA methods. The real difference lies in the calculation of regulatory capital. However, the standardized approach seems particularly attractive for traditional banks, as the activities of « retail banking » and « retail brokerage » weigh up to 12% in the calculation of regulatory capital against 15% with a BIA approach.

[1] Basel II considers a matrix division of the bank. It is divided into eight categories or lines of business: Corporate Finance, Sales & Trading, Retail Banking, Commercial Banking, Agency Services, Asset Management, Retail Brokerage.

The standardized approach is in fact a finest extension of the BIA, by declining this type of calculation by type of activity. The regulatory capital of the bank for the operational risk (K) corresponds then to the sum of the regulatory capital of every category of activity, namely :

$$K_{SA} = \sum_i \beta_i \times GI_i$$

Where GI_i is the net banking income (Gross Income or IM) of the i-th row of activity[2]**.** Facteur β_i values (12%, 15% and 18%) were calibrated by the Basel Committee.

II.2. Advanced Measurement Approach (AMA)

The Basel Committee proposes several alternatives within the AMA system : a method based on internal parameters (Internal Measurement Approach or IMA), the RDCA (Risk Drivers and Controls Approach) method, formerly Scorecard, scenario analysis or sbAMA (Scenario -based AMA), and finally, the LDA (Loss Distribution approach) method, the more sophisticated technically. The practice of each of these methods is subject to a set of qualitative criteria, particularly in terms of operational risk assessment and procedure for collecting data loss. This is their common denominator. On the fund, the difference concerns essentially the type of privileged information in the calculation of regulatory capital. The LDA method is based on historical data loss [5], while sbAMA seeks to define scenarios ('what- if' scenarios). The value at risk is then calculated by a Monte Carlo method [6].

As part of the IMA (Internal Measurement Approach), the « average or expected loss » is calculated separately for each class or line of business. For a category of activity *i* and a type of risk *j*, the capital charge K, is defined by example follows this way :

$$K_{ij} = \gamma_{ij} \times EL_{ij}$$

Where EL is the average loss and γ is a scaling factor. The average loss can be calculated as the product of three terms:

$$EL\ \gamma = EI_{ij} \times PE_{ij} \times LGE_{ij}$$

Where EL is the exposure indicator, PE_{ij} is the probability of occurrence of an operational risk event, typifies j for the business line i (probability of event), and LGE_{ij} is the amount of loss associated (loss given event). The challenge is to calibrate the γ parameter. The assumption of this method is that there is a (linear or non-linear) relationship, via the gamma (γ), between the average loss and risk measurement.

The RDCA method (eg Scorecard approach) proceeds by a series of weighted questions, some of which may resemble to scenarios. A score is determined on the basis of the obtained answers, that will help to break the total regulatory capital between the different business lines. The Basel Committee [7] has provided no mathematical formulation for this approach. However, the working groups within banks have proposed formulas for calculating the regulatory capital (K) of the form:

$$K_{Scorecard} = EI_{ij} \times \omega_{ij} \times RS_{ij}$$

With EI the Exposure Indicator, RS the Risk Score (Risk Score) and ω a Scale Factor.

II.3. The Scenario analysis

Scenario analysis (sbAMA) is actually an extension of the RDCA. The risk is considered as a combination of the severity and frequency of potential losses over a given period [8]. The frequency and severity (potential) loss can be measured in monetary units and number of annual occurrences. The risk somehow reflects the vulnerability of the bank. The risk assessment should therefore focus on the vectors of this vulnerability. Now, this one comes for the underlying risk factors. Reduce the level of operational risk imposes a good readability of the portfolio of the bank exposure to various risk factors previously defined.

To be really useful for purposes of decision regarding risk, a scenario analysis must be able to answer to these two questions: With what frequency does the scenario X may occur? What is the amount of the loss if the scenario X occurs?

On operational risk, the scenarios are generally derived from the critical resources on which support various business lines of the bank.

These resources correspond actually to operational risk factors. Among the most common, we list the level of competence / qualifications of staff, internal organization / transfers of information, IT infrastructure (eg,

[2] The Basel Committee holds seven events of operational risk: Internal Fraud, External Fraud, Employment Practices & Workplace Safety, Clients, Products & Business practices, Damage to Physical assets, Business Disruption and System Failures, Execution, delivery & process Management.

system security), procedures for control of unauthorized activities /theft and fraud / unintentional errors (eg, seizure, execution and monitoring of transactions), protective measures against disasters and other disasters, or the compliance with legal requirements (eg, compliance, information dissemination and fiduciary duty). The challenge is to determine how we can extract useful information scenarios. For example:
- What is the probability that one or several of these resources or risk factors are lacking on a time interval considered critical for the bank?
- What negative impact results from it?
If the probability of failure of risk factors or the impact on the operation of the bank is low, it is understood that it is obviously exposed to any real operational risk.

II.4. Modeling LDA

The general idea of the LDA method (Loss Distribution Approach) is to model the loss of operational risk for a given period (eg, one year), and deduct the value at risk. Frachot et al. (2003) propose to proceed in five steps to implement this method [9] :

- Estimation of the severrity distribution ;
- Estimation of the frequency distribution ;
- Calculation of the Capital charge ;
- Calculation of confidence intervals ;
- Incorporation of expert opinion.

It is not about getting into the mathematical formulation of these several steps, but simply to understand the general idea of the LDA method. Like most models of operational risk measurement, the LDA is based on a very old actuarial approach (frequency / severity) widely used in the field of insurance to model similar problems. So that the LDA model can turn, it is necessary to provide two key elements: loss severity distribution, and loss frequency distribution. These two distributions, which form the historical losses are then combined by a Monte Carlo simulation to obtain the distribution of the total loss. This is the result of several successive losses, it is a loss aggregate (aggregate loss distribution). From the total loss, we divert then the expected or average loss, and unexpected loss, for a given confidence level. The Fig1 illustrates the principle of the LDA method [9].

All this seems very simple : build an internal loss history , use usual statistical techniques to adjust the data to a standard distribution of the frequency of the losses (eg , Poisson); adjust historical data processed on a standard distribution of the severity of the losses (eg, lognormal) by a Monte Carlo simulation, integrating the effects of the key indicators of risk so as to take into account the possibility that potential future losses differ materially from historical losses; consider insurance to reduce the amount of loss in case of occurrence , and finally derive the distribution of the aggregate loss from which is determined the capital charge or regulatory capital required to cover the expected loss and exceptional loss. Could we imagine a clearer process? In fact, the difficulty does not lie in the different stages of the LDA method, but in the notorious lack of credible data regarding operational risk.

To stick to the Poisson distribution, the most commonly used in practice, no less than 1,082 observations of individual losses are necessary to obtain an estimate of the average number of casualties, with an error margin of 5 % and a level of only 90 % confidence. With the exception of very frequent loss events whose amount is necessarily weak, it is unlikely that a bank may have an internal history long enough to estimate the frequency distribution with a degree of confidence acceptable[3] losses. The problem of lack of data (or the necessary number of data) are exponentially more complicated when it comes to estimating the distribution of severity.

Must then indeed reasonable estimates not only of the average severity but also its variance. For example, a simple simulation of the lognormal law shows that it will take more than a million points to produce an acceptable estimate of the distribution of severity, with a confidence level of only 90% . This simply means that the number of available data is still insufficient to obtain an estimate of the capital charge not too far from its true value. However, the uncertainty of capital charge is directly related to the calculation of the average loss and especially the exceptional losses, two quantities necessary for the implementation of the LDA method.

III. THE LOAD CALCULATION CAPITAL

The **own funds** are one of the liabilities of a bank. They can be calculated in the prescribed manner. In this case, it is called standard own funds or regulatory capital. They can also be calculated using internal models which take account of diversification effects, the nature of the bank's portfolio, etc. In this case, we speak of own funds

[3] The frequent losses (high-frequency) must necessarily be associated with small amounts (low-severity). Otherwise, the bank may go bankrupt pretty quickly, which makes no sense from the perspective of operational risk measurement.

or Economic capital. The idea of Basel II is to converge the regulatory capital - concern of regulators - and economic capital - concern for banks.

III.1. Definition of Capital-at-Risk

The capital charge (Capital-at-Risk or CaR) is the share of the own funds intended to preserve the bank of the insolvency in case of exceptional losses. This hedging is of course subject to a certain level of confidence or probability. The capital charge CaR expresses the amount of the total potential loss (or severity) for a specified occurrence probability a priori. Capital-at-Risk is actually the output of a risk model. This notion of capital charge is rather indistinct in the area of operational risk. Following Roncalli (2004, p.175), we can hold the following three definitions [10] :

– Definition 1 (Value at Risk or *OpVaR*) : The capital charge is the 99.9% quantile of the distribution of the total loss or aggregate (obtained once the distributions of frequency and severity sized). *N* is the number of random events, the total loss is $L = \sum_{n=0}^{N} \varsigma_n$

Which ς_n represents the amount of the loss *n*. The capital charge is then written :

$$\Pr\{L > OpVaR\} = 0.1\%$$

– Definition 2 (*OpVaR unexpected loss* only) : it is about the previous definition from which we shield the average total loss or expected loss. The capital charge becomes :

$$\Pr\{L > \text{UL} + \text{EL}\} = 0.1\%$$

or: UL = *OpVaR* − E[*L*].

– Definition 3 (*OpVaR* or Value at risk beyond a threshold) : In this case, the capital charge is the 99.9% quantile of the distribution of the aggregate loss defined as the loss of over a certain threshold *H*. We then have :

$$\Pr\{\sum_{n=0}^{N} \varsigma_n \times \mathbf{1}\{\varsigma_n \geq H\} > OpVaR\} = 0{,}1\%$$

Where the term $1\ \{\zeta n \geq H\}$ is equal to 1 if the loss exceeds the threshold H and equal to 0 otherwise.

The calculation of the capital charge CaR occurs in three cases with the Monte Carlo method, but produces significantly different results depending on the definition used. In the third consultative document, the Basel Committee uses the first definition. He stated that the bank must calculate its capital requirement by aggregating the Expected Loss (EL) and Unexpected Losses (UL), except for being able to demonstrate that its internal systems cover adequately EL.

III.2. Aggregation of capital charges and correlation

In the framework of the LDA (Loss Distribution Approach) method, the total or aggregate loss $L_{i,j}$ is the random sum of the individual losses. The probability distribution of the aggregate loss, denoted $G_{i,j}$, is a compound distribution. The capital charge for CaR business line *i* and the type of risk *j* (ie, the *ij* matrix element of operational risk) corresponds then to the α quantile of G_{ij} :

$$CaR_{ij}(\alpha) = G_{ij}^{-1}(\alpha) = \inf\{x | G_{ij}(x) \geq \alpha\}$$

Equivalently, we can write that the capital charge CaR for the ij element of the matrix of operational risk is equal to the sum of the Expected Loss (EL) and the unexpected loss (UL), namely:

$$CaR_{ij}(\alpha) = EL_{ij} + UL_{ij}(\alpha) = G_{ij}^{-1}(\alpha)$$

This expression, shown in a simplified manner in Fig 2**,** can be calculated easily by the Monte Carlo method. The Basel Committee suggests that the capital charge for bank corresponds to the sum of all capital charges CaR_{ij} (α) :

$$CaR_{ij}(\alpha) = \sum_{i=1}^{I} \sum_{j=1}^{J} CaR_{ij}(\alpha)$$

Naturally, it is about a model of allowance of own funds of bottom-up type. The principle is to consolidate operational risk in the banking portfolio from the finest level, until the unity of allowance. By its nature, the bottom-up approach allows to track the consumption of own funds.

This method of calculating the capital charge CaR is particularly attractive, but not quite as simple as it seems. Confidence interval for α equal 99.9% set by the Basel Committee [11], a considerable number of simulations is required (several million) to expect a realistic estimate of economic capital.

IV. PITFALLS TO AVOID DURING THE IMPLEMENTING OF A MODEL OF OPERATIONAL RISK

Once it is specified in its outline, the measurement model - regardless of its form and its degree of sophistication - must be anchored in an integrated operational risk management system. This allows to feel "comfortable" in two respects. As with the development of the measurement model, it is ensured that the different assumptions, modifications and fittings are considered consistent with the guideline set by the risk management (most likely, improve the management of operational risk). And it is also a guarantee that these adjustments align on management processes already in place in the institution.

Again, Basel II is a convenient starting point. An integrated operational risk management system consists of five steps [2] :

- ✓ Step 1: identification ;
- ✓ Step 2: measure ;
- ✓ Step 3: monitoring ;
- ✓ Step 4: capital requirement ;
- ✓ Step 5: control.

Fig3 shows the integrated system, and highlights three essential properties of the latter : (1) it applies to all business lines within the institution, that they are or are not included in the proposed classification Basel II ; and (2) it applies to all new banking products and new initiatives prior to their launch.

The Fig3 also illustrates the need to continuously improve the system. This principle of operational risk management also deserves to be elevated to the golden rule. Without this process of improvement with continuous cycle, the system shown in Figure 3 can quickly disintegrate. More precisely, it is easy to fall into an Endless spiral of pseudo-improvements - in the vain hope of fully define a "perfect" system - without ever get something really useful on a practical level. While it is tempting to specify at first a measurement model which is expected to offer all the risk factors that may affect the level of operational risk [12]. The problem is that it unnecessarily lengthens the period of availability of the model.

V. FIGURES AND TABLES

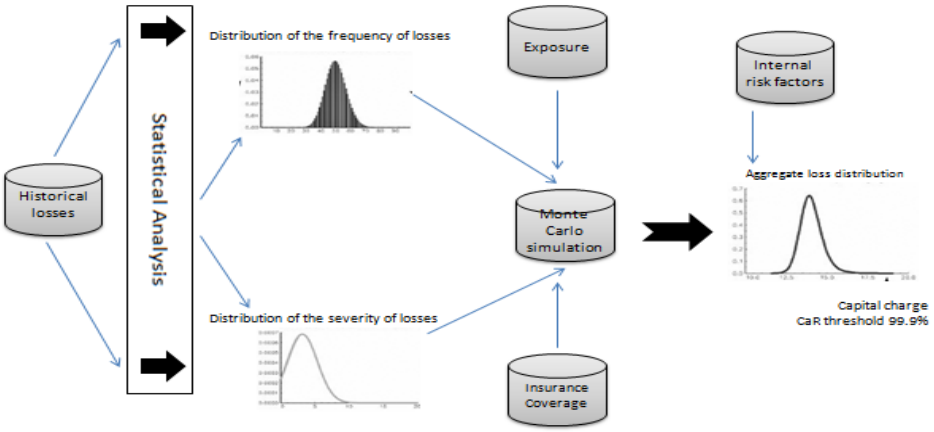

Fig1. Loss Distribution Approach (LDA)

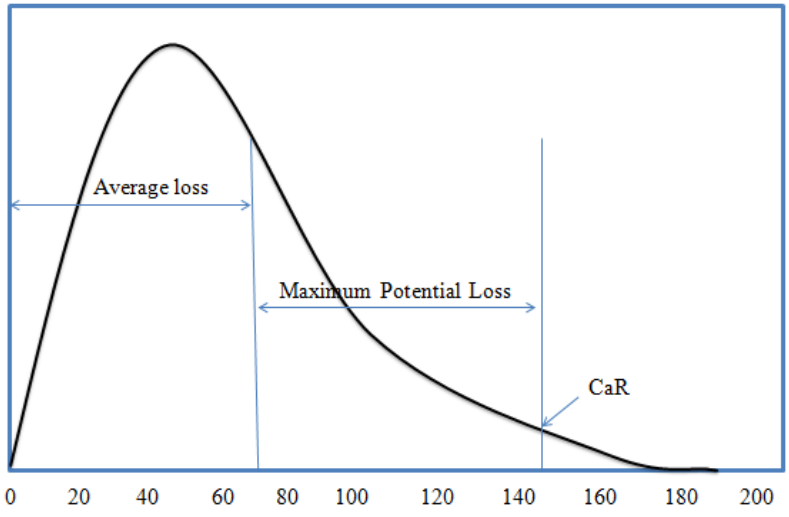

Fig2. Capital at Risk (CaR) and Operational Risk

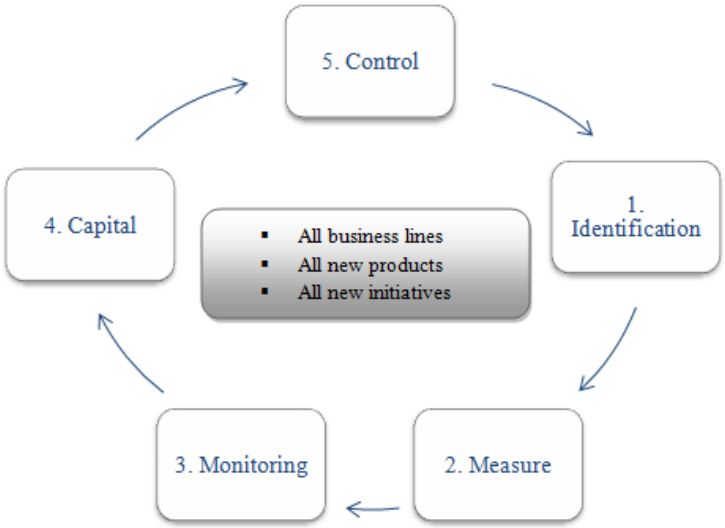

Fig3. Plan of an integrated management system of operational risk

VI. CONCLUSION

The operational risk management is relatively new in banks. In this article, we mainly approached the problem of the measure of this risk. It is necessary to wish that the models of operational risk in the near future provide the same level of transparency and accessibility as those used in market or credit risk. This is a must if we want to effectively integrate operational risk in a comprehensive system of risk management. Of course, it is always possible to improve a measurement model, whether or not operational risk. However, it is necessary to remain careful in front of the methodological arms race of these last years.

There is no denying that the level of technicality required from a risk manager sharply higher. Simply, it must be remembered that a "good" model is primarily a useful model in practice.

REFERENCES

[1] Basel committee on Banking Supervision, International Convergence of Capital measurement and Capital Standards. *Bank for international settlements*, June 2004

[2] Basel committee on Banking Supervision, Operational Risk Management, *Bank for international settlements*, September 1998.

[3] Basel Committee on Banking Supervision, Working Paper on the Regulatory Treatment of Operational Risk, *Bank for international settlements*, September 2001.

[4] Chavez-Demoulin, V., P. Embrechts et J. Nešlehová, "Quantitative Models for Operational Risk: Extremes, Dependence and Aggregation", *Journal of Banking and Finance*, *30, 10*, 2006, 2635-2658.

[5] Nešlehová, J., P. Embrechts et V. Chavez-Demoulin, Infinite mean models and the LDA for operational risk, *Journal of Operational Risk*, *1, 1*, 2006, 3-25.

[6] Chernobai, A., C. Menn, S. T. Rachev et C. Trûck, Estimation of Operational Value-at-Risk in the Presence of Minimum Collection Thresholds, *Technical Report*, University of California Santa Barbara, 2005c.

[7] Moscadelli, M., The Modelling of Operational Risk: Experience With the Analysis of the Data Collected by the Basel Committee, *Working Paper*, Banca d'Italia, 2004.

[8] Chernobai, A., C. Menn, S. Trûck et S. T. Rachev, A Note on the Estimation of the Frequency and Severity Distribution of Operational Losses, *Mathematical Scientist*, 30, 2, 2005a, 87-97

[9] Frachot, A., O. Moudoulaud et T. Roncalli, Loss Distribution Approach in Practice, in The Basel Handbook : A Guide for Financial Practioners, edited by Micheal Ong, *Risk Books*, 2004.

[10] Frachot, A., T. Roncalli et E. Salomon, The Correlation Problem in Operational Risk, Groupe de Recherche Opérationnelle, Crédit Lyonnais, France, 2004.

[11] Embrechts, P., H. Furrer et R. Kaufmann, Quantifying Regulatory Capital for Operational Risk, *Derivatives Use, Trading and Regulation*, *9, 3*, 2003, 217-233.

[12] Chernobai, A., C. Menn, S. T. Rachev, C. Trûck et M. Moscadelli, Treatment of Incomplete Data in the Field of Operational Risk : The Effects on Parameter Estimates, EL and UL Figures, The Advanced Measurement Approach to Operational Risk, edited by E. Davis, *Risk Books*, London, 2006.

American Journal of Engineering Research (AJER)
e-ISSN : 2320-0847 p-ISSN : 2320-0936
Volume-03, Issue-03, pp-245-250
www.ajer.org

Research Paper Open Access

Maternal Stress and Mother-Child Interaction Style Amon the Mothers of Cerebral Palsy Children – A Qualitative Study

Nisha Rani, Dr. Nishi Tripathi, Shailly Singh
Research Scholar (Psychology) SHIATS
Faculty & Incharge Dept of Psychology SHIATS, Allahabad
Research Scholar (Psychology) SHIATS

***Abstract:* - Objective:** To study the relationship between parenting stress and mother-child interaction style among the mothers of cerebral palsy children**. Methods:** The study was conducted in Samvedna Trust for handicapped in the Allahabad city. A purposive sample of 38 children with cerebral palsy within the age group of 5- 12 years was selected. Parenting stress was measured by using Parenting Stress Index Short-Forem (Abidin, 1995) Mother-child interactions were videotaped for 7 minutes during an unstructured play and was rated on three dimensions of responsiveness, affect and directive-ness, which are the subscales of the Maternal Behavior Rating Scale (MBRS, Mahoney 1992). Qualitative analysis was used to study the relationship. Each mother-child dyad was observed separately for the quality of interactions demonstrated in relation to mothers' stress level in each dyad**. Results:** The findings from this qualitative analysis suggested that the mothers who were experiencing a high stress level were found to be less effective during interaction. This means that mothers were less responsive to their child's behavior and actions; exhibited less warmth, enjoyment and approval of the child during interaction; and more controlling than the mothers who were not under much stress. **Conclusion:** Strong association between parenting stress and interaction style suggests the need for the therapists to develop and implement interventions to enhance the quality of mother-child interaction along with other rehabilitation services provided to these children with cerebral palsy.

***Keywords:* -** *Cerebral Palsy, Maternal Stress, Mother-Child Interaction.*

I. INTRODUCTION

Parenting stress is defined as the negative mental response parents ascribe to themselves and/or their child, created by a series of appraisals made by each parent in the context of his or her level of commitment to the parent role. One factor that has been reported to affect the level of stress that parents experience is severity of their children's disability (Keller &Hong 2004; Margalit, Leyser, Ankonia& Avraham, 1991). Thus the cerebral palsy which is the most severe disabilities children can have, is generally believed to place parents at even greater risk for debilitating level of stress than parents of children with, developmental disabilities (Bouma & Schweitzer, 1990;Hasting & Johnson, 2005;Herring, Gray, Taffe, Tonge, Sweeney & Einfeld, 2002) . Psychological state of mothers and primary caregiver is a significant consideration for early development of children with disabilities because this is another factor that appears to affect parents interaction with their children (Konstantarea & Homatides, 1992). Results from an observational study of mothers of children with disabilities who had high and low levels of depression indicated that more depressed mothers interacted less with their children and were less contingently responsive more irritable and had more negative affect and were likely to use harsh discipline than mothers with low level of depression. There is increasing research evidence that the developmental and socio emotional outcomes that children attain in their lives are greatly affected by style of interaction they have with their mothers or other primary care giver through- out the course of their routine activities (Bron fenbrenner,1992;Kochensta, Forman &Coy, 1999;Shonkoff & Phillips, 2000). This evidence indicates that a parent - child interaction is not only critical to the development of typically functioning children, but is also critical to the developmental outcomes attained by children who have disabilities like cerebral palsy.

Until now, various studies have been reported on the stress of mothers of the children with Cerebral palsy, which have evidenced the increased levels of stress among these mothers. Several studies have shown the negative correlations between parenting stress and various measures of child development. Although, these studies do not directly assess parent-child interaction, they either postulate or imply that the observed relationships between parenting stress and child development are mediated by the negative impact that high levels of stress have on parent-child interactions. Only a few studies have been reported that have attempted to determine whether the relationship between parenting stress and child behavior are mediated by reliable and valid measures of parent-child interaction. The assumption that parent-child interaction does in fact mediate the cause and effects of parenting stress (Sameroff & Feil, 1985), remains to be validated empirically. Although, few studies have reported the results, in support of this assumption, but those studies were based on the children with socio-emotional, and behavioral disorders. This study has attempted to determine the relationship between parenting stress and parent-child interaction through a reliable and valid measure if parent child interaction, in order to add to the literature.

Purpose: The purpose of this study was to examine how the mother's psychological status is related to mothers' style of interacting with their children.

II. HYPOTHESIS

Hypothesis 1: mothers with high levels of stress will be less responsive to their child's behavior during interaction than the mothers with low levels of stress.
Hypothesis 2: mothers with high levels of stress will demonstrate low degree of affect during interaction than the mothers with low levels of stress.
Hypothesis 3: mothers with high levels of stress will be more directing to their child's behavior during interaction than the mothers with low levels of stress.

III. METHOD

The study was conducted in Samvedna Trust for handicapped in the Allahabad city where the cerebral palsy children visit from various regions as well as states. A purposive sample of 38 children with cerebral palsy within the age group of 5- 12 years was selected from a population of nearby 80 cases of multiple disorders who were visiting the Samvedna trust and were getting various kinds of rehabilitation therapies. Data used in this study was collected in two phases. In the first phase mothers were asked to complete the demographic questionnaire and assessed for their stress level using the Parenting Stress Index-short form (PSI-SF) by Abidin, 1995. In the second phase mother-child interaction was videotaped for 7 minutes in the special education room where mother interacted with their children during an unstructured play using various physical and cognitive games and activities. This videotaping was done for rating the interaction style on three dimensions of responsiveness, affect and directive-ness, which are the subscales of the Maternal Behavior Rating Scale (MBRS, Mahoney 1992). The rating was done by the research practitioners in the field of psychology.
Data Analysis: First of all the Pearson's correlation coefficient (r = 0.60) was computed to determine the inter-rater reliability between the raters of maternal behavior patterns on MBRS (Mahoney, 1992). Second, the videos recorded for mother-child interaction patterns were subjected to qualitative analysis in relation to the mothers' stress level for each case under study.

IV. RESULTS

Demographic characteristics:
The sample comprised of mothers in their early adulthood period (Age group 20-40 years). The mean score for mother's age (30.92) suggests that most of the mothers belong to early adulthood period. Findings for the Mother's educational qualification indicate that 13 % mothers were educated up to primary school, 19 % up to high school, 21 % up to secondary education and 47% up to higher education, which means that maximum no. of mothers were well qualified as graduate and postgraduate. Mean score for the educational qualification (12.18) suggests that most of the mothers are educated up to secondary education and higher education. Findings for the no. of children indicate that 23 % mothers have one child, 45 % mothers have two children, and 24 % mothers have more than three children to take care in their routine.
The children's chronological ages ranged from 5 to 12,where 29 % children belonged to early childhood period (2-6 years), 66 % children belonged to middle childhood period (6-11 years), and only 5 % children belonged to adolescent age (12-18 years). The mean value for children's age (8.3) suggested that most of the children belonged to middle childhood period. The findings for the gender of the children indicate that more than 68% of the children were boys and 32 % of the children were girls.

Mother's Characteristics on Parenting Stress Index

The findings in Table 1 present the Frequency and percentages of levels of stress the mothers experience. The findings in the table indicated that in sample, 34 % mothers lies in the normal range, 6 % mothers lies in the risk range and 50 % mothers lies in the clinical range, which suggests that more than 50 %, i. e. most of the mothers are either in the risk of developing depressive symptoms or suffering from depressive symptoms. The mean score for total stress, (92.9) was found to be above the normative value and is above normative range (90), which suggests that according to the norms of the PSI-SF, mother's level of stress is in the clinical range.

V. QUALITATIVE ANALYSIS:

In this study mother child interaction was videotaped for seven minutes in order to assess the quality of maternal interaction style through an unstructured play. The qualitative analysis was done on the basis of the ratings, given by the research practitioners in psychology. These raters gave their ratings on each item of the maternal behavior rating scale (MBRS Mahoney, 1992), according to the interaction patterns observed in video recording. The ratings used for the qualitative analysis are based on the consistency of the ratings of these three raters. The maternal and child related factors behind the problem of the child as indicate by the qualitative analysis are; delayed cry after birth, obstructed labor, vacuum delivery, forceps delivery, fall accidents, jaundice after birth and maternal infection during pregnancy. The children in the sample were suffering from the distinct types of cerebral palsies such as, spastic quadriplegia, spastic paraplegia, dystonia; and the problems associated commonly with the type of cerebral palsy were dysarthria and seizures. As these children were receiving the special education for gross motor and fine motor activities through various types of block games, the video recording was based on the mother's behavior patterns with the child, while playing and doing activity on these block games, which was an unstructured process. After analyzing all the mother-child dyads (n=38) distinctly, in relation to mother-child interaction patterns following results were found.

First, the moderate degree of responsiveness was demonstrated by mothers with a stress level within the risk group. Low degree of responsiveness was demonstrated by the mothers with clinically significant, as well as normal levels of stress. Some mothers with high levels of stress demonstrated an effective responsive behavior. These findings indicated that the degree of responsiveness in parenting behavior was not found to be associated typically with any of the three levels of maternal stress. Responsiveness was associated with maternal stress in distinct ways.

Second the degree of affect demonstrated by most of the mothers was low to moderate. A few mothers demonstrated a high level of affect also. When these trends of affect were analyzed in relation to the maternal stress it was found that moderate and low degree of affect was demonstrated by the mothers who were experiencing stress level within the range of risk group or the clinical significant. The high degree of affect was demonstrated by the mothers with a stress level within the normal range. Though a few mother demonstrated a high degree of affect with increased stress level, but their frequency was negligible. All these findings suggested that the most of the mothers, who were experiencing a high level of stress, were not effective in demonstrating warmth, enjoyment and approval of the child.

Third, the findings observed from the mother-child interaction indicated that most of the mothers demonstrated a moderate and high degree of directive-ness. The low degree was also demonstrated by few mothers whose stress level was within the normal range. On relating each mother's degree of directive-ness with their stress level it was found that mothers demonstrating moderate and low degree of control were experiencing a stress level with in the risk group range or the clinical range. These findings suggested that mothers who were experiencing a high level of stress were more controlling than the mothers who were experiencing stress level within the normal range.

To summarize the findings of all three components of interaction style, mothers stress level was associated with quality of parenting style during mother-child interaction. The findings from this qualitative analysis suggested that the mothers who were experiencing a high stress level were found to be less effective during interaction. This means that mothers were less responsive to their child's behavior and actions; exhibited less warmth, enjoyment and approval of the child during interaction; and more controlling than the mothers who were not under much stress.

The findings from the qualitative analysis are consistent with study based on quantitative analysis depicting the relationship between child's functional disability, maternal stress and mother-child interaction style (Nisha Rani, Dr. Nishi Tripathi, 2013) which showed that parenting stress was having significant negative correlation ($r=-0.48$, $p< 0.01$), with maternal affect and a significant positive correlation ($r=0.40$, $p< 0.05$), with maternal directive-ness. However, there was non-significant correlation with maternal responsiveness. These findings suggest that highly stressed mothers are less effective in expressing their feelings, enjoyment, warmth, and are less inventive and less accepting to the actions of their children during their interaction, than the mothers who experience low levels of stress. Likewise, mothers experiencing high levels of stress are more likely to

control and direct their children during one to one interaction, than the mothers with low levels of stress. The findings of this study also suggest that parenting stress is unrelated to the maternal responsiveness which means that mothers are appropriately sensitive to their children's needs and effective in expressing her responsiveness while interacting with their children irrespective of their levels of stress they experience. These findings from both quantitative and qualitative analysis are highly compatible with results that have been reported in the literature which suggest that the high levels of parenting stress interfere with the ability of mothers to interact effectively with their children (Guralnick, 2005: Woolfson & Grant, 2006). This belief is most commonly based on the research findings which indicate the high levels of parenting stress are associated with lower levels of child development (Landry, et al., 2001; Neece & Baker, 2008; Noel, et al., 2008). Authors of these studies have proposed that highly stressed parents may be unable to engage in the quality or frequency of one to one interactions that are needed to support and nurture children's development which results in decreased child development and increased social emotional problems (Floyd & philippe' 1993; Hastings & Beck, 2004).

VI. CONCLUSION

One major finding of this study was that parenting stress was related to the mother's style of interaction (affect and directive-ness) with their children, which means that high level of maternal stress interferes with mother's effectiveness at engaging in quality interaction with their children Children with cerebral palsy are at extremely high risk for academic failure, and/or special education placement as well as dropping out of school. Since there is increasing evidence that the first five years of children's lives are critical period for addressing these developmental, and social emotional problems it becomes crucial to enhance the effectiveness of parents. Strong association between parenting stress and interaction style suggests the need for the therapists to develop and implement interventions to enhance the quality of mother-child interaction along with other rehabilitation services provided to these children with cerebral palsy.

REFERENCES

[1] Abidin, R. R. (1992). The determinants of parenting behavior. *Journal of Clinical Child Psychology, 21*, 407-412.

[2] Keller, D., & Honig, A. (2004). Maternal and paternal stress in families with school-aged children with disabilities. *American Journal of Orthopsychiatry, 74, (3),* 337-348.

[3] Margalit, M., Leyser, Y., Ankonina, D. B., & Avraham, Y. (1991).Community support in Israeli kibbutz and city families of disabled children: family climate and parental coherence. *Journal of Special Education 24, (4*), 427-440.

[4] Bouma, R., & Schweitzer, R. (1990). The impact of chronic illness on family stress: a comparison between autism and cystic fibrosis. *Journal of Clinical Psychology, 46*, 722-730.*Education, 24, (4),* 427-440.

[5] Hastings, R. P., & Beck, A., & Hill, C. (2005). Positive contributions made by children with an intellectual disability in the family: Mothers' and fathers' perceptions.*Journal of Intellectual Disabilities, 9*, 155-165.

[6] Herring, S., Gray, K., Taffe, J., Tonge, B., Sweeney, D., & Einfeld, S. (2006). Behavior and emotional problems in toddlers with pervasive developmental disorders and developmental delay: associations with parental mental health and family functioning. *Journal of Intellectual Disability Research, 50*, 874-882.

[7] Konstantareas, M. M., Homatidis, S., & Plowright, C. M. S. (1992). Assessing resourcesand stress in parents of severely dysfunctional children through the ClarkeModification of Holroyd's Questionnaire on Resources and Stress. *Journal of Autism and Developmental Disorders, 22 (2),* 217-234.

[8] Bronfenbrenner, U. (1992). Ecological systems theory. In R. Vasta (Ed.) *Six theories of child development: Revised formulations and current issues* (pp 187-248). Philadelphia: Jessica Kingsley.

[9] Shonkoff, J. P., & Phillips, D. A. (Eds.) (2000). From neurons to neighborhoods: The science of early childhood development. Washington, DC: National Academy Press.

[10] Kochanska, G., Forman, D. R., & Coy, K. C. (1999). Implications of the mother-child relationship in infancy for socialization in the second year of life. *Infant Behavioral Disorders, 22*, 249-265.

[11] Sameroff, A. J., & Fiel, L. A. (1985). Parental concepts of development. In I. E. Siegel (Ed.), *Parental belief systems* (pp83-105). Hillsdale, NJ: Erlbaum.

[12] Abidin, R. R. (1995). Parenting Stress Index Manual, (3rd edition). Odessa, FL: Psychological Assessment Resources.

[13] Mahoney, G. (1999). The Maternal Behavior Rating Scale-Revised. Cleveland, Ohio: Case Western Reserve University.

[14] Guralnick, M. J. (2005) An overview of the developmental systems model for early intervention. In:Guralnick, M. (Ed.). The developmental systems approach to early intervention. Baltimore, MD: Paul H. Brookes, 3-28

[15]. Woolfson, I., & Grant, E. (2006). Authoritative parenting and parental stress in parents of preschoolers and older children with developmental disabilities. *Child: Care,Health and Development, 32, 2,* 177-184.
[16] Landry, S. H. Smith, K. E., Swank, P. R., Assel, M. A., & Vellet, S. (2001). Does early responsive parenting have a special importance for children's development or it is consistency across time early childhood necessary? Developmental Psychology, 37, 387-403.
[17] Neece, C., & Baker, B. (2008). Predicting maternal parenting stress in middle childhood: the roles of child intellectual status, behavior problems and social skills. *Journal of Intellectual Disability Research, doi: 10.1111/j.1365-2788.2008.01071.x* Downloaded on July 21, 2008.
[18] Noel, M., Peterson, C., & Jesso, B. (2008). The relationship of parenting stress and child temperament to language development among economically disadvantaged preschoolers. *Journal of Child Language,* 35, 823-843.
[19] Floyd, F. J., & Phillippe, K. A. (1993). Parental interactions with children with or without mental retardation: behavior management, coerciveness and positive exchange. American *Journal on Mental Retardation, 6,* 673-684.
[20] Hastings, R. P., & Beck, A., & Hill, C. (2005). Positive contributions made by childrenwith an intellectual disability in the family: Mothers' and fathers' perceptions. *Journal of Intellectual Disabilities, 9,* 155-165.

Table I: Sample characteristics on Parenting Stress Index Short-form.

Level of Parenting Stress	Percentile Score Range	Frequency	Percentage
Normal Range	15-80th	13	34
Risk Range	<90th	6	16
Clinical Range	>90th	19	50

Appendix
Sample Illustration of Mother-Child Dyad

□ □ Mother's prenatal & intranatal history…Antenatal history was normal but intra-natal history of vacuum delivery was present.
□ □ History of the child's problem…Birth history of oxygenation and much delayed cry. Problem was identified at the age of one year.
□ □ Diagnosis…Spastic quadriplegia.
□ □ Associated problems…Visual impairment.
□ □ Maternal stress level (PSI-SF Score)…Normal range.

Interaction Patterns observed in video-recording:

1. Degree to which mother monitors child's behavior and all verbal and non-verbal subtle communication----------**High.**
2. Frequency of mother's responses to child's play, social activities, facial expressions, vocalizations and gestures----------**High**.
3. Effectiveness in engaging children in reciprocal interaction- whether the interactive sequences are dominated by either mother, child or there is balanced reciprocal exchange of turns------ ----**Moderate.**
4. Degree to which mother shows (by gesture, facial expressions, or tone of voice) or talks directly about feelings, thought, pleasure, or pain) ----------**High.**
5. Degree to which mother enjoys interaction with the child; display playfulness and humor; takes pleasure in child's accomplishments and express happiness either verbally or non-verbally-- ---- --------**High.**
6. Degree of expression of warmth through touches and Positive regard and affection for the child; emotional support and encouragement in an ego-enhancing way----------**Moderate.**
7. Degree to which mother is creative in her interaction with the child (comes up with novel ideas or suggestions) and degree of absence of stereotyped and repetitive actions----------

Moderate.

8. Degree of delight, admiration and positive affect for the child's actions and communicate in legitimate and worthwhile manner----------**High.**
9. Degree of physical activity and manipulation of the objects during interaction; and degree to which mother talks to the child and is engaged with the child----------**Moderate**.
10. Degree of interruptions (instructions, training, eliciting and control) during the child's free play and interaction----------**Moderate.**

CONCLUSION

Mother –child interaction patterns demonstrated a high degree of responsiveness and moderate degree of affect and directive-ness. Though the mother' stress level is within the normal range and the child here has modified functional dependence (need supervision), the degree of control demonstrated is high. These findings suggest that mother with normal stress level is more controlling, while being highly responsive and warm and enjoying and approving of the child.

American Journal of Engineering Research (AJER)
e-ISSN : 2320-0847 p-ISSN : 2320-0936
Volume-03, Issue-03, pp-251-263
www.ajer.org

Research Paper Open Access

Perceptron system to assist in decision making and monitoring of quality of software development in Information Technology environments

Chau Sen Shia, Ivanir Costa
Doctor, Production Engineering, Department of Postgraduate Production Engineering, University Paulista UNIP. São Paulo, SP - Brazil,
Doctor, Production Engineering, Department of Postgraduate Production Engineering, University Paulista UNIP. São Paulo, SP - Brazil,

Abstract: - Classical methods for *software* development require high costs and problems of communication between development teams, project risks and delays in the delivery of its services.
In this work, the aim is to develop a *perceptron* model to demonstrate the ability to control, service quality assessment and decision-making in IT (Information Technology). For this, we used perceptron network techniques, standards of service quality measures and risk analysis model of applied projects in software engineering.
With the network *perceptron* model implementation was possible to simulate the application of development in several requests for applications for *software*, in order to meet the management of schedules in all phases of the life cycle of the projects carried out. The tests with the *perceptron* model were applied in it environments to meet service requests from various fields. The results and analyses presented in these projects demonstrate that communication between development teams were more consistent. It was also possible to predict with more accuracy the delivery of services, decision making and risk reduction projects.

Keywords*: - software quality, measurement of services, indicator of quality of software, perceptron network.*

I. INTRODUCTION

Requests for services are often held for several consultancies and many of these processes requests are evaluated negatively, not satisfying the needs of its customers, (SANTOS, 2000). This shows that to meet customer needs, we need to identify the main risk factors that may contribute to the delay of projects and scale qualitative values to improve the preparation of solicitation of business proposals.

A competitive company focused on customer satisfaction should consider the participation and integration of its customers from the initial stages of the development process of its products (AGUIRRE CARLOS GONZALEZ and TOLEDO, 2012).

Aiming to improve the quality in service delivery, the proposed model of software allowed teams to better integrate various areas of the IT environment, as well as track the life cycle of a project from its initial phase. Constantly knowledge base perceptron network and service quality indicator were compared with the proposed phases of requirements gathering schedule.
The main objective of this work is the development of a perceptron model to assist in decision making in the provision of software services environments. In this form is possible to aim for better control the quality and the interaction of all the teams involved by computing and managing the lifecycle of a software project.

II. THEORETICAL REFERENCE

This section describes the main aspects related to the concepts and rationale for building the system proposed in this paper.

2.1. The role of quality and services

The importance of the quality and value of the service is the measure of the degree of customer satisfaction in relation to the requirements of price, reliability, durability, aesthetics, timeliness, taste, comfort. As the value of the service, can be quantified by the weighted sum of grades that are assigned by the data collection by weight assignments to the notes in this way good or service receives a value, while the quality is established during the design phase (COAST; EPPRECHIT and CARPINETTI, 2008).
To ISO 9126, the fundamental attributes of software quality can be classified into:

a) Functionality: is the degree to which the software meets the stated needs as indicated by attributes: suitability, accuracy, interoperability, compliance and security.
b) Reliability: is the amount of time the software is available for use as indicated by the attributes: maturity, fault tolerance, ease of retrieval.
c) Usability: is the ease of use of the software as indicated by the attributes: ease of understanding, learning, and operability.
d) Efficiency: the degree of optimization of the use, software, system resources as attributes: behavior over time and in relation to resources.
e) Ease of Maintenance: is the ease with which a correction can be made in software as attributes: ease of analysis, implementation of change, stability, testability.
f) Portability: the ease with which software can be transposed from one environment to another as attributes: adaptability, ease of installation, compliance, eases of replacement.

2.2. The Likert scale

The measurement based on a Likert type scale (created in 1932 by American educator and social psychologist Likert Rensis) is an instrument that features a cast of sentences for which the respondent expresses their degree of agreement , indicating values on a scale such as: (1) fully disagree , (2) disagree, (3) neither agree nor disagree (4) agree, (5) fully agree. The Likert scale has several advantages: a) it is easy formulation and implementation, b) is more objective, c) is more homogeneous and increases the probability of measuring unit attitudes. As a disadvantage, the scale turns out to quantify and standardize responses, making it impossible to detect nuances and subtleties of attitudes, which in turn are perceived in interviews and open questionnaires (SCOLARIS , 2009) .

On the Likert scale responses for each item varies according to the degree of intensity. This scale with ordered, equally spaced categories and with the same number of items in all categories , is widely used in organizational research investigating the practices of TQM (Total Quality Management) (SARAPH , 1989) , (BADRI , 1995) , (TAMIMI , 1995) and (ALEXANDRE , 1995).

2.3. The dividing line or boundary decision

Conform to Tan, Steinbach and Kumar (2006), the limit being two border regions of different classes is known as decision limit. The test condition involves only one attribute; the decision boundaries are straight, parallel to the coordinate axes. There are many metrics that can be used to determine the best way to break the records. These metrics are defined in terms of the distribution of the class of the registers before and after the division. According to Medeiros (2006), if a problem can be separated by a straight line, representing the division between classes, says that such a problem is linearly separable, otherwise it is not told linearly separable.

2.4. The GQM (Goal-Question-Metric) method

The difficulties of obtaining measurements for the software are varieties of aspects and the presence of many intangibles. In software projects, measurements can already be used in the requirements analysis (stage of development) to determine how the software should work. Another way to measure is the software application of GQM method (Goal -Question -Metric), consisting in organizing planning a software measurement in stages: a) goals that are established according to the needs of stakeholders and must be fixed depending on the software requirements (time , number of users employed to test) , b) issues that are set to perform work measurement and that the questions should bring useful information to improve the product , c) categories that divide the set, d) forms that drive the work of evaluators (KOSCIANSKI and SOARES, 2006) .

As Basilis and Weiss (1984), the method GQM (Goal -Question -Metric) is an organized way of dealing with the planning work of a measurement. The method organizes the planning of a software measurement in steps, with each step defines the following elements: a) objectives, b) questions, c) categories, d) forms.

2.4.1. The *SQuaRE* norm

The square model based on ISO / IEC 25000 defines the quality and focuses on a specific problem of measuring the quality of software products. This standard contains several examples of external and internal metrics that can be used as a starting point for building a system of quality assessment software (KOSCIANKI and SOARES , 2006) .

The square norm (Software Product Quality Requirement and Evaluation - Quality Requirements and Evaluation of Software Products), according Koscianski and Soares (2006), is an evolution of ISO / IEC 9126 and ISO / IEC 14598 standards. According to Garcia (2009), the norm square reunites the processes of software quality (ISO standard 9126) and product evaluation (default 14598) using as a base the measure of quality. The advantages offered by Square are: a) to coordinate measures and evaluation of software quality , b) provide a guide for specifying requirements of software quality , c) harmonize the existing rules with respect to ISO / IEC 15939 , by the reference model for measuring quality belonging to the ISO / IEC 25020 standard.

2.4.2. The spiral software development model

Proposed by Boehm (1988), the spiral model of evolutionary process is software that couples the iterative nature of a prototype system aspects and controlled cascade model. Provides potential for rapid development and increasingly more complete versions of software. The main features of the spiral model are described as:

a) is a generator of different processes directed to scratches and is used to guide the engineering software intensive systems, which occurs concurrently and has multiple involved.
b) It is a cyclic approach toward expanding incrementally, the degree of definition and implementation of a system, while decreasing its degree of risk. It is a series of anchor points of control to ensure the involvement of stakeholders as to find solutions for systems that are mutually satisfactory and practicable.

2.5. Mathematical neuron

According to Ludwig and Montgomery (2007), a mathematical neuron receives one or more input signals and returns a single output signal, and can be delivered as output of the network, or as an input signal to one or more other neurons of layer later. Input signals arrive simultaneously to neurons. Dendrites and axons are represented mathematically by synapses and intensity of bond is represented by synaptic weight. The neuron totals multiplications of entries with their respective synaptic weights generating weighted inputs (v1.w1, v2.w2, ..., xn. Wn) and the aggregation of all products is the result of the sum $v = \sum_{i=0}^{n} w_i x_i$

The activation function is compared with the transfer function, which aims to prevent the progressive increase of the output values throughout the network layer (LUDWING and MONTGOMERY, 2007).
The main transfer functions used are the sigmoid Gaussian and hyperbolic tangent type, as shown in Figure 1.

- Função sigmóide:

$$\varphi(v) = \frac{1}{1+e^{-v}}$$

- Função gaussiana:

$$\varphi(v) = e^{-v^2}$$

- Função tangente hiperbólica:

$$\varphi(v) = \tanh(v)$$

Figure 1 Functions transfers and Montegomery Ludwig (2007).

2.6. Artificial Neural Network

The ability of computers based on the Von Neumann architecture, which consists of central processing units that execute instruction sequences are not able to perceive and think of how the human mind multiprocessors (BROOKSHEAR , 2005) . Thus, many researchers focus their research applying theories of RNA (Artificial Neural Networks). The building is constructed using RNAs from many individual processors known as processing units.

Its basic function is similar to the biological network systems, composed of cell dendrites that are responsible for the information and axon inputs that are outputs of the information generated. To Palma Neto and Nicoletti (2005), Neural Networks is a general and practical approach for learning the functions of examples method. Can be characterized as:

a) Basic processors called neurons.
b) The activation function (representing the state of the neuron).
c) The existing pattern of connections between neurons.
d) For its training algorithm (or learning algorithm).

According to Nunes da Silva, and Spatti Flauzino (2010), the strategy of supervised training is to have affordable, considering each sample of the input signals, their desired outputs, where each training sample is composed of the input signals and their corresponding outputs. The synaptic weights and thresholds are then continuously adjusted by applying comparative actions executed by the learning algorithm itself, which oversee the discrepancy between the responses produced by the network in relation to those desired, and this difference was used in the fitting procedure.

Described below are the principal features of neural network adapted (LUDWING and Montgomery 2007).

a. A RNA should have an input layer or distribution, however has no neuron, only a number of nodes with the same number of input signals in the network. No computation is performed in this layer.
b. Should contain a layer, zero or more hidden layers and consist of one or more hidden neurons. These layers allow the network to extract statistics and represent problems that are not linearly separable.
c. Should contain a layer that has a number of neurons equal to the number of output signals from the network.
d. Should allow adjustment of the values of its synaptic weights, because that way the network is able to memorize the relationships among the input data with the output, thus represented an associative memory.

2.7. Perceptron learning algorithm

A neural network typically has two processing stages: the learning and use. These two moments of operation are distinct and applied in different periods.

Learning is a process of adjusting the weights of connections in response to stimuli presented to the network (the properties are modified due to the need to learn the information presented). The process of use is the way in which the network responds to a stimulus input occurs without changes in their structure. The models of artificial neural networks manipulate information by the interaction of a large number of basic processing units (AGUIAR and OLIVEIRA JUNIOR, 2007). The architecture of an artificial neural network defines how many neurons are arranged in relation to each other. These arrangements are essentially structured to directing synaptic connections from neurons (NUNES SILVA, SPATTI and FLAUZINO, 2010).

In a neural network, the synaptic weights are adjusted so that a given set of input signals can be processed by your neurons and present a set of output signals since your level of error is acceptable. The adjustment is made via a learning algorithm of type delta rule for perceptron network. The methodology for this type of neural network (as shown in Figure 2) is performed as described below:

a) Assign weights to random values.
b) Place a set of input signals.
c) Calculate values as supervised training.
d) Compare the calculated values with the desired values.
e) If the error obtained is not acceptable, adjust the weights according to the proportion of the error and the value of the corresponding input signal (the larger the error, more should be done to fix the weights).

$$w(i,j)_{T+1} = w(i,j)_T + \eta E(j)_T x(i)$$

- $w(i,j)_{T+1}$ = valor do peso corrigido;
- $w(i,j)_T$ = valor do peso na iteração anterior;
- $E(j)_T$ = Valor do erro para o neurônio j;
- i = índice do sinal de entrada;
- T = iteração;
- j = índice do neurônio;
- η = taxa de aprendizado;
- $x(i)$ = sinal de entrada.

Figura 2 Função de transferência, Ludwing e Montegomery (2007).

The error E (j) is the difference between the output signal (desired) to neuron j, represented by d (j). As y (j) is the output signal calculated by the neuron network for that, as shown in Equation 2. For the average error of all the neurons of the output layer interaction T is: $\varepsilon(T) = \frac{\sum_{j=1}^{n}|E(j)|}{n}$, where n equals the number of neurons of the output layer. The average error for the entire training set is: $\varepsilon_{med} = \frac{\sum_{T=1}^{n}\varepsilon(T)}{n}$.

The value of the mean error (as shown in Figure 3) can be used as a reference for termination of training and assessment for fine tuning the network.

$$E(j)=d(j)-y(j). \quad ; \quad \varepsilon(T) = \frac{\sum_{j=1}^{n}|E(j)|}{n} \quad ; \quad \varepsilon_{med} = \frac{\sum_{T=1}^{n}\varepsilon(T)}{n}$$

Figure 3 Transfer function, Montegomery and Ludwig (2007).

According to Aguiar and Oliveira Jr. (2007), the type of training can be supervised or unsupervised. Training is supervised when the parameter setting is done on presentation of a set of pairs of inputs and outputs standard. In this process, a default entry is presented to the network and an output is calculated. You unsupervised learning the set of training patterns has only entries. In this process, there is no standard output is not shown to the network a known standard. To Nunes da Silva, and Spatti Fauzino (2010), the process of training a neural network consists of the application of ordered steps that are necessary for synchronization of synaptic weights and thresholds of their neurons, with the ultimate goal to generalize solutions to be produced by their exits and their responses are representative of the physical system that are called mapping and learning algorithm.

2.8. Integrating perceptron network as quality classification and analysis of project risk

At this stage it creates the internal structure of a perceptron (as shown in Figure 4), with their respective binary values and relations between the models and the square spiral model (for risk analysis of projects) used in software engineering. Relations (according to studies established between the two models and their main characteristics) existing between their classes and subclasses of the square model proposed by Boehm (1988) model are structured according to the phases and project risks. Established the relationship of the classes he attributes of square model with its subclasses of the model *SQuaRE* to assign their corresponding binary values. Then, also the binary values have been assigned to the phases of the Boehm spiral model, so to describe the relationship between the two models using binary structure. The attributes of the structure of the perceptron neuron to the system is show in the figure 4.

SQuaRE	Binario	Atributos	Pesos	Fases				Relação SQuaRE x Modelo Espiral			
				fase1	fase2	fase3	fase4	RF1	RF2	RF3	RF4
1-Funcionalidade	000000	Adequabilidade		00	01	10	11	00000000	00000001	00000010	00000011
1-Funcionalidade	000000	Acurácia		00	01	10	11	00000000	00000001	00000010	00000011
1-Funcionalidade	000000	Interoperabilidade		00	01	10	11	00000000	00000001	00000010	00000011
1-Funcionalidade	000000	Segurança		00	01	10	11	00000000	00000001	00000010	00000011
2-Manutenibilidade	000001	Testabilidade		00			11	00000100			00000111
2-Manutenibilidade	000001	Estabilidade		00			11	00000100			00000111
2-Manutenibilidade	000001	Modificabilidade		00			11	00000100			00000111
2-Manutenibilidade	000001	Analisabilidade		00			11	00000100			00000111
3-Usabilidade	000010	Atratividade		00		10	11	00001000		00001010	00001011
3-Usabilidade	000010	Compreensibilidade		00		10	11	00001000		00001010	00001011
3-Usabilidade	000010	Apreensibilidade		00		10	11	00001000		00001010	00001011
3-Usabilidade	000010	Operabilidade		00		10	11	00001000		00001010	00001011
4-Confiabilidade	000011	Maturidade		00	01		11	00001100	00001101		00001111
4-Confiabilidade	000011	Tolerância a Falhas		00	01		11	00001100	00001101		00001111
4-Confiabilidade	000011	Recuperabilidade		00	01		11	00001100	00001101		00001111
5-Eficiencia	000100	Comportamento Temporal		00	01	10	11	00010000	00010000	00010010	00010011
5-Eficiencia	000100	Utilização de Recursos		00	01	10	11	00010000	00010000	00010010	00010011
6-Portabilidade	000101	Adaptabilidade				10	11			00010110	00010111
6-Portabilidade	000101	Instabilidade				10	11			00010110	00010111
6-Portabilidade	000101	Co-existência				10	11			00010110	00010111
6-Portabilidade	000101	Substitubilidade				10	11			00010110	00010111

Figure 4 Structure-square model and compared with the spiral model of Boehm, author.

III. METHODOLOGY

For software development proposed in this paper, we applied the methodology of exploratory, descriptive, explanatory, quantitative, and qualitative literature to achieve the research objectives to be achieved. The approach was based on literature searches the "state of art" in quality management software

development services, software measures, standards Square, Boehm spiral model of software and technical network perceptron. After the literature review, the risk factors of projects were identified, the negative evaluation process of service requests and software problems in measurements of impacts.

Upon approach , we identified the main characteristics of measuring quality of software product proposed by the international standard ISO / IEC 25000 , the spiral model proposed by Boehm (1988) , for risk analysis software design , technical network perceptron to assist in project risk analysis , using as a basis the opinions of experts , transforming the data collected by checklist form the basis of learning for risk assessment of projects aided by the perceptron network capacity rating risk impacts project (OLIVEIRA JUNIOR , 2007) .

Was applied in this work, a list of issues with the quality attributes presented by Square model are: functionality, maintainability, usability, reliability, efficiency and portability. Data collection was performed using the experiences of experts in the field of development consisting of a project manager, a system analyst and software developer.

The questionnaire was also applied in other types of projects such as Inventory Control, Real Estate, Service Delivery, Weights and Measures, Call Center, and Medical Diagnosis. For this, analysis and simulations of the data collected by IT experts and then were used for testing, simulations and validations that occurred during all phases of the development of software applications have been developed, as shown in Figure 5 (activity stream) below:

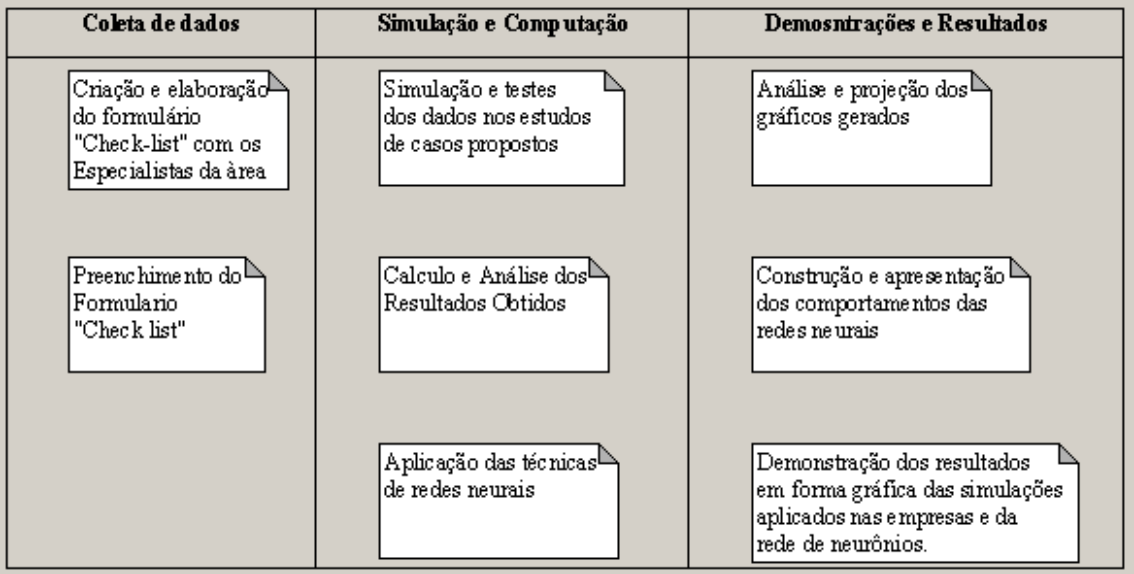

Figure 5 - Diagram of proposed development activities that work, the author.

Fase I

3.1. Collecting and analyzing data

For the insertion of the data collected , automated forms were used (to accept the entries of the data collected) developed the proposed application using the concepts presented by the authors of quality management and process management (CARVALHO; PALADINI; KOSCIANSKI AND SOARES; LAS CASAS; PALADINNI; SORDI; SPHAINER). The information collected through quality metrics Square service (or past projects) was obtained by the development team who contributed to this work.

The application of the research was conducted with experts from the development of small businesses (applied in segments from different areas) software. National and international journals to better understand the techniques of descriptive and exploratory studies were analyzed. Were used at the beginning of this study, interviews with experts in the field of software development (programmers, systems analysts and project managers). Then the forms (Check List) were completed, for a certain period of time (over a month). We used the Likert scale as measurement (grading between 1 and 5). Key attributes for measuring the quality of services are the norm square of: functionality, maintainability, usability, reliability, efficiency and portability.

Fase II

3.2. Practice Simulations

The practice of drills and tests in IT environments, were performed using data collection (check-list type) and attributes that qualify the quality measures for services obtained from the norm square (Software Product Quality Requirements and Evaluation). Perceptron techniques to meet the requirements and service

requests in IT network environments were applied. During the risk assessment project we used the spiral model proposed by Boehm with the participation of specialists of IT field for analysis and management of software projects. The following describes the main techniques and resources used to develop the proposed application of this work.

3.2.1. The application of the perceptron network with the square model

The structure of Multilayer Perceptron network was used for the integration of attributes that define the square model for assessing the quality of services. The attributes of entries are: functionality (000000), maintainability (000001), usability (000010), reliability (000011), efficiency (000100) and portability (000101), which has their corresponding binary values. As Medeiros (2006), in a multilayer perceptron model can contain many internal layers, besides the input and output layers. Weight values, bias, and references to settings and shots of the transfer functions of neurons as the values of the weighted sums thresholds are assigned. The functions used for the thresholds of shots are the step type: $y = f(x) = \begin{Bmatrix} -1, x < 0 \\ 1, x \geq 0 \end{Bmatrix}$.

Fase III

3.3. The application form check-list

The check-list (Figure 6) form also consists of assigning values "notes" using a Likert scale with 5 notes to the level of impact of project risk. Experts attributed the levels of project risk (qualitatively) during the life cycle of the project. Are described (in the checklist) the corresponding department for collecting and subject specialists responsible for assessing. Field of the weighted average and the dividing line was calculated by the system.

Formulario para Análise de "Modelo de Qualidade SQuaRE para Processo de Software"						
Questões (Níveis de Impactos de Riscos de Projeto)	Atribuição de Notas					Média
	1	2	3	4	5	Pondera
1-Funcionalidade : Adequabilidade, Acurácia, Interoperabilidade, segurança.		x				
2-Manutenibilidade: Testabilidade, Estabilidade, Modificabilidade, Analisabilidade.			x			
3-Usabilidade: Atratividade, Compreensibilidade, Apreensibilidade, Operabilidade.			x			
4-Confiabilidade: Maturidade, Tolerância a Falhas, Recuperabilidade.		x				
5-Eficiência: Comportamento Temporal, Utilização de Recursos.				x		
6-Portabilidade: Adaptabilidade, Instabilidade, Co-existência, Substitubilidade.		x				
			Linha Divisória			

Departamento :

Especialista da Área :

Cancelar Enviar

Figure 6 - Form Check List for collecting data on the levels of impact of project risks (normaSQuaRE), author.

The form (Figure-7) has been used since the service request with the participation of staff and during the construction phases of the software. The sequences of completing the forms were week.1 (2 forms), week 2 (3 forms), week 3 (2 forms) and week 4 (2 forms). Marking risk impacts was totaled as the notes and weighted averages.

Formulario para Análise de "Modelo de Qualidade SQuaRE para Processo de Software"						
Questões (Níveis de Impactos de Riscos de Projeto)	Atribuição de Notas					Média
	1	2	3	4	5	Ponderada
1-Funcionalidade : Adequabilidade, Acurácia, Interoperabilidade, segurança.	3	1	4	2		2,50
2-Manutenibilidade: Testabilidade, Estabilidade, Modificabilidade, Analisabilidade.	2		5	1	2	2,38
3-Usabilidade: Atratividade, Compreensibilidade, Apreensibilidade, Operabilidade.	4	1	2	3		2,40
4-Confiabilidade: Maturidade, Tolerância a Falhas, Recuperabilidade.	3	1	3	2	1	1,80
5-Eficiência: Comportamento Temporal, Utilização de Recursos.	3	1	3	3		2,60
6-Portabilidade: Adaptabilidade, Instabilidade, Co-existência, Substitubilidade.	3	1	3		3	2,64
			Linha divisória			2,39

Figure 7 - Form filled square analysis and generated average real estate project author.

The result of the collection presented (used in a Real Estate company), have their values computed in relation to the items of the risks Square model, where their weighted averages are described in their respective rows and columns. The result of the weighted average (all attributes) are described in the "dividing line",

representing an overview of project risk with the value of 2.35 (below the average level of the impact of risk was set at a value 2.5 by the experts as the Likert scale).

IV. PRESENTATION AND DISCUSSION

Using the tool of the model proposed in this paper, for the collection, analysis, simulation and generation of results are described and represented in graphical form to assist in monitoring the implementation of the technical proposal and the logic of perceptron network with the square model. Figure 8 shows the proposed training of the perceptron network system.

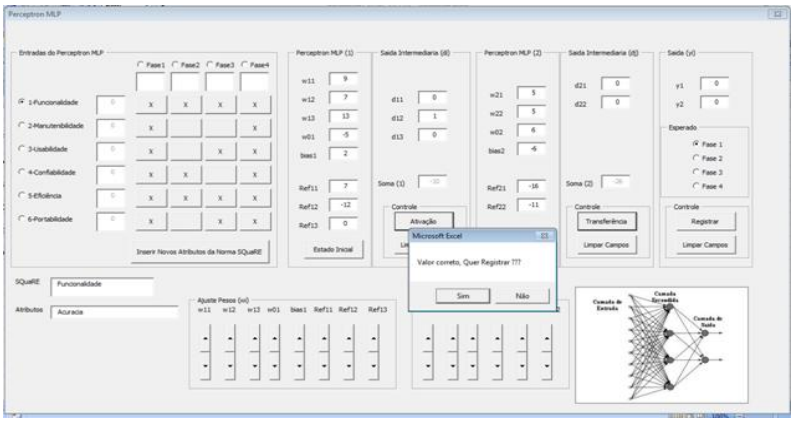

Figure 8 - Interface model proposed Layered Perceptron (system "PerceptronSQuaREBoehm"), author.

This application contains the interface interaction of Square attributes, their respective weights adjustments to the phases of the Boehm model for correcting the impacts of project risks. Through the system interface, insert the values of the adjustment of weights for the desired outputs to the phases provided by IT specialists and application of the learning algorithm. If the outputs are in accordance with pre-established values values are confirmed and thus are recorded in the knowledge base, otherwise the values must be rejected.

w11	w12	w13	w01	bias1	ref11	ref12	ref13	d11	d12	d13	soma1	w21	w22	w02	bias2	soma2	ref21	ref22	d21	d22	y1	y2	Fases	Atributos	SQuaRE
5	4	6	3	3	4	0	0	1	1	1	18	-3	-1	0	0	0	0	0	0	-12	0	0	fase 1	Testabilidade	Manutenibilidade
5	4	6	3	3	4	0	0	1	1	1	18	-3	-8	-3	0	0	0	0	0	-33	0	0	fase 1	Estabilidade	Manutenibilidade
5	4	6	3	3	4	0	0	1	1	1	18	-3	-12	-6	-1	0	0	0	0	-39	0	0	fase 1	Modificabilidade	Manutenibilidade
5	4	6	3	3	4	0	0	1	1	1	18	-3	-14	-8	-4	0	0	0	0	-19	0	0	fase 1	Analisabilidade	Manutenibilidade
5	4	6	3	3	4	0	0	1	1	1	18	7	3	4	1	-1	-1	1	1	34	1	1	fase 4	Testabilidade	Manutenibilidade
5	4	6	3	3	4	0	0	1	1	1	18	4	9	8	1	-3	-1	1	1	47	1	1	fase 4	Estabilidade	Manutenibilidade
5	4	6	3	3	4	0	0	1	1	1	18	6	9	8	9	-3	-5	1	1	117	1	1	fase 4	Modificabilidade	Manutenibilidade
5	4	6	3	3	4	0	0	1	1	1	18	5	7	-1	9	-2	-5	1	1	36	1	1	fase 4	Analisabilidade	Manutenibilidade

Figure 9-Base perceptron learning for maintainability, author.

Figure 9 shows part of the knowledge base already inserted as the adjustment of synaptic weights and the relationship of the square model (with the phase of the project risks Boehm model) for maintainability and its subclasses: stability, stability, modifiability and analyzability. Also be described by setting values of weights, bias, summations and references, with their respective values of intermediate outputs (d11, d12, d21, d22) and network outputs (y1 and y2). A Figure 10 shows the behavior of an analysis on the maintainability regarding the "testability" of phase 1 of the project.

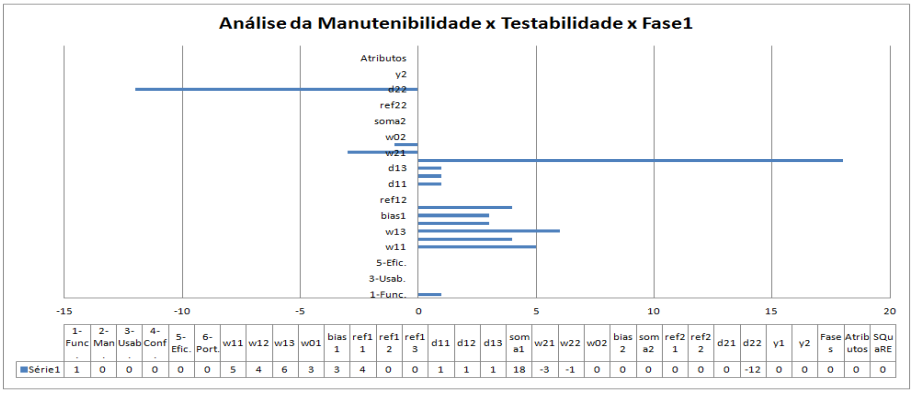

Figure 10 - Graph presented by behavioral testability attribute on an analysis of maintainability, author.

The values of the weights, bias, summations and references are set to the output values of the network are: y1 = 0 and y2 = 0. Variations occur for values of weights w21 = -3, -1 = w22, w02 = 0, = 0 bias2, soma2 = 0, = 0 ref21, ref22 = 0 and intermediate outputs, whose values are: d21 = 0, d22 = -12. Under these conditions, the learning of the network is recorded as the ratio of output set at y1 = 0 and y2 = 0 (relative to phase 1 of the spiral model) for specialists in IT.

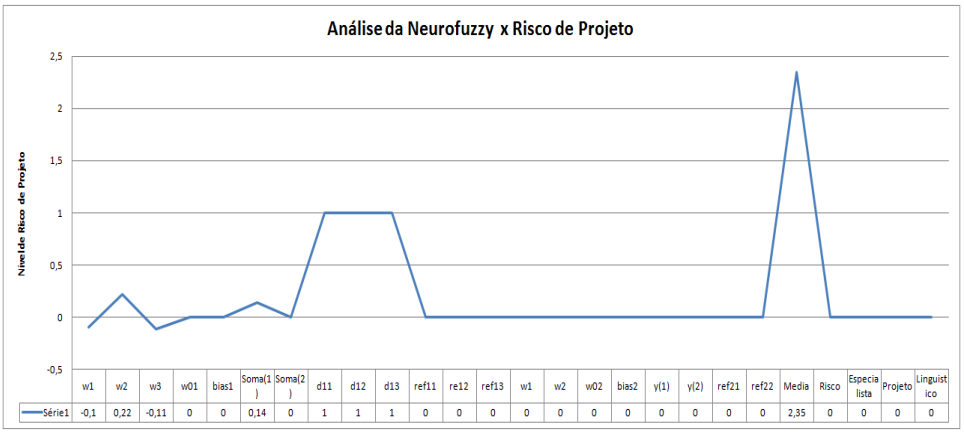

Figure 11 - Curve adjustment of network perceptron learning for system control "stock" view of the manager, author.

Figure 11 shows the levels of the perceptron network (occurred during training) and adjustments of values internal behavior, according to the vision of the project manager for "inventory control". Figure 12 shows the behavior of the perceptron network and the risk class in view of high "risk" and low "risk." = 0 and y2 = 0 (relative to phase 1 of the spiral model) for specialists in IT.

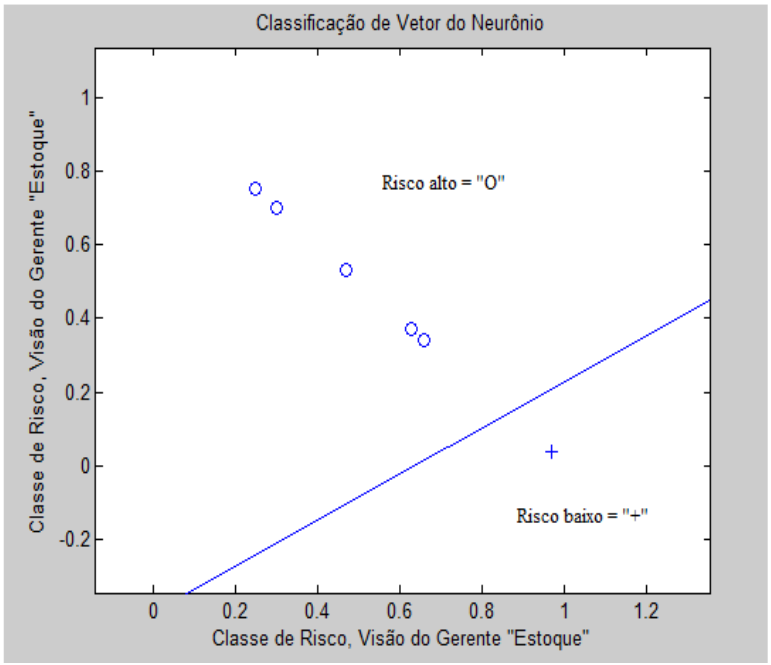

Figure 12 - Risk class risk to "high" and "low" risk to the system control "stock" view of the manager, reviewed by the perceptron, author network.

The levels of "high" risk concentrated between the values [0.3, 0.8], while the level of "low" risk is concentrated among the value "1" in the view of the project manager control "stock". Were developed with Matlab and C programming language, an artificial neuron for analysis of data generated by training the proposed system for comparison of these results, and generated a vision of pattern classification.

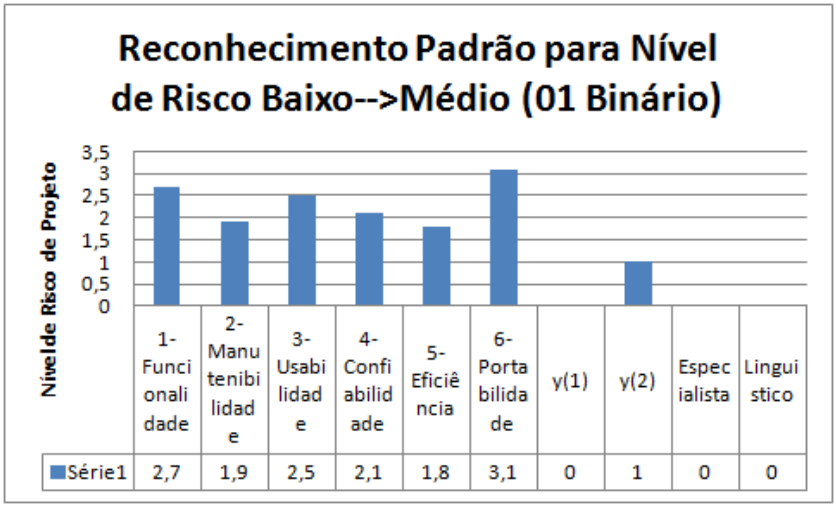

Figure 13 - Square Pattern Recognition of attributes in relation to the output level of project risk, author.

Figure 13 shows the result of pattern recognition of all the attributes of the square model (risk levels of each attribute relative to the average risk of default value "2.5") and binary output levels registered as the values assigned by the experts: very low risk = 00, 01 = low risk, medium risk = 01 and 11 = high risk. Figure 14 shows the interface of the results of the risk analysis of the draft risk assessment ("real" design) software, showing the level of risk above the average standard (value of 2.5) of the square and the main attributes phases of the project (according to the risk model project Boehm), which should be reviewed for adjustments that are close to the acceptable level.

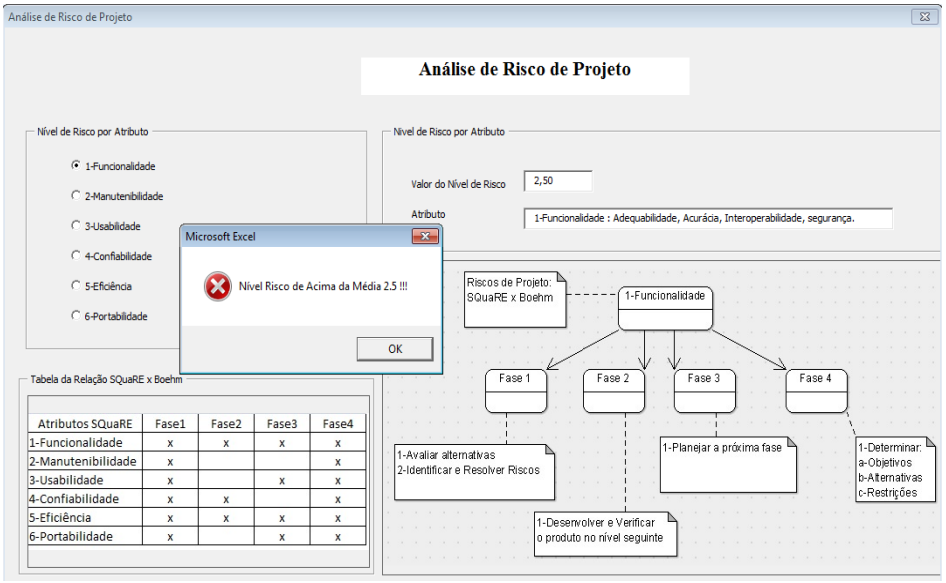

Figure 14 - Application of Risk Analysis, Value Model Square x model Boehm, High Risk Review, author.

The interface (risk analysis project) shows the main stages of project risk (the Boehm model) which are: Phase 1 (evaluate alternatives, identify and resolve risks), stage 2 (develop and check the product at the next level) , 3 phase (planning the next phase) and phase 4 (determine: objectives, alternatives and constraints). It is also shown the message that the level of project risk is above the acceptable limit.

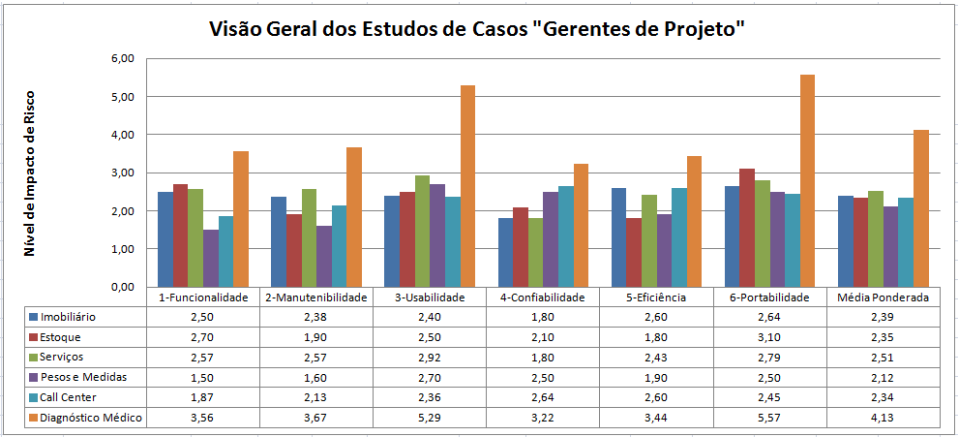

	1-Funcionalidade	2-Manutenibilidade	3-Usabilidade	4-Confiabilidade	5-Eficiência	6-Portabilidade	Média Ponderada
Imobiliário	2,50	2,38	2,40	1,80	2,60	2,64	2,39
Estoque	2,70	1,90	2,50	2,10	1,80	3,10	2,35
Serviços	2,57	2,57	2,92	1,80	2,43	2,79	2,51
Pesos e Medidas	1,50	1,60	2,70	2,50	1,90	2,50	2,12
Call Center	1,87	2,13	2,36	2,64	2,60	2,45	2,34
Diagnóstico Médico	3,56	3,67	5,29	3,22	3,44	5,57	4,13

Figure 15 - Graph of Results of Case Studies Searches "Project Managers", author.

Figure 15 shows the results (square of attributes) analyzed by all project managers for their respective case study (real estate, stock, Services, Weights and Measures, Call Center and Medical Diagnostics), a graphical view with the numerical results and weighted averages.

Atributos SQuaRE x Empresas Pesquisadas x Visão Analistas						
Atributos SQuaRE	Imobiliário	Estoque	Serviços	Pesos e Medidas	Call Center	Diagnóstico Médico
1-Funcionalidade		2,70	2,57	1,90	2,57	3,58
2-Manutenibilidade		2,40	2,14	1,70	2,29	2,86
3-Usabilidade		3,00	2,33	2,00	2,33	2,50
4-Confiabilidade		2,00	2,36	2,20	2,64	2,93
5-Eficiência		2,00	2,57	1,90	2,57	2,86
6-Portabilidade		2,20	3,42	1,50	1,73	2,27
Média Ponderada	0,00	2,38	2,57	1,87	2,36	2,83

Figure 16 - Table of Results of Case Studies Searches "Analysts Project" author.

Figure 16 shows the results (square of attributes) analyzed by all analysts project to their respective case study (real estate, stock, Services, Weights and Measures, Call Center and Medical Diagnostics) with the numerical results and the their weighted averages.

V. CONCLUSION

During the writing of this study, was defined as important: a) the quality of software development services, b) the need for a measure of this quality computerized form to assist specialist and managers during the life cycle of project software. Thus establishing the concept of involvement of people and technology within an environment of quality, production and service quality, to measure the qualitative results, while production, the quantitative values generated for services already running within the time or schedule.

The application of neural network allowed us to establish a new form of project evaluation based on perceptron learning network and classification of quality standards for services (*SQuaRE*) to the levels of risk impacts of software projects. After the phase of the network structure and the perceptron learning network, it was possible to train the network to evaluate and analyze neuron situations unforeseen risks during the course of the project life cycle. In order to answer the main questions raised in the introduction, the following main conclusions are:

a) the results obtained from the development of the proposed system show that the mechanisms adopted improved the way specialists in IT interact to establish a pattern of communication;
b) realize the proposed system, with the techniques of perceptron network and the standard square allow the assessment of quality of services;

c) quality measurement GQM (indicator of software quality) to ISO / IEC 9126and 14598 standard, IEEE 1044.1 1995 classification) risk, the Likert type scale, the weighted sum (serving size) and divide (metric distribution of the classes of records) are the elements responsible for the solutions:

c.1) requisition requests for software services;
c.2) in reviews of processes requisitions.;
c.3) in making decisions changing environment;
c.4) the compliance of proposed services (as to the timing and delivery dates);
c.5) quality of service (satisfaction to meet the need of the client);
c.6) in process management (assist in the management of indecision); c.7) Establishment of standards (standardization in the assessment and measurement of service quality);
c.8) in project risk analysis (identification of the impact of project risk factors), this concept aim minimize and propose the solutions to reduce many risks of projects.

A methodology was defined using: a) the standard measure of service quality (standard square), b) techniques for decision making in indecision (fuzzy logic), c) instrument of qualitative measurement (Likert scale), d) for default project risk analysis Model (Boehm). The results were demonstrated through the proposed and developed with a determination to submit their application results. As limiting the model was applied in the provision of small service businesses. In this sense, it is suggested that the software proposed in this paper, is extended with the application of wider areas and larger companies. It is also suggested integration with neural networks and implementation of a neural network system.

The proposed system, contribute to the minimization of the risks of software development. Assisted in the analysis of the main impact factors of risk based on the standards of quality of service (its realization was founded through the experiences of experts in IT). Also allowed to administer the proposed pursuant to the requirements raised during the early stages of projects that met the expectations of IT experts timeline. Critical factors were identified and, in addition, set a standard of communication between the teams participating in the development of projects. Aligned with the strategic objectives of the development and production of services, and agrees with the proposal of this paper.

REFERÊNCIAS

[1] AGUIAR e OLIVEIRA Jr. **Inteligência Computacional aplicada à administração, economia e engenharia em Matlab**. São Paulo: Thomson Learning, 2007.

[2] AGUIRRE GONZALÉZ, Mario Orestes e CARLOS de TOLEDO, Jose; **A Integração do Cliente no Processo de Desenvolvimento de Produto: Revisão Bibliográfica Sistemática e Temas para Pesquisa**, Produção, Natal – RN, Brasil, 2012.

[3] ALEXANDRE, J. W. C. **Uma investigação das práticas da gestão da qualidade total no setor manufatureiro do estado do Ceará**. 1999. Tese (Doutorado) – Departamento de Engenharia de Produção, Escola Politécnica, USP, São Paulo.

[4] BADRI, M. A.; DONALD, D.; DONNA, D. **A study of measuring the critical factors of quality management**. *International Journal of Quality & Reliability Management*, v. 12, n. 2, p. 36-53, 1995.

[5] BASILI, VR, WEISS, D. **A Methodology for Collection Valid *Software* Engineering Data. IEEE Trans. *SoftwareEng*** 10: 728-738, 1984.

[6] BOEHM, Barry W.A **Spiral Model of *Software* Development and Enhancement, IEEE**, May, 1988.

[7] BROOKSHEAR J. G; **Ciência da Computação uma Visão Abrangente**, Porto Alegre, Editora Bookman, 2005.

[8] CARVALHO , M. M.; e PALADINI, E. P. **Gestão da Qualidade Teoria e Casos**. Rio de Janeiro: Eliesevier Editora Ltda, 2006.

[9] COSTA, A. F B.; EPPRECHIT E. K. e CARPINETTI, L. C. R; **Controle Estatístico de Qualidade**; São Paulo,Editora Atlas S.A, 2008.

[10] COSTA, D. C de S.; **Tomada de Decisão Baseada em Lógica *Fuzzy* e na Distribuição Espacial da Mortalidade por Acidentes de Trânsito na Cidade de João Pessoa** – PB, João Pessoa-PB, 2011.

[11] CURY, M. V. Q. **Método para avaliar a percepção do usuário sobre a qualidade de sistemas de transporte urbano sobre trilhos com utilização da tecnologia *neuro - fuzzy***; Rio de Janeiro – RJ, 2007.

[12] FERNANDES, Ana Maria da Rocha. **Inteligência artificial: noções gerais**. Santa Catarina, Visual Books, 2003.

[13] FONSECA, F. E. A. da e ROZENFELD, H., **Medição de Desempenho para a Gestão do Ciclo de Vida de Produtos**: Uma Revisão Sistemática da Literatura, Revista Científica Eletrônica da Engenharia de Produção, Produção Online, Universidade de São Paulo, São Carlos, SP, 2012.

[14] GARCIA, Oscar Gomes *SQuaRE*: **Uma Unificação de Normas para a Especificação de Requisitos e a Avaliação da Qualidade**, Universidade de Castilha da mancha, Madri – Espanha, 2009.

[15] ISO/IEC 14598-1:1999, **Information technology - *Software* product evaluation** - part 1: General overview. Technical report, International Organization for Standardization, Geneva, Switzerland, 1999.
[16] ISO/IEC 25000:2005 http://iso.org./iso/catalogue detail?csnumber=35683 acessado em 10/09/2012.
[17] ISO/IEC 9126-1:2001, ***Software* engineering - Product quality** - Part 1: Quality model. Technical report, International Organization for Standardization, Geneva, Switzerland, 2001.
[18] KOSCIANSKI, A. e SOARES M. dos SANTOS **Qualidade de *software*: Aprenda as metodologias e técnicas mais modernas para o desenvolvimento de *software***, São Paulo, editora NovatecLtda, 2006.
[19] LAS CASAS, ALEXANDRE L. **Qualidade Total em Serviços**, São Paulo, Editora Atlas, 2007.
[20] LIKERT, Rensis; LIKERT, Jane Gibson. **Administração de conflitos: novas abordagens**. São Paulo: Mcgraw-Hill, 1979.
[21] LUDWING Jr., O. e MONTGOMERY E., **Redes Neurais Fundamentos e Aplicações com Programas em C**, Rio de Janeiro – RJ, Editora Ciência Moderna Ltda, 2007.
[22] MORAES, O. B. **Método de Análise de Dados para Avaliação de Áreas Urbanas Recuperadas – Uma Abordagem – Utilizando a Lógica *Fuzzy***, São Paulo – SP, 2008.
[23] MORAES, O. B. **Método de Análise de Dados para Avaliação de Áreas Urbanas Recuperadas – Uma Abordagem – Utilizando a Lógica *Fuzzy***, São Paulo – SP, 2008.
[24] NASCIMENTO Jr., C. L., YONEYAMA, T. (2000). **Inteligência Artificial em Controle e Automação**, São Paulo – SP, Editora Edgard Blücher, 2004.
[25] OLIVEIRA JUNIOR, W. **Estudo comparativo entre modelos lineares e redes neurais artificiais como tecnologias geradoras de previsões de valores financeiros**. 2007. Dissertação (Mestrado em Gestão do Conhecimento e Tecnologia da Informação) – UCB, Brasília.
[26] OLIVEIRA JUNIOR, W. **Estudo comparativo entre modelos lineares e redes neurais artificiais como tecnologias geradoras de previsões de valores financeiros**. 2007. Dissertação (Mestrado em Gestão do Conhecimento e Tecnologia da Informação) – UCB, Brasília.
[27] OLIVEIRA, Francisco Correia de; SANTOS, Carlos Augusto Parente Neiva. ***Terceirização no processo de desenvolvimento de sistemas de informações***. In: XXIV ENCONTRO NACIONAL DA ASSOCIAÇÃO NACIONAL DOS PROGRAMAS DE PÓS-GRADUAÇÃO EM ADMINISTRAÇÃO, 2000, Florianópolis. Anais. Rio de Janeiro: ANPAD, 2000. 1 CD-ROM.
[28] PALADINI E. P; **Gestão Estratégica da Qualidade Princípios, Métodos e Processos**; Editora Atlas S.A; São Paulo – SP, 2008.
[29] SANTOS, Joel J. **Análise de custos: Remodelando com ênfase para custo marginal, relatórios e estudos de casos**. 3. ed. São Paulo: Atlas, 2000.
[30] SARAPH, J. V.; BENSON, P. G.; SCHROEDER, R. G. **An instrument for measuring the critical factors of quality management.** *Decision Sciences*, v. 20, n. 4, p. 810-829, 1989.
[31] SCHILDT, H., **Inteligência Artificial Utilizando Linguagem C** – Tradução de Cláudio Gaiger Silveira, São Paulo – SP, Editora McGraw – Hill, São Paulo – SP, 1989.
[32] SCOARIS, Raquel Carmen de Oliveira; PEREIRA BENEVIDES, Ana Maria Teresa e SANTIN, Filho Ourides, **Elaboração e validação de um instrumento de avaliação de atitudes frente ao uso de história da ciência no ensino de ciências**, Revista Electrónica de Enseñanza de las Ciencias, Vol.8 Nº3 , 2009.
[33] SHAW I. S. e SIMÕES, M. G. **Controle e Modelagem *Fuzzy***, São Paulo – SP, Blücher Ltda, 2004.
[34] SILVA, Ivan Nunes; SPATTI, Danilo Hernane; FLAUZINO, Rogério Andrade, **Redes Neurais Artificiais para Engenharia e Ciências Aplicadas – Curso Prático**, São Paulo – SP, Editora ARTLIBER EDITORA LTDA, 2010.
[35] SORDI, J. O. **Gestão por Processos uma abordagem da moderna administração**, São Paulo – SP, Editora Saraiva, 2005.
[36] SPHAIER, A. A. **Adaptação de um Modelo para Avaliação da Qualidade de Serviços Prestados por uma Empresa de Tecnologia da Informação**, Rio de Janeiro – RJ, 2009.
[37] TAMIMI, N.; GERSHON, M. **A tool foi assessing industry TQM practice versus the Deming philosophy. *Production and Inventory* *Management Journal***, first quarter, v. 36, n. 1, p. 27-32, 1995.
[38] TAN, Pang-Ning; STEINBACH, Michael e KUMAR, Vipin, **Introdução ao DATA MINING**, Rio de Janeiro – RJ, Editora Ciência Moderna, 2006.
[39] WEBER, L.; KLEIN, P.A.T., **Aplicação da lógica *fuzzy* em *software* e hardware**. 1.ed, Canoas: Ulbra, 2003.

American Journal of Engineering Research (AJER)
e-ISSN : 2320-0847 p-ISSN : 2320-0936
Volume-03, Issue-03, pp-264-266
www.ajer.org

Research Paper Open Access

Synthesis And Characterization of Biodiesel From Nigerian Palm Kernel oil.

IGBOKWE, J. O. and Nwafor, M. O. I.
[1]*Department of Mechanical Engineering, Federal University of Technology, Owerri,Imo State, Nigeria.*
[2] *Department of Mechanical Engineering, Federal University of Technology, Owerri,Imo State, Nigeria.*

Abstract: **-** Biodiesel was produced from Nigerian Palm kernel oil through direct base- catalyzed transesterification process using methanol and sodium hydroxide as alcohol and catalyst respectively. The trans-esterification process involved 1 liter of Palm kernel oil, 200ml of methanol, 1.0% NaOH, reaction temperature of 65 degree Celsius and reaction time of 90mins and an average biodiesel yield of 87.67% was obtained. The produced biodiesel was blended with diesel fuel at a ratio of 20% biodiesel to 80% diesel fuel (by volume). The neat biodiesel and its blend were characterized using the ASTM methods. The results showed that the properties of the neat palm kernel oil biodiesel and its blend fall within the American Society for Testing and Materials (ASTM) specifications for Biodiesel fuels hence confirming their suitability as alternative fuels for modern diesel engines.

Keywords: - *Biodiesel, Characterization, Fuel Blend, Diesel fuel, Trans-esterification,*

I. INTRODUCTION

The use of fuels from bio-resources has been widely acknowledged as panacea to the global twin-problem of fuel crisis and environmental pollution informed by over dependence on fossil fuels (Barman, et al. 2010). Fossil fuels like petroleum, coal and natural gas have limited life and the fast depletion of their reserves has raised the fear of their exhaustion and possible fuel crisis in the near future. Besides, the combustion of these fossil fuels has been identified as the major source of emissions that cause air pollution and global warming. These challenges have engineered a global search for alternative fuels that are both renewable and environmentally friendly. For diesel engines, raw vegetable oils were used as alternative fuels in place of the diesel fuel. This however was found to cause some engine problems like injector cooking, high engine deposits and piston ring sticking due to high viscosity and low volatility of these oils. (Konis,et al, 1982). These problems were reduced or eliminated by chemical modification of the oils through the process of transesterification (Perkins,et al,1991). Transesterification involves the reaction of vegetable oils or fats with an alcohol in the presence of a catalyst to produce biodiesel and glycerol. The triglyceride is converted stepwise to diglyceride, monoglyceride and finally glycerol. (Ulf Schuchardt, et. al 1998). Currently, there is a growing interest in the production of biodiesel from various crop oils and others bio-sources because of its attractive features. Biodiesel fuels are non-toxic, biodegradable, sulphur and aromatics free. They have high cetane numbers and 11% oxygen content which enhance combustion. They have similar engine performances and lower engine emissions compared with diesel fuel (Rodjanakid ,et,al, 2004; Canakci, et al, 2003, Sugozus, et al.,2010; Nagarhalli,et al 2010).

The properties of the PKO biodiesel and its blend were determined using the ASTM characterization methods in order to determine their compliance with international standards and hence the suitability of the fuels for modern diesel engines.

II. MATERIALS AND METHODS

The palm kernel oil used was purchased from local market in Owerri in Nigeria while the methanol and sodium hydroxide pallets were bought from a standard chemical shop in owerri. The transesterification was done with a batch reactor equipped with a stirrer, thermometer and a heater. One liter high density plastic vessel

was used for catalyst/methanol mixing. The characterization was carried out at the laboratory of the Petroleum Training Institute Warri, Nigeria.

2.1 EXPERIMENTAL METHODS

200mlof methanol was measured and poured into a high density plastic vessel and 8.12g of NaOH was added to the methanol. The mixture was shaken vigorously till the sodium hydroxide was completely dissolved in the methanol resulting to a strong base known as sodium methoxide. 1000ml of palm kernel oil was poured into the reactor and was preheated to 65 degrees Celsius. The sodium methoxide was added to the oil. The reactor lid was closed and the mixture was stirred for 90minutes and later allowed to settle overnight. The fluid separated into two layers with the biodiesel floating on top. The biodiesel was decanted carefully and washed with warm water in order to remove the impurities. The experiment was repeated for three and an average yield 87.67% was obtained. A portion of the biodiesel was blended with diesel fuel at a volume ratio 20% biodiesel and 80% petrodiesel (B20). Both the pure biodiesel and its blend were characterized using the ASTM methods.

III. RESULTS AND DISSCUSSION

The transesterification process gave an average yield of 87.67% with catalyst concentration of 1%, reaction temperature of 65 degrees Celsius and reaction time of 90 minutes. This level of yield is considered reasonably high when compared with other similar works. The results of the characterization of pure biodiesel produced (B100) and its blend with petrodiesel (B20) are shown on Table 1. It is interesting to observe from the results that all the determined properties of biodiesel produced from Nigerian palm kernel oil and its blend fall within the ASTMD 6751 specifications for biodiesel fuels. It can also be observed that the cetane numbers and the flash points of B100 and B20 are higher than that of diesel fuel. This is in agreement with that of biodiesel fuels produced from other vegetable oils. High cetane number shortens the engine delay period and promotes smooth combustion while high flash point reduces fire risk.

TABLE 1: Physical Properties of The Produced PKO Biodiesel, Blend and Diesel Fuel

PROPERTY	TEST METHOD	ASTM SPECIFICATION FOR BIODIESEL	B100 PURE BIODIESEL	B20 BLEND	D2 DIESEL FUEL
Density@$_{15}{}^{o}$c kg/m ^{3}	D1298	0.8833	0.865	0.846	0.8368
Cloud point ^{0}c	D2500	-3 to 12	7.5	3.0	-15 to 5
Pour point^{0}c	D97	-15 to 10	0.0	-12	-35 to i5
Kinematic viscosity@40^{0}c	D445	1.9 to 6.0	2.99	2.04	1.3 to 4.1
Flash point^{0}c	D93	100 to 170	150	123	60 to 80
Iodine No.	DIN 53241-2	7.5 to 8.6	15.35	17.2	11.7 to16.3
Cetane No.	D613	48 to 65	54.57	51.2	40 to 53
Ash content	D482	0.02	0.02	0.02	<0.01
H.Value(MJ/Kg)	D3338	37-40.8	38.6	42.47	43.4 to 44.9.

IV. CONCLUSION

From the results of this work it can be concluded that:

An average biodiesel yield of 87.67% or more can be achieved by direct- base catalyzed transesterification of palm kernel oil produced in Nigeria.

The physical properties of Nigerian Palm kernel oil biodiesel and its blend with diesel fuel (B20) conform to the ASTMD6751 Specifications for biodiesel fuels. This makes it a potential feedstock for biodiesel production.

Biodiesel from Nigerian palm kernel oil is a suitable alternative fuel for modern diesel engines.

Fuel blend (B20) has properties that are closer to those of diesel fuel than the pure biodiesel thus suggesting a better engine performance potential.

REFERENCES

[1] Barman, S. C., Kumar, R., Singh, G. C., Kisku, A. H., Khan, M. M., Kidwai, R. C., Murthy, M. P. S., Negi, P., Randay, A. K., Verma, G. Y. and Bhargava, S. S. (2010) Assessment of Urban air pollution and its possible Health impact. Journal of Environmental Biology. 31,913-920

[2] Konis, R. A., Mousetis, T.I. and Lioyd, I. (1982) Polymerization of vegetable oils. in Vegetable Oils fuels. Proceedings of the International on Plant s and Vegetable oils as fuels. American Society of Agricltural Enginers. Furga, ND, USA. 218-223

[3] Perkins, I. A. and Peterson, C. I. (1991). Durability Testing of Transesterified Water rape oil as Fuels in Small bore multi-cylinder DI compression-ignition engine. SAE Paper 911764.

[4] Ulf Schuchardt, R. S. and Rogerio, M. V. (1998). Transesterification of Vegetable Oil: A Review. Journal of Brazilian Chemical Society. Vol. 9. No.1. 199-210.

[5] Rodjanakid, K.and Chinda, C. (2004) Performance of Engine using Biodiesel from Refined Palm oil stearin and Biiodiesel from crude coconut oil. The Joint International Conference on Sustainable Energy and Envirinment. Hua, Hin. Thailand.

[6] Canakci, M. and Van Gerpen J. (2003) Comparision of Engine Performance and Emissions for Petroleum diesel fuel, yellow grease biodiesel and soybean oil biodiesel. American Society of Aricultral Engieers. 46(4) 937- 944.

[7] Sugozus, I., Oner, C., Altun, S. (2010) The Performance and Emission Characteristics of a Diesel Engine Fueled with Biodiese and Diesel Fuels . International Journal of Engineering Research and Development. Vol.2, No 1.

[8] Nagarhalli, M. V., Nandedkar, V, M. and Molute, K. C. (2010) Emission and Performance Characteristics of Karanja Biodiesel and its blends in a CI Engine and its Economics. ARPN Journal of Engineering and Applied Sciences Vol. 5. No. 2.

American Journal of Engineering Research (AJER)
e-ISSN : 2320-0847 p-ISSN : 2320-0936
Volume-03, Issue-03, pp-267-273
www.ajer.org

Research Paper Open Access

Effect of Microwave on Fluidized Bed Drying of Beetroot *(Beta vulgaris L.)*

Yashwant Kumar[1], Mohammad Ali Khan[1] and Krishna Kumar Patel*[1]
[1]*Department of Post Harvest Engineering and Technology, Aligarh Muslim University, Aligarh-202002 (India)*

Abstract: - In the present work, an attempt has been made to study the effect of inlet air temperature and velocity on the drying characteristics of beetroot's (*Beta vulgaris L.)* pieces in microwave assisted fluidized bed drying (MAFBD) system. The results were compared with samples of beetroot dried in a fluidized bed dryer (FBD) at the same combination of temperatures and air velocities. The selected inlet air temperatures and inlet air velocities were 60°C, 67.50°C and 75°C and 9 m/s, 10.50 m/s and 12 m/s, respectively. Moisture content and outlet air humidity was measured at 5 minutes interval. The MAFBD method offered two to three times reduction in drying time as compared to the FBD method. It was also observed that the beetroot samples obtained from the MAFBD system had lower final moisture content than those obtained from the FBD system.

Keywords: - *Microwave assisted fluidized bed drying, Fluidized bed drying, Beetroots, etc.*

I INTRODUCTION

The excellent way to preserve foods is drying that is an oldest method of preserving high moisture foods [1]. With the several advantages, drying can add variety to meals and provide delicious and nutritious foods. Among them, dried foods take much less storage space than canned or frozen foods. Drying, however, is a difficult and complicated food processing operation because it brings about undesirable changes in quality. The extent of changes in quality depends on the care taken in preparing the material before drying and on the drying process used. Dried foods keep well because the moisture content is so low that spoilage organisms cannot grow. It also creates a hard outer-layer, help to stop micro-organisms from entering the food.

Moreover to above, the study by [3] on the dehydration of aonla fruits using FBD at 80°C with 115 m/min air velocity, 120 minutes (min) revealed that the retention of ascorbic acid is greater than sun and hot air tray dried samples. Thus, using FBD, the drying time can be considerably reduced and uniform drying of the whole material can be achieved [4, 5, 6]. With due to the several advantages, the fluidized bed drying process is now widely used for various applications in several agricultural sectors. For instance, in food processing, to dry many agricultural products of different particle sizes (ranging from 10 mm to 20 mm) such as wheat and corn grains; and green peas [7]; in the dairy and pharmaceutical industries, for drying, granulation, and coating operations [8].

In, fluidized bed drying process, the drying completed mostly in falling rate period that can be subdivided into unsaturated surface drying region and internal movement of moisture-control region [9, 10]. On the other hand, in microwave drying, the drying facilitates heat transmission and mass transfer in the same direction, from the inside to outwards, because heat generation occurs not only at the surfaces but at inner sections of foods [11]. Microwave heating is rapid and more energy efficient compared to hot air drying. The amount of heat generated depends on the strength of the microwave field and the dielectric properties of the material being heated [12]. Microwave drying also presents several advantages such as speeded heating (time saving), uniform volumetric heating, self regulating and automatic system, higher efficiency, lower cost of processing (low energy consumption) and compatibility with conventional heating over conventional thermal heating/drying methods [13].

Reference [14] dried macaroni beads from about 20% to 12% moisture content using microwave assisted fluidized bed (a fluidized bed of 7.6 cm dia and a domestic microwave oven with a power of 609 W) drier. To study MAFBD, they placed fluidized bed dryer in the household microwave oven and reported that at the first stage of the MAFBD, liquid water transports from the interior to the exterior of the particle by Darcy's

flow and as the temperature inside the material approaches to the boiling point of water, pressure development occurs pushing the moisture toward the surface. As the drying time proceeds, the liquid water supply cannot maintain the evaporation rate at the surface, and the moisture content near the surface decreases below critical moisture content. Darcy's flow disappears so that liquid water has to be evaporated and then transported to the particle surface by vapor diffusion [15]. Combination of the these two methods can give rise to several desired results. Thus, the uniformity of the temperature among the particles can be provided by well mixing due to fluidization [16] and the drying times can be reduced by the utilization of microwave energy [17, 18].

In the present study, focus is on the drying of beetroot using FBD and MAFBD. Beetroot (*Beta vulgaris L.*) commonly known as *chukander*, is mainly cultivated in India for its juice and vegetable value. It is a member of the flowering plant family Chenopodiaceae. The green leafy part of the beetroots is also of nutritional value, containing beta-carotene and other carotenoids. The nutritional benefits of beetroot are very well known. They are loaded with vitamins A, B_1, B_2, B_6 and C. The greens have a higher content of iron compared to spinach. They are also an excellent source of calcium, magnesium, copper, phosphorus, sodium and iron. Beetroot coupled with carrot juice, the excellent cleansing virtues are exceptional for curing ailments [19]. It contains high amounts of boron, which is directly related to the production of human sex hormones [20]. These findings suggest that beetroot ingestion can be a useful means to prevent development and progression of cancer. Extracts of beetroot also showed some antimicrobial activity on *Staphylococcus aureus* and on *Escherichia coli* and also antiviral effect was observed [21]. This nutrient is valuable for the health of the cardiovascular system [22]. The interest of the food industry in betalains has grown since they were identified as natural antioxidants [23] which may have positive health effects on humans [24]. Given the importance of beetroot, its drying by the two methods was undertaken.

The main purpose of this research was to fabricate a microwave assisted fluidized bed drier, to study the drying characteristics of beetroot at various combinations of air temperature and velocity using FBD and MAFBD.

II MATERIALS & METHODS

Material collection

Fresh and good quality beetroots of unknown variety were purchased from local market in Aligarh. By visual inspection damaged, immature and dried fruits were sorted out, manually. Beetroot of uniform size, free from pest and disease were selected for current research. After cleaning, washing, peeling and slicing, a laboratory fluidized bed dryer and self fabricated microwave assisted fluidized bed dryer (Fig. 1) were used for drying of the beetroot samples.

Microwave assisted fluidized bed drying

The fundamental fabrication criteria of microwave assisted fluidized bed drying is based on the study of [14]. The setup (Fig.1) was provisioned for air heating and air velocity control system. A domestic kitchen microwave oven (LG convection MWO type: Model: MC 9287 BQ, Korea) with a frequency of 2450 MHz was used. A drying chamber of circular cross section fabricated from perspex pipe fitted with a perforated perspex plate having an open area of about 50% of the base plate at the bottom was placed in a domestic kitchen microwave oven (LG convection MWO type: Model: MC 9287 BQ, Korea) with a frequency of 2450 MHz. This was used to accommodate the food material to be dried. The air velocity and the temperature distributions across the container were found to be uniform. Details of the experiments are given in Table 2. The drying was continued until the equilibrium moisture content was reached. The schematic of the experimental setup is depicted in Figure 1. The measurements were made for (1) initial moisture content of the sample (2) variation in moisture content of the product with drying time and (3) total drying time for reducing moisture level up to equilibrium moisture content. The initial and final moisture contents of the sample were determined according to the standard oven drying method [25]. The drying calculations were done by the formula as given below:

$$\text{Moisture Ratio} = \frac{Mt - Me}{Mo - Me} \times 100 \quad \text{..... (1)}$$

Where,

Mt = Moisture content at any time t
Mo = Initial moisture content
Me = Equilibrium moisture content

$$\text{Drying rate} = \frac{\text{Wt. of water removed}}{\text{Wt. of dry matter} \times \text{Time interval (min)}} \times 100 \quad \text{..... (2)}$$

$$\text{Moisture content (\%, db)} = \frac{\text{Wt. of moisture}}{\text{Wt. of dry matter}} \text{ x } 100 \quad \text{..... (3)}$$

$$\text{Moisture content (\%, Wb)} = \frac{\text{Wt. of moisture}}{\text{Wt. of sample (dry matter + water)}} \text{ x } 100 \quad \text{.....(4)}$$

III RESULTS & DISCUSSION

Fig. 2 to 4 represent the effect of air velocities (9, 10.50 and 12 m/s) on relationship between moisture content and drying times at different air temperatures viz. 60°C, 67.50°C and 75°C for both FBD and MAFBD. The moisture content decreased very rapidly during the initial stage of drying, as there was fast removal of moisture from the surface of the product in both cases. Initial moisture content of beetroot for all samples was found between 483.772 and 654.717 (%, db). As drying progressed, the available moisture content on the surface of the beetroot decreases. Consequently, the drying rate of beetroot also decreases with respect to time in both drying methods. The trends of drying rates can be explained with respect to constant rate period and falling rate period [10]. Most food materials have short constant rate periods and they dry mostly in the falling rate period [5, 26, and 27].

Fluidized bed drying

At 60°C air temperature (Fig. 2) in FBD, the moisture content of beetroot decreases from 5.663 to 5.332 then 4.151 (%, db) while the drying time first increases then became constant from t_1 (75 min) to t_2 (80 min) and t_3 (80 min) as the air velocity increases from 9 to 10.50 then 12 m/s, respectively. However, when the temperature of air increase to 67.50°C (Fig. 3) both the moisture content and drying time decreases as per the air velocity increases. The moisture content of beetroot was recorded as 5.485, 5.133 and 3.75 (%, db) with respect to air velocity 9, 10.50 and 12 m/s at the end of 65 min, 60min and 60 min, respectively.

Similarly, at 75°C air temperature, the moisture content of beetroot was reduced to 5.417 (%, db), 4.618 (%, db) and 3.517 (%, db) as velocity increased from 9 to 10.50 then 12 m/s at the end of 75 min, 75 min and 70 min drying time, respectively.

Microwave assisted fluidized bed drying (MAFBD)

In MAFBD at 60°C air temperature and 9 m/s air velocity, the moisture content of beetroots was reduced to 5.244 (%, db) at the end of 30 min drying, but when air velocities increased to 10.50 m/s and 12 m/s, the values of moisture content were recorded as 4.478 (%, db) and 3.618 (%, db) at the end of 30 min for both cases. However, at 67.50°C drying air temperature and 9 m/s air velocity, the moisture content of beetroot was reduced to (4.851%, db) at the end of 30 min drying but at this temperature when air velocity increased to10.50 m/s and 12 m/s, the values of moisture content were 4.21 (%, db) and 3.425 (%, db) at the end of 25 min in both cases.

Furthermore, at 75°C for air velocity 9 m/s, the moisture content of beetroots was reduced 4.651 (%, db) at the end of 30 min drying while at same temperature when air velocity increased to 10.50 m/s then 12 m/s, the values of moisture content were noticed 3.933 (%, db) and 3.313 (%, db), respectively at the end of 25 min in both cases.

Thus, for all air temperatures, the minimum moisture content was recorded at 12 m/s air velocity as compared to the other air velocities.

Comparison between FBD and MAFBD

In FBD, during the initial stage of drying (up to 40-50 min), the moisture content of sample decreased rapidly with increase in drying time. Similarly, in MAFBD, during the initial stage of drying (up to 20-25 min) the moisture content of sample decreased rapidly with increase in drying time. Thereafter, the moisture content of samples decreased slowly with increase in drying time and attained final equilibrium moisture content. This may be due to the partial vapor- pressure of water present in sample; initially being more in comparison to that of the external environment (surroundings of the sample). At the initial stage of drying, moisture starts migrating rapidly from the sample to the external environment because of higher partial vapor pressure difference between sample and environment. As a result, the partial vapor pressure difference between the product and environment decreases rapidly, which leads to slower removal of moisture from the product and becomes constant at the end of drying. The equilibrium moisture content values were higher for sample dried at 60°C as compared to those dried at 67.50°C and 75°C.

IV CONCLUSION

Microwave assisted fluidized bed drying can greatly reduce the drying time of food materials with internal resistance to mass transfer. In the present preliminary study, beetroot (*Beta vulgaris L.*) has been dried by two different methods, viz., microwave assisted fluidized bed drying and fluidized bed drying. In both methods, moisture is lost in good extent. But the microwave assisted fluidized bed drying proved better than the FBD method in terms of reduced drying time and lower final moisture content, as per the results obtained. The future research on food drying will inevitably focus on lower energy costs, less reliance on fossil fuels, and reduced greenhouse gas emissions. In the attainment of these objectives MAFBD is expected to play a meaningful role as an attractive option for drying fruits and vegetables.

REFERENCES

[1] Chauhan A.K.S. and Srivastava A.K. (2009). Optimizing Drying Conditions for Vacuum-Assisted Microw.ave Drying of Green Peas (*Pisum sativum L.*), Drying Technology, 27(6):761-769.

[2] Sablani S.S. (2006). Drying of fruits and vegetables: Retention of nutritional/functional quality. Drying Technology, 24 (2): 123–135.

[3] Murthy Z.V.P. and Joshi D. (2007). Fluidized Bed Drying of Aonla (*Emblica officinalis*). Drying Technology, 25 (5): 883 – 889.

[4] Tirawanichakul S., Prachayawarakorn S., Varanyanond W., Tungtrakul P. and Soponronnarit S. (2004). Effect of fluidized bed drying temperature on various quality attributes of paddy. Drying Technology, 22: 1731-1754.

[5] Bauman I., Bobic Z., Dakovic Z. and Ukrainczyk M., 2005. Time and speed of fruit drying on batch fluid-beds. Sadhana, 30: 687–698.

[6] Kwauk M., Li, J. and Liu D. (2000). Particulate and aggregative fluidization-50 years in retrospect. Powder Technology, 111: 3–18.

[7] Law C.L. and Majumdar A.S. (2006). Fluidized bed dryers. In Handbook of Industrial Drying; Mujumdar, A.S., Ed.; CRC Press: Boca Raton, FL: 173–201.

[8] Sokhansanj, S. and Jayas, D.S. (2006). Drying of foodstuff. In Handbook of Industrial Drying; Mujumdar, A.S., Ed.; CRC Press: Boca Raton, FL, pp. 521–546.

[9] Kundu K.M., Datta A.B. and Chatterjee P.K. (2001). Drying of oilseeds. Drying Technology, 19: 343–358.

[10] Tanfara H., Pugsley T. and Winters C. (2002). Effect of particle size distribution on local voidage in a bench-scale conical fluidized bed dryer. Drying Technology 20: 1273–1289.

[11] Bonafonte A.B., Iglesias, O. and Bueno J.L. (2007) Effects of operating conditions on the combined convective-microwave drying of agar gels. Drying Technology, 25 (11): 1867–1873.

[12] Gracia A., Iglesias, O. and Roques M. (1992). Microwave drying of agar gels. In: Drying 92; Mujumdar, A.S., Ed.; Elsevier: New York: 595–606.

[13] Sanga E., Mujamdar A.S. and Raghavan G.S.V. (2000). "Principals and application of Microwave Drying". In: Drying technology in agriculture and food sciences. Edited by A. S. Mujumdar. Enfiled N. H.: Science publishers. Inc.

[14] Goksu E.I., Sumnu G. and Esin A. (2005). Effect of microwave on fluidized bed drying of macaroni beads. Journal of Food Engineering 66(4):463-468.

[15] Chen G., Wang, W. and Mujumdar. A.S. (2001). Theoretical study of microwave heating patterns on batch fluidized bed drying of porous material. Chemical Engineering Science, 56: 6823-6835.

[16] Feng H. and Tang J. (1998). Microwave finish drying of diced apple slices in a spouted bed. Journal of Food Science, 63(4): 679-683.

[17] Jumah R.Y. and Raghavan G.S.V. (2001). Analysis of heat and mass transfer during combined microwave-convective spouted-bed drying. Drying Technology, 19(3&4): 485-506.

[18] Wang W., Bhraskar N.T., Chen G. and Mujumdar A.S. (2002). Simulation of fluidized-bed drying of carrot with microwave heating. Drying Technology 20(9): 1855-1867.

[19] Grubben G.J.H. and Denton O.A. (2004). Plant Resources of Tropical Africa 2. Vegetables. PROTA Foundation, Wageningen; Backhuys, Leiden; CTA, Wageningen.

[20] Socaciu C. (2008). Food colorants: chemical and functional properties. Washington, DC: Taylor & Francis: 169.

[21] Rauha J.P., Remes S., Heinonen M., Hopia A. and Kahkonen M., et al. (2000). Antimicrobial effects of Finnish plant extracts containing flavonoids and other phenolic compounds. Intl. J. Food Microbiol. 25: 3-12.

[22] Anonymous (2002). Betaine. University of Maryland Medical Center (UMMC). Retrieved September 6: 2007.

[23] Escribano J., Pedreno M. A., García-Carmona, F. and Muñoz R. (1998). Characterization of the antiradical activity of betalains from Beta vulgaris L. roots. Phytochem. Anal, 9: 124–7.
[24] Tesoriere L., Mario A., Daniela B., Maria A. and Livrea (2004). Absorption, excretion, and distribution of dietary antioxidant betalains in LDLs: potential health effects of betalains in humans. American Journal of Clinical Nutrition, 80(4): 941–5.
[25] Ranganna S. (1994). hand book of analysis and quality control for fruits and vegetables products, 2nd edn. Tata McGraw Hill Pub. Co. New Delhi.
[26] Stanislawski, J. (2005). Drying of diced carrot in a combined microwave fluidized bed dryer. Drying Technology, 23: 1711–1721.
[27] Saravacos, D.G. and Maroulis, B. (2001). Transport Properties of Food; Marcel Dekker: New York.

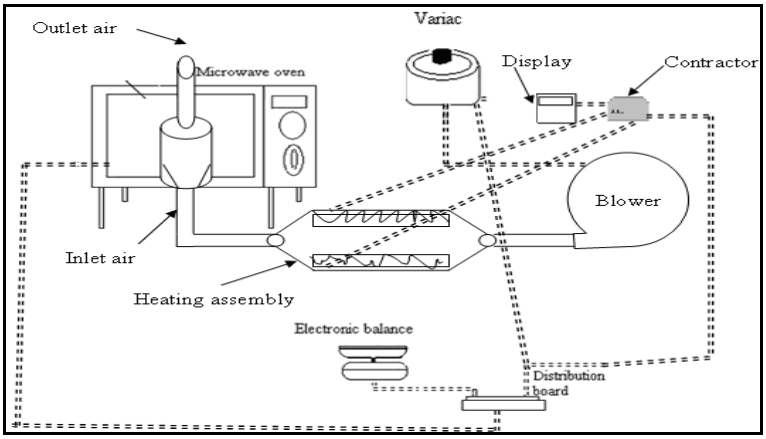

Fig. 1a Schematic diagram of microwave assisted fluidized bed drying system

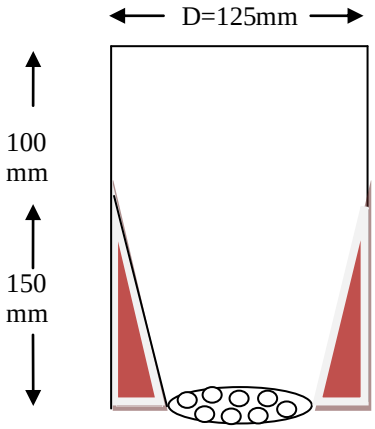

Fig. 2b Drying chamber in microwave assisted fluidized bed drying system

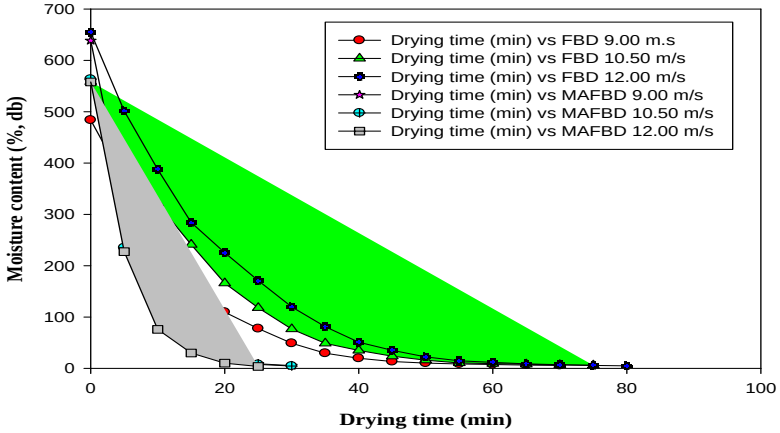

Fig. 2. Effect of velocity on moisture content during drying of beetroot in FBD and MAFBD at 60°C air temperature

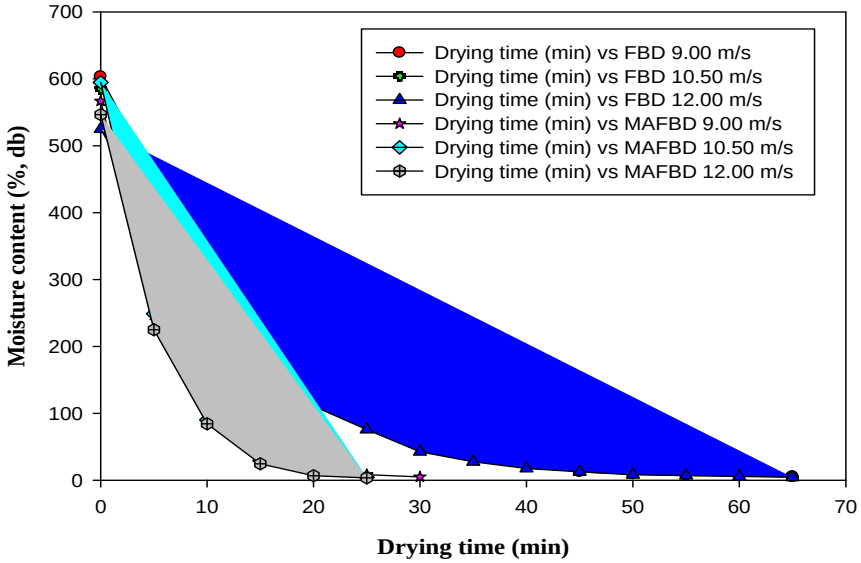

Fig. 3. Effect of velocity on moisture content during drying of beetroot in FBD and MAFBD at 67.50°C air temperature

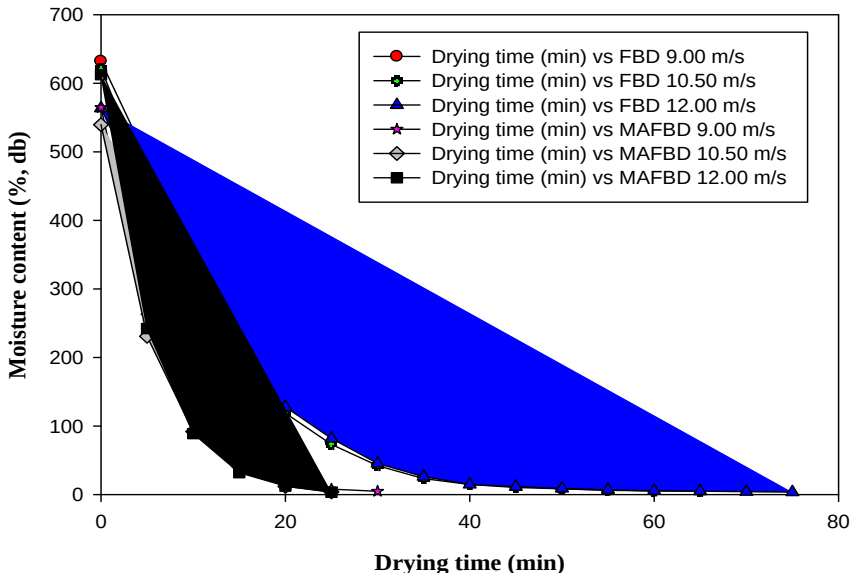

Fig. 4. Effect of velocity on moisture content during drying of beetroot in FBD and MAFBD at 75°C air temperature

Table 1. Nutritional value of beetroot per 100 g

Constituents	Amount	Constituents	Amount
Carbohydrates	9.96 g	Vitamin B_6	0.067 mg
Sugars	7.96 g	Folate (Vit. B_9)	80 µg
Dietry fiber	2.0 g	Vitamin C	3.6 mg
Fat	0.18 g	Calcium	16 mg
Protein	1.68 g	Iron	0.79 mg
Vitamin A equiv.	2 µg	Magnesium	23 mg
Thiamine (Vit. B_1)	0.031 mg	Phosphorus	38 mg
Riboflavin (Vit. B_2)	0.027 mg	Potassium	305 mg
Niacin (Vit. B_3)	0.331 mg	Zinc	0.35 mg
Pantothemic acid (B_5)	0.145 mg	Sodium	77 mg

Source: USDA national nutrient data base for standard reference, release 22 (2009)

Table 2. Technical details of microwave assisted fluidized bed drying equipment

Components and subcomponents of MAFBD		Technical details
1. Microwave (Model: MC 9287BQ, Made by Korea)		➢ Type: LG CONVECTION MWO (a domestic kitchen) ➢ Input and output power: 1950 and 900 watt ➢ Frequency: 2450 MHz ➢ Dimension: 574 mm x 376 mm x 505 mm.
2. Drying chamber	➢ Material used in construction	➢ Perspex and plaster of parish (POP)
	➢ Length of pipe,	➢ Total height 250 (100+150) mm (Fig.)
	➢ Top diameter,	➢ 125 mm
	➢ Distribution plate	➢ Made of perspex
	➢ Diameter of plate	➢ 60 mm
	➢ Diameter of hole	➢ 1 mm
	➢ Perforation	➢ 50%
	➢ Angle of taperness from the bottom	➢ 45^0 created by POP
2. Heating device/ assembly		Two electric heater
3. Motorized Blower (Made by Lama Electricals Azad factory and Model: 75 impellers)		➢ Used for fluidization of beetroots using air ➢ Horse power: 1,Voltage: 180-230 and Frequency: 50 cycle
4. Variac (Made by B. R. Trading Company, India)		➢ Used to adjust AC voltage ➢ Maximum load: 10 Amps (for input 240 V, 50/60 Hz) ➢ Output varied between 0 to 270 volt
5. Data logger		➢ Used to measure the outlet temperature and humidity ➢ Input: .230-240 V AC, Fuse: 200ml, Frequency: 50 Hz
6. Voltage Stabilizer (Made by CYBEX)		➢ to maintain the constant voltage supply to experimental setup ➢ Capacity: 3 kVA, servo type
7. Electronic balance (Made by Atcom Technologies Ltd.		➢ Capacity: 0.1 g to 5000g ➢ Voltage supply: 9V

Table 3. Details of experiments

Particulars	Details
Crop taken	Beetroot (Sanguina variety)
Pretreatment	Slicing to 7 mm x 7 mm x 1 mm size
Drying	Microwave assisted fluidized bed drying
Air velocity (A.V)	9 m/s, 10.50 m/s and 12 m/s
Air temperature	60°C, 67.50°C, and 75 °C
Control	Fluidized bed drying at same combination
Total number of experiments	21
Size of sample	200 g for microwave assisted fluidized bed drying and 500 g for fluidized bed drying.

American Journal of Engineering Research (AJER)
e-ISSN : 2320-0847 p-ISSN : 2320-0936
Volume-03, Issue-03, pp-274-279
www.ajer.org

Research Paper Open Access

Stochastic Analysis of Benue River Flow Using Moving Average (Ma) Model.

A Saminu[1], R L Batagarawa[2],I Abubakar[3]U Tsoho[4], H Sani[5]
**1, 2,, 4,5Department of civil Engineering, Nigerian Defence Academy, Kaduna*
3Department of Water Resources and EnvironmentalEngineering, ABU Zaria

Abstract :-Stochastic analysis is an established method of generating data,this was used to analyze 31 years of average monthly stream flowsof Benue River, the popular model known as Moving average (**MA)** was fitted to the data .The Parametersfor the model was estimated accompanied bydiagnostic checks, which showed the model fitness to the dataadequately, also the histogram of the residuals revealed that themodel assumption was correct (i.e. residualsare normally distributed), this was further tested by forecasting of10 years of stream flows at 95% confidence. The resultsdemonstrated the usefulness of the method in generatingadditional data in watersheds where there is paucity of time series data.

Keywords:-*Stream flow, Analysis , Water management*

I INTRODUCTION

Inadequacy and paucity of data has resulted in improper planning. Thus, in order to bridge this gap, stochastic analysis has been introduced into watershed forecasting. Stochasticanalysis is an established method of forecasting in hydrology. The pioneering works of Thomas and Fiering (1962), Matalas (1967) and Box and Jenkins (1976) and several other researchers brought to light, its importance in water resources management, planning and design. Stochastic analysis is the probabilistic analysis of time dependent random variable In which the variable is broken into its components: mean, cyclical or periodic and purely random components The mean and cyclical components are usually removed before application of well-known stochastic models to the purely-random components, for this reason, it is essential that the data be stationary. A data is said to be stationary, if there is no systematic change in variance and the mean is constant. Where the data are non-stationary, method proposed by Box and Jenkins (1976) and Chatfield (1992) can be used to convert the series into stationary one. Stochastic analysis is very useful in understanding the underlying process ofhydrological data and forecasting. This tool is therefore important in situations where there is paucity of data, required for planning and water resources management it is for this reason that we analyzed the monthly average stream flow records of River Benue, in view of its importance in water supply and waste watermanagement of Benue city.

II LITERATURE

There is extensive literature on the application of stochastic modeling in hydrology, Rao (1974) has successfullydeveloped model for monthly river flow analysis, whileClarke (1984) and Hurst and Bowles (1979) developedrainfall model, and water quality models respectively by modifying the theory of Box and Jenkins (1970) Thomasand Fiering (1962), through their pioneering work, have shown that stream flows can be generated using stochasticmodels this was further demonstrated by Okuta (1988), who used the model to generate stream flows In southernGhana, Stochastic analysis had previously been applied to some aspect of stream flow of River Kaduna. Oni (1990)developed a water quality management model for the river, while Harrison (1980) proposed a water supply protectionmodel earlier application was the stochastic modeling of sediment load of the southern water works of River Kadunaby Gleave (1971).

III MATERIALS AND METHOD

The simplest of the stochastic models is the Markov model, which correlates the value of the random variable at a current time to the value of earlier time The first order Markov process is used when serial correlations for lags greater than one are not important and is of the form:

$X_{i+1} = \mu_x + \rho_x(1)(X_i - \mu_x) + \varepsilon_{i+1}(1)$

Where:

X_{i+1}= The value of the process at time I,$\mu = The\ mean\ of\ X.\rho_x(1) = The\ first\ order\ serial\ correlation.$

$\varepsilon_{i+1} = Random\ component\ with\ E(\varepsilon) = 0\ and\ var(\varepsilon) = \sigma_\varepsilon^2$

$\bar{X}_t = \emptyset_{p,1}\bar{X}_{t-1} + \emptyset_{p,2}\bar{X}_{t-2} + \ldots \emptyset_{p,p}\bar{X}_{t-p} + a_t - \emptyset_{p,1}a_{t-1}\emptyset_2 a_{t-2} - \ldots - \emptyset_a a_{t-q}(2)$

The Auto correlation of the process is:

$\rho_1 = \frac{(1\emptyset_{1.1}\theta_{1.1})(\emptyset_{1.1}-\theta_{1.1})}{1+\theta_{1.1}^2-2\emptyset_{1.1}\theta_{1.1}}$

(3)

And $\rho_k = \emptyset_{1.1}\rho_{k,1}$

The stationarity and invertibility constraint to be satisfied are:

$-1 < \emptyset_{1.1} < 1\ and\ -1 < \emptyset_{1.1} < 1(4)$

O'Connell (1974) found that the value of $\emptyset$andθ, used for modeling stream flow time series are in the range where both parameter are positive and $\emptyset_1$ greater than θ. The relation $(\emptyset_{1.1} - \theta_{1.1})$ determines the sign of the lag-one autocorrelation, ρ is always positive.A general Model can be of the form:

$\check{Z}t = a_t - Ø_1a_{t-1} - Ø_2a_{t-2} - \ldots - Ø_qa_{t-q}(5)$

This model type is called moving average (MA) process of order q. The name "moving average" is somewhat misleading because the weights 1,- **Ø$_1$**, – **Ø$_2$**,... , - **Ø$_q$**, Which multiply the a's, need not total unity nor need they be positive. However, this nomenclature is in common use, and therefore we employ it**.**

If we define moving average operator of order q by

$Ø(B) = 1 - Ø_1B - Ø_2B^2 - \ldots - Ø_qB^q(6)$

Then the MOVING AVERAGE MODEL may be written economically as:

$\check{Z}t = Ø(B)a_t$ (7)

It contains q +2 unknown parameters μ, andØ1 ... $Ø_q\sigma^2$ a which in practice have tobe estimated from the data.

The likelihood estimates of the parameters of MA (p,q) and the conditional sum of square (ss) are obtained using these equations

$L_{.(\emptyset,\theta,r_a)} = nL_\theta r_a - \frac{S.(\emptyset,\theta)}{2r_a^2}8)$

$S.(\emptyset,\theta) = \sum_{t=1}^{n} at\left(\frac{\emptyset,\theta}{w.,a.,w}\right)(9)$

Where:

*L.*and*S.* are the conditional likely hood and sum of square of the model also:

The auto correlation at lag k is computed as:

$\frac{\sum_{i=1}^{N-K}(x_1-\bar{x})(x_{1+k}-\bar{x})}{\sum_{i=1}^{N}(x_1-\overline{x})^2)}(10)$

K= 0, 1, 2, 3, 4, ……..k

This model can be applied, and parameters estimated using available statiscal software. For this work MINITAB R14 and STATISTICA.

Stochastic analysis of stream flow requires unbroken record of flow data, collected over a period of time at the gauging station. The monthly mean daily discharge average stream flow was collected for 31 years between 1973 and 2003, with sample size N = 492 from preliminary checks, it was discovered that earlier data between 1973 were collected in ft/s; these were harmonized with later data and analyzed with homogenous units. A plot of the stream flow showed an increasing trend, probably due to urbanization and deforestation in the watershed this would make the data non- stationary, this was corrected by removing the trend and differencing of data with lag 12, this is seasonal differencing of lag 1.

The recommended procedures for Stochastic modeling was adopted which included the following (Box and Jenkins 1970)

(a) Determination of suitability of data for analysis through plotting of series

(b) Identification of models by examination of the autocorrelation function, ACF, and partial autocorrelation function, PACF, plots

(C) Estimation of model parameters

(d) Diagnostic check of the model to verify whether it complies with certain assumptions for the model.

(e) Model Calibration by plotting observed and filled dated.

These steps were carried out for this work using two readily available statistical software MINITAB R 14 and STATISCA.

Moving average MA (1) model was fitted to the data, we performed the time-series plots, model identification and estimation of parameters, diagnostic checking using the normal probability plot of the residuals detrended normal plot and histogram plot of the autocorrelation functions, We also conducted model calibration by comparing original and computed data, which were plotted for all the models Finally ten-year forecasts of stream flows using the models were made.

IV RESULTS AND DISCUSSION

The plots of the original data were shown in fig1 and of transformed data in fig2 the former showed an increasingtrend, which was muffled after logarithmic transformation

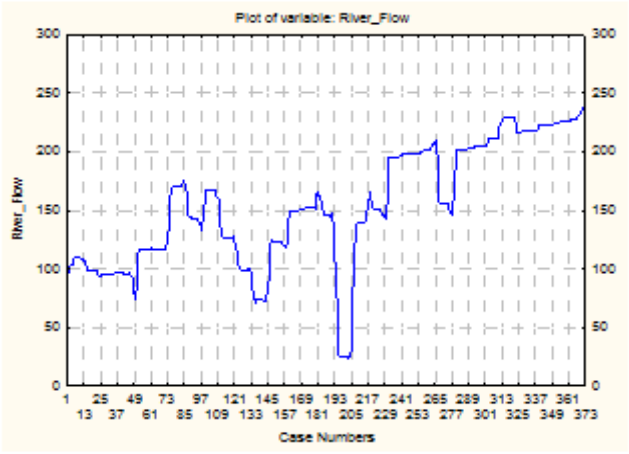

Fig1: The monthly stream flow data Benue River

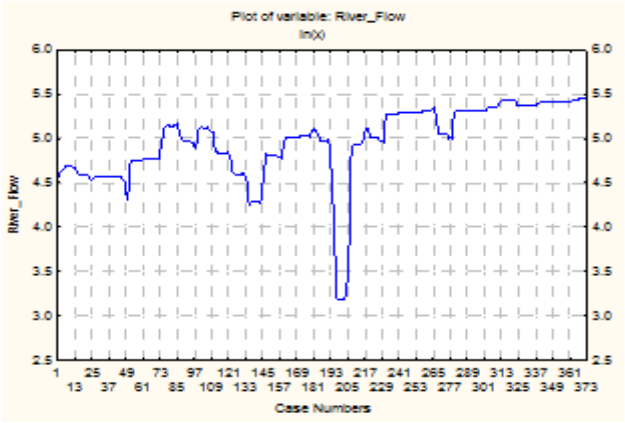

Fig 2: The transformed monthly stream flows of Benue River

In addition, in fig3 and 4 shows the autocorrelation and partial correlation plots of transformed data

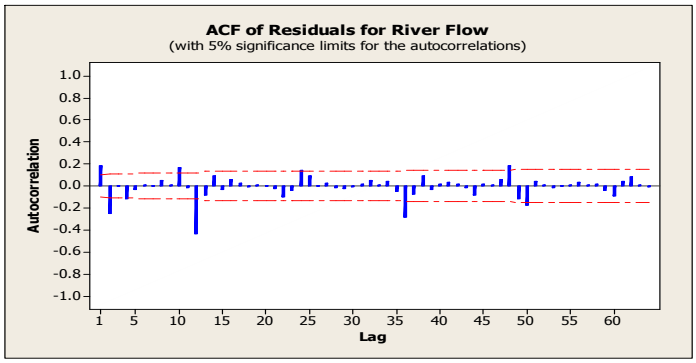

Fig 3: Autocorrelation function of the transformed data

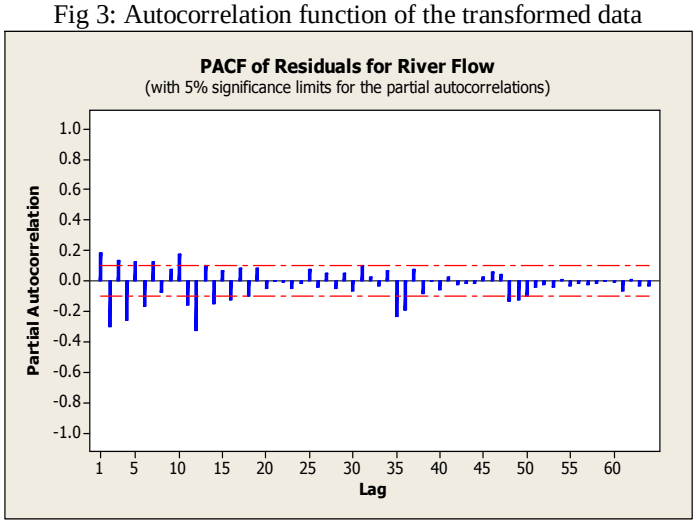

Fig4. Partial autocorrelation function of the transformed data

Diagnostic checks were carried out on the model by plotting the residuals and the order of the data asshown in Fig 5, also Histograph is shown in Fig 6. The Plots of the ACF of the residuals were also made earlier, to test the independence of the residuals, as a necessary condition for acceptance of model.

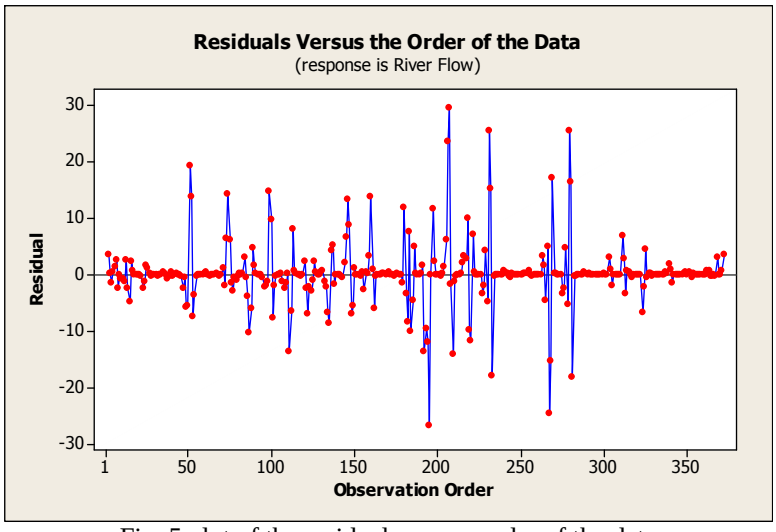

Fig. 5 plot of the residuals versus order of the data

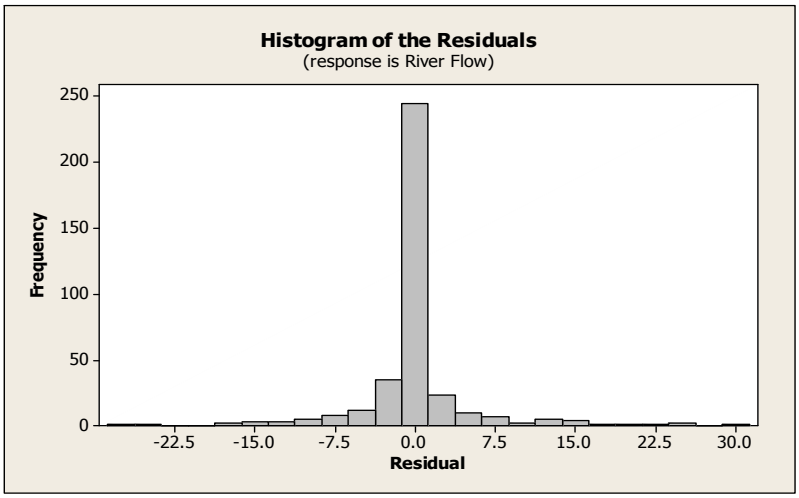

Fig. 6 Histogram plot of the residuals

The plots of the original and computed data are shown in Fig 7, while ten years forecasts are given in Fig 8.

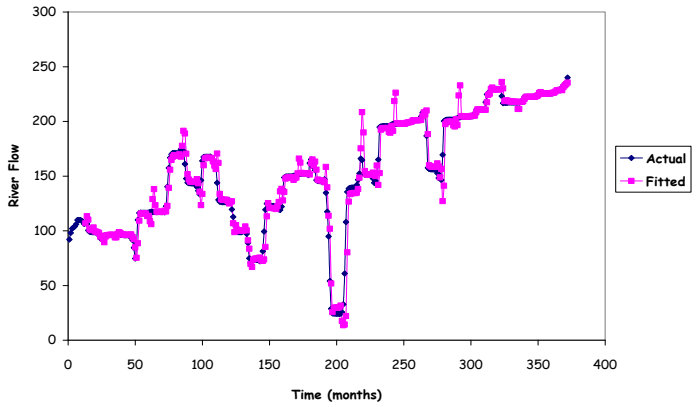

Fig.7 Actual and predicted monthly stream flows of Benue River.

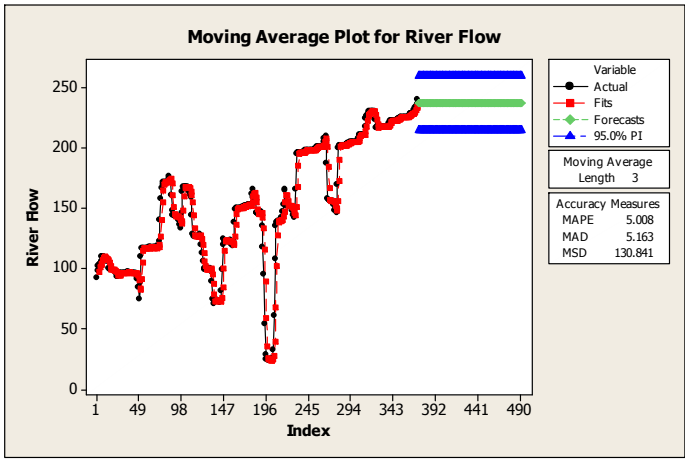

Fig.8: Actual, predicted 10-years forecast of stream flows.

Below is the estimation of parameters yielded the results for MA (1) Model:
Data: River Flow
Length: 372
NMissing: 0
Accuracy Measures:
Mean Absolute Percentage Error (MAPE) =5.008

Mean Absolute Deviation (MAD) = 5.163

Mean Square Deviation (MSD) = 06.6224

The transformation of the data and seasonal differencing reduced the serial autocorrelations. This fulfilled the model
assumptions; this is evident in the normal plots of the residuals, which showed independence. The histograph of the residuals also showed that the assumption was correct for the moving average model. The model calibrations showcased the capability of the model to generate the original data .The increasing flows may be due to increasing urbanization and deforestation in the catchments of the River Benue. Deforestation has the tendency of reducing infiltration and increasing runoff, as noticed in the watershed. There had been significant changes in land use patterns within the period of study i. e 1973 – 2003.

V CONCLUSION

The application of stochastic analysis of stream flows on River Benue was considered. A single model known as Moving Average (MA) was fitted to the data, using standard procedures enunciated by researchers. Diagnostic checks showed the model fitted the data adequately and this was tested by forecasting of 10 years of stream flows. This highlighted the importance and usefulness of the model in areas where we have paucity of data.

REFERENCES

[1] **Box G. E. P. and Jenkins G. M. (1976**): Time Series Analysis: Forecasting and Control, Holden Day Press. San Francisco.

[2] **Chatfield C. (1992):** The Analysis of Time Series An Introduction, Chapman and Hall, London.

[3] **Clarke R. T. (1984):** Mathematical Models in Hydrology, Institute of Hydrology, Wallingford, United Kingdom, pp51, 119 -123

[4] **Gleeve A.D.(1971):** Stochastic modeling of the sediment load of the southern water works of Kaduna River.(Msc Dissertation, unpublished).

[5] **Hurst J.A and Bowles H.T (1979):**Model choice: An operational comparisons of stochastic modeling pp 11-21.

[6] **Jenkins G. M. and Watts (1968**): Spectral Analysis and Its Applications, Holden Day Inc San Francisco.

[7] **Matalas G.F (1967):** Mathematical Assessment of Synthetic Hydrology

[8] **0' Connel F.G (1974):** A Simple Stochastic Modelling of Hur~t'S Range, Symposium on Mathematical Models in Hydrology.

[9] **Okuta T. N. (1988):** Application of Thomas –Fiering Model for Stream Flow Generation in Southern Ghana, Natural Water Bulletin, Vol. 3, No.1, Jan.

[10] **Oni A.D (1990):** River Water Quality Management Programme, A Proposal for River Kaduna Unpublished MSc Dissertation. Ahmadu Bello University, Zaria, Nigeria

[11] **RAO A.T (1974):** Linear statistical inference and its applications.

[12] **Thomas G.B and Fiering D.F (1962):** Mathematical Synthetic Stream Flow Sequences for the Analysis, of River Basin by Simulation

American Journal of Engineering Research (AJER)
e-ISSN : 2320-0847 p-ISSN : 2320-0936
Volume-03, Issue-03, pp-280-286
www.ajer.org

Research Paper Open Access

Electrical Fault Analysis of 33KV Distribution Network (A Case Study of Ekiti State 33KV Distribution Network)

Kehinde Olusuyi , Temitope Adefarati, Ayodele Sunday Oluwole, Adedayo Kayode Babarinde

[1] *(Department of Physical Planning, Federal University Oye Ekiti, Nigeria)*
[2]*(Department of Electrical/Electronic Engineering, Federal University Oye Ekiti, Nigeria)*

Abstract: - The aim of this research work is to carry out a fault analysis of 33KV distribution system using Ekiti state as a case study. Based on the available statistical data, Ekiti State is reported to suffer from severe shortages of electric power due to dilapidated and outdated electrical power infrastructures. In this research work, electric power infrastructure and energy availability in Ekiti State is studied since the state is one of the principal economic and political hubs of Nigeria. During the study, the conditions of all relevant electrical facilities for distributing power at the 33 KV level were assessed. Power availability in the 33/11kv injection stations in the state was considered by collecting data about energy supplied, faults and other outages. The outcome of the research indicated that the probability of having 2 consecutive hours of power was less than 25% in either year for most of the feeders indicating a very poor situation for consumers, especially small scale industries and commercial enterprises can only succeed using other sources of electricity. Faults on the feeders manifest a log-normal shape of the distribution which exhibited about 3000 earth faults over a nine year period corresponding to about $9x10^{-3}$ earth faults per MVAhr. Based on these findings, it can be deduced that not only is the physical equipment in need of serious rehabilitation and normalization, but also that even the power supplied requires better maintenance management to ensure delivery when available.

Keywords - Distribution, *Over-current, Feeder, Earth Fault, Load demand, Transformer*

I INTRODUCTION

In recent years electric power has become the most ubiquitous form of energy used for production, recreation, control and for carrying out most activities because of the ease with which it can be produced, transported and converted to various applications. Gordon Clapp, a former General Manager of the Tennessee Valley Authority (U.S.A) once said- "If you would destroy a region, you destroy its power supply. If you would hold a region to a lower standard of living, you can do it by placing a limit on its supply of electric power" (Uwaifo, 1994). Given its benefits to mankind, it was not long before electricity was regarded as an infrastructure, i.e. a basic necessity for man's socioeconomic well-being. It is now universally accepted that the social and economic factors which define the level of prosperity, are highly correlated with the level of demand for electric power.Ekiti State is an agrarian state in the southwestern part of Nigeria. The State lacks most of the infrastructures which is common in most of the developing countries. Of these is the poor state of electric power distribution, electric Power distribution system in Ekiti State is something of a major concern. There are more outages than uninterrupted power supply in most parts of the state all the year round. It is a known fact that electricity plays a dominant role in the socioeconomic development of any community. In view of the foregoing, this project seeks to identify the problems militating against regular, good quality of electric power supply in Ekiti-State with a view to proffering solutions and suggestions where necessary. This is to improve the socioeconomic life of the Power Holding Company of Nigeria (PHCN)'s customers in the state. Given this unsatisfactory state of affairs and the lack of comprehensive studies to formally guide the development of electric power in the state, there is a dire need for an assessment of the Ekiti-state electric power distribution with a view to quantifying the availability of electric power and examining some of the physical factors that may contribute to the poor state of the electric power infrastructure so that remedial suggestions may be preferred for improved system performance. It is in the light of this situation that this research has been

conceived so as to provide useful information about the present condition from which rational and well-thought out improvements can be planned and implemented.

II MATERIALS AND METHODS

A BRIEF PROFILE OF EKITI STATE

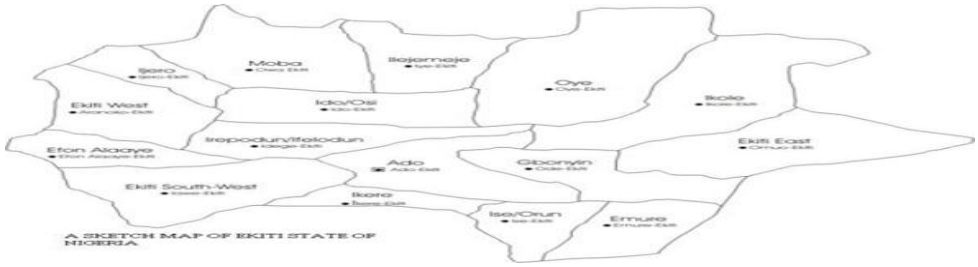

Map of Ekiti-State

2.1 Historical Background of Ekiti State

Ekiti State of Nigeria was created on 1st October, 1996 by the late Head of State and Commander-in-Chief of the Armed Forces of the Federal Republic of Nigeria, General Sani Abacha(GCON) .The State capital is located in Ado Ekiti.

2.2 The Ado- Ekiti District of the PHCN

The electric power distribution network of Ekiti State is under the management of the Power Holding Company of Nigeria (PHCN), Benin Distribution Zone and is referred to as Ado–Ekiti Business Unit. Ekiti-State which has no power generating capability is supplied from four different sources with capacities as shown in the table1.0.

Table 1.0: Ekiti-State 33kV Sources

S/N	Source	Transformer Capacity	Load Demand (MW)
1	Akure	2x30MVA	15
2	Omu Aran	2x1.5MVA	12
3	Okene	2x30MVA	3
4	Ilesa	2x30MVA	4

An estimated load demand of 34 MW can be satisfied from the sources as shown in table 1.0. Power distribution in Ekiti-State radiates outwards from a backbone and the distribution lines pass through thick vegetation/difficult terrain. This arrangement results in a fragmented supply to different areas of the state with different reliabilities, thus making maintenance and fault tracing on the network very tedious. Persistent low voltage due to the poor supply conditions has forced artisans and big electricity consumers depend on generators for their products and services. Ekiti State is serviced by 10 major injection substations and over 300 distributions. The main injection substations are highlighted in table 2.

Table 2: Injection Substations in Ekiti-State

S/N	Substation	Type KV)	Transformer Rating (MVA)	Source
1	Ijero	33/11	2.5	Ilesha
2	Oye	33/11	1	Omu-Aran
3	Ikole 1	33/11	2.5	Omu-Aran
4	Ikole 2	33/11	2.5	Omu-Aran
5	Ado	33/11	15, 7.5	Akure
6	Ise	33/11	2.5	Akure
7	Ikere 1	33/11	2.5	Akure
8	Ikere 2	33/11	2.5	Akure
9	UNAD	33/11	2.5	Akure
10	FED POLY	33/11	2.5	Akure

2.3 General Description of 33 kV Distribution Networks in Ekiti State

The 33 KV and 11 KV distribution networks in Ekiti-State are radial. The radial type system is the simplest and the one most commonly used. It comprises separate feeders or circuits radiating out of the substation or source, each feeder usually serving a given area (Pansini, 1986). The 33 KV network covers a

substantial part of Ekiti-State, this being fed from the four (4) sources of electric power. Ado, Ise-Orun, Emure, part of Gbonyin, Ikere, Irepodun/Ifelodun, Ekiti West and Ekiti South West Local Government areas receive supply via Akure-Ado 33kV line. The supply from Omu-Aran transmitting station covers Moba, Ikole, Ilejemeje, Ido/Osi and Oye Local Government areas. 33kV line tee-off from Kabba/Isanlu feeder from Okene transmitting station supplies power to Ekiti East Local Government Area while the Ikare feeder supplies power to part of the Gbonyin Local Government Area. Ado-Ekiti feeder, radiating from Ilesha transmitting station covers areas like Aramoko, Osi, Awo, Iropora, Eyio, Epe, Ado-Ekiti and environs. Ikogosi /Erijiyan 33kV line Tee-off from Efon Feeder supplies Ipole-Iloro, Ikogosi and Erijiyan-Ekiti.

There are two consumers that are fed at 33 KV. These are the Ero dam with 2 X 1.6 MVA operating 33/11 KV and the Ayetoro water booster station with 2 X 1.6 MVA also operates 33/11 KV. There are Ring Main Units (RMUs) at Ikere main substation No 1, Ikere main substation No 2 and Ikole main substation. These RMUs provide an arrangement for switching at the injection substations. There are also J and P/ 'D' fuses strategically located on the networks in order to provide protection against overload or over-current faults on the distribution transformers. The distribution transformers range from 50 KVA to 500 KVA ratings. Similarly, there are circuit breakers to interrupt fault currents and Isolators to physically open lines when necessary. There are also some arrangements for switching (jumper points) which can be closed in order to provide emergency supply to a feeder from an adjacent one. In the Ado main substation / control room, SF6 gas circuit breakers are installed for both of the 7.5 MVA and the 15 MVA transformers. The conductor sizes of the overhead lines are either 70mm2 or 100mm2. However, the Ido – Aaye – Ifaki – Oye route which is almost 32 km in length uses 150mm2 Aluminum conductor size while Ilupeju – Ire route which is 15km in length uses 35mm2 Aluminum conductor size.

III RESEARCH METHODOLOGY

3.1 Study Process for Assessment

The process of study of the assessment started with the evaluation of the physical condition of the distribution system with specific reference to the type and size of conductors, pole supports, spans and clearances, cross-arms, type of insulators and route length. A study of the operational and failure features of the network in terms of availability and quality of power, types of fault and frequency of occurrence of faults then followed.

Direct patrol and inspection of the 33 KV distribution network of Ekiti-State, as well as personal visits to injection substations for on–the-spot assessment of the state of equipment and installations of the injection substations were carried out. Fault data obtained from the Power Holding Company of Nigeria (PHCN), Ekiti State district for three consecutive years (2011- 2013) were collected and analyzed. Daily, hourly feeder loadings of the 11 KV distribution network in the district for two consecutive years (2009 – 2010) were obtained and analyzed. Also additional information was also obtained from interviews conducted with PHCN's staff and management and staff of Ekiti-State Electricity Board.

Table 3: 33kV Akure-Ado-Ekiti Route

ITEM	DESCRIPTON	QUANTITY	CONDITION	REMARKS
33kV line			Exposure to forest encroachment	Route not cleared.
Sag			About 80% of the spans met standard requirement	Improper construction and damaged cross arms and insulators are likely causes.
Distance		65 km in length	Only about 18 km of the route length is cleared.	Poor maintenance of the right-of-way by the PHCN due to inadequate funding and staffing.
Conductor	Aluminum	100 mm^2 in diameter	Loose strands are present	This is due to expansion of conductors as a result of overheating resulting from overload.
Sampled Poles	Tubular steel poles	489	134* (27%) poles were defective.	*The condition of the poles is due to either traffic accident or other factors like poor erection. Some of the concrete bases require re-construction.
Insulators	Post and pin type	1467	146 (10%) insulators were defective.	Insulators were affected due to rotten and broken cross arms. Some are also cracked due to old age, flashover and weather conditions.
Cross arms	Wooden	489	161 (33%) cross arms were defective.	Wooden cross arms are rotten, broken as a result of old age over-exposure to rainfall and sunlight.

Table 4: 33kV Ado-Ikere-Emure Route

ITEM	DESCRIPTION	QUANTITY	CONDITION	REMARKS
Line	33 kV		Line is exposed to forest encroachment.	The route is not cleared.
Sag			About 55% of the spans met standard requirement	The causes are likely the effects of damaged cross-arms, insulators and improper construction.
Distance		53.2 km in length	Only about 24 km (45%) is cleared	Negligence of the right-of-way by the PHCN due to inadequate funding and staffing.
Conductor	Aluminum	100 mm^2 in diameter	Loose strands are present	The loose strands are consequences of overload on the line conductors which cause them to expand.
Sampled Poles	Concrete	315	135 (43%) poles were defective.	The defects are due to poor erection and vandalism by trees during rainfall.
Insulators	Pin type	945	66 (7%) insulators were defective.	Displaced and broken insulators were due to rotten and broken cross-arms.
Cross arms	Wooden and steel	315	113 (33%) cross arms were defective.	Wooden cross arms are rotten, broken as a result of old age over-exposure to rainfall and sunlight.

Table 5: 33kV Ado-Aramoko Route

ITEM	DESCRIPTION	QUANTITY	CONDITION	REMARKS
Line	33 kV		Exposure to forest encroachment	The route was not cleared.
Sag			About 60% of the spans met standard requirement	Effects of damaged insulators and cross-arms.
Distance		32 km in length	Only about 26 km was not cleared.	Negligence of right-of-way by the PHCN due to inadequate funding and staffing.
Conductor	Aluminum	100 mm2 in diameter	Loose strands are present	This is due to expansion of conductors as a result of overheating resulting from overload.
Sampled Poles	Concrete	150	57 (38%) poles were defective.	The pole defects are due to the lack of concrete base of the poles and poor maintenance of route.
Insulators	Pin type	450	36 (8%) insulators were defective.	Some insulators were broken while some displaced due to rotten and broken cross-arms
Cross arms	Wooden	489	161 (33%) cross arms were defective.	The wooden cross-arms were rotten and broken as a result of old age and over-exposure to rainfall and sunlight.

Table 5: 11kV Ado-Iyin-Igede Route

ITEM	DESCRIPTION	QUANTITY	CONDITION	REMARKS
Line	11 kV		Line is exposed to forest encroachment	The route was not cleared.
Sag			About 60% of the spans met standard requirement	Poor construction and damaged cross-arms and insulators are likely causes.
Route		17.2 km in length	About 7 km (41%) was not cleared.	Negligence of the right-of-way by the PHCN inadequate funding and staffing.
Conductor	Aluminium	100 mm2 in diameter	Loose strands are present	This is due to expansion of conductors as a result of overheating resulting from overload.
Sampled Poles	Concrete and wooden	105	48 (46%) poles were defective.	Some poles were attacked by termite while some were not properly erected.
Insulators	Pin type	315	37 (12%) insulators were defective.	Some insulators were displaced due to rotten and broken cross-arms while some were broken due to weather condition.
Cross arms	Wooden and steel	105	45 (43%) cross-arms were defective.	The wooden cross-arms were rotten and broken as a result of old age and over-exposure to rainfall and sunlight.

Table 6: 33kV Ado-Ilawe Route

ITEM	DESCRIPTION	QUANTITY	CONDITION	REMARKS
Line	33 kV		Line is exposed to forest disturbance	The route was not cleared.
Sag			About 60% of the spans metstandard requirement	Effects of damaged insulators and cross-arms.
Distance		17 km in length	About 7 km (41%) was not cleared.	Poor maintenance of the right-of-way by PHCN due to inadequate funding and staffing.
Conductor	Aluminium	100 mm2 in diameter	Loose strands are present	This is due to expansion of conductors as a result of overheating resulting from overload.
Sampled Poles	Concrete	125	50 (40%) poles were defective.	The defects are due to destruction by trees during rainfall and poor erection of poles.
Insulators	Pin type	375	23 (6%) insulators were defective.	Some insulators were broken while some were displaced due to rotten and broken cross-arms.
Cross arms	Wooden and steel	125	41 (33%) cross-arms were defective.	The wooden cross-arms were rotten and broken as a result of old age and over-exposure to rainfall and sunlight.

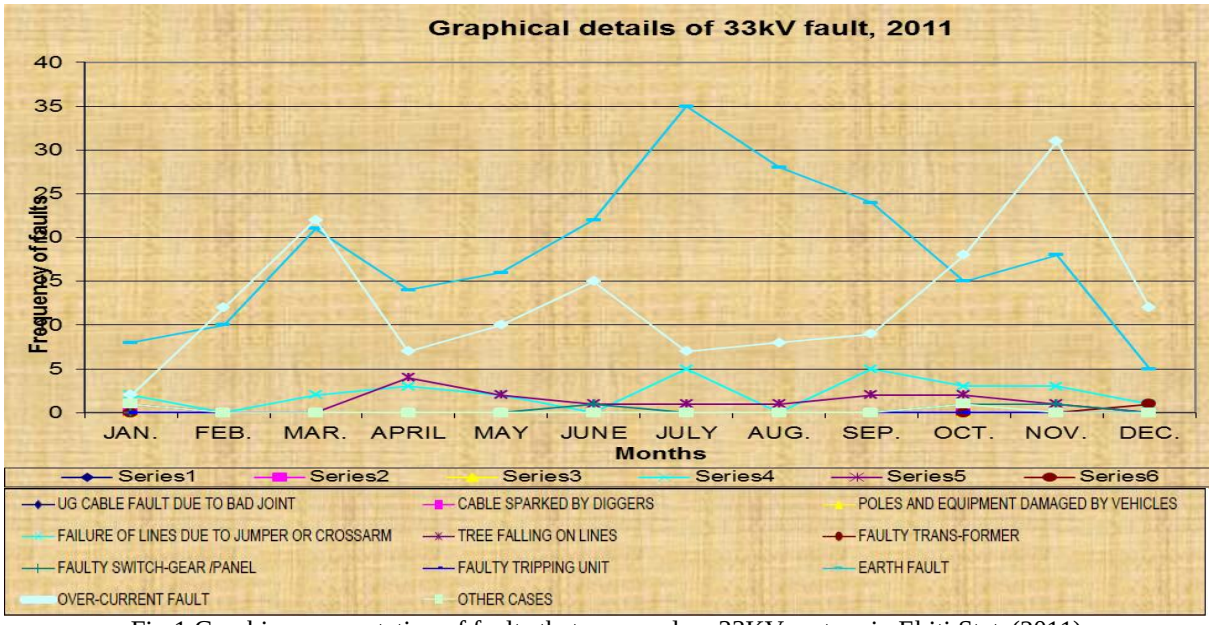

Fig 1:Graphic representation of faults that occurred on 33KV system in Ekiti State(2011)

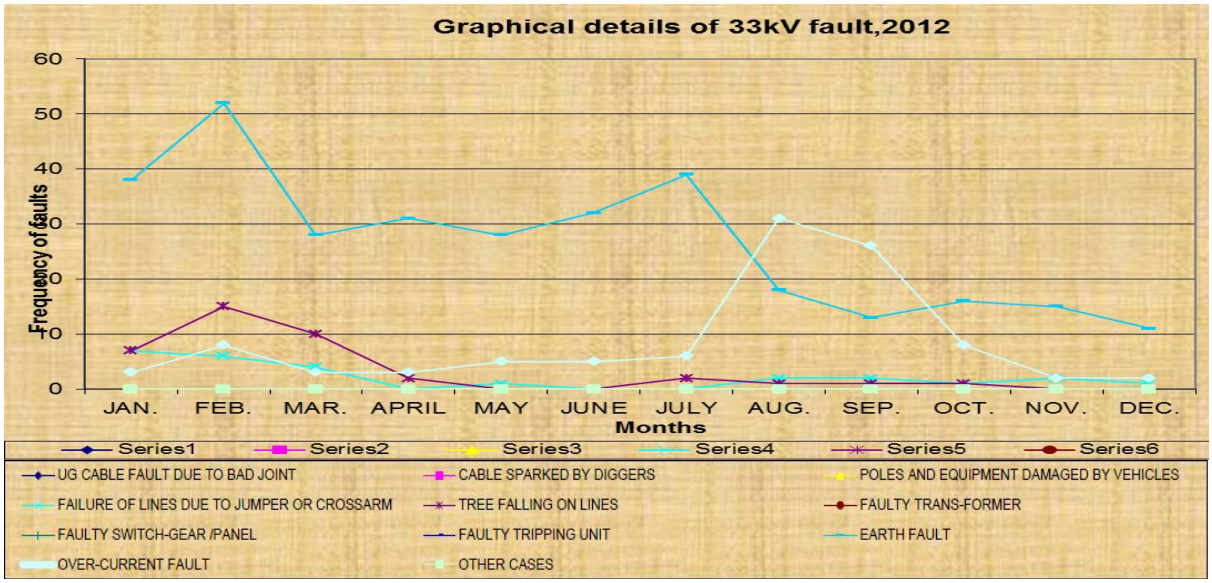

Fig 2:Graphic representation of faults that occurred on 33KV system in Ekiti State(2012)

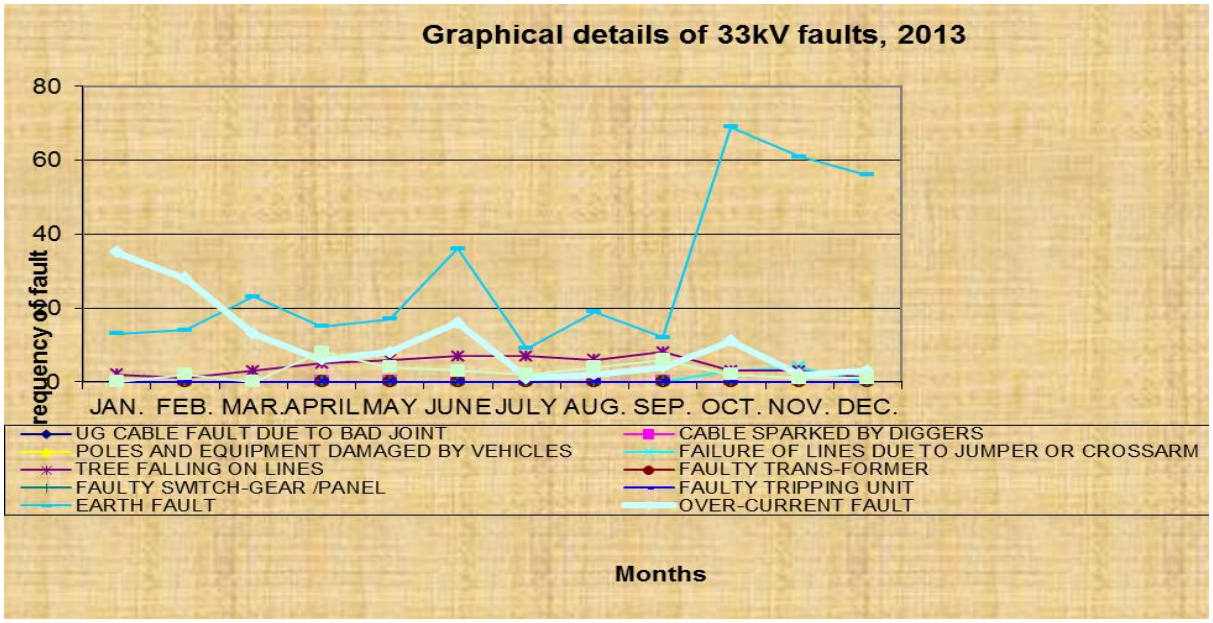

Fig 3:Graphic representation of faults that occurred on 33KV system in Ekiti State(2013)

IV RESULTS AND DISCUSSION

The following tables provide a graphic representation of the physical state of the components of the 33kV network in Ekiti State. The poor state of the lines accounts for the incessant outages and faults observed as shown in fig 1-fig 3 and Table 1-Table6.Inspection of the overhead lines revealed that in Ekiti-State, the supporting structures of the distribution systems are predominantly either reinforced concrete or wooden poles with a few steel towers, similarly with either wooden or steel cross-arms. The abundance of trees in Ekiti-State's forest makes the use of wood as supporting structures very economical. Most of the 'right-of-ways' in Ekiti-State pass through the forest due to the nature and topography of the state. However, the distribution networks were characterized by leaning poles or crooked structures, shattered insulators, broken or decayed cross-arms and vegetation encroachment. The data collected was compiled into a spreadsheet resident database from which many scenarios and analyses were deduced. Based on the findings in the data collected, the physical condition of the overhead lines, the substations as well as other relevant system components were assessed so that remedial measures could be determined. Power availability, loading characteristics of the district and probabilistic characterization of faults in the state were also carried out. Faults experienced on the 33kV distribution network of Ekiti State district between 2011 and 2013 were obtained from the Power Holding Company of Nigeria PLC (PHCN); the database contains details of types of fault cleared on a monthly basis for the period 2011 and 2013 on the 33kV network.

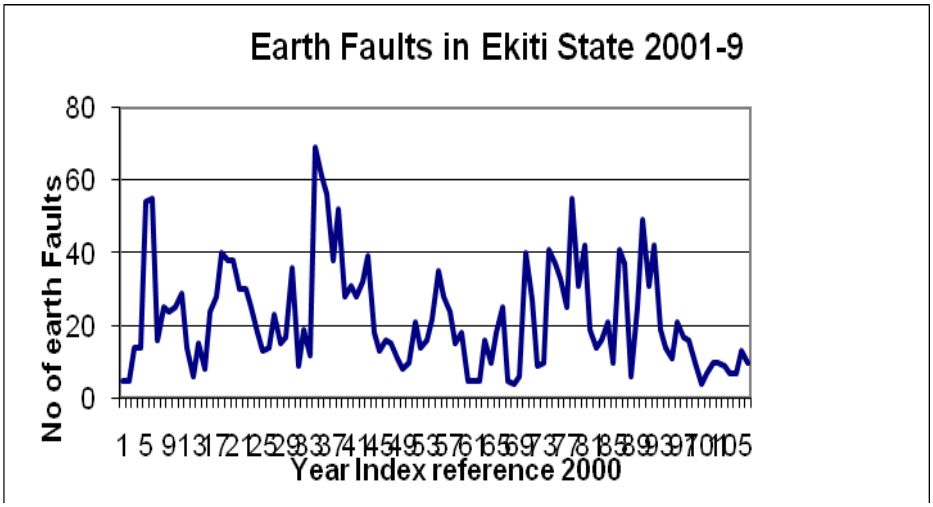

Fig 4: Earth Faults on 33kV network between 2001 and 2009

The fig 4 gives a plot of the frequency of earth faults observed on the 33kV network with year index reference 2000.

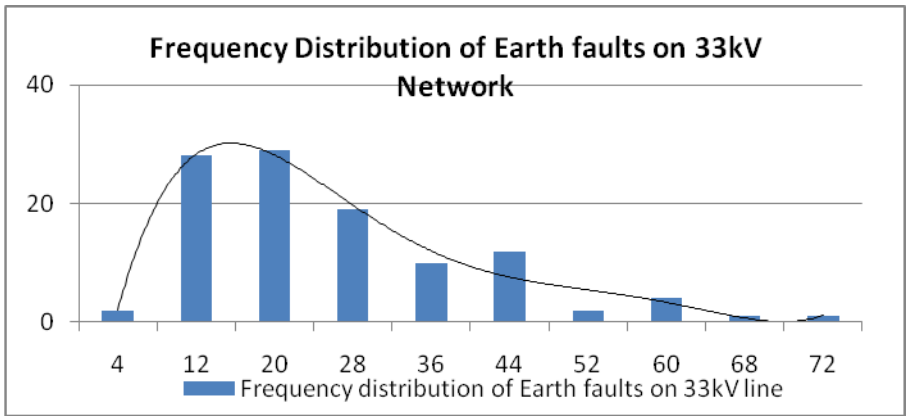

Figure 5: Frequency Distribution of Earth Faults on 33kV Network

The frequency distribution for the earth faults observed on the 33kV network is shown in fig 5.

V CONCLUSION AND RECOMMENDATIONS

S

REFERENCES

[1] Adegboye, B.A. (1998): "Failure Analysis of the 11kV Primary Distribution Feeders" National Engineering Conference Series vol. 5 No. 1, pp47-52

[2] Aduloju, A.O. (2003): "Electrical Power Systems" Evidence Nigeria Ventures, Ilorin, Nigeria

[3] Akinsanya, O.A.(2005): "Electrical Power system in Ekiti-State Problems and Suggestions" Proceedings of 1st Engineering Forum, School of Engineering, The Federal Polytechnic, Ado- Ekiti on Capacity Building in Infrastructural Maintenance. Pp28-32

[4] Allan, Ron and Billinton, Roy (2000): "Probabilistic Assessment of Power Systems" Proceedings of the IEEE, vol. 88, No. 2

[5] Billinton, Roy and Allan N Ronald (1984): "Reliability Evaluation of Power Systems" London, England: Pitman Advanced Publishing Program, 1984.

[6] Billinton, R and Allan R.N (1992): "Reliability Evaluation of Engineering Systems: Concepts and Techniques" Second Edition,New York: Plenum

[7] Brass, D.F.S et al (1966): "Electric Power Distribution, 415V-33kV" E.O Taylor and G.A Boal (eds), London: Edward Arnold, p272

[8] Brown, E Richard (1988): "Electric Power Distribution Reliability" Second Edition, New York: John Wiley & Sons

[9] Brown, R.E, Gupta, S, Christie, R.D, Venkata, S.S and Fletcher, R (1996): "Distribution System Reliability Assessment Using Hierarchical Markov Modelling" IEEE Transactions on Power Delivery, vol. 11 No.4

[10] Burke, J. James (1994): "Power Distribution Engineering– Fundamentals and Applications" Marcel Dekker, Inc

[11] Da Silva, M.G, Rodrigues, A.B, de Castro, C.L.C, Neto, A.C, Moutinho, E.A, Neto, N.S.A and Cavalacante, A.B (2004): "Reliability Assessment of Distribution Networks in Brazil's northeast" 8th International Conference on probabilistic Methods Applied to Power Systems, Iowa State University, September 12-16

[12] Davies, T (1984): "Protection of Industrial Power Systems" Pergamon Press.

[13] Debs, A.S. (1988): "Modern Power Systems Control and Operation" New York: Kluwer Academic Publishers.

[14] Uwaifo, S.O (1994): "Electric Power Distribution Planning and Development" Malthouse Press Limited.

[15] Villemeur, A (1992): "Reliability, Availability, Maintainability and Safety Assessment, volumes I and II" New York: John Wiley & Sons

[16] Pansini, A.J (1991): "Power Transmission and Distribution" Liburn, Ga: The Fairmont Press Pecht M. G. and Nash F.R (1994): "Predicting the Reliability of Electronic Equipment" Proceedings of the IEEE, vol. 82 No. 7, 994-1004

American Journal of Engineering Research (AJER)
e-ISSN : 2320-0847 p-ISSN : 2320-0936
Volume-03, Issue-03, pp-287-309
www.ajer.org

Research Paper Open Access

Corporate Networks: a Proposal for Virtualization with Cloud Computing

Chau Sen Shia, Mario Mollo Neto
Doctor, Production Engineering, Postgraduate Department of Production Engineering, University Paulista UNIP. São Paulo, SP – Brazil
Doctor, Production Engineering, Postgraduate Department of Production Engineering, University Paulista UNIP. São Paulo, SP – Brazi

Abstract: - Most Educational Universities encounter difficulties in developing a work of integration when need to do planning: allocation of classes, distribution of rooms, allocation of classes and establish better communication between the coordinators of other units belonging to the same institution (geographically distributed). According to Veras (2010) as a way to react to the increased competition, many companies have sought to use a more flexible organizational format. Currently, the use of business networking alliances has become an option in the search of this flexibiildade. The networks that interconnect, organizations offer support for processes, in response to the new times of this competitiveness. It may be noted that the inter-organizational networks supported by information technology (it), allow organizations to act together as a great value system. According to Fusco and Sacomano (2009), alliances may develop in any supply chain, provided the environment in which they occur, operations tasks, and processes to be developed, the qualities required, and available and the objectives to be developed. The performance of each part is what will make the difference in getting the results of the companies involved in the business. In order to better meet the studies related to behavioral analysis of alliances in enterprise networks with the use of technologies of *cloud computing* (cloud computing), this project applies the structure of how virtualization assessment tool for analysis of relationships between companies and the strategic alignment in organizations. In this context, this project intends to propose an architecture of integration of technology *cloud computing* with SOA (*Service Oriented Architecture* – service-oriented architecture) using *web services* (WEB Services) to assist in the execution of strategic business processes within the organizations aimed at universities that have multiple geographically distributed units.

Keywords*: - performance, virtualization, web services, cloud computing, service-oriented architecture.*

I. INTRODUTION

Reality increasingly dynamic and volatile and that configures the competitive assumptions and paradigms of competitiveness, have brought the need to speed up processes, business and organizations, therefore internationalize should be the presence of thought competitive and the strategic alignment of that reality (FUSCO and SACOMANO, 2009). Conform Tonini, Carvalho and Spinola (2009), for competitive advantage, companies must continually update themselves on technology, get maturity in processes and eliminating operational inefficiencies. This requires an engagement ads people, processes and the Organization as a whole.

Currently the companies are organizing network format, and business processes among the organizations increasingly use the applications that process and provide information for the operation of this new arrangement. The new organization, is a combination of various organizations, composed of interconnected cells with several access points provided by infra-structure information technology (IT), while the central element of processing and storage of information and data in the cloud is the *DATACENTER* (VERAS, 2009).

Aiming to establish a model of integration of alliances in corporate networks and the application of technologies *cloud computing*, SOA and *web services* to assist in strategic business processes of organizations into networks of relationships, the proposed project features the use of these technologies. Checks the possibility

of alliances and resource to sharing, to enter into multilateral agreements, the organizational relationships, interpersonal and inter-organizational.

The SOA is an architectural model agnostic to any technology platform and causes a company to have the freedom to get constantly the strategic objectives associated with service-oriented computing, taking advantage of the technology. The *web services* platform is defined by several industry standards supported by all communities, suppliers can be distributed and provide a *framework* for communication based on physically decoupled service contracts. To enable the business processes of a company the implementation of the strategy depends on your infra-structure information technology (IT). The infrastructure is the part of YOU that supports applications that support business processes is the Foundation of the Organization's operational model based on information. Can also be seen as the set of shared services, available for your entire organization, because it has the role of enabling the Organization to function and grow without large interruptions. A *cloud computing* is a set of virtual resources easily usable and accessible (*hardware*, *software*, and services development platform), which can be dynamically reconfigured to fit a workload (*Workload*) variable, allowing for optimization of the use of resources such as virtualization, application architectures, service-oriented infrastructure and technologies based on the Internet (VERAS, 2009).

To developer an architectural model will use the implementation on *web services*, the SOA, and the *cloud computing* for the strategic simulation on intra-organizational networks in the departments of an educational institution of higher education to planning and formation of new courses and adapting existing courses. The proposal established in this project is related to an IES (Higher Education Institution), aiming at the studies in corporate networks, production engineering and analysis of application of new technologies used for strategic planning within companies.

II. THEORETICAL FRAMEWORK

This section describes the main aspects and justifications for the construction of the system proposed in this paper and related to: cloud computing, service-oriented architecture, *web services* and University Educational Center as companies in networks.

2.1. Application of alliances in enterprise networks

The role of the Alliance will make the difference in getting the results of the companies involved in the business. Thus it is important to create solid alliances, but well developed, sufficiently flexible to include changes, as the market environment and corporate objectives change and the relationship evolve. The rings can be threatened only if the expected benefits of the relationship growing ever smaller, or if the behavior of any of the parties is considered opportunistic, (FUSCO and SACOMANO, 2009).

In this context, the relationship and the types of relationships should establish the density, the centralization and fragmentation of the network, establishing measures of position of the actors in the network. Figure 1 shows a model of communication with firms in networks, where using contracts for systems of cooperation and alliance relationships between organizations.

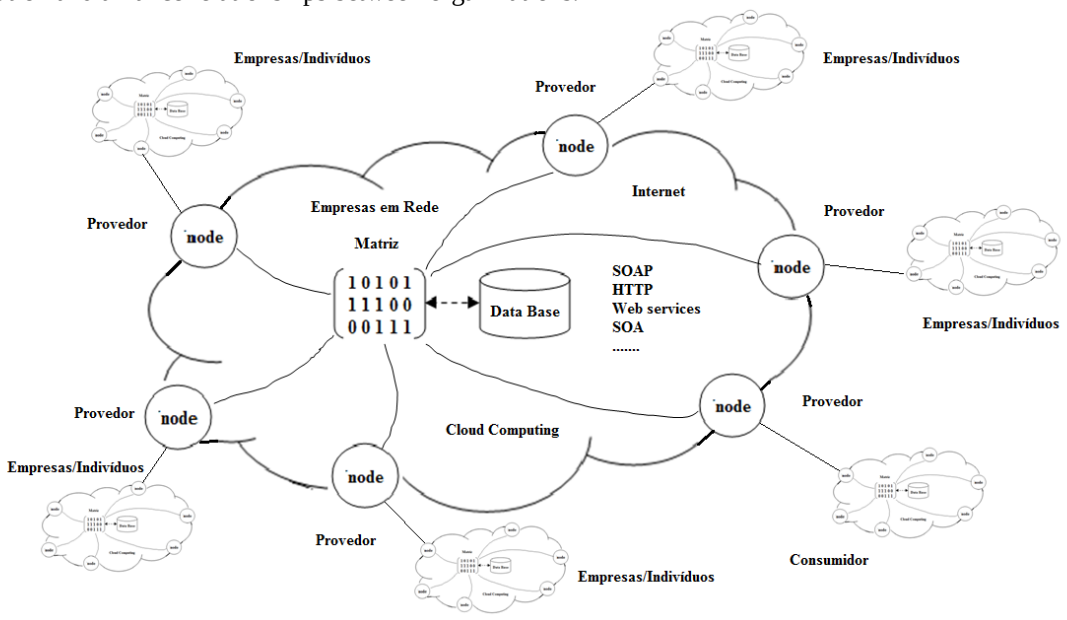

Figure 1-business networks, Contracts, Departments, Teams and Individuals, author.

The model presented in Figure 1 (proposal of this work) represents a set of *nodes* (nodes) or cloud computing providers that interconnect dynamically through a structure of type array. This structure is the mechanism responsible for locating services between providers and its main components are the array (static structure), in the tree structure (structure dynamic), graphs (search techniques and locations) and database (or knowledge base) where are located the services described using the architecture SOA (*Service Oriented Architecture*), *web services*technologies, protocols, HTTP (*Hypertext Transfer Protocol*), SOAP (*Simple Object Access Protocol*) and features of the *internet* itself. Subnets are comprised of companies or individuals that can be of type consumer or supplier of services and are responsible for the exchange of communication within the network (network Companies).

2.2 Practice of service design principles

A design paradigm, in the context of business automation is considered the approach that governs the design of logic, which consists of set of rules (or principles) complementary that define collectively the broad approach represented by paradigm. The fundamental unit of service-oriented logic is the *service* and by itself represents a distinct design paradigm. Each service gets its own distinct functional context and has a set of capabilities related to this context via public service contract (ERL, 2009).

In this context, the practice and the fundamentals of service contracts allow for greater interoperability, alignment of business and technology domain, greater organizational agility, greater diversification of suppliers, lower workload, low service coupling, service abstraction, and reuse of service and reduced amount of application-specific logic.

2.3. Application of integration of cloud computing and networking companies

Cloud computing is a set of virtual resources easily usable and accessible *hardware* (physical), *software* (logical), and services development platform. Its resources can be dynamically reconfigured to fit a workload (*Workload*) variable, allowing the optimization of the use of resources and replace it assets. These features and services are developed using new virtualization technologies, which are: application architectures and service-oriented infrastructure and technologies based on the internet as a means to reduce the resource usage costs of hardware and software you used for processing, storage and networking, (ERL, 2009). For the purposes of integration with corporate networks are analyzed the fundamentals the inter-organizational network, intra-organizational and inter-personal.

Inter-and intra-organization networks are special cases of interpersonal networks. In business, relationships are conducted between individuals (interpersonal network), because they are the ones who start an Alliance or contact between these companies. The inter-organizational network is networks based on the relationship between companies or organizations in General. Already the inter-organizational network is networks of individuals in organizations, (LAZZARINI, 2008). In this context, the use of infrastructure virtualization allows establishing flexible structures to meet the demands of business and structure dynamically strategies and corporate goals, as shown in the figures 2 (classic networking companies) and Figure 3 (proposed model of networking companies).

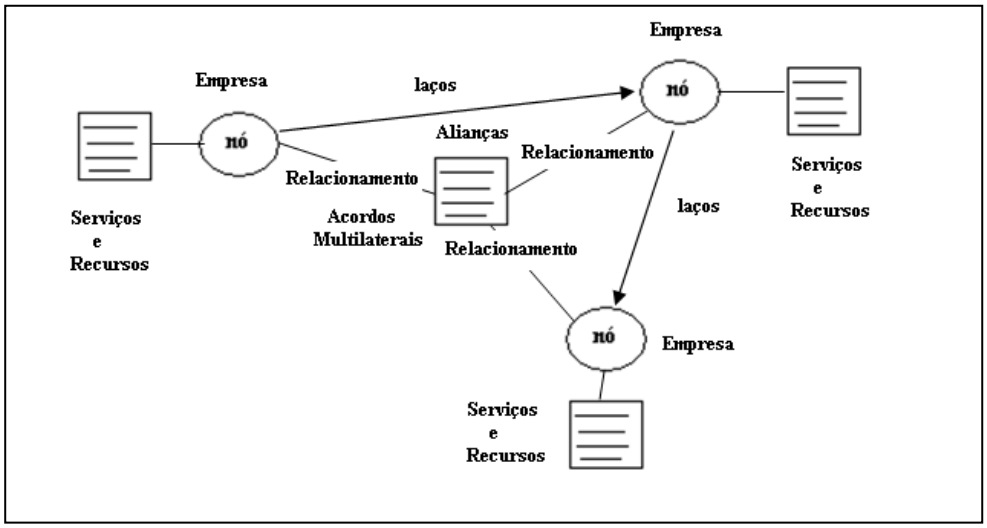

Figure 2-Business networking and relationships between businesses, the classical model, author.

Figure 2 shows the classic model of a relationship structure of firms in networks, where the nodes are companies where each one of them describe their services and provide their resources to be shared. In the Centre of the relationship are the alliances that are established between companies and multilateral agreements in accordance with the rules and policies of relationships established between these companies that must be met. The problem observed for this type of model is the static relationship, lack of control and transaction management services. There is no application of technological resources available in the market and many ties clusters as shown in Figure 3 below.

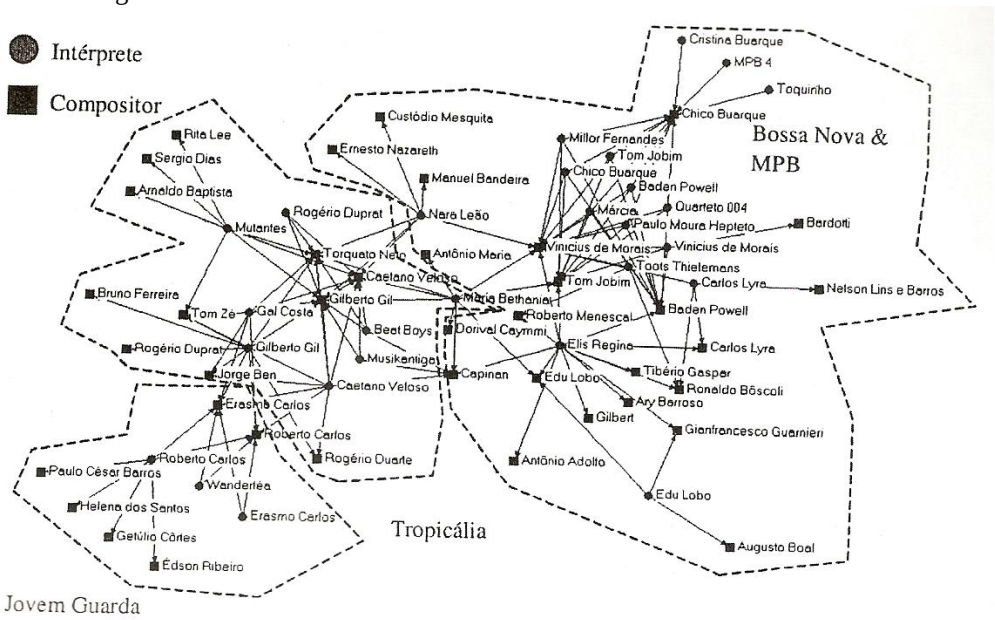

Figure 3-Network intérptretes and composers of Brazilian music period 1958-1961. Source: Kirschbaum and Vasconcelos (2007).

The figure 3 shows a network of interpreter of composers of Brazilian music using a model of relationship and interconnection between music styles and compositions of the 1958 and 1961 season. The figure 4 shows an improvement relation using the techniques of cloud computing and web service where companies, individuals or groups of individuals who can form alliances or service contracts using the resources of service orientation (SOA) technologies and communication protocols available over the internet.

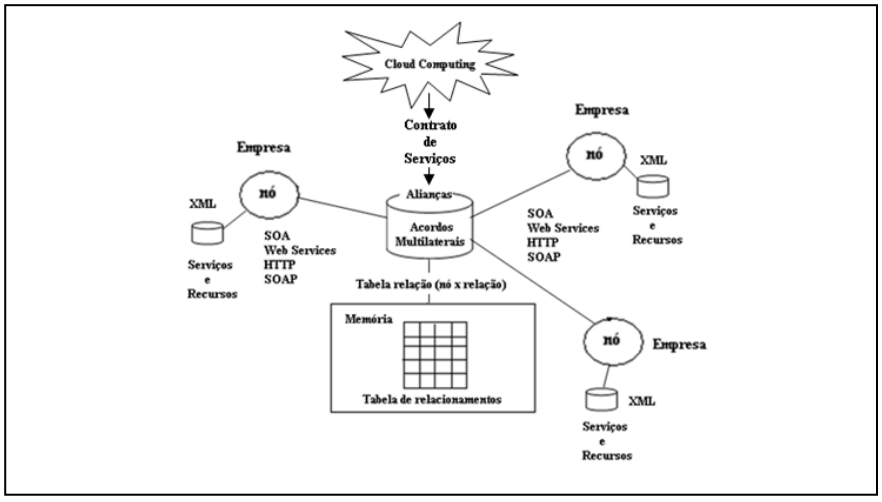

Figure 4-Companies in networks and relationships between the companies, proposed model, author.

Figure 4 represents a proposed model for setting up companies in network with the use of web technologies, service-oriented architecture, cloud computing and communication protocols for exchanging information and messages between the enpresas. The nodes represent companies, where each one of them have their own services and resources in their own bases. At the center of this control are multilateral agreements

where are established alliances and service contracts using virtualization techniques of cloud computing. The main search engine is responsible for the relationship table cotnrole and dynamic management of firms that tracks the relationship between the nodes for the exchange of information using the techniques of transaction services.

2.4. *Web services* integration with service-oriented architecture

The SOA is an architectural model agnostic to any technology platform, in this way companies can get their strategic objectives associated with service-oriented computing. In the current market, the platform of more associated with technology? , realization of SOA is the *web services*. This platform can be distributed e possui collections of standards and specifications that provide service description language, definitions from schemas, protocols of accesses to simple objects, Integration and discoveries of universal basic Profiles descriptions, message level security, transactions, cross-service and reliable message exchanges. All this are being provided by the technology of *web services* platform, (ERL, 2009).

In this context the following communication standards interfaces based on service contracts and independent implementation technologies given the loosely coupled paradigm. Coupling is the relationship established between the service contract, the logic and the resources that are encapsulated.

III. METHODOLOGY AND MATERIALS

Models will be developed and made available in cloud computing applications, for depends on of the foundations proposed in this project. In addition will be monitored and simulated in a intraorganizacional network within the IES (higher education Institution) in the undergraduate program in computer science and information system.

3.1. Scope of the experimental work

Will be built an application with service orientation structures (SOA) and development platforms (*web services* and *cloud computing*) based on the fundamentals presented according to the main authors of literature FUSCO and SACOMANO, (2009); ERL (2009); VERAS (2009 and 2010); LAZZARINI (2008); DEITEL (2005) and JORGESEN (2002).

The system will be analyzed and compared with the concepts of networking companies according to their use in cloud computing and virtualization technologies of *web services*. The application of time planning for the courses of computer science and information system is part of the proposed system and allows them to be shared among engineers using the distribution and d virtualization to cloud computing. Apply the features of intra-organizational networks according to the organizational structure of each unit who are geographically distributed that IES (Higher Education Institution).

3.2. Project architecture

Figure 5 shows the architecture of the integration *cloud computing* with companies in networks, using *web services* with SOA model, the communication protocol HTTP (*Hypertext Transfer Protocol*), the interfaces WSDL (*Web service Description Language*) and the default language XML (Extensible Markup Language).

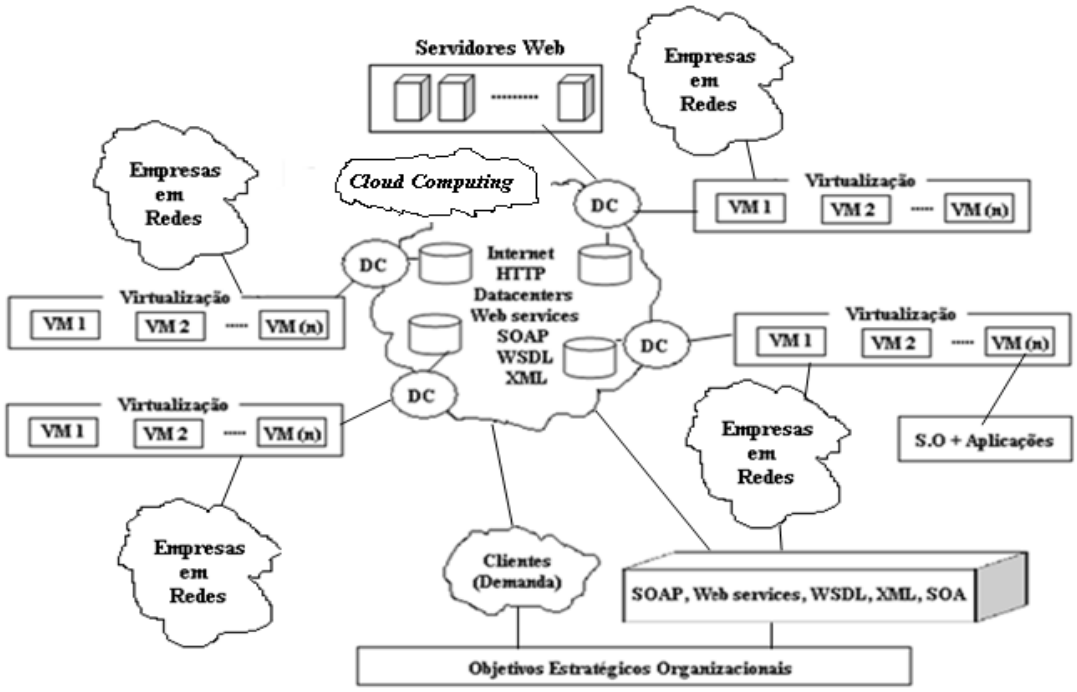

Figure 5 - Architecture integration companies in networking, cloud computing, web services and SOAP, author.

Figure 5 shows the architecture of the proposal of this work and its principal components. In the Centre is implementing ads techniques and resources available by cloud computing that are the *internet*, HTTP protocols, the *datacenters*, technologies *web services* SOAP protocols (*Web Services Object Access Protocol*), WSDL, and XML.

3.3. Details of the components

The infrastructure will be developed and the key components to extend the capabilities of communication between companies and networks enable service transactions between organizations.

In this project the main components are: the doors of communication between the structures of clouds Computing Virtualization, networking organizations, SOA service models and technologies of *web services*.

3.4. Tools used

The main tools used are: the hosting cloud computing, *web services*technologies, the SOA services models and techniques of intelligent search and dynamics of the tree and graphs.

3.5. Application environments

The environment for realization will be built on a network of educational company of type intraorganizacional. The infrastructure for the implementation of the case study should be built within a University where the departments need to be interconnected on networks of computers. Aiming at the implementation of this work is its implementation with cloud computing and the demonstration of its advantages.

3.5.1. Measure of network structure

The structure of a network can be characterized by their general structure or the way the ties are established between nodes (actors) of a network. However the assessment of the structure of this network can be accomplished through the density, centralization and fragmentation. A network is dense when several actors are connected to each other. The measure of density can be easily computed. Considering that there are no actors for certain context and ties not directional, the maximum number of links that it is possible to be established can be applied using the formula is N(N-1)/2 this occurs when all actors are connected to each other. Already the measure of density represents the number of observed network ties, dividing by the maximum number of links that is allowed for this network. However, if the actors don't have a bow to each other, the measure of density is equal to zero and if all actors were connected to each other, the density is equal to one (LAZZARINI, 2008).

A network can be coordinated by applying the concepts of network centralization. In this case the central actor joining several other actors who are not connected with other groups, this central actor then plays

the role of coordinating and controlling other actors. According to Lazzarini (2008), the central actor can add to the actors don't low density plants offering guidance to perform certain task. Density and centralization indicate how the network (as a whole) is structured. Already a fragmentation are disconnected subnets where the actors don't relate to other groups of actors. A high fragmentation means that there exists a strong cohesion, but locally the actors may be strongly cohesive.

Regarding the measurement of position of the actors in the network (known as positional indicators), she shows how a given actor can extract benefits according to their position in the network and the main indicators used are classified as grade and centrality of middle (LAZZARINI, 2008). Degree centrality evaluates the number of ties that an actor has with other actors. Already the centrality of middle, evaluates the degree as a particular actor is linked, directly or indirectly (actors who are located in different parts of the network). According to Wasserman and Faust (1994) the calculation of centrality of means to evaluate the measure for each actor, verifies that this actor is part of the minor road that connects each pair with other actors in the network, because the smaller the path, the greater its centrality to middle. So an actor with high centrality of middle allows this actor is connected directly or indirectly to various parts of the network.

The figure 6 show the model architecture (octal) proposed for the construction of enterprises in service networks, in the form "*octal*", graphs, trees and arrays. However the mathematical formula used was N(N-4.5)/2 for numbers of bonds observed (totaling 20 actors from the root) and the measure of density, the number observed on the network divided by the maximum number of links. The value of 4.5 is the result of the total number of elements in the first row divided by 2, which corresponds to the maximum number of main actor's relationship with the other actors in the network.

	A	B	C	D	E	F	G	H	I		
A		1		1		1		1		A	
B	1		1		1		1		1	B	
C		1		1		1		1		C	0,5
D	1		1		1		1		1	D	
E		1		1		1		1		E	1
F	1		1		1		1		1	F	
G		1		1		1		1		G	1
H	1		1		1		1		1	H	
I		1		1		1		1		I	1
	A	B	C	D	E	F	G	H	I		
											1
										Total =	4,5

Figure 6 Matrix octal structure of an enterprise networking, author

Figure 7 represents the array and network configuration "octal" balanced in relation to the actors connected on that network. The merged form defines the control mechanism of trade in communication with reducing conflicts between these actors. Then define the octal structure as shown in Figure 6. The structure can be increased or decreased in accordance with the existing interactions between actors. The general formula for calculation can be defined as N (N-(N-d))/2, where “d” is the total number of diagonals counting from the main diagonal. For N = 11 (number of actors in the network) the number of observed ties has approximately 30 related actors (above the main array), represents (11 (11-5.5))/2 = 30.25 relationships between actors.

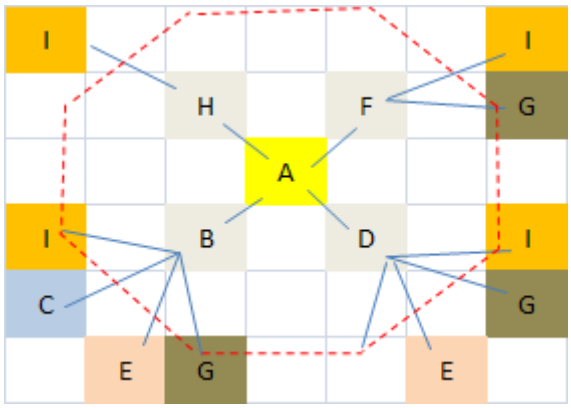

Figure 7 octal structure of an enterprise networking, author

Figure 7 shows the structure in octal format of actors, relations between these actors that determine the measures of network structure "octal" proposed in this work. The setting was obtained of the array shown in Figure 6, which determines the balanced relationship based on the concepts of density, centrality and of fragmentation. For this it is necessary to establish the new configuration (based on the array of figure 6) forming the octal model.

The actors B, C, G and I are connected directly or indirectly to the actors of the inner layer which are the actors B, D, F and H and with the central actor, moreover, can be connected or disconnected from the network to establish their communications and exchanges of information. On the new architecture can exist several different ways of settings, keeping the consistency of the initial structure. The new structure may be linked to their peers that have the same types of businesses or services (played by the American actors that has the same color) or to connect with groups that perform services or sell different products (represented by actors who have different colors), as shown in Figure 8.

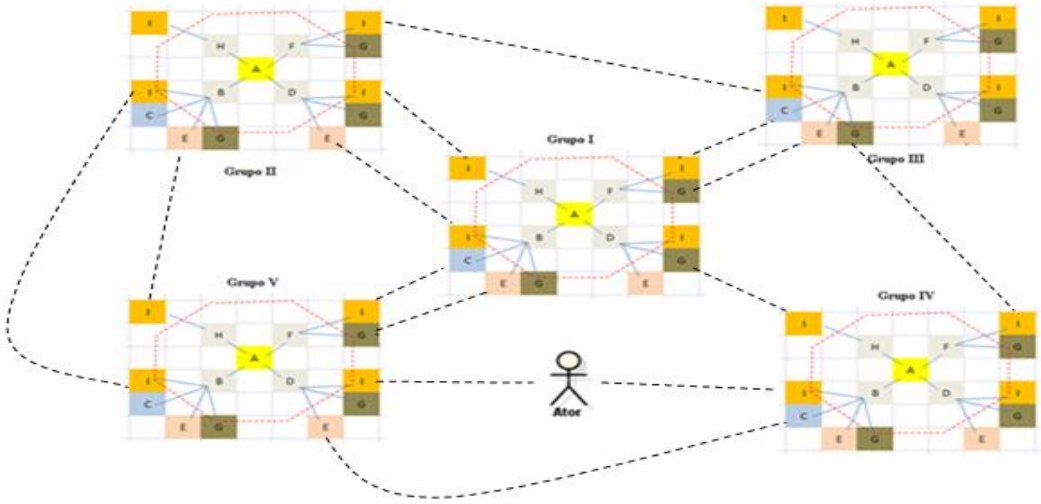

Figure 8 Architecture octal structure of a company in interconnected networks to other networks, author

The architecture of figure 8 shows the exchange of services between actors of different groups to achieve their common goals. Each group has its main actor by applying the techniques of measures of density, centralization, fragmentation, and degree of centrality. In this way it is possible to apply also the techniques of structural holes in order to obtain advantages in the negotiations. The actor (represented in Figure-8) shows how can extract more benefits according to its positioning between the groups on the network. The nodes (*nodes*) that have the same colors have in common the same interests and types of services or products in common (companies in the same sector), nodes (*nodes*) of different colors (interconnected) represent alliances with adjacent sectors companies but which complement each other.

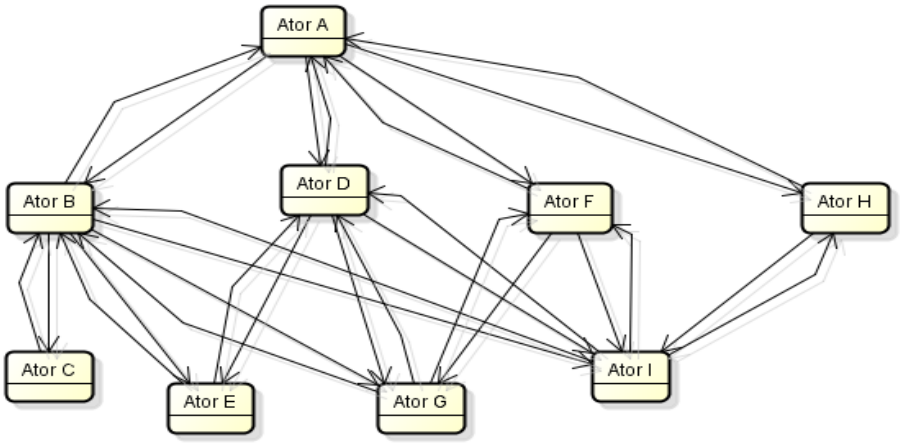

Figure 9 Structure Structural Holes company networks, author

In Figure 9 actors represent behaviors (Exchange or sharing services) of the companies or individuals belonging to companies in networks. Right now there is Exchange of information in the search or location of services provided between the actors to combine existing resources and obtain advantages in distinct parts that are disconnected from the network. Conform Lazzarini (2008), the lack of links between actors creates a structural hole that can be exploited. The benefits of this exploration (using the graph in Figure 8) may also allow the actors to combine existing resources in others parts of the network.

Networks with different levels of density correspond to the number of loops observed in the network about the maximum possible number of ties that can be established between actors (LAZZARINI, 2008). The results obtained from the comparison between the "classic" model and the model "octal" have as values for the densities (for a total of 20 actors and 9 ratios) of 99.87% for model performance "octal", while the "classic" model a value of 55.55% of performance. According to Coleman (1988), the density has a fundamental theoretical significance, because it attaches to dense networks a peculiar function, allowing the maximum flow of information between actors.

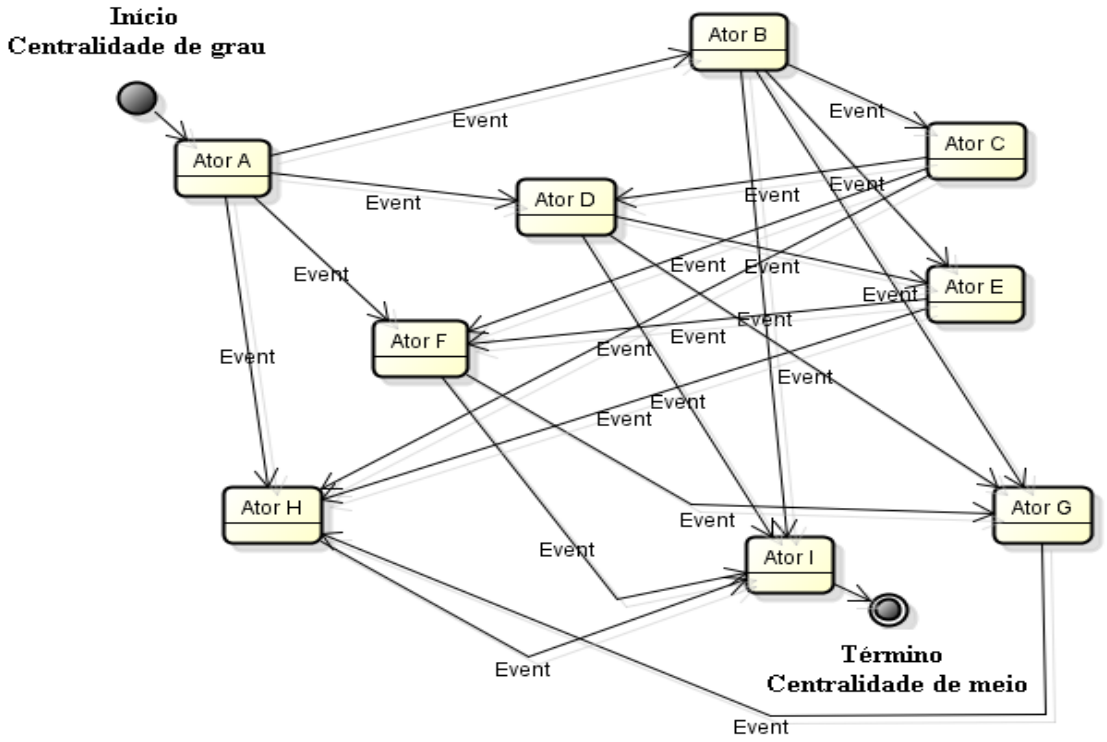

Figure 10 octal graph structure of a company in networks, author

Figure 10 shows the actors, and state transitions between these actors to Exchange or share services and in addition, define the behavior of firms in networks. In this phase it is possible to establish the types of possible relationships to network and establish the position of the actors and the measures of centrality of these actors to configure the best alliances and ties.

Figure 11 shows the tree structure of an octal architecture. The structure allows analyzing the intensity of relations in horizontal and vertical levels, as shown in the degrees of intensity of colors in horizontal line 1 level of the hierarchy.

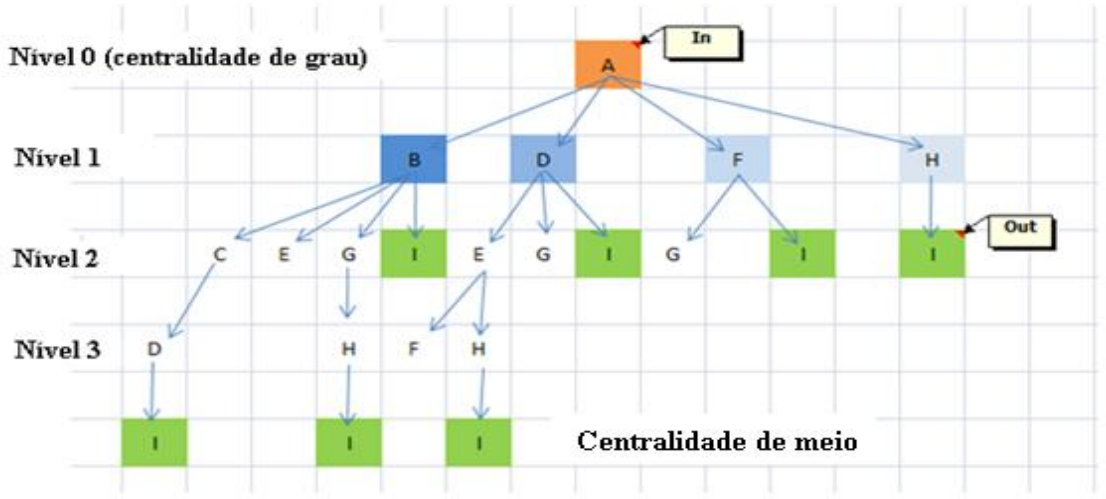

Figure 11 An octal tree structure of an enterprise networking, author

Figure 11 shows the structure in hierarchical levels, where represent the measures of position of the actors according to their centrality that can be of degree or of kind. Centrality of maximum degree centrality of the central actor (root), already the centrality of middle evaluates the maximum degree of interconnectedness that an actor is connected directly or indirectly with other actors that are disconnected in different parts of the network, where all entrances and exits are focused on a specific actor (in the example in Figure xx, corresponds to the actor "I"). The darker blue color shows that has a centralized of greater degree, since there is a larger number of ties that the actor has in relation to other actors and the lighter blue color less number of interconnected ties to this actor.

Structural holes is the absence of a bond between disconnected networks. According to Burt (1992), the non-existence of ties between actors of disconnected networks creates a structural hole and allows opportunities in negotiations to be presented. Actors must seek positions on your network in order to avoid redundant links (must make contacts with actors who do not have ties with each other). An actor can be represented by individuals or businesses that relate to other networked enterprises to obtain benefits and resources by connecting to the various portions of this network as shown in Figure 12.

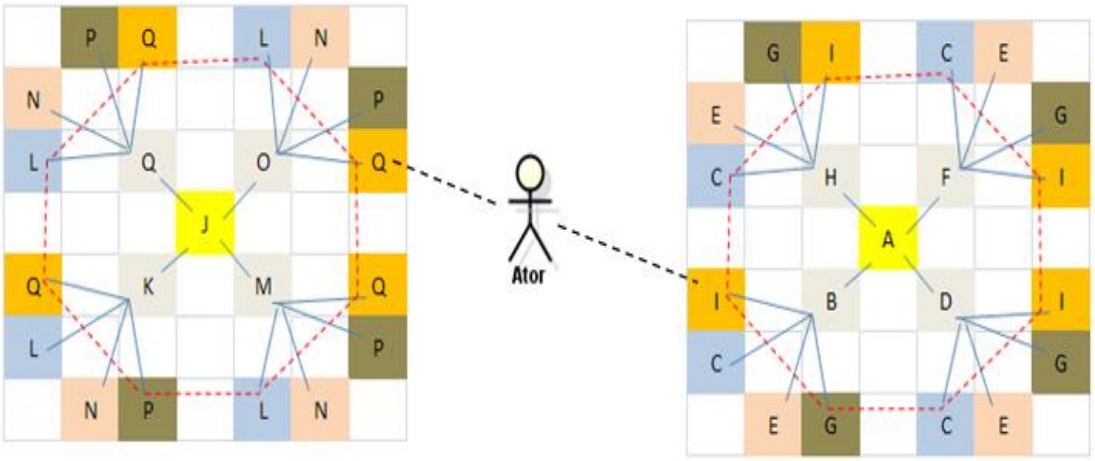

Figure 12 structural hole in a company "octal" network, author

Figure 12 shows the octal structure where the actor (can be individuals or companies) connected to the other companies of different networks but that has in common services that can be shared. This actor has just interconnection using informal structures of relationship with high centrality of middle.

Actors must seek positions in your network and get contacts with actors who do not have ties with each other, because it allows actors can combine existing resources in separate parts and disconnected from a particular network (BURT, 1992).

An organization that wants to develop a new product or service can form alliances with companies of different sectors initially disconnected (LAZZARINI, 2008). Networks of small firms allow company to preserve their specialization in a particular area and reduce contractual risks in market transactions (GETS WORSE, and SABEL, 1984; POWELL, 1990). Thus, an inter-organizational network can be considered as a new type of organization of several autonomous units and connected by means of links of different types. These types of bonds can be of type vertical or horizontal (ZENGER and HESTERLY, 1997). A vertical chain is a network of ties sequentially chained (LAZZARINI 2008). A vertical chain allows you to manage sequential interdependencies between the various actors involved, where each actor forensics a product or service that is the input of the other actor (THOMPSON 1967). Several authors have analyzed how to organize vertical chains: what types of agreements between actos can be established, to ensure that there is compliance with these agreements and how to provide changes to increase the quality or reduce costs along the chain (ZYLBERSZTAJN, 1995; ZYLBERSZTAJN and FARINA, 1999; NICKERSON et al., 2001).

A horizontal network occurs between companies of the same sector or companies of adjacent sectors (LAZZARINI, 2008). Horizontal networks may establish relationships with companies belonging to sectors that are complementary to each other (BRANDENBURGER and NALEBUFF, 1996). Horizontal networks feature two types of interdependencies between actors that sãod and aggregation and reciprocal. A inter-dependencies of type aggregation are weaker (THOMPSON 1967). Contact resulting from common interests, it is not necessary to question and develop intense relations since they may be momentary (SCHNEIDER, 2004). Figure 13 shows the octal structure that aggregates the concepts of vertical and horizontal networks and dynamic management utilizing control techniques for cloud computing, SOA and *web services*.

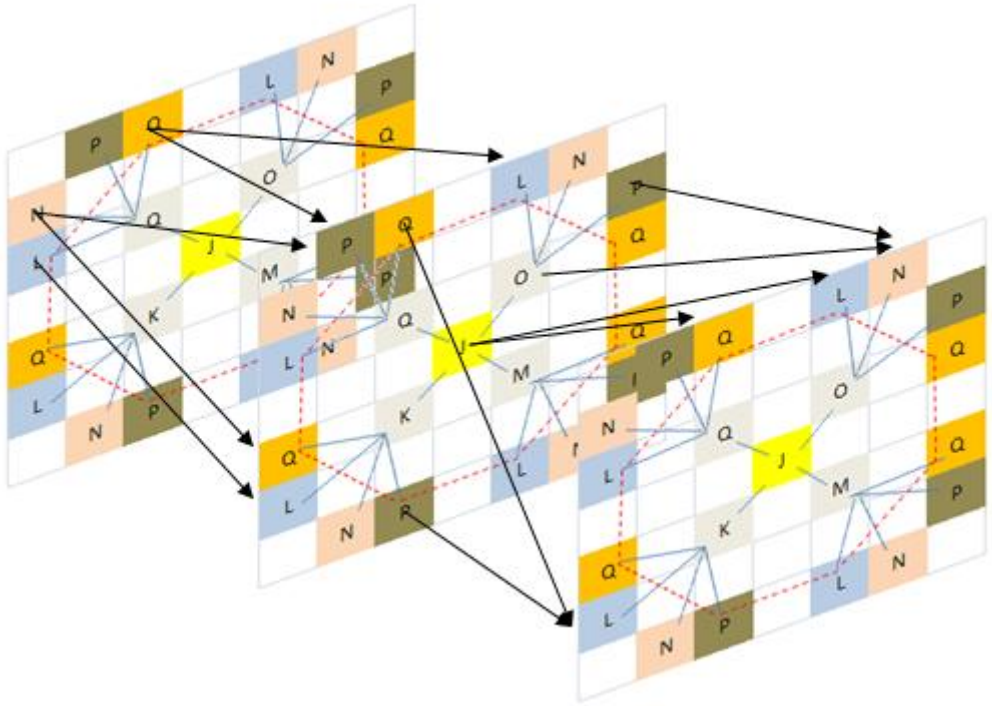

Figure 13- Structure of a network enterprise "octal" in the vertical, horizontal and netchains networks format, author

With the goal of establishing and structuring a more stable network, the purpose of this work presents the results of an analysis for enterprise configuration on networks for the distribution of services using *web services* and cloud computing techniques. The table 1 uses the shape of calculation model density maximum number of loops and the measure of density proposed by Lazzarini (2008). Then apply the calculation model for

distribution of services of the *octal* architecture and the graphic models resulting from its calculations as a comparison of their results, in addition to their comments and discussions.

Medidas	Atores (nós)	Modelo clássico (resultado) "laços x densidade"	Modelo Proposto (Resultado) "laços x intensidades"	Observações
Número máximo de laços	2	1 (laço)	1 (laço)	A relação dos laços e a densidade permanecem iguais.
Medida de densidade		2 (densidade)	2 (densidade)	
Número máximo de laços	3	3 (laços)	3 (laços)	A relação dos laços e a densidade permanecem iguais.
Medida de densidade		1 (densidade)	1 (densidade)	
Número máximo de laços	4	6 (laços)	6 (laços)	A relação dos laços e a densidade permanecem iguais, porém com aumento de densidade para ambos.
Medida de densidade		0,666666667 (densidade)	0,666666667 (densidade)	
Número máximo de laços	5	10 (laços)	10 (laços)	A relação dos laços e a densidade sofrem alteração, no entanto o modelo proposto mantém o valor anterior e ocorre a diminuição do valor para o modelo "clássico".
Medida de densidade		0,5 (densidade)	0,666666667 (densidade)	
Número máximo de laços	6	15 (laços)	10 (laços)	A relação dos laços e a densidade sofrem alteração, no entanto o modelo proposto mantém o valor anterior e ocorre a diminuição do valor para o modelo "clássico".
Medida de densidade		0,4 (densidade)	0,666666667 (densidade)	
Número máximo de laços	7	21 (laços)	10 (laços)	A relação dos laços e a densidade sofrem alteração, no entanto o modelo proposto mantém o valor anterior e ocorre a diminuição do valor para o modelo "clássico".
Medida de densidade		0,333333333 (densidade)	0,666666667 (densidade)	
Número máximo de laços	8	28 (laços)	10 (laços)	A relação dos laços e a densidade sofrem alteração, no entanto o modelo proposto mantém o valor anterior e ocorre a diminuição do valor para o modelo "clássico".
Medida de densidade		0,285714286 (densidade)	0,666666667 (densidade)	
Número máximo de laços	9	36 (laços)	10 (laços)	A relação dos laços e a densidade sofrem alteração, no entanto o modelo proposto mantém o valor anterior e ocorre a diminuição
Medida de densidade		0,25 (densidade)	0,666666667 (densidade)	

				do valor para o modelo "clássico".

Table 1 Comparative Table of Companies in networks (classical model) and distribution services in cloud computing, the author.

Table 1 shows the results obtained from the comparison between the measurements of maximum figures and ties in relation to densities of classical models and model "octal" by the amount of a company's existing actors in networks. From the aggregation of 4 actors and 6 ties, the network suffers change compared to densities. In the classic model network performance begins to decrease while the performance of the model "octal" holds steady as the numbers of actors and increase ties. The increase of number of nodes does not allow calculating the extent necessary when the actors in the network increase with the analyses of the actual performance of the network. As the authors Lazzarini, Greift, Holf, Stiglitz and Jones, the values obtained from densities of a network establish measures and levels of relationships of important information in a network and this justifies the importance of the results of the density of a network. The results generated by the octal model shows the critical limits to establish links between the nodes that can be a relationship between individuals or companies.

In dense networks it is possible to apply sanctions to groups of people who do not comply with the rules established by the groups. In dense networks allow the actors to apply collective sanctions, because this type of service (LAZZARINI, 2008). As (Greif ET al., 1994), this type of mechanism is the basis on which the informal groups of trade and strengthening of credit (HOLF and STIGLITZ, 1990). So the more dense is a local community, the easier it will be to support cooperative relations, because the density aims to facilitate cooperation between the actors (LAZZARINI, 2008). In addition to facilitate communication among the actors in creating a culture based on norms and values developed over time, in pursuit of common goals (JONES, 1997).

The table 2 describe the results obtained from the analysis of the density of the "classic" model in relation to the proposed model of density by applying the model of enterprises in services distributed networks with the SOA, *web services* and cloud computing. The work also has the aim of showing the benefits of this new architecture for a service delivery configuration using dynamic virtualization techniques, autonomous which can behave in the form synchronized or not, according to the needs of resources sharing in cloud computing.

	Modelo de cálculo ("clássico")			
		LaçoMax=	36	Número máximo de laços (Não Direcionais)
nós (atores)	laços(Obs)			
9	20			Não pode haver atores sem laços.
		Densidade=	0,555555556	Medida de densidade
			0,277777778	

Figure 14 -Model (classical) calculation of a company's networks, author

Figure 14 shows the calculation model used for definitions and analyses of comparisons of maximum densities and ties for quantities of actors and established ties between them. The results are generated as shown in the table 2.

Modelo "clássico"			
nós(atores)	Densidade(50%)	LaçoMax	Densidade
1			
2	0,50	1	1,00
3	0,50	3	1,00
4	0,50	6	1,00
5	0,10	10	0,20
6	0,24	15	0,47
7	0,24	21	0,47
8	0,25	28	0,50
9	0,25	36	0,50

Table 2 results obtained from the model (classical) calculation of a company's networks, author

In table 2 shows the values of the simulations and the values generated for maximum density limits and of 50% of its value. For we (actors) and ties maximum establish down between the actors (total 9 actors), interdependencies increase exponentially and the describe flow of information quickly. In this way communication and the exchange of transaction services are unstable. Figure 15 graphically shows the results generated by the simulation.

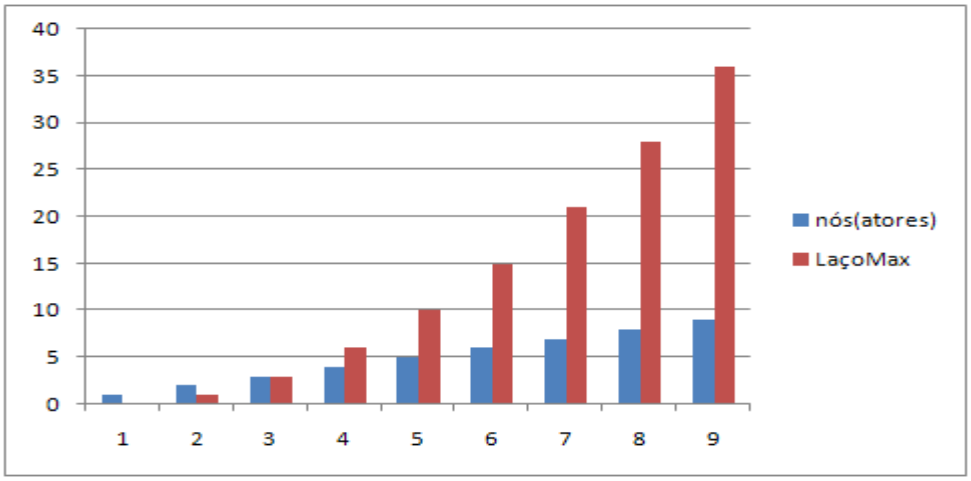

Figure 15 - Model (classical) graph of the calculations of a company in networks of actors in relation to bonds, author

Figure 15 represents the results of the analysis of the numbers of nodes in relation to bonds or relationships established between nodes. As there is an increase in the numbers of us there is a growth in the amount of necessary links required to establish communication or exchange of services, which is reduced in proportion to 8/36 (for a total of 9 us) the intensity of this relationship as you increase the number of nodes. In Figure 16 shows the results generated for the increase of us relative density (information flow).

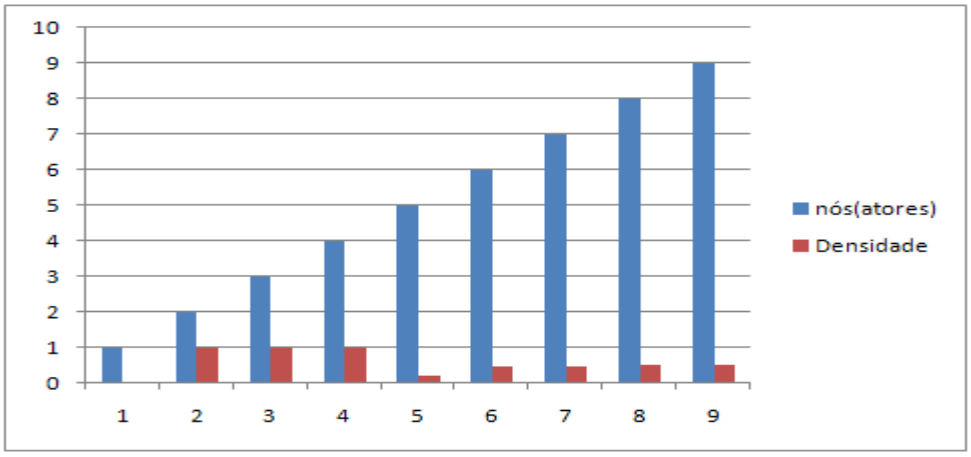

Figure 16 - Model (classical) graph of the calculations of a company in networks of actors in relation to densities author

Figure 16 shows that the increase of us above 50% there is a significant drop in the density. To maintain the stability of information flow between these actors, the limit of reliability of the relationship remains around 1/4 and 0.5/9 (for a total of 9 actors) of that relationship, which equates to 25% and 0.5% risk analysis analysis (margin of error = 20%). The figura 17 shows the calculation model to generate an analysis between the two models presented (classic and octal).

	Modelo de cálculo("octal")			
		LaçoMax=	20,0025	Número máximo de laços (Não Direcionais)
nós (atores)	laços(Obs)			
9	20			Não pode haver atores sem laços.
		Densidade=	0,999875016	Medida de densidade
			0,499937508	

Figure 17 - Model (octal) of calculating a company's networks, author

Figure 17 shows the application to simulate the calculations generated in relation to the numbers of actors and ties established between them, beyond the values of the measures of densities. Table 3 shows the results applied to the octal model.

modelo proposto "octal"			
nós(atores)	Densidade(50%)	LaçoMax	Densidade
2			
3			
4			
5	0,45	1	0,89
6	0,14	4	0,92
7	0,47	8	0,93
8	0,48	13	1,30
9	0,49	20	0,99

Tabela 3 - Resultados obtidos do modelo (octal) de cálculo de uma empresa em redes, autor

In table 3 notes the implementation of the proposed model (octal) increases the value of its density with increasing of number of nodes and links, also sets a limit of ties to the maximum use of information flow (or exchange of services and resources) between the actors. Figure 18 shows graphically the results generated from the proposal of this work.

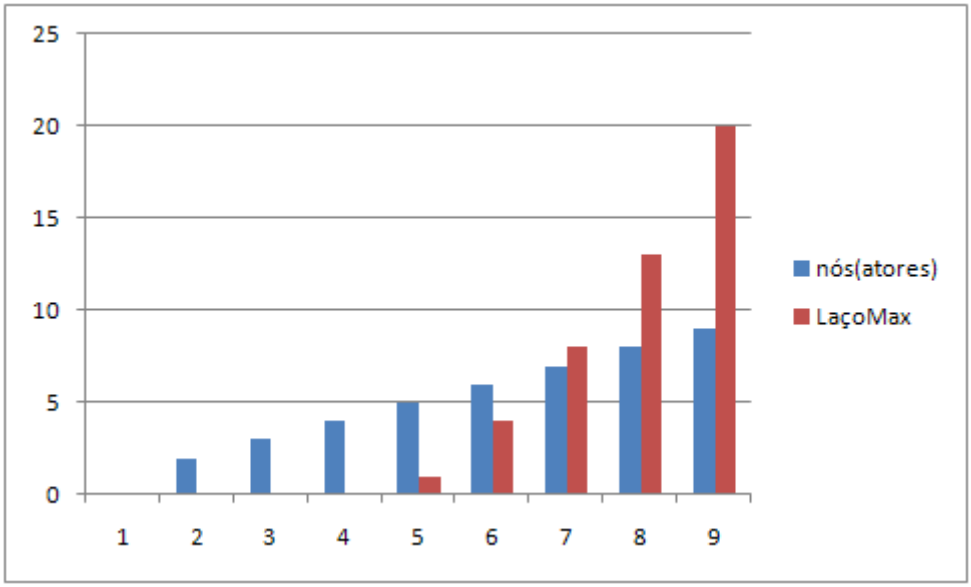

Figure 18 - Model (octal) chart of the calculations of a company in networks of actors in relation to bonds, author

Figure 18 shows the results generated by the simulation and the relationship of nodes and ties established between these actors to the octal model. It is observed that the increase of the influence ties only when the amount is above 50% of the total number of nodes on the network at a maximum ratio of 8/20 or 8 nodes to 20 ties (for a total of 9 nodes). This shows that the octal model has increased efficiency in its application to relations number above 50% of relationship between individuals or companies. Figure 19 shows graphically the results generated by the model octal.

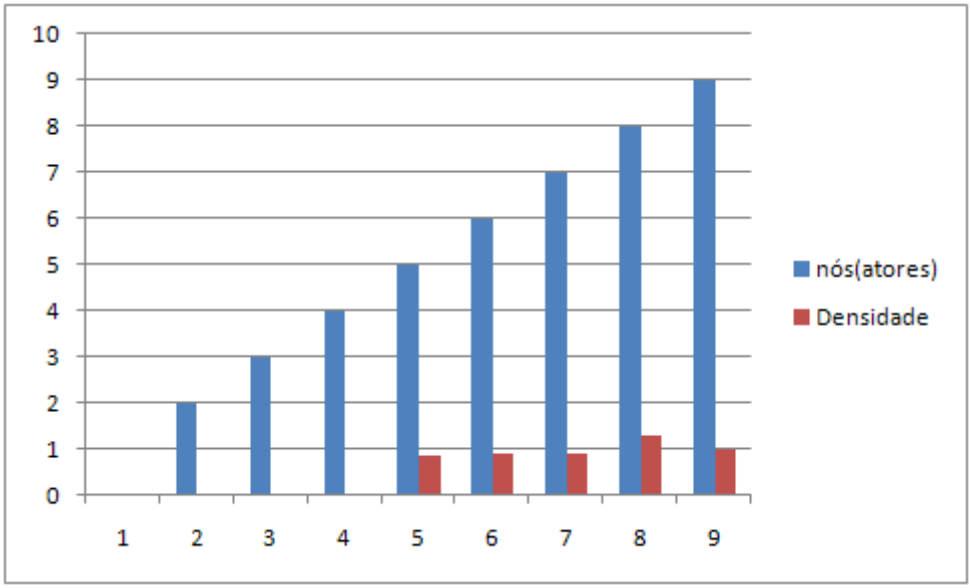

Figure 19 Model (octal) chart of the calculations of a company in networks of actors in relation to densities author

Figure 19 shows the generated results to the analysis of the simulations between actors and density (information flow) for model octal. It is observed that the increase of us regarding the density remains stable or establishes a limit to establish service contracts between individuals or companies of 0.9/5 and 1/9 (for a total of 9 actors) which equates to 18% and 11% of risk analysis of contracts (margin of error = 7%).

nós	Num. de laços máximo "Clássico"	Cáculos (densidade) "Clássico"	Num. de laços máximo "Octal"	(Cálculos de densidade) "Octal"
1				
2	1	1,00		
3	3	1,00		
4	6	1,00		
5	10	0,20	1	0,89
6	15	0,47	4	0,92
7	21	0,47	8	0,93
8	28	0,50	13	1,30
9	36	0,50	20	0,99

Comparative Table 4 - obtained from the model (classical) relative to the model "Octal" a business networking, author

The table 4 shows the results of the simulation loops and densities for the octal model. For a total of 9 we the density for the classic template has greater efficiency when the numbers of links are below 50% of the totality of its nodes. So for quantities of us above 50% of the total of us the octal model has its improved efficiency in almost 100% of its implementation and performance, also sets a limit for the intensity of their relationship. Figure 20 shows the result of the comparison charts of two model.

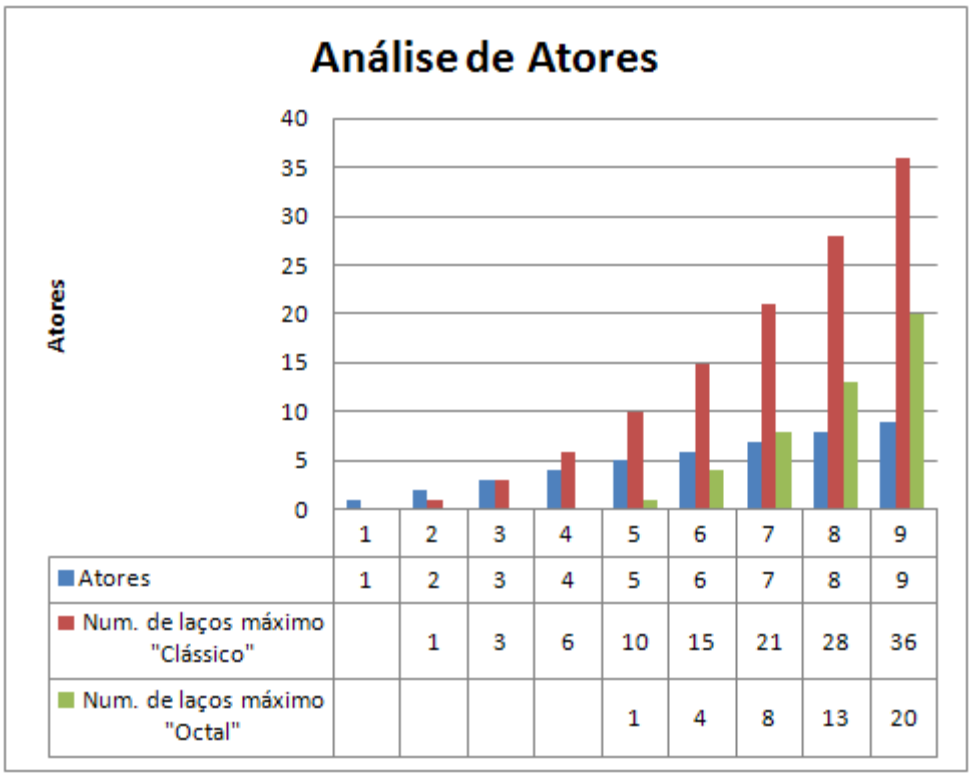

Figure 20 - comparison chart obtained from the model (classical) relative to the model "Octal" Actors and maximum bond of a company in networks, author

Figure 20 shows the results of the comparison between the two models presented (for a total of 9 nodes). In the classic model network performance begins to be perceived already in the early ties or service contracts. The landmark and leveling the network happens to the classic model when the network reaches 30%, for model octal your performance starts from 70%. The ratio of the intensity of relationship in average is 8/21 for the two models presented (40% efficiency for model octal), besides the octal model sets a limit of interconnection between individuals or companies. Figure 21 shows the relationship of density and actors of a network.

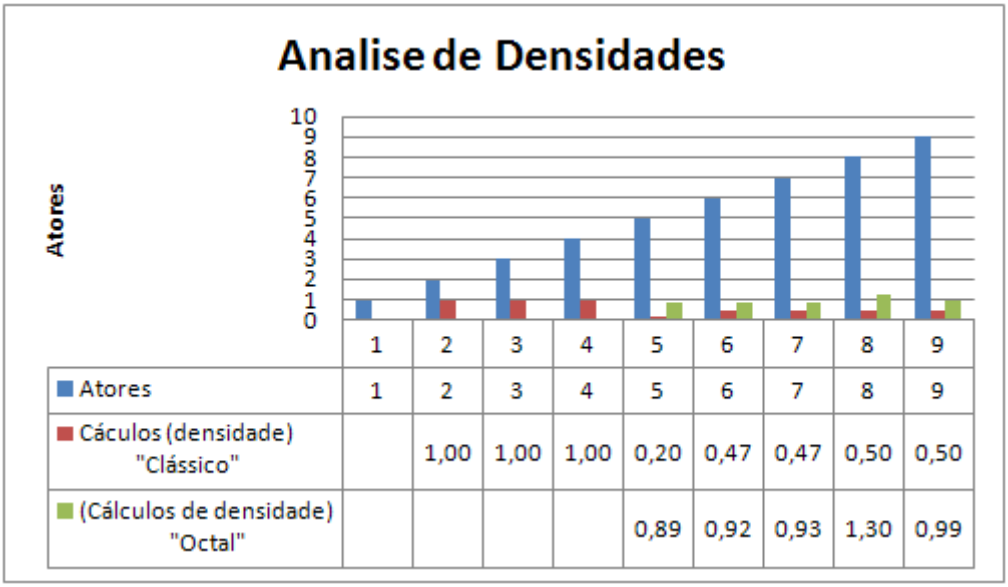

Figure 21 comparison chart obtained from the model (classical) relative to the model "Octal" actors and densities of a company in networks, author

Figure 21 shows the results of density in the graphic form of the models presented (for a total of 9 knots). While the model remains stable the octal interdependency the relationship between the actors in a network there is a reduction of density or flow of information between the network actors when numbers of actors achieve 50% of its entirety. To the octal model its density or information flow capacity increases when the number of actors increases. Figure xx shows the performance between the two models presented.

Análise comparativa de desempenho das densidades do modelo "Clássico" e "Octal"						
Atores utilizados na configuração	Num. De laços utilizados	Valor da densidade "Clássica"	Desempenho da densidade em % "Clássica"	Valor da densidade "Octal"	Desempenho da densidade em % "Octal"	Observações
9	1	0,027	2,7	0,049	4,9	
9	2	0,055	5,5	0,099	9,9	
9	3	0,083	8,3	0,149	14,9	
9	4	0,111	11,1	0,199	19,9	
9	5	0,138	13,8	0,25	24,9	
9	6	0,166	16,6	0,30	29,9	
9	7	0,194	19,4	0,35	34,9	
9	8	0,222	22,2	0,40	39,9	
9	9	0,25	25	0,449	44,9	
9	10	0,277	27,7	0,499	49,9	
9	11	0,305	30,5	0,549	54,9	
9	12	0,333	33,3	0,599	59,9	
9	13	0,361	36,1	0,649	64,9	
9	14	0,388	38,8	0,699	69,9	
9	15	0,416	41,6	0,749	74,9	
9	16	0,444	44,4	0,799	79,9	
9	17	0,472	47,2	0,849	84,9	
9	18	0,5	50	0,899	89,9	
9	19	0,527	52,7	0,949	94,9	
9	20	0,555	55,5	0,99	99	

Table 5 - results obtained from the analysis of the performance of the densities of the model "Classic" model with the "octal" a business networking, author

The table 5 shows the results of the performances of the two model for performance analysis and density of a network when there is an addition of ties (for a total of 20 bonds) that network. It is observed that there is a performance reduction (on average of 27.7/49.9 or 55%) to the classical model in relation to the octal model. Figure xx graphically shows this relationship.

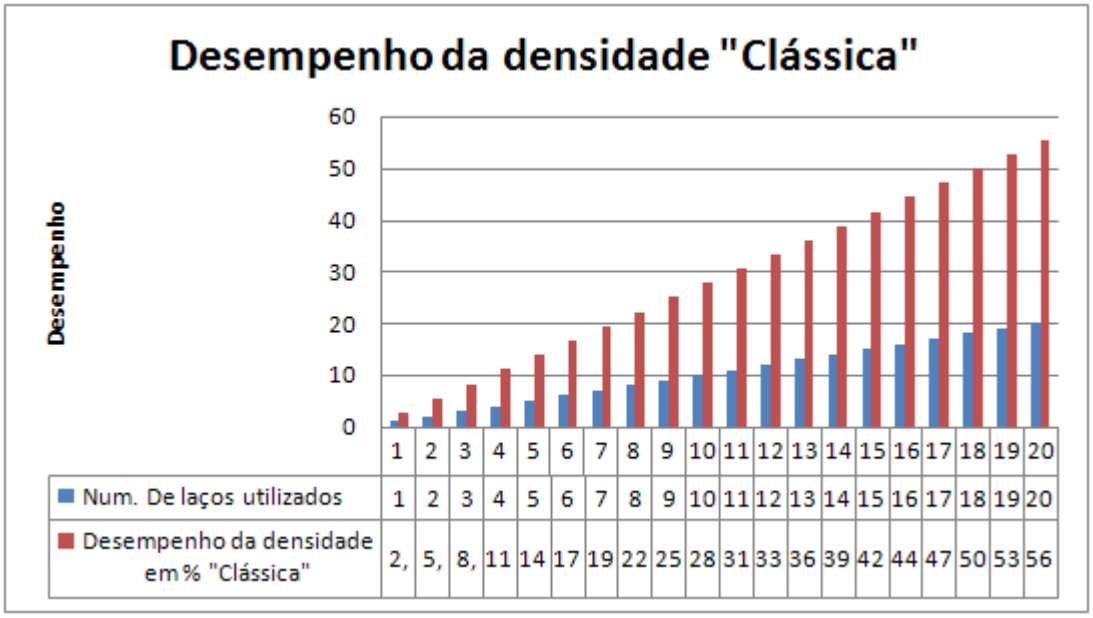

Figure 22 - Comparative graph of the performance model for the (classical) relative to the amount of a company of actors used in networks, author

Figure 22 shows the evolution of the number of ties to the classical model in relation to increased ties and performance loss (maximum) this network, in a proportion of 20/55 or 36%, and performance (minimum) of 1/2 or 50% (margin of error = 14%), for a total of 20 ties of a total of 9 nodes. Figure 23 shows the results generated by the model octal.

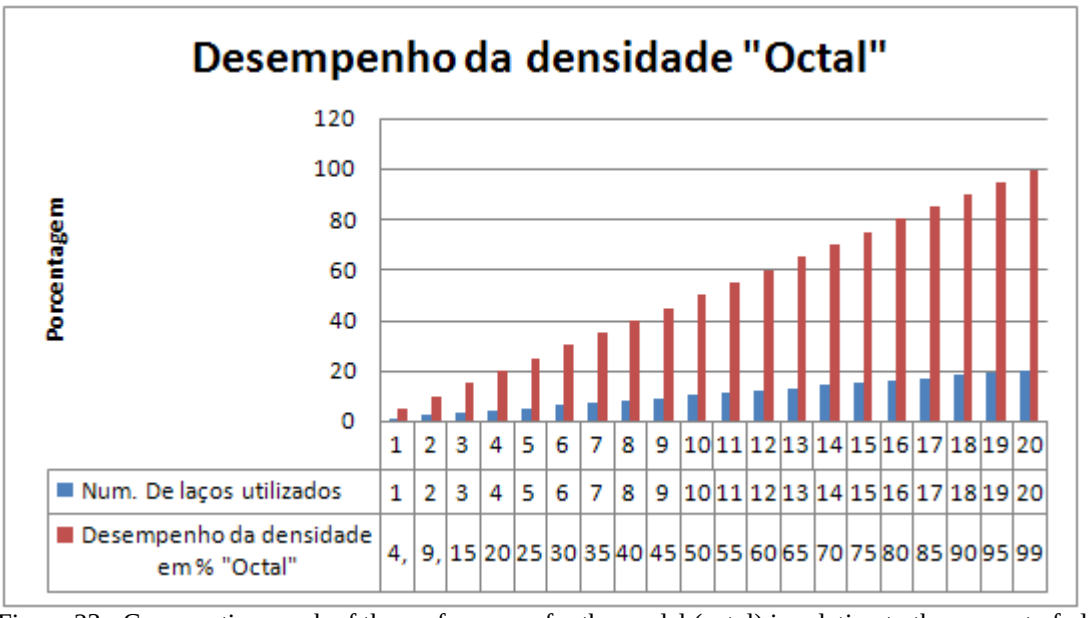

Figure 23 - Comparative graph of the performance for the model (octal) in relation to the amount of players used a company in networks, author

Figure 23 shows the evolution of bond numbers to octal model in relation to increased ties and performance loss (maximum) this network, in a proportion of 20/100 or 20% and performance (minimum) of 1/4 or 25% (margin of error = 5%) for a total of 20 ties of a network with 9 nodes.

3.5.2. Application and simulation

The simulation of the proposal was performed using a planning schedule, availability of teachers, disciplines as the available courses, schedules, shifts of classes and the rooms as each campus allocations of the IES. The figure 24 shows the application used for simulation and application of the proposal of this work.

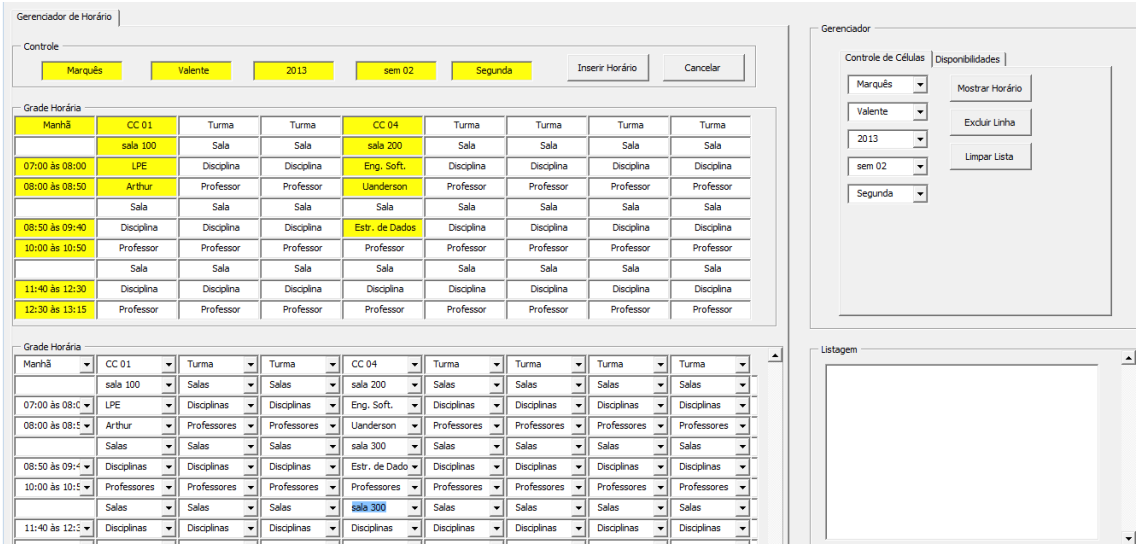

Figure 24 - main application screen distribution of classes, author

Figure 24 is the interface used for the application of the techniques of cloud computing, SOA and *web services*. The main services are contracts of teachers, availability of time and subjects designated for teaching, student enrolment and registration location, availability of rooms of the campus, planning schedules made by the coordination, the specific areas of expertise offered by half the year. The service contracts are based on SOA architecture and is based on the design of services, purpose, ability to reuse, strategic goals and service-oriented computing. In the implementation of the application uses the techniques of *web services* and cloud computing (through the virtualization of *datacenters*). The Foundation of web services is linked to the service logic, logic of processing messages, service contract and exchange of messages, which are responsible for building service-oriented solutions. The main components of the service oriented architecture are the inventories of services and resources for reuse. Communication between components using the proctocolos HTTP (*Hypertext Transfer Protocol*), HTTPS (*Hypertext Transfer Protocol Secure*), SMTP (*Simple Mail Transfer Protocol*) and Internet. Descriptions of message exchanges are performed by SOAP (*Simple Object Access protocol*), JMS (*Java Message Service*), request/response protocol that can be synchronously and asynchronously. The registration of services are business components (name, description, and contracts), techniques of information (languages, technologies and infrastructure access) and services (operations, taxonomies, rules, procedure and service elements). The SOA is the alignment between business model (processes) and IT, as it involves the model of governance, business requirements and IT capabilities. SOAP (*web services Access Protocol*) is the Protocol of access to services and their structure described using XML (*Extensible Markup Language*) responsible for communication between *web* applications and *web services*applications. The communication interface is performed through the WSDL (*Web Services Description Language*) which describes a *web service* that contains the operations and the input and output formats of each operation. Registering a web services in UDDI (*Universal Description Discovery and Integration*) of a *web services*provider, where are registered and published, because the UDDI are directories of *web services*.

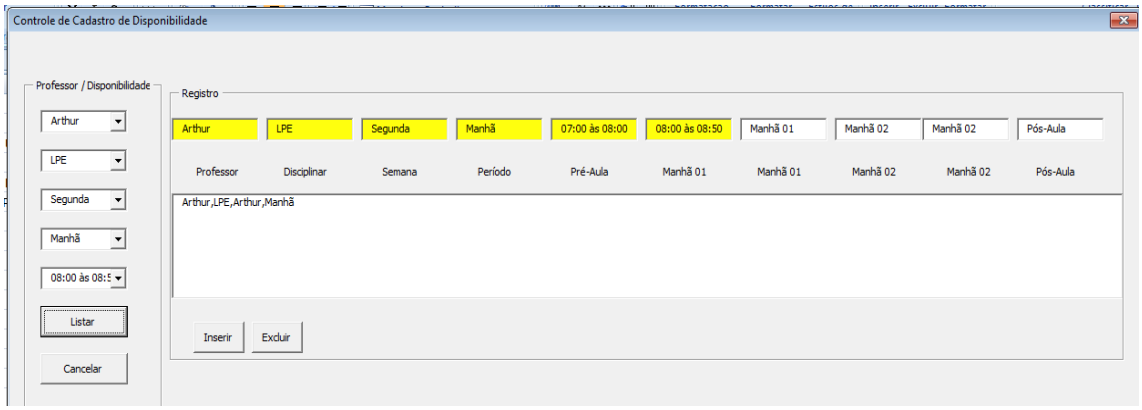

Figure 25 - Screen Application availability of teachers and classes, author

Figure 25 show a communication interface for control and management of schedule and availability fill disciplines input by teachers. This is the main component for the creation of the distribution schedule, classes, subjects and classes each semester of the academic year of an IES.

IV. ANALYSIS OF THE RESULTS

In relation to the analysis of the results, are monitoring the application performance of enterprise networking (it takes into account the analysis of the readings, the causes and effects of communication and efficiency compared to the costs involved). This is also indispensable for the verification of the benefits of new infrastructure with cloud computing and *web services*technologies, beyond the control of services using SOA design patterns.

Modeling of service-oriented computing and services, it should provide the results obtained and their advantages experiementais expected according to the studies carried out within the criteria and limits, as shown in the results below.

 Network configuration "octal" balanced in relation to the actors connected on that network from the array.
 The merged form defines the control mechanism of trade in communication with reducing conflicts between these actors
 The new architecture can exist several different ways of settings, keeping the consistency of the initial structure.
 The configuration can be obtained from matrix that determines the balanced relationship based on the concepts of density, centrality and of fragmentation.
 The actors are connected directly or indirectly to the actors of the inner layer of the octal model with the central actor, moreover, can be connected or disconnected from the network to establish their communications and exchanges of information.
 The new structure may be linked to their peers that have the same types of businesses or services (played by the American actors that has the same color) or to connect with groups that perform services or sell different products (represented by actors who have different colors),
 Each group has its main actor by applying the techniques of measures of density, centralization, fragmentation, and degree of centrality. In this way it is possible to apply also the techniques of structural holes in order to obtain advantages in the negotiations.
 The nodes (*nodes*) that have the same colors have in common the same interests and types of services or products in common (companies in the same sector), nodes (*nodes*) of different colors (interconnected) represent alliances with adjacent sectors companies but which complement each other.
 The mechanisms of state transitions between these actors allows show Exchange or sharing of services and in addition, define the behavior of firms in networks or individuals. It is possible to establish the types of possible relationships to network and establish the position of the actors and the measures of centrality of these actors to configure the best alliances and ties.
 The structure in hierarchical levels, where represent the measures of position of the actors according to their centrality that can be of degree or of kind.
 The intensity of the colors of the hierarchical levels shows that has a centralized of greater degree, since there is a larger number of ties that the actor has in relation to other actors and the lighter blue color less number of interconnected ties to this actor.
 The octal structure aggregates the concepts of vertical and horizontal networks and dynamic management using control techniques for cloud computing, SOA and *web services*.
 The new architecture allows you to establish service delivery configuration using dynamic virtualization techniques and autonomous which can behave in the form synchronized or not, according to the needs of resources sharing in cloud computing.
 The calculation presented in model allows you to define and analyze the maximum ties comparisons and densities in relation to quantities of actors and ties established between them
 The octal model sets a limit of interconnection between individuals or companies.
 The octal model its density or information flow capacity increases when the number of actors increases.
 Allows you to calculate the density, the number of ties, the intensity of relationship and the performance of a network.

V. CONCLUSION

Due to the evolution of the various modeling techniques of them stand out in the current times is the SOA, because it allows to relate business and IT services. Strategic alignment of an organization can be used. Have the web services are implemented allows the idea of services through the internet and be accessed anywhere in the world business logic and its realization with the use of web technology. For this virtualization of datacenters has the role to consolidate IT infrastructure to increase the performance and availability of

application offering a dynamic configuration to meet the new demands and requirements with low investment cost. The aim of this study was to propose a model for deploying networking companies in applying the architecture of service orientation and cloud computing techniques with web services for control and management planning academic schedule an IES. The research method was a case study of a set of units, or geographically distributed campus where many teachers teach in different units and coordinators also coordinate several units located in different regions. In relation to the practice and application of simulation - highlight the interdependence of services and cooperation agreements on integration and sharing of resources employed.

The results indicate the implementation of business policies with the IT environment and implementation distribution and technology services. In the management of academic planning results indicate a practice of sustainability and low cost. Thus the results obtained allowed to put into practice the concepts and theories applied in business networking. It was also possible to determine gain time and generate results even with the limitations presented that restricted their automation, efficiency and performance. However there is also evidence that it is possible to deepen the research that leads to even better results with the performance and involvement of more engineers and teachers who participate in the network. Furthermore the impact it has proved possible to facilitate resource allocation geographically distributed datacenters with virtualization. Finally, it should be emphasized that the inter - organizational networks are placed in the context of the current reality and in that sense to be competitive organizations must be aligned with the new technologies and management models for organizations .

BIBLIOGRAPHICAL REFERENCES

[1] BRANDENBURGER, A.; NALEBUFF, B. J. **Co-opetition**. New York: Currency Doubleday, 1996.

[2] BURT, R. S. **Cooptive corporate actor networks: a reconsideration of interlocking directorates involving american manufacturing**. Administrative Science Quartely, v.25, p.557-582, 1980.

[3] COLEMAN, J. S. **Social capital in the creation of human capital**. American Journal of Sociology, v.94, p. 95-120, 1988.

[4] DEITEL, H. M. **C# Como Programar**, Pearson Education do Brasil Ltda. São Paulo – SP, 2005.

[5] ERL, Thomas. **SOA Princípios de Design de Serviços**, Pearson Education do Brasil, São Paulo- SP, 2009.

[6] FUSCO, José Paulo Alves e SACOMANO, José Benedito. **Alianças em redes de empresas: modelo de redes simultâneas para avaliação competitiva**, Editora Arte & Ciência, São Paulo – SP, 2009.

[7] GREIF, A. **On the interrelations and economic implications of economic, social, political, and normative factors**: Reflection from two late medieval societies. In: DROBAK, J. N.; NYE, J. V. C.. The frontiers of the new institucional economics, San Diego: Academic Press, 1997. P.57-94.

[8] GREIF, A. **On the interrelations and economic implications of economic, social, political, and normative factors: Reflection from two late medieval societies**. In DROBAK, J. N.; NYE, J. V. C. **The frontiers of the new institutional economics**. San Diego: Academic Press, 1997. P. 57-94.

[9] HAMMERSLEY, Eric; **Profissional VMware Server**, Wiley Publishing. Inc., Indianapolis, Indiana, USA, 2007.

[10] HOLF, K.; STIGLITZ, J. E**. Imperfect information and rural credit markets: Puzzles and policy perspectives.** In: HOFF, K. **The economics of rural organization: theory, practice, and policy**. Oxford: Oxford Univeresity Press, 1993.

[11] JONES, C. **A general theory of network governance: Exchange conditions and social mechanisms**. Academy of Management Review, v. 22, n. 4, p. 911-945, 1997.

[12] JORGESEN, David. **Desenvolvendo Serviços Web .NET com XML**, Editora Alta Books Ltda. Rio de Janeiro – RJ, 2002.

[13] KIRSCHIBAUM, C.; VASCONCELOS, F. C. D. **Tropicália: Manobras estratégicas em redes de músicos**. Revista de Administração de Empresas, v.47, n.3, p.-26, 2007.

[14] LAZZARINI, Sérgio G. **Empresas em rede**, Cengage Learning, São Paulo – SP, 2008.

[15] NICKERSON, J. A. et al. **Market position, resource profile, and governance: Linking Porter and Williamson in the context of International Courier and Small Package Services in Japan**. Strategic Management Journal, v. 22, p. 251-273, 2001.

[16] PIORE, M. J.; SABEL, C. F. P. **Administrative Organization**. Englewood Cliffs: Prentice-Hall, 1960.

[17] POWELL, W. W. **Neither market nor hierarchy: Network forms of organization. Research in Organization Behavior**, v. 12, p. 295-336, 1990.

[18] SCHNEIDER, B. R. **Business politics and the State in twentieth-century Latin America**. Cambridge: Cambriedge University Press, 2004.

[19] THOMSOM, J. D. **Organizations in action: Social science bases of administrative theory**. New York: McGraw-Hill, 1967.

[20] TONINI, A. C.; CARVALHO, M. M.; SPINOLA, M. M.**; Contribuição dos modelos de qualidade e maturidade na melhoria de software. Revista Produção**, v.18, n. 2, p. 275 – 286, 2008.
[21] TONINI, Antonio Carlos; CARVALHO, Marly Monteiro de e SPINOLA, Mauro de Mesquita. **Contribuição dos modelos de qualidade e maturidade na melhoria dos processos de *software***, ABEPRO Produção, v18. São Paulo – SP, 2008.
[22] VERAS, Manoel. **Datacenter Componente Central da Infraestrutura de TI** (Tecnologia da Informação), Brasport Livros e Multimídia Ltda. Rio de Janeriro – RJ, 2010.
[23] VERAS, Manoel. **Virtualização Componente Central do Datacenter**, Brasport Livros e Multimídia Ltda. Rio de Janeiro – RJ, 2011.
[24] WASSERMAN, S.; FAUST, K. **Social network analysis**. Cambrigde: Cambridge University Press, 1994.
[25] ZENGER, T. R.; HESTERLY, W. S. **The disaggregation of corporations:Selective intervation, high-powered incentives, and molecular units.** Organization Science, v. 8, n. 3, p.209-222,1997.
[26] ZYLBERSZTAJN, D. **Governance structures and agribusiness coordination: Transaction cost economics based approach**. **In:** GOLDBERG, R. A**. Research in Domestic and International Agribusiness Management**. Boston: JAI Press, 1996. P. 245-310.
[27] ZYLBERSZTAJN, D.; FARINA, E. M. M. Q. **Strictly coordinated food systems: Exploring the limits of the Coasian firm.** International Food and Agribusiness Management Review, v. 2, p. 249-265, 1999.

American Journal of Engineering Research (AJER)
e-ISSN : 2320-0847 p-ISSN : 2320-0936
Volume-03, Issue-03, pp-310-316
www.ajer.org

Research Paper Open Access

Performance Evaluation of 25MLD Sewage Treatment Plant (STP) at Kalyan

Prachi N. Wakode, Sameer U. Sayyad
[1]*Post Graduate Student of Civil and Environmental Engineering Dept., Veermata Jijabai Technological Institute, Mumbai - 400019*
[2]*Assistant Professor, Dept. of Civil and Environmental Engineering, Veermata Jijabai Technological Institute, Mumbai - 400019*

Abstract: - The present study has been undertaken to evaluate the performance of 25 MLD Sewage Treatment Plant (STP) located at Adharwadi, Kalyan of Thane district which is based on Sequential Batch Reactor (SBR) process. Performance of this plant is an essential parameter to be monitored as the treated effluent is discharged into River Ulhas. The Performance Evaluation will also help for the better understanding of design and operating difficulties (aeration, blowers, etc.) in Sewage Treatment Plant. Sewage samples were collected from different locations i.e. Inlet, Distribution Chamber and Outlet of the Treatment Plant and analysed for the major waste-water quality parameters, such as pH, Biological Oxygen Demand (BOD), Dissolved Oxygen (DO), Chemical Oxygen Demand (COD), Total Suspended Solids (TSS), MLSS, Total Nitrogen and Total Phosphates. Actual efficiency of the 25 MLD STP will be evaluated by collecting samples (36 in all) for the period of 3 months (December to February). The conclusions of these evaluations may determine required recommendations and focus on modification requirements for the STP and will also determine whether the effluent discharged into the water body are under limits given by MPCB. The conclusions drawn from this study will outline the need for continuous monitoring and performance analysis by removal efficiencies of each and every unit of STP. Administrative capability and adequacy of maintenance systems were evaluated using questionnaires and by conducting staff interviews.

Keywords: - *domestic waste water, efficiency, evaluation, performance, sequential batch reactor, total nitrogen*

I INTRODUCTION

The main function of wastewater treatment plants is to protect human health and the environment from excessive overloading of various pollutants. Due to industrial development in MIDC, domestic effluent and urban run-off contribute the bulk of wastewater generated in Kalyan city. Domestic wastewater usually contains grey water (sullage), which is wastewater generated from washrooms, bathrooms, laundries, kitchens etc. It also contains black water made up of urine, excreta and flush water generated from toilets.

Physical, chemical and biological processes are applied to remove physical, chemical and biological contaminants. Its objective is to produce a waste stream (or treated effluent) and a solid waste or sludge also suitable for discharge or reuse back into the environment [1]

In Kalyan city, the common treatment technologies adopted for domestic sewage treatment are sequential batch reactors. According to KDMC city sanitation plan, the sewage collection system is decentralized one in KDMC area due to new town planning and topographic conditions. Each node has its own sewage collection network and sewage treatment plants. The efficiency of sewage treatment plants can be illustrated by a study on the evaluation of pollutant levels of the influent and the effluent at the treatment plant of sewage treatment plants discharging into the environment [1]

The treatment plant at Adharwadi is designed to treat 25MLD sewage. The efficiency of performance of the plant in stabilizing the sewage to the required standard has not been assessed since its operation. There has not been any research conducted on the plant to ascertain the impact of the final effluent being discharged

into River Ulhas. State and Local authorities with statutory authority in pollution control have established standards of purity that are necessary to prevent pollution of natural waters.

1.1 Present Scenario

Municipal wastewater is one of the largest sources of pollution, by volume. Municipal waste-water normally receives treatment before being released into the environment. "The higher the level of treatment provided by a wastewater treatment plant, the cleaner the effluent and the smaller the impact on the environment". [2]

Despite treatment, some pollutants remain in treated wastewater discharged into surface waters. Treated wastewater may contain grit, debris, disease-causing bacteria, nutrients, and hundreds of chemicals such as those in drugs and in personal care products like shampoo and cosmetics. Nowadays, society demands that all processes, product or services must also be analyzed from an environmental point of view. Therefore it is necessary to analyse the system to determine the overall pollution associated to these activities. [3]

Rapid growth and urbanization of city over past few decades has given rise to innumerable problems. One of the major problems is the deterioration of water quality in River Ulhas due to more or less unrestricted disposal of large volumes of domestic and industrial wastewater.

II SEWAGE TREATMENT PLANT AT KALYAN

Today, treating wastewater is generally a complex, multi-step industrial process. [1] The first step in a sewage treatment plant is generally some kind of mechanical treatment, where large objects and heavy materials are removed. The mechanical treatment may consist of a screening chamber (coarse and fine screening) and a degritor. To remove soluble organic matter and possibly also nitrogen from the wastewater, biological treatment is often the second step and followed by disinfection unit (Chlorine contact tank)

Figure 1: Google Earth Image of the Treatment Plant

Wastewater treatment plants are constructed to protect the environment from excessive overloading from different kinds of pollutants. These plants must meet the appropriate effluent standards. Abnormal process conditions at sewage treatment plants result in the release of effluent that may contain toxins and unacceptably high levels of dangerous organic and inorganic materials into various water bodies and the general environment [4]. This study is based on sequential batch reactor wastewater treatment systems because they are among the most widely-used systems.

2.1 Sequencing Batch Reactors for wastewater treatment

Discharge of domestic waste water in any water body can be harmful to the environment. Therefore, treatment of any kind of waste water to produce effluent with good quality is necessary. In this regard choosing an effective treatment system is important. Waste water discharge permits are becoming more stringent and SBR's offer a cost-effective way to achieve lower effluent limits. Sequencing batch reactor is a modification of activated sludge process which has been successfully used to treat municipal waste water [5].Of the process advantages are single tank configuration, easily expandable, simple operation and low capital costs. Improvements in aeration devices and controls have allowed SBRs to successfully compete with conventional activated sludge systems. A U.S.EPA report summarized this by stating that, *"The SBR is no more than an activated sludge system which operates in time rather than in space."*

2.2 SBR Operating Principles

Conventional activated sludge systems require separate tanks for the unit processes of biological reactions (aeration of mixed liquor) and solids-liquid separation (clarification) and also require process mixed liquor solids (return activated sludge) to be returned from the final clarification stage to the aeration tanks.

In contrast, SBR technology is a method of wastewater treatment in which all phases of the treatment process occur sequentially within the same tank. Hence, the main benefits of the SBR system are less civil structures, inter-connecting pipework, and process equipment and the consequent savings in capital and operating costs.

The sequencing batch reactor utilizes the Mix Air system by providing separate mixing with the direct drive mixer (DDM) and an aeration source such as jet surface aerator or Aerobic diffused-aeration. This system has the capability to cyclically operate the aeration and mixing to promote anoxic/aerobic and anaerobic environments with low energy consumption. In addition, the Mix Air system can achieve and recover alkalinity through denitrification, prevent nitrogen gas disruption in the settle phase, promote biological phosphorus removal. The Aerobic floating decanter follows the liquid level, maximizing the distance between the effluent withdrawal and sludge blanket. It is an integral component to the SBR system and provides reliable, dual barrier subsurface withdrawal with low entrance velocities to ensure surface materials will not be drawn into the treated effluent. The decanter option is easily accessible from the side of the basin and require minimal maintenance.

2.3 Phases of Operation

The sequencing batch reactor system features time-managed operation and control of aerobic, anoxic and anaerobic processes within each reactor. Equalization and clarification takes place within a reactor itself.

The SBR system utilizes five basic phases of operation to meet advanced wastewater treatment objectives. The duration of any particular phase may be based upon specific waste characteristics and/or effluent objectives.

1. **Mix-Fill**

- It is the phase when influent flow enters the reactor.
- In mix-fill phase, mixing is initiated with the (Direct Drive Mixer) DDM mixer to achieve complete mix of the reactor contents in the absence of aeration.It establishes a powerful down-flow mixing pattern that transports surface liquid downward and increases mass transfer. Flow entrainment and regenerative flow create high reactor turnover rates for efficient mixing.
- Anoxic conditions are created which facilitate removal of any residual nitrites/nitrates (NO_X) via the process of denitrification.
- In systems requiring phosphorus removal, the Mix-Fill phase is extended to create anaerobic conditions where phosphorus accumulating organisms (PAO) release phosphorus then ready for subsequent luxury uptake during aeration times.
- Anoxic conditions assist in the control of some types of filamentous organisms

2. **React-Fill**

- In this phase the influent flow continues under mixed and aerated conditions
- React-fill phase is as phase in which oxygen is supplied (i.e. diffused aeration) along with the fill process. Intermittent aeration may promote aerobic or anoxic conditions.
- Biological/chemical oxygen demand (BOD/COD) and ammonia nitrogen (NH_3) are reduced under aerated conditions
- Luxury uptake of phosphorus is produced under aerated conditions
- NO_X is reduced under anoxic conditions

3. **React**

- The Influent flow is terminated creating true batch conditions in React phase.
- Mixing and aeration continue in the absence of influent flow
- Biological/chemical oxygen demand (BOD/COD) and ammonia nitrogen (NH3) reduction continue under aerated conditions
- Oxygen can be delivered on a “as needed” basis via dissolved oxygen probes while maintaining completely mixed conditions
- Provides final treatment prior to settling to meet targeted effluent objectives.

4. **Settle**

- Influent flow, mixing and aeration are terminated in settle phase.
- Ideal solids/liquid separation is achieved due to perfectly quiescent conditions.
- Adjustable time values allow settling time to match prevailing process conditions.

5. Decant/Sludge Waste

- Decantable volume is removed by subsurface withdrawal with the help of floating decanters.
- Floating decanter follows the liquid level, maximizing distance between the withdrawal point and the sludge blanket.
- Usually the sludge blanket formed is of 1.5 m to 2 m; therefore decanting level should be fixed by help of PLC.
- Small amount of sludge is wasted near the end of each cycle.

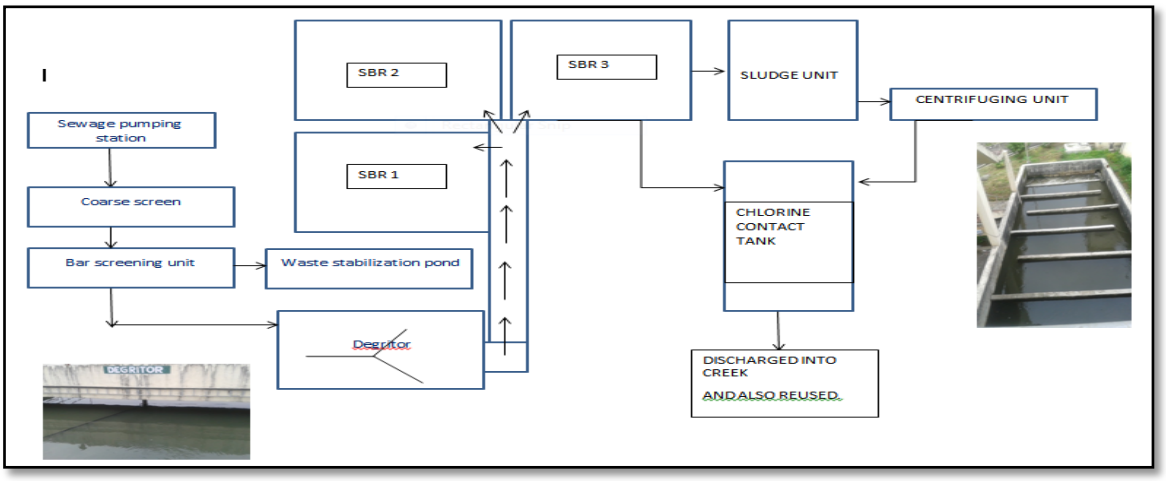

Figure 2: Flowchart of Treatment Plant

III METHODOLOGY

The Sewage treatment plant at Adharwadi is being designed to treat 25 MLD of sewage from area of Kalyan city. The flow chart is as shown in Figure 2:

3.1 Specifications of plant

1. Capacity of plant: 25 MLD
2. BOD considered at inlet- 150 mg/l
3. Screens
- Type: Mechanically cleaned bar screen
- Bar Screens: 2 no.s of 1 m x 2.3 m inclined at 60˚to horizontal, clear opening of 20 mm.
4. No. of reactors: 3 no.s
5. Size of reactor: 3.3 m x 3.3 m x 7.5 m
6. For process:
- In Fill phase, the influent is filled upto 6.5 m – 7 m.
- Decant level is upto 5 m. (i.e. 2 m sludge blanket)
7. The total cycle time for completing the process is **6 hours** at 25 MLD Adharwadi STP.
- Mix fill phase : 60 minutes
- React fill phase : 120 minutes
- React phase : 60 minutes
- Settle phase : 60 minutes
- Decanting phase : 60 minutes
8. The STP consists of 3 reactors; in which daily about 2-3 MLD of sewage is treated in each reactor. About 8 cycles take place on a daily basis.
9. The Working of the Plant is totally based on PLC (Programmable Logic Control) and the process in controlled over SCADA system.
10. The 25 MLD Adharwadi plant having "Sequential batch reactor technology" produce an effluent of less than: (as per MPCB)

- 10 mg/L BOD
- 20 mg/L TSS
- 5- 8 mg/L TN
- 1 - 2 mg/L TP

3.2 On-Site Procedure

1. Conducted a short meeting between administration staff and the operators by means of questionnaires.
2. To explain the purpose of performance evaluation and the evaluation process itself and its advantages.
3. To obtain information on maintenance and operational problems at the treatment plant.
4. Amount of process control routinely applied at plant should be noted and to be followed.

3.3 Sampling locations

Samples were collected after every unit of treatment raw water sump (inlet), SBR tank, and chlorine contact tank (outlet).

3.4 Sampling period

36 samples (12 sets of 3 samples) were collected for period of December to February.

3.5 Laboratory analysis

Collected samples will be tested by standard methods in the laboratory for the parameters:
Sample 1: Raw water: BOD, COD, pH, Total suspended solids, Total Nitrogen, Total Phosphorous.
Sample 2: SBR tank: BOD, COD, Total suspended solids, DO
Sample 3: CCT tank: pH, BOD, COD, Total suspended solids, Total Nitrogen, Total Phosphorous

IV OBSERVATION AND RESULTS

Table 1Test Observations

Date	Sample	Parameters						
		pH	BOD (mg/l)	COD (mg/l)	TSS (mg/l)		Total Nitrogen (mg/l)	Total Phosphorous (mg/l)
1	2	3	4	5	6		7	8
01.12.2013	1	6.8	137	415	139		7	4.3
	2	-	84	254	115		-	-
	3	7.1	6	16	11		1.3	0.9
06.12.2013	1	6.9	139	325	146		7.1	4.2
	2	-	82	244	124		-	-
	3	7.2	4	15	10		1.5	0.9
12.12.2013	1	7.2	146	440	144		7.4	4.1
	2	-	86	256	126		-	-
	3	7.4	5	18	9		1.7	1.1
19.12.2013	1	6.9	148	447	147		7.9	4.7
	2	-	88	264	128		-	-
	3	7.1	7	20	10		1.5	0.8
26.12.2013	1	6.9	151	450	152		7.6	4.5
	2	-	90	268	130		-	-
	3	7.2	5	17	8		1.7	0.9
02.01.2014	1	6.9	138	420	142		7.1	4.3
	2	-	85	250	119		-	-
	3	7.2	6	18	9		1.4	0.9
09.01.2014	1	7	119	363	127		5.9	1.9
	2	-	80	245	101		-	-
	3	7.1	5	15	10		1.5	0.8
16.01.2014	1	6.8	126	390	125		6	2.4
	2	-	83	240	98		-	-
	3	7.3	5	14	9		1.9	0.8
24.01.2014	1	6.9	130	400	130		6.1	2.5
	2	-	96	288	110		-	-
	3	7.2	6	17	10		1.8	0.8
28.01.2014	1	6.9	134	410	131		6.5	2.6
	2	-	110	320	100		-	
	3	7	5	20	11		2.1	1.1
01.02.2014	1	6.7	113	335	109		6.0	1.2
	2	-	80	234	76		-	-
	3	7.4	5	15	10		1.5	0.4
02.02.2014	1	0.2	150	324	154		7.5	4.8
	2	-	126	256	98		-	-
	3	7.3	6	21	10		2.34	0.8

Table 2 BOD Removal Efficiency

Date	Inlet (mg/l)	Outlet (mg/l)	Efficiency
01.12.2013	137	6	95.62 %
06.12.2013	139	4	97.12 %
12.12.2013	146	5	96.57 %
19.12.2013	148	7	95.27 %
26.12.2013	151	5	96.69 %
02.01.2014	138	6	95.65 %
09.01.2014	119	5	95.79 %
16.01.2014	126	5	96.03 %
24.01.2014	130	6	95.38 %
28.01.2014	134	5	96.26 %
01.02.2014	113	5	95.57 %
02.02.2014	150	6	96.00%

Table 3 TSS Removal efficiency

Date	Inlet	Outlet	Efficiency
01.12.2013	139	11	92.08 %
06.12.2013	146	10	93.15 %
12.12.2013	144	9	93.75 %
19.12.2013	147	10	93.19 %
26.12.2013	152	8	94.73 %
02.01.2014	142	9	93.66 %
09.01.2014	127	10	92.12 %
16.01.2014	125	9	92.8 %
24.01.2014	130	10	92.30 %
28.01.2014	131	11	91.60 %
01.02.2014	109	10	90.82 %
02.02.2014	154	10	93.51 %

Table 2: COD Removal efficiency

Date	Inlet	Outlet	Efficiency
01.12.2013	415	16	96.14 %
06.12.2013	325	15	95.38 %
12.12.2013	440	18	95.90 %
19.12.2013	447	20	95.52 %
26.12.2013	450	17	96.22 %
02.01.2014	420	18	95.71 %
09.01.2014	363	15	95.86 %
16.01.2014	390	14	96.41 %
24.01.2014	400	17	95.75%
28.01.2014	410	20	95.12 %
01.02.2014	335	15	95.52 %
02.02.2014	324	21	93.52 %

Table 3: Total Nitrogen and Total Phoshorus removal Effciency

Date	Total Nitrogen		TN Removal Efficiency	Total Phosphorous		TP Removal Efficiency
	Inlet	Outlet		Inlet	Outlet	
01.12.2013	7	1.3	81.43 %	4.3	0.9	79.06 %
06.12.2013	7.1	1.5	78.87 %	4.2	0.9	78.57 %
12.12.2013	7.4	1.7	77.02 %	4.1	1.1	73.17 %
19.12.2013	7.9	1.5	81.01 %	4.7	0.8	82.97 %
26.12.2013	7.6	1.7	77.63 %	4.5	0.9	80 %
02.01.2014	7.1	1.4	80.28 %	4.3	0.9	79.07 %
09.01.2014	5.9	1.5	74.57 %	1.9	0.8	57.89 %
16.01.2014	6	1.9	68.33 %	2.4	0.8	66.67 %
24.01.2014	6.1	1.8	70.49 %	2.5	0.8	68 %
28.01.2014	6.5	2.1	67.69 %	2.6	1.1	57.62 %
01.02.2014	6	1.5	75 %	1.2	0.4	66.67 %
02.02.2014	7.5	2.34	68.80 %	4.8	0.8	83.33 %

V CONCLUSIONS

Bases on the laboratory analysis and the operating data of sewage treatment plant, it is concluded that,

1. Average BOD at inlet is 134.63 mg/l with maximum of 151 mg/l and minimum of 113 mg/l respectively. After the advanced treatment, average BOD at outlet was observed to be 5.36 mg/l. Maximum BOD at effluent is 7 mg/l. Effluent BOD is within standard limits of discharging in the creek.
2. The overall BOD removal efficiency is 96 %.

3. The concentration of total suspended solids at inlet was observed to be 135.64 mg/l with the removal efficiency of 92.74% of which about 18.67 % of suspended solids were removed in degritor (primary treatment) itself.
4. The overall total suspended solids removal efficiency is 92.74 %.
5. The removal efficiencies of total nitrogen and phosphates were 75.67 % and 71.79 % respectively.

Following observations were made during the onsite survey and questionnaires session:

1. **Screening unit** : As per the CPHEEO manual [6], the head loss at screen should be 5 cm, but here it was observed as 25 cm, which is due to the clogging of organic/suspended matter/floating matter carried with the sewage. Screens need to be cleaned regularly with proper schedule.
2. **Degritor unit**: The sewage consists of sand, egg shells, many other inert materials. Rotations within the degritor is 2 rev/min. The degritor should be maintained properly. If the grit goes into the SBR process, it can affect the process by reducing the efficiency. There is a provision of waste stabilization pond just adjacent to degritor, which is used when the maintenance work of degritor is in process. The detention period is 15 days.
3. **SBR Tank**: The major criteria in this treatment is removal of BOD, removal of nitrates and phosphates. We have observed the BOD removal efficiency as 96 %. The higher efficiency is due to the proper maintenance of aeration equipment's (blowers and diffused aerators).

After discussion of the survey, proper scheduling was planned and was followed till present.

VI ACKNOWLEDGMENT

I wish to express my sincere thanks to the Head of Department, **Dr. Sumedh Y. Mhaske** and with deep sense of gratitude to my guide **Mr. Sameer U. Sayyad,** without whom, the work would have not been possible. The confidence with which **Mr. Sameer U. Sayyad** guided the work requires no elaboration. His timely suggestions given and encouragement shown, made me more confident in successfully carrying out my project work.

I am also thankful to KDMC officials and staffs for receiving the valuable cooperation from time to time during the project.

REFERENCES

[1] Metcalf and Eddy, Wastewater Engineering, treatment and reuse, New Delhi: Tata McGraw-Hill Publishing Company Limited, 2003.
[2] Wastewater technology factsheet - Sequencing batch reactor," EPA, 1999.
[3] A. Gallego, A. Hospido, M. T. Moreira and G. Feijoo, "*Environmental Performance of Wastewater Treatment Plant*," Resources, Conservation and Recycling, vol. 52, pp. 931-940, 2008.
[4] D. Nolasco, D. Irvine, M. Manoharan and E. Giroux, "Evaluation and Optimization of Design/ Operation of Sequencing batch Reactors for Wastewater treatment".
[5] A. H. Mahvi, "*Sequencing Batch Reactor- A Promising Technology in Wastewater Treatment*," Iran Journal of Environmental Health Sciences and Engineering, vol. 5, no. 2, pp. 79-90, 2008.
[6] EPA, "Manual on Procedures for evaluating performance of wastewater treatment plants".
[7] C.P.H.E.E. Organization, "Manual on Sewerage and Sewage Treatment," Ministry of Urban Development, New Delhi.
[8] N. E. I. W. P. Control, "Sequencing Batch Reactor Design and Operational Consideration," Sept, 2005.

American Journal of Engineering Research (AJER)
e-ISSN: 2320-0847 p-ISSN: 2320-0936
Volume-03, Issue-03, pp-317-321
www.ajer.org

Research Paper Open Access

Effect of primary materials ratio and their stirring time on SiC Nanoparticle production efficiency through sol gel process

Vahid Mazinani, Mahdiyeh Mallahi, Soheil Saffary, Mohammadamir Mohtashami, Saeed Maleki

[1,5]*Department of Mining and Metallurgical Engineering, Amirkabir University of Technology (Tehran Polytechnic), Hafez Ave., P.O. Box 15875–4413, Tehran, Iran*
[2]*Mechanical Engineering Department, K. N. Toosi University of Technology, Tehran, Iran*
[3]*School of Metallurgy & Materials Science, Iran University of Science & Technology (IUST), P.O. Box: 16845-161, Tehran, Iran*
[4]*College of Engineering, University of Miami, 1251 Memorial Drive, Coral Gables, FL, 33146, United States*

Abstract: **-**In this article, SiC (silicon carbide) Nanopowder was synthesized by sol-gel method. TEOS and sucrose were used as pricier source. Final gel were prepared by mixing in different stirring times and different ratio in pH=4 and drying. This mixture was heated at 650°C and carbothermal reduction was carried out at 1500 °C. XRD analyses showed that produced powder in this condition are only β-Sic. Investigating SEM and TEM images and PS diagrams for different samples one can realize that in TEOS/sucrose=4 and stirring time, 5 hours, maximum efficiency and minimum grain size and minimum agglomeration occurs. Experiment result indicated that nano silicium carbide along with tetraethoxysilane, ethanol, sucrose and water can be used as carbon supply. Average grain size which has been seen by SEM was less than 100 nm.

Keywords:-*sol-gel, nanopowder, synthesize, SiC*

I. INTRODUCTION

SiC is one of the most important none oxide ceramics which is produced in the powder form in a wide range, because of having excellent mechanical property, high electron conductivity, high thermal conductivity, high chemical resistance against oxidation possess wide range of application in industry such as high thermal application, semiconductors and so on. The main process of SiC production is carbothermal reduction which is known as Acheson process. Produced powder through this process is coarse. This is obvious that micro structured materials have great properties. These properties include improvement in strength, wear resistance, corrosion resistance and toughness. To produce SiC a lot of methods have been reported like sol-gel, plasma, laser and microvio. Nanopowder production through sol-gel process is a quite new process which will possess high potential in industry in future. This paper represents effect of important parameter on SiC production by sol-gel process.

SiC as a ceramic material has been noted a lot in the last decades due to unique properties such as stability in high temperatures. But low toughness is one the most important downside of SiC and other ceramics [1].

In the last years a lot efforts have been made to solve this problem Due to planting fibers and viscures to produce multiphase structure. Although toughness of SiC and other ceramics improved to some extent, toughness of these materials is less than applied metals. By producing nano particles and controlling particle size bonding energy in structure, surface and grain interfaces, the hope of producing strong ceramic ceramics with high toughness has been achieved [2].

SiC nanopowder, because of having special property such as high hardness and strength, high corrosion and oxidation resistance ,low thermal expansion quotient and high thermal conductivity is a suitable substance for improving complex materials and high temperature application such as thermal elements and fireproof [3,4,5].On the other hand, SiC as a semiconductor in designing electronic pieces with the ability of working in high temperatures, electric power and frequencies and high stressed media has attracted attention [6].

Conventional method of producing SiC which is famous in industrial scale is carbothermal reduction between Silica and petroleum coke in high temperature (about 2500 °c). Resultant SiC by this method is so 888grain and has a lot of impurities [1]. To produce piece with high quality, powder with high purity, spherical shape, small particle size, limited size distribution and low agglomeration intensity is needed. Nanopowder with these property can be produced through process like: carbonization of metals having Si [7], CVD [8], sol gel [9], heat plasma [10], grinding [6] and SiO2 carbothermal reduction [4]. Among these methods sol gel and carbothermal reduction are alike. But regarding different mixing condition of two reactors (SiO2 and carbon) , in sol gel method much more homogenous mixture is produced by having homogenous mixture, reaction rate increases and reaction temperature decreases so that producing fine grained powder is possible [11].

II. MATERIALS AND EXPERIMENT

In this research TEOS (Tetron Etil Ortho Silicate) with chemical formula Si (C2H5O4), ethanol, Sacarose (c12H22O11) and distilled water used as primary materials. Primary materials are mixed according to ratios in table 1 and were stirred with the speed of 250 rpm in 30˚Caccording to times in table2 in pH=4.5. Prepared solution was kept in an isolated place for 18 hours in order to finish hydrolysis reaction. Resultant gels were kept in the extraction fan for 4 hours in 60° C to dry. In order to perform paralysis, samples were kept in furnace with 888 atmospheres at 650˚ C at 15˚ C min-1 for 1.5 hours. For carbothermal reduction samples were kept in argon atmosphere. To remove remained Si and SiO2 pickling by HF was performed because of samples agglomeration a grinding process in neutral environment was done. After sorting the samples phase analyze through XRD was carried out. Then samples were studied by SEM and TEM images has been prepared in order to get information about morphology and different phase distribution and also approve or reject of presumption. After that PS test has been done to investigate grain size distribution in samples.

III. RESULTS AND DISCUSSIONS

3.1. Effect of TEOS/Eth ratio on produced SiC quantity

Figure 1 shows XRD spectrum related to TE1 sample. Presence of TEOS and carbon source leads to SiC production any way which spectrum above proves it. Since picks intensity are too close phase quantity cannot be obtained. But we have analyses like this:

According to the studies, equilibrium diagram for TEOS and water mixing can be plotted as figure2.

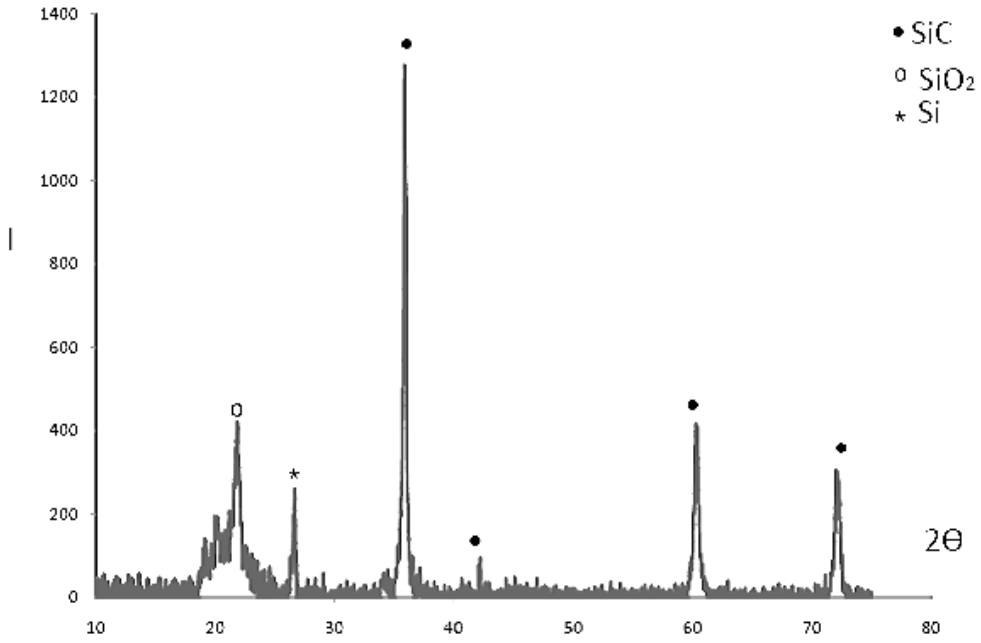

Fig.1 XRD spectrum for TE1 sample with T/E=6.

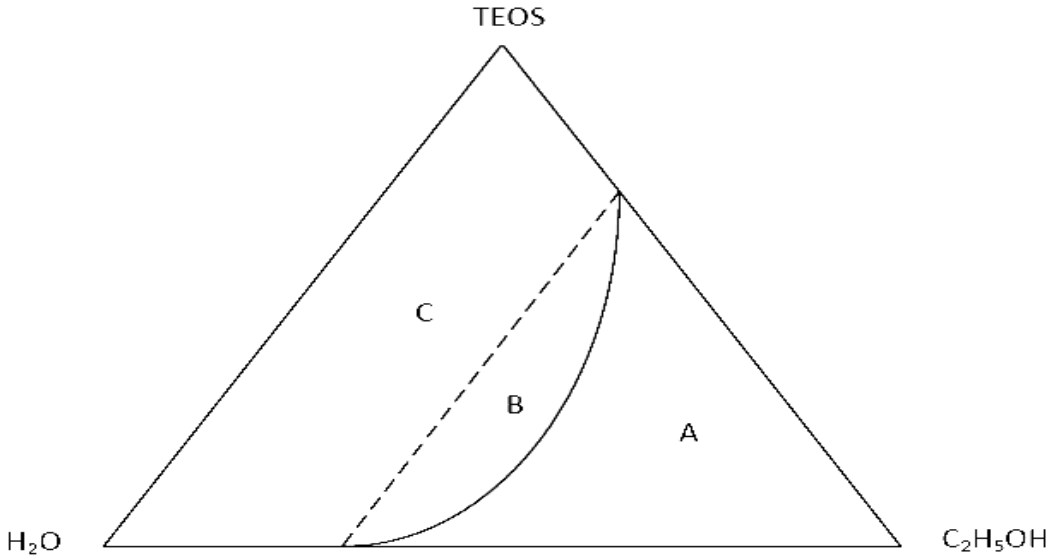

Fig.2. water and alcohol and TEOS mixing

In above mixing diagram region A is the main mixing region which can be developed to A_B region by increasing acid or decreasing alcohol amount. In fact by increasing alcohol so much it is deviated from ideal line hydrolysis reactions rate decrease and the amount of final phases will decline. Also decreasing solvent so much leads to increasing cross links and not occurring equilibrium reaction, so decreasing expected phases [6].

3.2. Effect of TEOS/Eth ratio on produced SiC particle shape

Figure 3 and 4 show SEM images for samples TE2 and TE4. SEM images indicate that in bigger grain size which growth nucleation powder shape changes from spherical shape to flat shape. Growth here is increasing cross links and chain length. Increasing particle size and getting out of Spherical shape with changing in alcohol ratio should be searched in mixing diagram. Figure 5 and 6 show TEM images for the same samples. Bigger flat shape grains are clear.

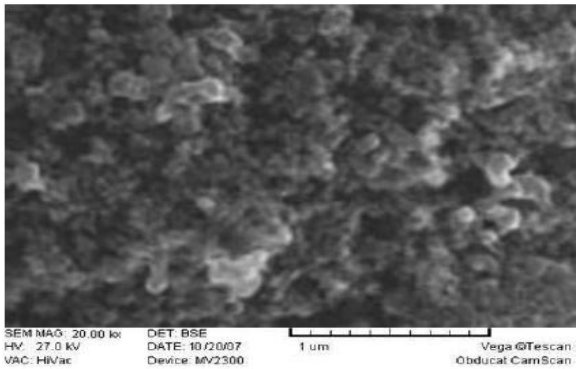

Fig.3. SEM image for TE2 with T/E=5**.**

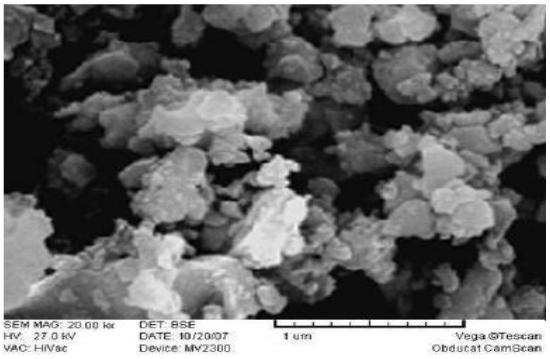

Fig.4. SEM image for TE4 with T/E=3**.**

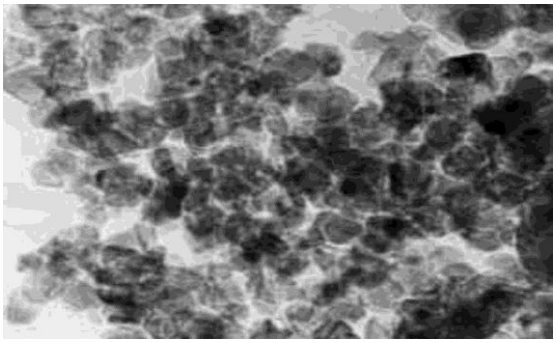

Fig.5. TEM image for TE2 with T/E=5**.**

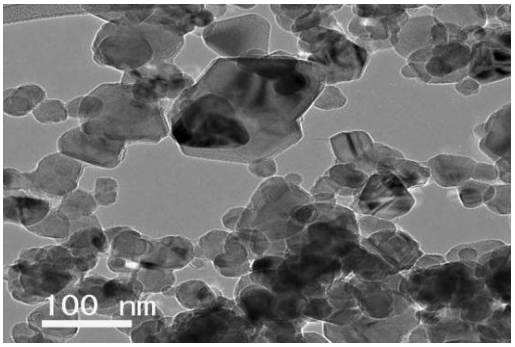

Fig.6. TEM image for TE2 with T/E=3**.**

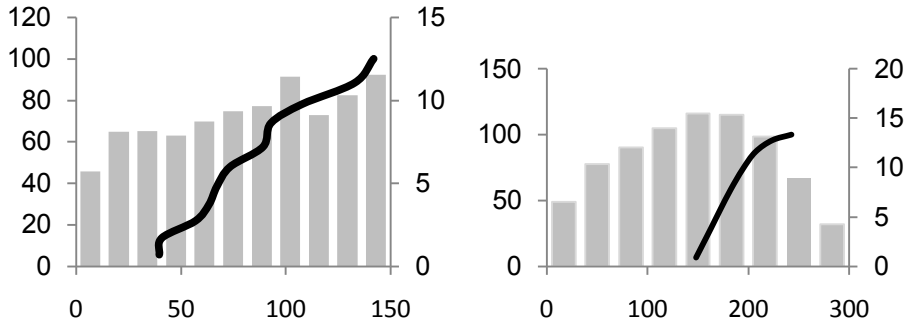

TE1 sample with T/E=6 TE2 sample with **T**/E=5

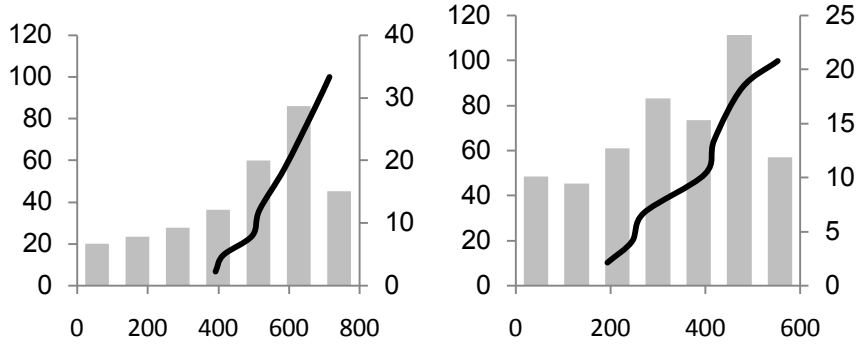

TE2 sample with **T**/E=3 TE2 sample with **T**/E=4

Fig.7. PS diagram

According to PS diagrams, average size for each sample is obtained. And effect of alcohol ratio on particle size can be figured. As one can see in diagram, best applied ratio in this ratio research has been 5. By decreasing alcohol, since it has the roll of solvent, particles are formed faster and by increasing micro cross links make bigger molecules which have led to bigger grain size. By increasing alcohol reactions rate decline and there is more gel than precipitate.

3.3. Effect of stirring time

Hydrolysis reactions are performed in 4 stages in following order:

$$Si(OC_2H_5)_4 + H_2O \rightarrow Si(OH)(OC_2H_5)_3 + C_2H_5OH$$
$$Si(OC_2H_5)_4 + 2H_2O \rightarrow Si(OH)_2(OC_2H_5)_2 + 2C_2H_5OH$$
$$Si(OC_2H_5)_4 + 3H_2O \rightarrow Si(OH)_3(OC_2H_5) + 3C_2H_5OH$$
$$Si(OC_2H_5)_4 + 4H_2O \rightarrow Si(OH)_4 + 4C_2H_5OH$$

Completing these reactions requires enough time. In short mixing times, these reactions are not completed so final phases mount decreases. By increasing mixing time so much reactions were completed and increasing time has caused increasing cross links and bigger micro molecules, these micro molecules cause SiO_2production in bigger sizes and trapping carbon source in them. In higher temperatures carbonization reaction occurs with lower diffusion and total amount of phases has declined.

By performing experiment according to table 2 with the same route, the best mixing time obtained as 4 hours which has been already mentioned in references and there is no need to repeat.

IV. CONCLUSIONS

Maximum efficiency SiC production is obtained in T/E ratio 5. By changing this ratio production efficiency decreases. By deviation from this ratio primary sol solvent, resultant powder shape has changed from spherical shape to flat shape. By obtaining average particle size from bar diagram, decrease or increase in this ratio effects on primary molecules size. In all XRD spectrums other phases exist which in some points are amorphous and by pickling, these phases will remove to some extent. It should be mentioned that resultant data in this experiment have some deviation, due to some limitation and difficulties.

Table1. Materials ratio with different TEOS/Eth

Sample	TEOS/Eth	TEOS/Sac	Sac/H_2O	TEOS/H_2O	Time
TE1	6	4	0/5	2	**4**
TE2	5	4	0/5	2	**4**
TE3	4	4	0/5	2	**4**
TE4	3	4	0/5	2	**4**

Table2. Materials ratio with different stirring time

Sample	TEOS/Eth	TEOS/Sac	Sac/H_2O	TEOS/H_2O	Time
T1	5	4	0/5	2	**3**
T2	5	4	0/5	2	**4**
T3	5	4	0/5	2	**5**
T4	5	4	0/5	2	**6**

REFERENCES

[1] V. Raman, O.P. Bahl, and U. Dhavan, "Synthesis of Silicon Carbide through the Sol-Gel Process from Different Precursors", National Physical Laboratory, New Delhi, India (1995).

[2] L. Tong, Ramana, and G. Reddy, "Thermal Plasma Synthesis of SiC Nano-Powders/Nano-Fibers", Department of Metallurgical and Materials Engineering, The University of Alabama, USA (2005).

[3] R. Pampuch, G. Gorny, and L. Stobierski, "Synthesis of One-Dimensional Nanostructured Silicon Carbide by Chemical Vapor Deposition", University of Science and Technology, AGH, Krakow, Poland (2004).

[4] H. Konno, T. Kinomura, H. Habazaki, and M. Aramata, "Synthesis of Sub micrometer-Sized SiC Particles from the Precursors Composed of Exfoliated Graphite and Silicone", Lab. Of Advanced Materials Chemistry, Japan (2003).

[5] Raman, V., O. P. Bahl and U. Dhawan, "Synthesis of silicon carbide through the sol-gel (1995).

[6] Ronald William, R.W., "Fundamental Principles of sol-gel Technology" (1989).

[7] K.J. Konsztowicz, Dispersion of SiC whisker in water, in: G. deWith, R. A. Terpstra, R. Metselaar (Eds.), Euro Ceramics, Vol.1, Processing of Ceramics, Elsevier Applied Science, London, pp. 1.169-1.173 (1989).

[8] R.A. McCauley, Rheology. Ceramic Monographs ~Handbook of ceramics, supplement to Interceram 32, 1-7(1983).

[9] J. Li, J. Tian and L. Dong, "Synthesis of SiC Precursors by a two-step Sol-Gel Process and their conversion to SiC powders", Journal of the European Ceramic Society, pp 1853-1857, 77 (2000).

[10] A.C. Pierre, Sol-Gel Processing of Ceramic Powders, Ceramic Bulletin, 70:1281–1288 (1991).

[11] C. J. Brinker, and G. W. Sherrer, Sol-Gel Science, Academic Press, NY (1990).

American Journal of Engineering Research (AJER)
E-ISSN: 2320-0847 P-ISSN: 2320-0936
Volume-03, Issue-03, pp-322-329
www.ajer.org

Research Paper Open Access

Analysis urban life quality, case study residents of Rostamabad City

Akram Ali Reza poor[1], Hojjat Allah Sharafi[2], Hossein Ghazanfarpour[2]
[1]*MSc student in Department of Geography and Urban Planning, College of human science, Zahehan Branch, Islamic Azad University, Zahedan, Iran, (Corresponding author)*
[2] *Assistant professors of Geography and Urban Planning, Shahid Bahonar University of Kerman, Iran*

Abstract: - One of the main issues raised about sustainable development and the quality of human life. Life quality, economic, social, physical, biological, cultural and political advocacy. City Rostamabad Narmashir city center, which is located in the South East province. Based on the material provided above, the present study is the evaluation of quality of life in the city Rostamabad. The purpose of this studies the physical aspects of quality of life, economic, social and Rostamabad is in the city. Research question is: subjective quality of life of residents in the city Rostamabad (Narmashir) How so? This study is a descriptive analysis. Data collection methods include observation, enterprise statistics, and library resources, and Inventory. Quality of Life Questionnaire research tool households. They Collection data by, correlations Statistical tests, Binomial T test, Wilcoxon, and one sample T- test were analyzed. Findings indicated the objective quality of life of city residents Rostamabad is desirable and less desirable in some areas. The results showed the following subjective satisfaction with the quality of this type of service, cost, access time, and so is low. The subjective quality of life in the next few social good and is close to the average. While the have become more favorable for quality of life in all three dimensions of economic, social, and spatial - ecological status of the city.

Keywords: - Urban life quality, Rostamabad city, residents

I. INTRODUCTION

One of the main issues raised about sustainable development and the quality of human life. Life quality, economic, social, physical, biological, political, cultural, and it can be said. That quality of life is one of the main areas of study in science, human geography; urban planners have a serious want to explain their research into this area. Smith was the first geographer quality of life, prosperity and social justice, as discussed in geography (Mohammadi Savadkoohi, 2011, 16). Since the late 1960s, the concept of quality of life in terms of social justice, social welfare, public life, quality of living environment and geographical science literature was compiled. Meanwhile, Liberal and Radical Geographers than other Schools of thought were affected. Issues such as social welfare, inequality, extreme poverty, disease, racism, crime, life expectancy, housing and were quickly attracted the attention of geographers (Shakui, 2007, 141).

Quality word in Latin (qual) means "what and how" of quality in the sense of "how" and qol the meaning of the word "quality" of life, and comprise the difference is that each individual is unique and different from others. Brown believes that quality of life means having fun and favorite work, a sense of security, inner joy, a feeling of closeness with those who share. Their lives with confidence and self-satisfaction, having fun and living with the values and beliefs of important (Brown and et al, 2003, 20).

One of the fundamental characteristics of quality of life is a multidimensional being. Those of It All experts agree that world. And despite all the efforts of many researchers have identified these dimensions, but overall, but they opened it can be said common is that they differ more from (Kurd zanganeh, 2007). Quality of life can be classified into two groups based on a shared objective and subjective. In concrete, there are objective indicators that point to an aspect of urban life are visible and obvious. These indicators quantitatively and in terms of numbers, figures and statistics (secondary data) are investigated and displayed. The second category is the subjective indicators in the form of mental retardation that are usually the same people through a questionnaire to measure satisfaction (Lotfy, 2010, 75). The broadest and most differentiated in quality of life,

clean the objective and subjective quality of life (Lee, 2008, 1206). Subjective than objective indicators index is more suitable for planning purposes.

Objectively necessary for the provision of basic necessities of life, personal and material resources to meet the social needs of citizens. And after having autonomy in mind: 1 - increasing mental well-being, including sensuality, satisfaction, purpose in life and personal growth; 2 - growth and prosperity in the course of prosperity and other pro 3 - participation in a wide range of social activities concerns. (Yung-Jaan Lee, 2008. 1206-1209). Various methods for studying the quality of life in rural and urban areas are employed. However, no comprehensive framework for the study of life quality integrated and holistic and based on physical characteristics, and social location is (Kamp et al, 2003, 5) it is therefore necessary to examine the quality of life in different parts. Among the nearly 200 countries, Iran ranked 150 among 2010's in terms of quality of life. This ranking indicated in the cost of living has increased 71 percent. According to Middle Eastern countries can be said the quality of life in Iran is moderate.

City Rostamabad is a center of Narmashir County, which is located in the South East province. Based on the material provided above, the present study is the evaluation of quality of life in the city Rostamabad. The purpose of this studies the physical aspects of quality of life, economic, social and Rostamabad is in the city.

II. THE NECESSITY AND IMPORTANCE OF RESEARCH

Because the debate on sustainable development, quality of life, including the issues raised in today's scientific study on this subject in each region and in each period, it seems imperative. In fact, it is the quality of life of people in any place, in any time period are reviewed.

Research on quality of life in a community, as can be assessed, and a description of the nature or circumstances of life in a particular region or country to be considered. Quality of life, social groups or individuals by external factors such as technology, manufacturing, infrastructure, communication with other groups or countries, different organizations in the community, the natural environment as well as internal factors that reflect the interaction between personal values and cultural values are determined by (Fattahi and et al, 2011, 9).

Quality of life in its collective dimension of the physical environment and social stability, social resources within communities in which they live are emphasized. Social resources include civil cohesion, Cooperation, integration, extensive network of connection and temporal connection at all levels of society, and society's norms and values such as trust, altruism and altruistic behavior, fairness, social justice and the equality(Phillips, 2006, 242).

Rostamabad city as a center of Narmashir County, less than 5 years, the city has become the center is a deprived area. To the current status of objective and subjective quality of life in the city will be investigated.

III. THY HISTORY OF RESEARCH

Perhaps the most famous of the highest quality ever taken place. The United Nations Human Development Report, the Human Development Report by the WHO in 1990 and successively developed as far as the most comprehensive studies on quality of life was raised. Quality of Life in New Zealand reported in 2007 showed a picture of life in New Zealand and was characterized by an improved quality of life, in what areas or areas where improvement is needed. This report covers 68 key indicators of quality of life. The purpose of this report was to provide information that could explain the perceived economic and environmental conditions, to describe and quantify the quality of life for residents living in urban areas in New Zealand, to be used.

Projects in the United States of America Jacksonville's quality of life, quality of life as "a feeling of well-being or satisfaction resulting from factors that are present in the external environment" are defined. External environment is divided into nine factors, and each factor is a target image. And indicators to measure progress toward these goals are determined. The nine factors are: economic, political / governmental, environmental, health, education, social, cultural - recreational, public safety and transport (Fattahi et al, 2011, 29-23). Since the late 1960s, the concept of quality of life in terms of social justice, social welfare, public life, quality of living environment and geographical sciences, literature and extensive research was conducted by researcher's worldwide geography. Iranian globally and multiple studies have been conducted on the quality of life in urban areas:

In the Yeager Study (1962), quality of the environment based on the structural condition of the existing facilities (including the number of inhabitants per square foot) was measured.

In the O'Connor Study (1978), housing quality index of the number of persons per room and bedroom crowding in Florida were examined.

In the Nelson et al Study (2005), the presence or absence of hot water and other facilities index to measure the quality of urban housing is considering.

In the Harris study (1976), in this study, the connection between housing quality and the characteristics of the housing price is to be created.
In the Ha and Weber Study (1994), 1040 people through questionnaires in order to assess the current situation and living conditions of living index is based on 77 questions and answers were in terms of satisfaction. Furthermore, given the importance of ideal and actual situations presented.
In the Carp and et al study (1976), Evaluation of a rapid transit system in coastal area residents was conducted on the environmental quality of life. This study evaluated the audience about their current living situation based on more than 100 properties in question were settled.

In the Bonaiuto and et al study (2003), as indicators of environmental quality perception of residence and neighborhood associations in urban areas, two instruments measuring quality connection with the residents live in urban environments is presented. These tools include the 11 criteria that perception of the environment in urban residential environment measures and criteria to measure the dependence of a neighborhood has been applied.

Moloudi (2010), the criteria and sub-criteria indicate that the consent of any of the physical characteristics of spatial structure - there is no content and performance at low quality of the new city Hashtgerd is many reasons.
Rezvani et al (2010), Quality of life domains were identified as follows: housing, water, light, food, fuel for cooking and heating, collection and disposal of garbage and sewage networks, health, safety, employment, ownership of the goods durable, education, information and communication, participation, freedom, fun and leisure.
Kokabee (2008), indicators and measures of quality of urban life in multiple dimensions and studies worldwide have examined.

Research questions:

- The objective quality of life of residents in the city Rostamabad (Narmashir) How so?
- Subjective quality of life of residents in the city Rostamabad (Narmashir) How so?
- The quality of the objective and subjective quality of life of residents in the city Rostamabad (Narmashir) is there a difference?

Research theories:

It seems the objective quality of life of residents in the city Rostamabad (Narmashir) is not desirable.
It seems the subjective quality of life of residents in the city Rostamabad (Narmashir) is not desirable.
Appears between the objective and subjective quality of life quality of residents in the city Rostamabad (Narmashir) There is a difference.

IV. RESEARCH MATERIALS AND METHODS

This study is a descriptive analysis. Data collection methods include observation, enterprise statistics, and library resources, and Inventory. Quality of Life Questionnaire household survey tool that has been developed in three dimensions and is capable of measuring all aspects of the lives of the citizens remaining Rostamabad evaluation.
In Rostamabad almost 1540 families live in the city. In the present study, using the estimation method chosen by 15 % of the population (about 225 households) was measured. While we have tried to sample each of the four main areas of town are randomly selected.
Data from field operations was analyzed using SPSS software, and then statistical tests (Binomial T test, Wilcoxon, and one sample T test) were analyzed. The two main methods of data analysis are:

- Statistical tests for assessing connection such as correlations Statistical tests
- Appropriate statistical tests to examine differences: like the one sample T test, and the Binomial T test

The study area

City Rostamabad between longitudes 58 ° 20 'to 58 degrees 46 minutes east and latitude 28 degrees 52 minutes north and 17 degrees and is accurate to 28. The city is located in the southeastern province of Kerman. From the north to the Dasht-e Lut, in the east city Fahraj, on the south west part of the city Rigan and Rud Ab and Bam city limits. (Kerman province Governor. Deputy of Planning. Office of Statistic, information and GIS).

V. RESULTS

In order to test the first theory, which says: "It seems that visual quality is not optimal Narmashir residents living in the city," the library is used in the field and the objective quality of life in the city Rostamabad (services utilities applications infrastructure production and consumption) show. The results show a

good level of service to citizens residing Rostamabad enjoy life. Only two of the "Recreation and sewage networks' have absent or weak. Also, since the table (1) the inhabitants of the city in the aftermath of the civil service have increased, we can conclude the objective quality of life of residents in the city Rostamabad is desirable.

Table (1) - Quality of life (Enjoyment or Lack enjoyment)

Row	Topic	Before becoming city	After becoming city
1	Banks and credit institutions	Lack enjoyment	Enjoyment (4 Bank)
2	Adequate Housing	Enjoyment 47.3%	Enjoyment 95.6%
3	Beautiful passages and quality	Enjoyment 18%	40% Enjoyment
4	Asphalted streets	Enjoyment 40 %	70% Enjoyment
5	The proper way of communicating	Enjoyment	Enjoyment
6	with the outside locations	Lack enjoyment	Enjoyment
7	Water supply network	Lack enjoyment	Enjoyment The cylinder supply of centers
8	Gas pipeline or gas cylinder the supply	Lack enjoyment	Enjoyment
9	Post and Post Bank	Lack enjoyment	Enjoyment
10	Landfills Center	Lack enjoyment	Lack enjoyment
11	Proper sewage network	Lack enjoyment	Enjoyment
12	Rubbish transfer trucks	Lack enjoyment	Enjoyment
13	Public library	Lack enjoyment	Enjoyment
14	Culture Centers	enjoyment	Enjoyment
15	New school with a capacity	Lack enjoyment	enjoyment
16	Academic institutions and higher	Lack enjoyment	Enjoyment
17	education	Lack enjoyment	Enjoyment
18	Health centers and pharmacies	Lack enjoyment	Enjoyment
19	Hospitals Hostels	Lack enjoyment	Enjoyment weak

Source: research results

In order to test the theory that says "subjective quality of life of residents in the city Rostamabad (Narmashir) is not desirable" test one sample T test, and the Binomial T test, were used.

The results of Tables (2), and Table (7), we can conclude subjective quality of life of residents in the city Rostamabad not desirable. Only the social dimension of satisfaction is slightly more than the average is desirable. In particular, the economic and physical - environmental, resident satisfaction, quality of life is low. The tables show the results of the city, residents ' satisfaction is greatly increased. Results Table (1) shows the values? Of items is done is winding down. And most of them are below average. It is noteworthy that all the items have improved during the Rostamabad to town.

Table (2) - Descriptive Results of the binomial T-test

Topic	Average	Number of respondents	Standard deviation
Quality of Economic life, before become city	2.0524	221	.72356
Quality of Economic life, After the become city	2.3928	221	.85510

Source: research results

Table (3) - Analytical results of the binomial T-test

Topic	Differences in the two samples before and after the becoming city					The value T	Degrees of freedom	Significance level
	Average Difference	Standard deviation	Average Standard deviation	Difference at 95% level probability				
				Lower limit	Upper limit			

Citizens' satisfaction in terms of life quality economical dimension	.34039	.57169	.03846	-.41618	-.26460	-8.851	220	.000

Source: research results

Table (4) - Descriptive Results of the binomial T-test

Topic	Average	Number of respondents	Standard deviation
Quality of social life, before become city	2.1965	222	.77886
Quality of social life, After the become city	2.8078	222	1.07358

Source: research results

Table (5) - Analytical results of the binomial T-test

Topic	Differences in the two samples before and after the becoming city					The value T	Degrees of freedom	Significance level
	Average Difference	Standard deviation	Average Standard deviation	Difference at 95% level probability				
				Lower limit	Upper limit			
Citizens' satisfaction in terms of life quality social dimension	-.61134	.71046	.04768	-.70531	-.51737	-12.821	221	.000

Source: research results

Table (6) - Descriptive Results of the binomial T-test

Topic	Average	Number of respondents	Standard deviation
life quality in dimension physical - environmental, before become city	2.1671	219	.91774
life quality in dimension physical - environmental, After the become city	2.6152	219	.94990

Source: research results

Table (7) - Analytical results of the binomial T-test

Topic	Differences in the two samples before and after the becoming city					The value T	Degrees of freedom	Significance level
	Average Difference	Standard deviation	Average Standard deviation	Difference at 95% level probability				
				Lower limit	Upper limit			
Citizens' satisfaction in terms of life quality in dimension physical - environmental	-.44810	.64490	.04358	-.53399	-.36221	-10.283	218	.000

Source: research results

VI. THE THIRD HYPOTHESIS TESTS

Between objective quality and subjective quality of life appears to be urban residents Rostamabad (Narmashir) There is a difference.

Results Table 1 shows the objective quality of life of residents Rostamabad is desirable. But the results of Tables (2) to (7) showed an objective quality of life of residents Rostamabad is not desirable. Therefore, we can conclude the objective quality and subjective quality of life of their citizens' lives are different.

VII. CONCLUSIONS

The quality of life of city residents Rostamabad results found desirable in some areas like entertainment and sewerage network is relatively good. Residents enjoy a relatively high because of the service. Especially social indicators such as access to health and education services are desirable. And people have the right level of service. The results showed that the subjective satisfaction of the people from this kind of quality, cost, access time, and so is low. The subjective quality of life in the next few social good and is close to the average. In interpreting these results, we deal with this question, which, despite many infrastructure services, communications, social and economic satisfaction with the services and quality of life is low, why?

Factors such as age and education level can be effective in reducing satisfaction, so if you want to be able to investigate the role of such factors as the results of correlations Statistical tests (Table 8, 9)'s satisfaction to be determined refer inhabited (subjective quality Living) communicative no age group and education level of residents.

Table (8) - Results of correlation test

Dimension	Topic	The correlation of age with any subject
economic	Pearson correlation	.052
	Sig	.438
	N	221
social	Pearson correlation	.061
	Sig	.370
	N	220
physical - environmental	Pearson correlation	.069
	Sig	.312
	N	216

Source: research results

Table (9) - Results of the correlation between education and quality of life

Dimension	Topic	Correlation between education level and any subject
economic	Pearson correlation	.148*
	Sig	.029
	N	218
social	Pearson correlation	-.059
	Sig	.384
	N	217
physical - environmental	Pearson correlation	1
	Sig	
	N	219

Source: research results

Finally, we stated that the city Rostamabad has a desirable effect on quality of life in the city. Tables 10 and 11 show the results of all quality of life indicators in all three dimensions of economic, social, and spatial - ecological status of the city have become more favorable.

Table (10) - Results of T-test analysis of binomial measure quality of life dimensions

Dimension	Indicators	Period before becoming city	Period after becoming city
economic	Quality of occupation	1.8374	2.2881
	Quality of earnings	1.8638	2.2612

	The quality of the urban economy	2.4395	2.6214
social	Access to quality social services	2.0922	2.7862
	lodging Quality of	2.2563	2.7837
	Quality of Urban Management	2.2355	2.8348
physical - environmental	Quality of the physical landscape	2.1345	2.5045
	Quality natural landscape	2.0580	2.4978
	Access to quality telecommunications services.	2.3605	2.8627
	Access to quality to urban services	2.1639	2.6601

Source: research results

Table 11 - Results of T-test analysis of binomial measure quality of life dimensions

Dimension	Period before becoming city	Period after becoming city
economic	2.0524	2.3928
social	2.1965	2.8078
physical - environmental	2.1671	2.6152

Source: research results

VIII. SUGGESTIONS

Now that quality of life was assessed in Rostamabad is necessary to provide recommendations based on the current status of this issue to be dealt with.

A - in economics

Developing industrial town in the area. Because it increases employment and income in the region. Processing of agricultural products in the region and will eventually lead to regional development.
Raising workshops and small factories, especially for women and youth.
Prevent land speculation and rein pressure groups that raise the price of land in the town and surrounding villages, have been followed by agriculture destroyed.

B - The social dimension

Improve administrative and cultural environment (cooling and heating work, etc).
Increased tourism and recreational services and facilities specially equipped beautiful park has a variety of features and attractive to people.
Sewer system and its development in the future.
Development of the housing sector, especially the old houses are built of mud brick. It is located on a fault zone with natural hazards such as earthquakes and floods combined.
Increased interaction with the public authorities, in particular the Council and Mayor.
Prepare for increased public participation in city development Rostamabad.

C - in the environmental and physical

Increase the brightness of the lights on the city streets.
Increase the quality of paths (Alleys and Streets).
Improvement of urban furniture painting, lighting, and design of buildings.

REFERENCE

[1] Bonaiuto. Marino and et al, (2004), "Neighborhood Evaluation within a Multi place perspective on Urban Activities", Environment and Behavior, Vol.36, No. 1, pp. 41-69.
[2] Brown and Roy I. Brown, (2003), Quality of Life and Disability an Approach for Community Practitioners, Jessica Kingsley Publishers, London and New York.
[3] Carp F M., Zawadski R. T. Shokrkon H, (1976); Dimensions of urban environmental quality; Environment and Behavior, Vol. 8, No. 2, pp: 239-264.
[4] Couper M (2000) Measuring the quality of community life: a program of longitudinal and comparative international research. In: Proceedings of the second international conference on the quality of life in cities, vol 2.pp 386–400. National University of Singapore, School of Real Estate and Building.

[5] Eftekhari, A.R. Tavakkoli, M, (2004), Rural social welfare, the cognitive approach in explaining social welfare, Modares Journal of Human Science Spatial Planning, Tehran.
[6] Fattahi, A. Khorasani, M.A. Paydar, A, (2013), Quality of Life and Human Development, Tehran, Entekhab publications.
[7] Ha, M., and Weber, M. J., (1994), Residential Quality and Satisfaction: Toward Developing, Residential Quality Indexes, Home Economics Research Journal, 22 (3), 296-308.
[8] Kamp, I., K, Van, Leidelmeijer, K., Marsman, G. and de Hollander, A., (2003), Urban environmental quality and human wellbeing: Towards a conceptual framework and demarcation of concepts; a literature study, Landscape and Urban Planning, 65(1-2).
[9] Kerman province Governor .Deputy of Planning. office of Statistic, information and GIS
[10] Kokabee, A, (2008), Measures of quality of urban life in urban centers, Journal of Hoviateshahr Number 1 / Fall-Winter 86.
[11] Lee, Y.-J., (2008), Subjective quality of life measurement in Taipei, Building and Marans RW.
[12] Lotfy, S, (2010), concept of quality of urban life: definitions, dimensions and measurements in urban planning, Journal of Human Geography, the first year, No. 14, pp. 82-64.
[13] Mohammadi Savadkoohi, Kh, (2011), the concept of quality of life in urban and countries involved in its promotion,, Journal of Shoraha , No. 55.
[14] Moloudi, J, (2010), master's thesis, geography and urban planning, urban environmental quality evaluation in the case of new cities: New City Hashtgerd, supervisor M. Rafieian, Tarbiat Modarres University.
[15] nelson, B, Jasvinder A. Singh, Howard A. Fink, Kristin L. Nichol, (2005), Health-related quality of life predicts future health care utilization and mortality in veterans with self-reported physician-diagnosed arthritis: The veterans arthritis quality of life study Original Research Article Seminars in Arthritis and Rheumatism, Volume 34, Issue 5, Pages 755-765.
[16] Pacione, M, (1995), The Use of objective and subjective measures of quality of life in human geography, Progress in Human Geography, No 6.
[17] Philips, D, (2006), Quality of life Concept, policy and Practice London Rutledge.
[18] Rafieian, M. Askari, A. Askarizadah, Z, (2010), Assessment of residential satisfaction residents Nawab district, Human Geography Research, No. 67, 68-53.
[19] Rafieian, M. Moloudi, J. Poortahery, M, (2011), measuring the quality of urban environment in new cities: New Town Hashtgerd, Modares Journal of Human Science Planning and Space Preparation, Volume 15, Number 3, pp. 20-39.
[20] Rezvani, M. Mitkan, A.A. Mansorian, H. Sattari . M.H, (2010), Development of indicators to measure the quality of urban life in the city Nurabad, Journal Urban - Regional Studies and Research, the first year , second edition.
[21] Shakui, H, (2007), new ideas in philosophy, Geography (volume I), Gitashenasi publications.
[22] Yung-Jaan Lee, (2008), Subjective quality of life measurement in Taipei, Building and Environment 43, pp 1205–1215.

American Journal of Engineering Research (AJER)
e-ISSN : 2320-0847 p-ISSN : 2320-0936
Volume-03, Issue-03, pp-330-338
www.ajer.org

Research Paper Open Access

Microalgae: An Alternative Source of Renewable Energy

A. Z. A. Saifullah, Md. Abdul Karim, Aznijar Ahmad-Yazid
Department of Mechanical Engineering, IUBAT – International University of Business Agriculture and Technology, Dhaka 1230, Bangladesh
Department of Mechanical Engineering, IUBAT – International University of Business Agriculture and Technology, Dhaka 1230, Bangladesh
Department of Engineering Design and Manufacture, University of Malaya 50603 Kuala Lumpur, Malaysia

Abstract:- This paper presents an overview on the potentiality of microalgae with particular emphasis as a sustainable renewable energy source for biodiesel. One of the most important dilemmas of the modern world is to supply maximal amount of energy with minimal environmental impact. The total energy demand of our planet is increasing with population growth whereas the fossil fuel reserves are dwindling swiftly. Biodiesel produced from biomass is widely considered to be one of the most sustainable alternatives to fossil fuels and a viable means for energy security and environmental and economic sustainability. But as a large area of arable land is required to cultivate biodiesel producing terrestrial plants, it may lead towards food scarcity and deforestation. Microalgae have a number of characteristics that allow the production concepts of biodiesel which are significantly more sustainable than their alternatives. Microalgae possess high biomass productivity, oils with high lipid content, fast growth rates, possibility of utilizing marginal and infertile land, capable of growing in salt water and waste streams, and capable of utilizing solar light and CO_2 gas as nutrients.

Keywords: – *Biodiesel, Energy security, Environment friendly, Microalgae, Sustainability*

I. INTRODUCTION

The global energy demand is expanding with rapid population growth. Almost 1.4 billion people of our planet face daily shortage of energy [1]. Estimate shows that the world would require 50% more energy in 2030 than it does today [2]. Adversely, the fossil fuel reserves are being exhausted day by day [3]. Fossil fuel meets about 80% of the world's energy demand [4]. The basic sources of this energy are wood, coal, petroleum oil and natural gas [5-10]. As these sources of energy are limited and cannot be reused, our planet is going to face energy scarcity. In addition, the emission produced by the combustion of fossil fuels also contributes to air pollution and global warming [11-14]. The combustion of fossil fuels is a major source of air contaminants including CO_x and SO_x [15-19]. Carbon dioxide contributes to greenhouse effect [20-23]. Sulfur dioxide leads to acid rain by forming sulfuric acid which changes the normal pH of soil [5, 22]. It can be assumed that the global consumption of energy will raise and lead to more environmental smash up [16]. The concern about rapid depletion of fossil fuels, energy security and climate change are forcing governments, scientist and researchers to explore alternative sources of energy. Presently many options are being studied and implemented including solar energy, hydroelectricity, geothermal energy, wind energy, ocean energy and biofuels [24, 25]. Only the transportation sector accounts for almost 30% of the world's energy consumption most of which is in the form of liquid fuels [26]. When energy consumption for transportation comes into consideration and as two thirds of global energy consumption is derived from petroleum based liquid fuels, more attention should be given on the renewable energy sources of liquid fuels, which is biomass derived liquid fuels or biofuels [27,28]. Biofuels can play a vital role in mitigating energy crisis and environmental pollution [29, 30]. The most common biofuels are ethanol produced from sugar and starch crops, and biodiesel produced from vegetable oils and animal fats [31, 32].

The objective of this study is to reveal microalgae as an alternative renewable energy source for producing biodiesel. Microalgae has been discussed in a broad broad-spectrum showing that microalgae is a

sustainable renewable energy source for biodiesel as other biomass sources of biodiesel need arable agricultural lands and sophisticated expensive technologies for their production on commercial basis.

II. BIODIESEL

Biodiesel is a non-toxic renewable energy source. It consists of monoalkyl esters of long chain fatty acids [33]. It is derived from vegetable oils and animal fats via transesterification reaction. The animal or vegetable oils are converted into biodiesel when one mole of triglyceride reacts with three moles of alcohol (such as methanol or ethanol) to produce a mole of glycerol and three moles of monoalkyl esters (biodiesel) [5]. Methanol is the most commonly used alcohol in the commercial production of biodiesel because of its low price [4, 34]. Biodiesel is usually blended with petroleum based diesel though it also can be used in pure form with some modifications of engines [35, 36]. Blends are indicated by the abbreviation B_{XX}, where XX is the percentage of biodiesel in the mixture.

2.1 Sources of Biodiesel

Biodiesel can be produced from both edible and non-edible sources of oil such as soybean oil [37-39], rapeseed [40,41], palm oil, maize[42], mahua[43], canola, coconut, corn oil [44], cotton seed [45], sunflower [44], fish oil, peanut, mustard oil, tobacco seed oil, jojoba oil, olive oil [46], pungam seed oil, linseed, groundnut oil, tall oil, fried oil, beef tallow, chicken fat, lard oil, animal fat, soapnut, Jatropha [47], pongamia, argemone, castor [46], karanja oil [48], algae, etc.

2.2 Creditability of biodiesel

Biodiesel has the potentiality to strengthen our energy security. It is an environmentally friendly energy source [49]. It is non-toxic and highly biodegradable [50-55]. The combustion of biodiesel emits less CO_x, SO_x, hydrocarbons, aromatic hydrocarbons, alkenes, aldehydes, ketones and particulate matter [56]. Biodiesel feedstock plants absorb CO_2 through photosynthesis, which is more than it discharges by the combustion process. Therefore, it can maintain ecological balance more effectively compared to petroleum diesel. Table 1 shows average emission impacts of biodiesel blends compared to petroleum diesel [57, 58].

Table 1. Average emission impacts of biodiesel blends compared to petroleum diesel

Biodiesel Blends	B20	B40	B60	B80	B100
Unburned hydrocarbons	-20%	-35%	-49%	-59%	-67%
Carbon Monoxide	-12%	-22%	-32%	-40%	-48%
Particulate Matter	-12%	-22%	-32%	-40%	-47%
NO_X	+2%	+4%	+6%	+8%	+10%

The production of biodiesel has the potentiality to generate new employment opportunity for developing country. Moreover, biodiesel has some technical advantages. Biodiesel gives more clean combustion than petroleum diesel. It possesses high cetane number. The cetane number is a measurement of the combustion quality of diesel fuel during compression ignition. So the flammability of biodiesel is better than that of diesel oil. Biodiesel can be transported safely due to its high flash point. Biodiesel acts as a better lubricant and detergent than petroleum diesel. Table 2 shows comparison of different properties of diesel and biodiesel [59, 60].

Table 2. Comparison of different properties of diesel and biodiesel

Fuel	Density at 15° C g/cm^3	Viscosity at 40°C mm^2/s	Sulfur, %	Carbon, %	Hydrogen, %	Oxygen, %	Flash point	Cetane Number	Lower calorific value MJ/kg
Diesel	0.834	2.83	0.034	86.2	13.8	—	62	47	42.59
Biodiesel	0.8834	4.47	< 0.005	76.1	11.8	12.1	178	56	37.243

The production and use of biodiesel involve multiple input and output to make a full assessment [61]. Nothing is wasted in the process of biodiesel production. Usually sodium hydroxide or potassium hydroxide is used as catalyst for biodiesel production. 4% alcohol can be extracted from the product and reused. 9% glycerin

is produced which can be used as raw material for toiletries industry. Table 3 shows reactants and products of transesterification reaction of biodiesel production [61].

Table 3. Reactants and products of transesterification reaction of biodiesel production [61]

Input(Reactants)	Output(Products)
1. Oil 87%	1. Methyl ester (Biodiesel) 86%
2. Alcohol 12%	2. Glycerin 9%
3. Catalyst 1%	3. Alcohol 4%
	4. Fertilizer 1%

2.3 Limitations of biodiesel

As arable lands are used for biodiesel production, it may lead to food scarcity. It also may cause deforestation because of the excessive demand of land for biodiesel production. The water demand for some biodiesel crops could put unsustainable pressure on local water resources. Using fertilizer for biodiesel production can have harmful effects on environment. The combustion of biodiesel increases nitrogen oxides emissions which creates smog and acid rain [62-68]. Biodiesel is less energy efficient than petroleum diesel. The content of a gallon of biodiesel is 11% less than the energy content of petro diesel. Biodiesel has higher viscosity than petro diesel [69, 70]. The viscosity of biodiesel is about 11-17 times greater than that of diesel fuel which leads to problem in pumping, atomization in the injector and combustion [71]. Biodiesel causes excessive engine wear. Biodiesel is corrosive against copper and brass [71].

2.4 Three generations of biodiesel feedstock

- First generation (Biodiesel produced from soybeans, coconut, sunflower, rapeseed, palm oil, etc.)
- Second generation (Biodiesel produced from jatropha, mahua, cassava, miscanthus, jojoba oil, salmon oil, tobacco seed, straw, etc.)
- Third generation (Biodiesel produced from microalgae)

The first generation Biofuels can assure the energy security and healthy environment. But the production of first generation Biofuels needs arable agricultural lands. Consequently, it may impact on global food security. As a large portion of land is required for global total fuel demand, it also may cause of deforestation. The second generation Biofuels is produced from non-edible components. It is intended to produce from woody part of non-edible plants that do not compete with food production. However, converting the woody biomass into fermentable sugars requires sophisticated and expensive technologies for commercial production. Therefore second generation Biofuels cannot be produced economically in large scale [72]. They also need arable lands which may cause food scarcity and deforestation. Biodiesel produced from microalgae is considered as the third generation of Biofuels. Microalgae can be a sustainable renewable energy source for biodiesel to overcome the limitations of first and second generation Biofuels [72].

III. MICROALGAE

Microalgae are prokaryotic or eukaryotic photosynthetic microorganisms. Naturally they can grow rapidly in fresh or salt water due to their unicellular or simple multi-cellular structure. Because of their simple cellular structure, they are very efficient converters of solar energy. As the cells of microalgae grow in aqueous suspension, they have efficient access of water, CO_2 and other nutrients [73]. Microalgae are one of the oldest living organisms in our planet. Microalgae have more than 300000 species. Several species of them have oil content up to 80% of their dry body weight. Table 4 shows lipid contents of different microalgal species [74, 80].

Table 4. Lipid contents of different microalgal species

Microalgae species	Lipid content (% dry weight)
Botryococcus braunii	25-75
Chlorella	18-57
Chlorella emersonii	25-63
Chlorella sp.	10-48
Dunaliella sp.	18-67
Dunaliella tertiolecta	18-71
Nannochloris sp.	20-56
Nannochloropsis sp.	12-53
Neochloris oleoabundans	29-65
Phaeodactylum tricornutum	18-57
Scenedesmus obliquus	11-55
Schizochytrium sp.	50-77

Many researches proved that microalgae have many advantages for biodiesel production in comparison with other conventional feedstock. Microalgae can be either autotrophic or heterotrophic. Autotrophs use inorganic compounds as a source of carbon. Autotrophs can be photoautotrophic, using light as a source of energy, or chemoautotrophic, oxidizing inorganic compounds for energy. Heterotrophs use organic compounds for growth. Heterotrophs can be photoheterotrophs, using light as a source of energy, or chemoheterotrophs, oxidizing organic compounds for energy [73]. Figure 1 shows different stages of production of microalgal biodiesel.

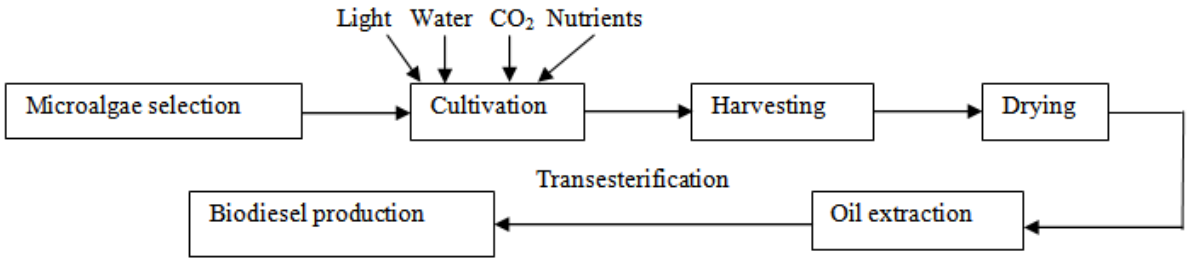

Figure 1. Different stages of production of microalgal biodiesel

3.1 Microalgal biodiesel creditability

Microalgae can be considered as a sustainable energy source of next generation biofuels [81]. Microalgae are capable of producing oil all year long. Oil productivity of microalgae is greater compared to conventional crops [82]. The oil content of microalgae is in the range of 20-50% which is greater than other competitors. Microalgae produce 15-300 times more oil for biodiesel production than traditional crops on an area basis. Biodiesel production from algal lipid is non toxic and highly biodegradable. Microalgae can grow in high rates which can be 50 times more than that of switchgrass, which is the fastest growing terrestrial crop [83]. They can complete an entire growth cycle in every few days via photosynthesis that converts sun energy into chemical energy. Microalgae have higher photon conversion efficiency; it is approximately 3-8% against 0.5% for terrestrial plants. Microalgae do not compete for land with food crops [84, 85]. They grow in fresh water, seawater, waste water or non-arable lands [86-88]. Therefore, they have minimal environmental effect such as deforestation. So microalgae are an alternative fuel feedstock that could avoid fuel versus food conflict [89]. The cultivation of microalgae needs less water than other energy oil crops. Table 5 shows comparison of different sources of biodiesel [90-100].

Table 5. Comparison of different sources of biodiesel

Biodiesel source	Oil yield (Liter oil/ha)	Land use (m^2/GJ)	Energy (GJ/ha)	Water required (m^3/GJ)
Soybean	446	689	15	383
Rapeseed	1190	258	39	383
Palm oil	5906	52	192	75
Sunflower	951	323	31	61
Jatropha	1896	162	62	396
Microalgae	24355-136886	2-13	793-4457	<379

Production of biodiesel from microalgae can fix CO_2 [101-103]. Roughly 1kg of algae biodiesel fixes 1.83 kg of CO_2. Microalgae cultivation has a higher CO_2 mitigation rate between 50.1 ± 6.5% on cloudy days and 82.3 ± 12.5% on sunny days for different algal species [104]. Some of the microalgae species are very efficient in capturing of CO_2 from high CO_2 streams such as flue gases. The CO_2 content in flue gases is usually 5-15%. The cultivation of Chlorella sp. in 55 m^2 culture area photo bioreactor mitigates 10-50% of CO_2 from flue gas (CO_2 content 6-8% by volume) [104]. Therefore, microalgae have the ability of decarbonization of flue gases. The cultivation of microalgae can utilize nitrogen and phosphorus as nutrients from waste water sources. So microalgae can give the additional benefit of wastewater bioremediation. Moreover, microalgal biodiesel can reduce the emission of NO_x. Microalgae produce valuable co-products or byproducts such as H_2, ethanol, biopolymers, proteins, cosmetic products, carbohydrates, fertilizer, animal feed, biomass residue etc. [105]. Microalgae cultivation does not require fertilizer, herbicides and pesticides. The heating value of Microalgal biodiesel is more than that of other terrestrial plants. The high heating value of biodiesel derived from rapeseed or soybean is 37 MJ/kg, while biodiesel derived from microalgae is 41 MJ/kg [106]. Table 6 shows properties of petroleum based diesel and microalgal biodiesel [107].

Table 6. Properties of petroleum based diesel and microalgal biodiesel

Energy source	Density (at 15°C) Kg / m^3	Kinematic viscosity (at 40°C) mm^2 / s
Diesel	836	3.03
Microalgal biodiesel	919	33.06

3.2 Limitations of microalgal biodiesel

Microalgae have low biomass concentration due to the limit of light penetration of algal cells. Therefore the cost of Microalgal biodiesel production is relatively higher compared to other feedstock. The drying process of harvested microalgae would be an energy consuming process due to the large water content. The heating value of Microalgal biodiesel is lower than that of petroleum based diesel fuel [108].

IV. CONCLUSION

Microalgal biodiesel is potentially alternative sustainable green energy. It is possible to produce microalgal biodiesel to satisfy the fast growing energy demand within the restraints of land and water resources. Microalgal farming can be coupled with flue gas CO_2 mitigation and wastewater treatment. Microalgae can produce a large variety of novel byproducts. Microalgae biodiesel is not yet economically viable enough to replace petroleum based fuels or compete with other renewable energy technologies such as wind, solar, geothermal and other forms of Bioenergy. Despite their high potential both in terms of productivity and sustainability, most algae based biofuel concepts still require significant investment to become commercially viable.

REFERENCES

[1] N. M. Komerath, P. P. Komerath, Terrestrial Micro Renewable Energy Applications of Space Technology, *Physics Procedia, 20,* 2011, 255-269.

[2] Yahaya Muhammad Sani, Wan Mohd Ashri Wan Daud, A.R. Abdul Aziz, Solid acid-catalyzed biodiesel production from Microalgal oil-The dual advantage, *Journal of Environmental Chemical Engineering,1,* 2013, 113-121.

[3] Saifuddin Nomanbhay, Refal Hussain, Md. Mujibur Rahman, Kumaran Palanisamy, Review Paper Integration of Biodiesel and Bioethanol Processes: Conversion of Low Cost Waste Glycerol to Bioethanol, *Advances in Natural and Applied Sciences, 6,* 2012, 802-818.

[4] Daming Huang, Haining Zhou, Lin Lin, Biodiesel: an Alternative to Conventional Fuel, *Energy Porcedia, 16,* 2012, 1874-1885.

[5] Demshemino S. Innocent, O'Donnell P. Sylvester, Muhammad F. Yahaya, Isioma Nwadike, and Linus N. okora, Comparative Analysis of biodiesel and petroleum Diesel, *International journal of Education and Research, 1(*8), 2013.

[6] Nivea De Lima Da Silva, Julian A. G. Garnica, Cesar B. Batistella, Maria Regina Wolf Maciel, Use of experimental design to investigate biodiesel production by multiple-stage Ultra-Shear reactor, *Bioresource Technology, 102,* 2011, 2672-2677.

[7] Surendhiran D. and Vijay M, Microalgal Biodiesel – A Comprehensive Review on the Potential and Alternative Biofuel, *Research Journal of Chemical Sciences, 2(11),* 2012, 71-81.

[8] Bajhaiya A.K., Mandotra S.K., Suseela M.R., Toppa K. and Ranade S., Algal Biodiesel: the next generation biofuel for India: Review Article, *Asian J. Exp.Biol.Sci., 1,* 2010, 728-739.

[9] Subramaniam R., Dufreche S., Zappi M. and Bajpai R., Microbal lipids from renewable resources: production and characterization, *J. Ind. Microbial Biotechnol., 37,* 2010, 1271-1287.

[10] David Painter, Are biofuels the future or a folly? : A review, *New Zealand Journal of Forestry, 53,* 2009.

[11] Zhou A., Thomson E., The Developments Of Biofuels in Asia, *Applied Energy, 86,* 2009, 11-20.

[12] Prabhakar, S. V. R. K., Elder M., Biofuels and resource use efficiency in developing Asia: Back to basics, *Applied Energy, 86,* 2009, 30-36.

[13] Agrawal A. K., Biofuels (alcohols and biodiesel) applications as fuels for internal combustion engines, *Progress in Energy and Combustion Science, 33,* 2007, 233-271.

[14] CheHafizan, Noor Zainon Zainura, Biofuel: Advantages and disadvantages based on life cycle assessment (LCA) perspective, *Journal of Environmental Research and Development, 7,* 2013.

[15] Quaye E. C., Energy Demands in the 21st century: The Role of Biofuels in a developing country, *Renewable Energy, 9,* 1996, 1029-1032.

[16] Basha S.A., Gopal K.R., Jebaraj S., A review on biodiesel production, combustion, emission and performance, *Renewable and Sustainable Energy Reviews, 13,* 2009, 1628-1634.

[17] Teresa M. Mata, Antonio A. Martins, Nidia. S. Caetano, Microalgal for biodiesel production and other applications: A review, *Renewable and Sustainable energy Reviews, 14,* 2010, 217-232.
[18] A. B. M. Sharif Hossain, Aishah Salleh, Biodiesel fuel production from algae as renewable energy, *American Journal of Biochemistry and Biotechnology, 4,* 2008, 250-254.
[19] Vishwanath Patil, Khanh-Quang Tran, Hans Ragnar Giselrød, Towards Sustainable Production of Biofuels from Microalgae, *International Journal of Molecular Sciences, 9,* 2008, 1188-1195.
[20] Amela Ajanovic, Biofuels versus food production: Does biofuels production increase food prices?, *Energy,* 2010, 1-7.
[21] S. N. Naik, Vaibhav V. Goud, Prasant K. Rout, Ajay K. Dalai, Production of first and second generation biofuels: A comprehensive review, *Renewable and Sustainable Energy Reviews, 14,* 2010, 578-597.
[22] R. Prakash, R. K. Shing, S. Murugan, Comparison of performance and emission parameters of a diesel engine fueled biodiesel and wood pyrolysis oil emulsions, *International Energy Journal, 13,* 2012, 123-132.
[23] Bruce Gardner, Wallace Tyner, Explorations in biofuels economics, policy, and history: Introduction to the special issue, *Journal of Agricultural and Food Industrial Organization, 5,* 2007.
[24] Gilbert R, Perl A., Transport revolutions: moving people and freight without oil, *Earthscan,* 2008.
[25] Dewulf J, Van Langenhove H., Renewables-based technology: sustainability assessment, Jhon Wiley & Sons, Ltd., 2006
[26] Parvatker A. G., Biodiesel from microalgae – A sustainability analysis using life cycle assessment, *International Journal of Chemical and Physical Sciences, 2,* 2013.
[27] Hagg A. L., Algae Bloom Again, *Nature, 447,* 2007, 520-521.
[28] Schneider D., Grow your Own? : Would the Wide Spread Adoption of Biomass-Derived Transportation Fuels Really Help the Environment, *American scientist, 94,* 2006, 408-409.
[29] Guanhua Huang, Feng Chen, Dong Wei, Xuewu Zhang, Gu Chen, Biodiesel production from microalgal biotechnology, Applied Energy, 87, 2010, 38-46.
[30] S. Kiran Kumar, Performance and Emission Analysis of Diesel Engine Using Fish Oil and Biodiesel Blends with Isobutanol as an Additive, *American Journal of Engineering Research, 2,* 2013, 322-329.
[31] Divya Bajpai, V. K. Tyagi, Biodiesel: Source, production, consumption, properties and its benefits, *Journal of Oleo Science, 55,* 2006, 487-502.
[32] Annisa Bhikuning, Engine Performance and Oil Analysis of Biodiesel from Bulk Oil, *Asian Transactions on Engineering, 1,* 2011.
[33] M. U. Kaisan, G. Y. Pam, D. M. Kulla, Physico–Chemical Properties of Bio–diesel from Wild Grape Seeds Oil and Petro–diesel Blends, *American Journal of Engineering Research, 2,* 2013, 291-297.
[34] Ramadhas A.H., Jayaraj S., Muraleedharan C., Biodiesel production from high FFA rubber seed oil, *Fuel, 84,* 2005, 335-340.
[35] Apostolakou A.A., Kookos I.K., Marazioti C., Angelopoulos K.C., Techno-economic Analysis of a biodiesel Production process from Vegetable oils, *Fuel Processing Technology, 90,* 2009, 1023-1031.
[36] Pedrojevic Z.J., The production of biodiesel from waste frying oils: A comparison of different purification steps, *Fuel, 87,* 2008, 3522-3528.
[37] Lepuerta M., Armas O., Fernandez J.R., Effect of Biodiesel Fuels on diesel Engine emissions, *Progress in Energy and Combustion Science, 34,* 2008, 198-223.
[38] A.L. Ahmad, N.H. Mat Yasin, C.J.C. Derek, J.K. Lim, Microalgae as a sustainable energy source for biodiesel production: A review, *Renewable and Sustainable Energy Reviews, 15,* 2011, 584-593.
[39] Celikten I., Koca A., Arslan MA., Comparison of performance and emissions of diesel fuel, rapeseed and soybean oil mythyl esters injected at different pressures, *Renew Energy, 35,* 2010, 814-820.
[40] Zankruti Patel, Krishnamurthy R., Biodiesel: Source Materials and Future Prospects, *International Journal of Geology, Earth and Enviromental Sciences, 3(2),* 2013, 10-20.
[41] Armen B. Avagyan, New Design & Build Biological System through the Use of Microalgae Addressed to Sustainable Development, *Journal of Environmental Protection, 1,* 2010, 183-200.
[42] Tahani S. Gendy, Seham A. El-Temtamy, Commercialization potential aspects of microalgae for biofuel production: An overview, *Egyptian Journal of Petroleum, 22,* 2013, 43-51.
[43] Sudheer Nandi, Performance of C. I. Engine by Using Biodiesel – Mahua Oil, *American Journal of Engineering Research, 2,* 2013, 22-47.
[44] Abu Yousuf, Mozammel Hoque, M. Asraful Jahan, Domenico Pirozzi, Technology and Engineering of Biodiesel Production: a Comparative Study between Microalgae and Other Non-Photosynthetic Oleaginous Microbes, *International Review of Chemical Engineering, 4(6),* 2012.
[45] Shashi Kumar Jain, Sunil Kumar, Alok Chaube, Technical Sustainability of Biodiesel and Its Blends with Diesel in C.I. Engines: A Review, *International Journal of Chemical Engineering and Applications, 2(2),* 2011.

[46] Bello Y. Makama, Bankefa Temitope, Nwaeburu Clifford, Linus N. Okoro, Synthesis and Calorific Value of Biodiesel by Methanolysis of Castor and Olive Oils in Admixture, *Australian Journal of Basic and Applied Sciences, 5(11),* 2011, 874-878.
[47] K. Sudhakar, M. Rajesh, M. Premalatha, Carbon mitigation potential of Jatropha Biodiesel in Indian context, *Energy Procedia, 14,* 2012, 1421-1426.
[48] S. Jaichandar1, K. Annamalai, The Status of Biodiesel as an Alternative Fuel for Diesel Engine – An Overview, *Journal of Sustainable Energy and Environment, 2,* 2011, 71-75.
[49] C.G. Tsanaktsidis, S.G. Christidis, G.T. Tzilantonis, Study about Effect of Processed Biodiesel in Physiochemical Properties of Mixtures with Diesel Fuel in order to Increase Their Antifouling Action, *International Journal of Environmental Science and Development, 1,* 2010.
[50] Parag Sexena, sayali Jawale, Milind H Joshipura, A review on prediction of properties of biodiesel and blends of biodiesel, Procedia Engineering, 51, 2013, 395-402.
[51] M. R. Jakeria, M. A. Fazal, A. S. M. A. Haseeb, Influence of different factors on the stability of biodiesel: A review, Renewable and Sustainable Energy Reviews, 30, 2014, 154-163.
[52] Fangrui Ma, Milford A. Hanna, Biodiesel production: A review, *Bioresource Technology, 70,* 1999, 1-15
[53] Hossain A. B. M. S., Nasrulhaq Boyce A., Salleh A., Chandran S., Biodiesel production from waste soybean oil biomass as renewable energy and environmental recycled process, *African Journal of Biotechnology, 9,* 2010, 4233-4240.
[54] A. P. Sathiyagnanam, Member, Iaeng, C. G. Saravanan, Experimental Studies on the Combustion Characteristics and Performance of A Direct Injection Engine Fueled with Biodiesel/Diesel Blends with SCR, *Proceedings of the World Congress on Engineering, 3,* 2011.
[55] Xiaohu Fan, Rachel Burton, Recent Development of Biodiesel Feedstocks and the Applications of Glycerol: A Review, *The Open Fuels and Energy Science Journal, 2,* 2009, 100-109.
[56] L. G. Anderson, Effects of Biodiesel Fuels Use on Vehicle Emissions, *Journal of Sustainable Energy and Environment, 3,* 2012, 35-47.
[57] A Comprehensive Analysis of Biodiesel Impacts on Exhaust Emissions, *United States Environmental Protection Agency,* 2002.
[58] Idusuyi N. Ajide O. O. Abu R., Biodiesel as an Alternative Energy Resource in Southwest Nigeria, *International Journal of Science and Technology, 2,* 2012.
[59] Dongsheng Wen, H. Jiang, Kai Zhang, Supercritical fluids technology for clean biofuel production, *Progress in Natural science, 19,* 2009, 273-284.
[60] M. Sakunthala, V. Sridevi, K. Vijay Kumar, K. Rani, Biodiesel – Renewable Fuel, Environmental Implications and Its Handling, *Journal of Chemical, Biological and Physical Sciences, 3,* 2013, 1564-1571.
[61] Adriana Downie, David Lau, Annette Cowie, Paul Munroe, Approches to greenhouse gas accounting methods for biomass carbon, *Biomass and Bioenergy, 60,* 2014, 18-31.
[62] Xiaoyan Shi, Xiaobing Pang, Yujing Mu, Hong He, Shijin Shuai, Jianxin Wang, Hu Chen, Rulong Li, Emission reduction potential of using ethanol-biodiesel-diesel fuel blend on a heavy-duty diesel engine, *Atmospheric Environment, 40,* 2006, 2567-2574
[63] Jinlin Xue, Tony E. Grift, Alan C. Hansen, Effect of biodiesel on engine performances and emissions, *Renewable and Sustainable Energy Reviews, 15,* 2011, 1098-1116.
[64] Jon Van Gerpen, Biodiesel processing and production, *Fuel Processing Technology, 86,* 2005, 1097-1107.
[65] Ambarish Datta, Bijan Kumar Mandal, Biodiesel production and its emission and performance: A review, *International Journal of Engineering & Scientific Research, 3,* 2012.
[66] Gaurav Dwivedi, Siddharth Jain, M. P. Sharma, Diesel engine performance and emission analysis using biodiesel from various oil sources – Review, *Journal of Material and Environmental Science, 4,* 2013, 434-447.
[67] S. Oberweis, T. T. Al-Shemmeri, Effect of biodiesel blending on emissions and efficiency in a stationary diesel engine, International Conference on Renewable Energies and Power Quality, 2010.
[68] James W. Richardson, Joe L. Outlaw, Marc Allison, The Economics of Microalgae Oil, *AgBioForum, 13(2),* 2010, 119-130.
[69] Mustafa E. Tat, Jon H. Van Gerpen, The Kinematic Viscosity of Biodiesel and Its Blends with Diesel Fuel, *Journal of the American Oil Chemists' Society, 76(12),* 1999.
[70] Pooja Ghodasara, Mayur Ghodasara, Experimental Studies on Emission and Performance Characteristics in Diesel Engine Using Bio–Diesel Blends and EGR (Exhaust Gas Recirculation), *International Journal of Emerging Technology and Advanced Engineering, 2(2),* 2012.

[71] M. Mofijur, H. H. Masjuki, M. A. Kalam, A.E. Atabani, M. Shahabuddin, *Effect of biodiesel from various feedstocks on combustion characteristics, engine durability and materials compatibility: A review, Renewable and Sustainable Energy Reviews, 28,* 2013, 441-455.
[72] Firoz Alam, Abijit Date, Roesfiansjah Rasjidin, Saleh Mobin, Hazim Moria, Abdul Baqui, Biofuel from algae- Is it a viable alternative?, *Procedia Engineering 49,* 2012, 221-227.
[73] Giuliano Dragone, Bruno Fernandes, Antonio A. Vicente, Jose A. Teixeira, Third generation biofuels from microalgae, Institute for Biotechnology and Bioengineering, Centre of Biological Engineering, University of Minho, Portugal.
[74] Suphi S. Oncel, Microalgae for a macroenergy world, *Renewable and Sustainable Energy Reviews, 26,* 2013, 241-264.
[75] S. Karthikeyan, A critical review: Microalgae as a renewable source for biodiesel production, International *Journal of Engineering Research & Technology, 1,* 2012.
[76] Yusuf Chisti, Biodiesel from microalgae, *Biotechnology Advances, 25,* 2007, 294-306.
[77] Liam Brennan, Philip Owende, Biofuels from microalgae – A review of technologies for production, processing, and extraction of biofuels and co-products, *Renewable and Sustainable Energy Reviews,* 2009.
[78] Xiaodan Wu, Rongsheng Ruan, Zhenyi Du, Yuhuan Liu, Current status and prospects of biodiesel production from microalgae, *Energies, 5,* 2012, 2667-2682.
[79] Luisa Gouveia, Ana Cristina Oliveira, Microalgae as a raw material for biofuels production, *Journal of Industrial Microbiology and Biotechnology, 36,* 2009, 269-274.
[80] Ramasamy Sakthivel, Sanniyasi Elumalai, M. Mohommad Arif, Microalgae lipid research, past, present: A critical review for biodiesel production, in the future, *Journal of Experimental Sciences, 2,* 2011, 29-49.
[81] P. Hyka, S. Lickova, P. Pribyl, K. Melzoch, K. Kovar, Flow cytometry for the development of biotechnological processes with microalgae, *Biotechnology Advances, 31,* 2013, 02-16.
[82] Rudras Baliga, Susan E. Powers, Sustainable Algae Biodiesel Production in Cold Climates, *International Journal of Chemical Engineering,* Volume 2010.
[83] Patrick E. Wiley, J. Elliott Campbell, Brandi Mckuin, Production of Biodiesel and Biogas from Algae: A Review of Process Train Options, *Water Environment Research, 83,* 2011, 326-338.
[84] Kalpesh K. Sharma, Holger Schuhmann, Peer M. Schenk, High Lipid Induction in Microalgae for Biodiesel Production, *Energies, 5,* 2012, 1532-1553.
[85] Janusz Jakóbiec, Mariusz Wądrzyk, Microalgae as a Potential Source for Biodiesel Production, *Agricultural Engineering, 6(124),* 2010.
[86] N. Abdel-Raouf, A. A. Al-Homaidan, I. B. M. Ibraheem, Microalgae and Wastewater Treatment, *Saudi Journal of Biological Sciences, 19,* 2012, 257-275.
[87] Andrzej Lewicki, Jacek Dach, Damian Janczak, Wojciech Czekala, The experimental photoreactor for microalgae production, *Procedia Technology, 8,* 2013, 622-627.
[88] Raphael Slade, Ausilio Bauen, Micro-algae cultivation for biofuels: Cost, energy balance, environmental impacts and future prospects, *Biomass and Bioenergy, 53,* 2013, 29-38.
[89] Wanchat Sawaengsak, Thapat Silalertruksa, Athikom Bangviwat, Shabbir H. Gheewala, Life cycle cost of biodiesel production from microalgae in Thailand, *Energy for Sustainable Development, 18,* 2014, 67-74.
[90] J.E. Andrade, A. Perez, P.J. Sebastian, D. Eapen, A review of bio-diesel production processes, *Biomass and Bioenergy, 35,* 2011, 1008-1020.
[91] A. E. Atabani, A. S. Silitonga, Irfan Anjum Badruddin, T. M. I. Mahlia, H. H. Masjuki, S. Mekhilef, A comprehensive review on biodiesel as an alternative energy resource and its characteristics, *Renewable and Sustainable Energy Reviews, 16,* 2012, 2070-2093.
[92] S. Kent Hoekman, Amber Broch, Curtis Robbins, Eric Ceniceros, Mani Natarajan, Review of biodiesel composition, properties, and specifications, *Renewable and Sustainable Energy Reviews, 16,* 2012, 143-169.
[93] Aninidita Karmakar, Subrata Karmakar, Souti Mukherjee, Properties of various plants and animals feedstocks for biodiesel production, *Bioresource Technology, 101,* 2010, 7201-7210.
[94] Anita Kirrolia, Narsi R. Bishnoi, Rajesh Singh, Microalgae as a boon for sustainable energy production and its future research & development aspects, *Renewable and Sustainable Energy Reviews, 20,* 2013, 642-656.
[95] Shalini Rajvanshi, Mahendra Pal Sharma, Microalgae : A Potential Source of Biodiesel, *Journal of Sustainable Bioenergy Systems, 2,* 2012, 49-59.
[96] Xiaodong Deng, Yajun Li, Xiaowen Fie, Microalgae: A Promising Feedstock for Biodiesel, African Journal of Microbiology Research, 3, 2009, 1008-1014.

[97] Baljeet Singh Saharan, Deepansh Sharma, Rajender Sahu, Ozlem Sahin, Alan Warren, Towards Algal Biofuel Production: A Concept of Green Bio Energy Development, *Innovative Romanian Food Biotechnology, 12,* 2013.
[98] Md.Imran Kais, Farsad Imtiaz Chowdhury, Kazy Fayeen Shahriar, Biodiesel from Microalgae as a solution of third world energy crisis, Bioenergy Technology, World Renewable Energy Congress 2011.
[99] Peer M. Schenk, Skye R. Thomas-Hall, Evan Stephens, Ute C. Marx, Jan H. Mussgnug, Clemens Posten & Olaf Kruse, Ben Hankamer, Second Generation Biofuels: High Efficiency Microalgae for Biodiesel Production, *Bioenergy Research, 1,* 2008, 20-43.
[100] Sushant S. Satputaley, Chetan Chawane, N. V. Deshpande, A Critical Review of Biofuels from Algae for Sustainable Development, *International Journal of Computer Applications,* National Conference on Innovative Paradigms in Engineering & Technology 2012.
[101] Lingling Wang, Bingtao Zhao, Yixin Zhang, Prediction of energy microalgae production under flue gas using response surface methodology, *Energy Procedia, 16,* 2012, 1066-1071.
[102] Razif Harun, Manjinder Singh, Gareth M. Forde, Michael K. Danquah, Bioprocess engineering of microalgae to produce a variety of consumer products, *Renewable and Sustainable Energy Reviews, 14,* 2010, 1037-1047.
[103] M. S. Ghayal, M. T. Pandya, Microalgae biomass: a renewable source of energy, *Energy Procedia, 32,* 2013, 242-250.
[104] Yanqun Li, Mark Horsman, Nan Wu, Christopher Q. Lan, Nathalie Dubois-Calero, Biofuels from Microalgae, American Chemical Society and American Institute of Chemical Engineers, 2008.
[105] Emma Suali, Rosalam Sarbatly, Conversion of microalgae to biofuel, *Renewable and Sustainable Energy Reviews, 16,* 2012, 4316-4362.
[106] Matthew N Campbell, Biodiesel: Algae as a Renewable Source for Liquid Fuel, *Guelph Engineering Journal, 1,* 2008, 2-7.
[107] Yi-Hung Chen, Bo-Yu Huang, Tsung-Han Chiang, Ting-Cheng Tang, Fuel properties of microalgae (Chlorella protothecoides) oil biodiesel and its blends with petroleum diesel, *Fuel, 94,* 2012, 270-273.
[108] GuanHua Huang, Feng Chen, Dong Wei, Xuewu Zhang, Gu Chen, Biodiesel production by microalgal biotechnology, *Applied Energy, 87,* 2010, 38-46.

American Journal of Engineering Research (AJER)
e-ISSN : 2320-0847 p-ISSN : 2320-0936
Volume-03, Issue-03, pp-339-345
www.ajer.org

Research Paper Open Access

Correlation Development for Sauter Mean Diameter of Rotary Atomizer

Murali.K[1], S.Maya Kannan[1], M.Sivanesh Prabhu[1],Senthil Kumar SK [1]
B.Aathitha chozhan[2], N.Ashok kumar[2], T.Charlin devadoss[2], P.Jeya kumar[2]
1- Assistant Professor, MAM School of Engineering, Trichy,Tamil Nadu,India.
2- Under Graduate Students, MAM School of Engineering, Trichy,Tamil Nadu,India.

Abstract: - Atomizers are of many types, among that simplex and duplex types of atomizers are used and recognized often as fuel injectors in aircrafts. Types of atomizers and features are read. Among many types of atomizer, rotary type of atomizer is selected due to its naked evident like easy retrofit to existing spreading system , able to handle large quantities, feed is possible, better economy, high peripheral speed and spread of droplets, uniform liquid feed rate, uniform distribution of feed, higher level of atomization etc., The rotary atomizer specifications and its features are listed, the droplets of rotary atomizer are visualized and readings are taken from experimental methods, such as Laser visualization method .After the droplets data alignment, the (SMD) Sauter Mean Diameter is to be taken in and considered, SMD means it is a average particle (droplet) size of a given particles, and it is further explained with its given relation. By SMD's given equated form it is used to compare data between rotary atomizer particles and given particle size. By SMD it is simplified further and used to create a co-relation between SMD and rotary atomizer. The rotary atomizer data values are taken through out with the SMD to find and form a co-related derived pattern for ROTARY ATOMIZER.

Keywords: *Co-relations, Droplets, Injectors, Rotary atomizer, SMD Sauter Mean Diameter, Types of atomizer*

I INTRODUCTION

Atomization
The development of the jet or sheet and the growth of small disturbances, which eventually leads to disintegration into ligaments and then small droplets.

Atomizer
Atomizer is a device for emitting water, perfume, or other liquids as a fine spray.

Types of Atomizer
1.Pressure Atomizer,
Plain Orifice,
Pressure Swirl,
Square Spray,
Dual Orifice,
Duplex,
Fan Spray.
Rotary Atomizer,
Air – Assist Atomizer,
Air Blast Atomizer.

Rotary Atomizer
One widely used type of atomizer comprises a high speed rotating disk with means for introducing liquid at it center. The liquid flow radially outward across the disk and is discharges at high velocity from it periphery.()
At high flow rate, ligaments or sheets are generated at the edges and disintegrate into droplets. Small disk operating at high rotational speeds and low flow rate are capable of producing spray in which drop size are fairly uniform at low flow rate droplets from near the edge of the disk. The sizes of the liquid droplet diminish with increase rotational speed, increases with flow rate. Rotary atomizers are used throughout the process and allied industries to produce a spray of relatively small mean droplet diameter. A typical application of atomizer is

atomization of feedstock in spray dryer. The principle of operation of centrifugal atomizers is the addition of centrifugal energy of liquid feed to increase the surface area. Disintegration of liquid film results in the formation of droplets stream. Rotary atomization has been widely studied and today it is well-known that the degree of atomization depends on the speed, feed rate, liquid properties, and atomizer design.

The majority of experimental conditions under which spray analysis studies have been conducted neglect influences of drying air entry around the atomizer and air flow produced by wheel rotation.A detrimental effect of wheel rotation is generation of a region of low pressure air at the wheel center. This region establishes an air flow that flows radially inward through clearance gap between wheel and atomizer body and on reaching the cavity in wheel center, the flow then changes direction and flows radially outward through the ports.

This air stream typically draws air from hot inlet air in dryer roof and can simultaneously aerate and partially dry feedstock within atomizer wheel. Dried particles deposited on wheel will over dry and can constitute a source of product contamination and potential ignition for fire and explosions.Pumped air stream, which possesses a largeamount of radial momentum, can significantly affect dryer flow pattern in pilot plants in diameter up to 2 m.

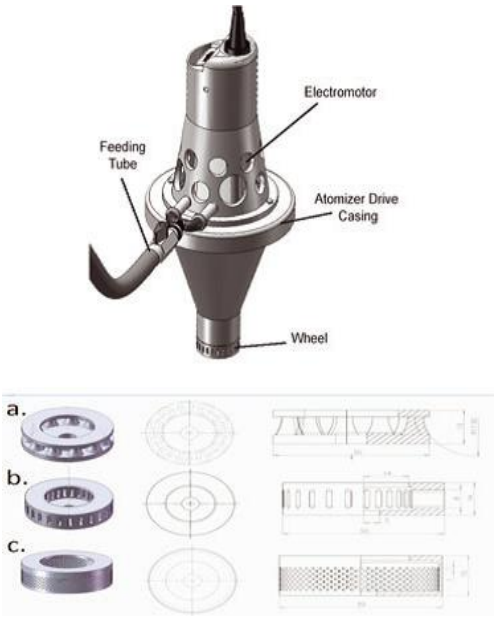

Figure 1. Rotary atomizer and wheels

II METHODOLOGY

Dimensional Analysis:

$SMD = 0.26N^{-0.79}Q^{0.32}d^{-0.69}\rho_L^{-0.29}\sigma^{0.26}(1+1.027\mu_L^{0.65})$

The above equation is taken from the following journal Bachalo, W.D, and Houser, M.J, Phase Doppler Spray Analyzer for Simultaneous Measurements of Drop Size and Velocity Distributions Opt.Eng., Vol.23, No.5, 1984, PP 583-590

$SMD = f[Q\sigma\mu_L/Nd\rho_L]$

$n = 7$

$Q = m^3/sec = L^3T^{-1}$

$\sigma = N/m = Kgm/sec^2m = MT^{-2}$

$\mu_L = Kg/msec = ML^{-1}T^{-1}$

$N = 1/sec = T^{-1}$

$d = m = L$

$\rho_L = Kg/m^3 = ML^{-3}$

$j = n-K = 3$

We take N, d, ρ_L as not as π form.

$\pi_1 = N^a.d^b.\rho_L^c.Q = M^0L^0T^0$

$T^{-a}.L^b.M^cL^{-3c}.L^3.T^{-1} = M^0L^0T^0$

$M = c = 0$

$L = b-3c+3 = 0$

$T = -a-1 = 0$

$a = -1$

$b = -3$

c = 0
$\pi^1 = N^{-1}d^{-3}\rho_L{}^0$
$= d^{-3}/N$
$= Q/Nd^3$
$\pi_2 = N^a d^b \rho_L{}^c \sigma$
$= [T^{-1}]^a[L]^b[ML^{-3}]^c \cdot MT^{-2}$
$= M^0L^0T^0$
$= T^{-a}L^bM^cL^{-3c}ML^{-2}$
M = c+1 = 0
L = b-3c = 0
T = -a-2 = 0
a = -2
b = -3
c = -1
$\pi_2 = N^{-2}d^{-3}\rho_L{}^{-1}\sigma$
$= \sigma/N^2d^3\rho_L$
$\pi_3 = N^a d^b \rho_L{}^c.\mu_L$
$= [T^{-1}]^a[L]^b[ML^{-3}]^c[ML^{-1}T^{-1}] = M^0L^0T^0$
$= T^{-a}L^bM^cL^{-3c}ML^{-1}T^{-1}$
M = c+1 = 0
L = b-3c-1 = 0
T = -a-1 = 0
a = -1
b = -2
c = -1
$\pi_3 = N^{-1}d^{-2}\rho_L{}^{-1}.\mu_L$
$= \mu_L/Nd^2\rho_L$
$\pi_4 = N^a d^b \rho_L{}^c.SMD$
$= [T^{-1}]^a[L]^b[ML^{-3}]^c[L]$
$= T^{-a}.L^b.M^cL^{-3c}.L$
M = c = 0
L = b-3c+1 = -1
T = -a = 0
a = 0
b = -1
c = 0
$\pi_4 = N^0d^{-1}\rho_L{}^0.SMD$
$= SMD/d$
f (π1, π2, π3/π4)
$= Q/Nd^3 * \sigma/N^2d^3\rho_L * \mu_L/Nd^2\rho_L * d/SMD$
$SMD = Q\sigma\mu_L/N^4d^7\rho_L{}^2m$

III RESULT & DISCUSSION

$SMD = 0.26N^{-0.79}Q^{0.32}d^{-0.69}\rho_L{}^{-0.29}\sigma^{0.26}(1+1.027\mu_L{}^{0.65})$

Table 1. Volumetric flow rate Vs SMD at 7000 rpm

Volumetric Flow Rate (Q) ($\times10^{-7}m^3/s$)	**SMD ($\times10^{-5}m$)**
54	7.26
108	9.08
162	10.5
216	11.6

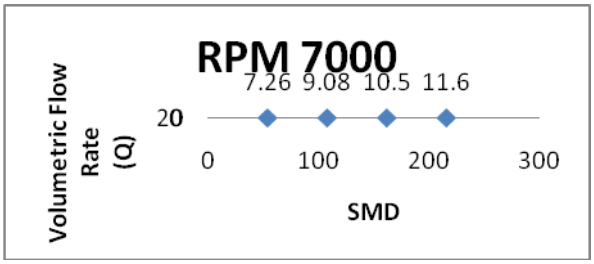

Graph 1. volumetric flow rate Vs SMD at 7000 rpm

Table 2. volumetric flow rate Vs SMD at 12000 rpm

Volumetric Flow Rate (Q) ($\times 10^{-7} m^3/s$)	SMD ($\times 10^{-5} m$)
54	4.73
108	5.92
162	6.87
216	7.61

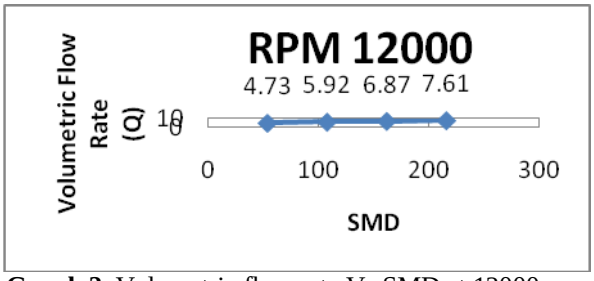

Graph 2. Volumetric flow rate Vs SMD at 12000 rpm

Table 3. Volumetric flow rate Vs SMD at 16000 rpm

Volumetric Flow Rate (Q) ($\times 10^{-7} m^3/s$)	SMD ($\times 10^{-5} m$)
54	3.79
108	4.73
162	5.4
216	6.06

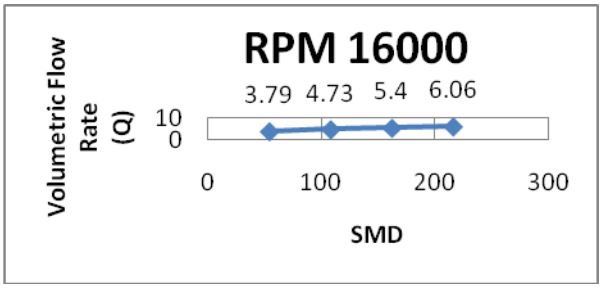

Graph 3. Volumetric flow rate Vs SMD at 16000 rpm

Table 4. Volumetric flow rate Vs SMD at 20000 rpm

Volumetric Flow Rate (Q) ($\times 10^{-7} m^3/s$)	SMD ($\times 10^{-5} m$)
54	3.15
108	3.94
162	4.58
216	5.05

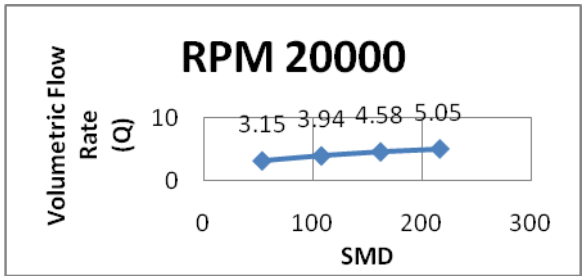

Graph 4. Volumetric flow rate Vs SMD at 20000 rpm

Table 5. volumetric flow rate Vs SMD at various rpm

Q RPM	7000	12000	16000	20000
	SMD			
54	7.26	4.73	3.79	3.15
108	9.08	5.92	4.73	3.94
162	10.5	6.87	5.4	4.58
216	11.6	7.61	6.06	5.05

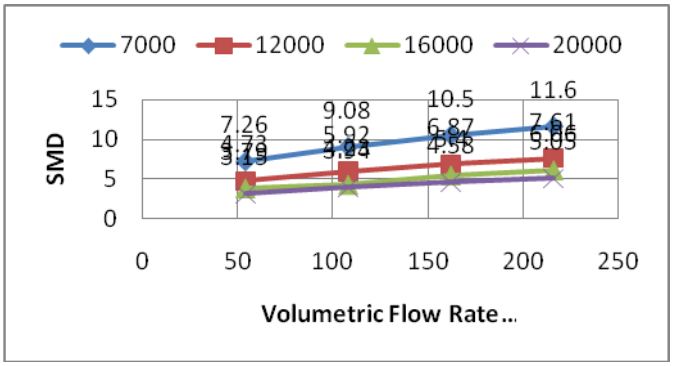

$$SMD = Q\sigma\mu_L/N^4d^7\rho_L{}^2m$$

Table 6. Volumetric flow rate Vs SMD at 7000 rpm

Q(*10^-7) m^3/sec	SMD(*10^-5) m
54	9.74
108	19.4
162	29.2
216	38.9

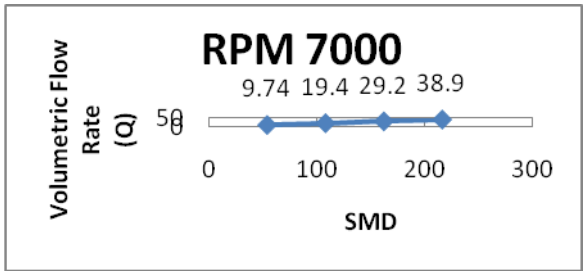

Graph 6. volumetric flow rate Vs SMD at 7000 rpm

Table 7. volumetric flow rate Vs SMD at 12000 rpm

Q(*10^-7) m^3/sec	SMD(*10^-5) m
54	5.67
108	11.3
162	17
216	22.6

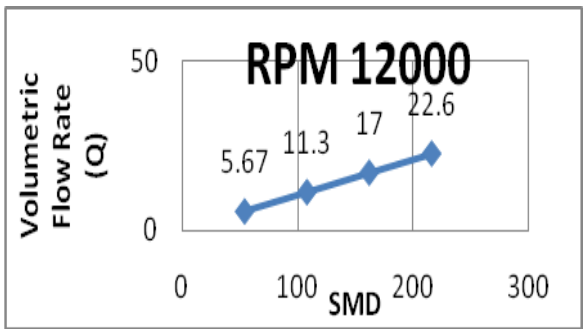

Graph 7. volumetric flow rate Vs SMD at 12000 rpm

Table 8. volumetric flow rate Vs SMD at 16000 rpm

Q(*10^-7) m^3/sec	SMD(*10^-5) m
54	4.88
108	9.7
162	14.6
216	19.5

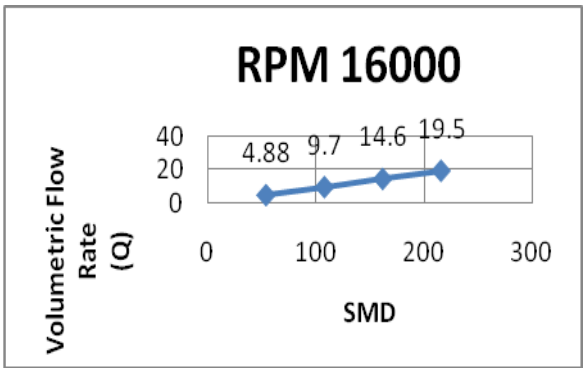

Graph 8. volumetric flow rate Vs SMD at 16000 rpm

IV CONCLUSION

From the study of atomization and types of atomizer, Rotary atomizer is selected for naked evidence and results as:-

Data are collected for kerosene and its properties to use on rotary atomizer of SMD.Then we applied the data in a journal about SMD of rotary atomizer. fter substitute the values for various rpm & volumetric flow rate Vs SMD, by the acquired value graph I has been plotted. Equation taken from the journal and by solving it, we get a correlated pattern using Bucking π Theorem under dimensional analysis. From the taken values of kerosene & substituting in the correlated pattern graph II is plotted for various rpm and volumetric flow rate Vs SMD. Then by comparing graph I and graph II we get similar plotations, where our correlation is proved and unique for SMD of ROTARY ATOMIZER.

REFERENCES

[1] Farmer,W.N (1976).Sample space for particle size and velocity measuring interferometers, Appl opt,vol:15,PP.1984-1989.

[2] Yule.A,Chigier.N,Atakan.S, and Ungut.A (1977).Particle size and velocity measurement by laser anemometry,AIAA,15th Aerospace science meeting.PP.77-214.

[3] Bachalo,W.D,Hess,C.F and Hartwell,C.A (1979).An instrument for spray droplet size and velocity measurement,ASME winter annual meeting.PP.79.

[4] Jackson,T.A, and Samuelson,G.S (1985).Spatially resolved droplet size measurement,ASME.PP.85.

[5] Hess,C,F (1984).A technique combining the visibility of a dropper signal with the peak intensity of the pedestal to measure the size and velocity of the droplets in a spray, AIAA 22nd Aerospace science meeting.

[6] Mularz,E.J,Bosque,M.A, and Hamenik,F.M (1983).Detailed fuel spray analysis technigue,NASA Technical Memorandum 83476.

[7] Bachlo,W.D and Houser,M.J (1984).Phase doppler spray analyzer for simultaneous measurements of drops size and velocity distribution.23(5).PP.583-590.

[8] Bachlo,W.D and Houser,M.J (1985).Spray drop size and velocity measurements using the phase/doppler particle analyzer,3rd International conference on liquid atomization and spray system,London.2.PP.1-12.

[9] Dr.Corso,S.M and Kemeny,G.A (1957).Effect of ambient and fuel pressure on nozzle spray angle,ASME.vol:79(3),PP.607-615.

[10] Holve,D.J (1980).In site optical particle sizing technique,J.Energy,vol:4(4),PP.176-182.

[11] Holve,D.J and Amen.K (1984).Optical particle counting and sizing using intensity DE consolation,opt.eng,vol:23(5),PP.591-603.

[12] Holve,D.J and Dayis,G.W (1985).Sample volume and alignment analysis for an optical particle counter size and other applications,opt.vol:24(7).PP.998-1005.

[13] Holve,D.J (1982).Transit timing velocimetry for two phase reacting flows,vol:48,PP.105-108.

American Journal of Engineering Research (AJER)
e-ISSN : 2320-0847 p-ISSN : 2320-0936
Volume-03, Issue-03, pp-346-358
www.ajer.org

Research Paper Open Access

A Review on Drapeability of Natural Fibre-made Fabrics

Dr. Swapan Kumar Ghosh[1], Chinmoy Dey[2], Kalyan Ray Gupta[3]
[1]*Associate Professor, Department of Jute and Fibre Technology, University of Calcutta,35, Ballygunge Circular Road, Kolkata- 700019, West Bengal, India*
[2]*Junior Research Fellow, Department of Jute and Fibre Technology,University of Calcutta, 35, Ballygunge Circular Road, Kolkata- 700019, West Bengal,India*
[3]*Assistant Professor, Department of Jute and Fibre Technology, University of Calcutta,35, Ballygunge Circular Road, Kolkata- 700019, West Bengal, India*

Abstract: - Amongst the different property parameters of the produced fabric, drapeability of fabric is one of the crucial parameters with respect to end uses. It is the ability of fabric to hang freely in graceful folds when some area of it is supported over a surface and the rest is unsupported. During the application of different fabrics, both in industrial and apparel sector, it has been observed that the ability of the fabric to assume a graceful appearance of the contour is very vital conveying the significance of drapeability of the fabric. With the growing environmental concerns and eco-sustainability, the global emphasis is towards the application of eco-concordant, bio-degradable, renewable green products and this has inclined towards the natural fibre-made fabrics scoring them over their manmade counter parts and making them a natural choice for the mankind. The natural fibre-made fabrics have proven records of efficacy to prove their mettle match with manmade fabrics in different areas of application. This paper has reviewed and analyzed the various attributes of natural fibre-made fabrics such as jute, cotton, silk and wool focusing mainly on their draping behavior, determining their strengths and weakness considering the future direction of research to overcome their deficiencies.

Keywords: -*bending behavior, bending length,bending stiffness,drape,drapemeter, drape coefficient*

I. INTRODUCTION

Drape of a fabric refers to the manner in which the fabric falls, shapes, gathers or flows with gravity on the model form or on a human body, as well as on furniture and wall hangings, when only part of it is directly supported. Drape of a fabric is an important cloth property in apparel as well as in industrial uses. The ability to fold gracefully in two directions simultaneously distinguishes fabrics from other sheet materials. The folding takes a complex three-dimensional form with double curvature. The research into fabric drape dates back to the classic paper published by Pierce [1] in 1930s with the title "The Handle of Cloth as a Measurable Quantity."Chuet.al. [2] and Cusick [3] made a great contribution to the practical determination of this fabric property by measuring three-dimensional draping. In 1986, Hearle and Amirbayat [4] made a theoretical investigation on drapeability of fabric, and gained some insight into the nature of this property from a study of complex buckling using a different approach. Niwa and Seto [5] published a paper about the relationship between drapeability and mechanical properties. They derived the parameter combinations of bending rigidity, bending hysteresis, weight per unit area, shear stiffness and shear hysteresis from an analysis of bending of a fabric cantilever with hysteresis in bending and shear by applying the heavy elastic theory. Other researchers who have contributed to this area include Sudnik [6], Morooka and Niwa [7],Gaucher et.al. [8], and Collier et.al.[9], [10]. Sudnik [6] correlated fabric drapeability with bending length and in 1978, he confirmed the importance of bending length in predicting fabric drape. Peirce [1] commented that bending length from the cantilever test is strictly a measure of the draping property and simultaneously an instrument was decided to measure the angle through which a specimen of cloth drooped when a definite length was held out over an edge, based on the recognition that stiffness has a large effect on drapeability. He concluded, by means of a mathematical formula, this angle was converted into "bending length", defined as the length of fabric that will bend under its own weight to a definite extent. It is a measure of the draping quality of a sheet material. He also observed that bending length or bending rigidity is only a partial predictor of drape behavior for many fabrics.

Sudnik [6] determines that shear resistance was also a factor, although not as important as bending resistance. Morooka and Niwa [7], generated an equation to predict fabric drape using data from the Kawabata Evaluation System for Fabrics (KES-F) system and they concluded that fabric weight and bending modulus were the most important factors. They also reported that shear resistance was not a significant factor in draping behavior for the fabrics. However, research by Collier et.al. [11] indicated that shear properties are more significant predictors of fabric drape than bending properties and shear hysteresis, and that shear hysteresis is more closely related to drape coefficient. Chu et.al [2] found that in general, drapeability depends on three basic fabric parameters i.e. Young's Modulus (Y), the cross-sectional moment of inertia (I), and the weight (W). They also have generated an equation in which the drape coefficient equals to f (B/W), where the bending stiffness B = YI. In Cusick's original work, he measured the drape coefficient, bending length, and shear stiffness (the shear angle at which a fabric begins to buckle; fabrics with higher shear stiffness buckle at lower angles). Other mechanical properties such as tensile strength were not considered in his study. He also found that theoretical drape coefficients were lower than the measured values for the majority of fabrics tested, when ignoring shear stiffness. In later work, Cusick [3] used statistical evidence to prove that fabric drape involves curvature in more than one direction, and that the deformation depends on both shear stiffness and bending length. He also formulated an equation for the relationship between drape coefficient and bending length and shear angle. The bending properties of fabrics govern many aspects of fabric performance, such as hand and drape, and they are an essential part of the complex fabric deformation analysis. Peirce [1] produced a formula for calculating the stiffness of a fabric in any direction in terms of the stiffness in the warp and weft direction. This was derived from the theory for homogenous elastic material and it was found to be empirically satisfactory. It is suggested that the reason for this is that most of the fabrics which Peirce tested were made from cotton. He first introduced the bending rigidity of a fabric by applying the equation, $B = wc^3 \times 10^3$mg-cm in his classical paper, where B is the bending rigidity, w is the weight of the fabric in grams per square cm and c is the bending length. He also introduced another equation for bending rigidity in various directions which is $B_\theta = \{(\cos^2\theta/\sqrt{B_1}) + (\sin^2\theta/\sqrt{B_2})\}^{-2}$, where B_1, B_2 and B_θ are bending rigidities in warp, weft and θ directions respectively. This equation enabled the value for any direction to be obtained when the values in the warp and weft directions were known. Go et al. [12] measured the bending stiffness of fabrics using the heart loop method. They also indicated that the bending stiffness of the fabric is dependent on the bending model of the test piece. The bending stiffness of fabric having long floats on its surface was smaller in face-to-face bending than back-to-back. The effect of the crimp of the component yarn of fabric on the fabric bending stiffness was generally small. Later, Go and Shinohara [13] reported that on the polar diagram of bending stiffness there was minimum presented at 45° to the warp when the fabric was bent. Their formula neglected the restriction at the interaction of the warp and weft directions. They concluded that the stiffness of textile fabrics depended upon their bending directions and that, in general, the stiffness in bias directions was relatively small. Cooper [14] used cantilever methods to determine fabric stiffness and stated that there was no evidence to suggest that there was any appreciable shearing of the fabric caused by its own weight. He presented an equation including twist effect. The results of the twisting effect were found to be valuable in practical applications and so equation was derived $B_\theta = \{B_1 \cos 4\theta + B_2 \sin 4\theta + (J_1 + J_2) \cos^2\theta \sin^2\theta\}$, where J_1 and J_2 are constants due to torsional moment. Cooper concluded that the stiffness of a fabric may vary with direction of bending in different ways, but for most practical purposes measurement along warp, weft and one other direction was sufficient to describe it. Cooper conducted a detailed study of the stiffness of fabrics in various directions and has produced polar diagrams of bending stiffness. He found that some fabrics had a distinct minimum value at an angle between the warp and weft direction while others had similar values between the warp and weft. In general, viscose rayon fabrics provided an example of the former and cotton fabrics an example of the latter. These effects were explained in terms of the fabric bending stiffness in the warp and weft direction and the resistance offered by the yarns to the torsional effects which are inseparable from bending at an angle to warp and weft. He also concluded that the resistance offered by the yarns to the torsional deformation is low when the interaction between the yarns is low and vice versa. Shinohara et.al. derived an equation empirically which is similar to the equation introduced by Peirce and analyzed the problems using three dimensional elastics. They assumed the constituent yarns of woven fabrics to be perfectly elastic, isotropic, uncrimped and circular in cross-section and to behave in a manner free from inter-fibre friction. In addition, they also presented another equation containing a parameter n which was related to V introduced by Cooper [14] in order to predict the shape of a polar diagram. In addition, although Peirce's, Shinohara et.al.'s and Cooper's models can all be applied to the prediction of polar diagrams of bending hysteresis for loose to tight plain woven fabrics, amongst these three models, Cooper's model presents the lowest deviation from the experimental results. Therefore, it can be seen that the twist and frictional effects in Cooper's model play an important role in the prediction of bending hysteresis on either loose or tight plain woven fabrics. Moreover, when comparing the bending hysteresis of loose and tight plain woven fabrics, the deviation in loose plain woven fabric is smaller than that in tight plain woven fabric. From the above analysis,

we may conclude that Cooper's model is the most reliable in the prediction of bending hysteresis in both loose and tight plain woven fabrics.

Amirbayat and Hearle [15] reviewed several research works relating the simulation of fabric drape. They implied that the membrane strains are important in fabrics, observing that the uniqueness of fabric drape is the formation of double curvatures. Thus, in addition to tensile characteristics, shear rigidity and Poisson's ratio play important roles in the drape process. Amirbayat and Hearle also computed theoretical values of deformation for an isotropic material and analyzed the effects of Poisson's ratio, which is the combined effect of in-plane stiffness relative to bending stiffness and weight of the material. Bending and shear properties were confirmed as significant when measuring fabric drape and contributed to the understanding of drape to some extent. But two-dimensional drape in the cantilever cannot reflect the nature of drape because it involves three-dimensional double curvature deformations. Simultaneously, Lo et.al. [16] had developed a model for predicting the drape behavior. Chen found that Young's modulus, shear modulus, and thickness affect the extent of drape, but Poisson's ratio, in the usual range of 0.0 to 0.5, does not show any appreciable effect on drape. The shape attained by a fabric after drape is influenced by the orthotropy of fabric, but they observed that the asymmetry due to orthotropy is greatly influenced by shear modulus and thickness. It was concluded by them that the fabrics with low shear modulus do not exhibit asymmetry, even if the Young's modulus values are quite different in the warp and weft directions. Similarly, thin fabrics do not show the effect of orthotropy as much as thick fabrics.

The work of GulcanSule has been conducted to investigate drape and bending properties of gray plain woven fabrics and the effect of weft density, weft yarn count and warp tension on these properties. In his work, warp and weft yarn type, warp count and warp density were kept constant, while weft count, weft density and warp tension were varied in manufacturing the fabrics. At the end of the study, they concluded that higher values were found for bending rigidities of the fabrics woven with thicker weft yarns and at higher weft densities in the warp, weft and overall bending rigidities. It was observed that bending rigidities of the fabrics in the warp direction had increased as warp tension was increased. This increase occurred at higher levels in fabrics woven with thicker weft yarns and at higher weft densities. Considering warp crimps of these fabrics, having the same structural parameters but woven under different warp tensions as the only exception, where warp crimp had decreased as warp tension was increased. This made these yarns more resistant to bending in the fabric and thus, higher bending rigidity was achieved in the warp direction. Bending rigidity in the weft direction did not show any significant change, i.e. no increase or decrease with the change in warp tension. In the case of fabrics woven with thinner weft yarns, bending rigidity in the weft direction decreased as the warp tension increased. This decrease was explained depending on the increase in weft crimp against the increase in the warp tension in the case of fabrics woven with thinner weft yarns and/or at higher weft densities. The increase, which occurred at higher levels, in the weft crimp, reduced resistance of the weft yarns in the fabric for bending, especially in the case of fabrics woven with thinner weft yarns and/or at higher weft densities. This had caused a reduction in bending rigidity of these fabrics in the weft direction. Overall fabric bending rigidity is the geometrical mean of bending rigidity in the warp direction and bending rigidity in the weft direction. In the case of fabrics woven with thicker weft yarns, as warp tension had increased, overall fabric bending rigidity got increased. The increase in bending rigidity in the warp direction of the fabrics woven with the thinnest weft yarn, depending on the increase in the warp tension, increased at lower levels compared with the increase that had occurred in bending rigidities of the fabrics woven with other weft yarns, while bending rigidity in the weft direction did not vary significantly as the warp tension increased and therefore, overall fabric bending rigidity did not vary significantly despite a very insignificant increase. Considering drape coefficients of the fabrics, it was observed that the drape coefficient increased as the weft density increased and weft yarn became thicker. The drape coefficient did not significantly vary depending on the variations in the warp tension. This study has evidenced once more that the effect of the bending rigidity of a fabric on its drape feature is quite significant. In this study, the fabrics woven with thicker weft yarns at higher weft densities gave higher bending rigidities and drape coefficients.

Bijian Chen and Muthu Govindaraj [17] in their research work, have shown the effect of changing the thickness of the fabric while keeping the stiffness values and weight constant for the simulations. It is their observation that for a small change in thickness, there is a significant change in drape. The reason is that thickness of the fabric has a large influence on the bending stiffness of the fabric. It has been depicted in their research work that when the thickness of the fabric is of the order 0.03 cm, the corners of the fabric appear to be collapsed. This indicates that the fabric has a low stiffness. The drape also appears symmetric in spite of the differences in the warp and weft Young's modulus values. As thickness increases to 0.04cm and later to 0.05cm, the fabric takes on an asymmetric drape. This explains why thin fabrics usually assume a symmetric drape.

Bijian Chen and Muthu Govindaraj [18] have also reflected the effect of shear modulus on drapeability of fabrics in their work where they have kept Young's modulus and Poisson's ratio values constant for the different simulations. Different Young's modulus values have been chosen in the warp and weft directions to study the

effect of change in shear modulus on an orthotropic fabric. Nevertheless, the effect of increasing of shear stiffness on drape can be seen from the simulations using the same Young's modulus values giving rise to occurrence of orthotropy only in combination with higher shear modulus. Jute woven fabrics usually have a low shear modulus compared to the tensile modulus, which is perhaps the reason that most fabrics assume a symmetric drape.

Chen and Llyod [18] and later on Collier et.al. concluded that Poisson's ratio has a significant effect on the drape coefficient and also found that the Poisson's ratio for fabrics is not easy, and even if some measurements can be made, the definition of Poisson's ratio may not be totally applicable to fabrics. De Jong and Postle [19] showed that theoretical and experimental values of Poisson's ratio for fabrics rarely agree. Their findings show that as Poisson's ratio increases from 0.0 to 0.5, there is no appreciable change in either extent of drape or the shape of the folds.

Weidong Yu and Zhaoqun Du studied the Bending Evaluation System of Fabric and Yarn (BES-FY) can measure the bending, weight, friction, and tensile properties of fabric and yarn through a pull-out test and delineate the relationship between the mechanical geometry and the corresponding deforming process, so as to quantify the comprehensive hand of fabrics and yarns. The bending process of the BES-FY system was mainly investigated in their study. Two bending models were developed under different conditions and the corresponding formulae for bending rigidity were also obtained. The optimum point and range for calculating the bending rigidity was acquired by experimental and analytical investigation, which involved the study of the relationship of bending rigidity-curvature. These can be divided into three sections, namely, linear, quadratic and constant function, through the comparisons between the bending rigidity of the two bending models and that of KES-FB2 and FAST-2, the better bending model was selected to characterize the bending properties of the fabrics and the yarn.

II. METHODS TO DETERMINE DRAPEABILITY OF TEXTILE FABRIC

Traditionally, the textile technologists, researchers, manufacturers and end-users assess fabric drape [20] subjectively and by practical experience. This qualitative assessment of fabric drape sometime may result in errors. Therefore, the textile researchers realized the importance of understanding the phenomenon of drape and desired to be able to measure it quantitatively and objectively. The different methods of measuring drape of a fabric improvised over the years have been included in this review.

Cantilever methods were first introduced' by Peirce (1930) [1] for the evaluation of fabric drape, his methods were based on the recognition that stiffness has large effect on drapeability. The standard tester, called flexometer which became the standard Shirley Stiffness Tester, had been described in details by Peirce. The bending / drooping angle of fabric subjected to test can be measured, when a definite length of fabric specimen droops over an edge of the instrument. The specimen is a rectangle with ratio of length to its width (6: 1). By means of a mathematical formula, the bending angle has been converted into a term called "bending length", which is a measure of fabric drapeability in two dimensions and stated as drape stiffness by Peirce. Later on with the passage of time various modifications of the method had been worked out to make the method suitable for different types of fabrics. For example, for very stiff fabrics such as starched and ironed, a weight called weighted rectangle can be added to the free-end of the specimen. Again, for a very flimsy fabric, a triangle cantilever may be used. Peirce also suggested another cantilever with wider strip of 6 in. wide.

Chu et.al. (1950) [2] and Cusick (1961) [3] made their great contribution to the measurement of fabric drape. The standard drapemeter, which is in current use, determines the drape coefficient, which is the ratio of projected area with specimen's original area. The drape coefficient can provide an objective description of the deformation. This method scores over the cantilever method because of its capability to test the three dimensional drape feature and thus can differentiate the paper web and a textile fabric.

F. R. L. Testing Machines Inc. (1980) [21] reported that the F.R.L. Cantilever Bending Tester is capable of testing thin sheet material, textiles, and other flexible materials including carpets. Kalyanaraman and Siveramakrishnan (1984) [22] designed an electronic cantilever meter based on opto-electronic principles. Their instrument has the same accuracy as the Shirley Stiffness Meter and works on measurement is objective and could easily be automated.

Clapp et.al. (1990) [23] developed an indirect method of measuring the moment-curvature relationship for fabrics.

Collier et.al. (1991) [24] designed a digital drapemeter to measure fabric drape co-efficient by using photo-voltaic cells. The drapemeter utilizes the principle of the standard experimental drapemeter and applies a bottom surface of photo-voltaic cells to determine the amount of light blocked by a fabric specimen draped on a pedestal. A digital display gives the amount of light being absorbed by the photo-voltaic cells, which is related to the amount of drape of the fabric specimen. This principle was earlier adapted by textile researchers in China.

The Fabrics Assurance by Sample Testing (FAST) system developed by CSIRO consists of a cantilever bending meter (1993). The principle for FAST 2 is very similar to that of Shirley Stiffness Tester in which the fabric

bends under its own weight until its leading edge intercepts a plane at an angle of 41.5 degrees from the horizontal. Compared with Shirley Stiffness tester, the FAST 2 was designed to test a wider specimen (50mm), even though any sample width from the standard 2.45cm up to 50mm can be employed. In addition this instrument encloses totally the electronics and detection apparatus.

Russel (1994) [25] reported an alternative instrument for the measurement of the fabric bending length in contrast with the commercial Shirley Stiffness Tester and the FAST 2 bending meter.

Potluri et.al. (1996) [26] also improvised an experimental technique to verify their numerical method for the capability to compute for general situations. A laser triangulation sensor, attached to a robot arm, had been used for measuring the cantilever profile of the fabric samples. A manipulating device positions the fabric sample as a cantilever of specific length.

Stylios et al (1996) [27] developed a new type of drapemeter, which measures both static and dynamic drape in true three dimension by using CCD camera as a vision sensor. This system, called the Marilyn Monroe Meter (M3) has been used to measure real fabric drape behavior, and is being used to verify their theoretical prediction model. The drape profile of the specimen can be taken and presented on computer.

Matsudaira et.al. (2000) studied the static and dynamic drape behavior of polyester shingosen fabrics using the dynamic drape coefficient with swinging motion. The dynamic drape coefficient D_d of peach face shingosen fabric was small and that of new worsted was large. In this study the two-dimensional projection of the hanging shape of fabrics was measured by an image analysis system by Library Co. in Japan.

The image analysis method had been developed to overcome the constraints in measuring the drape coefficient of fabric. Vangheluwe and Kiekens (1993) [28], Jeong and Phillips (1998), Lo, Hu and Li (2002) have all used image analysis for the measurement of drape of fabrics. Jeong and Phillips (1998) studied the fabric drape behavior with image analysis. The effects of fabric structure and its mechanical properties on the draping characteristics of fabric had been studied with a systematically designed range of fabrics. According to Jeong and Phillips, the fabric cover factor influences the drapeability of the fabric by increasing the fabric bending rigidity. However, fabrics with different but similar cover factors showed differences in their drapeability which was due to the influence of weave structure on the thread interaction and related shear properties of the fabrics. It has been shown that the instability of fabric drape increases as the residual bending curvature and residual shear angle increases. Cover factor increased drape instability by increasing the residual bending curvature.

An automatic fabric evaluation system has been developed to analyze the structure of woven fabric and to objectively evaluate the fabric quality. Fabric images have been captured by a Charge Couple Device (CCD) camera and preprocessed by Gaussian filtering and histogram equalization. Fabric construction parameters such as count, cloth cover, yarn crimp, fabric thickness, and weight per unit area are measured automatically from planar and cross-sectional images of woven fabric with image processing and image analysis.

Lo et.al. (2002) have studied modeling of a fabric drape profile. The drape coefficient (DC %), node numbers, and node shape in the fabric drape profile can be predicted accurately with this model. Polar coordinate fitting is used to determine the constants in the drape profile model, and good agreement has been obtained between the theoretical and experimental drape profiles of thirty-five woven fabric specimens. In addition, constants in the drape profile model may also be obtained by bending and shear hysteresis using regression analysis. Good agreements are found between the calculated DC% and the experimental DC% for the fabric specimens examined in this study. Moreover better predictions of the fabric drape profile may be obtained from the mean value taken in the warp, weft and 45˚ directions than those in the warp and weft directions.

III. NATURAL FIBRES

The backdrop of growing global concern for environment concomitant with the alarming danger of carbon foot-print generation amalgamated with non-biodegradability and higher toxicity generation from the use of manmade-fibres have created an urge to come back to natural fibres, thereby opening new market opportunities. The growing disinclination to use artificial fibres and an increasing preference for natural fibres is reviving the importance of the latter like jute, cotton, silk, wool, flax, sisal, hemp, coir etc.

Jute [29], a lingo-cellulosic bast fibre belonging to botanical genus Corchorus (Family Tiliaceae) includes about 40 species available almost throughout the tropics, out of which C. capsularis linn and C. olitorius linn were found to be as economic plants and became commercially important. C. capsularis is known as ‘White’ jute and C. olitorius as ‘Tossa’ jute. Jute is grown abundantly in Bengal and adjoining areas of Indian subcontinent. Jute is widely used in production of packaging and wrapping textiles (sacking and hessian) besides its additional uses as carpet backings, decorative / furnishing fabrics, designed carry bag fabrics, geotextile fabrics, as well as for manufacture of high quality paper and composites etc. its main advantages are its renewable agro – origin, bio – degradability, high strength and high moisture regain, medium to good affinity for dyes, good heat and sound insulation properties and ready availability at low cost.

Cotton is the oldest natural fibre used for textile purpose. The cotton plant (shrubs) belongs to the family, Gossypium and the different species of this family constitutes the different varieties of cotton e.g. ordinary American Cotton is Gossypium Hirsutum, Asiatic Indian Cotton is Gossypium Herbaccum and Gosypium Arboretum, while Sea-Island, Egyptian and Peruvian Cotton are Gosypium Barbadense. The major use of cotton fibre is in making clothes in apparel sector including the areas of medical textiles, sports textiles, industrial textiles and other categories of technical textiles.

Silk is a very fine, regular and translucent, natural, protein filament. Silk filament comes from the cocoons built by 'silkworms', which are not worms at all, but silk moth pupae. The scientific name of one of the important domestic silk moth is Bombyx Mori. The silk fibre is mainly produced in China, India, Thailand, Europe, North America, Vietnam, and Malaysia in large quantity. The silk fibre may be up to 600 m long, but averages about 300 m in length. Depending upon the health, diet and state under which the silk larvae extrude the silk filaments, their diameter may be vary from 12 -30 µm. This gives a fibre length to breadth ratio well in excess of 2000:1. The beauty and softness of silk's luster is due to the triangular cross-section of the silk filament. As the silk filament is usually slightly twisted about itself, the angle of light reflection changes continuously. As a result, the intensity of the reflected light is broken, resulting in a soft, subdued luster. The silk fibre is mainly used in making clothes in apparel sector as well as in production of furnishing fabrics.

Wool is the fibre extracted from the fleece of domesticated sheep mostly. Apart from sheep, wool also comes from the angora goat, yak, llama, alpaca, and even camels. It is natural, proteinous, multicellular, staple fibre. It is largely produced in Australia, New Zealand United States and in China etc. The length of the wool fibre ranges from about 5 cm for the finest wools to 35 cm for the longest and coarsest wools. Wool fibres vary greatly in their fibre diameter, ranging from about 14 µm for the very finest wools to more than 45 µm for the coarsest wools. Fine, lightweight, pleasant handling fabrics can be manufactured from the finer wools. Fibre length to breadth ratio can be critical with wool, since the short, coarse fibres spin into less attractive yarns than do those of fine wools. In general, fibre length to breadth ratio ranges from 2500:1 for the finer, shorter wools to about 7500:1 for the coarser, longer wools. Wool fibre may vary from off-white to light cream in colour. In addition to clothing, wool has been used for blankets, horse rugs, saddle cloths, carpeting, felt, woolinsulation and upholstery. The chemical composition, physical properties and chemical properties of the natural fibres jute, cotton, silk and wool fibres have been discussed in tables 1, 2, 3 respectively. The morphological diagram of the four natural fibres is shown in the Fig. 1.

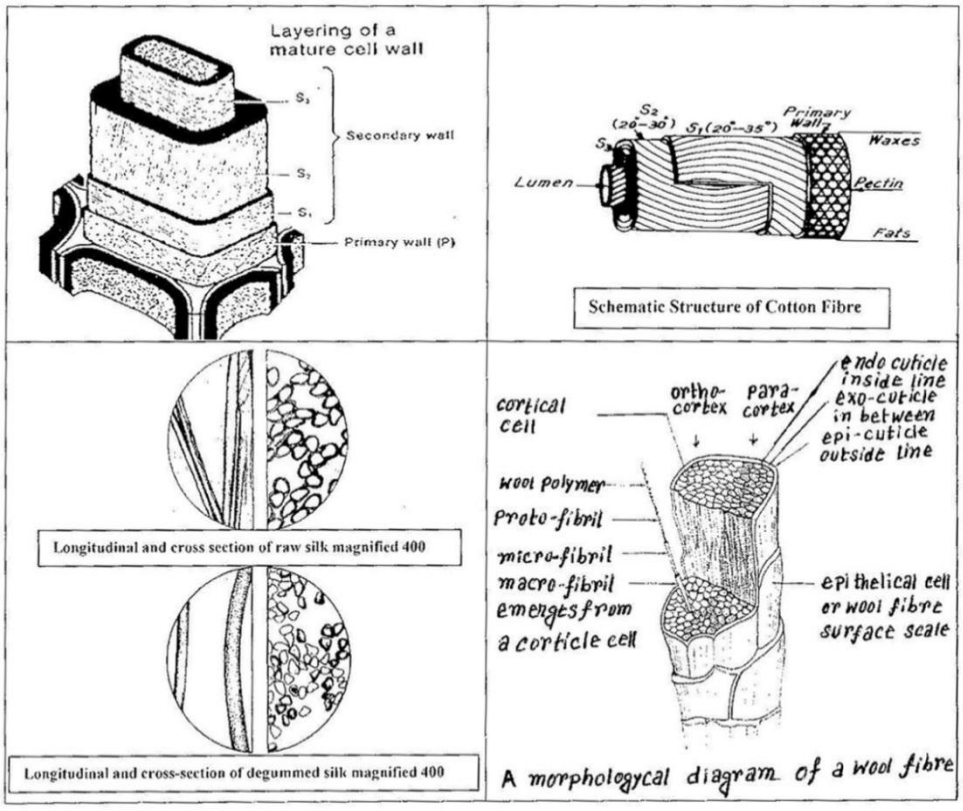

Fig.1Longitudinal and cross-sectional views of the natural fibres – jute, cotton, silk and wool

Table 1 Average chemical composition (%bone dry weight of the fibre) of jute, cotton, silk and wool fibre

Constituent	Jute	Cotton	Silk	Wool
Cellulose	60-63	95.5(94-97)	-	-
Hemi-cellulose	21-24	Nil/traces (sometimes reported to< 0.3)	-	-
Lignin	12-13	Nil	-	-
Protein or nitrogenous matter	0.8-1.87	1.1(0.3-2.5)	-	-
Pectins	0.2-0.5	0.9(0.6-1.2)	-	-
Mineral matter (Ash)	0.7-1.2	0.8(0.2-1.8)	-	-
Maleic, Citric and other organic acid residue	-	0.8(traces to 0.8)	-	-
Fat and waxes	0.4-1.0	0.4-1.6	1.5	-
Fibroin	-	-	75	-
Ash of silk fibroin	-	-	0.5	-
Sericin	-	-	22.5	-
Mineral salt	-	-	0.5	-
Keratin	-	-	-	33
Grease	-	-	-	28
Suint	-	-	-	12
Different impurities	-	-	-	26
Mineral water	-	-	-	1

Table 2 Comparison of physical properties of jute, cotton, silk and wool fibres

Fibres	Fibre Density (g/cm^3)	Tenacity (g/den*)	Elongation at break (%)	Specific Gravity	Moisture Regain% (at 65 % RH)	Crystallinity (%)
Jute	1.48	2.7 – 5.5	1.7	1.50	13.75	50 - 55
Cotton	1.55	3.5 – 3.8	5-10	1.54	8.50	60 - 65
Silk	1.34	3.33-4.56	20-25	1.25-1.34	11	65-70
Wool	1.32	1.0- 2.0	25-35	1.30-1.32	17	25-30

* cN/tex = 8.83 x (g/den);

Table 3 Comparison of chemical properties of jute, cotton, silk and wool fibres

Fibre	Jute	Cotton	Silk	Wool
Effect of acids	Easily damaged by hot dilute acids and conc. Cold acid.	Not affected by acids	Decomposed by strong acids.	Decomposed by hot conc. H_2SO_4.
Effect of alkali	Damaged by strong alkali, losses weight when heated with caustic soda.	Has excellent resistance to alkali.	Less readily damaged by alkali than wool fibre.	Strong alkaline effect on wool fibre. Dissolved in NaOH.
Effect of light	Colour changes slightly in sun light because of lignin.	Due to UV rays and infrared rays the cotton polymers degrade.	Decomposed in presence of atmospheric oxygen.	Affected by sun light.
Effect of micro-organism	Good prevention ability.	Attacked by fungi and bacteria.	Affected by mildew slightly.	Affected by mildew if remains wet for long time.
Dyeability	Easy to dye (using direct and basic dye normally).	Direct, reactive, sulphur, vat and azoic dyes is used to dye.	Acid dye is used to dye.	Could be dyed with direct, basic and acid dyes.
Solubility	Dissolved in 72% H_2SO_4.	Dissolved in Conc. 70% H_2SO_4.	Soluble in 5% NaOH (hot).	Soluble in 5% NaOH at room temperature.

IV. EMPIRICAL STUDY OF FABRIC DRAPE USING NATURAL FIBRE-MADE FABRICS

Dhingra and Postle (1980-1981) [30] investigated seam bending rigidity. They used wool woven fabric with 2/2 twill structure. It was found that a seam has a little effect on fabric shear rigidity and hysteresis, but has a significant effect on bending rigidity. When a seam is perpendicular to the axis of bending with 1 mm seam allowance, bending rigidity is 3-4 times greater than the bending rigidity with no seam. When a seam is parallel to the axis of bending with seam allowance 1 mm, there is a little effect on bending rigidity. When seam allowance is greater than 2.5 mm, bending resistance increases, but the effect is not as significant as in the perpendicular direction. Bending takes place more easily in the parallel direction than in the perpendicular direction when a seam is imposed on it. It is because more freedom area of un-sewn part is found in the former.
Hu and Chung (1998) [31] have published a paper on drape behavior of woven fabrics with seams. This paper presents a fundamental drape analysis of seamed fabrics using Cusick's drapemeter. Simple plain and twill woven fabrics with various fibres content of cotton, linen, silk, and wool and polyester are given radical and circular seams. The effects of seam allowance and seam positions are investigated experimentally. Drape behavior is determined and compared in terms of drape coefficient, node analysis, and drape profile. Investigating drape on seamed fabrics can improve apparel design and fabric end use applications. Moreover it contributes to garment drape prediction for the clothing CAD system.

Itagi and Rao (2012) [32] have highlighted an experimental investigation into the drape behavior of silk fabrics with the circular seams using Cusick's drapemeter. They have studied the effects of seam positioning on the drape behavior. Varying positions of a circular seam in the fabric specimens show varying effects on drape coefficient percentage of light and heavy weight fabrics. Fabrics of medium weight have shown gradual increase in drape coefficient percentage. Drape profiles more or less show consistency with changed seam positions for light and medium weight fabrics but heavy weight fabrics show disturbed profile. Investigations of Itagi and Rao on fabric drape value for silk apparel fabrics with seams have a significant value for both textile and garment industries because it provides a realistic drape study with respect to garment appearance. The researchers believe that their findings can be applied to computer simulations of drape in the silk apparel industries.

Hu and Chan (1998) [33] have investigated that that relation between the fabric drape coefficient and from that Cusick drapemeter and mechanical properties tested on Kawabata Evaluation System for Fabrics (KES-F) for woven fabrics. This is first attempt at determining comprehensive relationship between the fabric drape coefficient and mechanical properties. Drape coefficient is the dependent variable. Sixteen mechanical properties tested on the KES-F system and their transformed forms are independent variables. Four regression models are proposed: the multiple linear regression of the drape coefficient with KES-F original data, Niwa's model, logarithm for KES-F data and logarithm for both drape coefficient and KES-F data. Except for an initial run with Niwa's model, the mechanical properties correlated to drape coefficient are reduced to three or four by screening out inter-correlated parameters using stepwise regression. The regression results are analyzed in terms of correlation coefficients, residual and T values. The version with logarithms for mechanical properties and drape coefficient seems to be more accurate. We know that bending and shear properties are close related to drape coefficient, and this analysis shows that two other parameter-mean deviation of friction coefficient and tensile linearity – are also highly correlated with drape coefficient and may be independent.

Stylios, Powell and Cheng (2002) [34] on their paper have proposed a powerful predictive tool to determine both the drape attributes and the drape grade from the mechanical properties of a fabric. Combining this with a novel feedback system (Stylios and Cheng, in preparation), there is now the possibility of modifying the drape grade or drape attributes of a fabric to be more desirable, and then finding the changes to the material properties required to achieve them. This opens up the possibility of re-engineering fabrics to match changing fashion and market requirements. The system consists of neural networks, which predict the drape attributes from the natural logarithm of the material properties divided by the weight, and that predict the subjective drape of a fabric from the drape attributes. A comparison had been made between these neural networks with linear regression models and discriminate analysis. The drape coefficient was found to be a principal factor in the prediction of the subjective drape. However, the incorporation of the drape attributes allows quantities that relate directly to the aesthetic qualities of a fabric's drape to be related to the mechanical properties of the fabric.

Shyr, Wang and Cheng (2007) [35]have investigated the comparison of the key property parameters affecting the dynamic and static drape co-efficient of four natural-fibre woven fabrics (cotton, linen, silk and wool fabrics) by a newly devised dynamic drape automatic measuring system integrating Cusick's drapemeter principle with the image analysis technique. The relationship for four natural-fibre woven fabrics between the fabric drape coefficient and sixteen physical property parameters, based on the Kawabata Evaluation System for Fabrics (KES-F), have been investigated. Results show that the experimental data of the dynamic drape coefficient versus the rotating speed can be well fitted to a Boltzman function. The correlation coefficient analysis showed that the static drape coefficient and the dynamic drape coefficients of these four natural-fibre

woven fabrics, at 100 and125 r.p.m. did not have a very good correlation, apart from the wool fabric. The key parameters for the static drape coefficient and dynamic drape coefficient at 100 r.p.m. of each natural-fibre fabric were selected from sixteen physical properties using a stepwise regression method. Results showed that the selected key parameters of different natural-fibre fabrics were not entirely the same, and that the static drape coefficient of a fabric could not show dynamic performance. However, the bending and shearing blocked properties were found to be most closely associated with the static and dynamic drape coefficient for the test fabrics.

Fathy and Ebrahim (2011) [36] have made a paper on prediction of garment drapeability based on fabric properties. The drape coefficient alone is not sufficient information about a fabric, so the number of folds, their wavelength, distribution and amplitude is specified as well. In case of cloths the position compared to the projection and warp line is also specified for these data. The investigation of the drape properties of 100% cotton fabrics has shown high correlation between various fabric structure parameters and the fabric drape. The drape coefficient values for most of the sample varies from 29.77 to 56.86% which is expected value for the woven fabric for outerwear women's tailored clothing. The sample that has much greater drape value has also much higher bending stiffness (length & rigidity), warp formability, shear rigidity, and weight. The highest correlation has been found between the fabric drape and stiffness and the parameters which indicate fabric tightness.

GülcanSüle (2012) [37] has made an investigation of bending and drape properties of woven fabrics and the effects of fabric constructional parameters and warp tension on these properties. This study was conducted to investigate drape and bending properties of grey plain woven fabrics and the effect of weft density, weft yarn count and warp tension on these properties. The particular of warp yarns like type, count, density and weft yarn type have been kept constant while weft count, weft density and warp tension were varied in manufacturing of the fabrics. At the conclusion, higher values had been observed for bending rigidities of the fabrics woven with thicker weft yarns. It was seen that bending rigidities of the fabrics in the warp direction increased as warp tension increased. Considering warp crimps of these fabrics, having the same structural parameters but woven under different warp tensions as the only exception, warp crimp decreased as warp tension increased. This made these yarns more resistant to bending in the fabric and, thus, higher bending rigidity was achieved in the warp direction. Bending rigidity in the weft direction did not show any significant change. In the case of fabrics woven with thinner weft yarns at a weft density of 26 threads/cm, bending rigidity in the weft direction decreased as the warp tension had increased. This decrease was explained depending on the increase in weft crimp versus the increase in the warp tension in the case of fabrics woven with thinner weft yarns. Overall fabric bending rigidity is the geometrical mean of bending rigidity in the warp direction and bending rigidity in the weft direction. Considering drape coefficients of the fabrics, it had been observed that the drape coefficient increases as the weft density increases and weft yarn becomes thicker. The drape coefficient did not significantly vary depending on the variations in the warp tension. This study has evidenced once more that the effect of the bending rigidity of a fabric on its drape feature is quite significant.

El-Sabbagh and Taha (2013) [38] have investigated the draping behavior of jute woven fabric to study the feasibility of using natural fabrics in place of synthetic glass-fibre fabrics. Draping behavior describes the in-mould deformation of fabrics, which is vital for the end appearance and performance of polymer composites. The draping coefficient was determined with a common drapemeter for fabrics with densities of 228–765 gsm and thread counts under different humidity and static dynamic conditions. The results were compared with that of glass-fibre fabrics with close areal densities. Characterization of the jute fabrics was carried out to fill the knowledge gap about natural fibre-made fabrics and to ease their modeling. The tensile and bending stiffness and the shear coupling have been also characterized for a plain woven jute fabric with a tensile machine, Shirley bending tester, and a picture frame respectively. As a case study, the draping and resin-transfer moulding of the jute fabric over a complex asymmetric form was performed to measure the geometrical conformance. The adoption of natural fibres as a substitute for synthetic fibres, where the strength requirements are satisfied, would thus require no special considerations for tool design or common practices. However, the use of natural fibres would lead to weight and cost reductions.

Ghosh et.al. (2014) [39] have studied on the evaluation of the drapeability of the jute fabrics. They have tested some conventional jute woven and nonwoven fabrics, jute geotextile fabrics along with some woven and nonwoven synthetic fabrics. After performing the tests for the physical properties along with drapeability related properties of the different supplied fabric specimens and analyzing their test results, they have observed that the drapeability of the double warp woven jute geotextile specimen of area density 805 gsm (having a drape co-efficient value of 0.882) was more than that of the double warp woven jute geotextile fabric specimen of area density 627 gsm amongst the three jute geotextile specimens. It was also found that among the conventional jute woven fabric specimens hessian fabric specimen has the superior draping phenomena (having a minimum drape co-efficient value of 0.928).Comparing the conventional jute woven fabric specimens with the jute woven geotextile specimens with respect to the drape co-efficient value, it had been observed that the jute woven

geotextile specimens have comparatively high drapeability than that of the conventional jute woven fabric specimens. The property parameters of the supplied fabric specimens some jute nonwoven fabric specimens along with some synthetic nonwoven fabric specimens, namely, polyester and polypropylene fabrics, had been also tested. During testing the different mechanical property parameters (such as bending length, flexural rigidity, bending modulus) of the different selected fabric specimens it had been observed that most of the property parameters were showing their responses beyond the range of the measuring capacity of the testing instruments which were used to carry out the testing of the property parameters of the different supplied fabric specimens in their study. Test results of the different supplied jute woven fabric specimens and synthetic woven fabric specimens as well as jute and synthetic nonwoven fabric specimens reveal the fact that woven jute geotextile specimens, having comparatively high area density in terms of gsm as compared to that of the conventional jute and synthetic woven fabrics and the jute and synthetic nonwoven fabric specimens show superior drapeability than the rest of the supplied fabric specimens.

Robson and Long (2000) [40], in their study investigated the application of an imaging system to the detailed objective measurement of the drape profiles of a range of wool fabrics, captured from a traditional drape tester. Image processing and software techniques are successfully implemented to enable, by the measurement of number of key parameters, a full and automatic characterization of the drape profiles reflecting visual impression. Drape coefficient values gathered via the instrumental technique correlate strongly with those established using the traditional cut and weigh approach. Strong parameter relationships are identified, and it is established that a three parameters combination of drape coefficient, numbers of nodes and variation in node severity would be required to enable good discrimination between the drape profiles of the fabric range under study.

Chen, Hu, and Ten (2001) [41] have authored a paper, dealing with the formulation of a "finite-volume method for contact drape simulations of woven fabrics and garments". A simple and easily achievable approach for handling the contact process between a fabric sheet and a rigid object has been proposed. A number of numerical examples demonstrating the capability of the method for various drape problems and different fabric materials (cotton, wool and polyester) have been given. Based on the results and discussions presented in that paper, they proposed that the conclusions may be drawn as the validity and accuracy of the present finite-volume method together with the proposed contact determination algorithm have been demonstrated through numerical comparisons with available numerical and experimental results; among the three different fabric materials studied, the numerical simulations have shown that the wool fabric has a better drapeability than the polyester or the cotton fabric; a drape simulation of fabric sheets or garments using the present method can be easily achieved on a computer within a reasonably short period of time, which demonstrates the efficiency of the proposed method. The computer time required for the drape simulation of the softer wool fabric is generally less than that for the stiffer polyester or cotton fabric; the proposed method is not only capable of accurate and efficient simulations of contact drape deformations of simple fabric sheets but also provide realistic predictions for the drape behavior of garments such as skirts in contact with body forms.

Abdin, Taha, El-Sabbagh and Ebeid (2012) [42] have published a paper on description of draping behavior of woven fabrics over single curvatures by image processing and simulation techniques. The conclusions that they have made is about the draping ability of woven fabrics like jute and glass fibre-made fabrics which is found to improve with decreased fabric cover factor. This is reflected in low drape coefficient and high Drape Distance Ratio (DDR) values. Although the current study evidences no clear relationship between the cover factor and the number of folds created when fabric is draped, the depth of each fold, in terms of the Fold Depth Index (FDI), is observed to decrease with increasing cover factor. Experimental observations can be easily predicted with finite element tools, like PamForm2G software.

In another paper (2012) [43] Taha, Abdin and Ebeid have made a paper on the prediction of draping behavior of woven fabrics over double-curvature moulds using finite element techniques. Increased cover factor (implying increased areal density and fabric tightness) results in increased shear resistance, and hence poor draping qualities. In addition to shear behavior, out-of-plane bending properties additionally contribute to final draping. Thus, to avoid wrinkling of reinforcement fabrics in moulding operations, fabrics of low in-plane shear and high bending resistance are to be favored. Whenever possible, acute angles and large edge curvatures should be avoided in mould design. The interaction of different mould geometries is also to be avoided. Simulation techniques for the optimization of mould design and material selection have been proven to be a successful tool.
Wang and Cheng (2011) [44] have published a paper on dynamic drape property evaluation of natural fibre woven fabrics using a novel automatic drape-measuring system. In this study, static and dynamic drapeability testing values of spring/summer natural fibre woven fabrics are analyzed. The weights of the tested fabrics range from 11.0 to 18.3 mg/cm2. The 'Four-in-One' Automatic Measuring System for dynamic drape is used to measure fabric drapeability. The drape-testing instrument is employed with forward rotation, reciprocating motion, and swinging motion, simulating the changes in the dynamic drape of fabric when people walk at different speeds. The results of this study indicate that the dynamic drape coefficient (D_c) and dynamic drape

coefficient of fabric in forward rotation (D_{cr}) can be used to determine the dynamic drape liveliness of four types of natural fibre woven fabrics in forward rotation, the dynamic drape coefficient with reciprocating motion (D_d) can be used to determine the dynamic drape liveliness of the four fabrics in reciprocating motion, and the dynamic drape coefficient with swinging motion (D_{sr}) can be used to determine the dynamic drape liveliness of the four fabrics in swinging motion.

Lin, Wang and Shyr (2008) [45] on their investigation compared and prepared model of the dynamic drape of four natural fibre-made (cotton, linen, silk and wool) fabrics. They have primarily analyzed the dynamic drape coefficient of four natural-fibre fabrics at speeds of 0–450 rpm. A tangent partition method was used to divide the drape coefficient curve into four regions, characterized as drape coefficient increment initial growth, fast growth, slow growth and dynamic stable regions. The ANOVA test was used for validation. The dynamic drape coefficients of these four natural fibre-made fabrics were then compared. The order of the drape coefficient of these fabrics changed three times in the fast growth region and then remained unchanged throughout the slow growth and dynamic stable regions. The order of the static drape coefficient of fabrics could not represent the drape coefficient of fabrics in dynamic performance. Therefore, a linear model, a growth model and a nonlinear logistic model were used to analyze the dynamic drape coefficient curve. The results showed that the nonlinear logistic function could be used to fit the drape coefficient curves throughout the static state and the dynamic stable region.

V. COMPARATIVE ANALYSIS OF THE DRAPING BEHAVIOR OF DIFFERENT NATURAL FIBRE-MADE FABRICS

The review work shows that the draping property of fabric is an important phenomenon to satisfy the end-use requirement of the fabric both in industrial and apparel sectors and to understand their suitability as per the specific end uses. This review work shows the different methods of measuring drape of a fabric improvised over the years starting from the Peirce Cantilever Method to the modern Image Analysis Technique. These modern instruments help to reduced error to evaluate drape of fabric both qualitatively as well as quantitatively. The drapeability of natural fibre-made fabric has made them unique in their own sectors, depending on their end-use requirements. It has been observed that the drape coefficient of jute fabrics is comparatively high than the other natural fibre-made fabrics like cotton, silk and wool considering the effective property parameters of fabrics and this makes the fabrics suitable in the field of geotextile applications such as road construction, river embankment, soil erosion control in the hill slope etc. as well as in agrotextile applications like mulching, weed management etc. While, cotton, wool and silk fabrics having a comparatively low drape coefficient value than that of the jute fabric, are much more drapeable, due to which the former are very much suitable to be used in apparel sector. Again, amongst cotton, silk and wool fabrics, the later are suitable to be used as winter garments while silk fabrics are suitable in producing furnishing products along with dress wear.

VI. CONCLUSION

The results of comprehensive review shows shortcomings and constraints that have been encountered during the performance of the experiments to evaluate the drape and related property parameters of certain natural fibre-made fabrics such as jute nonwoven fabrics. It has been observed that the bending phenomenon of those fabric specimens is occurring in a region beyond the scope of measurable zone of the existing instrument, disabling to record the readings of bending property parameters of the fabric specimens. So, there lies a possibility to design and develop an instrument for precisely evaluating the draping related property parameters of jute or alike natural fibre-made fabrics. Again, during evaluation of drape and its related property parameters of coarser fibre-made fabrics, using a standard stiffness tester and drapemeter, it has been found that the number of yarns per unit length of the fabric specimen in the width direction of the instrument template is not sufficient to give a satisfactory reading due to very small size of the template width as compared to its length, which is generally 1:6 in a standard stiffness tester. Hence, it is very difficult to analyze and assess the bending behavior related to draping behavior of the fabrics within the scope of such instruments. Therefore, an instrument is required to be engineered so that true draping behavior can be evaluated for such fabrics.

VII. ACKNOWLEDGEMENTS

The authors convey their regards to the Honorable Vice Chancellor and Pro Vice Chancellor (academic), University of Calcutta, West Bengal, India for their kind consent to allow this review paper for publication in the scholarly journal and valuable guidance to carry out this paper.

REFERENCES

[1] F.T. Peirce, “The Handle of Cloth as a Measurable Quantity”, *Journal of Textile Institute*, 21, 1930, T 377-417.

[2] C.C. Chu, C.L. Cummings and N.A. Teixeira, "Mechanics of Elastic Performance of TextileMaterials, Part-V: A Study of the Factors Affecting the Drape of Fabrics", *Textile ResearchJournal*, Sage Publisher, vol. 20, 1950, pp 539-548.

[3] G.E. Cusick, "The Resistance of Fabrics to Shearing Forces", *Journal of Textile Institute*, 52, 1961,T 395-406.

[4] J.W.S. Hearle and J. Amirbayat, "Analysis of Drape by means of Dimensionless Groups", *TextileResearch Journal*, Sage Publisher, vol. 56, 1986, pp 727-733.

[5] M. Niwa and F. Seto, "Relationship between Drapeability and Mechanical Properties of Fabrics",*Journal of Textile Machine, Soc*. Jpm.39 (11), 1986, pp 161- 168,.

[6] Z.M. Sudnik, "Objective Measurement of Fabric Drape –Practical Experience in the Laboratory",*Textile Institute*, vol. 59(1), 1972, pp 14-18.

[7] H. Morooka and M. Niwa, "Relation between Drape Coefficients and Mechanical Properties ofFabrics", *Journal of Textile Machine, Soc*. Jpm.22 (3), 1976, pp 67-73.

[8] M.L. Gaucher, M.W. King, and B. Johnson, "Predicting the Drape Coefficient of KnittedFabrics", *Textile Research Journal*, Sage Publisher , vol. 53, 1983, pp 297-303.

[9] J.R. Collier, B.J. Collier, G. O'Toole and S.M. Sargand, "Drape Prediction by means of FiniteElement Analysis", *Journal of Textile Institute*, 82, 1991, T96-107.

[10] J.R. Collier, B.J. Collier, G. O'Toole and S.M. Sargand, "Development of a Digital Drape Tester"ACPTC Combined Proceedings, 1991, pp 35.

[11] J.R. Collier and B.J. Collier, "CAD/CAM in the Textile and Apparel Industry", *Clothing TextilesJournal*, vol.8 (3), 1990, pp 7-13.

[12] Y. Go, A. Shinohara and F. Matsuhashi "Viscoelastic studies of textile fabrics part VI: anisotropyof the stiffness of textile fabrics", *J Text Mach Soc Japan*, vol.14, 1958, pp 170–174.

[13] Y. Go and A. Shinohara, "Anisotropy of the crease recovery of textile fabrics", *Journal of TextileMachine, Soc Japan*, vol.8, 1962, pp 33–38.

[14] D.N.E. Cooper, "The stiffness of woven textiles", *Journal of Textile Institute*, vol.51, 1960, ppT317–335.

[15] J. Amirbayat, and J. W. S. Hearle, "The Anatomy of Buckling of Textile Fabrics: Drape andConformability", *Journal of Textile Institute*. vol.80 (1), 1989pp 51-70.

[16] W.M. Lo, J.L. Hu and L.K. Li, "Modeling a Fabric Drape Profile", *Textile ResearchJournal*, vol.72, 2002, pp 454 – 463.

[17] C. Bijian and M. Govindaraj, "A Parametric Study of Fabric Drape", *Textile Research Journal*,vol.66, 1996, pp17-24.

[18] Y. Chen, D. W. Lloyd, and S. C. Harlock, "Mechanical Characteristics of Coated Fabrics",*Journal of Textile Institute*, vol.86, 1995, pp 690-700.

[19] S. De Jong and R. Postle, "An Energy Analysis of Woven Fabric Mechanics by Means of Optimal-Control Theory, Part I: Tensile Properties", *Journal of Textile Institute*, vol. 68, 1977, pp 350-361.

[20] H. Jinlian and C. Yuk Fung, "Effect of Fabric Mechanical Properties on Drape", *Textile Research Journal*, Sage Publisher, vol. 68, 1998, pp 57.

[21] F. R. L. Cantilever bending tester, Testing Machines Inc. 400 Bayview ave. Amityville, New York, 11701, 1p. News Release Literature, 1980.

[22] A. R. Kalyanaraman, and A. Siveramakrishnan, "Electronic fabrics stiffness meter-performance evaluation with the known instruments", *Textile Research Journal*, 54, No. 7, 1984, pp 479-484.

[23] T.G. Clapp, H. Peng, T. K. Ghosh, and J. W. Eischen, "Indirect Measurement of the moment-curvature relationship for fabrics", *Textile Research Journal*, 60, No. 9, 1990, pp 525-533.

[24] B. J. Collier, "Measurement of fabric drape and its relation to fabric mechanical properties and subjective evaluation", *Clothing and Textile Research Journal*, 1991, pp 46-52.

[25] S. J. Russell, "Alternative Instrument for the Measurement of Fabric Bending Length, (Univ of Leeds); (Letter to Editor)", *Journal of the Textile Institute*, 85, No. 1, 1994, pp82-83.

[26] P. Potluri, J. Atkinson, and I. Porat, Departments of Textile and Mechanical Engineering, "Large deformation modeling of flexible materials", *J. Text. Inst.*, 87, pp 129-151.

[27] G. Stylios, International Journal of Clothing Science and Technology, 1996.

[28] L. Vangheluwe, and Kiekens, "Time dependence of the rape coefficient of fabrics",*International Journal of Clothing Science and Technology*, 5, 1993, pp 5-8.

[29] S. Bhargava, "Jute: A Strategy for Growth", Indian Jute-A New Symphony, published by Jute Manufacturers Development Council, February 2003, pp 2.

[30] Dhingra and Postle, "Some aspects of the tailorability of woven and knitted outwearFabrics", *Clothing Research Journal*, 8-9, 1980-1981, pp 59-76.

[31] J. Hu, and S. Chung, "Drape behavior of woven fabrics with seams", *Textile Research Journal*,68, 1998, pp. 913.

[32] A. A. Itagi, and P. M. D. Rao, "Study on effects of circular seam on drape of silk apparelFabrics", *International Journal of Engineering Research & Technology (IJERT*), vol. 1 Issue 5, July2012.
[33] J. Hu, and Y. F. Chan, "Effect of fabric mechanical properties on drape", *Textile Research Journal* 68, 1998, pp. 57-64.
[34] G. K. Stylios, N. J. Powell, and L. Cheng, "An investigation into the engineering of the drapeabilityof fabric", Transactions of the Institute of Measurement and Control 24,1, 2002, pp. 33–50.
[35] T. W. Shyr, P.N. Wang, K.B. Cheng, "A comparison of the key parameters affecting the dynamic and static drape coefficients of natural-fibre woven fabrics by a newly devised dynamic drape automatic measuring system", *FIBRES & TEXTILES in Eastern Europe*, vol. 15, No. 3 (62).July / September 2007.
[36] F. Fathy, S. Ebrahim, "Prediction of garment drapeability based on fabric properties", *Journal of*American Science,7(9), 2011.
[37] GülcanSüle, "Investigation of bending and drape properties of woven fabrics and the effects offabric constructional parameters and warp tension on these properties", *Textile Research Journal*, 82: 810 originally published online 13th February 2012.
[38] *A. El-Sabbagh and I. Taha,* "Characterization of the draping behavior of jute woven fabrics forapplications of natural-fibre epoxy Composites", *Journal of Applied Polymer Science*, Publishedonline 26 April 2013.
[39] S. K. Ghosh, R. Bhattacharyya, C. Dey, B. Mukherjee, "An evaluation of drapeability of jute fabric",*Journal of Natural fibres*, accepted online on 29th January, 2014, in press.
[40] D. Robson, and C. C. Long, "Drape analysis using imaging techniques", *Clothing and Textiles*Research Journal, 18: 1, 2000.
[41] S.F. Chen, J.L. Hu, J.G. Ten, "Finite-volume method for contact drape simulations of woven fabricsand garments", Elsevier Science, Finite Elements in Analysis and Design 37, 2001, pp 513-531.
[42] Y. Abdin, I. Taha, A. El-Sabbagh, S. Ebeid, "Description of draping behaviour of woven fabricsover single curvatures by image processing and simulation techniques", *Elsevier science*,*Composites*: Part B 45, 2012, pp. 792–799.
[43] Y. Abdin, I. Taha, A. El-Sabbagh, S. Ebeid, "Prediction of draping behavior of woven fabrics overdouble-curvature moulds using finite element techniques", *International Journal of Material and*Mechanical Engineering, 1, 2012, pp. 25-31.
[44] P. N. Wang, and K. B. Cheng, "Dynamic drape property evaluation of natural fibre woven fabricsusing a novel automatic drape-measuring system", *Textile Research Journal*, 81: 1405, Originally published online 5 May 2011.
[45] J. Y. Lin, P. N. Wang, and T.W. Shyr, "Comparing and modeling the dynamic drape of fournatural-fibre fabrics", *Textile Research Journal*,78: 911,Sep 23, 2008.

American Journal of Engineering Research (AJER)
e-ISSN : 2320-0847 p-ISSN : 2320-0936
Volume-03, Issue-03, pp-359-364
www.ajer.org

Research Paper Open Access

Detrimental effect of Air pollution, Corrosion on Building Materials and Historical Structures

N. Venkat Rao, M. Rajasekhar, Dr. G. Chinna Rao
[1](Civil Engineering, Vardhaman College of Engineering, Shamshabad, Andhra Pradesh, India)
[2](Civil Engineering, Vardhaman College of Engineering, Shamshabad, Andhra Pradesh, India)
[3](Science and Humanities, Vardhaman College of Engineering, Shamshabad, Andhra Pradesh, India)

Abstract: - *The economy of any country would be drastically changed if there were no corrosion. The annual cost of corrosion world wise is over 3 % of the worlds GDP. As pet the sources available, India losses $ 45 billion every year on account of corrosion of infrastructure, Industrial machinery and other historical heritage. Keeping this critical and alarming situation in view, this paper focuses on how all these forms of corrosion affect building materials and historical structures. It also tries to bring awareness among the stakeholders of the environment and national heritage. The process of corrosion may be initiated in the form of chemical corrosion and electrochemical corrosion. The chemical may be witnessed in the form of direct oxidation, corrosion by liquid metals, fused halides and non aqueous solutions. Electrochemical corrosion may be seen in the form of immersion corrosion, underground corrosion and atmospheric corrosion.*

Keywords: - *Air pollution, Corrosion, Historical monuments, electrochemical corrosion, Oxidation.*

I. INTRODUCTION

With the advent of industrial revolution degradation of buildings has been identified. Though there are many reasons for degradation the principal reason may be attributed to air pollution. The air pollution in the form of acid rain may be chiefly responsible. The pollutants that are principally responsible for acid rain are sulphur dioxide and nitrogen dioxides. These two are emitted from the combustion of fossils fuels like coal and oil. The rapid industrialization has encouraged the quantity of these emissions. The quantity of these emissions has enormously increased in industrialized countries like UK, USA, Germany, France, Japan etc. The information on materials damage due to air pollution is very scanty. However, the information on corrosive effects of acid precipitation on metals is available for a few cities. Due to high concentration of industrial discharges and salinity and humidity in the air, corrosion rates in Mumbai are reported to be 3 to 6 times higher than those in other similar coastal areas of the country.

II. MATERIALS AFFECTED

In fact, all most all materials are affected by the deposition of acid, but the degree of damage or intensity may be varied. Some of them are more susceptible to the affect such are Carbon, Steel, Zinc, Nickel, Limestone, Marble, Paints and some plastics. Basically metallic materials are spoiled due to corrosion. Oxygen and moisture are the chief agents responsible for corrosion. Submerged structures like foundations and pipes will also be affected by acidified waters due to corrosion caused by acid attack.

2.1. THE CHEMISTRY OF CORROSION

Corrosion causing acids may attack the material both in wet and dry form. Some of the pollutants in the gaseous form may fall close to the source of emissions causing direct damage. Sulphur dioxide frequently falls as dry deposition within 30 km of its source. Wet deposition of acids occurs when the pollutants are released in to atmosphere. They react with water vapor present in clouds to form dilute acids. Sulphur dioxide, nitrogen dioxide, carbon dioxide are the most responsible pollutants causing damage to the material. The intensity of damage caused by sulphur dioxide is more compared to the other pollutants. In fact in the reaction of the materials with pollutants many variables take place. The atmospheric concentration may play a major role in the

deposition of pollutants on to the surface of materials. When the pollutants fall on to the surface of the material the intensity of reaction depends on the nature of the material and amount of moisture content present in when So_2 falls as dry deposition on the material, it is oxidized to sulphuric acid in the presence of moisture in the surface.

III. AFFECT OF AIR POLLUTION ON MATERIALS

The damage due to air pollution on materials is really a serious concern since the service life of buildings is remarkably reduced. It is true that the intensity of manmade pollutants on building degradation is more than the impact of natural pollutants. Most importantly the affects of soiling, degradation, corrosion and erosion caused by So2 are very much serious. The effect of air pollution on materials may be seen in terms of discoloration, material loss, structural failing and soiling. Both discoloration and structural failure due to air pollution on buildings may be insignificant and that may not involve huge coasts. But the effect of corrosion due to acidic deposition costs a lot. Especially the effect of sulphur dioxide and nitrogen dioxide emissions is very much significant. The effect of calcium sulphate has been very significant and may be continued for fairly long time. When calcium carbonate dissolves in sulphuric acid leads to the formation of calcium sulphate. The calcium sulphate when it falls on stone breaks the surface of the building blocks.

IV. MAJOR AIR POLLUTANTS – AFFECT

Air pollutants deteriorate by five ways such as abrasion, deposition and removal, direct chemical attack, indirect chemical attack and corrosion. Air pollution is directly responsible for economic losses in urban areas. The atmospheric deterioration of materials are caused due to moisture, temperature, sunlight, air movement and the position of the materials.

TABLE1: The effect of air pollution on materials

MATERIAL EFFECTED	RANGE OF SENSITIVITY
Brick	very low
Concrete	low
Mortar	moderate to high
sandstone, limestone, marble	high
Unalloyed steel	high
Stainless steel	very low
Nickel and nickel-plated steel	high
Zinc and galvanised steel	high
Aluminium	very low
Copper	low

4.1. OXIDES OF NITROGEN

It is produced from burning of fossil fuels and is responsible for acid rain when it reacts with atmosphere. Acid rain causes tremendous impact on the surface of material.

TABLE 2: NO_2 levels in Indian cities

CITY	RANGE OF AVG. CONC. (PPM)	RANGE OF MAX. CONC. (PPM)
Mumbai	0.008-0..13	0.013-0.05
Delhi	0.008-0..13	0.016-0.035
Kolkota	0.006-0..17	0.023-0.051
Kanpur	0.01-0..095	0.02-0.013

4.2. OXIDES OF SULPHUR

It is a corrosive gas comes from chemical, paper industries when it reacts with atmosphere it causes acid rain. The most notorious pollutant responsible for metallic corrosion is sulphur dioxide, it has been reported that corrosion of hard metals such as steel begins at annual mean concentrations of 0.02 ppm. Sulphuric acid mist in the atmosphere causes deterioration of structural materials such as marble sculptures and buildings have suffered damage in the last 30 years as a result of increased SO_2 content in the atmosphere.

TABLE 3: Sulphur Dioxide levels in Indian cities

CITY	SULPHUR DIOXIDE LEVEL ($\mu G/M^3$)
Mumbai	47
Kolkota	33

Delhi	41
Chennai	8
Hyderabad	5
Kanpur	16
Ahmedabad	11

4.3. CORBON MONOXIDE

The combustion of fossil fuels results in the emission of a variety of pollutants in to the atmosphere of which the major ones are Sox, NOx and CO. Particularly the main sources of CO in the urban air are smoke and exhaust fumes of many devices, burning coal., gas or oil. These pout comes show a big impact on the structures exclusively located near by the factories from where they are emitted.

TABLE 4: Carbon Monoxide levels in urban areas

City	Max. 1 hour CO (ppm)
London	58
Chicago	46
Los Angles	43
New York	27
Kolkota	35

4.4. PARTICULATE MATTER

Particulates such as soot, dust and fumes soil painted surfaces, fabrics and buildings, and because of their abrasive nature, particulates can cause damage to exposed surfaces when they are driven by wind at high velocities. Through their own corrosiveness or in the presence of SO2 and moisture, they can accelerate the corrosion of steel, copper, zinc and other metals.

TABLE 5: Particulate matter levels in Indian cities

City	Particulate level ($\mu g/m^3$)
Mumbai	240
Kolkota	340
Delhi	601
Chennai	100
Hyderabad	146
Kanpur	543
Ahmedabad	306

4.5. OZONE

Ozone is a very reactive substance. Much of the degradation of materials, such as fabrics and rubber, now attributed to weathering caused primarily by Ozone. Ozone present in two layers of atmosphere. The part of Ozone that present in lower layer of atmosphere (Troposphere) is more dangerous than the part present in Stratosphere. The Ozone present in the Stratosphere prevents the fall of Ultra violet radiation on to the earth as it shows an adverse affect on structures.

4.5. INDIAN AMBIENT AIR QUALITY STANDARDS

The Central Pollution Control Board in India has set up ambient air quality standards with regard to permissible concentration of the following pollutants:

TABLE 6: Indian Ambient air quality standards

POLLUTANT	INDUSTRIAL AREA ($\mu G/M^3$)	RESIDENTIAL AREA ($\mu G/M^3$)	SENSITIVE AREA ($\mu G/M^3$)
Sulphur dioxide			
Annual Avg.	80	60	15
24 hrs	120	80	30
Oxides of Nitrogen as NO_2			
Annual Avg.	80	60	15
24 hrs	120	80	30
Suspended Particulate Matter (SPM)			

Annual Avg.	360	140	70
24 hrs	500	200	100
Carbon Monoxide			
8 hrs	5000	2000	1000
1 hr	10000	4000	2000

V. INTENSITY OF DAMAGE

Most of the research studies revealed the effect of acid deposition on modern structures is significantly less than the effect on ancient monuments. All most all heritage structures are built up with lime stone and calcareous stones which are most vulnerable to corrosion. Hence continuous renovation and retrofitting is a must to protect our heritage. The historic structures all around the world are affected by acid rain. Most of the studies for the long time focused on the effect of sulphur pollutants, later the interest was diverted to the effect of nitrogen residues on the structures. Many of the researchers carried out studies on sulphur and nitrogen pollutants individually, they found their intensity of damage on materials. But in the recent past they could identify the effect of ozone and its acidifying air pollutants: in fact the effect of acid deposition on material can be studies under two important heads

The Taj Mahal, one of the Seven Wonders of the World, and India's pride, greatest land mark is also being threatened from air and water pollution. The report submitted by National Environment Engineering Research Institute deliberately shows that the 17th century monument is being damaged by air and water pollution. This is being happened even after the remedial measures taken by the government. The Ministry of Environment, Government of India has conducted a survey to find out the facts of pollution on the historical tomb. The report has revealed that the pollution levels in terms of both air and water had rose to most significant and dangerous level ,as a result of revolutionary growth in industry, traffic and population. Illegal and irrational constructions are springing up around the Taj Mahal, the heavily polluted water of the river Yamuna also causing a serious damage to the monument. An air pollution control programme was launched in 1998 when it was found the monuments famous and peculiar white marble was seen to be turning yellow. The then president Bill Clinton made an interesting statement that pollution had done "what 350 years of wars, invasions and natural disasters have failed to do and begun to mar the magnificent walls of the Taj Mahal". A series of serious banning measures have been taken including avoiding running of vehicles 500 meters away from the structure and sophisticated devices are arranged to provide running count of air pollution. It was also noticed that the fluctuations in ground water table have been threatening the structure, the water in the river Yamuna is continuously polluted by the discharge of effluents. Many experts declared that the measurable Total Particulate Suspended Matter (TSPM), Respirable Suspended Particulate Matter (RSPM) and Oxides of sulphur and nitrogen are all posing huge threats to the ancient monumental structures. The blackening of surface of structures due to the formation of dust layer over a period of time. According to Suryanarayana Murthy, a conservation architect, the organic matter that settle on the structure along with the dust leads to moth formation due to rains.

FIGURE 1: Pollution turning Taj Mahal yellow

Charminar, one of the greatest monuments in India, is being threatened by air pollution. Charminar was in most polluted area the TSPM recorded in 2010 was 267.5 and in 2012 it was 287. Some of the other oldest structures like Jama Masjid, Mecca Masjid and Badeshali Ashoorkhana are all affected by dust particulates. Architects notice that high levels of the TSPM are the biggest threat to monuments. It was also identified by Murthy that the formation of the layer happens much faster on structures with a rough surface as in the case of

Mecca Masjid, compared to the structure with smooth and plastered surface like Charminar. It has also been identified that it may take about eight to twelve month for a layer of 1 mm to form over the surface of Charminar, but it happens faster on structures like Mecca Masjid where the rugged stone is exposed. Charminar is the most famous icon of Hyderabad, now it has been suffering from deadly effect of air pollution. It was identified that the minarets of the monuments have developed air cracks at some places. Moss and Lichen growth has been identified on the walls facing the mosque on the second floor and it was also noticed on the steps leading to the upper portions. It was decided by Archaeological Survey of India (ASI) to take up repair activities at a cost of Rs 10 lacks. In fact ASI is authorized to look after its maintenance and it was also planned to take up chemical wash of charminar.

According to the available sources it was believed that the air cracks formed might be the result of climatic change. The heavy rains that lashed the city recently were believed to form precipitated matters on the surface of the structure. The seepage of rain water and the dampness have also shown their impact on air cracks. Dr. Das, the Official of ASI said during 2001,one of the minarets had suffered damage, but ASI had initiated an immediate action and rectified the problem.

The ASI has also identified that the vibrations produced by relentless movement of vehicles around it. ASI started an awareness programme called Charminar Pedestranisation Project, in concerned with this project, some of the traffic volume has been diverted.

FIGURE 2: Air cracks on Charminar

FIGURE 3: Pollution on Statue of Liberty

VI. CONCLUSION

The present contribution showed a general description on the current state of some of the historical structures. As far as the pollution on materials is concerned the tropical climate with the presence of natural pollutants create conditions for deterioration of both metals and rocky materials. In fact the present situation of historical structures is at critical junction. It is necessary that the appropriate governments should initiate substantial measures to control the damage of structures. The awareness among the public is also important to stimulate the concerned authorities to initiate control and remedial measures. This paper tries to place the facts and bring awareness among the public and custodian authorities.

REFERENCES

[1] P.Watkiss, N. Eyre, M.Holland, A. Rabl, N.Short, (2000), Impacts of air pollution on building materials, Now at the Energy Savings Trust, 21 Dartmouth Street, London, UK.

[2] C.S. Rao (2014), Environmental Pollution control Engineering, New Age international Publishers, New Delhi.

[3] S. Jacobs and C. P. Bean, "Fine particles, thin films and exchange anisotropy," in Magnetism, vol. III, G. T. Rado and H. Suhl, Eds. New York: Academic, 1963, pp. 271–350.

[4] G.S.Birdie, J.S.Birdie (2013), Water Supply and Sanitary Engineering (including Environmental Engineering and Pollution control Acts), Dhanpat Rai Publications, New Delhi

[5] E.Robinson and RC Robbins (1970), Gaseous Sulphur Pollutants from urban and natural sources J. Air Pollut. Contr. Assoc. vol. 20, pp. 303-306

[6] S. Syed (2006), Corrosion of Materials, Emirates Journal for Engineering Research, 11 (1), 1-24.

[7] ECOTEC (1996). An evaluation of the benefits of reduced sulphur dioxide emissions from reduced building damage. Ecotec Research and Consulting Ltd., Birmingham, UK.

[8] Gas (EUR 16523); Vol.5: Nuclear (EUR 16524); Vol.6: Wind and Hydro Fuel Cycles (EUR 16525). Published by European Commission, Directorate-General XII, Science Research and Development. Office for Official Publications of the European Communities, L-2920 Luxembourg.

[9] Hamilton, R.S. and Mansfield, T.A. (1992). The Soiling of Materials in the Ambient Atmosphere. Atmospheric Environment, **26A**, 3291-3296.

[10] Harter, P. (1986). Acidic Deposition - Materials and Health Effects. IEA Coal Research TR36.

[11] Holland, M.R. and Haydock, H. (2001) Economic consequences of ozone damage to paint and rubber. *In preparation.*

[12] Kucera, V. (1994). The UN ECE International Cooperative Programme on Effects on Materials, Including Historic and Cultural Monuments. Report to the working group on effects within the UNECE in Geneva, Swedish Corrosion Institute, Stockholm, 1994.

[13] Lee, D.S., Holland, M.R. and Falla, N. (1996) The potential impact of ozone on materials. Atmospheric Environment, 30, 1053-1065.

[14] NAPAP (1990) National Acid Precipitation Assessment Programme. 1990 Integrated Assessment Report. NAPA, Washington D.C.

[15] Webster, R. P. and Kukacka, L. E. (1986). Effects of Acid Deposition on Portland Concrete. In Materials Degradation Caused by Acid Rain. American Chemical Society, 1986, pp. 239-249.

[16] Tolstoy, N., Andersson, G., Sjöström, Ch., and Kucera, V. (1990). External Building Materials - Quantities and Degradation. Research Report TN:19. The National Swedish Institute for Building Research, Gävle, Sweden, 1990.